Introduction to the THERMODYNAMICS OF MATERIALS

SEVENTH EDITION

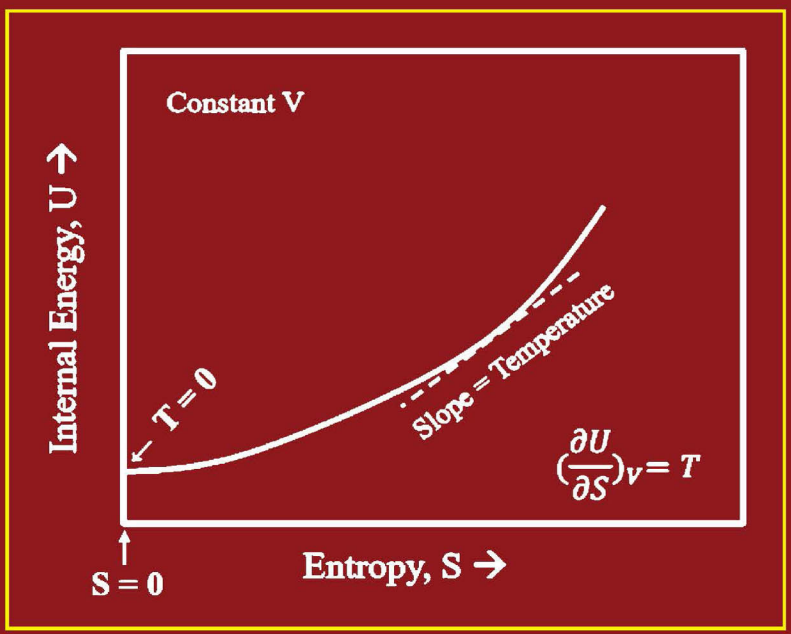

David R. Gaskell
and **David E. Laughlin**

CRC Press
Taylor & Francis Group

The Laws of Thermodynamics

- **Zeroth Law**
  Introduces the thermodynamic intensive variable of temperature (***T***)
- **First Law**
  Conservation and conversion of energy
  Defines extensive thermodynamic state variable of internal energy (***U***)
  $d\boldsymbol{U} = \delta q - \delta w'$
- **Second Law**
  Defines the extensive thermodynamic state variable of entropy (***S***)
  $d\boldsymbol{S}_{universe} \geq 0$
- **Third Law**
  For systems in internal equilibrium, sets the zero of entropy at the minimum in temperature (0K) and at the minimum in internal energy

The Three *TdS* Equations

$$TdS = c_v dT + \frac{T\alpha_P}{\beta_T} dV$$

$$TdS = c_p dT - TV\alpha_P dP$$

$$TdS = c_v \frac{\beta_T}{\alpha_P} dP + \frac{c_P}{\alpha_P V} dV$$

Fundamental Equations (extensive) for Magnetic Materials

$$dU' = TdS' - PdV' + V'\mu_0 \mathcal{H} dM + \Sigma \mu_i dn_i$$

$$dH' = TdS' + V'dP - V'\mu_0 Md\mathcal{H} + \Sigma \mu_i dn_i$$

$$dA' = -S'dT - PdV' + V'\mu_0 \mathcal{H} dM + \Sigma \mu_i dn_i$$

$$dG' = -S'dT + V'dP - V'\mu_0 Md\mathcal{H} + \Sigma \mu_i dn_i$$

Maxwell Relations for Single Component

$$\left(\frac{\partial T}{\partial V}\right)_S = -\left(\frac{\partial P}{\partial S}\right)_V$$

$$\left(\frac{\partial T}{\partial P}\right)_S = \left(\frac{\partial V}{\partial S}\right)_P$$

$$\left(\frac{\partial S}{\partial V}\right)_T = \left(\frac{\partial P}{\partial T}\right)_V$$

$$\left(\frac{\partial S}{\partial P}\right)_T = -\left(\frac{\partial V}{\partial T}\right)_P$$

Values of Selected Physical Constants

Absolute temperature of the ice point (0°C) = 273.15 K

Absolute temperature of the triple point of H_2O (by definition) = 273.16000 K

Faraday's constant f = 96,487 coulomb/mole

Avogadro's number N_o = 6.0232×10^{23}/gram•mole

Boltzmann's constant k_B = 1.38054×10^{-23} joules/degree
= 8.61733×10^{-5} ev/degree

Atmosphere 1 atm = 1.01325 bar
= 101.325 kPa
= 760 mm Hg

Gas constant R = 8.3144(6) joules/degree•mole
= 82.06 cm^3•atm/degree•mole
= 1.987 cal/degree•mole

Planck constant h = 6.6261×10^{-34} joule•sec

Permeability of vacuum μ_0 = $4\pi \times 10^{-7}$ Henry/meter

Permittivity of vacuum $\varepsilon_0 = \frac{1}{c^2 \mu_0}$ = $8.8542\ 10^{-12} \frac{coulomb^2}{joule \bullet m}$

Introduction to the Thermodynamics of Materials

Maintaining the substance that has made *Introduction to the Thermodynamics of Materials* a perennial bestseller for decades, the Seventh Edition is updated to reflect the broadening field of materials science and engineering. Chapters are updated and revised throughout to be more useful and logical for students.

- Features more than 60 new homework problems for the students, a listing of terms and concepts introduced, and a summary section
- Includes more on mathematical and graphical analysis of the various state functions utilized in classical thermodynamics
- Includes a more extensive discussion of the third law of thermodynamics
- Features a new appendix on exact differential equations and mathematical relationships, including all mathematical relations among differentials of homogeneous functions utilized in the text

Written as the definitive introduction to the thermodynamic behavior of materials systems, this text presents the underlying thermodynamic principles of materials and their applications and continues to be the best undergraduate textbook in thermodynamics for materials science students. An updated solutions manual is also available for qualifying adopting professors.

Taylor & Francis
Taylor & Francis Group
http://taylorandfrancis.com

Introduction to the Thermodynamics of Materials

Seventh Edition

David R. Gaskell and David E. Laughlin

CRC Press
Taylor & Francis Group
Boca Raton London New York

CRC Press is an imprint of the
Taylor & Francis Group, an **informa** business

Seventh edition published 2025
by CRC Press
2385 NW Executive Center Drive, Suite 320, Boca Raton FL 33431

and by CRC Press
4 Park Square, Milton Park, Abingdon, Oxon, OX14 4RN

CRC Press is an imprint of Taylor & Francis Group, LLC

© 2025 David R. Gaskell and David E. Laughlin

Sixth edition published by CRC Press 2018

Reasonable efforts have been made to publish reliable data and information, but the author and publisher cannot assume responsibility for the validity of all materials or the consequences of their use. The authors and publishers have attempted to trace the copyright holders of all material reproduced in this publication and apologize to copyright holders if permission to publish in this form has not been obtained. If any copyright material has not been acknowledged please write and let us know so we may rectify in any future reprint.

Except as permitted under U.S. Copyright Law, no part of this book may be reprinted, reproduced, transmitted, or utilized in any form by any electronic, mechanical, or other means, now known or hereafter invented, including photocopying, microfilming, and recording, or in any information storage or retrieval system, without written permission from the publishers.

For permission to photocopy or use material electronically from this work, access www.copyright.com or contact the Copyright Clearance Center, Inc. (CCC), 222 Rosewood Drive, Danvers, MA 01923, 978-750-8400. For works that are not available on CCC please contact mpkbookspermissions@tandf.co.uk

Trademark notice: Product or corporate names may be trademarks or registered trademarks and are used only for identification and explanation without intent to infringe.

Library of Congress Cataloging-in-Publication Data
Names: Gaskell, David R., 1940-2013 author. | Laughlin, David E., 1947- author.
Title: Introduction to the thermodynamics of materials/David R. Gaskell and David E. Laughlin.
Other titles: Introduction to metallurgical thermodynamics
Description: Seventh edition. | Boca Raton, FL: CRC Press, 2024. | Includes index.
Identifiers: LCCN 2023053230 | ISBN 9781032450995 (hbk) | ISBN 9781032451015 (pbk) | ISBN 9781003375388 (ebk)
Subjects: LCSH: Thermodynamics. | Materials–Thermal properties. | Metallurgy.
Classification: LCC TN673.G33 2024 | DDC 620.1/1296–dc23/eng/20231122
LC record available at https://lccn.loc.gov/2023053230

ISBN: 978-1-032-45099-5 (hbk)
ISBN: 978-1-032-45101-5 (pbk)
ISBN: 978-1-003-37538-8 (ebk)

DOI: 10.1201/9781003375388

Typeset in Times
by codeMantra

Access the Support Material: www.routledge.com/9781032450995

Diane
Our boundary lines have fallen to us in pleasant places.

Psalm 16.6
We have walked together *in the* Grace of Life

Taylor & Francis
Taylor & Francis Group
http://taylorandfrancis.com

Contents

Preface xviii
Authors xix

PART I Thermodynamic Principles

Chapter 1 Introduction and Definition of Terms 3

1.1 Introduction 3
1.2 The Concept of State 4
1.3 Example of Equilibrium 8
1.4 The Equation of State of an Ideal Gas 9
1.5 The Units of Energy and Work 12
1.6 Extensive and Intensive Thermodynamic Variables 13
1.7 Equilibrium Phase Diagrams and Thermodynamic Components 13
1.8 Laws of Thermodynamics 16
1.8.1 The First Law of Thermodynamics 17
1.8.2 The Second Law of Thermodynamics 17
1.8.3 The Third Law of Thermodynamics 17
1.9 Summary 17
1.10 Concepts and Terms Introduced in This Chapter 18
1.11 Qualitative Example Problems 19
1.12 Quantitative Example Problems 20
Problems 21

Chapter 2 The First Law of Thermodynamics 23

2.1 Introduction 23
2.2 The Relationship between Heat and Work 23
2.3 Internal Energy and the First Law of Thermodynamics 25
2.3.1 Adiabatic Changes of State 26
2.3.2 Changes of State with No Work 26
2.3.3 Changes of State with Both Work and Heat Processes 27
2.4 Constant Volume Processes 29
2.5 Constant Pressure Processes and the Enthalpy, *H* 30
2.5.1 Application of the First Law to Chemical Reactions 31
2.6 Heat Capacity 32
2.6.1 Application of the First Law to Enthalpy Changes 33

2.6.2 Relationship between C_P and C_V 34
2.6.2.1 Free Expansion of a Gas: Joule Expansion ... 36
2.6.2.2 Adiabatic Expansion of a Gas: Joule Thomson Expansion 36
2.7 Reversible Adiabatic Processes 37
2.8 Reversible Isothermal Pressure or Volume Changes of an Ideal Gas 38
2.9 Other Forms of Work 40
2.9.1 Magnetic Work on a Paramagnetic Material 40
2.9.2 Electrical Work on a Dielectric Material 41
2.9.3 Work to Create or Extend a Surface 41
2.10 Summary 42
2.11 Concepts and Terms Introduced in This Chapter 44
2.12 Qualitative Example Problems 45
2.13 Quantitative Example Problem 46
Problems 52
Appendix 2A: Note on the Sign Convention of δw 56

Chapter 3 The Second Law of Thermodynamics 57

3.1 Introduction 57
3.2 Spontaneous or Natural Processes 57
3.3 Entropy and the Quantification of Irreversibility 59
3.4 Reversible Processes 61
3.5 Illustration of Reversible and Irreversible Isothermal Processes 61
3.5.1 The Reversible Isothermal Expansion of an Ideal Gas 61
3.5.2 The Free Expansion of an Ideal Gas 63
3.5.3 Summary of the Isothermal Reversible versus Irreversible Expansion of Ideal Gas 63
3.6 Further Differences between Reversible and Irreversible Expansions 64
3.7 Compression of Ideal Gas 64
3.7.1 Reversible Compression of Ideal Gas 65
3.8 Illustration of Reversible and Irreversible Adiabatic Expansion Processes 65
3.8.1 Reversible Adiabatic Expansion 66
3.8.2 The Adiabatic Irreversible Expansion of an Ideal Gas 66
3.8.2.1 Adiabatic Free Expansion 66
3.8.2.2 Adiabatic Irreversible Expansion but Not Free Expansion 67
3.8.3 Summary of the Adiabatic Reversible versus Irreversible Expansion of Ideal Gas 67

3.9 Summary Statements 68
3.10 The Properties of Heat Engines 68
3.11 The Thermodynamic Temperature Scale 71
3.12 The Second Law of Thermodynamics 74
3.13 Maximum Work 77
3.14 Entropy and the Criterion for Equilibrium 79
3.15 The Combined Statement of the First and Second Laws of Thermodynamics 80
3.16 Summary 82
3.17 Concepts and Terms Introduced in This Chapter 83
3.18 Qualitative Example Problems 84
3.19 Quantitative Example Problems 86
Problems 91

Chapter 4 The Statistical Interpretation of Entropy 94

4.1 Introduction 94
4.2 Entropy and Disorder on an Atomic Scale 95
4.3 The Concept of Microstate 96
4.4 Isolated Systems 97
4.4.1 Distinguishable Sites with Different Assigned Energies 98
4.4.2 Configurational Entropy of Differing Atoms in a Crystal: Entropy of Mixing 100
4.4.2.1 Mixing of a Generalized Crystal 103
4.4.3 Configurational Entropy of Magnetic Spins on an Array of Atoms 105
4.4.4 Summary of the Microcanonical Approach 106
4.5 The Boltzmann Distribution 107
4.6 The Influence of Temperature 111
4.7 The Two State System 113
4.8 Application to the Heat Capacity of Solids at Low Temperatures 115
4.9 Heat Flow and the Production of Entropy 120
4.10 Summary 123
4.11 Concepts and Terms Introduced in This Chapter 124
4.12 Qualitative Example Problems 124
4.13 Quantitative Example Problems 126
Problems 129

Chapter 5 Fundamental Equations and Their Relationships 131

5.1 Introduction 131
5.2 The Enthalpy, H 132
5.3 The Helmholtz Free Energy, A 133
5.4 The Gibbs Free Energy, G 137
5.5 The Fundamental Equations for a Closed System 139

5.6 The Variation of the Composition within a Closed System ... 140
5.7 The Chemical Potential ... 140
5.8 Thermodynamic Relations ... 143
5.9 Maxwell's Relations ... 144
5.10 Examples of the Application of Maxwell Relations ... 146
5.10.1 The First *TdS* Equation ... 146
5.10.2 The Second *TdS* Equation ... 148
5.10.3 The Third *TdS* Equation ... 150
5.10.4 Entropy and Volume as Dependent Variables and Temperature and Pressure as Independent Variables ... 152
5.10.5 A Magnetic Maxwell Relation ... 153
5.10.6 *S*, *V*, and *M* as Dependent Variables with Independent Variables *T*, *P*, and $\mathcal{H}$ ... 154
5.11 An Energy Equation (Internal Energy) ... 157
5.12 Another Energy Equation (Enthalpy) ... 157
5.13 Gibbs–Helmholtz Equations ... 158
5.14 Summary ... 159
5.15 Concepts and Terms Introduced in This Chapter ... 161
5.16 Qualitative Example Problems ... 161
5.17 Quantitative Example Problems ... 163
Problems ... 166

Chapter 6 Heat Capacity, Enthalpy, Entropy, and the Third Law of Thermodynamics ... 169

6.1 Introduction ... 169
6.2 Temperature Dependence of the Heat Capacity ... 170
6.3 Enthalpy as a Function of Temperature ... 174
6.4 The Third Law of Thermodynamics ... 184
6.4.1 Historical Development of the Third Law of Thermodynamics ... 184
6.4.1.1 Another Statement of the Third Law of Thermodynamics ... 186
6.4.2 Experimental Verification of the Third Law ... 186
6.4.3 Some Physical Consequences of the Third Law of Thermodynamics ... 188
6.4.3.1 Thermal Expansion Coefficient ... 188
6.4.3.2 The Thermal Coefficient of Pressure ... 189
6.4.3.3 Heat Capacities ... 189
6.4.3.4 Magnetization versus Temperature Plot ... 189
6.4.3.5 Energy Plots versus Entropy ... 189
6.4.3.6 Stable Phases at 0 K ... 190
6.4.3.7 Approaching 0 K ... 191
6.4.4 Apparent Contradictions to the Third Law of Thermodynamics ... 192

6.5 Temperature Dependence of Entropy at Higher Temperatures 194
6.5.1 Richard's Rule for Entropies of Melting 195
6.5.2 Trouton's Rule for Entropies of Boiling 196
6.6 The Influence of Pressure on Enthalpy and Entropy 198
6.6.1 Example Calculations 199
6.7 Summary 200
6.8 Concepts and Terms Introduced in This Chapter 202
6.9 Qualitative Example Problems 202
6.10 Quantitative Example Problems 203
Problems 209

PART II Phase Equilibria

Chapter 7 Phase Equilibrium in a One-Component System 215

7.1 Introduction 215
7.2 The Variation of Gibbs Free Energy with Temperature at Constant Pressure 216
7.3 The Variation of Gibbs Free Energy with Pressure at Constant Temperature 221
7.4 The Gibbs Free Energy as a Function of Temperature and Pressure 222
7.5 Equilibrium between the Vapor Phase and a Condensed Phase 225
7.6 Graphical Representation of Vapor Phase and Condensed Phase Equilibria on Pressure Temperature Phase Diagrams 229
7.7 Solid–Solid Equilibria 229
7.7.1 Solid–Solid Equilibria in Iron 231
7.7.2 Solid–Solid Equilibria in Zirconia 233
7.8 The Effect of an Applied Magnetic Field on the *P-T* Diagram 234
7.9 Summary 235
7.10 Concepts and Terms Introduced in This Chapter 237
7.11 Qualitative Example Problems 238
7.12 Quantitative Example Problems 240
Problems 244
Appendix 7A: Derivation of the Gibbs Equilibrium Phase Rule 248
7A.1 One Component System 248
7A.2 System with *C* Components 249

Chapter 8 The Behavior of Gases 250

8.1 Introduction 250
8.2 The *P-V-T* Relationships of Gases 250
8.3 The Thermodynamic Properties of Ideal Gases and Mixtures of Ideal Gases 251
8.3.1 Mole Fraction 251
8.3.2 Dalton's Law of Partial Pressures 252
8.3.3 Partial Molar Quantities 253
8.4 Mixing of Ideal Gases 255
8.4.1 The Internal Energy of Mixing of Ideal Gases 255
8.4.2 The Enthalpy of Mixing of Ideal Gases 255
8.4.3 The Gibbs Free Energy of Mixing of Ideal Gases 256
8.4.4 The Entropy of Mixing of Ideal Gases 257
8.5 Deviation from Ideality and Equations of State for Real Gases 257
8.6 The van der Waals Fluid 262
8.6.1 The van der Waals Equation for CO_2 267
8.6.2 Summarizing Remarks on the van der Waals Equation 270
8.7 Other Equations of State for Nonideal Gases 271
8.8 Further Thermodynamic Treatment of Nonideal Gases 272
8.8.1 Numerical Examples Using Fugacity 274
8.9 Summary 280
8.10 Concepts and Terms Introduced in This Chapter 282
8.11 Qualitative Example Problems 282
8.12 Quantitative Example Problems 284
Problems 287

Chapter 9 The Behavior of Solutions 290

9.1 Introduction 290
9.2 Raoult's Law and Henry's Law 290
9.3 The Thermodynamic Activity of a Component in Solution 294
9.4 The Gibbs–Duhem Equation 296
9.5 The Gibbs Free Energy of Formation of a Solution 298
9.5.1 The Molar Gibbs Free Energy of a Solution and the Partial Molar Gibbs Free Energies of the Components of the Solution 298
9.5.2 The Change in Gibbs Free Energy due to the Formation of a Solution (Mixing) 299
9.5.3 The Method of Tangential Intercepts 301
9.6 The Properties of Ideal Solutions 301
9.6.1 The Change in Volume Accompanying the Formation of an Ideal Solution 301
9.6.2 The Enthalpy of Formation of an Ideal Solution 303
9.6.3 The Entropy of Formation of an Ideal Solution 304

9.6.4 The Gibbs Free Energy of Formation of an Ideal Solution 307
9.7 Nonideal Solutions 307
9.8 Application of the Gibbs–Duhem Relation to the Determination of Activity 310
9.8.1 The Relationship between Henry's and Raoult's Laws 312
9.8.2 Direct Calculation of the Total Molar Gibbs Free Energy of Mixing 312
9.9 Regular Solutions 314
9.10 The Gibbs Free Energy of Formation of Regular Solutions ... 321
9.11 Criteria for Phase Stability in Regular Solutions 324
9.12 The Flory–Huggins Regular Solution Model for Application to Polymers 329
9.13 Summary 331
9.14 Concepts and Terms Introduced in This Chapter 333
9.15 Qualitative Example Problems 334
9.16 Quantitative Example Problems 336
Problems 338

Chapter 10 Gibbs Free Energy Composition and Phase Diagrams of Binary Systems 342

10.1 Introduction 342
10.2 Gibbs Free Energy and Thermodynamic Activity 343
10.3 Liquid and Solid Standard States 345
10.3.1 Analysis of the Development of Solidus and Liquidus Curves for Ideal Solutions 345
10.4 Phase Diagrams, Gibbs Free Energy, and Thermodynamic Activity 351
10.5 Calculations of Portions of Phase Diagrams 353
10.5.1 Calculations of a Portion of the Bi-Cd Phase Diagram 358
10.5.2 Calculations of Liquidus Lines with Varying Positive Deviations from Ideality 358
10.6 The Phase Diagrams of Binary Systems That Exhibit Regular Solution Behavior in Both the Liquid and Solid States 362
10.6.1 Solution with $\alpha_l = -20{,}000\,\text{J}$ and $\alpha_s = 0$ 362
10.6.2 Solution with $\alpha_l = -20{,}000\,\text{J}$ and $\alpha_s = +10{,}000\,\text{J}$ 364
10.6.3 Solution with $\alpha_l = +20{,}000\,\text{J}$ and $\alpha_s = +30{,}000\,\text{J}$ 366
10.6.4 Concluding Remarks on Section 10.6 369
10.7 Slopes of the Temperature Composition Curves Involving First-Order Transformations 370

10.8 Examples of Incorrect Binary Phase Diagram Configurations 372
10.9 Magnetic Transformations and the Phase Diagram 373
10.10 Summary 374
10.11 Concepts and Terms Introduced in This Chapter 375
10.12 Qualitative Example Problems 376
10.13 Quantitative Example Problems 377
Problems 383
Appendix 10A 386
Appendix 10B 388

PART III Reactions and Transformations of Phases

Chapter 11 Reactions Involving Gases 393

11.1 Introduction 393
11.2 Reaction Equilibrium in a Gas Mixture and the Equilibrium Constant 394
11.3 The Effect of Temperature on the Equilibrium Constant 400
11.4 The Effect of Pressure on the Equilibrium Constant 402
11.5 Reaction Equilibrium as a Compromise between Enthalpy and Entropy 403
11.6 Reaction Equilibrium in the System $SO_{2(g)}$–$SO_{3(g)}$–$O_{2(g)}$ 406
11.6.1 The Effect of Temperature in the System $SO_{2(g)}$–$SO_{3(g)}$–$O_{2(g)}$ 407
11.6.2 The Effect of Pressure in the System $SO_{2(g)}$–$SO_{3(g)}$–$O_{2(g)}$ 408
11.6.3 The Combined Effect of Temperature and Pressure Changes in the System $SO_{2(g)}$–$SO_{3(g)}$–$O_{2(g)}$ 409
11.7 Equilibrium in H_2O–H_2 and CO_2–CO Mixtures 411
11.8 Summary 413
11.9 Concepts and Terms Introduced in This Chapter 415
11.10 Qualitative Example Problems 415
11.11 Quantitative Example Problems 417
Problems 423

Chapter 12 Reactions Involving Pure Condensed Phases and a Gaseous Phase 426

12.1 Introduction 426
12.2 Reaction Equilibrium in a System Containing Pure Condensed Phases and a Gas Phase 427

12.3 The Variation of the Standard Gibbs Free Energy Change with Temperature 432
12.4 Ellingham Diagrams 433
12.4.1 Ellingham Diagram of the Oxidation of Silver 434
12.4.2 Some General Features of Ellingham Diagrams 435
12.4.3 Ellingham Diagrams with Intersecting Stability Lines 436
12.5 The Effect of Phase Transformations 441
12.5.1 Example of the Oxidation of Copper 442
12.6 The Oxides of Carbon 444
12.6.1 The Effect of Pressure on the Oxidation of Carbon 445
12.6.2 The Effect of P_{CO_2}/P_{CO} on the Equilibrium Reaction $2CO + O_2 = 2CO_2$ 447
12.7 Graphical Representation of Equilibria in the System Metal–Carbon–Oxygen 450
12.8 Summary 455
12.9 Concepts and Terms Introduced in This Chapter 456
12.10 Qualitative Example Problems 457
12.11 Quantitative Example Problems 458
Problems 465
Appendix 12A: Determination of I in Equation 12.10 467

Chapter 13 Reaction Equilibria in Systems Containing Components in Condensed Solution 469

13.1 Introduction 469
13.2 The Criteria for Reaction Equilibrium in Systems Containing Components in Condensed Solution 470
13.3 Alternative Standard States 479
13.4 Phase Stability Diagrams: Si-C-O 486
13.4.1 Plots of $\log a_C$ and $\log p_{O_2}$ for Si-C-O 487
13.4.1.1 The Equilibrium Si–SiO_2–Gas Phase 487
13.4.1.2 The Equilibrium Si–SiC–Gas Phase 488
13.4.1.3 The Equilibrium SiC–SiO_2–Gas Phase 488
13.4.1.4 The Equilibrium SiC–C–Gas Phase 488
13.4.1.5 The Equilibrium SiO_2–C–Gas Phase 490
13.4.1.6 The Equilibrium Si–C–Gas Phase 490
13.4.2 Plots of $\log p_{CO} = \log p_{CO_2}$ Stability Diagram for Si-C-O 492
13.4.3 Plots of $\log p_{CO}$ versus $\frac{1}{T}$ for Si-C-O 496
13.4.3.1 The Equilibrium $Si_{(s)}$–SiO_2–Gas Phase 496
13.4.3.2 The Equilibrium $Si_{(s)}$–SiC–Gas Phase 498

13.4.3.3 The Equilibrium $Si_{(l)}$–SiC–Gas Phase 498
13.4.3.4 The Equilibrium SiC–SiO_2–Gas Phase 498
13.5 Binary Systems Containing Compounds 499
13.5.1 Example Problem: The Binary Ga–GaP System 507
13.6 Graphical Representation of Phase Equilibria 508
13.6.1 Phase Equilibria in the System Mg–Al–O 508
13.6.2 Phase Equilibria in the System Al–C–O–N Saturated with Carbon 513
13.7 The Formation of Oxide Phases of Variable Composition 516
13.7.1 The Fe-O System 518
13.8 The Solubility of Gases in Metals 525
13.9 Summary 529
13.10 Concepts and Terms Introduced in This Chapter 531
13.11 Qualitative Example Problems 531
13.12 Quantitative Example Problems 533
Problems 536

Chapter 14 Electrochemistry 542

14.1 Introduction 542
14.2 The Relationship between Chemical and Electrical Driving Forces 544
14.3 The Effect of Concentration on EMF 549
14.4 Formation Cells 550
14.5 Concentration Cells 552
14.6 The Temperature Coefficient of the EMF 558
14.7 Thermal Energy (Heat) Effects 560
14.8 The Thermodynamics of Aqueous Solutions 561
14.9 The Gibbs Free Energy of Formation of Ions and Standard Reduction Potentials 564
14.9.1 Single Electrode Potential 567
14.9.2 Solubility Products 569
14.9.3 The Influence of Acidity 573
14.10 Batteries 574
14.10.1 Lead-Acid Battery 574
14.10.2 Nickel Cadmium Battery 575
14.10.3 Lithium Ion Batteries 576
14.11 Pourbaix Diagrams 576
14.11.1 The Pourbaix Diagram for Aluminum 579
14.11.1.1 The Equilibrium between the Two Dissolved Substances 579
14.11.1.2 The Equilibrium between the Two Solids 580
14.11.1.3 One Solid in Equilibrium with a Dissolved Substance 581
14.11.1.4 The Solubility of Alumina in Aqueous Solutions 585

14.12 Summary 586
14.13 Concepts and Terms Introduced in This Chapter 588
14.14 Qualitative Example Problem 589
14.15 Quantitative Example Problems 590
Problems 593

Chapter 15 More Binary System Solution Models 596

15.1 Introduction 596
15.2 Review of Ideal and Regular Solution Models 596
15.2.1 The Gaseous State: Ideal Solutions 596
15.2.2 The Condensed State: Ideal Solutions 597
15.2.3 The Condensed State: Regular Solutions 597
15.2.3.1 Regular Solutions with Positive Deviation from Ideality 598
15.2.3.2 Regular Solutions with Negative Deviation from Ideality 599
15.3 Sub-Regular Solution Models 599
15.4 Statistical Models of Solutions 602
15.5 The Atomic Order Parameter 606
15.5.1 Statistical Models Including Second-Neighbor Interactions 610
15.6 Landau Theory of Ordered Solutions 611
15.6.1 The 2-4 Model 612
15.6.1.1 Excursus on T_C 615
15.6.2 The 2-3-4 Model 616
15.6.3 The 2-4-6 Model 620
15.6.4 Concluding Remarks on the Landau Model 623
15.7 Summary 623
15.8 Concepts and Terms Introduced in This Chapter 624
15.9 Qualitative Example Problems 624
Problems 626

Appendix A: Selected Thermodynamic and Thermochemical Data 629

Appendix B: Useful Mathematical Relationships 636

Appendix C: The Generation of Additional Thermodynamic Potentials as Legendre Transformations 639

Nomenclature 647

Answers to Selected Problems 649

Index 663

Preface

This seventh edition of *Introduction to the Thermodynamics of Materials* is published 51 years after the first edition (titled *Introduction to Metallurgical Thermodynamics*), written by David R. Gaskell. Over the years, the book has grown in size and expanded in coverage. The flavor of the seventh edition is still somewhat *Metallurgical*, but the topics have expanded to include a more general materials accent. As stated in the preface to the sixth edition, I used the first edition in 1975, when teaching my first thermodynamics course at Carnegie Mellon University. In 2022, I retired from Carnegie Mellon University after 48 years of teaching and research, but not before collating many of my homework and exam questions, some of which I have added to this edition.

There is no space to mention all the people who have given me comments and suggestions over the past 7 years. But special thanks must go to Prof. J.K. Chen, Dean of the College of Engineering, National Taipei University of Technology, who translated the text into Chinese, and in the course of his translation, he found many errors. My former PhD student, Prof. Huseyin Ucar, of California State Polytechnic University supplied me with typos he found in his lecturing on thermodynamics. Anthony P. Petric, Emeritus Professor, McMaster University, gave me some good suggestions. Finally, thanks to Drs. George Shannon and Piyamanee Komolwit, who helped with the proofreading of this edition.

Of course, I gladly acknowledge the love and encouragement I have received from my wife, Diane. Our 4 children, their spouses, and our 9 grandchildren have been a constant source of inspiration and delight to us. Truly, as the psalmist of old wrote: "Our boundary lines have fallen to us in pleasant places".

I count it a privilege to write this seventh edition of *Thermodynamics*, some 11 years after David R. Gaskell's death. May the text continue to train students well in the basics of materials thermodynamics.

David E. Laughlin
ALCOA Professor of Physical Metallurgy, Emeritus
Department of Materials Science and Engineering
Carnegie Mellon University

Authors

David R. Gaskell earned a BSc in metallurgy and technical chemistry at the University of Glasgow, Scotland, and a PhD at McMaster University, Hamilton, Ontario, Canada. Dr. Gaskell's first faculty position was at the University of Pennsylvania, where he taught from 1967 to 1982 in metallurgy and materials science. In 1982, he was recruited at the rank of professor by Purdue University, West Lafayette, Indiana, where he taught until his death in 2013. During Dr. Gaskell's career, he served as a visiting professor at the National Research Council of Canada, Atlantic Regional Laboratory, Halifax, Nova Scotia (1975–1976), and as a visiting professor at the G. C. Williams Co-operative Research Centre for Extraction Metallurgy, in the Department of Chemical Engineering, University of Melbourne, Australia (1995). He also held a position during his sabbatical in Australia as a visiting scientist at the Commonwealth Scientific and Industrial Research Organisation (CSIRO) in Clayton, Victoria. Dr. Gaskell authored the textbooks *Introduction to Metallurgical Thermodynamics*, *Introduction to the Thermodynamics of Materials*, and *Introduction to Transport Phenomena in Materials Engineering.*

David E. Laughlin is the ALCOA Professor of Physical Metallurgy Emeritus in the Department of Materials Science and Engineering at Carnegie Mellon University (CMU), Pittsburgh, Pennsylvania. He also had a courtesy appointment in the Electrical and Computer Engineering Department. He was the principal editor of *Metallurgical and Materials Transactions* from 1987 to 2016. David is a graduate of Drexel University, Philadelphia, Pennsylvania (1969), and the Massachusetts Institute of Technology, Cambridge, Massachusetts (1973). He is a fellow of the Minerals, Metals and Materials Society (TMS), an honorary member of the American Institute of Mining, Metallurgical, and Petroleum Engineers (AIME), and a fellow of ASM International. He is also the recipient of several CMU awards for teaching and research excellence and was named a distinguished scientist of the TMS Electronic, Magnetic, and Photonic Materials Division. He presented the 2017 ASM Campbell Memorial Lecture and is the recipient of the 2025 ASM International J. W. Gibbs Award. He has authored more than 500 technical publications in the field of phase transformations, physical metallurgy, and magnetic materials; has been awarded 12 patents; and has edited or coedited seven other books, including the fifth and sixth editions of *Physical Metallurgy.*

Taylor & Francis
Taylor & Francis Group
http://taylorandfrancis.com

Part I

Thermodynamic Principles

Taylor & Francis
Taylor & Francis Group
http://taylorandfrancis.com

1 Introduction and Definition of Terms

1.1 INTRODUCTION

The term *thermodynamics* was derived from the two Greek words *therme* and *dynamikos*, which were translated into English as "heat" and "power" (or "movement"), respectively. Originally, thermodynamics was the physical science that focused on the relationship between heat (a form of energy) and work. It has since increased its area of application to include all the *equilibrium states* and *variables* of systems that are being investigated. Importantly, thermodynamics defines heat and identifies it as the process in which energy is transferred from one region to another down a temperature gradient. In this text, we will mainly use the phrase *thermal energy* to identify this form of energy transfer, but sometimes the word *heat* will be used. Thermodynamics deals with the *conservation* of energy as well as the *conversion* of the various forms of energy into each other or into work.

Thermodynamics is concerned with the behavior of and interactions between portions of the universe denoted as *systems* and those portions of the universe not included in the system, called the *surroundings* or the *environment*. The system is that part of the universe we wish to investigate in detail, and the surroundings is that part of the universe outside the system which may interact with it by exchanging energy or matter. The system may perform work on the surroundings or have work performed on it by the surroundings. The boundary or wall between the system and the surroundings allows or forbids such interactions. In what we will call *simple thermodynamic systems*, the surroundings interacts with the system only *via* pressure and temperature changes. The chemical composition remains constant in simple systems.

It is convenient to characterize systems by the kinds of interactions that are allowed between them and their surroundings:

1. *Isolated systems*: In these systems, no work can be done on or by the system. In addition, energy or matter may not enter or leave it. Thus, the energy of these systems remains constant, as does the overall composition. Isolated systems are therefore unaffected by changes in the surroundings. Macroscopic changes can occur within the system if it is not at equilibrium.
2. *Closed systems*: These are systems in which the boundaries are impermeable to matter; therefore, the amount and composition of the systems are constant. Closed systems may receive (or give off) energy from (or to) the surroundings. The boundaries are called *diathermal*; that is, they allow (thermal) energy to transfer through them into or out of the system. Work may be performed on or by these systems.

DOI: 10.1201/9781003375388-2

3. *Open systems*: These are systems that can exchange both energy and matter with the surroundings. Neither the energy nor the amount of or composition of the matter in these systems needs to remain constant. The boundaries are both permeable (to matter) and diathermal.

The boundaries or walls of the system are classified as follows:

- *Adiabatic*: No thermal energy can pass through.
- *Diathermal*: Thermal energy can pass through.
- *Permeable*: Matter can pass through.
- *Impermeable*: Matter cannot pass through.
- *Semipermeable*: Some components are able to pass through, while others are not.

It is evident that when evaluating a system, it is important that its interactions with the surroundings be either known or determined.

The macroscopic property of systems called *temperature* is a distinguishing aspect of the subject of thermodynamics. Temperature is not utilized in the mechanical description of matter (mass, velocity, momentum, etc.) encountered in introductory physics courses. The discovery that mechanical energy could be *converted* to thermal energy (*via* friction) was an important early step in the development of thermodynamics. Later, the conversion of thermal energy into mechanical work, or other forms of energy, became a focus of classical thermodynamics. This will be discussed in the introduction to the First Law of Thermodynamics in Chapter 2.

A *system* may be a machine (e.g. heat engine) or a device (e.g. transducer) of interest to us. In the study of the thermodynamics of materials, the system is composed of matter, which is anything that has mass and occupies space. Matter has a given temperature, pressure, and chemical composition, as well as physical properties such as the coefficient of thermal expansion, compressibility, heat capacity, and viscosity. A central aim of applied thermodynamics is the determination of the effect of the surroundings on the equilibrium state of a given system. Since the surroundings interacts with the system by transferring or receiving various forms of energy or matter with it, another focus of applied thermodynamics is the establishment of the relationships that exist between the equilibrium state of a given system and the influences that have been brought to bear on it. *Equilibrium* is the *state* of macroscopic rest from which no spontaneous changes can occur without interactions with the surroundings.

1.2 THE CONCEPT OF STATE

A fundamental concept in thermodynamics is that of the thermodynamic *state*. If it were possible to know the masses, velocities, positions, and all modes of motion (translational, rotational, etc.) of all of the constituent particles in a system, as well as any possible interactions among them, this knowledge would serve to describe what is called the *microscopic state* of the system. In turn, this would determine, in principle, all of the thermodynamic variables of the system that can be measured (energy, temperature, pressure, etc.). For systems with macroscopic dimensions, this

would entail more than 10^{24} coordinates, which is clearly an impossible task. In the absence of such detailed knowledge as is required to determine the microscopic state of the system, classical thermodynamics begins with a consideration of the variables of the system, which, when determined, completely define the *macroscopic state* of the system; that is, when all of the thermodynamic variables are fixed, the macroscopic state of the system is fixed and is said to be in equilibrium. It is found that when the values of a small number of thermodynamic variables are fixed, the values of the rest of the thermodynamic variables are also fixed. Indeed, when a *simple system* such as a given quantity of a substance of fixed composition is being considered, the fixing of the values of two of the thermodynamic variables fixes the values of the rest of the thermodynamic variables. Thus, only two thermodynamic variables are independent, which, consequently, are called the *independent thermodynamic variables* of the system. All of the other variables are *dependent variables.* The thermodynamic state of a system of a given quantity of the substance is thus uniquely determined when the values of the two independent variables (often chosen to be the field variables temperature and pressure) are fixed. This has been called the *Duhem postulate* (Pierre Maurice Marie Duhem (1861–1916)). There are situations, however, when more independent variables are needed—for example, when external fields other than temperature and pressure are present. Such *fields* include electric or magnetic fields.

The values of the equilibrium thermodynamic variables of a system are not functions of the history of the system; that is, they are *independent* of the path over which the process has taken the system in changing it from its previous state to its present equilibrium state. These thermodynamic variables are thus *intrinsic* to the state of the system. Such thermodynamic variables are functions of state and can be expressed as *exact differentials*[1] of their dependent variables. There are, of course, times when a system has properties that depend on its history; these properties are commonly called *extrinsic* properties. They are *not equilibrium* properties of the system and depend on, for example, the *microstructure* of the system. Given time, they may change. It should be noted that some of these extrinsic properties often can be manipulated to produce materials with optimum characteristics.

Consider the volume, V, of 1 mole of a simple gas (i.e. one made up of atoms or molecules that do not interact with each other). The value of the volume is dependent on the values of the pressure, P, and temperature, T, of the gas. The relationship between the dependent variable V and the independent variables P and T can be expressed as

$$V = V(P,T) \tag{1.1}$$

According to Herbert Bernard Callen (1919–1993),[2] this is an example of an *equation of state*, that is, a functional relationship that expresses the extensive variables in terms of the *intensive variables* (which were called *field variables* above). In a three-dimensional diagram, the coordinates of which are volume, pressure, and

[1] See Appendix B for some properties of exact differential equations.

[2] H. B. Callen, *Thermodynamics and an Introduction to Thermostatistics*, Wiley, Hoboken, NJ, 1991.

temperature, the points in *V-P-T* space, which represent the equilibrium states of existence of the system, lie on a surface. This is shown in Figure 1.1 for 1 mole of a simple gas. Fixing the values of any two of the three variables fixes the value of the third variable of the system when it is in equilibrium.

Consider a process that changes the state of the gas from state 1 to state 2. This process causes the volume of the gas to change by

$$\Delta V = V_2 - V_1$$

The process could proceed along many different paths on the *V-P-T* surface, two of which, $1 \rightarrow a \rightarrow 2$ and $1 \rightarrow b \rightarrow 2$, are shown in Figure 1.1.

Consider the path $1 \rightarrow a \rightarrow 2$. The change in volume is

$$\begin{aligned}\Delta V &= \Delta V_{1\rightarrow a} + \Delta V_{a\rightarrow 2} \\ &= (V_a - V_1) + (V_2 - V_a) \\ &= V_2 - V_1\end{aligned}$$

where:

$1 \rightarrow a$ occurs at the constant pressure, P_1

$a \rightarrow 2$ occurs at the constant temperature, T_2

We can express these changes as:

$$\Delta V_{1\rightarrow a} = V_a - V_1 = \int_{T_1}^{T_2} \left(\frac{\partial V}{\partial T}\right)_{P_1} dT$$

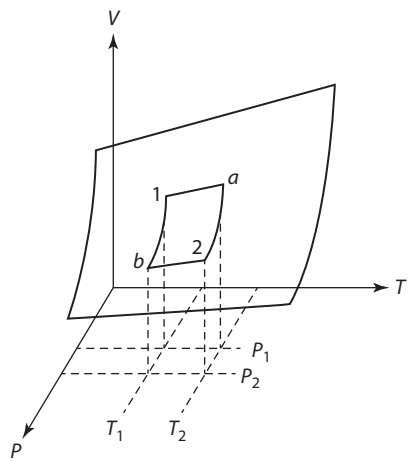

FIGURE 1.1 The equilibrium states of existence for 1 mole of gas in *V-P-T* space are shown to lie on a surface.

and

$$\Delta V_{a\to 2} = V_2 - V_a = \int_{P_1}^{P_2} \left(\frac{\partial V}{\partial P}\right)_{T_2} dP$$

Thus,

$$\Delta V_{1\to 2} = \int_{T_1}^{T_2} \left(\frac{\partial V}{\partial T}\right)_{P_1} dT + \int_{P_1}^{P_2} \left(\frac{\partial V}{\partial P}\right)_{T_2} dP \tag{1.2}$$

Similarly, for the path $1 \to b \to 2$:

$$\Delta V_{1\to b} = V_b - V_1 = \int_{P_1}^{P_2} \left(\frac{\partial V}{\partial P}\right)_{T_1} dP$$

and

$$\Delta V_{b\to 2} = V_2 - V_b = \int_{T_1}^{T_2} \left(\frac{\partial V}{\partial P}\right)_{P_2} dT$$

Hence,

$$\Delta V_{1\to 2} = \int_{P_1}^{P_2} \left(\frac{\partial V}{\partial P}\right)_{T_1} dP + \int_{T_1}^{T_2} \left(\frac{\partial V}{\partial T}\right)_{P_2} dT \tag{1.3}$$

Equations 1.2 and 1.3 must yield the same value of $\Delta V_{1\to 2}$. In the limit of an infinitesimal change in volume, these equations yield the complete or total differential of Equation 1.1:

$$dV = \left(\frac{\partial V}{\partial P}\right)_T dP + \left(\frac{\partial V}{\partial T}\right)_P dT \tag{1.4}$$

The change in volume caused by changing the state of the gas from state 1 to state 2 depends only on the volumes at states 1 and 2 and is independent of the path taken by the gas between the states. This is because the volume of the gas is a *state function*, and Equation 1.4 is an exact differential of the volume, which is a thermodynamic state variable.

The partial differentials that relate the change in volume to changes in the *intensive thermodynamic variables* (P and T) are related to the properties of the gas, namely,

$$\beta_T \equiv -\frac{1}{V}\left(\frac{\partial V}{\partial P}\right)_T, \text{ the isothermal compressibility with dimensions of } P^{-1}$$

and

$$\alpha_P \equiv \frac{1}{V}\left(\frac{\partial V}{\partial T}\right)_P, \text{ the coefficient of thermal expansion with dimensions of } T^{-1}$$

Thus, the complete differential of Equation 1.4 can be written as

$$dV = \alpha_P V dT - \beta_T V dP$$

This equation can be easily integrated over the ranges in T and P, when β_T and α_P are approximately constant.

1.3 EXAMPLE OF EQUILIBRIUM

In Figure 1.1, the equilibrium states of the system are shown to lie on a surface in V-P-T space. This means that equilibrium exists at unique combinations of P and T such that P and T satisfy the equation of state of the gas and therefore lie in the $V(P,T)$ surface. Any point $(P_i V_i)$ not lying on the surface is not in an equilibrium state.

A particularly simple system is illustrated in Figure 1.2. In this figure, 1 mole of a gas (which is the quantity of the gas that contains Avogadro's number of particles, Lorenzo Avogadro, 1776–1856) is shown to be contained in a cylinder by a movable piston.

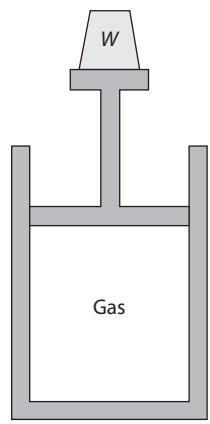

FIGURE 1.2 One mole of a gas is shown to be contained in a cylinder by a piston. The walls of the cylinder are diathermal, and W is the mass that is exerting pressure on the gas.

The system is at equilibrium when:

1. The pressure exerted *by* the gas *on* the piston equals the pressure exerted *by* the piston *on* the gas.
2. The temperature of the gas is the same as the temperature of the surroundings (since the thermal energy can be transferred through the diathermal boundaries of the cylinder).

The state of the gas is thus fixed, and equilibrium occurs as a result of the establishment of a balance between the tendency of the external influences acting on the system to cause a change in the system (i.e., the temperature and pressure) and the tendency of the system to resist such a change. Fixing the pressure of the gas at P_1 and T_1 determines the state of the system and hence fixes the volume at the value V_1. If, at constant temperature, by a suitable *increase* in the weight placed on the piston, the pressure exerted on the gas is increased to P_2 (Figure 1.1), the resulting imbalance between the pressure exerted by the gas and the pressure exerted on the gas causes the piston to move into the cylinder. This process decreases the volume of the gas and hence increases the pressure of the gas which it exerts on the piston until equalization of the pressures is restored. As a result of this process, the volume of the gas decreases from V_1 to V_b. Thermodynamically, the *isothermal* change of pressure from P_1 to P_2 *changes the state* of the system from state 1 (characterized by P_1, T_1) to state b (characterized by P_2, T_1), and the volume, as a dependent variable, decreases from the value V_1 to V_b. This shows that work was performed on the gas by the piston.

If the pressure exerted by the piston on the gas is maintained constant at P_2 and the temperature of the surroundings is raised from T_1 to T_2, the consequent temperature gradient across the cylinder wall causes the transfer of thermal energy (heat) from the surroundings into the gas. The increase in the temperature of the gas at the constant pressure P_2 causes the expansion of the gas, which pushes the piston out of the cylinder. When the gas is uniformly at the temperature T_2, the volume of the gas is V_2. Again, thermodynamically, the increasing of the temperature from T_1 to T_2 at the constant pressure P_2 changes the state of the system from state b (P_2, T_1) to state 2 (P_2, T_2), and the volume as a dependent variable increases from V_b in the state b to V_2 in the state 2. In this case, work was performed *on* the piston by the expanding gas. Since volume is a *state function*, the final volume V_2 would be the same if the state were first changed from 1 to a and then from a to 2.

1.4 THE EQUATION OF STATE OF AN IDEAL GAS

The pressure–volume relationship of a gas at constant temperature was determined experimentally in 1660 by Robert Boyle (1627–1691), who found that, at constant T,

$$P \propto \frac{1}{V}$$

This is known as *Boyle's law*. Similarly, the volume–temperature relationship of a gas at constant pressure was determined experimentally in 1787 by

Jacques-Alexandre-Cesar Charles (1746–1823). This relationship, which is known as *Charles' law*, is that, at constant pressure,

$$V \propto T$$

Thus, in Figure 1.1, which is drawn for 1 mole of a gas, sections of the *V-P-T* surface drawn at constant *T* produce rectangular hyperbolae that asymptotically approach the *P* and *V* axes in a *P* versus *V* plot, and sections of the surface drawn at constant *P* produce straight lines in a *V* versus *T* plot. These sections are shown in Figure 1.3a and b.

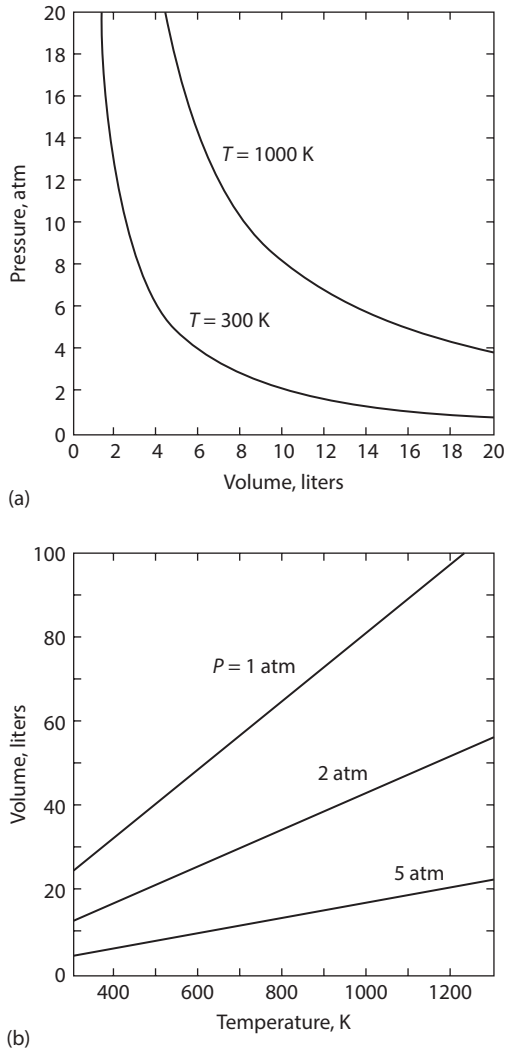

FIGURE 1.3 (a) The variation, with pressure, of the volume of 1 mole of ideal gas at 300 and 1000 K. (b) The variation, with temperature, of the volume of 1 mole of ideal gas at 1, 2, and 5 atm.

In 1802, Joseph-Luis Gay-Lussac (1778–1850) observed that the coefficient of thermal expansion of what were at the time called *permanent gases* was a constant. Previously, it was noted that the coefficient of thermal expansion, α_P, is defined as the fractional increase of the volume of the gas, with the change in temperature at constant pressure; that is,

$$\alpha_P \equiv \frac{1}{V}\left(\frac{\partial V}{\partial T}\right)_P \tag{1.5}$$

where V is the volume of 1 mole of the gas at 0°C. Gay-Lussac obtained a value of $1/267$ for α_P, but more refined experimentation by Henri Victor Regnault (1810–1878) in 1847 showed α_P to have the value $1/273$.

Later, it was found that the accuracy with which Boyle's and Charles' laws describe the behavior of different gases varies from one gas to another. Generally, gases with lower boiling points obey the laws more closely than do gases with higher boiling points. It was also found that the laws are more closely obeyed by all gases as the pressure of the gas is decreased. It was thus found convenient to invent a hypothetical gas that obeys Boyle's and Charles' laws exactly *at all temperatures and pressures*. This hypothetical gas is called the *perfect* or *ideal gas*, and it has a value of $\alpha_P = 1/273$.

The existence of a finite coefficient of thermal expansion therefore sets a limit on the thermal contraction of the ideal gas; that is, since $\alpha_P = 1/273.15$, the fractional decrease in the volume of the gas, per degree decrease in temperature, is $1/273.15$ of the volume at 0°C. Thus, at −273.15°C, the volume of the ideal gas would be zero, and hence, the limit of temperature decrease, −273.15°C, is the *absolute zero* of temperature (Anders Celsius, 1701–1744):

$$T\left(\text{degrees absolute}\right) = T\left(\text{degrees celsius}\right) + 273.15$$

A combination of Boyle's law:

$$P_0 V\left(T, P_0\right) = PV\left(T, P\right)$$

and Charles' law:

$$\frac{V\left(P_0, T_0\right)}{T_0} = \frac{V\left(P_0, T\right)}{T}$$

where:

P_0 = standard pressure (1 atmosphere [atm])
T_0 = standard temperature (273.15 degrees absolute)
$V(P,T)$ = volume at pressure P and temperature T
gives

$$\frac{PV}{T} = \frac{P_0 V_0}{T_0} = \text{constant} \tag{1.6}$$

From Avogadro's hypothesis, the volume per gram mole[3] of all ideal gases at 0°C and 1 atm pressure (termed *standard temperature and pressure* [STP]) is 22.414 liters. Thus, the constant in Equation 1.6 has the value

$$\frac{P_0V_0}{T_0} = \frac{1\text{ atm} \cdot 22.414\text{ liters}}{273.15\text{ K} \cdot \text{mole}} = 0.082057\ \frac{\text{liter} \cdot \text{atm}}{\text{degree} \cdot \text{mole}}$$

This constant is given the symbol R, the *gas constant*, and, being applicable to all ideal gases, it is a universal constant. Equation 1.6 can thus be written as

$$PV = RT \tag{1.7}$$

which is the equation of state for 1 mole of ideal gas. Equation 1.7 is also called the *ideal gas law*. Because of the simple form of its equation of state, the ideal gas is used extensively as a system in thermodynamic discussions.

The existence of an absolute temperature scale shows that different systems can be assigned a single-valued function to designate the *intensity* of their thermal energy. The Zeroth Law of Thermodynamics can be stated as follows: if system A is in thermal equilibrium with system B, and system B is in thermal equilibrium with system C, then system A is in thermal equilibrium with system C. Thus, all three systems must have the same absolute temperature, and therefore, the temperature of a system is a thermodynamic *intensive state variable*. If the temperature gradient between two systems is equal to zero, the systems are in thermal equilibrium. If the temperature gradient is nonzero, there is a tendency for energy to transfer from the high-temperature system to the low-temperature system, commonly called *heat transfer*. We will see that temperature is a measure of the energy of the particles that compose the system.

1.5 THE UNITS OF ENERGY AND WORK

The unit *liter·atm* occurring in the units of R is an energy term. Work is done when a force moves a body through a distance. *Work* and *energy* have the dimensions force·distance. Pressure is force per unit area; hence, work and energy can have the dimensions pressure·area·distance or pressure·volume. The unit of energy in SI units[4] is joule, which is the work done when a force of 1 newton moves a distance of 1 meter.

The unit *liter·atm* is converted to joule as follows:

$$1\text{ atm} = 101{,}325\ \frac{\text{newton}}{\text{meter}^2}$$

[3] A gram mole (g mole or mole) of a substance is the mass of Avogadro's number of molecules of the substance expressed in grams. Thus, a g mole of O_2 has a mass of 32 g, a g mole of C has a mass of 12 g, and a g mole of CO_2 has a mass of 44 g.

[4] *Système International*, The International System of Units. There are seven basic units in the SI system, namely, seconds, s, the unit of time; meters, m, the unit of length; kilograms, kg, the unit of mass; amperes, A, the unit of current; Kelvin, K, the unit of temperature; moles, mol, the amount of a substance; candel, cd the luminous intensity. All other units are combinations of these basic units. For example, the joule, J, is the unit of energy given as kg·m

Multiplying both sides by liters (10^{-3} meter^3) gives

$$1 \text{ liter} \cdot \text{atm} = 101.325 \text{ newton} \cdot \text{meters} = 101.325 \text{ joules}$$

Thus,

$$R = 0.082057 \frac{\text{liter} \cdot \text{atm}}{\text{degree} \cdot \text{mole}}$$
$$= 8.3144 \frac{\text{joules}}{\text{degree} \cdot \text{mole}}$$

Other forms of work, such as magnetic and electrical, and their conversions will be discussed as they arise in the course of the text.

1.6 EXTENSIVE AND INTENSIVE THERMODYNAMIC VARIABLES

Thermodynamic state variables are either *extensive* or *intensive*. Extensive variables have values that depend on the size of the system, whereas values of intensive variables are independent of the size of the system. Volume is an extensive variable, and temperature and pressure are intensive variables. The values of extensive variables, expressed per unit volume or unit mass of the system, have the characteristics of intensive variables; for example, the volume per unit mass (specific volume) and the volume per mole (molar volume) are variables whose values are independent of the size of the system.

For a system of n moles of an ideal gas, the equation of state is

$$PV' = nRT$$

where V' is the total volume of the system.[5]

Per mole of the system, the equation of state reduces to Equation 1.7:

$$PV = RT$$

where V, the molar volume of the gas, equals V'/n. The molar volume of an ideal gas at standard temperature pressure (STP) is 22.414 liters (one *liter* equals 10^{-3}m^3).

1.7 EQUILIBRIUM PHASE DIAGRAMS AND THERMODYNAMIC COMPONENTS

Of the several ways to represent the equilibrium states of the existence of a system graphically, the *constitution* or *equilibrium phase diagram* is the most popular and convenient. The complexity of a phase diagram is determined primarily by the number of *components* that occur in the system, where components are chemical

[5] In this text, *Primed* values of extensive variables denote the *total* value of the variable. Unprimed values of extensive variables denote the *molar*

species of fixed composition. The simplest components are chemical elements and molecules. Systems are primarily categorized by the number of components they contain—for example, one-component (unary) systems, two-component (binary) systems, three-component (ternary) systems, four-component (quaternary) systems, and so on.

The phase diagram of a *one-component* system with only two independent state variables is a two-dimensional representation of the dependence of the equilibrium state, with the two independent variables as the coordinate axes. Pressure and temperature are normally chosen as the two independent variables. Figure 1.4 shows a schematic representation of part of such a phase diagram for H_2O. The full curves in Figure 1.4 divide the diagram into three areas, designated solid, liquid, and vapor. If a quantity of pure H_2O is at some temperature and pressure which is represented by a point *within* the area *AOB*, the equilibrium state of the H_2O is a liquid. Similarly, within the area *COA* and below the *COB curve*, the equilibrium states are, respectively, the solid and vapor states of water. When the equilibrium state lies within one of these regions, it is said to be *homogeneous*; that is, it consists of only one phase of water.

If the state of existence lies on a curve, the equilibrium state consists of two phases. On the curve *AO*, the liquid and solid H_2O coexist in equilibrium with one another. States such as these are called *heterogeneous*. A *phase* is a finite volume in the physical system within which the thermodynamic variables are uniformly constant; that is, the variables do not experience any abrupt change in passing from one point in the volume to another.[6]

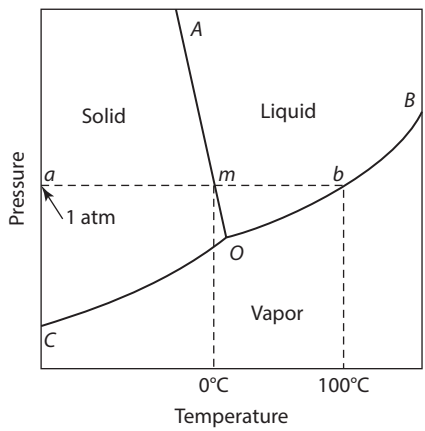

FIGURE 1.4 Schematic representation of part of the pressure–temperature equilibrium phase diagram for H_2O. The melting point is designated as *m,* and the boiling point is designated as *b*.

[6] More fully, "a phase is a physically distinct homogeneous portion of a thermodynamic system delineated in space by a bounding surface, called an interphase interface, and distinguished by its state of aggregation (solid, liquid or gas), crystal structure, composition and/or degree of order. Each phase in a material system generally exhibits a characteristic set of physical, mechanical and chemical properties and is, in principle, mechanically separable from the whole", from W. A. Soffa and D. E. Laughlin, "Diffusional Phase Transformations in the Solid State," in *Physical Metallurgy*, vol. 1, edited by D. E.

The curve *AO* represents the simultaneous variation of *P* and *T* required for the maintenance of the equilibrium between solid and liquid H_2O and thus represents the influence of pressure on the melting temperature of ice. Similarly, the curves *CO* and *OB* represent the simultaneous variations of *P* and *T* required, respectively, for the maintenance of the equilibrium between solid and vapor H_2O and between liquid and vapor H_2O. The curve *CO* is thus the variation, with temperature, of the saturated vapor pressure of solid water (ice) or, alternatively, the variation, with pressure, of the sublimation temperature of water vapor. The curve *OB* is the variation, with temperature, of the saturated vapor pressure of liquid water or, alternatively, the variation, with pressure, of the dew point of water vapor. The three two-phase equilibrium curves meet at point *O* (the triple point), which thus represents the unique values of *P* and *T* required for the establishment of the three-phase (solid + liquid + vapor) equilibrium.

The path *amb* indicates that if a quantity of ice is heated at a constant pressure of 1 atm, melting occurs at the state *m*, which, by definition, is the normal melting temperature of ice. Boiling occurs at the state *b*, which is the normal boiling temperature of water.

Phases may be solids, liquids, or gases. Gases are single-phase *solutions* and, hence, are homogeneous phases. Liquids may be homogeneous and single phase, or they may divide into regions of different composition and therefore be composed of two or more phases. Likewise, solids may be single phase or may also be composed of more than one phase. It is common to call a metal composed of more than one component an *alloy*. Alloys may be single phase or multiphase. A single-phase crystalline alloy consists of many grains, each of the same composition. Such single-phase alloys are called *solid solutions*.

If the system contains two components, a composition axis must be included, and consequently, the complete diagram is three-dimensional, with the coordinates composition, temperature, and pressure. In most cases of condensed phases, however, it is sufficient to present a binary phase diagram as a constant-pressure section of the three-dimensional diagram. The constant pressure chosen is normally 1 atm, and the coordinates are composition and temperature. Figure 1.5, which is a typical simple binary phase diagram, shows the phase relationships occurring in the system Al_2O_3–Cr_2O_3 at 1 atm pressure. This phase diagram shows that, at temperatures below the melting temperature of Al_2O_3 (2050°C), solid Al_2O_3 and solid Cr_2O_3 are completely miscible in all proportions and form a solid solution. This can occur because Al_2O_3 and Cr_2O_3 have the *same crystal structure* (corundum, space group $R\bar{3}c$), and the Al^{3+} and Cr^{3+} ions are of similar size. The Al^{3+} and Cr^{3+} ions are considered to be randomly distributed on the *c* sites of the space group $R\bar{3}c$. At temperatures above the melting temperature of Cr_2O_3 (2265°C), liquid Al_2O_3 and liquid Cr_2O_3 are completely miscible in all proportions and form a liquid solution.

The equilibrium phase diagram shown in Figure 1.5 contains areas of complete solid solubility and complete liquid solubility, which are separated from one another by a two-phase area in which solid and liquid solutions coexist in equilibrium with one another. For example, at the temperature T_1, the Al_2O_3–Cr_2O_3 system of composition between *X* and *Y* exists as a two-phase system comprising a liquid solution of composition *l* in equilibrium with a solid solution of composition *s*. The relative

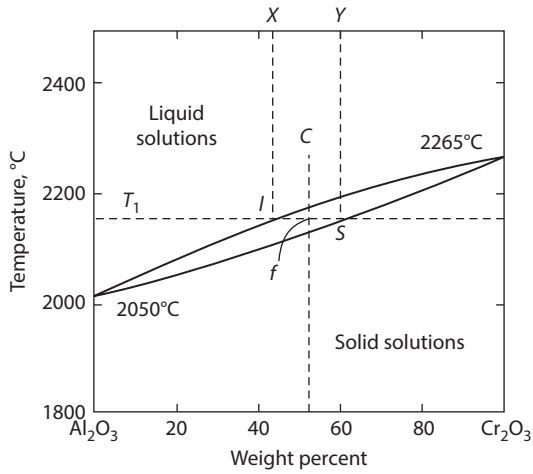

FIGURE 1.5 The temperature composition equilibrium phase diagram for the system Al_2O_3–Cr_2O_3 at a constant pressure of 1 atm.

proportions of the two phases present in equilibrium depend only on the overall composition of the system in the range *X*–*Y* and are determined by the lever rule, as follows:

For the overall composition *C* at the temperature T_1, the fraction of solid in equilibrium at T_1 is given as lC/lS, and the fraction of liquid is given as CS/lS, where the numerator and denominators of the expressions are the length of the cords denoted on the phase diagram.

Because the only requirement of a component is that it has a fixed composition, the designation of the components of a system is somewhat arbitrary. In the system Al_2O_3–Cr_2O_3, the obvious choice of the components is Al_2O_3 and Cr_2O_3. However, the most convenient choice is not always as obvious, and the general arbitrariness in selecting the components must be considered when dealing with oxide phase diagrams.

1.8 LAWS OF THERMODYNAMICS[7]

Sometimes, thermodynamics is summarized by stating its laws, which can be treated either as experimentally determined *facts of nature* or as *axioms* from which other thermodynamic relationships can be derived.

The so-called Zeroth Law introduces the important *intensive* thermodynamic variable temperature, *T*, which is a measure of the thermal intensity of a material and allows the determination of thermal equilibrium. The other three laws are summarized in the following subsections and will be the subject of study throughout the text.

[7] A very good summary of the Laws of Thermodynamics is found in P. Atkins, *The Laws of Thermodynamics: A Very Short Introduction*, Oxford University Press, Oxford, UK, 2010.

1.8.1 The First Law of Thermodynamics

The First Law not only states that the energy of the universe is *conserved* but also posits that the various forms of energy (e.g., thermal, electrical, magnetic, and mechanical) can be *converted* into other forms of energy. When first delineated, it was the fact that *thermal energy* (heat) could be converted to *mechanical work* that was of special interest (heat engines). This law also defines the important extensive thermodynamic state function called the *internal energy*, U', of the system under investigation.

1.8.2 The Second Law of Thermodynamics

Although the Second Law is the one that often gets the most attention in popular discussions of science, it is often incorrectly understood! Care must be taken in applying the law by delineating the system and the surroundings. This law allows us to make important predictions of the direction in which a system will evolve with time during spontaneous processes, if other important caveats are taken into account. The Second Law introduces another important extensive thermodynamic state function called *entropy*, S'. A short version of the Second Law is that the entropy of the universe never decreases.

1.8.3 The Third Law of Thermodynamics

In its strongest form, the Third Law states that when a system, which is in complete internal equilibrium, approaches the absolute zero in temperature, all of the aspects of its entropy approach zero. Sometimes, the Third Law is stated as follows: a system can never be taken to the absolute zero in temperature. This is also called the *unattainability principle.*

The Laws of Thermodynamics will be discussed in the following chapters and applied to the thermodynamic stability of systems in later chapters of the text.

1.9 SUMMARY

1. In thermodynamics, the universe is divided into the system (that part of the universe of interest to us) and the surroundings. There are several kinds of walls between the system and the surroundings, and each type gives rise to a system with specific characteristics.
2. In thermodynamics, the equilibrium of the system is of interest in that, if it is known, one can determine if the current state of the system will change and in which direction such a change would go.
3. The state of a *simple system* is determined by its temperature and pressure, the two intensive independent variables of the system.
4. Other thermodynamic variables are functions of pressure and temperature. Graphs may be plotted which display the equilibrium states of the system as a function of the independent variables.
5. The Zeroth Law of Thermodynamics introduces the intensive variable temperature, T.

6. The First Law of Thermodynamics states that the energy of the universe is constant, shows that different forms of energy may be converted into one another, and introduces the extensive thermodynamic variable internal energy, U'.
7. The Second Law of Thermodynamics defines which processes may occur spontaneously and introduces the extensive thermodynamic variable entropy, S'. The entropy of the universe can never decrease.
8. The Third Law of Thermodynamics states that all aspects of entropy approach the value of zero as the temperature of the system approaches zero, if the system is in *complete internal equilibrium*.

1.10 CONCEPTS AND TERMS INTRODUCED IN THIS CHAPTER

The reader should write out brief definitions or descriptions of the following terms. Where appropriate, equations may be used.

Adiabatic boundary
Alloy
Avogadro's hypothesis
Boyle's law
Charles' law
Closed system
Coefficient of thermal expansion
Components
Conservation of energy
Conversion of energy
Diathermal boundary
Energy/work
Equation of state
Equilibrium phase diagram
Exact differentials
Extensive/intensive thermodynamic variables
Gas constant, R
Homogeneous/heterogeneous systems
Ideal gases/ideal gas law
Independent/dependent thermodynamic variables
Isolated system
Isothermal compressibility
Laws of Thermodynamics
Microscopic/macroscopic thermodynamic variables
Open system
Permeable boundary
Semipermeable boundary
Simple system
Solid/liquid solutions
System/surroundings

Thermodynamic field variables
Thermodynamic state
Thermodynamic state functions
Thermodynamic state variables
Triple point
Unattainability principle
Universe
Vapor pressure
V-P-T space

1.11 QUALITATIVE EXAMPLE PROBLEMS

QUALITATIVE PROBLEM 1

Obtain simplified expressions for β_T and α_P of an ideal gas.

SOLUTION TO QUALITATIVE PROBLEM 1

$$\beta_T = -\frac{1}{V}\left(\frac{\partial V}{\partial P}\right)_T, \quad \text{but } V = \frac{RT}{P}: \quad \left(\frac{\partial V}{\partial P}\right)_T = -\frac{RT}{P^2}:$$

$$\beta_T = \left(-\frac{1}{V}\right)\cdot\left(-\frac{RT}{P^2}\right) = \frac{1}{P}$$

$$\text{and} \quad \alpha_P = \frac{1}{V}\left(\frac{\partial V}{\partial T}\right)_P, \quad \text{but } V = \frac{RT}{P}: \quad \left(\frac{\partial V}{\partial T}\right)_P = \frac{R}{P}:$$

$$\alpha_P = \frac{1}{V}\cdot\frac{R}{P} = \frac{1}{T}$$

QUALITATIVE PROBLEM 2

Another property of a simple system is defined as: $\gamma_V = \frac{1}{P}\left(\frac{\partial P}{\partial T}\right)_V$

Determine the value of the expression $\frac{\alpha_P}{\beta_T \gamma_V}$

SOLUTION TO QUALITATIVE PROBLEM 2

$$\frac{\alpha_P}{\beta_T \gamma_V} = \frac{\frac{1}{V}\left(\frac{\partial V}{\partial T}\right)_P}{-\frac{1}{V}\left(\frac{\partial V}{\partial P}\right)_T \frac{1}{P}\left(\frac{\partial P}{\partial T}\right)_V} = -P\left(\frac{\partial V}{\partial T}\right)_P \left(\frac{\partial P}{\partial V}\right)_T \left(\frac{\partial T}{\partial P}\right)_V$$

$$\frac{\alpha_P}{\beta_T \gamma_V} = P \quad \text{since} \quad \left(\frac{\partial V}{\partial T}\right)_P \left(\frac{\partial P}{\partial V}\right)_T \left(\frac{\partial T}{\partial P}\right)_V = -1$$

See Appendix B.

1.12 QUANTITATIVE EXAMPLE PROBLEMS

QUANTITATIVE PROBLEM 1

Consider 1 mole of an ideal gas. Using a *y*-axis of pressure and an *x*-axis of temperature, plot the variations of pressure with temperature for volumes of 11.2, 22.4, and 44.8 liters. Use ranges of pressure and temperature consistent with Figure 1.3.

SOLUTION TO QUANTITATIVE PROBLEM 1

States of constant volume can be calculated using the ideal gas law ($PV' = nRT$). The following table summarizes the calculations. The plot is found in Figure 1.6.

	Pressure (atm)		
Temperature (K)	**$V = 11.2$ liters**	**$V = 22.4$ liters**	**$V = 44.8$ liters**
300	2.20	1.10	0.55
400	2.93	1.47	0.73
500	3.66	1.83	0.92
600	4.40	2.20	1.10
700	5.13	2.56	1.28
800	5.86	2.93	1.47
900	6.59	3.30	1.65
1000	7.33	3.66	1.83
1100	8.06	4.03	2.01
1200	8.79	4.40	2.20
1300	9.52	4.76	2.38

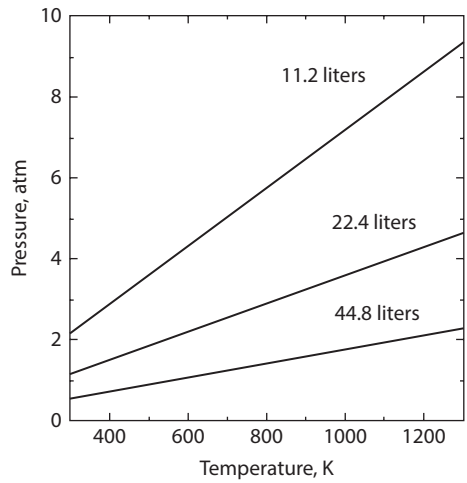

FIGURE 1.6 Pressure–temperature plots for 1 mole of an ideal gas at three different volumes.

QUANTITATIVE PROBLEM 2

A balloon containing one mole of an ideal gas at 273 K and pressure of one atmosphere is slowly compressed at constant temperature to one half of its initial volume. Calculate how much work was done on the balloon.

SOLUTION TO QUANTITATIVE PROBLEM 2

$$\text{Work} = \text{Force} \times \text{distance}$$
$$\text{Force} = \text{Pressure} \times \text{area}$$

$$\text{Thus, Work} = \text{Pressure} \times \text{area} \times \text{distance} = \text{Pressure} \times \Delta V$$

Since the gas is ideal, for one mole, $P = \dfrac{RT}{V}$

$$\text{Thus,} \quad \text{work} = \int_{V_1}^{V_2} P dV = \int_{V_1}^{V_2} \frac{RT}{V} dV = RT \ln \frac{V_2}{V_1} = -RT \ln 2$$

The minus sign shows that work was performed on the balloon.

PROBLEMS

1.1 The plot of $V = V(P,T)$ for a gas is shown in Figure 1.1. Determine the expressions of the two second derivatives of the volume of this plot (*note*: the principal curvatures of the surface are proportional to these second derivatives). What are the signs of the curvatures? Explain.

1.2 The expression for the total derivative of V with respect to the dependent variables P and T is:

$$dV = \left(\frac{\partial V}{\partial P}\right)_T dP + \left(\frac{\partial V}{\partial T}\right)_P dT$$

Substitute the values of β_T and α_P obtained in Qualitative Problem 1 into this equation and integrate them to obtain the *equation of state* for an ideal gas.

1.3 The pressure–temperature phase diagram in Figure 1.4 has no two-phase areas (only two-phase curves), but the temperature composition diagram in Figure 1.5 does have two-phase areas. Explain.

1.4* Calculate the value of the ratio $\dfrac{\alpha_P}{\beta_T}$ for an ideal gas in terms of its volume.

1.5* Obtain an expression for the isobaric thermal expansion of a van der Waals gas.

The equation of state of a van der Waals gas is: $\left(P + \dfrac{a}{V^2}\right)(V - b) = RT$

1.6* Obtain an expression for the isothermal compressibility of a van der Waals gas.

The equation of state of a van der Waals gas is: $\left(P + \frac{a}{V^2}\right)(V - b) = RT$

1.7* Show that the expression $\frac{\alpha_P}{\beta_T \gamma_V} = P$ is valid for an ideal gas.

1.8* The isothermal compressibility of a certain solid is given as:

$$\beta_T = -\frac{1}{V}\left(\frac{\partial V}{\partial P}\right)_T$$

It is found to be a constant over a certain range of V and T.

Determine the equation of state for the solid in the range in which β_T is constant.

* New problem in this edition.

2 The First Law of Thermodynamics

2.1 INTRODUCTION

The First Law of Thermodynamics is sometimes thought to be merely an extension of the Law of Conservation of Energy, which was discovered in the late seventeenth century for mechanical systems. It is, however, much more! The First Law of Thermodynamics introduces the important thermodynamic state variable *internal energy*, U (also called a *thermodynamic potential*). The law also posits that energy may be converted from one of its forms to another form. Furthermore, the law introduces the important concept that the transfer of thermal energy (heat) is of a different quality of energy than that which is done during a process of *work*. First, we start with a review of basic mechanics.

Kinetic energy is conserved in a frictionless system of interacting rigid elastic bodies. A collision between two of these bodies results in a transfer of kinetic energy from one to the other; the work done *by* one equals the work done *on* the other. Consequently, the total kinetic energy of the system is unchanged as a result of the collision. If the kinetic system is under the influence of a gravitational field, then the sum of the kinetic and potential energies of the bodies is constant. Changes in the position of the bodies in the gravitational field, in addition to changes in the velocities of the bodies, do not alter the total *dynamic energy* of the system. As a result of possible interactions, kinetic energy may be *converted* to potential energy and *vice versa,* but the sum of the two remains constant. If, however, *friction* occurs in the system, then with continuing collision and interaction among the bodies, the total *dynamic energy* of the system *decreases* and thermal energy (heat) is produced. It is thus reasonable to expect that a relationship exists between the amount of dynamic energy *dissipated* and the thermal energy *produced* as a result of the effects of friction.

The establishment of such a relationship laid the foundations for the development of the thermodynamic method. As a subject, this has now gone far beyond simple considerations of the transformation of energy from one form to another—for example, from dynamic energy to thermal energy. The development of thermodynamics from its early beginnings to its present state was achieved as a result of the *invention* of convenient thermodynamic *functions of state*. In this chapter, two of these thermodynamic functions—the *internal energy*, U, and the *enthalpy*, H—are introduced.

2.2 THE RELATIONSHIP BETWEEN HEAT AND WORK

The relationship between heat (thermal energy) and work was suggested in 1798 by Count Rumford (aka Sir Benjamin Thomson, 1753–1814), who, during the boring of cannons at the Munich Arsenal, noticed that the heat, q, produced during the boring was roughly proportional to the work, w, performed during the boring.

DOI: 10.1201/9781003375388-3

This suggestion was novel, as hitherto, heat had been regarded as being an invisible *fluid* (or gas) called *caloric*, which resided between the constituent particles of a substance. In the caloric theory of heat, the temperature of a substance was considered to be determined by the quantity of caloric gas which it contained. It was thought that when two bodies of differing temperature were placed in contact with one another, they came to an intermediate common temperature as the result of caloric flowing between them. Thermal equilibrium was thought to be reached when the pressure of caloric gas in one body equaled that in the other.

Some 40 years would pass before the relationship between heat and work suggested by Rumford was placed on a firm quantitative basis, as a result of a series of experiments carried out by James Prescott Joule (1818–1889). Joule conducted experiments in which work was performed in a certain quantity of adiabatically[1] contained water, and he then measured the resultant increase in the temperature of the water. He observed that a direct proportionality existed between the work done and the resultant increase in temperature and that the same proportionality existed no matter what means were employed in the work production. Methods of work production used by Joule included the following:

1. Rotating a paddle wheel immersed in the water
2. An electric motor driving a current through a coil immersed in the water
3. Compressing a cylinder of gas immersed in the water
4. Rubbing together two metal blocks immersed in the water

This proportionality between the work performed and the rise in temperature gave rise to the notion of a *mechanical equivalent of heat*, and for the purpose of defining this figure, it was necessary to define a unit of thermal energy. This unit is the *calorie* (or 15° *calorie*), which is the quantity of thermal energy needed to be transferred to 1 gram of water to increase the temperature of the water from 14.5°C to 15.5°C. On the basis of this definition, Joule determined the value of the mechanical equivalent of heat to be 0.241 calories per *joule* (J). The presently accepted value is 0.2389 calories (15° calories) per joule. Rounding this to 0.239 calories per joule defines the *thermochemical calorie*, which, until the introduction in 1960 of SI units, was the traditional energy unit used in thermochemistry.

From the preceding discussion, it is seen that the transfer of thermal energy, q, and the performance of work, w, are *processes* that occur on or to a system and are not intrinsic to the system; that is, they are not variables of the system. When performed on a system, they do, however, change the state of the system, and therefore, they change the *properties* of the system.

[1] An adiabatic vessel is one which is constructed in such a way as to prohibit, or at least minimize, the passage of thermal energy (heat) and matter through its walls. The most familiar example of an adiabatic vessel is the *Dewar flask* (known more popularly as a *thermos flask*). Thermal energy transmission by conduction into or out of this vessel is minimized by using double glass walls separated by an evacuated space, and a rubber or cork stopper. Thermal energy transmitted by radiation is minimized by using highly polished mirror surfaces.

2.3 INTERNAL ENERGY AND THE FIRST LAW OF THERMODYNAMICS

From Joule's experiments, it can be said that "the change of a body inside an adiabatic enclosure from a given initial state to a given final state involves the same amount of work by whatever means the process is carried out."[2] The statement is a preliminary formulation of the *First Law of Thermodynamics*, and in view of this statement, it is necessary to define some function that depends only on the *internal state* of a body or system. Such a function is the internal energy, *U*. We will see that the internal energy is related to the system's capacity to do work. Internal energy is best introduced by means of comparison with more familiar concepts.

When a body of mass m is lifted in a gravitational field from height h_1 to height h_2, the work w done on the body is given by

$$\begin{aligned} w &= \text{Force} \times \text{distance} \\ &= mg \times (h_2 - h_1) \\ &= mgh_2 - mgh_1 \\ &= \text{Potential energy at position } h_2 - \text{potential energy at position } h_1 \end{aligned}$$

Since the *potential energy* of the body of a given mass m depends only on the position of the body in the gravitational field, it is seen that the work done on the body is dependent only on its final and initial positions. Therefore, the work performed is independent of the path taken by the body between the two positions—that is, between the two states.

Similarly, the application of a force f to a body of mass m causes the body to accelerate according to Newton's law:

$$f = ma = m\frac{dv}{dt}$$

where the acceleration a equals dv/dt. The work done on the body is thus obtained by integrating

$$dw = fdl$$

where dl is the distance that the force moves the body.

$$\therefore dw = m\frac{dv}{dt}dl = m\frac{dl}{dt}dv = mvdv$$

[2] K. Denbigh, *The Principles of Chemical Equilibrium*, Cambridge University Press, Cambridge, UK, 1971.

Integration gives:

$$w = \frac{1}{2}mv_2^2 - \frac{1}{2}mv_1^2$$

$$= \text{The kinetic energy of the body at velocity } v_2 \left(\text{state } 2\right)$$

$$-\text{the kinetic energy of the body at velocity } v_1 \left(\text{state } 1\right)$$

Again, the work done on the body is the difference between the values of a function of the state of the body and is *independent of the path* taken by the body between the states. In this case, the change in *the potential energy* is equal to the change in the kinetic energy of the system.

Likewise, in electrical processes, the work needed to move a charged particle between two points in an electric field depends only on the difference in the *electric potential* between the two points and not on its path.

2.3.1 Adiabatic Changes of State

In the case of work being done on an adiabatically contained body of constant gravitational potential and kinetic energy, the function that describes the state of the body, or the change in the state of the body, is the internal energy, *U*. Thus, the work done on (or by) an adiabatically contained body equals the change in the internal energy of the body; that is, the work equals the difference between the value of *U* in the final state and the value of *U* in the initial state. In describing work, we will use the convention that assigns a negative value to work done *on* a body and a positive value to work done *by* a body. This convention arises because we often consider only the work done to be *PdV* work. When a gas expands, and hence does work against an external pressure, the integral $\int_1^2 P\,dV$, which is the work performed *by* the system, is a positive quantity that corresponds to a decrease in the internal energy of the system.

For an adiabatic process in which work *w* is done on the gas, as a result of which its state moves from *A* to *B*.

$$w = -\left(U'_B - U'_A\right)$$

If work *w* is done on the body ($w < 0$), then $U'_B > U'_A \left(w < 0\right)$. If the body itself performs work ($w > 0$), then $U'_B < U'_A$.[3]

2.3.2 Changes of State with No Work

In Joule's experiments, the work performed on the system caused a change in the state of the adiabatically contained water and was measured as an increase in the temperature

[3] The prime in *U'* indicates the total internal energy of the system. *U* is the internal energy per mole.

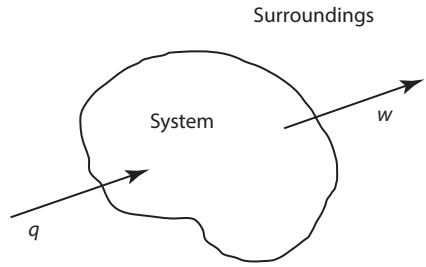

FIGURE 2.1 Schematic showing the sign convention for the work, w (positive), done by the system and energy transferred as heat, q, added to the system.

of the water. The same increase in temperature, and hence the same change of state, could have been produced by placing the water in thermal contact with a source that was hotter than the water, allowing energy to flow down the temperature gradient into the water. In describing the transfer of thermal energy, we will use the convention that assigns a negative value to thermal energy which transfers *out* of a body (an exothermic process) and a positive value to thermal energy which transfers *into* a body (an endothermic process). Hence,

$$q = \left(U'_B - U'_A\right)$$

Thus, when energy transfers into the body due to a thermal gradient, q is a positive quantity and $\left(U'_B > U'_A\right)$, whereas if energy transfers out of the body due to a thermal gradient, $\left(U'_B < U'_A\right)$ and q is a negative quantity. See Figure 2.1 for a schematic description of the sign conventions for heat and work used in the text.

2.3.3 Changes of State with Both Work and Heat Processes

It is now of interest to consider the change in the internal energy of a body which simultaneously performs work and absorbs thermal energy. Consider a body, initially in state A, which performs work, w, and absorbs energy, q, via a thermal gradient, and, as a consequence, moves to state B. The absorption of q *increases* the internal energy of the body by the amount q, and the performance of work w by the body *decreases* its internal energy by the amount w. Thus, the total change in the internal energy of the body, $\Delta U'$, is

$$\Delta U' = U'_B - U'_A = q - w \tag{2.1}$$

This equation summarizes the First Law of Thermodynamics for a system of fixed composition. We can see that while the internal energy of the system has changed by an amount $(q - w)$, the energy of the surroundings has changed by $-(q - w)$. Thus, the total energy of the universe (system plus surroundings) is unchanged.

For an infinitesimal change of state, Equation 2.1 can be written as a differential:

$$dU' = \delta q - \delta w \tag{2.2}$$

Notice that the left-hand side of Equation 2.2 gives the value of the increment in an already existing property of the system, whereas the right-hand side has no corresponding interpretation. U', the *total internal energy*, is an extensive state variable (function) of the system, which means that the integration of dU' between two states gives a value that is *independent of the path* taken by the system between the two states. Such is not the case when δq and δw are integrated. The thermal and work effects, which involve energy in transit, depend on the path taken between the two states, as a result of which the integrals of δw and δq cannot be evaluated without knowledge of the specific path. This is illustrated in Figure 2.2. Here, the value of $U_2' - U_1'$ is *independent* of the path taken between state 1 (P_1 V_1) and state 2 (P_2 V_2). However, the work done by the system, which is given by $w = \int_{V_1}^{V_2} P\,dV$ (the area under the curve between V_1 and V_2), varies, depending on the path. In Figure 2.2, the work done in process $1 \rightarrow 2$ *via* path *c* is less than that done *via* path *b*, which, in turn, is less than that done *via* path *a*. From Equation 2.1, it is seen that the δq must also depend on the path, and in the process $1 \rightarrow 2$, more thermal energy is absorbed by the system *via* path *a* than is absorbed *via* path *b*, which, again in turn, is greater than the heat absorbed *via* path *c*.

It should be noted that in Equation 2.2, the use of the symbol *d* indicates a differential element of a *state function* or *state variable*, the integral of which is independent of the path. The use of the symbol δ indicates a small change of some quantity which is not a state function. Of interest is that in Equation 2.1, the algebraic sum of two quantities, neither of which individually is independent of the path, gives rise to a quantity (in this case the internal energy) that is independent of the path.

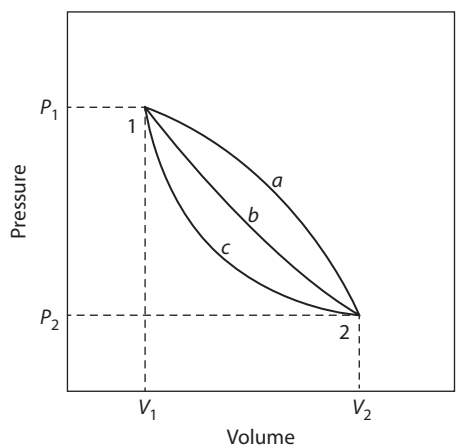

FIGURE 2.2 Three process paths taken by a fixed quantity of gas in moving from state 1 to state 2, showing that the work performed by the gas during expansion depends on the path traversed during the process.

In the case of a *cyclic process* that returns the system to its initial state—for example, the process $1 \rightarrow 2 \rightarrow 1$ in Figure 2.2—the change in U as a result of this process is zero; that is,

$$\Delta U' = \int_1^2 dU' + \int_2^1 dU' = \left(U_2' - U_1'\right) + \left(U_1' - U_2'\right) = 0$$

The vanishing of a cyclic integral $\oint dU' = 0$ *is a property of a state variable*.

In Joule's experiments, where $\left(U_2' - U_1'\right) = -w$, the process was adiabatic ($q = 0$), and thus, the path of the process was specified.

Since U' is an extensive thermodynamic state variable, for a simple system consisting of a given amount of substance of fixed composition, the value of U' is fixed once any two thermodynamic variables (the independent variables) are fixed. If temperature and volume are chosen as the independent variables, then

$$U' = U'\left(V', T\right)$$

The *complete differential* dU' in terms of the partial derivatives gives

$$dU' = \left(\frac{\partial U'}{\partial T}\right)_{V'} dT + \left(\frac{\partial U'}{\partial V'}\right)_T dV'$$

It should be noted that if the system is open to changes in the number of moles of the substance, this equation is rewritten to include such changes:

$$dU' = \left(\frac{\partial U'}{\partial T}\right)_{V',n} dT + \left(\frac{\partial U'}{\partial V'}\right)_{T,n} dV' + \left(\frac{\partial U'}{\partial n}\right)_{T,V'} dn$$

(Here the system is assumed to be composed of but one chemical component.)

Since the state of a closed system is fixed when the two independent variables are fixed, it is of interest to examine those processes that can occur when the value of one of the independent variables is maintained constant and the other is allowed to vary. In this manner, we can examine processes in which the volume V' is maintained constant (isochore or isometric processes), Section 2.4; the pressure P is maintained constant (isobaric processes), Section 2.5; or the temperature T is maintained constant (isothermal processes), Section 2.8. We can also examine adiabatic processes in which $\delta q = 0$, Section 2.7.

2.4 CONSTANT VOLUME PROCESSES

If the volume of a *simple system* is maintained constant during a process, then the system does no work ($\int P dV' = 0$), and from the First Law, Equation 2.2,

$$dU' = \delta q_v \tag{2.3}$$

where the subscript v indicates constant volume. Integration of Equation 2.3 gives

$$\Delta U' = q_v$$

for such a process. This shows that the increase or decrease in the internal energy of a closed system equals, respectively, the thermal energy absorbed or rejected by the system during the constant volume process. If thermal energy enters the system, the internal energy of the system increases. For this process,

$$\left(dU'\right)_V = \left(\frac{\partial U'}{\partial T}\right)_{V'} dT = \delta q_V$$

The thermodynamic property $\left(\partial U'/\partial T\right)_{V'}$ is the constant volume heat capacity of the system, Cv (see Section 2.6).

2.5 CONSTANT PRESSURE PROCESSES AND THE ENTHALPY, *H*

If the pressure is maintained constant during a process that takes the system from state 1 to state 2, then the work done by the closed system is given as

$$w = \int_{V_1}^{V_2} P dV = P \int_{V_1}^{V_2} dV = P \times \left(V_2 - V_1\right)$$

and the First Law gives

$$U_2' - U_1' = q_p - P\left(V_2 - V_1\right)$$

where the subscript P indicates constant pressure.

Rearrangement gives

$$\left(U_2' + PV_2\right) - \left(U_1' + PV_1\right) = q_p$$

Since the expression $(U' + PV')$ contains only thermodynamic state variables, the expression itself must be a thermodynamic state variable. This state variable is called the *enthalpy*, H', of the system; that is,

$$H' \equiv U' + PV' \tag{2.4}$$

Hence, the total derivative of the enthalpy is

$$dH' = dU' + PdV' + V'dP$$

and at constant pressure,

$$dH' = dU' + PdV'$$

Integrating, we obtain:

$$\Delta H' = H_2' - H_1' = q_P \tag{2.5a}$$

$$dH' = \delta q_P \tag{2.5b}$$

Thus, the enthalpy change during a constant pressure process is equal to the thermal energy admitted to or withdrawn from the system during the process.

2.5.1 Application of the First Law to Chemical Reactions

Suppose we need to know the enthalpy change, ΔH, for the oxidation of two moles of BCC iron (α) into solid hematite (Fe_2O_3).

$$2Fe(\alpha) + \frac{3}{2}O_2 \rightarrow Fe_2O_3$$

Some tables in the literature do not show the value of ΔH for this reaction. However, the molar values of ΔH for the following reactions are found in most of the tables found in the literature:

$$3Fe(\alpha) + 2O_2 \rightarrow Fe_3O_4 \qquad \Delta H_1$$

$$2Fe_3O_4 + \frac{1}{2}O_2 \rightarrow 3Fe_2O_3 \qquad \Delta H_2$$

Since enthalpy is a thermodynamic state variable, the value of its change from one state to another is independent of the path of the reaction. Thus, if we add two-thirds of the reaction

$$3Fe(\alpha) + 2O_2 \rightarrow Fe_3O_4 \qquad \Delta H_1$$

to one-third of the reaction

$$2Fe_3O_4 + \frac{1}{2}O_2 \rightarrow 3Fe_2O_3 \qquad \Delta H_2,$$

we get

$$2Fe(\alpha) + \frac{3}{2}O_2 \rightarrow Fe_2O_3$$

and

$$\Delta H = \frac{2}{3}\Delta H_1 + \frac{1}{3}\Delta H_2$$

This use of equivalent reactions is a direct consequence of the First Law of Thermodynamics and the path independency of enthalpy changes. It is called *Hess' law of constant heat summation* (Germain Hess, 1802–1850) and is commonly used in thermochemistry.

2.6 HEAT CAPACITY

Before discussing the adiabatic and isothermal processes, it is convenient to discuss the concept of *heat capacity*. The heat capacity, C, of a system is the ratio of the thermal energy added to or withdrawn from a system of fixed composition to the resultant change in the temperature of the system. Thus,

$$C \equiv \frac{q}{\Delta T}$$

or, if the temperature change is made vanishingly small, then

$$C \equiv \frac{\delta q}{dT}$$

The concept of heat capacity is only used when the addition of thermal energy to or withdrawal of thermal energy from the system produces a temperature change; the concept is not used when a phase change is involved. For example, if the system is a mixture of ice and water at 1 atm pressure and 0°C, then the addition of heat simply melts some of the ice and no change in temperature occurs and the heat capacity, as defined, would have an *apparent infinity*.

Note that if a system is in state 1 and the absorption of a certain quantity of thermal energy by the system increases its temperature from T_1 to T_2, then the statement that the final temperature is T_2 is insufficient to determine the final state of the system. This is because the system has two independent variables, and so, one other variable, in addition to the temperature, must be specified in order to define the state of the system. This second independent variable could be varied in a specified manner or could be maintained constant during the change. The latter possibility is the more practical, and so, the addition of thermal energy to a *simple system* to produce a change in temperature is normally considered at either constant pressure or constant volume. In this way, the path of the process is specified, and the final state of the system is known.

Thus, the heat capacity at constant volume, C_v, and the heat capacity at constant pressure, C_p, are defined as

$$C_v \equiv \left(\frac{\delta q}{dT}\right)_V$$

$$C_p \equiv \left(\frac{\delta q}{dT}\right)_P$$

From Equations 2.3 and 2.5b,

$$C_v = \left(\frac{\delta q}{dT}\right)_V = \left(\frac{\partial U'}{\partial T}\right)_V \quad \text{or} \quad dU' = C_v dT \tag{2.6a}$$

$$C_p = \left(\frac{\delta q}{dT}\right)_P = \left(\frac{\partial H'}{\partial T}\right)_P \quad \text{or} \quad dH' = C_p dT \tag{2.6b}$$

The heat capacity as defined above is seen to be dependent on the size of the system and is therefore an *extensive* property. However, in normal usage, it is more convenient to use the heat capacity per unit quantity of the system. Thus, the *specific heat* of the system is the heat capacity per gram at constant V or constant P, and the *molar heat capacity* is the heat capacity per mole at constant V or at constant P. Thus, for a system containing n moles,

$$nc_v = C_v$$

and

$$nc_p = C_p$$

where c_v and c_p are the *molar values* of the heat capacity.

2.6.1 Application of the First Law to Enthalpy Changes

Heat capacities can be used in conjunction with the First Law of Thermodynamics to calculate enthalpy changes of reactions as a function of temperature. Consider the solidification of 1 mole of a liquid to a solid at its equilibrium freezing temperature T_2 (Figure 2.3).

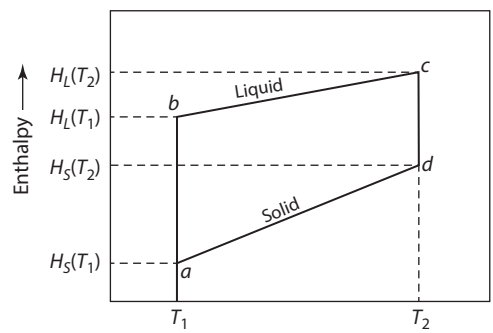

FIGURE 2.3 Enthalpy vs. temperature plots for 1 mole of a solid and liquid, showing that the enthalpy of transformation depends on temperature if the heat capacities differ. T_2 is the equilibrium solidification temperature.

The value of its enthalpy of freezing (or solidification) is seen to be

$$H_S(T_2) - H_L(T_2) < 0$$

since thermal energy leaves the substance and enters the surroundings (exothermic). This value is the negative of the length of the cord $\overline{cd}$ in Figure 2.3. If the liquid is supercooled to a temperature of T_1, the enthalpy change for freezing is seen now to be $H_S(T_1) - H_L(T_1)$. This value can be calculated as follows:

$$\text{The enthalpy of the liquid at } T_1 = H_L(T_2) + \int_{T_2}^{T_1} c_P^L dT = H_L(T_2) + c_P^L(T_1 - T_2)$$

$$\text{The enthalpy of the solid at } T_1 = H_S(T_2) + \int_{T_2}^{T_1} c_P^S dT = H_S(T_2) + c_P^S(T_1 - T_2)$$

$$\text{Thus,} \quad H_S(T_1) - H_L(T_1) = H_S(T_2) - H_L(T_2) + \int_{T_2}^{T_1} \left(c_P^S - c_P^L\right) dT$$

which is equal to the negative of the length of the cord $\overline{ba}$. This value is more negative (more thermal energy leaving the system: more exothermic) than that at T_2 because the temperature dependence of the enthalpy of the solid is greater than that of the liquid. The temperature dependence of the enthalpy is the heat capacity! The change in the enthalpy as a function of temperature can be written as

$$\left(\frac{\partial \Delta H}{\partial T}\right)_P = \Delta c_P$$

when the enthalpies vary linearly with temperature.

2.6.2 Relationship between C_P and C_V

In classical thermodynamics, we cannot calculate the exact values of the properties of matter, but we can calculate the relations *between* some of the properties. Although we *cannot calculate* C_P or C_V of an ideal gas in classical thermodynamics, we *can calculate their difference:* $C_P - C_V$

It is expected that, for any substance, c_p will be of greater magnitude than c_v. If it is required that the temperature of a system be increased by a certain amount, then, if the process is carried out at a constant volume, all of the thermal energy added to the system is used to raise the temperature of the system. However, if the process is carried out at constant pressure, then, in addition to raising the temperature by the required amount, the thermal energy added is required to provide the work necessary to expand the system at constant pressure. This work of expansion against the constant pressure per degree of temperature increase is calculated as

$$\frac{PdV'}{dT} \quad \text{or} \quad P\left(\frac{\partial V'}{\partial T}\right),$$

and hence, it might be expected that

$$c_p - c_v = P\left(\frac{\partial V}{\partial T}\right)_P \tag{2.7}$$

For 1 mole of an ideal gas,

$$\left(\frac{\partial V}{\partial T}\right)_P = \frac{R}{P},$$

and thus, $c_p - c_v = R$.

For any gas, the difference between c_p and c_v is calculated as follows:

$$c_p = \left(\frac{\partial H}{\partial T}\right)_P = \left(\frac{\partial U}{\partial T}\right)_P + P\left(\frac{\partial V}{\partial T}\right)_P$$

and

$$c_v = \left(\frac{\partial U}{\partial T}\right)_V$$

Hence,

$$c_p - c_v = \left(\frac{\partial U}{\partial T}\right)_P + P\left(\frac{\partial V}{\partial T}\right)_P - \left(\frac{\partial U}{\partial T}\right)_V$$

but

$$dU = \left(\frac{\partial U}{\partial V}\right)_T dV + \left(\frac{\partial U}{\partial T}\right)_V dT,$$

and therefore,

$$\left(\frac{\partial U}{\partial T}\right)_P = \left(\frac{\partial U}{\partial V}\right)_T \left(\frac{\partial V}{\partial T}\right)_P + \left(\frac{\partial U}{\partial T}\right)_V$$

Hence,

$$\begin{aligned} c_p - c_v &= \left(\frac{\partial U}{\partial V}\right)_T \left(\frac{\partial V}{\partial T}\right)_P + \left(\frac{\partial U}{\partial T}\right)_V + P\left(\frac{\partial V}{\partial T}\right)_P - \left(\frac{\partial U}{\partial T}\right)_V \\ &= \left(\frac{\partial V}{\partial T}\right)_P \left[P + \left(\frac{\partial U}{\partial V}\right)_T\right] \end{aligned} \tag{2.8}$$

The two expressions for $c_p - c_v$ (Equations 2.7 and 2.8) differ by the term

$$\left(\frac{\partial V}{\partial T}\right)_P \left(\frac{\partial U}{\partial V}\right)_T$$

2.6.2.1 Free Expansion of a Gas: Joule Expansion

In an attempt to evaluate the term

$$\left(\frac{\partial U}{\partial V}\right)_T$$

for gases, Joule performed an experiment that involved filling a copper vessel with a gas at some pressure and connecting this vessel *via* a stopcock to a similar but evacuated vessel. The two-vessel system was immersed in a quantity of adiabatically contained water and the stopcock was opened, thus allowing the *free expansion* of the gas into the evacuated vessel. After this expansion, Joule could not detect any change in the temperature of the system. Since the system was adiabatically contained and no work was performed, then from the First Law,

$$\Delta U = 0,$$

and hence,

$$dU = \left(\frac{\partial U}{\partial V}\right)_T dV + \left(\frac{\partial U}{\partial T}\right)_V dT = 0$$

Thus, since $dT = 0$ (*experimentally determined*) and dV is not 0, the term

$$\left(\frac{\partial U}{\partial V}\right)_T$$

must be zero. Joule thus concluded that the *internal energy* of a gas is a function only of *temperature* and is independent of the volume (and hence pressure).

This is true for an ideal gas. See Problem 2.18. Is it true for all gases?

2.6.2.2 Adiabatic Expansion of a Gas: Joule Thomson Expansion

In a more critical experiment performed by Joule and Thomson (William Thomson, aka Lord Kelvin, 1824–1907), in which an adiabatically contained gas of molar volume V_1 at the pressure P_1 was throttled through a porous diaphragm to the pressure P_2 and the molar volume V_2, a change in the temperature of the gas was observed, which showed that, for real gases,

$$\left(\frac{\partial U}{\partial V}\right) \neq 0$$

Thus for *real gases*, $U = U(T, P)$ or $U = U(T, V)$.

The reason Joule did not observe a temperature rise in the original experiment was that the heat capacity of the copper vessels and the water was considerably greater than the heat capacity of the gas, and thus, the small heat changes that actually occurred in the gas were absorbed in the copper vessels and the water. This decreased the actual temperature change to below the limits of the available means of temperature measurement at that time.

2.7 REVERSIBLE ADIABATIC PROCESSES

During a *reversible process* in which the state of a gas is changed, the gas never leaves the equilibrium surface shown in Figure 1.1. Consequently, during a reversible process, the gas passes through a continuum of equilibrium states, and the work, *w,* is given by the integral $\int_{V_1}^{V_2} P\,dV$. In a *reversible adiabatic process*, $q=0$, and thus, from the First Law, $dU=-\delta w$.

Consider a system comprising 1 mole of an ideal gas. From Equation 2.6a,

$$dU = c_v dT$$

and, for a reversible adiabatic process,

$$dU = -\delta w = -PdV$$

Thus,

$$c_v dT = -PdV$$

Since the system is 1 mole of an ideal gas, then

$$P = \frac{RT}{V},$$

and hence,

$$c_V dT = -\frac{RT}{V} dV$$

Integrating between states 1 and 2 gives

$$c_v \ln\left(\frac{T_2}{T_1}\right) = R \ln\left(\frac{V_1}{V_2}\right)$$

or

$$\left(\frac{T_2}{T_1}\right)^{C_v} = \left(\frac{V_1}{V_2}\right)^{R}$$

or

$$\left(\frac{T_2}{T_1}\right) = \left(\frac{V_1}{V_2}\right)^{\frac{R}{c_V}}$$

For an ideal gas, it has been shown that $c_p - c_v = R$. Thus, $\left(c_P/c_V\right) - 1 = R/c_V$, and if we set $c_P/c_V \equiv \gamma$, then $R/c_V = \gamma - 1$, and hence,

$$\frac{T_2}{T_1} = \left(\frac{V_1}{V_2}\right)^{\gamma-1}$$

From the ideal gas law,

$$\frac{T_2}{T_1} = \frac{P_2V_2}{P_1V_1} = \left(\frac{V_1}{V_2}\right)^{\gamma-1}$$

Thus,

$$\frac{P_2}{P_1} = \left(\frac{V_1}{V_2}\right)^{\gamma},$$

and hence,

$$P_2V_2^{\gamma} = P_1V_1^{\gamma} = PV^{\gamma} = \text{constant} \tag{2.9}$$

This is the relationship between the pressure and the volume of an ideal gas undergoing a *reversible adiabatic process* (Figure 2.4).

For an ideal monatomic gas, since

$$c_P = \frac{5}{2}R \quad \text{and} \quad c_V = \frac{3}{2}R,$$

we see that

$$\gamma = \frac{5}{3}$$

2.8 REVERSIBLE ISOTHERMAL PRESSURE OR VOLUME CHANGES OF AN IDEAL GAS

From the First Law,

$$dU' = \delta q - \delta w,$$

and for an isothermal process, $dT = 0$ and $dU' = 0$ for an ideal gas.

Therefore, $\delta w = \delta q = PdV = RT\,dV/V$ per mole of gas.

Integrating between the states 1 and 2 gives

$$w = q = RT\ln\left(\frac{V_2}{V_1}\right) = RT\ln\left(\frac{P_1}{P_2}\right) \tag{2.10}$$

Thus, for an ideal gas, an *isothermal* process is one of constant internal energy, during which the work done by the system equals the thermal energy absorbed by the system, both of which are given by Equation 2.10.

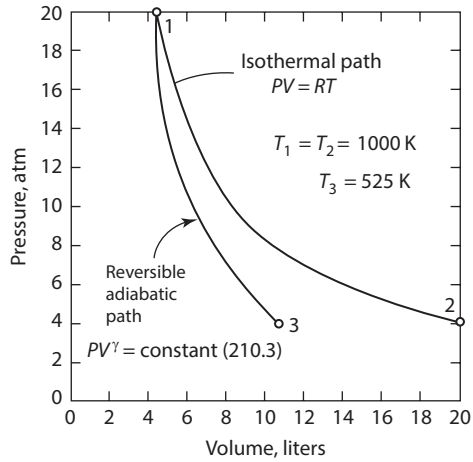

FIGURE 2.4 Comparison of the process path taken by a reversible isothermal expansion of one mole of an ideal gas with the process path taken by a reversible adiabatic expansion of an ideal gas between an initial pressure of 20 atm and a final pressure of 4 atm.

The plots of pressure versus volume for a reversible isothermal process and for a reversible adiabatic process are shown in Figure 2.4. It is seen that, for a given decrease in pressure, the work done by the *reversible isothermal* process (which is equal to the area under the curve) exceeds that done by the reversible adiabatic process. This difference is due to the fact that during the isothermal process, thermal energy is absorbed by the system in order to maintain a constant temperature, whereas during the adiabatic process, no thermal energy is admitted to the system. During the *isothermal expansion*, the internal energy of the gas remains constant, but during the *adiabatic expansion*, the internal energy decreases by an amount equal to the work done by the gas.

Example 2.1

For the reversible isothermal path shown in Figure 2.4, Equation 2.10 gives the work done by the gas as

$$w = RT\ln\left(\frac{P_1}{P_2}\right) = 8.3144 \times 1000 \times \ln\left(\frac{20}{4}\right) = 13.38 \text{ kJ}$$

For the reversible adiabatic path, the area under the curve is obtained as follows. Since PV^{γ} = constant = 210.3 and

$$\gamma = \frac{c_P}{c_V} = \frac{5/2R}{3/2R} = \frac{5}{3},$$

then

$$w = \int PdV = 210.3 \times \int dV$$

The volume of the gas in state 3 is obtained from Equation 2.9 as $V_3 = (210.4/4)^{3/5} =$ 10.78 liters, and the volume in state 1 is $V_1 = (210.3/20)^{3/5} = 4.10$ liters. Thus,

$$w = 210.3 \times \left(-\frac{3}{2}\right) \times \left(V_3^{-2/3} - V_1^{-2/3}\right)$$

$$= 210.3 \times (-1.5) \times \left(10.78^{-2/3} - 4.10^{-2/3}\right) = 58.41 \cdot \text{atm} = 5.92 \text{ kJ}$$

Alternatively, since $q = 0$, $w = -\Delta U = -c_v\ (T_3 - T_1) = -1.5 \times 8.3144 \times (525 - 1000) =$ 5.92 kJ.

Thus, more work is performed by an ideal gas during the isothermal expansion process than during the adiabatic expansion process for the same change in pressure.

2.9 OTHER FORMS OF WORK

Up to this point, we have only used PdV work in the First Law. We called these systems *simple systems*. There are, of course, other kinds of work that may be performed on or by a system. Here, we present three additional kinds of work.

To include other forms of work, the First Law can be written as

$$dU' = \delta q - \sum \delta w_i$$

It is important to remember that in this equation, each of the terms δw_i is the work done *by* the system.

2.9.1 Magnetic Work on a Paramagnetic Material

The work done *on* a material by an external magnetic field is given by

$$\delta w' = -V' \mu_0 \boldsymbol{\mathcal{H}} d\boldsymbol{M}$$

$$w' = -V' \mu_0 \int_{M_1}^{M_2} \boldsymbol{\mathcal{H}} d\boldsymbol{M}$$

$\boldsymbol{M}$ and $\boldsymbol{\mathcal{H}}$ have units of amp/m; μ_0, the permeability of vacuum, has units of N/amp^2; and V has units of m^3. The units of work in this equation are in joules. Both $\boldsymbol{\mathcal{H}}$ and $\boldsymbol{M}$ are axial vectors.

The First Law therefore becomes

$$dU' = \delta q - \sum \delta w_i = \delta q - PdV + V' \mu_0 \boldsymbol{\mathcal{H}} d\boldsymbol{M}$$

For an adiabatic process at constant volume,

$$(dU')_{q,V} = V' \mu_0 \boldsymbol{\mathcal{H}} d\boldsymbol{M}$$

Thus, under the specified conditions, the internal energy, U', of the paramagnetic material increases when an applied magnetic field increases its magnetization.

The temperature of the paramagnetic material also increases due to the applied magnetic field. Thus after the application of a magnetic field, the system is capable of doing more work, since the added internal energy is available to perform work.

2.9.2 Electrical Work on a Dielectric Material

The work done *on* a dielectric material by an external electric field is given by

$$\delta w' = -V' \boldsymbol{E} d\boldsymbol{D}$$

$$w' = -V' \int_{D_1}^{D_2} \boldsymbol{E} d\boldsymbol{D}$$

where $\boldsymbol{E}$ is the electric field intensity (N/coul) and $\boldsymbol{D}$ is the electric displacement (coul·m/m^3). The units of work are in joules. Both $\boldsymbol{E}$ and $\boldsymbol{D}$ are *polar* vectors.

The First Law in this case therefore becomes

$$dU' = \delta q - \sum \delta w_i = \delta q - PdV + V' \boldsymbol{E} d\boldsymbol{D}$$

For an adiabatic process at constant volume,

$$\left(dU'\right)_{q,V} = V\boldsymbol{E} d\boldsymbol{D}$$

Thus, under the specified conditions, the internal energy, U, of the dielectric material increases if an applied electric field increases its displacement field. The temperature of the dielectric material increases as well.

2.9.3 Work to Create or Extend a Surface

The reversible work done in *creating* a new surface (in joules) of area A is given as

$$\delta w' = -\gamma dA$$

γ has units of J/m^2 and A has units of m^2. The surface energy, γ, is a scalar. For liquids, the surface energy is isotropic. For solids, the surface energy has a symmetry that is at least that of the point symmetry of the solid. The First Law now becomes

$$dU' = \delta q' - \sum \delta w_i = \delta q' - PdV' + \gamma dA$$

For an adiabatic process at constant volume,

$$\left(dU'\right)_{q,V} = \gamma dA$$

Thus, under the specified conditions, the total energy of the system increases when a new surface area is created.

In the text to this point, we have ignored the surface energy of a material. Our implicit assumption has been that the volume terms are much larger than the surface terms, and hence, the surface terms may be neglected. Surface terms need to be included when the surface-to-volume ratio is not negligible, such as is the case for nano-size particles.

A related quantity of work is the reversible work necessary to *increase* the surface area by *stretching* it with a stress σ. This work is given as

$$\delta w' = -\sigma dA$$

Surface stress is a second-rank tensor, with units of N/m. For a liquid, the surface stress, σ, is isotropic and is numerically equal to the surface energy, γ, which is positive. This is not necessarily the case for crystalline solids, where the surface stress may take on positive or negative values.

2.10 SUMMARY

1. The establishment of the relationship between the work done on or by a system and the thermal energy entering or leaving the system is facilitated by the introduction of the thermodynamic function U, the internal energy.
2. U is a function of state, and thus, the difference between the values of U in two states depends only on the states and is independent of the process path taken by the system in moving between the states.
3. The relationship between the internal energy change, the work done, and the thermal energy absorbed per mole by a system of fixed composition in moving from one state to another is given as $\Delta U = q - w$, or, for an increment of this process, $dU = \delta q - \delta w$. This relationship summarizes the First Law of Thermodynamics.
4. The internal energy of an isolated system ($\delta q = 0$ and $\delta w = 0$) is constant.
5. The integrals of δq and δw can only be obtained if the process path taken by the system in moving from one state to another is known. Process paths that are convenient for consideration include the following:
   a. Constant volume processes (isochoric) in which $\int \delta w = \int P dV = 0$, if only PdV work is possible.
   b. Constant pressure processes (isobaric) in which $\int \delta w = P \int dV = P\Delta V$ if only PdV work is possible.
   c. Constant temperature (isothermal) processes.
   d. *Adiabatic* processes in which $q = 0$. For adiabatic processes, the work needed to take the system from $U' = U_1'$ to $U' = U_2'$ is independent of the path.
6. For a constant volume process in a simple system, $w = 0$ and $\Delta U' = q_v$. The definition of the constant volume molar heat capacity as

$$c_V = \left(\frac{\delta q}{dT}\right)_V = \left(\frac{\partial U}{\partial T}\right)_V$$

(which is an experimentally measurable quantity) facilitates the determination of the change in U resulting from a constant volume process, since

$$\Delta U = \int_{T_1}^{T_2} c_v dT.$$

7. Consideration of constant pressure processes is facilitated by the introduction of the thermodynamic function H; the enthalpy for 1 mole is defined as $H \equiv U + PV$. Since the expression for H contains only functions of state, H is also a function of state, and thus, the difference between the values of H in two states depends only on the states and is independent of the path taken by the system in moving between them.
8. For a constant pressure process, $\Delta H = \Delta U + P\Delta V = (q_p - P\Delta V) + P\Delta V = q_p$. The definition of the constant pressure molar heat capacity as

$$c_P = \left(\frac{\delta q}{dT}\right)_P = \left(\frac{\partial H}{\partial T}\right)_P$$

(which is an experimentally measurable quantity) facilitates the determination of the change in H as the result of a constant pressure process, since

$$dH = \int_{T_1}^{T_2} c_p dT.$$

9. For an ideal gas, the internal energy U' is a function only of temperature.
10. $c_p - c_v = R$ for an ideal gas.
11. The process path of an ideal gas undergoing a reversible adiabatic change of state is described by $PV^\gamma = \text{constant}$, where $\gamma = c_P/c_V$. During an adiabatic expansion, since $q = 0$, the decrease in the internal energy of the system equals the work done by the system.
12. Since the internal energy of an ideal gas is a function only of temperature, the internal energy of an ideal gas remains constant during an isothermal change of state. Thus, the thermal energy that enters or leaves the gas as a result of the isothermal process equals the work done by or on the gas, with both quantities being given by

$$w = q = RT \ln\left(\frac{V_2}{V_1}\right) = RT \ln\left(\frac{P_1}{P_2}\right)$$

13. Only the differences in the values of U' and H' between two states—that is, the values of $\Delta U'$ and $\Delta H'$—can be measured. The absolute values of U' and H' in any given state cannot be determined.
14. Other work terms include the work done on a material by the application of an external magnetic field or by an electric field. Also, the creation of a new surface must be done by doing work on the material.

15. A generalized First Law can be written as

$$dU' = \delta q - \sum \delta w_i$$

where $\sum \delta w_i$ is the total work done by the system.

2.11 CONCEPTS AND TERMS INTRODUCED IN THIS CHAPTER

The reader should write out brief definitions or descriptions of the following terms. Where appropriate, equations may be used.

Adiabatic process
Calorie
Conservation of energy
Cyclic process
Dissipated energy
Electric work
Enthalpy of melting/freezing
Enthalpy, H
Equation of state
First Law of Thermodynamics
Free expansion
Heat (thermal energy)
Heat capacity
Hess' law of constant heat summation
Internal energy, U
Isobaric process
Isochoric process
Isothermal process
Kinetic energy/potential energy
Magnetic field
Magnetic work
Mechanical equivalent of heat
Paramagnet
Process
Real gas
Reversible processes
Simple system
Specific/molar heat capacity
State variable
Surface energy/work
System variables
Thermodynamic potential
Thermodynamic state variable (function)
Work

2.12 QUALITATIVE EXAMPLE PROBLEMS

QUALITATIVE PROBLEM 1

One mole of an ideal gas at a pressure of 1 atm and temperature of 273 K is expanded to twice its volume at constant pressure.

a. In terms of P and V_1 and V_2, how much work was performed? Was the work performed on the gas or by the gas? Explain.
b. If two moles of an ideal gas at the same initial pressure and temperature were to double its volume under constant pressure, how much work would be performed on or by the gas? Compare the value with that in part (a).
c. In either case (a) or (b), does the temperature increase or decrease? Explain.

SOLUTION TO QUALITATIVE PROBLEM 1

a. The work is performed *by* the gas and equals $P\Delta V = P(V_2 - V_1) = PV_1$.
b. The starting volume for this part of the problem is twice what it was in case (a) Thus, it starts as $2V_1$. It also doubles during the process. Thus ΔV doubles to $4V_1$. Thus, the work performed by 2 moles of the gas is $2PV_1$, twice that of part (a) of the problem.
c. The temperature increases in both cases.

Case (a):

$$P_1V_1 = (1)RT_1 \quad \text{and} \quad P_2V_2 = (1)RT_2, \quad \text{but} \quad P_2 = P_1 \quad \text{and} \quad V_2 = 2V_1.$$

Thus, $T_2 = 2T_1$. The temperature doubles.

Case (b):

Since there are 2 moles in this case: at the same P and T as case (a), V must start off twice as large as the starting volume of case (a), that is, it starts as $2V_1$. This doubles to $4V_1$.

Thus, $P(2V_1) = (2)RT_1$ and $P(4V_1) = (2)RT_2$. The temperature also doubles.

Why does the temperature increase? In order to expand at constant pressure, more energy must be given to the gas to keep the pressure from decreasing.

QUALITATIVE PROBLEM 2

A magnetic field $\boldsymbol{\mathcal{H}}$ is applied to a material with a positive susceptibility χ. Assume $\boldsymbol{M} \,//\, \boldsymbol{\mathcal{H}}$ and that the $\boldsymbol{M}$ versus $\boldsymbol{\mathcal{H}}$ plot is linear with a slope χ (Figure 2.5a), where χ is the susceptibility of the material.

a. Determine the work done when $\boldsymbol{\mathcal{H}}$ varies from zero to $\boldsymbol{\mathcal{H}} = \boldsymbol{\mathcal{H}}_f$.
b. Sketch the area on the $\boldsymbol{\mathcal{H}} - \boldsymbol{M}$ plot that corresponds to the work done on the material.
c. The product of $V\mu_0$, $M_f \cdot \boldsymbol{\mathcal{H}}_f$, is an energy. Subtract your answer in part (a) from the value $V\mu_0 M_f \cdot \boldsymbol{\mathcal{H}}_f$. What is this energy?

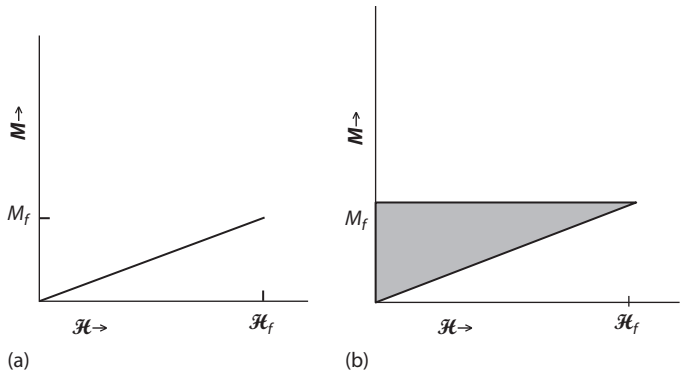

FIGURE 2.5 (a) Schematic showing $\boldsymbol{M}$ vs. $\boldsymbol{\mathcal{H}}$ plot for a material under the applied magnetic field. (b) Plot of Figure 2.6a, showing work done on the material as the shaded region.

SOLUTION TO QUALITATIVE PROBLEM 2

a. $$w = V\mu_0 \int_0^{M_f} \boldsymbol{\mathcal{H}} d\boldsymbol{M} = V\mu_0 \int_0^{M_f} \frac{\boldsymbol{M}}{\chi} d\boldsymbol{M} = \frac{V\mu_0 M_f^2}{2\chi} = \frac{V\mu_0 M_f \boldsymbol{\mathcal{H}}_f}{2}$$

b. Refer to Figure 2.5b.

c. This is the work that the moments, $\boldsymbol{M}$, performed against the applied magnetic field, $\boldsymbol{\mathcal{H}}$, in resisting magnetization. Since this was a reversible and linear process, the work is equal in magnitude and opposite in sign to the work applied to the material.

2.13 QUANTITATIVE EXAMPLE PROBLEM

QUANTITATIVE PROBLEM

Ten liters of a monatomic ideal gas at 25°C and 10 atm pressure is expanded to a final pressure of 1 atm. The molar heat capacity of the gas at constant volume, c_v, is 3/2 R and is independent of temperature. Calculate the work done, the heat absorbed, and the change in U and in H for the gas if the process is carried out as follows:

a. Isothermally and reversibly
b. Adiabatically and reversibly

Having determined the final state of the gas after the reversible adiabatic expansion, verify that the change in U for the process is independent of the path taken between the initial and final states by considering the process to be carried out as follows:

i. An isothermal process followed by a constant volume process
ii. A constant volume process followed by an isothermal process
iii. An isothermal process followed by a constant pressure process

iv. A constant volume process followed by a constant pressure process
v. A constant pressure process followed by a constant volume process

SOLUTION TO QUANTITATIVE PROBLEM

The size of the system must first be calculated. From consideration of the initial state of the system (the point *a* in Figure 2.6),

$$n = \text{The number of moles} = \frac{P_a V_a}{RT_a} = \frac{10 \times 10}{0.08206 \times 298} = 4.09$$

a. *The isothermal reversible expansion*: The state of the gas moves from *a* to *b* along the 298-degree isotherm. Along any isotherm, the product *PV* is constant:

$$V_b = \frac{P_a V_a}{P_b} = \frac{10 \times 10}{1} = 100 \text{ liters}$$

For an ideal gas undergoing an isothermal process, $\Delta U = 0$, and hence, from the First Law,

$$q = w = \int_a^b P dV = nRT \int_a^b \frac{dV}{V} = 4.09 \times 8.3144 \times 298 \times \ln \frac{100}{10} \text{ J}$$

$$= 23.3 \text{ kJ}$$

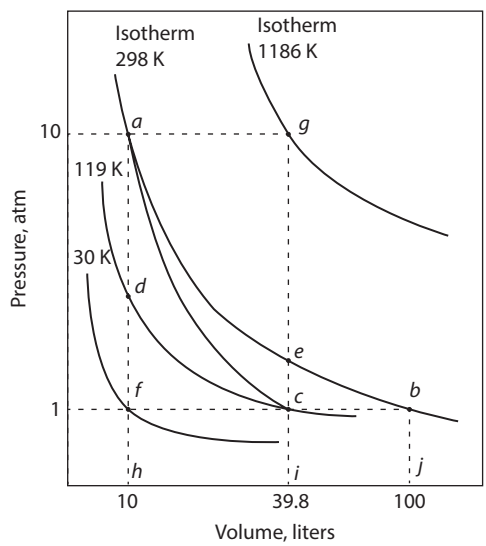

FIGURE 2.6 The five process paths considered in the numerical problem.

Thus, in passing from state a to state b along the 298-degree isotherm, the system performs 23.3 kJ of work and absorbs 23.3 kJ of heat from the constant temperature surroundings.
Since for an ideal gas, H is a function only of temperature, $\Delta H'_{(a\to b)} = 0$; that is,

$$\Delta H_{(a\to b)} = \Delta U_{(a\to b)} + \left(P_b V_b - P_a V_a\right) = \left(P_b V_b - P_a V_a\right)$$

$$= nRT_b - nRT_a = nR\left(T_b - T_a\right) = 0$$

b. *The reversible adiabatic expansion*: If the adiabatic expansion is carried out reversibly, then during the process the state of the system is, at all times, given by $PV^{\gamma} = \text{constant}$, and the final state is the point c in the diagram. The volume V_c is obtained from $P_a V_a^{\gamma} = P_c V_c^{\gamma}$ as

$$V_c = \left(\frac{10\times 10^{5/3}}{1}\right)^{3/5} = 39.8 \text{ liters}$$

and

$$T_c = \frac{P_c V_c}{nR} = \frac{1\times 39.8}{4.09\times 0.08206} = 119 \text{ degrees}$$

The point c thus lies on the 119-degree isotherm. As the process is adiabatic, $q = 0$, and hence,

$$\Delta U_{(a\to)} = -w = \int_a^c nc_v dT = nc_v\left(T_c - T_a\right)$$

$$= 4.09\times 1.5\times 8.3144\times\left(119 - 298\right) \text{ J}$$

$$= -9.13 \text{ kJ}$$

The work done by the system as a result of the process equals the decrease in the internal energy of the system = 9.13 kJ.

i. An *isothermal process followed by a constant volume process* (the path $a \to e \to c$; that is, an isothermal change from a to e, followed by a constant volume change from e to c).

$$\Delta U'_{(a\to e)} = 0, \quad \text{as this is an isothermal change of state}$$

$$\Delta U'_{(e\to c)} = q_v \left(\Delta V = 0, \text{ and hence, } w = 0\right)$$

$$= \int_e^c nc_v dT$$

and as the state e lies on the 298-degree isotherm, then

$$\Delta U'_{(e\to c)} = 4.09\times 1.5\times 8.3144\times(119-298)\text{ J} = -9.13\text{ kJ}$$

Thus,

$$\Delta U'_{(a\to c)} = \Delta U'_{(a\to e)} + \Delta U'_{(e\to c)} = -9.13\text{ kJ}$$

ii. *A* constant *volume process followed by an isothermal process* (the path $a \to d \to c$; that is, a constant volume change from *a* to *d*, followed by an isothermal change from *d* to *c*).

$$\Delta U'_{(a\to d)} = q_v\left(\Delta V = 0,\ \text{and hence, } w = 0\right)$$

$$= \int_a^d nc_v dT, \text{ and as the statedlies in the 119 - degree isotherm, then}$$

$$\Delta U'_{(a\to d)} = 4.09\times 1.5\times 8.3144\times(119-298)\text{ J} = -9.13\text{ kJ}$$

$$\Delta U'_{(d\to c)} = 0, \text{ as this is an isothermal process, and hence,}$$

$$\Delta U'_{(a\to c)} = \Delta U'_{(a\to d)} + \Delta U'_{(d\to c)} = -9.13\text{ kJ}$$

iii. *An isothermal process followed by a constant pressure process* (the path $a \to b \to$ c; that is, an isothermal change from *a* to *b*, followed by a constant pressure change from *b* to *c*).

$$\Delta U'_{(a\to d)} = 0,\ \text{as this process is isothermal}$$

$$\Delta U'_{(b\to cf)} = q_p - w,\quad \text{and as}\quad P_b = P_c,\ \text{then}\ \ w = P_b\left(V_c - V_b\right)$$

$$= \int_b^c nc_p dT - P_b\left(V_c - V_b\right)$$

Since $c_v = 1.5\ R$ and $c_p - c_v = R$, then $c_p = 2.5\ R$; and as 1 liter atm equals 101.3 J,

$$\Delta U'_{(b\to c)} = \left[4.09\times 2.5\times 8.3144\times(119-298)\right]$$

$$-\left[1\times(39.8-100)\times 101.3\right]\text{ J}$$

$$= -15.2 + 6.1 = -9.1\text{ kJ}$$

Thus,

$$\Delta U'_{(a\to c)} = U'_{(a\to b)} + U'_{(b\to c)} = -9.1\text{ kJ}$$

iv. *A* constant *volume process followed by a constant pressure process* (the path $a \rightarrow f \rightarrow c$; that is, a constant volume change from *a* to *f*, followed by a constant pressure change from *f* to *c*).

$$\Delta U'_{(a\rightarrow f)} = q_v \left(V_a = V_f, \text{and hence, } w = 0\right)$$

$$= \int_a^f nc_v dT$$

From the ideal gas law,

$$T_f = \frac{P_f V_f}{nR} = \frac{1\times 10}{4.09\times 0.08206} = 30 \text{ degrees}$$

That is, the state *f* lies on the 30-degree isotherm. Thus,

$$\Delta U'_{(a\rightarrow f)} = 4.09\times 1.5\times 8.3144\times(30-298)\text{ J} = -13.67\text{ kJ}$$

$$\Delta U'_{(f\rightarrow c)} = q_p - w = \int_f^c nc_p dT - P_f\left(V_c - V_f\right)$$

$$= \left[4.09\times 2.5\times 8.3144\times(119-30)\right] - \left[1\times(39.8-10)\times 101.3\right]\text{ J} = +7.57 - 3.02\text{ kJ}$$

Thus,

$$\Delta U'_{(a\rightarrow c)} = \Delta U'_{(a\rightarrow f)} + \Delta U'_{(f\rightarrow c)} = 13.67 + 7.57 - 3.02$$

$$= -9.12\text{ kJ}$$

v. *A constant-pressure process followed by a constant volume process* (the path $a \rightarrow g \rightarrow c$; that is, a constant pressure step from *a* to *g*, followed by a constant volume step from *g* to *c*).

$$\Delta U'_{(a\rightarrow g)} = q_p - w$$

From the ideal gas law,

$$T_g = \frac{P_g V_g}{nR} = \frac{10\times 39.8}{4.09\times 0.08206} = 1186 \text{ degrees}$$

and hence, the state *g* lies on the 1186-degree isotherm. Thus,

$$\Delta U'_{(a\rightarrow g)} = \left[4.09\times 2.5\times 8.3144\times(1186-298)\right]\text{ J}$$

$$-\left[10\times(39.8-10)\times 101.3\right]\text{ J} = 75.5 - 30.2\text{ kJ}$$

$$\Delta U'_{(g\rightarrow c)} = q_v = 4.09\times 1.5\times 8.3144\times(119-1186)\text{ J} = -54.4\text{ kJ}$$

Thus,

$$\Delta U'_{(a\to c)} = \Delta U'_{(a\to g)} + \Delta U'_{(g\to c)} = 75.5 - 30.2 - 54.4$$
$$= -9.1 \text{ kJ}$$

The value of $\Delta U'_{(a\to c)}$ is thus seen to be independent of the path taken by the process between the states *a* and *c*.

The change in enthalpy from a to c (Figure 2.6). The enthalpy change is most simply calculated from the consideration of a path that involves an isothermal portion, over which $\Delta H' = 0$, and an isobaric portion, over which $\Delta H = q_p = \int nc_p\, dT$. For example, consider the path $a \to b \to c$.

$$\Delta H'_{(a\to b)} = 0$$
$$\Delta H'_{(b\to c)} = q_p = nc_p\left(T_c - T_b\right)$$
$$= 4.09 \times 2.5 \times 8.3144 \times (119 - 298)\text{ J}$$
$$= -15.2 \text{ kJ}$$

and hence,

$$\Delta H'_{(a\to c)} = -15.2 \text{ kJ}$$

or alternatively

$$\Delta H'_{(a\to c)} = \Delta U'_{(a\to c)} + \left(P_c V_c - P_a V_a\right)$$
$$= -9.12 \text{ kJ} + \left[(1 \times 39.8 - 10 \times 10) \times 101.3\right]\text{ J}$$
$$= -9.12 - 6.10 = -15.2 \text{ kJ}$$

in each of the paths (i) to (v); the heat and work effects differ, although in each case the difference $q - w$ equals -9.12 kJ. In the case of the reversible adiabatic path, $q = 0$, and hence, $w = +9.12$ kJ. If the processes (i) to (v) are carried out reversibly, then

- For path (i), $q = -9.12 +$ the area *aeih*
- For path (ii), $q = -9.12 +$ the area *dcih*
- For path (iii), $q = -9.12 +$ the area *abjh* $-$ the area *cbji*
- For path (iv), $q = -9.12 +$ the area *fcih*
- For path (v), $q = -9.12 +$ the area *agih*

PROBLEMS

2.1 A monatomic ideal gas at 300 K has a volume of 15 liters at a pressure of 15 atm. Calculate

a. The final volume of the system
b. The work done by the system
c. The heat entering or leaving the system
d. The change in the internal energy
e. The change in the enthalpy when the gas undergoes
   i. A reversible isothermal expansion to a pressure of 10 atm
   ii. A reversible adiabatic expansion to a pressure of 10 atm

The constant volume molar heat capacity of the gas, c_v, has the value 1.5 R.

2.2 One mole of a monatomic ideal gas, in the initial state $T = 273$ K, $P = 1$ atm, is subjected to the following three processes, each of which is conducted reversibly:

a. A doubling of its volume at constant pressure
b. Then a doubling of its pressure at constant volume
c. Then a return to the initial state along the path $P = 6.643 \times 10^{-4} V^2 + 0.6667$

Calculate the heat and work effects that occur during each of the three processes.

2.3 The initial state of a quantity of monatomic ideal gas is $P = 1$ atm, $V = 1$ liter, and $T = 373$ K. The gas is isothermally expanded to a volume of 2 liters and is then cooled at constant pressure to volume V. This volume is such that a reversible adiabatic compression to a pressure of 1 atm returns the system to its initial state. All of the changes of state are conducted reversibly. Calculate the value of V and the total work done on or by the gas.

2.4 Two moles of a monatomic ideal gas are contained at a pressure of 1 atm and a temperature of 300 K; 34,166 J of heat is transferred to the gas, as a result of which the gas expands and does 1216 J of work against its surroundings. The process is reversible. Calculate the final temperature of the gas.

2.5 One mole of N_2 gas is contained at 273 K and a pressure of 1 atm. The addition of 3000 J of heat to the gas at constant pressure causes 832 J of work to be done during the expansion. Calculate

a. The final state of the gas
b. The values of ΔU and ΔH for the change of state
c. The values of c_v and c_p for N_2

Assume that nitrogen behaves as an ideal gas and that the change of state is conducted reversibly.

2.6 Ten moles of monatomic ideal gas, in the initial state $P_1 = 10$ atm, $T_1 = 300$ K, is taken round the following cycle:

a. A reversible change of state along a straight line path on the P-V diagram to the state $P = 1$ atm, $T = 300$ K
b. A reversible isobaric compression to $V = 24.6$ liters

c. A reversible constant volume process to $P = 10$ atm

How much work is done on or by the system during the cycle? Is this work done on the system or by the system?

2.7 One mole of a monatomic ideal gas at 25°C and 1 atm undergoes the following reversibly conducted cycle:

a. An isothermal expansion to 0.5 atm, followed by
b. An isobaric expansion to 100°C, followed by
c. An isothermal compression to 1 atm, followed by
d. An isobaric compression to 25°C

The system then undergoes the following reversible cyclic process:

a. An isobaric expansion to 100°C, followed by
b. A decrease in pressure at constant volume to the pressure P atm, followed by
c. An isobaric compression at P atm to 24.5 liters, followed by
d. An increase in pressure at constant volume to 1 atm

Calculate the value of P which makes the work done on the gas during the first cycle equal to the work done by the gas during the second cycle.

2.8 One mole of a monatomic ideal gas at standard temperature and pressure (STP) undergoes the following three processes:

a. At constant pressure, the temperature is doubled.
b. At constant temperature, the pressure is doubled.
c. The gas is returned to STP via a constant volume process.

Calculate ΔU, ΔH, Q, and W for each of the steps.

2.9 Paramagnetic salts often obey the Curie relation:

$$\frac{M}{\boldsymbol{H}} = \frac{\text{constant}}{T} = \frac{C}{T}$$

Obtain an expression for the work needed to change the magnetization from $M = 0$ to $M = M$ of such a material. Assume that the field and the magnetization are parallel.

2.10 One mole of a monatomic ideal gas is taken on the path $A \rightarrow B \rightarrow C \rightarrow D \rightarrow A$, as shown in Figure 2.7. All paths are reversible.

- $A \rightarrow B$ is a reversible isothermal expansion of the gas.
- $B \rightarrow C$ is a reversible adiabatic expansion of the gas.
- $C \rightarrow D$ is a reversible isothermal compression of the gas.
- $D \rightarrow A$ is a reversible adiabatic compression of the gas.

a. Derive expressions for ΔU, q, and w during each step in terms of V_a, V_b, V_c, V_d, t_1, t_2, and R. Determine the sign of each.
b. Determine the values of $\sum(w_i)$, $\sum(q_i)$, and $\sum(\Delta Ui)$ in terms of V_a, V_b, V_c, V_d, t_1, t_2, and R. Determine the sign of each.

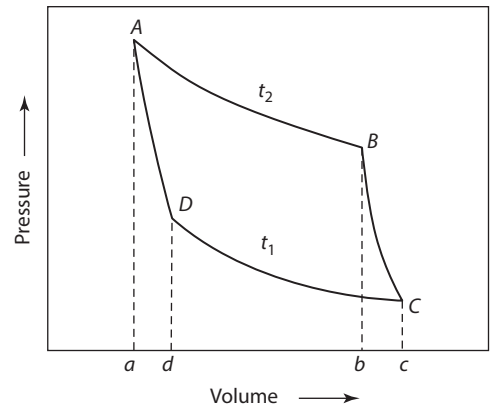

FIGURE 2.7 A cycle for one mole of a monatomic ideal gas with two isothermal paths and two adiabatic paths. The area enclosed by *ABCD* is the work done by the gas during the cycle.

2.11 The change in enthalpy when 1 mole of solid water (ice) is melted at 273 K is 6008 J.

a. Calculate the change in enthalpy when ice is melted at 298 K. Is this process possible at 1 atm?
b. Calculate the change in enthalpy when supercooled water solidifies at 260 K.
c. Sketch the *H* versus *T* plot for both solid and liquid water.

For this problem, take the heat capacity of liquid water to be 75.44 J/K and that of solid water to be 38 J/K over the range in temperatures of the problem. The enthalpy of liquid water at 298 K may be arbitrarily set equal to zero.

2.12 Three phases, α, β, and δ, meet as shown in Figure 2.8a, forming three interphase interfaces—namely, α/β, α/δ, and β/δ. It can be shown that the following holds.

$$\frac{\gamma_{\alpha/\beta}}{\sin\theta_3} = \frac{\gamma_{\alpha/\delta}}{\sin\theta_2} = \frac{\gamma_{\beta/\delta}}{\sin\theta_1}$$

Using this equation, determine the equation that relates the grain boundary grooving angle θ_{gb} to the interface energy $\gamma_{\alpha/L}$ and the grain boundary energy $\gamma_{\alpha/\alpha}$ (Figure 2.8b).

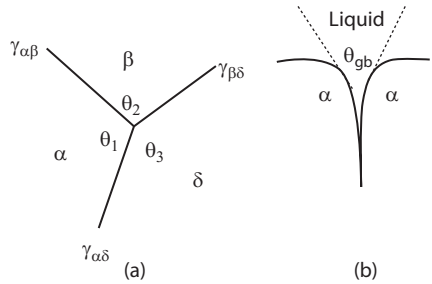

FIGURE 2.8 (a) Three phases meeting at a point, showing the angles between their surfaces. (b) A grain boundary groove showing the equilibrium groove angle.

2.13* Calculate the change in the enthalpy when 1 mole of SiC is heated from 25°C to 1000°C. The constant pressure molar heat capacity of SiC varies with temperature as

$$c_p = 50.79 + 1.97 \times 10^{-3} T - 4.92 \times 10^{6} T^{-2} + 8.20 \times 10^{8} T^{-3} \text{ J/mole} \cdot \text{K}$$

2.14* Derive an expression for the work performed by an ideal gas in expanding reversibly and adiabatically from P_1V_1 to P_2V_2.

2.15* It can be shown by the kinetic theory of gases that the internal energy of a monatomic ideal gas can be written as: $U = \frac{3}{2}PV$

Show that for a monatomic ideal gas : $c_V = \frac{3}{2}R$ and $c_P = \frac{5}{2}R$

2.16* It can be shown by the kinetic theory of gases that the internal energy of a monatomic ideal gas can be written as: $U = \frac{3}{2}PV = \frac{3}{2}RT$

Show that for an ideal gas : $\left(\frac{\partial U}{\partial V}\right)_T = 0$

2.17* Obtain an expression for the work performed by n moles of a van der Waals gas in expanding isothermally from a volume of V_1 to V_2.

The van der Waals' equation of state for n moles of a gas is given as:

$$\left(P + \frac{n^2 a}{V^2}\right)(V - nb) = nRT$$

* New problem in this edition.

APPENDIX 2A: NOTE ON THE SIGN CONVENTION OF δW

There are two sign conventions in the literature for the work term in the First Law. One convention is that work done by the system is considered positive, and therefore, since the internal energy, U, decreases, for $\delta q = 0$, we have

$$dU = -\delta w \left(\text{convention i}\right)$$

This is the convention used in this text.

The other convention is that work done on the system is positive work, and therefore, the internal energy of the system increases when positive work is performed (for $\delta q = 0$):

$$dU = +\delta w \left(\text{convention ii}\right)$$

In thermodynamic discussions that deal mainly with gases, the first convention is the best one to use. This is because when the system is a gas and pressure is applied to it, the gas contracts ($V_2 < V_1$). This means that the internal energy of the gas changes (for $\delta q = 0$) as

$$dU = -PdV = -P\left(V_2 - V_1\right) > 0$$

This convention is based on the fact that pressure applied to a gas is defined as positive, and therefore, the volume of the gas decreases.

The internal energy of the gas must decrease if the gas does work.

Using this convention, for work terms caused by the application of external magnetic fields or stress fields, the work term on the system is negative work. For example, we write

$$dU = \delta q - \delta w = \delta q - \left(-V\mu_0 \boldsymbol{H} d\boldsymbol{M}\right) = \delta q + V\mu_0 \boldsymbol{H} d\boldsymbol{M}$$

which shows that magnetic work done on the system increases the internal energy, as expected.

For stress, this is taken care of since the equivalent stress to hydrostatic pressure is a compressive stress:

$$P = -\frac{1}{3}\text{Trace}\begin{pmatrix} \sigma & 0 & 0 \\ 0 & \sigma & 0 \\ 0 & 0 & \sigma \end{pmatrix}$$

which is defined as negative stress, and tensile stress is positive.

3 The Second Law of Thermodynamics

3.1 INTRODUCTION

In Chapter 2, it was seen that when a system undergoes a change of state, the consequent change in the internal energy, U, of the system is dependent only on its initial and final states and is equal to the algebraic sum of the thermal energy, q, and work, w, effects. From this, it follows that the total energy of the universe (system plus surroundings) for an allowable change must remain constant.

Two questions now arise.

1. What magnitudes may the q and w effects have?
2. What criteria govern these magnitudes?

   Two extreme cases related to the first question can occur.

   - $w = 0$ and $q = \Delta U'$
   - $q = 0$ and $w = -\Delta U'$

   But if $q \neq 0$ and $w \neq 0$, a third question arises.
3. Is there a definite limit to the amount of work which the system can do during its change of state?

   The answers to these questions require an examination of the *nature* of the processes that affect q and w. This examination, which is made in this chapter, identifies two types of processes (*reversible* and *irreversible* processes) and introduces a state function called the *entropy* (S).

The development of the concept of entropy will be introduced from two different starting points. In Sections 3.2–3.8, entropy will be seen as a *quantification* of the degree of irreversibility of a process. In Sections 3.10–3.14, it will be seen that, as a result of an examination of the properties of *reversibly* operated heat engines, there naturally develops a quantity that has all the properties of a thermodynamic state function. This state function is the entropy. These findings lead to two statements of the *Second Law of Thermodynamics*, which, together with the other laws of thermodynamics, lay the foundation for the thermodynamic method of describing the behavior of matter to be discussed in the remainder text.

3.2 SPONTANEOUS OR NATURAL PROCESSES

A system left to itself will do one of two things: it may remain in the state in which it happens to be or it may change of its own accord to some other state. That is, if the system is initially in equilibrium with its surroundings, then, left to itself, it will remain in this equilibrium state. On the contrary, if the initial state is not the

DOI: 10.1201/9781003375388-4

equilibrium state, the system will spontaneously[1] (i.e., without any external influence) move toward its equilibrium state. The equilibrium state is a state of rest (at least at the macroscopic level), and thus, once at equilibrium, a system will only move away from equilibrium if it is acted on by some external agency. Even then, the combined system, comprising the original system and the external agency, is simply moving toward the equilibrium state of the new combined system. A process that involves the spontaneous movement of a system from a nonequilibrium state to an equilibrium state is called a *natural* or *spontaneous* process. Since such a process cannot be reversed without the application of an external agency which leaves a permanent change in this agency, such a process is said to be *irreversible*. The terms *natural*, *spontaneous*, and *irreversible* are synonymous in this context.

The mixing of gases and the transfer of energy down a temperature gradient are common examples of natural processes.

- If the initial state of a system consisting of two gases A and B is that in which gas A is contained in one vessel and gas B is contained in a separate vessel, then, when the vessels are connected to one another, the system *spontaneously* moves to the equilibrium state in which the two gases are completely mixed within the combined vessels. The composition of the gas mixture is homogeneous (uniform) throughout the volume which the gas occupies.
- If the initial state of a two-body system is that in which one body is at one temperature and the other body is at another temperature, then, when the bodies are placed in thermal contact with one another, a spontaneous process occurs in which energy is transferred from the hotter to the colder body. The equilibrium state is reached when both bodies attain a common uniform temperature.

In both of these examples, the reverse process (the unmixing of the gases and the transfer of thermal energy up a temperature gradient) will never occur *spontaneously*. Also, in both examples, common experience allows the equilibrium states to be predicted without any knowledge of the *criteria for equilibrium*. However, in more complex systems, the equilibrium state may not be able to be predicted from common experience, and thermodynamic criteria governing equilibrium must be established before a calculation of the equilibrium state can be made.

The determination of the equilibrium state is of prime importance in thermodynamics, since knowledge of this state for any materials system will allow the determination of the direction in which any change of state will proceed from any starting or initial state. For example, knowledge of the equilibrium state of a chemical reaction system such as

$$A + B = C + D$$

will afford knowledge of whether, from any initial state, which would be some mixture of A, B, C, and D, the reaction will proceed from right to left or from left to right. Also, knowledge of the extent to which the reaction will proceed before equilibrium is reached can be attained.

[1] In thermodynamics, a *spontaneous change* does not imply anything about the rate of change of the system, only that there is no energetic barrier to its occurrence.

If a system undergoes a spontaneous process involving the performance of *work* and the transfer of thermal energy, then, as the process continues, during which time the system approaches its equilibrium state, the capacity of the system for further spontaneous change decreases, as does its capacity to do further work. Once equilibrium is reached, the *capacity of the system* for doing further work is exhausted. In the initial nonequilibrium state of an isolated system (a system of constant internal energy), some of the energy of the system is available for doing useful work, and when the equilibrium state is reached, as a result of the completion of a spontaneous process, none of the energy of the system is available for doing further spontaneous useful work, even though the total energy of the system has not decreased. Thus, as a result of the spontaneous process, the energy of the system has become degraded, in the sense that energy, which was available for doing useful work, is now in a form that is not available for external purposes. Sometimes, this is referred to as the *dissipation* of energy.

3.3 ENTROPY AND THE QUANTIFICATION OF IRREVERSIBILITY

Two distinct types of spontaneous processes are given as follows:

1. The conversion of work into thermal energy—that is, the *degradation* of mechanical energy to thermal energy (heat)
2. The transfer of thermal energy down a temperature gradient

If an irreversible process is one in which the energy of the system undergoing the process is degraded, then the possibility that the extent of degradation can differ from one process to another suggests that a *quantitative measure* of the extent of degradation, or degree of irreversibility, can be developed.

The existence of processes that exhibit differing degrees of irreversibility can be illustrated as follows. Consider the weight–heat reservoir system shown schematically in Figure 3.1. This system consists of a weight–pulley arrangement that is coupled to a constant-temperature heat reservoir. The system is at equilibrium when an upward force acting on the weight exactly balances the downward force, *W*, of the

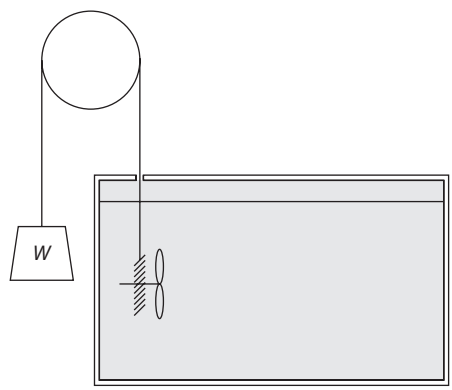

FIGURE 3.1 A weight–pulley–heat reservoir arrangement in which the work done by the falling weight is degraded to thermal energy, which appears in the heat reservoir.

weight. If the upward force is removed, the equilibrium is upset and the weight spontaneously falls, performing work, which is converted, by means of a suitable system of paddle wheels, into thermal energy, which enters the constant-temperature heat reservoir. Equilibrium is re-established when the upward force acting on the weight is replaced, and the net effect of this process is that mechanical energy is converted to thermal energy.

Lewis and Randall[2] considered the following three processes:

1. The heat reservoir in the weight–heat reservoir system is at the temperature T_2. The weight is allowed to fall, performing work, w, and the thermal energy produced, q, enters the heat reservoir.
2. The heat reservoir at the temperature T_2 is placed in thermal contact with another heat reservoir at a lower temperature T_1, and the same thermal energy, q, is allowed to be transferred from the reservoir at T_2 to the reservoir at T_1.
3. The heat reservoir in the weight–heat reservoir system is at the temperature T_1. The weight is allowed to fall, performing work, w, and the thermal energy produced, q, enters the reservoir.

Each of these processes is *spontaneous* and hence *irreversible*, and therefore, degradation of energy occurs in each of them. However, since process 3 is the sum of processes 1 and 2, the degradation of energy occurring in process 3 must be greater than the degradation occurring in each of the processes 1 and 2. Thus, it can be said that process 3 is *more irreversible* than either process 1 or process 2. An examination of the three processes indicates that both the amount of thermal energy transferred, q, and the temperatures between which this energy is transferred are important in defining a quantitative scale of irreversibility. In the case of comparison between process 1 and process 3, the quantity q/T_2 is smaller than the quantity q/T_1, which is in agreement with the conclusion that process 1 is less irreversible than process 3. The quantity q/T can thus be taken as a measure of the degree of irreversibility of the process, and the value of q/T is the increase in entropy occurring as a result of the process. Thus, when the weight–heat reservoir system undergoes a spontaneous process that causes the absorption of thermal energy q at the constant temperature T, the entropy produced by the system, $\Delta S'$, is given by

$$\Delta S' = \frac{q}{T} > 0 \tag{3.1}$$

This value is larger in the case of the lower-temperature reservoir. The increase in entropy caused by the process can be thus taken as a measure of the degree of irreversibility of the process.

[2] G. N. Lewis and M. Randall, *Thermodynamics*, revised by K. S. Pitzer and L. Brewer, 3rd ed., McGraw-Hill, New York, 1995, p. 78.

3.4 REVERSIBLE PROCESSES

Since the degree of *irreversibility* of a process is path dependent, it should be possible for the process to be conducted in such a manner that the degree of irreversibility is minimized. The ultimate of this minimization is a process in which the degree of irreversibility is zero and in which no degradation of energy occurs. This limit, which the behavior of real systems can be made to approach, is called a *reversible* process. If a process is reversible, then the concept of spontaneity is no longer applicable. Recall that spontaneity occurs as a result of the system moving, of its own accord (i.e., no external influences), from a nonequilibrium state to an equilibrium state. Thus, if the spontaneity is removed, it is apparent that, at all times *during* the process, the system is at equilibrium. A reversible process, then, is one during which the system is never away from equilibrium. A reversible process that takes the system from the state A to the state B is one in which the process path passes through a continuum of equilibrium states. Such a path is, of course, an idealization, but it is possible to conduct an actual process in such a manner that it is nearly reversible. Such an actual process (sometimes called a *quasi-static* process) is one which proceeds under the influence of an infinitesimally small driving force, such that, during the process, the system is never more than an infinitesimal amount from equilibrium. If, at any point along the path, the small external influence is removed, then the process ceases; if the direction of the small external influence is reversed, then the direction of the process is reversed.

Reversible and natural processes are illustrated in the following section.

3.5 ILLUSTRATION OF REVERSIBLE AND IRREVERSIBLE ISOTHERMAL PROCESSES

In this section, we will compare two processes: the *isothermal reversible* expansion of an ideal gas and the *free expansion* of an ideal gas.

3.5.1 The Reversible Isothermal Expansion of an Ideal Gas

Let us consider the reversible isothermal expansion of 1 mole of a monatomic ideal gas from the state (V_A, T) to the state (V_B, T), where $V_B > V_A$ (Figure 3.2). The gas is

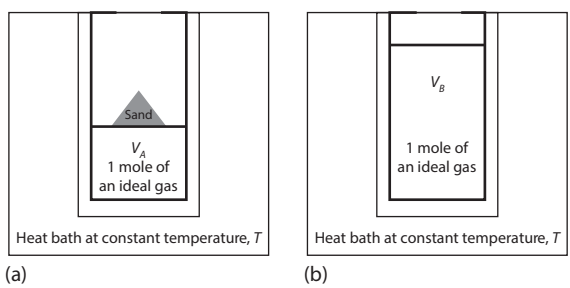

FIGURE 3.2 (a) One mole of a confined ideal gas being held at V_A by a mass of sand. The gas is in thermal equilibrium with the heat bath. (b) The mass of sand is removed one piece of sand at a time (reversibly) and the new volume of the gas is V_B. This is a reversible isothermal expansion process for the gas.

placed in thermal contact with a heat reservoir[3] at the temperature T, and by slowly reducing the weight on the piston by removing one grain of sand at a time, the pressure exerted by the gas is only infinitesimally greater than the instantaneous pressure exerted by the piston on the gas. The state of the gas thus lies, at all times, on a section at the constant temperature T of the V-P-T surface (Figures 1.1 and 1.3a), and hence, the gas passes through a continuum of equilibrium states in going from the state (V_A, T) to the state (V_B, T). Since the gas is never out of equilibrium, the process is reversible.

From the First Law,

$$\Delta U = q - w$$

The internal energy of an ideal gas depends only on its temperature. Hence, $\Delta U = 0$, and thus, $q = w$; that is, the work done by the expanding gas on the piston equals the thermal energy transferred from the constant-temperature heat reservoir into the gas.

We calculate the work done as

$$w_{\text{rev}} = \int_{V_A}^{V_B} P dV = \int_{V_A}^{V_B} \frac{RT dV}{V} = RT \ln \frac{V_B}{V_A}$$

Since $V_B > V_A$, w_{rev} is a positive quantity, in accordance with the fact that work is done *by* the gas. The transfer of thermal energy from the reservoir to the gas (at constant internal energy) causes a change in the entropy of the gas:

$$\Delta S_{\text{gas}} = S_B - S_A = \frac{q_{\text{rev}}}{T} = \frac{w_{\text{rev}}}{T} = R \ln \frac{V_B}{V_A}$$

which is also a positive quantity.

The change in the entropy of the reservoir is given by

$$\Delta S_{\text{heat reservoir}} = -\frac{q}{T} = -\Delta S_{\text{gas}} = R \ln \frac{V_A}{V_B} < 0$$

The total change in the entropy (gas plus heat reservoir) can be written as

$$\Delta S_{\text{total}} = \Delta S_{\text{gas}} + \Delta S_{\text{reservoir}} = 0 \tag{3.2}$$

[3] The pertinent feature of a constant temperature heat reservoir is that it experiences only heat effects and neither performs work nor has work performed on it. The *ice calorimeter*, which comprises a system of ice and water at 0°C and 1 atm pressure, is an example of a simple constant temperature heat reservoir. Thermal energy transferring into or out of this calorimeter at 0°C is measured as the change occurring in the ratio of the amount of ice to that of water present as a result of the thermal energy flow. Since the molar volume of ice is larger than that of water, the change in this ratio is measured as a change in the total volume of ice plus water in the calorimeter. Strictly speaking, if thermal energy flows out of the calorimeter, freezing some of the water, the volume of the system increases, and hence, the calorimeter does, in fact, perform the work of expansion against the atmospheric pressure. However, the ratio of the work done in expansion to the corresponding thermal energy leaving the

For the reversible isothermal expansion process of an ideal gas, the total change in entropy of the universe is zero: no entropy has been produced. The increase in entropy of the gas in enlarging its volume is exactly offset by the decrease in entropy of the surroundings in giving off heat.

3.5.2 The Free Expansion of an Ideal Gas

We now consider the free expansion (i.e., expansion against zero atmospheric pressure) of 1 mole of an ideal gas from V_A to V_B. We have seen in Chapter 2 that the free expansion of an ideal gas is also isothermal. Thus, the final state of the free expansion is the same as the state of the isothermal reversible expansion process (i.e., both states have the same V and T). In this case, however, no work is done by the gas against the piston, since the weight on the piston is rapidly removed. Thus, $\Delta U = 0$ and $w = 0$, which by the First Law means that $q = 0$ as well.

Since entropy is a state function, the change of entropy of the gas for the free expansion must be the same as that for the isothermal expansion.

$$\Delta S_{\text{gas}} = S_B - S_A = R \ln \frac{V_B}{V_A} > 0$$

Also, since no thermal energy leaves the heat reservoir, $\Delta S_{\text{reservoir}} = 0$. The total change in the entropy (gas plus heat reservoir) for the free expansion is

$$\Delta S_{\text{total}} = \Delta S_{\text{gas}} + \Delta S_{\text{reservoir}} = \Delta S_{\text{gas}} = R \ln \frac{V_B}{V_A} > 0 \tag{3.3}$$

In the case of free expansion, there is no decrease in entropy of the heat reservoir, since no thermal energy was absorbed by the ideal gas; it did no work. Thus, for the free expansion process, the entropy of the universe increases ($\Delta S_{\text{total}} > 0$). Note that the entropy of the gas increased without any heat entering into it. Thus, we see that entropy is a function of volume as well as temperature.

3.5.3 Summary of the Isothermal Reversible versus Irreversible Expansion of Ideal Gas

1. These two processes have the following in common:
   The temperature of the gas remains constant
   The internal energy of the gas remains constant
2. The processes differ in the following cases:
   In the reversible case,
   work is performed *by* the gas during its expansion
   the entropy of the universe (system plus surroundings) remains constant ($\Delta S_{\text{total}} = 0$)
   In the free expansion,
   no work is performed by the gas
   the entropy of the universe increases ($\Delta S_{\text{total}} > 0$).

3.6 FURTHER DIFFERENCES BETWEEN REVERSIBLE AND IRREVERSIBLE EXPANSIONS

We now look at the processes from the point of view of the thermal energy that was transferred from the heat reservoir to the gas and the work that was performed by the gas. For the reversible isothermal expansion case, $q_{rev} = w_{max}$. This process yields the maximum amount of work that can be performed by the gas during isothermal expansion. The reversible process also yields the most amount of thermal energy that can be transferred to the gas from the heat reservoir. The total change in entropy of the universe is zero for the reversible expansion.

For the case of the free expansion of the gas, we have seen that $w = q = 0$.

Overall, it can be seen that the work performed in the preceding two cases of the isothermal expansion of an ideal gas varies between 0 for free expansion (isothermal) and w_{max} for reversible isothermal expansion; that is,

$$0 \leq w \leq w_{max}$$

We also see that

$$0 \leq q \leq q_{rev}$$

This means that

$$0 \leq \Delta S_{total} \leq \frac{q_{rev}}{T}$$

$\Delta S_{total} = 0$ when the process is reversible. $\Delta S_{total} > 0$ when the process is irreversible. The maximum value of ΔS_{total} occurs for the irreversible free expansion case.

It is important to note that the difference in entropy between the final and initial states of an ideal gas is independent of whether the process is conducted reversibly or irreversibly. In going from state *A* to state *B*,

$$\Delta S = S_B - S_A = \frac{q}{T} + \Delta S_{irr} \tag{3.4a}$$

$$= \frac{q_{rev}}{T} \tag{3.4b}$$

Equation 3.4b indicates that, since the change in entropy can be determined only by the measurement of thermal energy transferred reversibly at the temperature *T*, then entropy changes can be measured *only for reversible processes*, in which case the measured thermal energy transferred is q_{rev} and $\Delta S_{irr} = 0$.

3.7 COMPRESSION OF IDEAL GAS

In this section, we compare the reversible and irreversible compressions of an ideal gas.

3.7.1 Reversible Compression of Ideal Gas

Consider the reversible *isothermal* compression of 1 mole of an ideal gas from the state (V_B, T) to the state (V_A, T) (Figure 3.2). The gas is placed in thermal contact with a heat reservoir at the temperature T, and, by adding one grain of sand at a time to the top of the piston, the gas is compressed slowly enough that, at all times during its compression, the pressure exerted on the gas is only infinitesimally greater than the instantaneous pressure of the gas, P_{inst}, where $P_{\text{inst}} = RT/V_{\text{inst}}$. The state of the gas thus lies, at all times, on a section at the constant temperature T of the *V-P-T* surface (Figures 1.1 and 1.3a), and hence, the gas passes through a continuum of equilibrium states in going from the state (V_B, T) to the state (V_A, T). Since the gas is never out of equilibrium, the process is reversible and no degradation of energy occurs. Entropy is not *created* during this process. Entropy is transferred from the gas to the heat reservoir, where it is measured as the thermal energy entering the reservoir divided by the temperature T.

Since the compression is conducted isothermally, $\Delta U = 0$; thus, the work done on the gas is equal to the thermal energy withdrawn from the gas; that is,

$$w_{\max} = q_{\text{rev}}$$

where

$$w_{\max} = \int_{V_B}^{V_A} P dV = \int_{V_B}^{V_A} \frac{RT dV}{V} = RT \ln \frac{V_A}{V_B}$$

Since the volume of the gas has decreased ($V_B > V_A$), $w_{\max}$ is a negative quantity, in accordance with the fact that work is done *on* the gas. The transfer of thermal energy from the gas to the reservoir causes a change in the entropy of the gas:

$$\Delta S_{\text{gas}} = \frac{q_{\text{rev}}}{T} = \frac{w_{\max}}{T} = R \ln \frac{V_A}{V_B}$$

which is also a negative quantity.

Since there is no change in the total entropy during the reversible compression, the change in the entropy of the reservoir is given by

$$\Delta S_{\text{heat reservoir}} = -\Delta S_{\text{gas}} = R \ln \frac{V_B}{V_A} > 0$$

3.8 ILLUSTRATION OF REVERSIBLE AND IRREVERSIBLE ADIABATIC EXPANSION PROCESSES

In this section, we will compare the *adiabatic reversible expansion* of an ideal gas and the *adiabatic irreversible expansion* of an ideal gas.

3.8.1 Reversible Adiabatic Expansion

Consider the reversible adiabatic expansion of 1 mole of an ideal gas from the state (P_A, T_A) to the state (P_B, T_B), where $P_B < P_A$. For the process to be reversible, it must be conducted slowly enough that, at all times, the state of the gas lies on its *V-P-T* surface. As has been shown in Chapter 2, this condition, together with the condition that $q = 0$ (an adiabatic process), dictates that the process path across the *V-P-T* surface follows the curve $PV^\gamma = \text{constant}$. Since the process is reversible, no degradation of energy occurs, and since the process is adiabatic, no thermal energy transfer occurs. The change in the entropy of the gas is therefore zero. Consequently, all states of an ideal gas lying on a $PV^\gamma = \text{constant}$ curve are states of equal entropy (cf. all states of an ideal gas lying on a $PV = RT$ curve are states of equal internal energy). A reversible adiabatic process is thus an *isentropic* process. During a reversible adiabatic expansion, the work done by the gas, $w_{\max}$, equals the decrease in the internal energy of the gas; that is,

$$\Delta U = -w_{\max}$$

We can write the following for the reversible process:

$$w = \int_{V_A}^{V_B} P dV \quad \text{and} \quad PV^\gamma = \text{constant (call it } K)$$

$$= K \int_{V_A}^{V_B} V^{-\gamma} dV = \left[\frac{KV^{-\gamma+1}}{(-\gamma+1)} \right]_{V_A}^{V_B} = \left[\frac{PV}{(-\gamma+1)} \right]_{P_A V_A}^{P_B V_B} = \frac{R(T_B - T_A)}{1-\gamma}$$

$$= \frac{3}{2} R(T_A - T_B)$$

Since the work done by the gas is positive, $T_B < T_A$; that is, the gas cools.

The change in the internal energy can be calculated as

$$\Delta U = \int_{T_A}^{T_B} c_v dT = \frac{3}{2} R(T_B - T_A) = -w$$

which is negative. The internal energy of the gas decreased by the amount of work that the gas performed.

3.8.2 The Adiabatic Irreversible Expansion of an Ideal Gas

3.8.2.1 Adiabatic Free Expansion

Now, consider the irreversible free expansion under adiabatic conditions of 1 mole of an ideal gas from the state (P_A, T_A) to the state (P_B, T_B), where $P_B < P_A$. The pressure exerted on the gas is suddenly decreased from P_A to $P_B = 0$, and the state of the gas moves off the *V-P-T* surface. Being out of equilibrium, the expansion occurs irreversibly. The process is adiabatic, $q = 0$, and since no work is performed, $w = 0$. By

the First Law, ΔU is zero as well and since the gas is ideal, there is no change in the temperature. Thus, the free expansion of an ideal gas under adiabatic conditions is *isothermal* and the entropy change can be calculated from the isothermal reversible expansion of an ideal gas derived in Section 3.5.1 to be $R \ln \frac{V_{\text{final}}}{V_{\text{initial}}}$. There is no change in the entropy of the surroundings ($q = 0$), so the total change in the entropy is positive.

3.8.2.2 Adiabatic Irreversible Expansion but Not Free Expansion

If instead of free expansion, the pressure of the gas decreased at a finite rate (not quasi statically) from P_A to P_B; the gas would perform some work during its expansion, but the work performed by the gas would be less than when the work was performed reversibly. The temperature of the gas would decrease, as in the reversible case, since some of the internal energy was converted to work. However, the decrease in temperature would not be as much as during reversible free expansion. Also, the entropy of the gas would increase, but not as much as when it freely expanded adiabatically because its temperature decreased.

3.8.3 Summary of the Adiabatic Reversible versus Irreversible Expansion of Ideal Gas

1. These processes have the following in common:
   - No heat leaves or enters the gas
   - The entropy change of the surroundings is zero
2. The processes differ in the following ways:
   In the reversible case,
   - The temperature of the gas decreases
   - The internal energy of the gas decreases
   - Work is performed *by* the gas during its expansion
   - The entropy of the gas does not change
   - The entropy of the surroundings does not change
   - The entropy of the universe remains constant ($\Delta S'_{\text{total}} = 0$).

   In the free expansion,
   - The temperature of the gas remains the same
   - The internal energy of the gas remains constant
   - No work is performed by the gas
   - The entropy of the gas increases
   - The entropy of the surroundings does not change
   - The entropy of the universe increases ($\Delta S'_{\text{total}} > 0$).

   In the general irreversible case (that is not free expansion),
   - The temperature of the gas decreases, but less than for reversible adiabatic expansion
   - Some work is performed but less than that of reversible adiabatic expansion
   - The internal energy of the gas decreases less than that in reversible adiabatic expansion
   - The entropy of the gas increases, but less than during free adiabatic expansion

The entropy of the surroundings does not change
The entropy of the universe increases ($\Delta S'_{\text{total}} > 0$).

3.9 SUMMARY STATEMENTS

The following points have emerged from the discussion so far:

1. Entropy is an extensive thermodynamic state variable (function).
2. Entropy is not created when a system undergoes a reversible process; entropy is transferred from one part of the system/surroundings to another part.
3. The total entropy of the universe increases when an irreversible process occurs.
4. For all processes, we can write $\Delta S'_{\text{system}} = q/T + \Delta S'_{\text{irr}}$ and $q \leq q_{\text{rev}}$.
5. For all processes, the entropy of the universe increases or stays the same. The total entropy of the universe never decreases.

3.10 THE PROPERTIES OF HEAT ENGINES

Traditionally, the concept of entropy as a thermodynamic state function is introduced by considering the behaviors and properties of heat engines. The author believes it is still a good way to learn about entropy and the conversion of one form of energy to another.

A *heat engine* is a device that converts thermal energy (heat) into work. It is interesting to note that steam engines were in operation for a considerable number of years before the reverse process—that is, the conversion of work into thermal energy—was investigated by Rumford in 1798. In the operation of a heat engine, *some* of the energy that has been transferred from a *high-temperature heat reservoir* is converted into work, with the remainder of the energy being transferred to a *low-temperature heat reservoir.* The process is shown schematically in Figure 3.3. Treating the engine as the system, the First Law gives

$$\Delta U' = q_2 - q_1 - w$$

Since an engine must return to its original state before its next cycle. We write:

$$\Delta U' = 0 \quad \text{and} \quad q_2 - q_1 = w$$

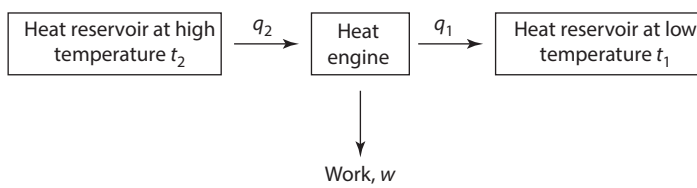

FIGURE 3.3 Schematic representation of the working of a heat engine, showing that the thermal energy q_2 is partially converted into work,

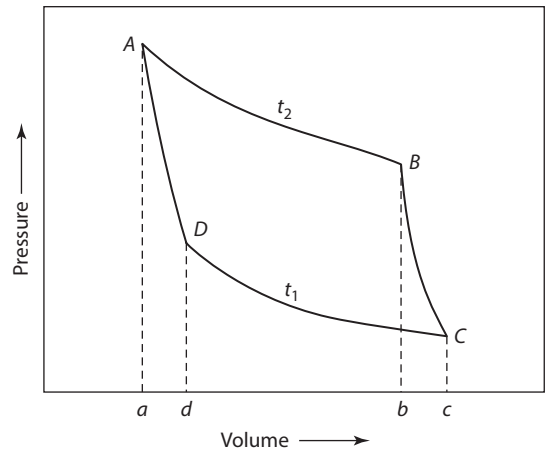

FIGURE 3.4 A pressure vs. volume plot of the four processes involved in a Carnot cycle.

This simple equation tells us that for this process, all of the heat is not transformed into work. Can we do better?

Consider the *steam engine*, which is a typical example of a heat engine. In a steam engine, *superheated steam* is passed from the boiler (the high-temperature heat reservoir) to the cylinders, where the steam performs work by expanding against the pistons (the engine). As a result of this expansion, the temperature of the steam decreases, and at the end of the piston stroke, the spent steam is exhausted to the atmosphere (the low-temperature heat reservoir). A flywheel returns the piston to its original position, thus completing the cycle and preparing for the next working stroke.

The *efficiency* of a heat engine is given by

$$\text{Efficiency} = \eta = \frac{\text{Work obtained}}{\text{Energy input}} = \frac{w}{q_2}$$

The factors governing the efficiency of this process were explained in 1824 by Carnot (Nicolas Léonard Sadi Carnot, 1796–1832), who considered the cyclic process illustrated in Figure 3.4.

In the step $A \rightarrow B$, thermal energy q_2 is isothermally and reversibly transferred from a heat reservoir at the temperature t_2 to a thermodynamic substance, as a result of which the thermodynamic substance isothermally and reversibly expands from the state *A* to the state *B* and performs work w_1 equal to the area *ABba*.

In the step $B \rightarrow C$, the thermodynamic substance undergoes a reversible adiabatic expansion from the state *B* to the state *C*, as a result of which its temperature decreases to t_1, and it performs work equal to the area *BCcb.*

In the step $C \rightarrow D$, energy q_1 is isothermally and reversibly transferred from the thermodynamic substance to a heat reservoir at the temperature t_1. Work w_3, equal to the area *DCcd*, is done on the substance.

In the step $D \rightarrow A$, the substance is reversibly and adiabatically compressed, during which its temperature increases from t_1 to t_2, and work w_4, equal to the area *ADda*, is done on the substance.

During this *cyclic process*, which has returned the thermodynamic substance to its initial state, the substance has performed the work $w = w_1 + w_2 - w_3 - w_4$ (equal to the area *ABCD*) and has absorbed thermal energy $q = q_2 - q_1$. For a cyclic process, $\Delta U = 0$, and thus, from the First Law,

$$\sum q_i = \sum w_i$$

Thus,

$$q_2 - q_1 = \sum w_i \equiv w$$

The efficiency of this cyclic process (which is known as a *Carnot cycle*) is given by

$$\text{Efficiency} = \eta = \frac{w}{q_2} = \frac{q_2 - q_1}{q_2} = 1 - \frac{q_1}{q_2}$$

This equation shows that even in this idealized Carnot cycle (all processes assumed to be reversible), the efficiency is less than unity for finite values of q_1, *the dissipated energy.*

The consequence of all of the steps in the cyclic process having been conducted reversibly is illustrated in the following discussion. Consider a second engine working with a different substance, again between the temperatures t_1 and t_2, and let this second engine be *more* efficient than the first one. This greater efficiency could be obtained in either of two ways:

1. The same amount of thermal energy, q_2, is withdrawn from the heat reservoir at t_2, and *more work*, w', is obtained from it than was obtained from the first engine; that is, $w' > w$. Thus, the second engine rejects less thermal energy, q_1', to the cold reservoir at t_1 than does the first engine; that is, $q_1' < q_1$.
2. The same work is obtained by withdrawing less thermal energy, q_2', from the heat reservoir at t_2; that is, $q_2' < q_2$. Thus, less thermal energy, q_1', is rejected into the heat reservoir at t_1; that is, $q_1' < q_1$.

Consider now that the second engine is run in the forward direction, and the first engine is run in the reverse direction; that is, it acts as a *heat pump*. Then, from case (1) above, for the second engine run in the forward direction, $w' = q_2 - q_1'$. For the first engine run in the reverse direction, $-w = -q_2 + q_1$. The sum of the two processes is

$$(w' - w) = (q_1 - q_1')$$

that is, an amount of work $(w' - w)$ has been obtained from a quantity of thermal energy $(q_1 - q_1')$ without any other change occurring in the system or its surroundings.

Although this conclusion does not contravene the First Law of Thermodynamics, it is contrary to all human experience. Such a process has been termed a *perpetual motion of the second kind*; that is, heat is converted to work without leaving a change in any other body. (Perpetual motion of the first kind is the creation of energy from nothing.)

From case (2) above, for the second engine run in the forward direction, $w = q_2' - q_1'$. For the first engine run in the reverse direction, $-w = -q_2 + q_1$. The sum of the two processes is

$$q_2' - q_2 = q_1' - q_1 = q$$

that is, an amount of thermal energy at the lower temperature has been transferred to a higher temperature without any other change occurring. This corresponds to the *spontaneous transfer of thermal energy* up a temperature gradient. This is even more contrary to human experience than is the perpetual motion of the second kind.

The preceding discussion gives rise to the following two formulations of the Second Law of Thermodynamics:

1. It is impossible, by means of a cyclic process, to transfer thermal energy from a hot reservoir and convert it to work without, in the same process, transferring thermal energy to a cold reservoir. This is known as the *principle of Kelvin and Planck* (Lord Kelvin, aka William Thomson, 1824–1907, and Max Karl Ernst Ludwig Planck, 1858–1947).
2. It is impossible to transfer thermal energy from a cold to a hot reservoir without, in the same process, converting a certain amount of work to thermal energy. This is the *principle of Clausius* (Rudolf Julius Emanuel Clausius, 1822–1888).

These two formulations of the Second Law of Thermodynamics are equivalent to each other: that is:

i. if one of them is shown to be true, the other one *must* be true
   and
ii. if one of them can be shown to be false, the other one *must* also be false.

After we discuss the *thermodynamic temperature* in the next section, we will be able to relate the Second Law of Thermodynamics more quantitatively and express it in terms of the Entropy function discussed in the earlier sections of this chapter.

3.11 THE THERMODYNAMIC TEMPERATURE SCALE

The foregoing discussion suggests that all reversible Carnot cycles operating between the same upper and lower temperatures must have the same efficiency—namely, the maximum possible. This maximum efficiency is independent of the working substance and is a function only of the working temperatures t_1 and t_2. Thus,

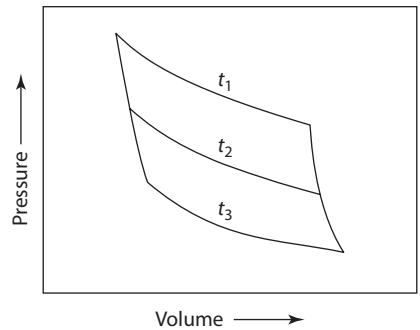

FIGURE 3.5 Carnot cycles operating between t_1 and t_2, t_1 and t_3, and t_2 and t_3.

$$\text{Efficiency} = \eta = \frac{q_2 - q_1}{q_2} = f'(t_1, t_2) = 1 - \frac{q_1}{q_2}$$

or

$$\frac{q_1}{q_2} = f(t_1, t_2)$$

Consider the Carnot cycles shown in Figure 3.5. The two cycles operating between t_1 and t_2, and between t_2 and t_3, are equivalent to a single cycle operating between t_1 and t_3. Thus,

$$\frac{q_1}{q_2} = f(t_1, t_2)$$

$$\frac{q_2}{q_3} = f(t_2, t_3)$$

and

$$\frac{q_1}{q_3} = f(t_1, t_3)$$

So,

$$\left(\frac{q_1}{q_3}\right) \times \left(\frac{q_3}{q_2}\right) = \frac{f(t_1, t_3)}{f(t_2, t_3)} = \frac{q_1}{q_2} = f(t_1, t_2)$$

Since $f(t_1, t_2)$ is independent of t_3, then $f(t_1, t_3)$ and $f(t_2, t_3)$ must be of the form

$$f(t_1, t_3) = \frac{F(t_1)}{F(t_3)}$$

and

$$f(t_2,t_3)=\frac{F(t_2)}{F(t_3)}$$

that is, the efficiency function $f(t_1, t_2)$ is the quotient of a function of t_1 alone and t_2 alone. Thus,

$$\frac{q_1}{q_2}=\frac{F(t_1)}{F(t_2)}$$

Kelvin took these functions to have the simplest possible form—namely, T_1 and T_2. Thus,

$$\frac{q_1}{q_2}=\frac{T_1}{T_2}$$

in which case the efficiency of a Carnot cycle is

$$\text{Efficiency}=\frac{q_2-q_1}{q_2}=\frac{T_2-T_1}{T_2}=1-\frac{T_1}{T_2} \tag{3.5}$$

This defines an *absolute thermodynamic scale of temperature* which is independent of the working substance. It is seen that the zero of this temperature scale is that temperature of the cold reservoir which makes the Carnot cycle 100% efficient.

The absolute thermodynamic temperature scale (or Kelvin scale) is identical to the ideal gas temperature scale discussed in Chapter 1. This can be demonstrated by considering 1 mole of ideal gas to be the working substance in a Carnot cycle.

Referring to Figure 3.4,

State A to state B. Reversible isothermal expansion at t_2:

$$\Delta U=0$$

and from Equation 2.10

$$q_2=w_1=Rt_2\ln\left(\frac{V_B}{V_A}\right)$$

State B to state C. Reversible adiabatic expansion:

$$q=0$$

and from Equation 2.6a,

$$w_2=-\Delta U=-\int_{t_2}^{t_1}c_v dT$$

State C to state D. Reversible isothermal compression at t_1:

$$q_1 = w_3 = Rt_1 \ln\left(\frac{V_D}{V_C}\right)$$

State D to state A. Reversible adiabatic compression:

$$q = 0$$

$$w_4 = -\int_{t_1}^{t_2} c_v dT$$

The total work done on the gas $= w = w_1 + w_2 + w_3 + w_4$

$$= Rt_2 \ln\left(\frac{V_B}{V_A}\right) - \int_{t_2}^{t_1} c_v dT + Rt_1 \ln\left(\frac{V_D}{V_C}\right) - \int_{t_1}^{t_2} c_v dT$$

The thermal energy transferred from the hot reservoir $= q_2 = Rt_2 \ln\left(\frac{V_B}{V_A}\right)$.

It can be shown (see Problem 3.7) that

$$\frac{V_B}{V_A} = \frac{V_C}{V_D}$$

and thus,

$$w = R(t_2 - t_1)\ln\left(\frac{V_B}{V_A}\right)$$

Finally,

$$\text{Efficiency} = \eta = \frac{w}{q_2} = \frac{(t_2 - t_1)}{t_2} = 1 - \frac{T_1}{T_2}$$

which is equivalent to Equation 3.5.

We conclude that the absolute thermodynamic temperature scale is the same as the ideal gas temperature scale.

3.12 THE SECOND LAW OF THERMODYNAMICS

The equation

$$\frac{q_2 - q_1}{q_2} = \frac{T_2 - T_1}{T_2}$$

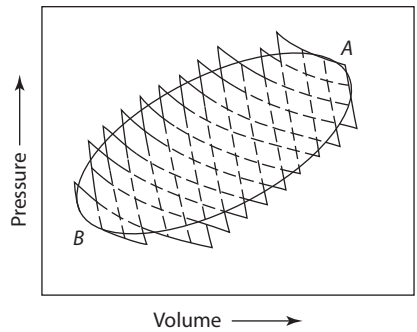

FIGURE 3.6 A cyclic process broken down into a large number of Carnot cycles.

can be written as

$$\frac{q_2}{T_2} - \frac{q_1}{T_1} = 0 \tag{3.6}$$

Any cyclic process can be broken down into a number of Carnot cycles, as shown in Figure 3.6. In going around the cycle *ABA* in a clockwise direction, the work done by the system equals the area enclosed by the path loop. This loop can be roughly approximated by a number of Carnot cycles as shown, and for the zigzag paths of these cycles, from Equation 3.6,

$$\sum \frac{q_i}{T_i} = 0$$

where the thermal energy being transferred into the system is positive and the thermal energy being transferred out of the system is negative. The zigzag path of the Carnot cycles can be made to coincide with loop *ABA* by making the Carnot cycles smaller and smaller, and in the limit of coincidence, the summation can be replaced by a cyclic integral; that is,

$$\oint \left(\frac{\delta q_i}{T} \right)_{\text{rev}} = 0$$

The vanishing of the cyclic integral indicates that the integral is an exact differential of some function of state of the system. This function is the entropy, *S*, and for the case of a reversible process, we can write

$$dS' = \frac{\delta q}{T} \tag{3.7}$$

where δq is the infinitesimal thermal energy transferred reversibly into (or out of) the system at temperature *T*. Thus, if thermal energy is transferred into the system, the entropy of the system increases.

For the loop *ABA*,

$$\oint dS' = 0 = \int_A^B dS' + \int_B^A dS' = (S_B - S_A) + (S_A - S_B) = 0$$

It is to be emphasized that q in Equation 3.7 is the reversible thermal energy increment, and thus, Equation 3.7 should be written properly as

$$dS' = \frac{\delta q_{\text{rev}}}{T} \tag{3.8}$$

Recall that this expression was derived from the consideration of Carnot cycles, in which all operations are performed reversibly.

The application of Equation 3.6 to a reversibly operated heat engine, in which q_2 is withdrawn from a constant-temperature source at T_2, work w is performed, and q_1 is rejected into a constant-temperature heat sink at T_1, shows that the decrease in the entropy of the high-temperature source, q_2/T_2, equals the increase in the entropy of the heat sink, q_1/T_1. That is, $\Delta S'_{\text{total}} = 0$, which is a consequence of the fact that the process is conducted reversibly.

The Second Law of Thermodynamics can thus be stated as follows:

1. The incremental change in entropy dS' of a system into which (or out of which) thermal energy has been reversibly added (or expelled) is given as $dS' = dq_{\text{rev}}/T$, and the entropy function S' is a *state function* of the system.
2. The entropy of a system in an adiabatic enclosure can never decrease.
   - The entropy increases during an irreversible process.
   - The entropy remains constant during a reversible process.
   - The entropy remains constant if the system was initially in equilibrium.

From (2), it is seen that, for an infinitesimal change of state of an adiabatically contained system,

$$\sum dS'_i \geq 0 \tag{3.9}$$

that is, the sum of the incremental changes in entropy of all i parts of the system which are in thermal contact with each other is zero if the infinitesimal change of state is reversible and is greater than zero if the infinitesimal change of state is irreversible.

Equation 3.9 can be converted to an equality by writing

$$\sum_i dS'_i = dS'_{\text{irr}} \tag{3.10}$$

where dS'_{irr} is the total entropy created in the given incremental irreversible process.

3.13 MAXIMUM WORK

For a change of state from A to B, the First Law gives

$$U'_B - U'_A = q - w$$

In Section 3.1, three questions were raised concerning this law. The third question was,

Is there a definite limit to the amount of work which the system can do during its change of state?

As we indicated in Section 3.1, the First Law gives no indication of the allowed magnitudes of q and w in the given process. Its only restriction is that the energy of the universe must remain constant. We have seen in the preceding discussion that, although the values of q and w can vary depending on the degree of irreversibility of the path taken between the state A and B, the Second Law sets a definite *limit* on the maximum amount of work which can be obtained from the system during a given change of state and, hence, sets a limit on the quantity of thermal energy which the system may absorb.

For an infinitesimal change of state, Equation 3.4a can be written as

$$dS'_{\text{system}} = \frac{\delta q}{T} + dS'_{\text{irr}}$$

and, from the First Law,

$$\delta q = dU'_{\text{system}} + \delta w$$

Thus,

$$dS'_{\text{system}} = \frac{dU'_{\text{system}} + \delta w}{T} + dS'_{\text{irr}}$$

or

$$\delta w = TdS'_{\text{system}} - dU'_{\text{system}} - TdS'_{\text{irr}}$$

and finally, since $TdS'_{\text{irr}} > 0$

$$\delta w \le TdS'_{\text{system}} - dU'_{\text{system}} \tag{3.11}$$

If the temperature remains constant throughout the process (and equal to the temperature of the reservoir supplying heat to the system), then the integration of Equation 3.11 from state A to state B gives

$$w \le T\left(S'_B - S'_A\right) - \left(U'_B - U'_A\right)$$

and since U and S are functions of state, then w cannot be greater than a certain amount, w_{max}, the work which is obtained from the system when the process is conducted reversibly; that is,

$$w_{max} = T\left(S'_B - S'_A\right) - \left(U'_B - U'_A\right)$$

This work, w_{max}, corresponds to the absorption of the maximum heat, q_{rev}, and is the most work that can be performed during the change of state.

Since entropy is a state function, then, in undergoing any specific change of state from A to B,

The change in the entropy of the system is the same whether the process is conducted reversibly or irreversibly.

The preceding discussion indicates that *it is the* heat effect *which is different* in the two cases; that is, if the process involves the absorption of thermal energy and is conducted reversibly, then the thermal energy absorbed, q_{rev}, is greater than the thermal energy which would have been absorbed if the process had been conducted irreversibly. As has been seen, when 1 mole of an ideal gas is isothermally and reversibly expanded from state A to state B, energy q, where

$$q = RT \ln \frac{V_B}{V_A}$$

is reversibly transferred from the heat reservoir to the gas, and the increase in the entropy of the gas, $S_B - S_A = R \ln V_B / V_A$. The entropy of the thermal reservoir decreases by an equal amount, and therefore, *entropy is not created*; that is, $\Delta S_{irr} = 0$. However, if the mole of gas is allowed to expand freely from P_A to P_B (as in Joule's experiment discussed in Section 2.6), then, since the gas performs no work, no thermal energy is transferred from the reservoir to the gas, and there is no change in the entropy of the reservoir. Since entropy is a state function, the value of $S_B - S_A$ is independent of the process path, and hence, the entropy created, ΔS_{irr}, equals $S_B - S_A$, which equals $R \ln V_B / V_A$. This entropy is created as a result of the degradation of the work that would have been performed by the gas had the expansion not been carried out against zero pressure. For the free expansion, this *degraded work* equals w_{max} as well as q_{rev}. That is, all of the potential work of expansion was lost!

The free expansion therefore represents the limit of *complete irreversibility*, during which all of the *potential* work is degraded because of the increase in volume of the gas. The degraded potential work in the gas accounts for the increase in the entropy of the gas. For the isothermal expansion of 1 mole of ideal gas from the state A to the state B, the value of ΔS_{irr} is

$$0 \le \Delta S_{irr} \le R \ln \frac{V_B}{V_A}$$

$\Delta S_{irr} = 0$ for a reversible isothermal expansion and $\Delta S_{irr} = R \ln V_B / V_A$ for a free expansion. The value of ΔS_{irr} is thus shown to depend on the degree of irreversibility of the process, and as discussed in Section 3.3, it is a measure of the degree of irreversibility of the process.

3.14 ENTROPY AND THE CRITERION FOR EQUILIBRIUM

At the beginning of this chapter, it was stated that a system, left to itself (i.e., no interactions with the surroundings, an isolated system), would either remain in the state in which it happened to be or would *spontaneously* change (that is, without any outside influence) to some other state. If the system is initially at equilibrium, then it will remain at equilibrium, and if it is not initially in equilibrium, it will change spontaneously toward its equilibrium state. This *spontaneous* process is, by definition, irreversible, and the movement of the system from its initial nonequilibrium state to its final equilibrium state is accompanied by an increase in the entropy of the *system*. The attainment of the equilibrium state coincides with the entropy reaching a *maximum value*, and hence, for such systems, entropy can be used as a *criterion* for determining the equilibrium state.

In an *isolated* system of constant internal energy, U, and constant volume, V, equilibrium is attained when the entropy of the system is at maximum, consistent with the fixed values of U and V. Consider the chemical reaction

$$A + B = C + D$$

occurring in an adiabatic enclosure at constant volume. Starting with A and B, the reaction will proceed from left to right as long as the entropy of the system is thereby increased; or, conversely, starting with C and D, the reaction will proceed from right to left, again provided that the entropy of the system is thereby increased. Figure 3.7 shows a possible variation of entropy with the extent of reaction. It is seen that a point is reached along the reaction coordinate at which the entropy of the system has its maximum value. This is the equilibrium state of the system, since further reaction in either direction would decrease the entropy and, hence, will not occur spontaneously. This concept will be utilized when we discuss the reactions of gases in Chapter 11.

The entropy is only defined when the system is at equilibrium, so only the maximum point on the curve is an equilibrium state.

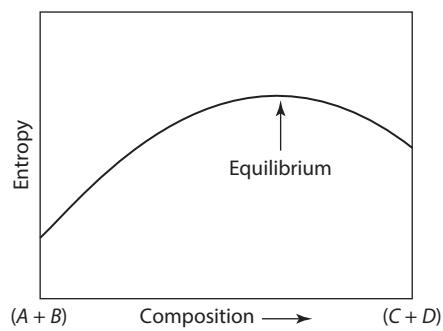

FIGURE 3.7 Schematic representation of the entropy of a closed system containing $A+B+C+D$ as a function of the extent of the reaction $A+B=C+D$ at constant internal energy and volume.

3.15 THE COMBINED STATEMENT OF THE FIRST AND SECOND LAWS OF THERMODYNAMICS

For an incremental change in the state of a closed simple system, the First Law of Thermodynamics gives

$$dU' = \delta q - \delta w$$

and, if the process occurs reversibly, the Second Law of Thermodynamics gives

$$dS' = \frac{\delta q}{T} \quad \text{or} \quad \delta q = TdS'$$

For a simple system,

$$\delta w = PdV'$$

A combination of the two laws gives the equation

$$dU' = TdS' - PdV' \tag{3.12}$$

Restrictions on the application of Equation 3.12 are

1. That the system is closed—that is, does not exchange matter with its surroundings during the process
2. That work due to change in volume is the *only form* of work performed by the system

Equation 3.12 relates the dependent variable of the system, U, to the independent variables, S and V; that is,

$$U' = U'(S', V')$$

The total differential of U' is written as

$$dU' = \left(\frac{\partial U'}{\partial S'}\right)_V dS' + \left(\frac{\partial U'}{\partial V'}\right)_S dV' \tag{3.13}$$

A comparison of Equations 3.12 and 3.13 shows that

$$\text{Temperature} = T = \left(\frac{\partial U'}{\partial S'}\right)_V$$

$$\text{Pressure} = P = -\left(\frac{\partial U'}{\partial V'}\right)_S$$

The particularly simple form of Equation 3.12 stems from the fact that, in considering variations in U as the dependent variable, the "natural" choice of independent

variables is S and V. The consideration of S as the dependent variable and U and V as the independent variables—that is,

$$S' = S'(U', V')$$

gives

$$dS' = \left(\frac{\partial S'}{\partial U'}\right)_V dU' + \left(\frac{\partial S'}{\partial V'}\right)_U dV' \tag{3.14}$$

Rearranging Equation 3.12 as

$$dS' = \frac{dU'}{T} + \frac{PdV'}{T}$$

and comparing it with Equation 3.14 shows that

$$\left(\frac{\partial S'}{\partial U'}\right)_V = \frac{1}{T} \quad \text{and} \quad \left(\frac{\partial S'}{\partial V'}\right)_U = \frac{P}{T} \tag{3.15}$$

From this equation, it can be seen that increasing the internal energy of the system at constant volume increases its entropy, since $1/T > 0$ (Figure 3.8). The curvature of the S versus U plot is negative.

$$\left(\frac{\partial^2 S'}{\partial U'^2}\right)_V = -\frac{1}{T^2}\frac{\partial T}{\partial U'} < 0$$

Also, since $P/T > 0$, increasing the volume increases the entropy of a system at constant U. The plot of S versus V (at constant U) is similar to the one of S versus U: S increases with V and the plot has negative curvature (if $\alpha_P > 0$. See Problem 3.13).

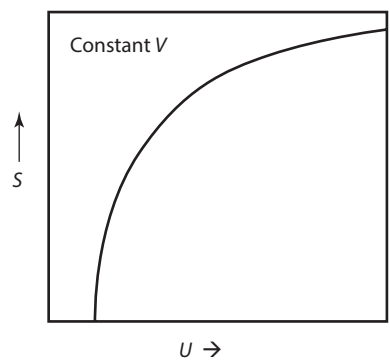

FIGURE 3.8 Plot of entropy vs. internal energy. Note that as U approaches its minimum value, S also approaches its minimum value.

It can also be seen that as *S (and hence T)* approaches zero, *U* approaches its minimum value. (more on this in Chapter 6, when the Third Law of Thermodynamics is discussed).

There is no need to have a δq transfer of energy to have entropy increase! This type of entropy is related to the increase in the *space the system occupies*. We will call this *configurational entropy* to distinguish it from the so-called thermal entropy.

The further development of thermodynamics is a consequence of the fact that *S* and *V* (or *S* and *P*) are an *inconvenient* pair of independent variables. In considering a real system, considerable difficulty would be encountered in arranging the state of the system such that, simultaneously, it has the required entropy and occupies the required volume. It would be much better to have temperature and pressure or temperature and volume be the two independent variables. In Chapter 5, we will introduce other thermodynamic state functions that will be of help to our study of thermodynamics.

In the next chapter, we present an atomistic interpretation of entropy and introduce basic concepts of statistical thermodynamics.

3.16 SUMMARY

1. The process paths taken by a system undergoing a change of state can be classified into two types: *reversible* and *irreversible*.
   - When the change in the state of the system occurs as the result of the application of a *finite driving force*, the process proceeds irreversibly, and the degree of irreversibility of the process increases with the increasing magnitude of the driving force.
   - For a process to occur reversibly, the driving force must be infinitesimal, and thus, a reversible process proceeds at an infinitesimal rate. The system is imagined to move through a continuum of equilibrium states during a reversible process.
2. When a system undergoes a change of state, during which it performs work and absorbs thermal energy, the magnitudes of the quantities w and q are maxima ($w_{\max}$ and q_{rev}), respectively, when the change of state occurs reversibly. For an irreversible path between the two states, less work is performed by the system, and correspondingly less thermal energy is absorbed.
3. There exists a state function called entropy, *S*, which can be written as

$$dS' = \frac{\delta q_{\text{rev}}}{T}$$

when δq_{rev} enters (or leaves) the system. The difference between the entropy in state *B* and that in state *A* is thus

$$\Delta S' = S'_B - S'_A = \int_A^B \frac{\delta q_{\text{rev}}}{T}$$

4. If, in moving between the two states, the temperature of the system remains constant, the change in the entropy of the system is $\Delta S' = q_{rev}/T$ where q_{rev} is the thermal energy absorbed or given off by the system in moving *reversibly* between the two states.
5. If q_{rev} is provided by a constant-temperature heat reservoir at the temperature T, the entropy of the reservoir decreases by the amount q_{rev} / T as a result of the system moving from A to B. The entropy of the combined system plus heat reservoir is thus unchanged as a result of the *reversible process*; entropy has simply been transferred from the heat reservoir to the system.
6. If the change in the state of a system from A to B were carried out *irreversibly*, then less thermal energy, q ($q < q_{rev}$), would be withdrawn from the heat reservoir by the system. Thus, the magnitude of the decrease in the entropy of the reservoir would be smaller (equal to q / T). However, since entropy is a state function, the change in entropy of the gas, $S'_B - S'_A$, is independent of the process path, and thus, $\Delta S'_{system} + \Delta S'_{heat\ reservoir} > 0$. Entropy has been created as a result of the occurrence of an irreversible process. The entropy created is termed $\Delta S'_{irr}$.
7. In the general case, $S'_B - S'_A = q / T + \Delta S'_{irr}$, and as the degree of irreversibility increases, the thermal energy, q, withdrawn from the heat reservoir decreases and the magnitude of $\Delta S'_{irr}$ increases.
8. The increase in entropy, due to the occurrence of an irreversible process, arises from the degradation of the energy of the system, wherein some of the internal energy, which is potentially available for the doing of useful work, is degraded.
9. A process occurring in an adiabatically contained system of constant volume (i.e., a system of constant U' and V') will proceed irreversibly with a consequent production of entropy until the entropy is *maximized*. The attainment of maximum entropy is the criterion for equilibrium. Thus, the entropy of an adiabatically contained system can never decrease; it increases as the result of an irreversible process and remains constant at its maximum value during a reversible process.
10. A combination of the First and Second Laws of Thermodynamics gives, for a closed system that does no work other than the work of expansion against a pressure, $dU = TdS - PdV$. S and V are thus the natural choices of independent variables for U as the dependent variables.
11. The equation $dU = TdS - PdV$ is valid for all reversible and irreversible processes, since all the variables are state functions. For irreversible processes, q need not be equal to TdS and the work need not be equal to PdV.

3.17 CONCEPTS AND TERMS INTRODUCED IN THIS CHAPTER

The reader should write out brief definitions or descriptions of the following terms. Where appropriate, equations may be used.

Absolute thermodynamic temperature scale
Adiabatic expansion of gas
Carnot cycle
Constant-temperature heat reservoir
Criterion for equilibria
Degree of irreversibility
Dissipation of energy
Driving force
Efficiency of engine
Entropy
Equilibrium state
Heat engine
Heat pump
Heat reservoir
Irreversible processes
Isentropic process
Isothermal expansion of gas
Maximum work
Natural processes
Nonequilibrium state
Perpetual motion
Principle of Clausius
Principle of Kelvin and Planck
Quasi-static process
Reversible processes
Second Law of Thermodynamics
Spontaneous processes
Steam engines
Superheated system
Thermodynamic temperature

3.18 QUALITATIVE EXAMPLE PROBLEMS

QUALITATIVE PROBLEM 1

A heat engine is operating in a Carnot cycle: all processes are reversible (Figure 3.4). For each of the processes, obtain expressions for the change in entropy of the engine and the change in entropy of the surroundings after one cycle. Assume one mole of an ideal monatomic gas.

SOLUTION TO QUALITATIVE PROBLEM 1

The values of q for each process can be found in Section 3.11.

The engine:

1. For the reversible isothermal expansion process from A to B:

$$\Delta S_{\text{engine}} = \frac{q_2}{T_2} = R \ln\left(\frac{V_B}{V_A}\right)$$

2 For the reversible adiabatic expansion process from B to C:

$$\Delta S_{\text{engine}} = 0, \text{ since } q = 0$$

3 For the reversible isothermal compression process from C to D:

$$\Delta S_{\text{engine}} = \frac{q_1}{T_1} = R \ln\left(\frac{V_D}{V_C}\right)$$

4. For the reversible adiabatic compression process from D to A:

$$\Delta S_{\text{engine}} = 0, \quad \text{since } q = 0$$

The total change in entropy of the engine is therefore

$$\Delta S_{\text{engine}}^{\text{total}} = R \ln\left(\frac{V_B}{V_A}\right) + R \ln\left(\frac{V_D}{V_C}\right) = 0, \quad \text{since} \quad \frac{V_B}{V_A} = \frac{V_D}{V_C}$$

see Problem 3.7

For each of the processes, the change in entropy of the surroundings is the negative of that for the engine. Thus, $\Delta S_{\text{surroundings}}^{\text{total}} = 0$.

Thus, for the Carnot cycle, $\Delta S_{\text{total}} = \Delta S_{\text{system}} + \Delta S_{\text{surrounds}} = 0$.

QUALITATIVE PROBLEM 2

Draw the entropy versus temperature diagram for the Carnot cycle depicted in Figure 3.4.

SOLUTION TO QUALITATIVE PROBLEM 2

See Figure 3.9

Start by choosing a position in the temperature–entropy space for that of state A.

- The first process is an isothermal ($dT = 0$) increase in entropy from state A to B.
- The second process is a constant entropy decrease in temperature from state B to C.
- The third process is an isothermal decrease in entropy from state C to state D.
- The last process is a constant entropy increase in temperature from state D to state A.

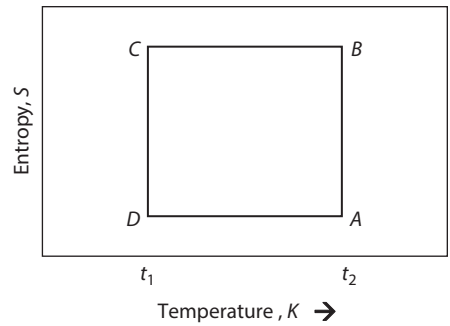

FIGURE 3.9 The temperature entropy diagram for the Carnot cycle of Figure 3.4.

Be sure you understand the sign of each of the changes in temperature and entropy (Figure 3.9).

3.19 QUANTITATIVE EXAMPLE PROBLEMS

QUANTITATIVE PROBLEM 1

Five moles of a monatomic ideal gas are contained adiabatically at 50 atm pressure and 300 K. The pressure is suddenly released to 10 atm, and the gas undergoes an irreversible expansion, during which it performs 4000 J of work.

a. Show that the final temperature of the gas after the irreversible expansion is greater than that which the gas would attain if the expansion from 50 to 10 atm had been conducted reversibly.
b. Calculate the entropy produced as a result of the irreversible expansion.

Given: The constant-volume molar heat capacity of the gas, c_v, has the value 1.5 R.

SOLUTION TO QUANTITATIVE PROBLEM 1

a. In the initial state 1:

$$V_1' = \frac{nRT_1}{P_1} = \frac{5 \times 0.08206 \times 300}{50} = 2.46 \text{ liters}$$

If the adiabatic expansion from 50 to 10 atm is carried out reversibly, then the process path follows $PV^{\gamma} = \text{constant}$, and in the final state 2:

$$V_2' = \left(\frac{P_1 V_1^{\gamma}}{P_2} \right)^{1/\gamma} = \left(\frac{50 \times 2.46^{5/3}}{10} \right)^{3/5} = 6.47 \text{ liters}$$

and

$$T_2 = \frac{P_2V_2}{nR} = \frac{10 \times 6.47}{5 \times 0.08206} = 158 \text{ K}$$

For the irreversible process, which takes the gas from the state 1 to the state 3, as $q = 0$:

$$\Delta U' = -w = -4000 = nc_v(T_3 - T_1) = 5 \times 1.5 \times 8.3144 \times (T_3 - 300)$$

and hence, $T_3 = 236$ K, which is higher than T_2.

b. As the irreversible expansion from state 1 to state 3 was conducted adiabatically, no thermal energy was transferred into the system, and hence, the difference between the entropy at state 3 and the entropy at state 1 is the entropy created, $\Delta S'_{\text{irr}}$, as a result of the irreversible process. This difference in entropy can be calculated by considering any reversible path from state 1 to state 3. Consider the reversible path $1 \rightarrow a \rightarrow 3$ shown in Figure 3.10, which is a reversible decrease in temperature from 300 to 236 K at constant volume, followed by a reversible isothermal expansion from V'_a and V'_3.

For a reversible constant-volume process,

$$\delta q_v = nc_v dT = TdS'$$

or

$$dS' = \frac{nc_v dT}{T}$$

the integration of which, from state 1 to state a, gives

$$S'_a - S'_1 = nc_v \ln \frac{T_a}{T_1} = 5 \times 1.5 \times 8.3144 \times \ln \frac{236}{300} = -15.0 \text{ J/K}$$

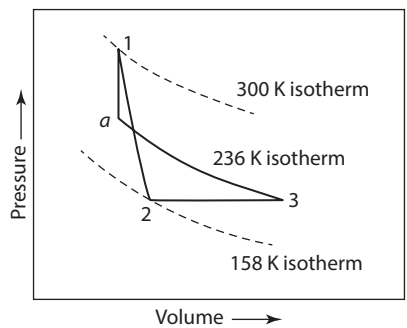

FIGURE 3.10 The process paths considered in Quantitative Problem 1.

For the reversible isothermal expansion from state a to state 3, as $\Delta U' = 0$:

$$q = w = nRT \ln \frac{V_3'}{V_a'}$$

where

$$V_3' = \frac{nRT_3}{P_3} = \frac{5 \times 0.08206 \times 236}{10} = 9.68 \text{ liters}$$

and thus,

$$S_3' - S_a' = \frac{q}{T} = nR \ln \frac{V_3'}{V_a'} = 5 \times 8.3144 \ln \frac{9.68}{2.46} = 56.95 \text{ J/K}$$

The entropy created during the irreversible expansion is thus

$$S_3' - S_1' = -15.0 + 57.0 = 42.0 \text{ J/K}$$

Alternatively, the state of the gas could be changed from 1 to 3 along the path 1 → 2 → 3. As the reversible adiabatic expansion from state 1 to state 2 is isentropic:

$$S_3' - S_1' = S_3' - S_2'$$

and, for the reversible isobaric expansion from state 2 to state 3:

$$\delta q_p = nc_p dT = TdS'$$

or

$$dS' = \frac{nc_p dT}{T}$$

the integration of which, from state 2 to state 3, gives

$$S_3' - S_2' = 5 \times 2.5 \times 8.3144 \times \ln \frac{236}{158} = 41.7 \text{ J/K}$$

which, again, is the entropy created by the irreversible adiabatic expansion of the gas from state 1 to state 3.

QUANTITATIVE PROBLEM 2

At a pressure of 1 atm, the equilibrium melting temperature of lead is 600 K, and at this temperature, the latent heat of melting of lead is 4810 J/mole.

Calculate the entropy produced when 1 mole of supercooled liquid lead spontaneously freezes at 590 K and 1 atm pressure.

Given: The constant-pressure molar heat capacity of liquid lead, as a function of temperature, at 1 atm pressure is given by

$$c_{p(l)} = 32.4 - 3.1 \times 10^{-3} T \text{ J/K}$$

and the corresponding expression for solid lead is

$$c_{p(s)} = 23.56 + 9.75 \times 10^{-3} T \text{ J/K}$$

SOLUTION TO QUANTITATIVE PROBLEM 2

The entropy produced during the irreversible freezing of the lead equals the difference between the change in the entropy of the lead and the change in the entropy of the constant-temperature heat reservoir (at 590 K) caused by the process.

First, calculate the difference between the entropy of 1 mole of solid lead at 590 K and 1 mole of liquid lead at 590 K. Consider the processes illustrated in Figure 3.11.

1. Step $a \rightarrow b$: 1 mole of supercooled liquid lead is heated from 590 to 600 K at 1 atm pressure.
2. Step $b \rightarrow c$: 1 mole of liquid lead is solidified reversibly at 600 K (the equilibrium melting or freezing temperature is the only temperature at which the melting or freezing process can be conducted).
3. Step $c \rightarrow d$: 1 mole of solid lead is cooled from 600 to 590 K at 1 atm pressure.

Since entropy is a state function,

$$\Delta S_{(a \rightarrow d)} = \Delta S_{(a \rightarrow b)} + \Delta S_{(b \rightarrow c)} + \Delta S_{(c \rightarrow d)}$$

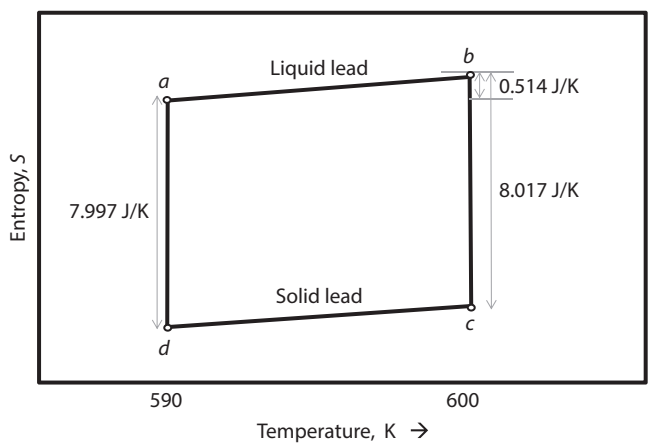

FIGURE 3.11 The changes of state examined in Quantitative Problem 2 depicted in an entropy vs. temperature diagram.

Step a → b

$$\Delta S_{(a\to b)} = \int_a^b \frac{\delta q_{\text{rev}}}{T} = \int_a^b \frac{\delta q_p}{T} = \int_{590\,\text{K}}^{600\,\text{K}} \frac{c_{p,\text{Pb}(l)}dT}{T}$$

$$= \int_{590\,\text{K}}^{600\,\text{K}} \left(\frac{32.4}{T} - 3.1\times10^{-3}\right)dT$$

$$= 32.4\ln\frac{600}{590} - 3.1\times10^{-3}\times(600-590) = +0.514\ \text{J/K}$$

Step b → c

$$\Delta S_{(b\to c)} = \frac{q_{\text{rev}}}{T} = \frac{q_p}{T} = \frac{\text{Latent heat of freezing}}{\text{Equilibrium freezing temperature}}$$

$$= -\frac{4810}{600} = -8.017\ \text{J/K}$$

Step c → d

$$\Delta S_{(c\to d)} = \int_c^d \frac{\delta q_{\text{rev}}}{T} = \int_c^d \frac{\delta q_p}{T} = \int_{600\,\text{K}}^{590\,\text{K}} \frac{c_{p,\text{Pb}(s)}dT}{T}$$

$$= \int_{600\,\text{K}}^{590\,\text{K}} \left(\frac{23.6}{T} + 9.75\times10^{-3}\right)dT$$

$$= 23.6\ln\frac{590}{600} + 9.75\times10^{-3}(590-600) = -0.494\ \text{J/K}$$

Thus,

$$\Delta S_{(a\to d)} = +0.514 - 8.017 - 0.494 = -7.997\ \text{J/K}$$

Consider the thermal energy entering the constant-temperature heat reservoir at 590 K. As the thermal energy is transferred at constant pressure, $q_p = \Delta H$, where ΔH is the difference between the enthalpies of states *d* and *a*. As *H* is a state function,

$$\Delta H_{(a\to d)} = \Delta H_{(a\to b)} + \Delta H_{(b\to c)} + \Delta H_{(c\to d)}$$

$$\Delta H_{(a\to b)} = \int_a^b c_{p,\mathrm{Pb}(l)}\,dT = \int_{590\ \mathrm{K}}^{600\ \mathrm{K}} \left(32.4 - 3.1\times 10^{-3}T\right)dT$$

$$= 32.4\times(600-590) - \frac{3.1\times 10^{-3}}{2}\left(600^2 - 590^2\right) = 30$$

$$\Delta H_{(b\to c)} = -4810J$$

$$\Delta H_{(c\to d)} = \int_c^d c_{p,\mathrm{Pb}(s)}\,dT = \int_{600\ \mathrm{K}}^{590\ \mathrm{K}} \left(23.6 + 9.75\times 10^{-3}T\right)dT$$

$$= 23.6\left(590-600\right) + \frac{9.75\times 10^{-3}}{2}\left(590^2 - 600^2\right) = -294\ \mathrm{J}$$

Thus,

$$\Delta H_{(a-d)} = -4799\ \mathrm{J}$$

and so, the heat reservoir absorbs 4799 J of thermal energy at 590 K. Consequently,

$$\Delta S_{\text{heat reservoir}} = \frac{4799}{590} = 8.134\ \mathrm{J/K}$$

Thus, the entropy created is

$$\Delta S_{\mathrm{irr}} = -7.994 + 8.134 = 0.137\ \mathrm{J/K}$$

An examination shows that the lower the temperature of the irreversible freezing of the supercooled liquid, the more irreversible the process and the larger the value of ΔS_{irr}.

PROBLEMS

3.1 The initial state of 1 mole of a monatomic ideal gas is $P = 10$ atm and $T = 300$ K. Calculate the change in the entropy of the gas for
- a. An isothermal decrease in the pressure to 5 atm
- b. A reversible adiabatic expansion to a pressure of 5 atm
- c A constant-volume decrease in the pressure to 5 atm

3.2 One mole of a monatomic ideal gas is subjected to the following sequence of steps:

a. Starting at 300 K and 10 atm, the gas expands freely into a vacuum to triple its volume.
b. The gas is next heated reversibly to 400 K at constant volume.
c. The gas is reversibly expanded at constant temperature until its volume is again tripled.
d. The gas is finally reversibly cooled to 300 K at constant pressure.

Calculate the values of q and w and the changes in U, H, and S.

3.3 One mole of a monatomic ideal gas undergoes a reversible expansion at constant pressure, during which the entropy of the gas increases by 14.41 J/K and the gas absorbs 6236 J of thermal energy. Calculate the initial and final temperatures of the gas. One mole of a second monatomic ideal gas undergoes a reversible isothermal expansion, during which it doubles its volume, performs 1729 J of work, and increases its entropy by 5.763 J/K. Calculate the temperature at which the expansion was conducted.

3.4 Calculate the change in the enthalpy and the change in entropy when 1 mole of SiC is heated from 25°C to 1000°C. The constant-pressure molar heat capacity of SiC varies with temperature as

$$c_p = 50.79 + 1.97 \times 10^{-3} T - 4.92 \times 10^{6} T^{-2} + 8.20 \times 10^{8} T^{-3} \text{ J/mole} \cdot \text{K}$$

3.5 One mole of copper at a uniform temperature of 0°C is placed in thermal contact with a second mole of copper which, initially, is at a uniform temperature of 100°C. Calculate the temperature of the 2-mole system, which is contained in an adiabatic enclosure, when thermal equilibrium is attained. Why is the common uniform temperature not exactly 50°C? How much thermal energy is transferred, and how much entropy is produced by the transfer? The constant-pressure molar heat capacity of solid copper varies with temperature as

$$c_p = 22.64 + 6.28 \times 10^{-3} T \text{ J/mole} \cdot \text{K}$$

3.6 A reversible heat engine, operating in a cycle, withdraws thermal energy from a high-temperature reservoir (the temperature of which consequently decreases), performs work w, and rejects thermal energy into a low-temperature reservoir (the temperature of which consequently increases). The two reservoirs are, initially, at the temperatures T_1 and T_2 and have constant heat capacities C_1 and C_2, respectively. Calculate the final temperature of the system and the maximum amount of work that can be obtained from the engine.

3.7 In deriving the equation for the efficiency of a Carnot engine in Section 3.11, it was stated that $V_B / V_A = V_C / V_D$. Show that this equality is valid.

3.8 This problem picks up from Problem 2.11. Use data from that problem for this one.

a. Calculate the change in entropy at 273 K for the freezing of water.

b. Calculate the change in entropy for the freezing of water at 260 K.

3.9 Calculate the work performed by the Carnot cycle shown in Figure 3.4 using the *T*-*S* diagram of Figure 3.9.

3.10* Calculate the change in the entropy of one mole of iron when it is heated from 300 K to 1500 K at one atmosphere pressure. See Table A.2

3.11* The Equation $dU' = TdS' - PdV$ (Equation 3.12 of the text) was derived for reversible processes. Can you use this equation for irreversible processes as well?

3.12* A famous nineteenth century scientist defined a thermodynamic function, ξ, as

$$\xi = H - TS$$

Where H is the enthalpy, S is the entropy and T is the temperature of the system.

Plot the function ξ versus temperature as well as ξ versus pressure, by determining the sign of the slope and curvature of each plot.

3.13* Sketch a plot of entropy, S versus volume, V for a simple system at constant internal energy. The signs of the slope and curvature must be determined.

* New problem in this edition.

4 The Statistical Interpretation of Entropy

4.1 INTRODUCTION

Classical thermodynamics is *phenomenological*; that is, it *studies* matter as it *appears* to our *senses*. In this regard, we use our *senses* to describe the properties of matter such as pressure, volume, and temperature.

Classical thermodynamics is *macroscopic*, that is, it does not delve into the more fundamental question, of what does matter consist?

In this chapter, we will use the understanding that matter consists of atoms and molecules and introduce the use of *statistics* to the approach of understanding thermodynamics at the microscopic level. This starting place moves us from the realm of Classical Thermodynamics to what is called *Statistical Thermodynamics*. Our excursion will be brief, with the goal of giving the reader a more comprehensive (and more physical) understanding of entropy.

In Chapter 3, the introduction of entropy as a *thermodynamic state function* was facilitated by the realization that there exist both *possible* and *impossible* spontaneous processes. This was done by the examination of the thermal energy and work effects occurring during these processes. From the formal statements of the *Second Law of Thermodynamics*, as developed from classical thermodynamics arguments, it is difficult to assign a *physical significance* or a *physical quality* to entropy. In this respect, entropy differs from internal energy in spite of the fact that, within the scope of classical thermodynamics, both properties are extensive thermodynamic functions of the state of a system. The ready acceptance of the First Law of Thermodynamics in the nineteenth century, after its enunciation, was due to the easily understood physical significance of internal energy, whereas the lack of a corresponding understanding of entropy caused the acceptance of the Second Law of Thermodynamics to be slower. A more physical interpretation of entropy had to await the development of Statistical Thermodynamics and the subsequent development of quantum mechanics.

By the middle of the nineteenth century, the Kinetic Theory of Gases was used to calculate the energy distribution of a given volume of gas as a function of temperature. A schematic of this distribution is shown in Figure 4.1. It can be seen that the gas molecules have a range of energies. This range of energies changes with temperature as does its spread. The average or the mean was utilized to estimate the *internal energy* of the gas. The *pressure* exerted by such a gas was estimated through the sum of average momentum changes per unit time of the gaseous particles as they struck the walls of their container. Starting from these and similar concepts, Boltzmann (Ludwig Eduard Boltzmann, 1844–1906) moved on to the task of understanding the *entropy* of gaseous matter from the point of view of the *mechanics* of the motion and collisions of the atoms or molecules that

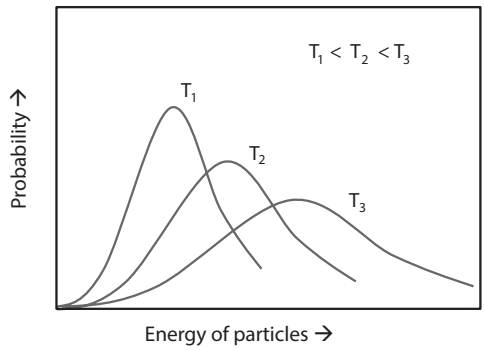

FIGURE 4.1 Schematic plot of the distribution of the probability of particles of a certain energy as a function of temperature. As the temperature increases, the maximum energy of the particles increases.

compose the gas. Later Gibbs (Josiah Willard Gibbs, 1839–1903) added his genius to the task of developing the topic of Statistical Thermodynamics (or statistical Mechanics) early in the first decade of the twentieth century.

4.2 ENTROPY AND DISORDER ON AN ATOMIC SCALE

Josiah Willard Gibbs described the entropy of a system as being its "mixed-up-ness."[1] We can understand this concept of *mixed-up-ness* to be applied at the atomic or molecular level; that is, the more "mixed up" the constituent particles of a system, the larger is the value of its entropy. For example, in the crystalline solid phase, most of the constituent particles are confined to vibrating about their regularly arrayed positions, whereas in the liquid phase, confinement of the particles to specific sites is absent. The particles in the liquid phase are relatively free to wander through the communal volume occupied by the liquid. The arrangement of the particles in the crystalline solid phase is thus said to be more ordered than that of the liquid phase, or alternatively, is *less mixed up* than that of the liquid phase. As a consequence, the *configurational entropy* of the liquid phase can be understood to be greater than that of the solid crystalline phase. Similarly, the atomic or molecular disorder in the gaseous phase is greater than that in the liquid phase, since, in the gaseous phase, there is more volume in which the molecules are free to move. Thus, the *configurational entropy* of the gaseous phase is greater than that of the liquid phase.

This *qualitative* understanding of entropy correlates with phenomena on a macroscopic level. For example, the transformation of a crystalline solid phase to a liquid phase at its equilibrium melting temperature, T_m, requires that the substance absorb a quantity of thermal energy, q, called the *enthalpy of melting*. The entropy of the substance being melted is thus understood to be increased. Indeed, if the melting process is conducted at constant pressure:

[1] J. W. Gibbs, *The Collected Works of J. W. Gibbs*, vol. 1, Yale University Press, New Haven, CT, 1928, unpublished fragments.

$$\Delta S'_{\text{melting}} = \frac{q}{T_m} = \frac{\Delta H'_{\text{melting}}}{T_m}$$

The increase in the entropy of the substance which accompanies melting correlates with the corresponding increase in the degree of disorder of the configurational states of its constituent particles.

Care must be taken, however, in using the concept of *mixed-up-ness*. An isolated supercooled liquid increases its entropy when it spontaneously transforms to its crystalline phase, since the process is an irreversible one. But a crystal seems to be less mixed up than a liquid! How can the entropy of the substance increase? This apparent anomaly exists because we have focused on only one of the *aspects of entropy*—namely, the *configurational* aspect. If we include in our examination the influence of the enthalpy of freezing (the thermal energy released during freezing), it is seen that this release of energy increases the temperature of the isolated system, resulting in a concomitant increase in the thermal entropy of the system. This increase in thermal entropy is greater than that of the decrease in configurational entropy during the liquid-to-crystal transformation. This illustrates that all aspects of the entropy of a system must be considered when evaluating changes in a system, just as all aspects of the energy of a system must be taken into account when applying the First Law of Thermodynamics.

If the transformation from liquid to solid is arranged to occur reversibly and *isothermally* at the equilibrium melting temperature of the substance, T_m, the increase in the degree of disorder of the heat reservoir equals the decrease in the degree of disorder of the substance. Thus, the total degree of disorder of the combined system plus heat reservoir is unchanged. Consequently, the entropy can be thought of as having been transferred from the system to the heat reservoir. The equilibrium melting or freezing temperature of a substance can thus be defined as that temperature at which no change in the entropy of the substance plus heat reservoir occurs as a result of the phase change. Only at this temperature are the solid and liquid phases in equilibrium with one another, and hence, only at this temperature can the phase change occur *reversibly*, with no net increase of entropy of the universe.

4.3 THE CONCEPT OF MICROSTATE

The *state* of a simple, single-component isolated system in Classical Thermodynamics can be denoted as its *macrostate*. The *macro*state is fixed with the knowledge of two of its macroscopic thermodynamic variables (e.g. temperature and pressure or energy and volume), which are its macroscopic *degrees of freedom*. However, when we consider the atomic and molecular makeup of the system, there are many more possible *degrees of freedom* of the microscopic constituents, which give rise to the *same macrostate* of the system. Each microscopic constituent has three coordinates for its position in space and three coordinates for either its momentum or kinetic energy. In addition, there is an enormous number of microscopic constituents in experimental systems, of the order of 10^{24} for a mole of particles. *Statistical thermodynamics* considers the various ways that the total number of constituents, N, and their degrees of freedom can be found in the macrostates we encountered in the first three chapters.

The following two systems have been studied in the previous chapters:

1. *Isolated systems*, where $S' = S'(U', V', N)$ or $U' = U'(S', V', N)$ and N is fixed.
2. *Closed systems* in equilibrium with a heat bath, where $S' = S'(T, V', N)$ and N is fixed.

Later in the text, **Open systems** where $S' = S'(T,V', \mu)$ and the number of particles may change will be examined. (μ is the chemical potential to be defined in Chapter 5.)

When considering the microstates of the above systems, special names have been given in the statistical thermodynamic formulation, such as the *microcanonical, canonical*, and *grand-canonical* formalisms, respectively. In this brief introduction to statistical thermodynamics, only the *microcanonical* (isolated systems) and *canonical* (closed systems) formulations will be considered.

The development of a quantitative relationship between entropy and the degree of *mixed-up-ness* requires the quantification of the term *degree of mixed-up-ness*. This can be obtained from a consideration of elementary statistical thermodynamics. Statistical thermodynamics postulates that the equilibrium state of a system is simply the *most probable* of all of its possible (i.e., accessible) microstates. Therefore, statistical thermodynamics is concerned with:

- The determination of the systems accessible microstates
- The criteria governing and the determination of the most probable microstate
- The resulting properties of this most probable microstate

Both Boltzmann and Gibbs found it convenient to examine the *distribution of the particles of the system* among the various accessible energy levels by considering the energy levels to be *discrete* values. This changed the distribution of energy of the particles from being a *continuous function* of state to a discrete function and made it more convenient to perform various statistical operations (averages, RMS deviations, etc.) on the system of interest. This method turned out to be similar (but not identical) to the results of quantum theory, which was developed several decades later. A postulate of quantum theory is that if a particle is confined to move within a given fixed volume, then its energy is quantized; that is, the particle may only have certain discrete values of energy, which are separated by *forbidden energy bands*. For any given particle, the spacing between the quantized values of energy (the allowed energy levels) decreases as the volume available to the movement of the particle increases. Considering the various *allowable states* of the system introduces another *aspect of the entropy* of a system—namely, the *degree of the spread* in the distribution of the particles among its possible energy levels. This spread can be considered the degree of *mixed-up-ness* of the occupied energy levels of the particles in the system and is related to what is its *thermal entropy.*

4.4 ISOLATED SYSTEMS

Simple examples of three systems that may occur in thermodynamic isolation and the calculation the number of microstates for each will now be examined. First, an *isolated system* that has *distinguishable microstates* that all have the same *energy* as

that of the macrostate will be examined. Next, a system with two kinds of particles (A and B atoms) which can have various *spatial arrangements* in a crystal but all having the same energy will be discussed.

As a final example of equilibrium in an isolated system, a collection of magnetic spins in a paramagnet will be considered.

4.4.1 Distinguishable Sites with Different Assigned Energies

The effect of the *discretation of energy* and its resulting distribution can be illustrated by considering a hypothetical system comprising a perfect crystal in which all of the distinguishable sites are occupied by n identical particles. The physical characteristics of the particles such as volume and mass, as well as the structure of the crystal, determine the quantization of the allowed energy levels, in which the lowest energy level, or the *ground state*, is designated ε_0, and the succeeding levels of increasing energy are designated ε_1, ε_2, ε_3, and so on. The n particles of the crystal have a total fixed energy U' and fixed volume V'. The system is therefore an *isolated* system: neither energy nor particles can enter or leave the system. We ask the following questions:

- In how many ways can the n particles be distributed over the available energy levels such that the total energy of the crystal (i.e., U') remains constant?
- Of the possible distributions, which is the most probable?

For simplicity, consider that the crystal contains three particles that are located on three distinguishable lattice sites A, B, and C. Suppose, again for simplicity, that the quantization is such that the energy levels are equally spaced, with the ground level being taken as $\varepsilon_0 = 0$, the first level $\varepsilon_1 = u$, the second level $\varepsilon_2 = 2u$, and so on. Let the total energy of the system be $U' = 3u$. This system has the three possible distributions shown in Figure 4.2.

a. All three particles in energy level ε_1
b. One particle in energy level ε_3, and the other two particles in energy level ε_0
c. One particle in energy level ε_2, one particle in energy level ε_1, and one particle in energy level ε_0

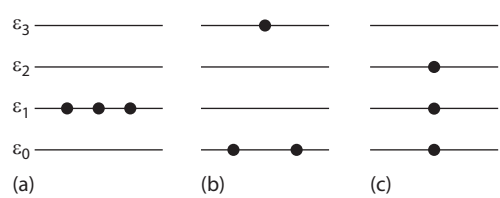

FIGURE 4.2 The three possible distributions of particles among energy levels in a system of constant energy. (a) All particles in ε_1, (b) one particle in ε_3 and two particles in ε_0, (c) one particle in each of the levels ε_0, ε_1, and ε_2.

These distributions are now examined to determine how many distinguishable arrangements (*complexions* or *microstates*) they individually contain.

- *Distribution a*: There is only one *microstate* of this distribution, since the interchange of the particles among the three sites does not produce a different microstate.
- *Distribution b*: Any of the three distinguishable sites can be occupied by any of the three particles of energy $3u$, and the remaining two sites are each occupied by a particle of zero energy. Since the interchange of the particles of zero energy does not produce a different arrangement, there are three microstates in distribution *b*.
- *Distribution c*: Any of the three distinguishable sites can be occupied by the particle of energy $2u$. Either of the two remaining sites can be occupied by the particle of energy $1u$, and the single remaining site is occupied by the particle of zero energy. The number of distinguishable microstates in distribution *c* is thus $3 \times 2 \times 1 = 3! = 6$.

These arrangements are shown in Figure 4.3. The ten arrangements are the ten *microstates* of the system. Since each of the microstates has the same energy, they correspond to one *macrostate* of the system.

The concept of macrostates lies within the domain of classical thermodynamics. The macrostate is fixed when the values of the independent variables are fixed. In this example, the system was considered to be isolated; that is, the values of U', V', and N are fixed (the constancy of volume is required in order that the quantization of the energy levels can be determined). Hence, the macrostate of the system is fixed. With respect to the occupancy of the microstates within the given macrostate (i.e., $U' = 3u$), in view of the absence of any reason to the contrary, it is assumed for the isolated systems that *each of the microstates is equally probable*, and thus, the probability (P_i) of observing the preceding system in any one of its ten possible microstates is 1/10.

$$P_i = 1/\Omega = 1/10$$

where Ω is the total number of microstates with the total energy U'.

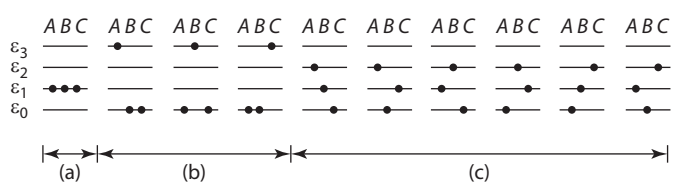

FIGURE 4.3 Illustration of the complexions or microstates within distributions of particles among energy levels in a system of constant energy. (a) One microstate with the distribution of Figure 4.2(a). (b) The three microstates with the distribution of Figure 4.2 (b). (c) The seven microstates with the distribution of Figure 4.2 (c).

However, the ten microstates occur in three distinct distributions, and hence, the probability that the system occurs

- In distribution *a* is 1/10
- In distribution *b* is 3/10
- In distribution *c* is 6/10

Distribution *c* is thus the *most probable*. The physical significance of these probabilities can be viewed in either of two ways:

1. If it were possible to make an instantaneous observation of the system, the probability of observing an arrangement in distribution *c* would be 6/10.
2. If the system were observed over a finite interval of time, during which the system rapidly changed from one microstate to another, the fraction of time which the system spends in all of the arrangements in distribution *c* would be 6/10.

For actual systems, the number of particles is much larger, as is the number of distinguishable microstates that are occupied for given values of U', V', and N. These microstates will still correspond to a single macrostate if the total energy of the system remains constant. Similarly, the number of possible distributions increases, and in such real systems—for example, 1 mole of a system that contains 6.023×10^{23} particles—the number of arrangements within the most probable distribution is very much larger than the number of arrangements in *all of the other distributions* ($\Omega \approx \Omega_{max}$). Thus, the *most probable microstate* is considered to be *the* equilibrium state in the macro-system. For macroscopic systems, the total number of possible arrangements, Ω, is set equal to the number of microstates with maximum probability, Ω_{max}. Since the equilibrium state in a closed system is the one of greatest entropy, the entropy, S' is a function of Ω_{max}:

$$S' = f(\Omega_{max}) \tag{4.1}$$

In this simplified example, the maximum probability occurs when the occupied energy levels of the particles are the most spread out (see Figure 4.3c).

4.4.2 Configurational Entropy of Differing Atoms in a Crystal: Entropy of Mixing

In the preceding section, the entropy of the system was considered in terms of the number of ways that the *energy* of the identical particles of the system could be distributed on distinguishable sites. The entropy was seen to be greatest when the occupancy of the energy levels was broadly distributed. The degree of *mixed-up-ness* corresponded to the *spread* of the distribution of energy among the microstates. This is commonly called the *thermal entropy* of the system. Entropy can also be considered in terms of the *number of ways* in which particles themselves can be *distributed in space*. This consideration gives rise to the concept of *configurational entropy* mentioned briefly in Section 4.1 and now exemplified.

Consider two crystals, one containing white atoms and the other containing gray atoms. Assume that there is no difference in the energy of white/white, white/gray, and gray/gray bonds. When the two crystals are placed in physical contact with one another, a *spontaneous process* may occur in which the white atoms diffuse into the crystal of the gray atoms and the gray atoms diffuse into the crystal of the white atoms.[2] Since this process is *spontaneous*, (irreversible) entropy must be produced. If the system is isolated, equilibrium will be reached when the entropy of the system reaches a maximum value. In such a case, the number of each type of atoms would be the same on either side of the original interface. Hence, the diffusion processes have occurred to the extent that all concentration gradients in the system have been eliminated. This is the mass transport analog of the heat transfer case, in which heat "flows" irreversibly between two bodies until the temperature gradients have been eliminated (see Section 3.2).

Consider the two crystals to be composed of four white atoms and four gray atoms, as shown in Figure 4.4, which shows the initial arrangement of the atoms. Assume the crystals are held at the same temperature and volume, and that a partition is placed between them so as to not allow interdiffusion. As stated previously, we assume that the bonding energy of the three types of bonds is the same and hence there are no *energetically favored* arrangements of the atoms.

If the partition is removed, the atoms are able to rearrange themselves by moving across the interface between the two crystals, i.e. by diffusion. We seek to determine the most probable state of the system; that is, where will the atoms reside with respect to the position of the barrier after equilibrium is attained (i.e., how many gray atoms will be on the left side and how many will be on the right side of the system)?

The use of combinatorics allows for the calculation of the number of distinguishable ways in which this arrangement can be realized. Recall that the number of ways that N atoms can be arranged into two groups of atoms, one group of n atoms and the rest in the other group, is given as

$$\Omega = \frac{N!}{n!\cdot(N-n)!} \tag{4.2}$$

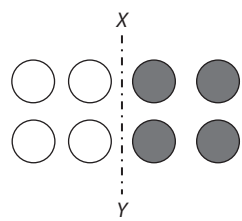

FIGURE 4.4 Representation of a crystal of white atoms in contact with a crystal of gray atoms.

[2] We ignore the mechanism of diffusion in this discussion.

First, consider the number of possible distributions of white atoms on the left side:

1. Four white atoms on the left: $\Omega_{4,0} = (4 \times 3 \times 2 / 4! \cdot 0!) = 1$ (in which the notation indicates four white atoms on the left of *XY* and none on the right).
2. Three white atoms on the left and one gray atom on the left: $\Omega_{3,1} = (4!/3! \cdot 1!) = 4$ (the gray atom could be in any of the four sites).
3. Two white atoms on the left and two gray atoms on the left: $\Omega_{2,2} = (4!/2! \cdot 2!) = 6$.
4. One white atom on the left and three gray atoms on the left: $\Omega_{1,3} = (4!/1! \cdot 3!) = 4$ (the one white atom could be on any of the four sites).
5. No white atoms on the left, and four gray atoms on the left: $\Omega_{0,4} = (4!/0! \cdot 4!) = 1$.

For each distribution of white atoms, there is a corresponding set of distribution of gray atoms on the right side:

1. For case 1, all gray atoms are on the right side: $\Omega_{0,4} = (4!/0! \cdot 4!) = 1$ (in which the notation indicates four gray atoms on the right of *XY* and none on the left).
2. For case 2, three gray atoms are on the right side and one white on the right: $\Omega_{1,3} = (4!/1! \cdot 3!) = 4$ (the "missing" gray atom could be on any of the four sites).
3. For case 3, two gray atoms are on the right side and two white atoms are on the right side: $\Omega_{2,2} = (4!/2! \cdot 2!) = 6$.
4. For case 4, one gray atom is on the right side and three white atoms are on the right side: $\Omega_{3,1} = (4!/3! \cdot 1!) = 4$.
5. For case 5, no gray atoms are on the right side and four white atoms are on the right side: $\Omega_{4,0} = (4!/4! \cdot 0!) = 1$.

Now consider the number of ways that each of the preceding configurations can be made. Starting with all white atoms on the left and all gray atoms on the right, clearly, there is only one way for this to occur, which can be found as $\Omega_{4,0} \cdot \Omega_{0,4} = 1$.

Next, consider three white atoms and one gray atom on the left: There are four ways to obtain the configuration on the left. There are also four ways to arrive at the corresponding configuration (three gray atoms and one white atoms) on the right. Thus, there are 16 ways of distributing one gray atom on the left and one white atom on the right. This can be found as $\Omega_{3,1} \cdot \Omega_{1,3} = 16$.

The case of two white atoms on the left and two gray atoms on the left is given as $\Omega_{2,2} \cdot \Omega_{2,2} = 36$.

Next, consider one white atom and three gray atoms on the left: There are four ways to obtain the configuration on the left. There are also four ways to arrive at the corresponding configuration (one gray atom and three white atom) on the right. Thus, there are 16 ways of distributing one gray atom on the left and one white atom on the right. This can be found as $\Omega_{1,3} \cdot \Omega_{3,1} = 16$.

Finally, with all gray atoms on the left and all white atoms on the right there is only one way for this to occur, which can be found as $\Omega_{0,4} \cdot \Omega_{4,0} = 1$.

These results are summarized in the following table:

Atoms on Left of Partition	Atoms on Right of Partition	No. of Ways (Complexions)
4 white	4 gray	1
3 white/1 gray	3 gray/1 white	16
2 white/2 gray	2 gray/2 white	36
1 white/3 gray	1 gray/3 white	16
4 gray	4 white	1

Thus, the total number of spatial configurations available in this isolated system is $1+16+36+16+1=70$, which is the number of distinguishable ways in which four atoms of one color and four atoms of the other color can be arranged on the eight sites; that is,

$$\text{Number of ways} = \frac{8!}{4!4!} = 70$$

For isolated systems, it is assumed that each of these configurations is *equally probable*. The probability of finding the system in the arrangements 4:0 or 0:4 is 1/70, the probability of arrangements 3:1 or 1:3 is 16/70, and the probability of arrangement 2:2 is 36/70. Arrangement 2:2 is thus the most probable state and this corresponds to the equilibrium state, in which the concentration gradients have been eliminated.

The *most likely* arrangement of atoms would be to have two gray atoms and two white atoms on both sides of the permeable partition. Other arrangements are possible, and since there is no energetic difference between the various microstates, all are *equally probable*. However, since there are 36 microstates with equal numbers of gray and white atoms on either side, that macrostate would be *most probable*. Once again, the most probable case is the one with the greatest *number of microstates* for the given conditions. This illustrates that Statistical Thermodynamics does not determine with *absolute certainty* what the final arrangement will be, but only that which is the *most probable configuration* and the most likely to be observed. Again, it must be emphasized that for large systems, there is negligible chance for the system to be found away from its maximum Ω.

In the case just discussed, the increase in entropy occurs as a result of the increase in the number of spatial configurations which become available to the system when the white crystal and the gray crystal are placed in contact with one another. The increase in the entropy of the system arises from an increase in its configurational entropy, S_{conf}. It must be kept in mind that this is for the case where there are no energetically favored bonds between or among the particles of the system. If, for example, the white/gray bond energy was much greater than the white/white and gray/gray bond energy, the system may have to remain as shown in Figure 4.4 in order to keep the *total energy* of the system constant.

4.4.2.1 Mixing of a Generalized Crystal

The mixing process can be expressed more generally as

$$A+B(\text{unmixed}) \rightarrow A+B(\text{mixed})$$

that is,

$$\text{State 1} \rightarrow \text{State 2}$$

$$\Delta S'_{\text{conf}} = S_{\text{conf(2)}} - S_{\text{conf(1)}} = k_B \ln \Omega_{\text{conf(2)}} - k_B \ln \Omega_{\text{conf(1)}}$$

$$= k_B \ln \left(\frac{\Omega_{\text{conf(2)}}}{\Omega_{\text{conf(1)}}} \right)$$

and, if n_a atoms of A are mixed with n_b atoms of B, then

$$\Omega_{\text{conf(2)}} = \frac{(n_a + n_b)!}{n_a!\, n_b!} \quad \text{and} \quad \Omega_{\text{conf(1)}} = 1$$

Thus,

$$\Delta S'_{\text{conf}} = k_B \ln \frac{(n_a + n_b)!}{n_a!\, n_b!} \tag{4.3}$$

If X_A and X_B are considered to be the mole fraction of A atoms and the mole fraction of B atoms, the expression can be reduced to

$$\Delta S_{\text{conf}} = -R\left[X_A \ln X_A + X_B \ln X_B\right] \tag{4.4}$$

for 1 mole of atoms (see Qualitative Problem 1a in this chapter). This equation gives the configurational entropy of a binary system containing two distinguishable kinds of atoms. It is plotted in Figure 4.5. The maximum configurational entropy of mixing can be seen to occur when equal numbers of the two kinds of atoms are mixed together to form a (solid) solution.

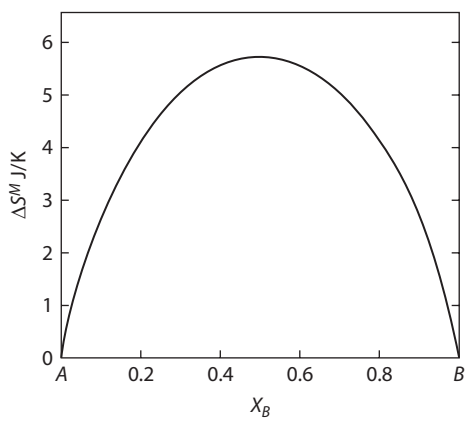

FIGURE 4.5 The molar configurational entropy of mixing for a binary solution with no preference for any type of bonds. The maximum value is $R \ln 2$.

4.4.3 Configurational Entropy of Magnetic Spins on an Array of Atoms

As a final example of equilibrium in an isolated system, consider a collection of magnetic spins in a paramagnet i.e. a substance in which the spins are randomly placed on the atoms. For simplicity, the only spins allowed take values of $\pm\frac{1}{2}m$. The spins will be called *up* and *down* spins.

If there is no external magnetic field applied and if there is no interaction energy between the spins (also called the *exchange energy*), each of the two spin quantum states (up or down) has the same energy. Since the total energy of the system is the sum of the individual energies of the spins, the energy remains constant. Now, all possible microstates of the system will be enumerated.

Consider a system consisting of eight sites on which magnetic spins will be placed. One microstate is that all atoms have their spins pointing up. There is only one such microstate state possible. Consider a microstate with one down spin. The down spin could be on any of the eight sites. Hence, there are eight such possible microstates with one down spin. Next, consider a microstate with two down spins. The first one could be on any of the eight atoms and the second could be on any of the remaining seven atoms. This would be 56 microstates, except that we have counted the states twice, since the order in which we placed the spins on the atoms could be switched without producing a new microstate. Hence, there are 28 microstates with two down spins. This can be calculated from the following formula:

$$6\text{ up and }2\text{ down} = \frac{8!}{6!\cdot 2!} = 28$$

The case for three down spins can be calculated from

$$5\text{ up and }3\text{ down} = \frac{8!}{5!\cdot 3!} = 56$$

The case for four up and four down can be determined as

$$4\text{ up and }4\text{ down} = \frac{8!}{4!\cdot 4!} = 70$$

The other cases can easily be seen by symmetry to be

- 3 up and 5 down = 56
- 2 up and 6 down = 28
- 1 up and 7 down = 8
- 0 up and 8 down = 1

Thus, there are a total of $2^8 = 256$ possible microstates[3] of the spins, which can be divided into nine distinct groups (Figure 4.6).

[3] In the case under considerations here, the spin on an atom may be either up or down. In the case of the four white atoms and four gray atoms, the atoms could not change "color." This accounts for the different number of microstates in the eight-atom spin system (256) versus the number in the eight-colored atom system of Section 4.4.2, which was found to have 70 microstates.

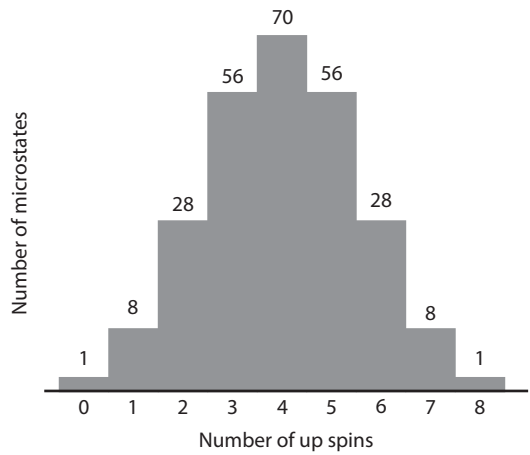

FIGURE 4.6 Plot of the number of microstates against the number of up spins in each microstate.

The magnetization of a material is defined as

$$M = \sum_i m_i$$

where:

M is the magnetization

and $\sum_i m_i$ is the sum of the $\pm m$ spins

It can be seen that the value of M in a microstate can be less than zero, equal to zero, or greater than zero. However, the most probable microstate has a total magnetization of zero, and this is considered to be the equilibrium state. It can also be seen that the average value of M over all microstates is also zero. A material in this state is called a *paramagnet*. If an external magnetic field is applied to the system, M would change to a nonzero value since the energies of the two spins would no longer be equal, due to their interaction with the applied magnetic field. However, when the field is removed, the spins will return to the paramagnetic configuration.

4.4.4 Summary of the Microcanonical Approach

The three *isolated systems* discussed in Sections 4.4.1–4.4.3 show that the microstate with the maximum number of ways of attaining it is the most probable state of the system. Boltzmann postulated that the entropy of one mole of an isolated system is a function of Ω:

$$S(U,V,N) \sim \ln(\Omega)$$

where Ω is the total number of ways that the microstates can be distributed to obtain the constant energy of the system. For large systems we can set, $\Omega = \Omega$.

The most probable microstate represents the equilibrium state. This differs from the statement of the Second Law in classical thermodynamics which states that in an isolated system, the equilibrium state *is the one with maximum entropy*. However, as we have stated above, for large systems there is very little chance that the most probable microstate is not the equilibrium state. This does, however, make us aware that if an isolated system is not very large, it may occur that the observable states are not ones of maximum probability (see Section 4.4.1).

4.5 THE BOLTZMANN DISTRIBUTION

The probability that a system resides in a particular microstate of an isolated system is the same for all microstates. This is so because the total energy of the isolated cannot change in an isolated system. But if the energy of a system can change, it is clear that all microstates will not have the same energy, and hence will not have the same probability of being occupied. Lower energy microstates will have a higher probability of being occupied. In this section, an expression for the probability of occupation of a microstate as a function of its energy will be derived. This general derivation arrives at what is called the *Boltzmann distribution*.

The *number of arrangements* within a given distribution, Ω, is calculated as follows: if n particles are distributed among the energy levels such that n_0 are on level ε_0, n_1 on level ε_1, n_2 on level ε_2,..., and n_r on ε_r, the highest energy level of occupancy, then the number of arrangements, Ω, is given by

$$\Omega = \frac{n!}{n_0!\,n_1!\,n_2!\cdots n_i!} = \frac{n!}{\prod_{i=0}^{i=r} n_i!} \tag{4.5}$$

For example, the system discussed in Section 4.4.1 gives

$$\Omega\left(\text{distribution } a\right) = \frac{3!}{3!0!0!} = 1$$

$$\Omega\left(\text{distribution } b\right) = \frac{3!}{2!1!0!} = 3$$

$$\Omega\left(\text{distribution } c\right) = \frac{3!}{1!1!1!} = 6$$

The most probable distribution is obtained by determining the set of numbers n_0, n_1,..., n_r, which maximizes the value of Ω. For large number of energy levels, this will be determined by maximizing the natural log of the expression. Also when the values of n_i are large, Stirling's approximation (James Stirling, 1692–1770) can be used.

$$\text{Thus for large numbers } \ln X! = X \ln X - X.$$

Taking the logarithms of the terms in Equation 4.5 gives

$$\ln \Omega = n \ln n - n - \sum_{i=0}^{i=r} \left(n_i \ln n_i - n_i \right) \tag{4.6}$$

Since the macrostate of the system is determined by the values of U', V', and n, any distribution of the particles among the energy levels must conform to the conditions

$$\begin{aligned} U' = \text{constant} &= n_0 \varepsilon_0 + n_1 \varepsilon_1 + n_2 \varepsilon_2 + \cdots + n_r \varepsilon_r \\ &= \sum_{i=0}^{i=r} n_i \varepsilon_i \end{aligned} \tag{4.7}$$

and

$$\begin{aligned} n = \text{constant} &= n_0 + n_1 + n_2 + \cdots + n_r \\ &= \sum_{i=0}^{i=r} n_i \end{aligned} \tag{4.8}$$

From Equations 4.7 and 4.8, any interchange of particles among the energy levels must conform to the conditions

$$\delta U' = \sum_i \varepsilon_i \delta n_i = 0 \tag{4.9}$$

and

$$\delta n = \sum_i \delta n_i = 0 \tag{4.10}$$

Also, from Equation 4.6, any interchange of particles among the energy levels gives

$$\begin{aligned} \delta \ln \Omega &= -\sum \left(\delta n_i \ln n_i + \frac{n_i \delta n_i}{n_i} - \delta n_i \right) \\ &= -\sum \left(\delta n_i \ln n_i \right) \end{aligned} \tag{4.11}$$

If Ω has the maximum possible value, then a small rearrangement of particles among the energy levels will not alter the value of Ω or the value of $\ln \Omega$. Thus, if the set of values of n_i is such that Ω has its maximum value, then

$$\delta \ln \Omega = -\Sigma \left(\delta n_i \ln n_i \right) = 0 \tag{4.12}$$

The set of values of n_i in the most probable distribution is obtained by the method of undetermined multipliers, in the following manner. Equation 4.9 is multiplied by the constant β, which has the units of reciprocal energy, to give

$$\Sigma\beta\varepsilon_i\delta n_i = 0 \tag{4.13}$$

Equation 4.10 is multiplied by the dimensionless constant α to give

$$\Sigma\alpha\delta n_i = 0 \tag{4.14}$$

and Equations 4.12–4.14 are added to give

$$\sum_{i=0}^{i=r}\left(\ln n_i + \alpha + \beta\varepsilon_i\right)\delta n_i = 0 \tag{4.15}$$

that is,

$$\begin{aligned}&\left(\ln n_0 + \alpha + \beta\varepsilon_0\right)\delta n_0 + \left(\ln n_1 + \alpha + \beta\varepsilon_1\right)\delta n_1\\ &+\left(\ln n_2 + \alpha + \beta\varepsilon_2\right)\delta n_2 + \left(\ln n_3 + \alpha + \beta\varepsilon_2\right)\delta n_3\\ &+\cdots+\left(\ln n_r + \alpha + \beta\varepsilon_r\right)\delta n_r = 0\end{aligned} \tag{4.15a}$$

The solution of Equation 4.15a requires that each of the bracketed terms be individually equal to zero; that is,

$$\ln n_i + \alpha + \beta\varepsilon_i = 0$$

or

$$n_i = e^{-\alpha}e^{-\beta\varepsilon i} \tag{4.16}$$

Summing over all r energy levels gives

$$\sum_{i=0}^{i=r} n_i = n = e^{-\alpha}\sum_{i=0}^{i=r} e^{-\beta\varepsilon_i}$$

The summation

$$\mathcal{Z} = \sum e^{-\beta\varepsilon_i} = e^{-\beta\varepsilon_0} + e^{-\beta\varepsilon_1} + e^{-\beta\varepsilon_2} + \cdots + e^{-\beta\varepsilon_r}$$

which is determined by the magnitude of β and by the quantization of the energy, is called the *partition function*, $\mathcal{Z}$ (from the German *Zustandssumme*, sum over the states). Thus,

$$e^{-\alpha} = \frac{n}{\mathcal{Z}}$$

and,

$$n_i = \frac{ne^{-\beta\varepsilon_i}}{\mathcal{Z}} \tag{4.17}$$

The condition that Ω has its maximum value for the given macrostate is thus that Equations 4.9, 4.10, and 4.12 are simultaneously satisfied.
The distribution of particles in the energy levels which maximizes Ω (i.e., the most probable distribution) is thus one in which the occupancy of the levels decreases exponentially with increasing energy, and the shape of this distribution is shown in Figure 4.7.

The actual shape of the exponential curve in Figure 4.7 (for a given system) is determined by the value of β. β is inversely proportional to the absolute temperature, being given by

$$\beta = \frac{1}{k_B T} \tag{4.18}$$

in which k_B is Boltzmann's constant, an expression of the gas constant per atom or molecule; that is,

$$k_B = \frac{R}{N_O} = \frac{8.3144(6)}{6.0221 \times 10^{23}} = 1.38065 \times 10^{-23}\,\text{J/K}$$

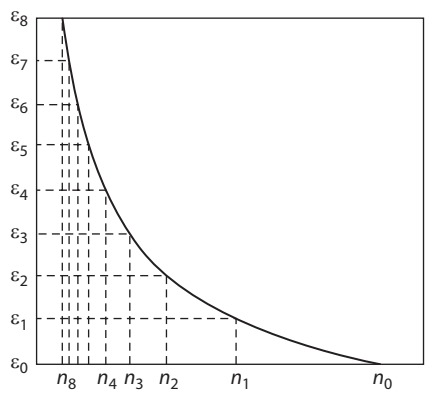

FIGURE 4.7 Schematic representation of the most probable distribution of particles among the quantized energy levels.

where N_O is Avogadro's number.

The partition function can therefore be written as:

$$\mathcal{Z} = \sum_{i=1}^{\Omega} \exp\left(-\frac{\varepsilon_i}{k_B T}\right)$$

This can be easily calculated for the isolated system, where all states have the same energy.

$$\mathcal{Z} = \sum_{i=1}^{\Omega} \exp\left(-\frac{\varepsilon_i}{k_B T}\right) = \Omega \exp\left(-\frac{\varepsilon_i}{k_B T}\right)$$

The probability P_i of finding a particle in a given state is thus

$$P_i = \frac{n_i}{n} = \frac{\exp\left(-\frac{\varepsilon_i}{k_B T}\right)}{\sum_{i=1}^{\Omega} \exp\left(-\frac{\varepsilon_i}{k_B T}\right)} = \frac{1}{\Omega}$$

Since Ω is a constant, each microstate has the same probability of being occupied in the isolated system.

4.6 THE INFLUENCE OF TEMPERATURE

The nature of the exponential distribution of particles in Figure 4.7 is determined by the temperature of the system. However, if the macrostate of the system is fixed by fixing the values of U', V', and n, then T, as a dependent variable, is also fixed. Equation 4.18 shows that T increases with decreasing β, and the shape of the exponential distribution changes as shown in Figure 4.8. An increase in temperature causes the population of

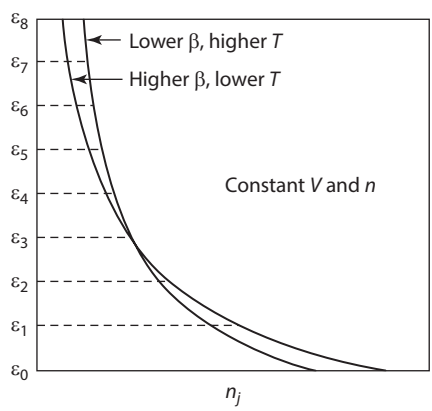

FIGURE 4.8 The influence of temperature on the most probable distribution of particles among energy levels in a closed system of constant volume.

the upper energy levels to become relatively more populated. This corresponds to an increase in the average energy of the particles; that is, to an increase in the value of U'/n, which, for fixed values of V and n, corresponds to an increase in U'.

When the number of particles in the system is very large, the number of arrangements within the most probable distribution, Ω_{max}, is the only term that makes a significant contribution to the total number of arrangements, Ω_{total}, which the system may have; that is, Ω_{max} is significantly larger than the sum of all of the other possible arrangements. Thus, when the number of particles is large, Ω_{total} can be equated with Ω_{max}.

Substituting $\beta = 1/k_B T$, Equation 4.6 can be written as

$$\ln \Omega_{total} = \ln \Omega_{max} = n \ln n - \sum n_i \ln n_i$$

in which the values of n_i are given by Equation 4.17. Thus,

$$\begin{aligned}
\ln \Omega_{total} &= n \ln n - \sum \frac{n}{\mathcal{Z}} e^{-\varepsilon_i / k_B T} \ln\left(\frac{n}{\mathcal{Z}} e^{-\varepsilon_i / k_B T}\right) \\
&= n \ln n - \frac{n}{\mathcal{Z}} \sum \left[e^{-\varepsilon_i / k_B T} \left(\ln n - \ln \mathcal{Z} - \frac{\varepsilon_i}{k_B T} \right) \right] \\
&= n \ln n - \frac{n}{\mathcal{Z}} (\ln n - \ln \mathcal{Z}) \sum e^{-\varepsilon_i / k_B T} + \frac{n}{\mathcal{Z} k_B T} \sum \varepsilon_i e^{-\varepsilon_i / k_B T}
\end{aligned}$$

But,

$$U' = \sum n_i \varepsilon_i = \sum \frac{n}{\mathcal{Z}} \varepsilon_i e^{-\varepsilon_i / k_B T} = \frac{n}{\mathcal{Z}} \sum \varepsilon_i e^{-\varepsilon_i / k_B T}$$

Therefore,

$$\sum \varepsilon_i e^{-\varepsilon_i / k_B T} = \frac{U' \mathcal{Z}}{n}$$

and thus,

$$\ln \Omega = n \ln \mathcal{Z} + \frac{U'}{k_B T}$$

or

$$k_B T \ln \Omega = n k_B T \ln \mathcal{Z} + U' \tag{4.19}$$

In Chapter 5, a function called the *Helmholtz free energy* will be defined as

$$A' \equiv U' - TS.$$

It can be seen from Equation 4.19 that

$$A' = -nk_B T \ln \mathcal{Z} \tag{4.20}$$

and that

$$S' = k_B \ln \Omega \tag{4.21}$$

Equation 4.21, which is called the *Boltzmann equation*, is the required quantitative relationship between the entropy of a system and its degree of mixed-up-ness, in which the latter, given by Ω, is the number of ways in which the energy of the system can be distributed among the particles. The most probable state of the system is that in which Ω has a maximum value, consistent with the fixed values of U', V', and n, and hence, the equilibrium state of the system is that in which S' is a maximum, consistent with the fixed values of U', V', and n. The Boltzmann equation thus provides a helpful mathematical and statistical understanding of entropy.

4.7 THE TWO STATE SYSTEM

Consider a system composed of two types of particles: those with an energy ε_0 and those with a higher energy ε_1. Such a system could be one of magnetic moments with a spin up or down in a small magnetic field, $\mathcal{H}$, or the system could be one electric dipoles with their positive regions up or down in a small electric field, E. The total number of particles is N.

The partition function for this system is written as:

$$\mathcal{Z} = \sum_{i=0}^{1} \exp\left(-\frac{\varepsilon_i}{k_B T}\right) = \exp\left(-\frac{\varepsilon_0}{k_B T}\right) + \exp\left(-\frac{\varepsilon_1}{k_B T}\right) \tag{4.22}$$

This can be rewritten by assigning the value of 0 to the energy ε_0 since only the difference between the values ε_0 and ε_1 is important.

The number of particles with energy $\varepsilon_0 = 0$ is:

$$n_0 = N \frac{\exp\left(-\frac{\varepsilon_0}{k_B T}\right)}{\exp\left(-\frac{\varepsilon_0}{k_B T}\right) + \exp\left(-\frac{\varepsilon_1}{k_B T}\right)} = \frac{N}{1 + \exp\left(-\frac{\varepsilon_1}{k_B T}\right)} \tag{4.23}$$

The number of particles with energy ε_1 is:

$$n_1 = N \frac{\exp\left(-\frac{\varepsilon_1}{k_B T}\right)}{\exp\left(-\frac{\varepsilon_0}{k_B T}\right) + \exp\left(-\frac{\varepsilon_1}{k_B T}\right)} = N \frac{\exp\left(-\frac{\varepsilon_1}{k_B T}\right)}{1 + \exp\left(-\frac{\varepsilon_1}{k_B T}\right)} = \frac{N}{1 + \exp\left(\frac{\varepsilon_1}{k_B T}\right)} \tag{4.24}$$

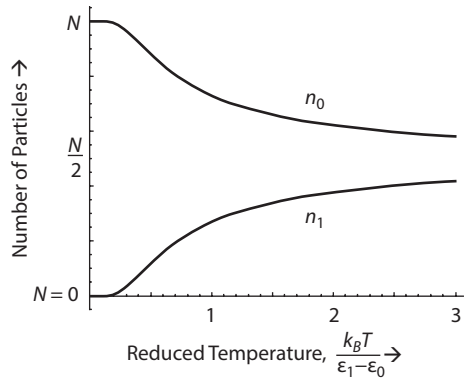

FIGURE 4.9 Number of particles occupying the states of the two-state system as a function of reduced temperature.

These values of the number of particles in the two states as a function of reduced temperature are plotted in Figure 4.9.

At high temperatures, the energy levels approach equal occupation. The small value of the difference in energy of the states ε_0 and ε_1 is not sufficient to bias their occupation.

At low temperatures, the term $\exp\left(-\frac{\varepsilon_1}{k_BT}\right)$ approaches zero, while the term $\exp\left(\frac{\varepsilon_1}{k_BT}\right)$approaches infinity. Thus, n_0 approaches N and n_1 approaches 0. As $T \to 0$, all particles tend to have the lowest possible energy. It can be seen that the entropy also approaches 0, since the particles are all going toward one state, namely, the low energy state. See Chapter 6 on the Third Law of Thermodynamics.

The internal energy of the system is $U' = n_o\varepsilon_0 + n_1\varepsilon_1 = n_1\varepsilon_1$. The shape of the plot of U' versus reduced temperature is thus the same as the bottom half of Figure 4.9, since only the higher energy particles have nonzero (relative) energy. Thus, the internal energy is:

$$U' = n_1\,\varepsilon_1$$

The derivative of the internal energy with respect to T is the constant volume heat capacity as a function of reduced temperature and is shown in Figure 4.10.

The maximum in the heat capacity is seen to occur at approximately $\frac{\varepsilon_1}{2}$. Here, the input energy in the form of heat is used to mix up the occupations of the two levels, which in turn increases the entropy of the system.

The slope of the heat capacity curve goes to zero at high temperatures since the internal energy related to the two states approaches a constant value. The slope of the curve also goes to zero at very low temperatures. This occurs because there is not enough thermal energy in the system at low temperatures to change the occupancy of the low energy level (n_0) to the higher energy level (n_1).

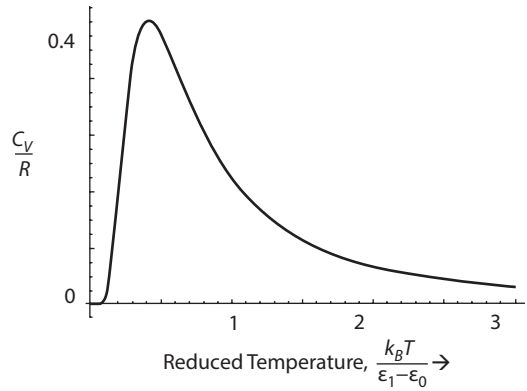

FIGURE 4.10 Specific heat of the two-state system as a function of reduced temperature.

4.8 APPLICATION TO THE HEAT CAPACITY OF SOLIDS AT LOW TEMPERATURES

The calculation of the heat capacity of a solid, as a function of temperature, was one of the early successful applications of quantum theory to the solid state. The first such calculation was published in 1907 by Einstein (Albert Einstein, 1879–1955), who considered the properties of a solid containing n atoms, each of which behaves as a quantum harmonic oscillator vibrating *independently* in three orthogonal directions about its position. Furthermore, he assumed the behavior of each of the $3n$ oscillators is not influenced by the behavior of its neighbors, and a single frequency v is assigned to each of the oscillators. Such a system of quantum oscillators is now called an *Einstein solid* (sometimes an *Einstein crystal*).

For a fixed frequency of vibration, the energy levels of a quantum harmonic oscillator take values of the ith energy level as

$$\varepsilon_i = \left(i + \frac{1}{2}\right)h\nu \tag{4.25}$$

In Equation 4.25, i is an integer that has values in the range zero to infinity, and h is Planck's constant (Max Karl Ernst Ludwig Planck, 1858–1947). Since each oscillator has three degrees of freedom (i.e., it can vibrate in the x, y, and z directions), the energy, U', of the Einstein solid (which can be considered to be a system of $3n$ linear independent [distinguishable] quantum harmonic oscillators) is given as

$$U' = 3\sum n_i\varepsilon_i \tag{4.26}$$

where, as before, n_i is the number of atoms in the ith energy level. Earlier in this chapter, we defined the partition function $\mathcal{Z}$ as

$$\mathcal{Z} \equiv \sum_i \exp\left(-\frac{\varepsilon_i}{k_BT}\right)$$

and the number of particles (n_i) with a given energy ε_i was written as

$$n_i = \frac{n \exp\left(-\frac{\varepsilon_i}{k_B T}\right)}{\mathcal{Z}} \tag{4.27}$$

since the quantum oscillators are *distinguishable*. Substituting Equations 4.25 and 4.26 and simplifying, we obtain

$$U' = \sum_i 3 n_i \varepsilon_i = \sum_i 3 n_i \left(i + \frac{1}{2}\right) h\nu$$

Now, substituting Equation 4.27 into this equation, we obtain

$$U' = \sum_i 3 \frac{n \exp\left(-\frac{\varepsilon_i}{k_B T}\right)}{\mathcal{Z}} \left(i + \frac{1}{2}\right) h\nu = 3nh\nu \sum_i \left(i + \frac{1}{2}\right) \left(\frac{\exp\left(-\frac{\varepsilon_i}{k_B T}\right)}{\sum_i \exp\left(-\frac{\varepsilon_i}{k_B T}\right)} \right) \tag{4.28}$$

This represents the total internal energy, U', of an Einstein solid.
This equation can be expanded to obtain

$$U' = 3nh\nu \left(\frac{\sum_i i \exp\left(-\frac{\varepsilon_i}{k_B T}\right)}{\sum_i \exp\left(-\frac{\varepsilon_i}{k_B T}\right)} + \frac{1}{2} \left(\frac{\sum_i \exp\left(-\frac{\varepsilon_i}{k_B T}\right)}{\sum_i \exp\left(-\frac{\varepsilon_i}{k_B T}\right)} \right) \right)$$

$$U' = 3nh\nu \left(\frac{\sum_i i \exp\left(-\frac{1}{k_B T}\left(i + \frac{1}{2}\right) h\nu\right)}{\sum_i \exp\left(-\frac{1}{k_B T}\left(i + \frac{1}{2}\right) h\nu\right)} + \frac{1}{2} \right)$$

$$= 3nh\nu \left(\frac{\sum_i i \exp\left(-\frac{ih\nu}{k_B T}\right)}{\sum_i \exp\left(-\frac{ih\nu}{k_B T}\right)} + \frac{1}{2} \right)$$

Now we let

$$\sum_i i \exp\left(-\frac{ih\nu}{k_B T}\right) = \sum i x^i = x\left(1 + 2x + 3x^2 + \cdots\right) = \frac{x}{(1-x)^2}$$

and let

$$\sum_i \exp\left(-\frac{ih\nu}{k_B T}\right) = \sum x^i = 1 + x + x^2 + \cdots = \frac{1}{1-x}$$

where $x = \exp(-h\nu / k_B T)$.

Then, U' becomes

$$U' = \frac{3nh\nu}{2}\left(\frac{2\dfrac{x}{(1-x)^2}}{\dfrac{1}{1-x}} + 1\right) = \frac{3nh\nu}{2}\left(\frac{1+x}{1-x}\right)$$

$$U' = \frac{3nh\nu}{2}\left(\frac{1+\exp\left(-\dfrac{h\nu}{k_B T}\right)}{1-\exp\left(-\dfrac{h\nu}{k_B T}\right)}\right)$$

$$U' = \frac{3nh\nu}{2}\left(\frac{1+\exp\left(-\dfrac{h\nu}{k_B T}\right)}{1-\exp\left(-\dfrac{h\nu}{k_B T}\right)}\right) = \frac{3}{2}nh\nu + \frac{3nh\nu}{\left(\exp\left(\dfrac{h\nu}{k_B T}\right)-1\right)}$$

$$U' = \frac{3}{2}nh\nu + \frac{3nh\nu}{\left(\exp\left(\dfrac{h\nu}{k_B T}\right)-1\right)} \tag{4.29}$$

U' is the total internal energy of a system composed of $3n$ quantum harmonic oscillators, which Einstein used to model the thermal properties of a solid with n atoms vibrating independently of each other. Equation 4.29 gives the variation of the energy of the system with temperature, and differentiation with respect to temperature at constant volume gives, by definition, the constant volume heat capacity c_v. Maintaining a constant volume causes constant quantization of the energy levels. Thus,

$$C_v = \left(\frac{\partial U'}{\partial T}\right)_V = 3nh\nu\left(\exp\left(\frac{h\nu}{k_B T}\right)-1\right)^{-2}\frac{h\nu}{k_B T^2}\exp\left(\frac{h\nu}{k_B T}\right)$$

$$= 3nk\left(\frac{h\nu}{k_B T}\right)^2\frac{\exp\left(\dfrac{h\nu}{k_B T}\right)}{\left(\exp\left(\dfrac{h\nu}{k_B T}\right)-1\right)^2}$$

Defining $h\nu / k_B = \theta_E$, where θ_E is the Einstein characteristic temperature, and taking n as equal to Avogadro's number, gives the constant volume molar heat capacity of the crystal as

$$c_v = 3R\left(\frac{\theta_E}{T}\right)^2\frac{e^{\frac{\theta_E}{T}}}{\left(e^{\frac{\theta_E}{T}}\right)^2} \tag{4.30}$$

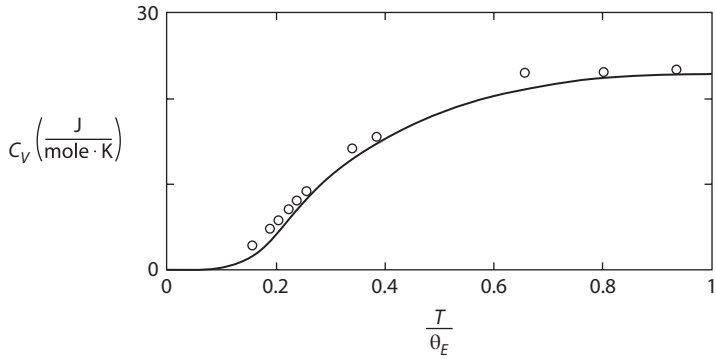

FIGURE 4.11A The experimental constant volume heat capacity for diamond, plotted with the best fit to the Einstein model of a solid, $\Theta_E = 1320$ K. (Adapted from R. DeHoff, *Thermodynamics in Materials Science*, CRC Press, Boca Raton, FL, 2006.)

The variation of c_v with T / θ_E is shown in Figure 4.11a which shows that as T / θ_E (and hence, T) increases, $c_v \rightarrow 3R$, in agreement with Dulong and Petit's law (see Chapter 6). We also see that as $T \rightarrow 0$, $c_v \rightarrow 0$, which is in agreement with experimental observations. The actual values of θ_E for any element and its vibration frequency, v, are obtained by curve-fitting Equation 4.30 to experimentally measure heat capacity data. Such curve fitting, which is shown in Figure 4.11a, shows that although the Einstein equation adequately represents actual heat capacities at higher temperatures, the theoretical values of the Einstein model approach zero more rapidly than do the actual values. For example, as T / θ_E decreases from 0.02 to 0.01, the theoretical molar heat capacity decreases from 1.2×10^{-17} to 9.3×10^{-39} J/K. This discrepancy is caused by the fact that the quantum oscillators do not vibrate with a single frequency, as was assumed by Einstein, as well as the fact that the vibrations are correlated with each other (i.e., they do not vibrate independently of each other, as was also assumed).

The next step in the theory was made in 1912 by Debye (Peter Joseph William Debye, 1884–1966), who assumed that the range of frequencies of vibration (phonons) available to the oscillators is the same as that available to the elastic vibrations in a continuous solid. The lower limit of the wavelength of these vibrations is determined by the interatomic distances in the solid. Taking this minimum wavelength, λ_{min}, to be in the order of 5×10^{-10} m, and the wave velocity, v, in the solid to be about 5×10^3 m/s, gives the maximum frequency of vibration of an oscillator to be of the order of

$$\nu_{max} = \frac{v}{\lambda_{min}} = \frac{5 \times 10^3 \text{ m/s}}{5 \times 10^{-10} \text{ m}} = 10^{13} \text{ s}^{-1}$$

Debye assumed that the frequency distribution is one in which the number of vibrations per unit volume per unit frequency range increases parabolically with increasing frequency in the allowed range $0 \leq v \leq v_{max}$, and, by integrating Einstein's equation over this range of frequencies, he obtained the heat capacity of the solid as

$$c_v = \frac{9nh^3}{k_B^2\theta_D^3}\int_0^{\nu_D}\nu^2\left(\frac{h\nu}{k_BT}\right)^2\frac{\exp\left(\frac{h\nu}{kT}\right)}{\left(1-\exp\left(\frac{h\nu}{kT}\right)\right)^2}d\nu$$

which, with $x = h\nu / k_BT$, gives

$$c_v = 9R\left(\frac{T}{\theta_D}\right)^3\int_0^{\theta_D/T}\frac{x^4e^{-x}}{\left(1-e^{-x}\right)^2}dx \tag{4.31}$$

where:

ν_D (the Debye frequency) $= \nu_{\max}$

and $\theta_D = h\nu_D/k_B$ is the characteristic Debye temperature of the solid

Equation 4.31 is compared with Einstein's equation in Figure 4.11b. Debye's equation approaches the Dulong and Petit limit at high temperatures and shows an excellent fit to the experimental data at lower temperatures. Figure 4.12 shows the curve fitting of Debye's equation to the measured heat capacities of Pb, Ag, Al, and diamond. The curves are nearly identical, except for a horizontal displacement. The relative horizontal displacement is a measure of θ_D. When plotted as c_v versus $\log T/\theta_D$, the data in Figure 4.12 fall on a single curve. This is an example of a *law of corresponding states*. We will see another example of this when we study the van der Waals gas in Chapter 8.

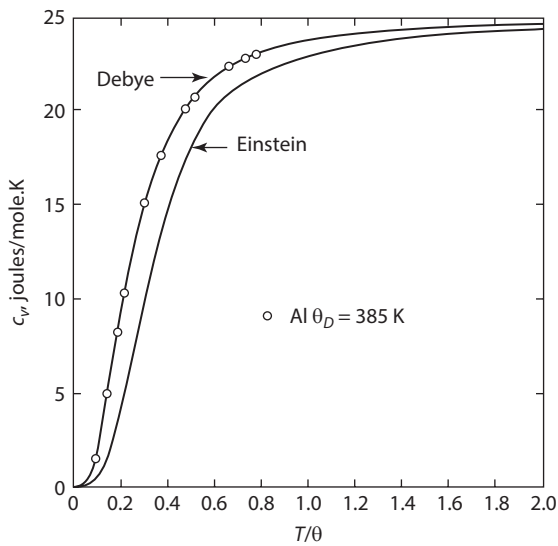

FIGURE 4.11B Comparisons of the Debye heat capacity, the Einstein heat capacity, and the actual heat capacity of aluminum.

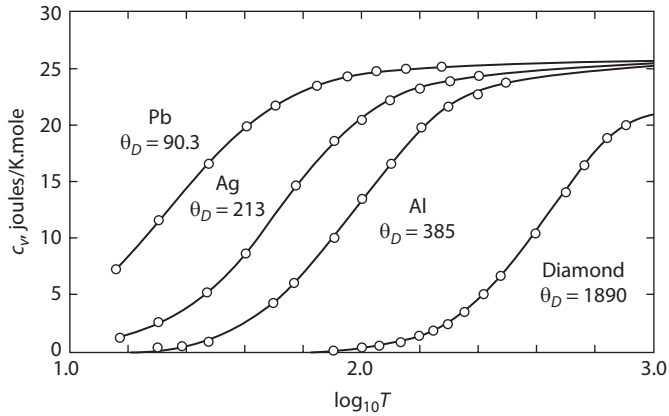

FIGURE 4.12 The constant volume molar heat capacities of several solid elements. The curves are the Debye equation with the indicated values of θ_D.

The value of the integral in Equation 4.31 from zero to infinity is 25.98, and thus, for very low temperatures, Equation 4.31 becomes

$$c_v = 9R \times 25.98 \left(\frac{T}{\theta_D} \right)^3 = 1944 \left(\frac{T}{\theta_D} \right)^3$$

which is called the *Debye T^3 law* for low-temperature heat capacities.

Debye's theory does not consider the contribution made to the heat capacity by the uptake of energy by free electrons at the Fermi level in a metal at low temperatures. For a metal at low temperatures, the heat capacity varies as

$$c_v = \gamma T + 1944 \left(\frac{T}{\theta_D} \right)^3$$

Thus, at temperatures approaching 0 K, c_v for a metal varies linearly with T.

Because of the various uncertainties in the theoretical calculation of heat capacities, it is normal practice to measure the variation of the constant pressure molar heat capacity with temperature and express the relationship analytically (see Section 6.4).

4.9 HEAT FLOW AND THE PRODUCTION OF ENTROPY

Classical thermodynamics shows that the transfer of thermal energy from a body at some temperature to a body at a lower temperature is an irreversible process which is accompanied by the production of entropy. It also shows that the reverse process—that is, the flow of thermal energy up a temperature gradient—is an *impossible* spontaneous process. An examination of microstates shows that a microstate in which variations in temperature occur within a system is *less probable* than a microstate in which the temperature of the system is uniformly constant.

Consider two closed systems, A and B. Let the energy of A be U'_A and the number of complexions of A be Ω_A. Similarly, let the energy of B be U'_B and its number of complexions be Ω_B. When thermal contact is made between A and B, the product $\Omega_A\,\Omega_B$ will, generally, not have its maximum possible value, and thermal energy will be transferred either from A to B or from B to A. Thermal energy flows from A to B if, thereby, the increase in Ω_B, caused by the increase in U'_B, is greater than the decrease in Ω_A, caused by the decrease in U'_A. Thermal energy continues to flow from A to B as long as the product $\Omega_A\,\Omega_B$ continues to increase, and the flow of thermal energy ceases when $\Omega_A\,\Omega_B$ reaches its maximum value—that is, when the increase in Ω_B caused by the transfer of an increment of thermal energy from A is exactly compensated by the decrease in Ω_A. The condition for A to be in thermal equilibrium with B is thus that the transfer of a quantity of thermal energy from one body to the other does not cause a change in the value of $\Omega_A\,\Omega_B$. That is,

$$\delta \ln \Omega_A \Omega_B = 0$$

Consider a rearrangement of the particles in the quantized energy levels in B which causes U'_B to increase by a certain amount, and consider a simultaneous rearrangement of the particles in the energy levels of A which causes U'_A to decrease by the same amount; that is, $\left(U'_A + U'_B\right)$ remains constant. If the levels of A are populated in accordance with $\delta \ln \Omega = \dfrac{\delta q}{k_B T}$ with $T = T_A$ and if the levels of B are also populated in accordance with $\delta \ln \Omega = \dfrac{\delta q}{k_B T}$ with $T = T_B$, then

$$\delta \ln \Omega_A = \frac{\delta q_A}{k_B T_A}$$

and

$$\delta \ln \Omega_B = \frac{\delta q_B}{k_B T_B}$$

When a quantity of thermal energy is transferred from A to B at total constant energy, then

$$\delta q_A = -\delta q_B$$

Thus,

$$\delta \ln \Omega_A \Omega_B = \delta \ln \Omega_A + \delta \ln \Omega_B = \left(\frac{1}{T_A} - \frac{1}{T_B}\right)\frac{\delta q}{k_B}$$

and hence, the condition that $\delta \ln \Omega_A\,\Omega_B$ be zero is that $T_A = T_B$. The *reversible* transfer of thermal energy from one body to another thus only occurs when the temperatures

of the bodies are equal, since only in such a case does $\Omega_A\,\Omega_B$—and hence, the total entropy of the combined system $\left(S'_A + S'_B\right)$—remain constant.

An irreversible transfer of thermal energy increases the value of the product $\Omega_A\,\Omega_B$, and hence, entropy is created. From the point of view of microstates, an irreversible process is one which takes the system from a *less probable state* to the *most probable state*. From the point of view of macrostates, an irreversible process takes the system from a nonequilibrium state to the equilibrium state. Thus, what is deemed in classical thermodynamics to be an *impossible process* is shown by the consideration of microstates to be a *highly improbable process*. As the size of the system increases, the probability of the "up-hill" flow of thermal energy approaches zero. For very small systems (clusters of atoms), these improbable processes must be considered.

The total entropy of a simple system consists of its thermal entropy, S'_{th}, which arises from the number of ways in which the energy of the system can be shared among the particles, and its configurational entropy, S'_{conf}, which arises from the number of distinguishable ways in which the particles can fill the space available to them. Thus,

$$\begin{aligned} S'_{\text{total}} &= S'_{\text{th}} + S'_{\text{conf}} \\ &= k_B \ln \Omega_{\text{th}} + k_B \ln \Omega_{\text{conf}} \\ &= k_B \ln \Omega_{\text{th}} \Omega_{\text{conf}} \end{aligned}$$

If two systems are placed together in thermal contact, the change in entropy is given as

$$\Delta S'_{\text{total}} = k_B \ln \frac{\Omega_{\text{th}(2)} \Omega_{\text{conf}(2)}}{\Omega_{\text{th}(1)} \Omega_{\text{conf}(1)}}$$

In the mixing of particles of A with particles of B, ΔS_{total} only equals $\Delta S'_{\text{conf}}$ if the mixing process does not cause a redistribution of the particles among the energy levels—that is, if $\Omega_{\text{th}(1)} = \Omega_{\text{th}(2)}$. This condition corresponds to the *ideal mixing* of the particles and requires that the quantization of energy be the same in crystals A and B. Ideal mixing is the exception rather than the rule, and, generally, when two or more components are mixed at constant U', V', and n, $\Omega_{\text{th}(2)}$ does not have the same value as $\Omega_{\text{th}(1)}$; thus, the completely random mixing of particles does not occur. In such cases, either the clustering of like particles (indicating difficulty in mixing) or ordering (indicating a tendency toward compound formation) occurs. In all cases, however, the equilibrium state of the system is that which, at constant U', V', and n, maximizes the product $\Omega_{\text{th}}\Omega_{\text{conf}}$. See Chapters 9 and 10 for more discussion on the interplay of energy (U' and/or H') and entropy on the stability of phases.

If, in addition to atoms or molecules, the system is composed of magnetic spins, electric dipoles, and so on, their entropy must be included in the consideration of the total entropy of the system.

4.10 SUMMARY

1. A single macrostate of a simple system, which is determined when the independent thermodynamic variables of the system are fixed, contains a very large number of microstates, each of which is characterized by the manner in which
   - The thermal energy of the system is distributed among the particles
   - The particles are distributed in the configurations available to them
2. Although the occurrence of a system in any one of its microstates is equally probable (for the case of the closed system), greatly differing numbers of microstates occur in differing distributions. The distribution which contains the largest number of microstates is the most probable distribution.
3. In real systems (with a very large number of particles) the number of microstates in the most probable distribution is significantly larger than the sum of all of the other microstates occurring in all of the other distributions. This most probable distribution is considered to be the equilibrium thermodynamic state of the system.
4. The relationship between the number of microstates available to the system, Ω, and the entropy of the system is given by the Boltzmann equation:

$$S' = k_B \ln \Omega$$

   in which k_B is Boltzmann's constant.
5. If a situation arises which allows an increase in the number of microstates available to the system (at constant energy), then spontaneous redistribution of the energy among the particles (or particles over the available configurations) occurs until the newly available most probable distribution occurs. The Boltzmann equation shows that an increase in the number of microstates made available to the system causes an increase in the entropy of the system.
6. The total entropy of a system is the sum of each of the aspects of entropy:
   - Thermal entropy, S_{th}
   - Configurational entropy, S'_{conf}
   - Any other aspect of entropy, such as spin entropy, electric dipole entropy, and so on
7. The thermal entropy arises from the number of ways in which the thermal energy available to the system can be shared among the constituent particles, Ω_{th}.
8. The configurational entropy arises from the number of ways in which the particles can be distributed over the configurations available to them, Ω_{conf}.
9. The spin entropy arises from the number of ways in which the spins can be distributed over the sites available to them, Ω_{spin}.
10. Since any of the thermal distributions can be combined with any of the configurational distributions, the total number of microstates available to the system is the product $\Omega_{\text{th}}\Omega_{\text{conf}}$ ($\Omega_{\text{th}}\Omega_{\text{conf}}\Omega_{\text{spin}}$ if spins are present), and hence, from the logarithmic form of the Boltzmann equation, the total entropy of the system is the sum of the individual entropies of the system.

11. The heat capacity of solids can be modeled by the statistical thermodynamic models of Einstein and Debye. The Debye model is best at low temperatures as it displays the experimentally observed T^3 dependence at low temperatures for non-conductors.

4.11 CONCEPTS AND TERMS INTRODUCED IN THIS CHAPTER

The reader should write out brief definitions or descriptions of the following terms. Where appropriate, equations may be used.

Aspects of entropy
Boltzmann distribution
Boltzmann equation for entropy
Bond energy
Classical thermodynamics
Configurational entropy
Debye model of heat capacity
Einstein model of heat capacity
Einstein solid (crystal)
Entropy as "mixed-up-ness"
Exchange field
External field
Kinetic theory of gases
Macrostate
Microcanonical ensemble
Microstate
Most probable state
Paramagnet
Partition function
Phenomenological
Spin entropy
Spin system
Statistical thermodynamics
Thermal entropy

4.12 QUALITATIVE EXAMPLE PROBLEMS

QUALITATIVE PROBLEM 1

One mole of a FeX alloy of 50 at% X has its Fe and X atoms randomly arranged on a body-centered cubic lattice (BCC). The magnetic moments (spin) on the Fe atoms are also randomly arranged. The X atoms do not have magnetic moments.

a. Calculate the atomic configurational entropy of the alloy.
b. Calculate the entropy of the alloy due to the magnetic moments, assuming only plus and minus orientations

c. Is the sum of the entropies for (a) and (b) the total entropy of the alloy? Explain.

SOLUTION TO QUALITATIVE PROBLEM 1

a. From Equation 4.3, we get

$$\Delta S_{\text{conf}} = k_B \ln \frac{(n_{\text{Fe}} + n_{\text{X}})!}{n_{\text{Fe}}! \cdot n_{\text{X}}!}$$

$$= k_B \left[(n_{\text{Fe}} + n_{\text{X}}) \ln (n_{\text{Fe}} + n_{\text{X}}) - (n_{\text{Fe}} + n_{\text{X}}) - (n_{\text{Fe}} \ln n_{\text{Fe}} - n_{\text{Fe}} + n_{\text{X}} \ln n_{\text{X}} - n_{\text{X}}) \right]$$

$$= k_B (n_{\text{Fe}} + n_{\text{X}}) \left[\ln (n_{\text{Fe}} + n_{\text{X}}) - \frac{(n_{\text{Fe}} \ln n_{\text{Fe}} + n_{\text{X}} \ln n_{\text{X}})}{(n_{\text{Fe}} + n_{\text{X}})} \right]$$

$$= k_B (n_{\text{Fe}} + n_{\text{X}}) \left[\ln (n_{\text{Fe}} + n_{\text{X}} - X_{\text{Fe}} \ln n_{\text{Fe}} - X_{\text{X}} \ln n_{\text{X}}) \right]$$

$$= -k_B (n_{\text{Fe}} + n_{\text{X}}) \left[X_{\text{Fe}} \ln X_{\text{Fe}} + X_{\text{X}} \ln X_{\text{X}} \right]$$

If $n_{\text{Fe}} + n_X = 1$ mole:

$$\Delta S_{\text{conf}} = -R (X_{\text{Fe}} \ln X_{\text{Fe}} + X_{\text{X}} \ln X_{\text{X}})$$

For a 50 atomic percent X alloy, we get :

$$\Delta S_{\text{conf}} = R \ln 2$$

b. The spin entropy is found by

$$\Delta S_{\text{spin}} = -k_B \ln \left(\frac{1}{2} \right)^{n_{\text{Fe}}} = n_{\text{Fe}} k_B \ln 2$$

Since n_{Fe} is 0.5 moles,

$$\Delta S_{\text{spin}} = \frac{R}{2} \ln 2$$

c. No, there is also thermal entropy, which must be included.

QUALITATIVE PROBLEM 2

We saw in Section 4.6 that

$$A' = -nk_B T \ln \mathcal{Z}$$

In the next chapter, we will show that $\left(\frac{\partial A'}{\partial T} \right)_V = -S'$

Take the derivative of A' with respect to T and obtain expressions for S' and U' in terms of the partition function $\mathcal{Z}$. Also obtain an expression for the constant volume heat capacity in terms of the partition function.

SOLUTION TO QUALITATIVE PROBLEM 2

$$\frac{\partial A'}{\partial T} = -S' = -nk_B \ln \mathcal{Z} - nk_B T \frac{\partial \ln \mathcal{Z}}{\partial T}$$

$$\therefore S' = nk_B \ln \mathcal{Z} + nk_B T \frac{\partial \ln \mathcal{Z}}{\partial T}$$

$$A' = U' - TS'$$

$$-nk_B T \ln \mathcal{Z} = U' - T\left(nk_B \ln \mathcal{Z} + nk_B T \frac{\partial \ln \mathcal{Z}}{\partial T} \right)$$

$$\therefore nk_B T^2 \frac{\partial \ln \mathcal{Z}}{\partial T} = U'$$

The expression for the constant volume heat capacity if found as follows:

$$C_V = \left(\frac{\partial U'}{\partial T} \right)_V = 2nk_B T \left(\frac{\partial \ln \mathcal{Z}}{\partial T} \right)_V + nk_B T^2 \left(\frac{\partial^2 \ln \mathcal{Z}}{\partial T^2} \right)_V$$

4.13 QUANTITATIVE EXAMPLE PROBLEMS

QUANTITATIVE PROBLEM 1

Spectroscopic observation of molecular N_2 in an electrical discharge shows that the relative numbers of molecules in excited vibrational states with energies given by

$$\varepsilon_i = \left(i + \frac{1}{2} \right) hv \tag{4.32}$$

are

i	0	1	2	3
$\frac{n_i}{n}$	1.00	0.250	0.062	0.016

Show that the gas is in thermodynamic equilibrium with respect to the distribution of vibrational energy, and calculate the temperature of the gas. In Equation 4.32, i is an integer that has values in the range zero to infinity, h is Planck's constant of action ($= 6.6252 \times 10^{-34}$ J·s), and the vibration frequency, v, is $7.00 \times 10^{13}\,s^{-1}$.

SOLUTION TO QUANTITATIVE PROBLEM 1

From Equations 4.17, 4.18, and 4.32,

$$\frac{n_i}{n} = \frac{\exp\left[-\left(i+\frac{1}{2}\right)\frac{h\nu}{k_B T}\right]}{\mathcal{Z}}$$

Observation shows that

$$\frac{n_1}{n_0} = 0.250$$

Thus,

$$\frac{n_1}{n_0} = \frac{\exp\left(-\frac{3}{2}\frac{h\nu}{k_B T}\right)}{\exp\left(-\frac{1}{2}\frac{h\nu}{k_B T}\right)} = \exp\left(-\frac{h\nu}{k_B T}\right) = 0.250$$

which gives

$$\frac{h\nu}{k_B T} = 1.386$$

Then, from Equation 4.17,

$$\mathcal{Z}\frac{n_0}{n} = \exp\left(-\frac{1}{2}\frac{h\nu}{k_B T}\right) = 0.5$$

$$\mathcal{Z}\frac{n_1}{n} = \exp\left(-\frac{3}{2}\frac{h\nu}{k_B T}\right) = 0.125$$

$$\mathcal{Z}\frac{n_2}{n} = \exp\left(-\frac{5}{2}\frac{h\nu}{k_B T}\right) = 0.031$$

and

$$\mathcal{Z}\frac{n_3}{n} = \exp\left(-\frac{7}{2}\frac{h\nu}{k_B T}\right) = 0.008$$

Normalizing gives

$$\frac{n_0}{n_0} = 0.5 / 0.5 = 1.0$$

$$\frac{n_1}{n_0} = 0.125 / 0.5 = 0.25$$

$$\frac{n_2}{n_0} = 0.031 / 0.5 = 0.062$$

$$\frac{n_3}{n_0} = 0.008 / 0.5 = 0.016$$

which shows that the gas is in equilibrium with respect to the distribution of vibrational energy. The temperature of the gas is obtained as

$$T = \frac{h\nu}{1.386 k_B} = \frac{\left(6.6262 \times 10^{-34}\right)\left(7.00 \times 10^{13}\right)}{1.386 \times 1.38065 \times 10^{-23}} = 2424 \text{ K}$$

QUANTITATIVE PROBLEM 2

The isotopic composition of lead in atomic percent is as follows:

Atomic Weight	Atomic Percent
204	1.5
206	23.6
207	22.6
208	52.3

Calculate the molar isotopic configurational entropy of lead.

SOLUTION TO QUANTITATIVE PROBLEM 2

The configurational isotopic entropy is obtained from the Boltzmann equation:

$$S = k_B \ln \Omega \tag{4.21}$$

where

$$\Omega = \frac{(N_O)!}{(0.015N_O)!(0.236N_O)!(0.226N_O)!(0.523N_O)!}$$

Stirling's approximation gives

$$\begin{aligned}\ln \Omega &= N_O \ln N_O - 0.015N_O \ln 0.015N_O - 0.236N_O \ln 0.236N_O \\ &\quad - 0.226N_O \ln 0.226N_O - 0.523N_O \ln 0.523N_O \\ &= 3.298 \times 10^{25} - 4.567 \times 10^{23} - 7.578 \times 10^{24} \\ &\quad - 7.251 \times 10^{24} - 1.704 \times 10^{25} \\ &= 6.498 \times 10^{23}\end{aligned}$$

Therefore, the molar isotopic configurational entropy is

$$S = k_B \ln \Omega = \left(1.38054 \times 10^{-23}\right) \times \left(6.498 \times 10^{23}\right) = 8.97 \text{ J/K}$$

PROBLEMS

4.1 A rigid container is divided into two compartments of equal volume by a partition. One compartment contains 1 mole of ideal gas *A* at 1 atm, and the other contains 1 mole of ideal gas *B* at 1 atm.
   a. Calculate the increase in entropy which occurs when the partition between the two compartments is removed.
   b. If the first compartment had contained 2 moles of ideal gas *A*, what would have been the increase in entropy when the partition was removed?
   c. and d. Calculate the corresponding increases in entropy in each of the above two situations if both compartments had contained ideal gas *A*.

4.2 Show that, when *n* atoms of *A* and *n* atoms of *B* form a randomly mixed solution, the fraction of the total number of distinguishable complexions that occur in the most probable distribution decreases with an increasing value of *n*.

4.3 Assuming that a silver-gold alloy is a random mixture of gold and silver atoms, calculate the increase in entropy when 10 g of gold is mixed with 20 g of silver to form a homogeneous alloy. The gram atomic weights of Au and Ag are, respectively, 198 and 107.9.

4.4 On the assumption that copper-nickel alloys are random mixtures of copper and nickel atoms, calculate the mass of copper which, when mixed with 100 g of nickel, causes an increase in entropy of 15 J/K. The gram atomic weights of Cu and Ni are, respectively, 63.55 and 58.69.

4.5 A weak magnetic field is applied to a system of up and down spins. The up spins have a slightly lower energy state than those with down spins. This is because the up spins are favored by the weak magnetic field. Thus,

$$\varepsilon^{\uparrow} < \varepsilon^{\downarrow}$$

   a. Determine the partition function for this system under the influence of the weak magnetic field.
   b. Determine the ratio of: $\frac{n^{\uparrow}}{n^{\downarrow}}$ for very high temperatures and very low temperatures.

4.6* Obtain an expression for the internal energy of an Einstein solid as the temperature gets very large, differentiate it with respect to *T*, and show that the Dulong and Petit value for the heat capacity is attained.

4.7* An expression for entropy of a mole of a certain substance has been determined to be:

$$S(U,V,N_A) = N_A k_B \left[\frac{5}{2} + \ln\left(\frac{V}{N_A} \left(\frac{4\pi m U}{3h^2 N_A} \right) \right)^{\frac{3}{2}} \right]$$

a. Obtain an expression for $U = U(T)$ for this substance.
b. Obtain an expression for the constant volume heat capacity of this substance.
Hint: Start from the Fundamental equation $dU = TdS - PdV$ and obtain the expression for $\left(\frac{\partial S}{\partial U} \right)_V$

4.8* The entropy of one mole of an ideal gas is given as:

$$S(U,V,N_A) = R \left[\frac{5}{2} + \ln\left(\frac{V}{N_A} \left(\frac{4\pi m U}{3h^2 N_A} \right) \right)^{\frac{3}{2}} \right]$$

Derive the Ideal Gas Law from this expression.
Hint: Start from the Fundamental Equation $dU = TdS - PdV$ and obtain the expression for $\left(\frac{\partial S}{\partial V} \right)_U$

4.9* One mole of an A_3B compound is formed from pure A and pure B. What is the entropy of formation of this compound?

4.10* Show that the internal energy of an isolated system is equal to:

$$-\frac{\partial \ln \mathcal{Z}}{\partial \beta} \quad \text{where} \quad \beta = \frac{1}{k_B T}$$

* New problem in this edition.

5 Fundamental Equations and Their Relationships

5.1 INTRODUCTION

The main power of the thermodynamic method stems from its provision of criteria for equilibrium in materials systems and for the determination of the effects that changes in the external influences acting on the system have on the equilibrium state. The practical usefulness of this power is, however, determined by the practicality of the *equations of state* for the system—that is, the relationships that can be established among the thermodynamic variables of the system.

Combining the First and Second Laws of Thermodynamics for one mole of a simple system leads to (see Equation 3.12):

$$dU = TdS - PdV$$

This fundamental equation gives the relationship between the dependent variable U (*molar internal energy*) and the independent molar variables S and V (entropy and volume) for a closed system, consisting of one mole of the material, which is undergoing a process involving a change of volume against the external pressure as the only form of work performed on, or by, the system.

In Chapter 3 it was shown that the entropy of an isolated system is maximum at equilibrium. In addition, the entropy of the universe (system plus surroundings) never decreases for any process.

The further development of thermodynamics beyond Equation 3.12 arises, in part, from the fact that, from a practical point of view, the choice of S and V as the independent variables is inconvenient. Although the volume of a system can be measured with relative ease and gases can be controlled, entropy can be neither simply measured nor simply controlled. It is thus desirable to develop a simple expression, similar in form to Equation 3.12, which contains a more convenient choice of independent variables. From a practical point of view, a convenient pair of independent variables would be temperature and pressure, since these variables are easily measured and controlled. The derivation of an equation of state of the simple form of Equation 3.12, but using P and T as the independent variables, and of a criterion for equilibrium in a constant-pressure, constant-temperature system, are thus desirable.

Alternatively, from the theoretician's point of view, a convenient choice of independent variables would be V and T, since constant-volume constant-temperature systems are easily examined by the methods of statistical mechanics. This arises because fixing the volume of a closed system fixes the quantization of its energy levels, and thus, the Boltzmann factor, $\exp(-\varepsilon_i / k_B T)$, and the partition function, both of which appear in Equation 4.17, have constant values in constant-volume constant-temperature systems.

DOI: 10.1201/9781003375388-6

Thus, the derivation of an equation of state using V and T as the independent variables and the establishment of a criterion for equilibrium in a system of fixed volume and fixed temperature are also desirable. In Sections 5.3 and 5.4, fundamental equations using these independent variables will be developed.

Equation 3.12 cannot be applied to systems that undergo changes in composition caused by chemical reactions or to systems that perform work other than the work of expansion against an external pressure (so-called *P-V* work). Since systems that experience changes in composition are of prime importance to the materials scientist and engineer, composition variables must be included in any equation of state and in any criterion for equilibrium. Also, any equation of state must be capable of accommodating forms of work other than *P-V* work, such as the electrical work performed by a galvanic cell or magnetic work performed on the system by an applied external magnetic field.

Thus, although Equation 3.12 lays the foundation of thermodynamics, it is necessary to develop other thermodynamic potentials (sometimes called *auxiliary functions*) which have *dependent variables*, which are related in simple form to more convenient choices of *independent variables*. With this increase in the number of thermodynamic functions, it is necessary also to establish the relationships which exist among them. It is often found that some required thermodynamic expression which itself is not amenable to experimental measurement is related in a simple manner to some measurable quantity. Examples of this have been presented in Chapter 3, where it was found that

$$\left(\frac{\partial U'}{\partial S'}\right)_V = T, \quad -\left(\frac{\partial U'}{\partial V'}\right)_S = P, \quad \text{and} \quad \left(\frac{\partial S'}{\partial V'}\right)_U = \frac{P}{T}$$

In this chapter, the *thermodynamic potentials* (state functions) H (the enthalpy), A (the Helmholtz free energy), G (the Gibbs free energy), and μ_i (the chemical potential of the species i) are defined and their properties and interrelationships examined.

5.2 THE ENTHALPY, *H*

Enthalpy has already been introduced as a state function in Section 2.5. It is defined as

$$H' \equiv U' + PV'$$

Its full differential is:

$$\begin{aligned} dH' &= dU' + PdV' + V'dP \\ &= TdS' + V'dP \end{aligned} \tag{5.1}$$

The natural thermodynamic independent variables for enthalpy, which itself is an extensive variable, are S' and P; $H' = H'(S', P)$. For a system undergoing a change of state at constant pressure and doing only *P-V* work, Equation 5.1 simplifies to

$$dH' = \delta q_P = TdS'$$

This equation shows that the change of state of a simple closed system at constant pressure, during which only *P-V* work is done, is the change in the enthalpy of the system and equals the thermal energy entering or leaving the system, q_P. For this reason, it was called the *heat function at constant pressure* by Gibbs (Josiah Willard Gibbs, 1839–1903), who introduced it in 1875[1]. More of the properties and applications of the enthalpy state variable will be examined in Chapter 6.

5.3 THE HELMHOLTZ FREE ENERGY, *A*

Changes in the internal energy, U', can be measured by processes involving heat and work. Changes in the enthalpy at constant pressure P quantify the changes in the thermal energy of the system. It may be asked, is there a thermodynamic potential that measures the maximum amount of work that a change in the internal energy of a system can perform? There is, and it is called the *Helmholtz free energy* or work function A'.

Consider a simple system that undergoes a spontaneous change of state at constant temperature T. Since the process is spontaneous, we can write

$$\Delta S'_{\text{tot}} = \Delta S'_{\text{system}} + \Delta S'_{\text{surroundings}} > 0$$

If the process is performed at constant volume, the change in the internal energy of the system is denoted as δq_V. This δq_V changes the entropy *of the surroundings* by the amount - $\delta q_V / T$. Thus, we can write

$$\Delta S'_{\text{tot}} = \Delta S'_{\text{system}} - \frac{\Delta U'_{\text{system}}}{T}$$

or

$$-T\Delta S'_{\text{tot}} = \Delta U'_{\text{system}} - T\Delta S'_{\text{system}} \tag{5.2}$$

Since the process is spontaneous, $\Delta U'_{\text{system}} - T\Delta S'_{\text{system}} < 0$. This yields a criterion for a *spontaneous change* of a system in thermodynamic variables that only apply to the system, namely U' and S'.

If $\Delta U'_{\text{system}} - T\Delta S'_{\text{system}} > 0$, no spontaneous change will occur, according to the Second Law of Thermodynamics, and the system is *stable*. Note that if, in addition, the entropy of the system is constant, $\Delta U'_{\text{system}} > 0$ and no spontaneous change will occur.

Defining the Helmholtz free energy, A', as

$$A' \equiv U' - TS'$$

For a system undergoing a change of state from state 1 to state 2,

[1] J. W. Gibbs, "On the Equilibrium of Heterogeneous Substances", *Trans. Conn. Acad.* (1875), vol. 3, pp. 108–248. See page 140 (Equation 89).

$$\left(A_2' - A_1'\right) = \left(U_2' - U_1'\right) - \left(T_2 S_2' - T_1 S_1'\right)$$

and, if the system is closed,

$$\left(U_2' - U_1'\right) = q - w$$

in which case

$$\left(A_2' - A_1'\right) = q - w - \left(T_2 S_2' - T_1 S_1'\right)$$

If the process is also isothermal—that is, $T_2 = T_1 = T$, which is the temperature of the heat reservoir which supplies or withdraws thermal energy to the system during the process—then, from the Second Law:

$$q \le T\left(S_2' - S_1'\right)$$

and hence,

$$\left(A_2' - A_1'\right) \le -w$$

A comparison with

$$\delta w \le T dS'_{\text{system}} - dU'_{\text{system}} \tag{3.11}$$

shows that the equality can be written as

$$\left(A_2' - A_1'\right) + T\Delta S'_{\text{irr}} = -w \tag{5.3}$$

and thus, during a *reversible isothermal process*, (that is: $\Delta S'_{\text{irr}}$ is zero), the amount of work done by the system is a *maximum* and is equal to the *decrease* in the value of the Helmholtz free energy. For this reason, the Helmholtz free energy is sometimes called the *work function*. It can be seen to be equal to the *available energy* of the system which is *free* to do work (hence it is a *free energy*!). Furthermore, for an isothermal process conducted at constant volume, which, necessarily, does not perform *P-V* work, Equation 5.3 gives

$$\left(A_2' - A_1'\right) + T\Delta S'_{\text{irr}} = 0 \tag{5.4}$$

or, for an increment of such a process,

$$dA' + T dS'_{\text{irr}} = 0$$

Since dS'_{irr} is always positive during a spontaneous process, it is seen that A' decreases during a spontaneous process, as shown above.

Since $dS'_{\text{irr}} = 0$ is a criterion for a *reversible process*, equilibrium requires that

$$dA' = 0 \tag{5.5}$$

Thus, in a closed system held at constant T and V', the Helmholtz free energy can only *decrease* (for spontaneous processes) or remain constant. Equilibrium is attained in such a system when A' achieves its *minimum* value. The Helmholtz free energy thus provides a criterion for equilibrium in a system at constant temperature and constant volume—namely,

$$dA'_{T,V} = 0 \quad \text{and} \quad d^2A'_{T,V} > 0$$

The natural independent thermodynamic variables for the Helmholtz free energy are seen to be T and V; that is, $A' = A'(T,V')$.

Consider a crystalline solid in equilibrium with its vapor (Figure 5.1b), the system being at constant volume and its pressure is below that of its triple point (see Figure 1.4). Since the slope of the solid vapor PT curve is positive, if the temperature is decreased, the vapor pressure must decrease in order to keep the two phases in equilibrium. This is done by decreasing the number of atoms in the gas. These atoms attach themselves to the solid. The *internal energy* of the two-phase system thus decreases and the entropy of the two-phase system approaches the entropy of the solid phase, since the vapor phase vanishes (Figures 5.1a and 5.2a).

On the other hand, as the temperature of the system becomes very high, the solid phase gives up atoms to the vapor phase and the solid eventually disappears, maximizing the entropy of the system (Figure 5.1c). At intermediate temperatures, there is an equilibrium between the vapor and solid phases. The number of atoms in the vapor phase in equilibrium with the solid can be determined from a plot of the Helmholtz energy versus n_v, since the Helmholtz energy is a minimum at equilibrium (Figure 5.3). This plot shows that the equilibrium is a trade-off between the system minimizing its internal energy, U', and maximizing its entropy. As the temperature rises from T_1 to T_2 (Figure 5.4), the minimum in the Helmholtz energy moves to a larger number of atoms in the vapor—namely, $n_v(T_2) > n_v(T_1)$. Eventually, at the limit of very high temperature, all the atoms are in the vapor phase. It should also be noted that the schematic plot of the Helmholtz free energy shows that its slope at $n_v = 0$ is large and negative, meaning for all temperatures >0 K, there will be a finite number of atoms in the vapor phase in equilibrium with the solid.

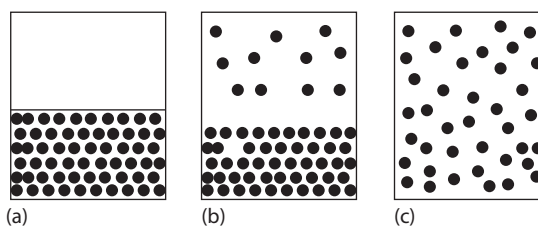

FIGURE 5.1 Schematic of a crystalline solid and its vapor at three different temperatures, where the pressure is below its triple point. (a) $T = 0$ K, (b) $0 < T$, (c) T very large. The volume of the system is fixed.

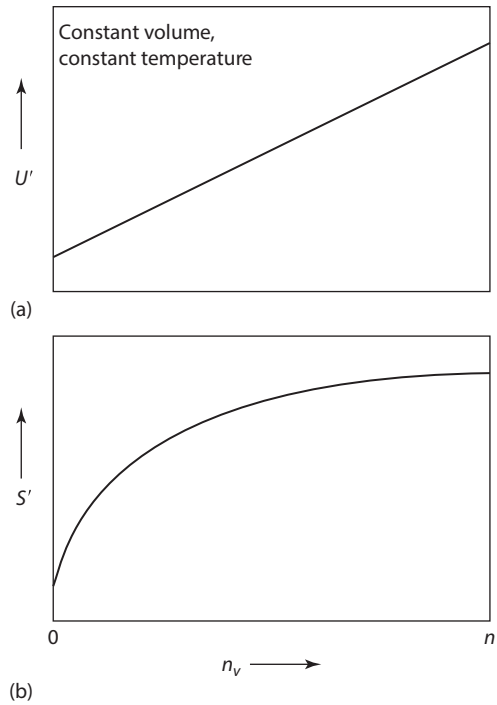

FIGURE 5.2 The variations of (a) internal energy, U', and (b) entropy, S', with the number of atoms in the vapor phase of a closed solid-vapor system at constant temperature and constant volume.

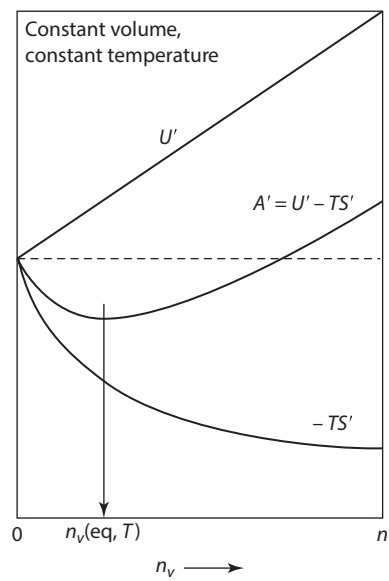

FIGURE 5.3 Illustration of the criterion for equilibrium in a closed solid-vapor system at constant temperature and constant volume.

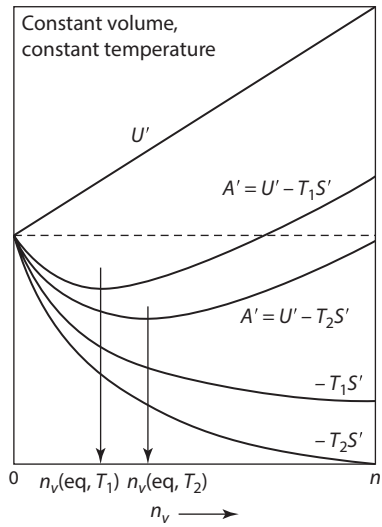

FIGURE 5.4 The influence of temperature on the equilibrium state of a closed solid-vapor system of constant volume.

5.4 THE GIBBS FREE ENERGY, *G*

The Gibbs free energy is defined as

$$G' \equiv H' - TS'$$

For a system of one mole, undergoing a change of state from 1 to 2, this yields

$$\begin{aligned}(G_2 - G_1) &= (H_2 - H_1) - (T_2S_2 - T_1S_1) \\ &= (U_2 - U_1) + (P_2V_2 - P_1V_1) - (T_2S_2 - T_1S_1)\end{aligned}$$

For a closed simple system, the First Law gives

$$(U_2 - U_1) = q - w$$

and thus,

$$(G_2 - G_1) = q - w + (P_2V_2 - P_1V_1) - (T_2S_2 - T_1S_1) \tag{5.6}$$

If the process is carried out such that $T_1 = T_2 = T$, which is the temperature of the heat reservoir that supplies or withdraws thermal energy from the system, and also, if $P_1 = P_2 = P$, which is the constant pressure at which the system undergoes a change in volume, then

$$(G_2 - G_1) = q - w + P(V_2 - V_1) - T(S_2 - S_1)$$

In the expression for the First Law, the work w is the *total* work done on or by the system during the process. Thus, if the system performs chemical, magnetic, or electrical work in addition to the work of expansion against the external pressure, then these work terms are included in w. Thus, w can be expressed as

$$w = w' + P(V_2 - V_1)$$

where:

$P(V_2 - V_1)$ is the P-V work done by the change in volume at the constant pressure P and w' is the sum of all of the *non–P-V* forms of work done

Substituting into Equation 5.6 gives

$$(G_2 - G_1) = q - w' - T(S_2 - S_1)$$

and again, since

$$q \le T(S_2 - S_1)$$

then

$$w' \le -(G_2 - G_1) \tag{5.7}$$

The equality can be written as

$$-w' = (G_2 - G_1) + T\Delta S_{\text{irr}}$$

Thus, for an isothermal, isobaric process, during which no form of work other than P-V work is performed (i.e., $w' = 0$),

$$(G_2 - G_1) + T\Delta S_{\text{irr}} = 0 \tag{5.8}$$

Such a process can only occur spontaneously (with a consequent increase in entropy) if the Gibbs free energy decreases. Since $\Delta S_{\text{irr}} = 0$ is a criterion for thermodynamic equilibrium, then an increment of an isothermal isobaric process occurring at equilibrium requires that

$$dG = 0 \tag{5.9}$$

Thus, for a system undergoing a process at constant T and constant P, the Gibbs free energy can only decrease or remain constant, and the attainment of equilibrium in the system coincides with the system having the minimum value of G consistent with the values of P and T; that is,

$$dG_{T,P} = 0 \quad \text{and} \quad d^2G_{T,P} > 0$$

This criterion of equilibrium, which is of considerable practical use, will be used extensively in the subsequent chapters.

5.5 THE FUNDAMENTAL EQUATIONS FOR A CLOSED SYSTEM

Using the aforementioned definitions for H, A, and G, we have the following four fundamental equations for one mole of a closed simple system:

$$dU = TdS - PdV \tag{5.10a}$$

$$dH = TdS + VdP \tag{5.10b}$$

$$dA = -SdT - PdV \tag{5.10c}$$

$$dG = -SdT + VdP \tag{5.10d}$$

As indicated earlier, work terms in addition to work against pressure may also be present. This adds terms to the fundamental equations. For example, if the system is also under the influence of an applied magnetic field, the work performed on the system is $V\mu_0 \boldsymbol{H}d\boldsymbol{M}$ (V is the molar volume) and must be added to the combined First and Second Laws expression (Equation 3.12) to obtain:

$$dU' = TdS' - PdV' + V'\mu_0 \mathcal{H} d\boldsymbol{M} \tag{5.11a}$$

The other three forms of the fundamental equation become[2]

$$dH' = TdS' + V'dP - V'\mu_0 \boldsymbol{M} d\mathcal{H} \tag{5.11b}$$

$$dA' = -S'dT - PdV' + V'\mu_0 \mathcal{H} d\boldsymbol{M} \tag{5.11c}$$

$$dG' = -S'dT + V'dP - V'\mu_0 \boldsymbol{M} d\mathcal{H} \tag{5.11d}$$

Let us look at the fundamental equation which uses G' as the dependent variable and temperature, pressure, and magnetic field as the *independent intensive variables.*

$$dG' = -S'dT + V'dP - V'\mu_0 \boldsymbol{M} d\mathcal{H}$$

The slope of the curve of the Gibbs free energy, G, versus temperature, T, at constant pressure and applied magnetic field, $\mathcal{H}$, is:

$$\left(\frac{\partial G'}{\partial T}\right)_{P,\mathcal{H}} = -S'$$

[2] The forms shown here are consistent with the modern texts of thermodynamics, using: $H = U + PV - V\mu_0 M d\mathcal{H}$; $A = U - TS$, and $G = H - TS$. See R. C. O'Handley, *Modern Magnetic Materials: Principles and Applications*, John Wiley, New York, 2000; and J. M. D. Coey, *Magnetism and Magnetic Materials*, Cambridge University Press, Cambridge, UK, 2010. Also see Appendix C.

The curvature of G versus T at constant pressure is proportional to

$$\left(\frac{\partial^2 G'}{\partial T^2}\right)_{P,\mathcal{H}}$$

which is

$$\left(\frac{\partial^2 G'}{\partial T^2}\right)_{P,\mathcal{H}} = -\left(\frac{\partial S'}{\partial T}\right)_{P,\mathcal{H}} = -\left(\frac{C_{P,\mathcal{H}}}{T}\right) < 0 \tag{5.12}$$

When there is no applied magnetic field, this reduces to the following equation:

$$\left(\frac{\partial^2 G'}{\partial T^2}\right)_{P} = -\left(\frac{\partial S'}{\partial T}\right)_{P} = -\left(\frac{C_P}{T}\right) < 0 \tag{5.13}$$

Since the heat capacity must be positive, the curvature of the G versus T plot is negative.

5.6 THE VARIATION OF THE COMPOSITION WITHIN A CLOSED SYSTEM

Thus far we have restricted our considerations to closed systems which were of fixed composition. In such cases, it was found that simple systems have two independent variables which, when fixed, uniquely determine the state of the system.

However, a closed system of a fixed amount of matter can still have changes in the composition of the phases that compose the system. The number of moles of the various species present can change as a consequence of a chemical reaction occurring in the system. Also, new phases can be formed by chemical reaction. Thus, the minimization of G at constant P and T occurs when the system has a unique number or ratio of moles of each phase. For example, if the system contains the gaseous species CO, CO_2, H_2, and H_2O, then, at constant T and P, the minimization of G will occur only when the reaction equilibrium $CO + H_2O = CO_2 + H_2$ is established (Figure 5.5). The oxide of carbon changes its composition, but the overall number of C, O, and H atoms stays the same in the container of the reacting gases.

5.7 THE CHEMICAL POTENTIAL

The Gibbs free energy of a simple closed system with no chemical reactions depends only on the temperature and the pressure. If the system is an open system, since the Gibbs free energy is an *extensive property*, its value is dependent on the amount of matter of the system. It is therefore necessary that the number of moles within the open system be specified. The Gibbs free energy is thus a function of the intensive thermodynamic variables T, P, and the *numbers* of moles of all of the species; that is,

$$G' = G'\left(T, P, n_i, n_j, n_k, \ldots\right) \tag{5.14}$$

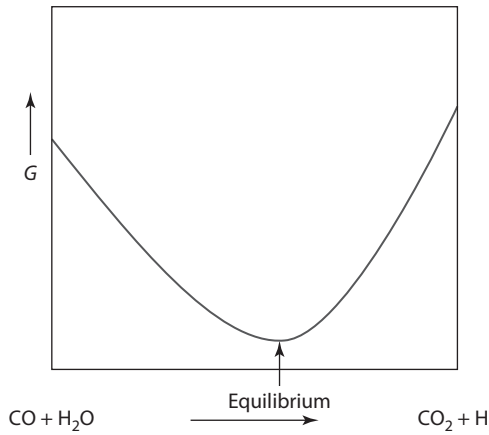

FIGURE 5.5 Schematic of the Gibbs free energy vs. degree of reaction completion for the $CO + H_2O \leftrightarrow CO_2 + H_2$ reaction.

in which G' is the total Gibbs free energy, and n_i, n_i, n_k, … are the numbers of moles of the species i, j, k, … present in the system.

The thermodynamic state of the system is only fixed when all of the independent variables are fixed. Differentiating Equation 5.14 gives

$$dG' = \left(\frac{\partial G'}{\partial T}\right)_{P,n_i,n_j,\ldots} dT + \left(\frac{\partial G'}{\partial P}\right)_{T,n_i,n_j,\ldots} dP + \sum_{i=1}^{i=k}\left(\frac{\partial G'}{\partial n_i}\right)_{T,P,n_j,\ldots} dn_i \qquad (5.15)$$

where

$$\sum_{i=1}^{i=k}\left(\frac{\partial G'}{\partial n_i}\right)_{T,P,n_j,\ldots} dn_i \qquad (5.16)$$

is the sum of k terms (one for each of the k species), each of which is determined by the partial differentiation of G' with respect to the number of moles of the ith species at constant T, P, and n_j, where n_j represents the numbers of moles of every species other than the ith species.

The term $\left(\partial G' / \partial n_i\right)_{T,P,n_j,\ldots}$ is called the *chemical potential* of species i, and is usually denoted as μ_i.

The chemical potential of the ith species in a homogeneous phase is thus the incremental change of the Gibbs free energy that accompanies an incremental increase of the species to the system at constant temperature, pressure, and numbers of moles of all of the other species. It is an *intensive thermodynamic variable*, and at equilibrium, the value of μ_i is the same in each of the phases that are present.

Alternatively, we can think of the chemical potential as follows: if the system is large enough that the addition of one mole of the ith species at constant temperature and pressure does not measurably change the composition of the system, then μ_i is

the change in the Gibbs free energy of the system caused by the addition of one mole of the *i*th species.

Equation 5.14 can be written as

$$dG' = -S'dT + V'dP + \sum_{1}^{k} \mu_i dn_i \tag{5.17}$$

in which G' is expressed as a function of T, P, the numbers of moles of each substance and the chemical potential μ_i of each species. Equation 5.17 can thus be applied to *open systems*, which exchange *matter* as well as *thermal energy* with their surroundings, and to *closed* systems, which undergo changes in composition caused by chemical reactions (Section 5.6).

Similarly, Equations 5.10a–c can be made applicable to open systems by including the terms describing the dependences on the composition of, respectively, U', H', and A':

$$dU' = TdS' - PdV' + \sum_{1}^{k} \left(\frac{\partial U'}{\partial n_i} \right)_{S,V,n_j,\ldots} dn_i \tag{5.18}$$

$$dH' = TdS' + V'dP + \sum_{1}^{k} \left(\frac{\partial H'}{\partial n_i} \right)_{S,P,n_j,\ldots} dn_i \tag{5.19}$$

$$dA' = -S'dT - PdV' + \sum_{1}^{k} \left(\frac{\partial A'}{\partial n_i} \right)_{T,V,n_j,\ldots} dn_i \tag{5.20}$$

Inspecting Equations 5.17 through 5.20 shows that

$$\mu_i = \left(\frac{\partial G'}{\partial n_i} \right)_{T,P,n_j} = \left(\frac{\partial U'}{\partial n_i} \right)_{S,V,n_j} = \left(\frac{\partial H'}{\partial n_i} \right)_{S,P,n_j} = \left(\frac{\partial A'}{\partial n_i} \right)_{T,V,n_j} \tag{5.21}$$

Note that the thermodynamic variables held constant in the partial derivatives of each of the energy functions are the *natural thermodynamic* variables of the specific energy in question.

Hence, the complete set of equations for open systems with only *P-V* work is as follows:

$$dU' = TdS' - PdV' + \Sigma \mu_i dn_i \tag{5.22}$$

$$dH' = TdS' + V'dP + \Sigma \mu_i dn_i \tag{5.23}$$

$$dA' = -S'dT - PdV' + \Sigma \mu_i dn_i \tag{5.24}$$

$$dG' = -S'dT + V'dP + \Sigma \mu_i dn_i \tag{5.25}$$

From Equations 5.22–5.25, we have the following:

- U' is the characteristic thermodynamic potential (state function) of the independent extensive variables S, V', and composition; that is, $U' = U'(S', V', n_i)$.
- H' is the characteristic thermodynamic potential (state function) of the independent variables S', P, and composition; that is, $H' = H'(S', P, n_i)$.
- A' is the characteristic thermodynamic potential (state function) of the independent variables T, V', and composition; that is, $A' = A'(T, V', n_i)$.
- G' is the characteristic thermodynamic potential (state function) of the independent intensive variables T, P, and composition; that is, $G' = G'(T, P, n_i)$.

Although all four of the preceding equations are basic in nature, Equation 5.25 is sometimes called ***the*** *fundamental equation* because of its practical usefulness.

A comparison of the First Laws

$$dU' = \delta q - \delta w$$

With Equation 5.18, indicates that, for a closed system undergoing a process involving a reversible change in composition (e.g., a reversible chemical reaction),

$$\delta q = TdS'$$

and

$$\delta w = PdV' - \Sigma \mu_i dn_i$$

The term $-\Sigma \mu_i dn_i$ is the *chemical work* done by the system, which was included as w' in Equation 5.7, and the total work w is the sum of the *P-V* work and the chemical work. Gibbs introduced this important term to thermodynamics in 1875.[3]

5.8 THERMODYNAMIC RELATIONS

Including the chemical potential terms in Equations 5.11a–d yields an open system:

$$dU' = TdS' - PdV' + V'\mu_0 \mathcal{H} d\boldsymbol{M} + \Sigma \mu_i dn_i$$

$$dH' = TdS' + V'dP - V'\mu_0 \boldsymbol{M}\, d\mathcal{H} + \Sigma \mu_i dn_i$$

$$dA' = -S'dT - PdV' + V'\mu_0 \mathcal{H} d\boldsymbol{M} + \Sigma \mu_i dn_i$$

[3] J. W. Gibbs, "On the Equilibrium of Heterogeneous Substances," *Trans. Conn. Acad.* (1875), vol. 3, pp. 108–248 See page 116 (Equation 12).

$$dG' = -S'dT + V'dP - V'\mu_0 \boldsymbol{M} d\boldsymbol{\mathcal{H}} + \Sigma \mu_i dn_i$$

The *intensive* thermodynamic state variables T, P, $\boldsymbol{\mathcal{H}}$, and μ_i are equal to the derivatives of an energy potential with respect to their *conjugate extensive* variables, S, V, $\boldsymbol{M}$, and n_i, respectively:

$$T = \left(\frac{\partial U'}{\partial S'}\right)_{V,M,n_i} = \left(\frac{\partial H'}{\partial S'}\right)_{P,H,n_i} \tag{5.26}$$

$$P = -\left(\frac{\partial U'}{\partial V'}\right)_{S,M,n_i} = -\left(\frac{\partial A'}{\partial V'}\right)_{T,M,n_i} \tag{5.27}$$

$$\boldsymbol{H} = \frac{1}{\mu_0 V'}\left(\frac{\partial U'}{\partial \boldsymbol{M}}\right)_{V,S,n_i} = \frac{1}{\mu_0 V'}\left(\frac{\partial A'}{\partial \boldsymbol{M}}\right)_{V,T,n_i} \tag{5.28}$$

$$\mu_i = \left(\frac{\partial G'}{\partial n_i}\right)_{T,P,n_j} = \left(\frac{\partial U'}{\partial n_i}\right)_{S,V,n_j} = \left(\frac{\partial H'}{\partial n_i}\right)_{S,P,n_j} = \left(\frac{\partial A'}{\partial n_i}\right)_{T,V,n_j} \tag{5.21}$$

Also, the *extensive* thermodynamic state functions are derivatives of a thermodynamic potential (energy) function with respect to their *conjugate intensive* state variables:

$$S' = -\left(\frac{\partial A'}{\partial T}\right)_{V,\boldsymbol{M},\text{comp}} = -\left(\frac{\partial G'}{\partial T}\right)_{P,\boldsymbol{M},\text{comp}} \tag{5.29}$$

$$V' = \left(\frac{\partial H'}{\partial P}\right)_{S,\boldsymbol{H},\text{comp}} = \left(\frac{\partial G'}{\partial P}\right)_{T,\boldsymbol{H},\text{comp}} \tag{5.30}$$

$$\boldsymbol{M} = -\frac{1}{\mu_0 V'}\left(\frac{\partial H'}{\partial \boldsymbol{\mathcal{H}}}\right)_{P,S,\text{comp}} = -\frac{1}{\mu_0 V'}\left(\frac{\partial G'}{\partial \boldsymbol{\mathcal{H}}}\right)_{P,T,\text{comp}} \tag{5.31}$$

5.9 MAXWELL'S RELATIONS

If Z is a state function and x and y are chosen as the independent thermodynamic variables in a closed system of fixed composition, then we write

$$Z = Z(x, y)$$

differentiation of which gives

$$dZ = \left(\frac{\partial Z}{\partial x}\right)_y dx + \left(\frac{\partial Z}{\partial y}\right)_x dy$$

(See also Appendix B, Criteria for an exact differential)

If the partial derivative $\left(\partial Z/\partial x\right)_y$ is itself a function of x and y, being given by $\left(\partial Z/\partial x\right)_y = L\left(x,y\right)$, and similarly, the partial derivative $\left(\partial Z/\partial y\right)_x = M\left(x,y\right)$, then

$$dZ = Ldx + Mdy$$

Thus,

$$\left[\frac{\partial}{\partial y}\left(\frac{\partial Z}{\partial x}\right)_y\right]_x = \left(\frac{\partial L}{\partial y}\right)_x$$

and

$$\left[\frac{\partial}{\partial x}\left(\frac{\partial Z}{\partial y}\right)_x\right]_y = \left(\frac{\partial M}{\partial x}\right)_y$$

But, since Z is a state function, the change in Z is independent of the order of differentiation; that is,

$$\left[\frac{\partial}{\partial y}\left(\frac{\partial Z}{\partial x}\right)_y\right]_x = \left[\frac{\partial}{\partial x}\left(\frac{\partial Z}{\partial y}\right)_x\right]_y = \frac{\partial^2 Z}{\partial x\,\partial y}$$

and hence,

$$\left(\frac{\partial L}{\partial y}\right)_x = \left(\frac{\partial M}{\partial x}\right)_y$$

Previously, the following equations of state for one mole of a closed simple system were seen to be:

$$dU = TdS - PdV \tag{3.12}$$

$$dH = TdS + VdP \tag{5.10b}$$

$$dA = -SdT - PdV \tag{5.10c}$$

$$dG = -SdT + VdP \tag{5.10d}$$

These equations yield the following Maxwell relations:

$$\left(\frac{\partial T}{\partial V}\right)_S = -\left(\frac{\partial P}{\partial S}\right)_V \tag{5.32}$$

$$\left(\frac{\partial T}{\partial P}\right)_S = \left(\frac{\partial V}{\partial S}\right)_P \tag{5.33}$$

$$\left(\frac{\partial S}{\partial V}\right)_T = \left(\frac{\partial P}{\partial T}\right)_V \tag{5.34}$$

$$\left(\frac{\partial S}{\partial P}\right)_T = -\left(\frac{\partial V}{\partial T}\right)_P \tag{5.35}$$

Additional Maxwell relations can be obtained by considering systems with variations in composition or with additional work terms (for example magnetic terms. See Problems 5.14 and 5.15).

The value of the preceding Maxwell relations lies in the fact that they contain many experimentally measurable quantities that can be used to determine quantities that are not easy to measure directly. For example, Equation 5.35 shows that increasing the pressure on a material at constant temperature changes the entropy of the material by an amount that is proportional to $-\alpha_P V dP$.

5.10 EXAMPLES OF THE APPLICATION OF MAXWELL RELATIONS

The entropy of a simple system can be written as a function of any two of the thermodynamic variables *T*, *V*, and *P*. We now look at each of these.

5.10.1 The First *TdS* Equation

Consider the dependence of the entropy of one mole of a substance on the independent variables *T* and *V*.

$$S = S(T,V) \tag{5.36}$$

differentiation of which gives

$$dS = \left(\frac{\partial S}{\partial T}\right)_V dT + \left(\frac{\partial S}{\partial V}\right)_T dV \tag{5.37}$$

At constant volume, the First Law can be written as

$$TdS = \delta q_v = dU = c_v dT \tag{5.38}$$

The partial derivative components of Equation 5.37 are:

$$\left(\frac{\partial S}{\partial T}\right)_V = \frac{c_v}{T} \text{ and } \left(\frac{\partial S}{\partial V}\right)_T = \left(\frac{\partial P}{\partial T}\right)_V$$

The second one is obtained from the Maxwell relation of Equation 5.34.

Thus, Equation 5.37 can be written as

$$dS = \frac{c_v}{T}dT + \left(\frac{\partial P}{\partial T}\right)_V dV \tag{5.39}$$

Multiplying the Equation 5.39 by T, the following is obtained.

$$TdS = c_v dT + T\left(\frac{\partial P}{\partial T}\right)_V dV \tag{5.40}$$

This equation is called the first TdS equation by Zemansky.[4] The term $\left(\partial P/\partial T\right)_v$ can be shown to equal α_P / β_T. So, the equation can be written as

$$TdS = c_v dT + \frac{T\alpha_P}{\beta_T}dV \tag{5.41}$$

We have the following cases, assuming that $\alpha_P > 0$

- For an *isothermal expansion*: $\Delta S = \int \frac{\alpha_P}{\beta_T}dV > 0$
- If the temperature is raised at constant volume: $\Delta S = \int \frac{c_v}{T}dT > 0$
- For an *isentropic expansion*:

$$0 = c_v dT + \frac{T\alpha_P}{\beta_T}dV$$

$$\left(\frac{dT}{dV}\right)_S = -\frac{T\alpha_P}{c_v\beta_T} < 0$$

This may at first glance seem to be incorrect, as we may think that increasing T should increase V and thus $\left(\frac{dT}{dV}\right)_S$ should be positive. But the derivative is taken at constant entropy, so if we increase T, we must decrease V to keep the entropy constant, and hence, the term $\left(\frac{dT}{dV}\right)_S$ is indeed negative.

If the substance is one mole of an ideal gas, we can write

$$\left(\frac{\partial P}{\partial T}\right)_V = \frac{R}{V} \tag{5.42}$$

and thus, Equation 5.39 can be written as

$$dS = \frac{c_v}{T}dT + \frac{R}{V}dV \tag{5.43}$$

[4] M. W. Zemansky, *Heat and Thermodynamics*, McGraw-Hill, New York, 1957.

the integration of which (assuming constant c_v) between the states 1 and 2 gives, for an ideal gas,

$$S_2 - S_1 = c_v \ln\left(\frac{T_2}{T_1}\right) + R\ln\left(\frac{V_2}{V_1}\right) \tag{5.44}$$

From Equation 5.44 we have the following three special cases for one mole of an ideal gas:

- For an *isothermal expansion* of an ideal gas:

$$\Delta S_{\text{gas}} = R\ln\left(\frac{V_2}{V_1}\right)$$

- If the temperature of an ideal gas is raised at constant volume:

$$\Delta S_{\text{gas}} = c_v \ln\left(\frac{T_2}{T_1}\right)$$

- For an *isentropic expansion* of an ideal gas:

$$S_2 - S_1 = 0, \text{ and thus, } c_v \ln\left(\frac{T_2}{T_1}\right) = -R\ln\left(\frac{V_2}{V_1}\right)$$

and since $\gamma = c_P/c_V$ and $c_P - c_V = R$, for an ideal gas, we obtain (cf. Section 2.7)

$$\frac{T_2}{T_1} = \left(\frac{V_1}{V_2}\right)^{\gamma-1}$$

5.10.2 The Second *TdS* Equation

Consider the dependence of the entropy of one mole of a substance on the independent variables T and P:

$$S = S(T, P)$$

differentiation of which gives

$$dS = \left(\frac{\partial S}{\partial T}\right)_P dT + \left(\frac{\partial S}{\partial P}\right)_T dP \tag{5.45}$$

But $\left(\frac{\partial S}{\partial T}\right)_P = \frac{c_P}{T}$ and, by Equation 5.35, $\left(\frac{\partial S}{\partial P}\right)_T = -\left(\frac{\partial V}{\partial T}\right)_P$

Using these relations, we can write Equation 5.45 in the form of the second *TdS* equation:

$$TdS = c_P dT - T\left(\frac{\partial V}{\partial T}\right)_P dP = c_P dT - \alpha_P VTdP \tag{5.46}$$

We have the following cases, assuming that $\alpha_P > 0$

- For an isothermal reversible change of pressure:

$$dS = -\alpha_P VdP$$

  which shows that an increase in P at constant T decreases the entropy of the substance (cf. Equation 5.35).
- For an isobaric reversible change in temperature:

$$dS = c_P \frac{dT}{T}$$

$$\Delta S = \int c_P \frac{dT}{T} = c_P \ln \frac{T_2}{T_1} \quad \text{over a range where } c_P \text{ is constant}$$

  Thus, increasing the temperature at constant pressure increases the entropy of the substance.
- For an isentropic process:

$$dS = 0 = \frac{c_P}{T} dT - \alpha_P VdP$$
$$\therefore \left(\frac{dT}{dP}\right)_S = \frac{\alpha_P VT}{c_P}$$

  This shows that if the entropy is held constant, and the temperature is raised, the pressure is also raised if $\alpha_P > 0$.

  These cases reduce to the following when we consider 1 mole of an ideal gas:
- For an isothermal reversible change of pressure of an ideal gas:

$$dS = -\alpha_P VdP = -\frac{V}{T} dP = -\frac{R}{P} dP$$
$$\Delta S_T = -R \ln \frac{P_2}{P_1} = R \ln \frac{P_1}{P_2} = R \ln \frac{V_2}{V_1}$$

- For an isobaric reversible change in temperature of an ideal gas:

$$\Delta S = c_P \ln \frac{T_2}{T_1} = \frac{5}{2} R \ln \frac{T_2}{T_1} = \frac{5}{2} R \ln \frac{V_2}{V_1}$$

- For an isentropic process of an ideal gas:

$$\frac{c_P}{T}dT = \alpha_P V dP$$

$$\left(\frac{dT}{dP}\right)_S = \frac{\alpha_P VT}{c_P} = \frac{V}{c_P}$$

Thus, if an ideal gas increases in temperature at constant entropy, the pressure must also increase. This can be rationalized as follows: increasing the temperature would increase the entropy of the gas, so the pressure must increase to keep the entropy constant.

5.10.3 The Third *TdS* Equation

Consider the dependence of the entropy of one mole of a substance on the independent variables *P* and *V*.

$$S = S(P,V)$$

Differentiation of which yields

$$dS = \left(\frac{\partial S}{\partial P}\right)_V dP + \left(\frac{\partial S}{\partial V}\right)_P dV \tag{5.47}$$

$$\text{But} \quad \left(\frac{\partial S}{\partial P}\right)_V = -\left(\frac{\partial V}{\partial T}\right)_S \quad \text{and} \quad \left(\frac{\partial S}{\partial V}\right)_P = \left(\frac{\partial P}{\partial T}\right)_S$$

$$\text{From the first } TdS \text{ equation :} \quad \left(\frac{\partial V}{\partial T}\right)_S = -\frac{c_V \beta_T}{T\alpha_P}$$

$$\text{From the second } TdS \text{ equation :} \quad \left(\frac{\partial P}{\partial T}\right)_S = \frac{c_P}{TV\alpha_P}$$

$$\text{Finally :} \quad TdS = \frac{c_V \beta_T}{\alpha_P} dP + \frac{c_P}{V\alpha_P} dV \tag{5.48}$$

which is the third *TdS* equation.

We have the following cases, assuming that $\alpha_P > 0$

- For an isobaric change of volume:

$$TdS = \frac{c_P}{V\alpha_P} dV$$

which shows that increasing the volume of a material at constant pressure increases the entropy, that is $\left(\frac{\partial S}{\partial V}\right)_P = \quad \frac{c_P}{} \quad > 0$

- For a constant volume change in pressure, the entropy of the material increases with increasing pressure, that is $\left(\frac{\partial S}{\partial P}\right)_V = \frac{c_V \beta_T}{T \alpha_P} > 0$
- For an isentropic process:

$$\frac{c_V \beta_T}{\alpha_P} dP = -\frac{c_P}{V \alpha_P} dV$$

$$\text{and therefore} \quad \left(\frac{\partial P}{\partial V}\right)_S = -\frac{c_P}{c_V V \beta_T} < 0$$

which shows that increasing pressure decreases the volume (as expected) at constant entropy.

These cases reduce to the following when we consider one mole of an ideal gas:

- For an isobaric change of volume, one mole of a monoatomic ideal gas:

$$\left(\frac{\partial S}{\partial V}\right)_P = \frac{c_P}{V} = \frac{5}{2}\frac{R}{V}$$

$$\text{Thus}: \ \Delta S_P = \frac{5}{2} R \ln \frac{V_2}{V_1}$$

- At constant volume, the change in the entropy of one mole of a monoatomic ideal gas changing its pressure from P_1 to P_2 is calculated to be:

$$\left(\frac{\partial S}{\partial P}\right)_V = \frac{3}{2} R: \quad \Delta S_V = \frac{3}{2} R \ln \frac{P_2}{P_1}$$

The increase in entropy with an increase in pressure is due to the increase in the temperature of the gas.

- For an isentropic process, the value of $\left(\frac{\partial P}{\partial V}\right)_S$ is seen to be:

$$\left(\frac{\partial P}{\partial V}\right)_S = -\frac{5}{3}\frac{P}{V} < 0$$

For a diatomic ideal gas $\left(\frac{\partial P}{\partial V}\right)_S = -\frac{7}{5}\frac{P}{V} < 0$

5.10.4 Entropy and Volume as Dependent Variables and Temperature and Pressure as Independent Variables

We can write the entropy and the volume of one mole of one-component simple system as a function of the intensive variables T and P (i.e., $S = S(T, P)$ and $V = V(T, P)$) and obtain the following equations to first order:

$$dS = \left(\frac{\partial S}{\partial T}\right)_P dT + \left(\frac{\partial S}{\partial P}\right)_T dP$$
$$dV = \left(\frac{\partial V}{\partial T}\right)_P dT + \left(\frac{\partial V}{\partial P}\right)_T dP$$

But we know that

$$\left(\frac{\partial S}{\partial T}\right)_P = \frac{c_P}{T}, \quad \left(\frac{\partial V}{\partial T}\right)_P = \alpha_P V, \quad \text{and} \quad \left(\frac{\partial V}{\partial P}\right)_T = -V\beta_T$$

and by a Maxwell relation (Equation 5.35):

$$\left(\frac{\partial S}{\partial P}\right)_T = -\left(\frac{\partial V}{\partial T}\right)_P = -\alpha_P V$$

Thus, we can write

$$\begin{aligned} dS &= \frac{c_P}{T} dT - \alpha_P V dP \\ dV &= \alpha_P V dT - V\beta_T dP \end{aligned} \tag{5.49}$$

or, in matrix notation:

$$\begin{pmatrix} dS \\ dV \end{pmatrix} = \begin{pmatrix} \frac{c_P}{T} & -\alpha_P V \\ \alpha_P V & -V\beta_T \end{pmatrix} \begin{pmatrix} dT \\ dP \end{pmatrix} \tag{5.50}$$

This set of equations shows that the response of a material to a rise in temperature at constant pressure is twofold: the entropy changes by an amount proportional to the material's heat capacity and the volume changes by an amount proportional to the coefficient of expansion of the material. Furthermore, a change in the pressure of the system at constant temperature changes the material's volume by an amount which is proportional to the negative of its isothermal compressibility, while its entropy changes proportional to the negative of its coefficient of expansion. Figure 5.6 shows in diagrammatic form the relationship among the four thermodynamic variables under discussion.

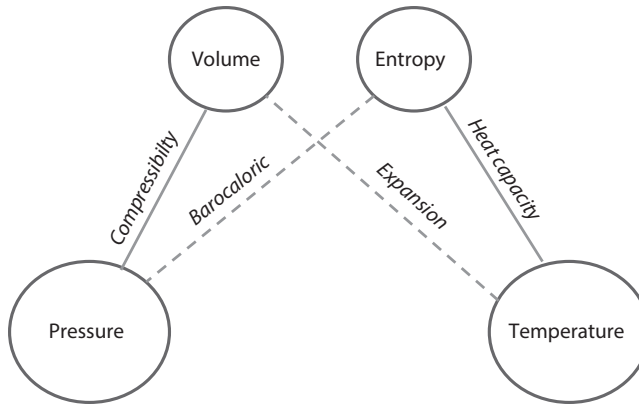

FIGURE 5.6 The intrinsic independent thermodynamic parameters T and P with their conjugate extrinsic thermodynamic parameters. Also shown are the properties that relate the various thermodynamic variables.

The matrix $\begin{pmatrix} \frac{c_P}{T} & -\alpha_P V \\ \alpha_P V & -V\beta_T \end{pmatrix}$ is sometimes called a property matrix. The terms along the diagonal represent *direct effect properties* where the conjugate variables are involved (T/S and P/V). The off diagonal terms measure the effect of one variable on another that is not its conjugate variable.

5.10.5 A Magnetic Maxwell Relation

As a final example, we obtain a Maxwell relation on the fundamental equation for a single-component material under the influence of an external magnetic field.

$$G' = G\left(T, P, \mathcal{H}\right)$$

$$dG' = -S'dT + V'dP - V'\mu_0 \boldsymbol{M} d\mathcal{H}$$

$$\left(\frac{\partial S'}{\partial \mathcal{H}}\right)_{T,P} = V'\mu_0 \left(\frac{\partial \boldsymbol{M}}{\partial T}\right)_{\mathcal{H},P}$$

Since increasing the applied field $\mathcal{H}$ decreases the spin entropy of a magnetic material, the plot of magnetization *versus* temperature must have a negative slope. We will use this equation later to discuss the magnetocaloric effect. The applied magnetic

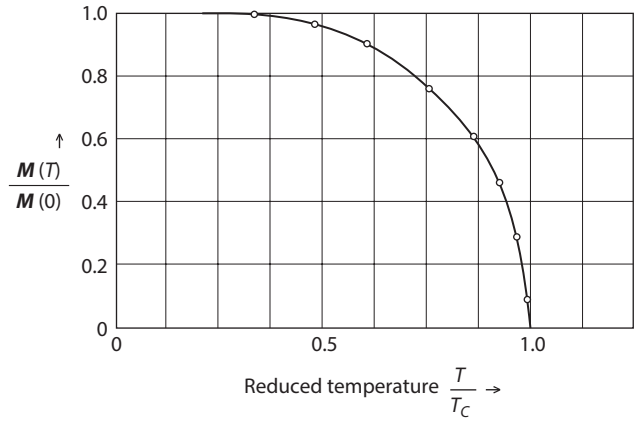

FIGURE 5.7 Reduced magnetization vs. reduced temperature for a magnetic material displaying a negative slope for $T > 0$.

field and the temperature oppose each other's effects on the ordering or disordering of the magnetic spins.

In ferromagnetic materials, the magnetization is an *order parameter* of the system. Above the Curie temperature (T_C), where the material is paramagnetic, $\boldsymbol{M} = 0$. Below the Curie temperature, the material is ferromagnetic, and with decreasing temperature the magnetization increases continuously until it reaches its maximum value, $\boldsymbol{M}(0)$ at 0 K. Thus, increasing the temperature of a ferromagnet decreases its magnetization and increases its entropy. Figure 5.7 plots $\boldsymbol{M}(T)/\boldsymbol{M}(0)$ versus T/T_C (the *reduced thermodynamic variables*). Note that on decreasing the temperature just below the Curie temperature the rate of increase in M is very high. The rate of change decreases until at 0 K the $\boldsymbol{M}$ vs. T plot has a zero slope. This is true for order parameters and is a consequence of the Third Law of Thermodynamics. See Chapter 6.

5.10.6 *S, V,* AND *M* AS DEPENDENT VARIABLES WITH INDEPENDENT VARIABLES *T, P,* AND $\mathcal{H}$

Writing the *extensive variables* entropy, volume, and magnetization for one mole of a one-component system as a function of the *intensive variables* T, P, and $\mathcal{H}$, yields the following:

$$
\begin{aligned}
dS &= \left(\frac{\partial S}{\partial T}\right)_{P,\mathcal{H}} dT + \left(\frac{\partial S}{\partial P}\right)_{T,\mathcal{H}} dP + \left(\frac{\partial S}{\partial \mathcal{H}}\right)_{T,P} d\mathcal{H} \\
dV &= \left(\frac{\partial V}{\partial T}\right)_{P,\mathcal{H}} dT + \left(\frac{\partial V}{\partial P}\right)_{T,\mathcal{H}} dP + \left(\frac{\partial V}{\partial \mathcal{H}}\right)_{T,P} d\mathcal{H} \\
d\boldsymbol{M} &= \left(\frac{\partial \boldsymbol{M}}{\partial T}\right)_{P,\mathcal{H}} dT + \left(\frac{\partial \boldsymbol{M}}{\partial P}\right)_{T,\mathcal{H}} dP + \left(\frac{\partial \boldsymbol{M}}{\partial \mathcal{H}}\right)_{T,P} d\mathcal{H}
\end{aligned}
\tag{5.51}
$$

These equations can be written in matrix form, as done previously for the two intensive variables case.

$$\begin{pmatrix} dS \\ dV \\ d\boldsymbol{M} \end{pmatrix} = \begin{pmatrix} \left(\frac{\partial S}{\partial T}\right)_{P,\mathcal{H}} & \left(\frac{\partial S}{\partial P}\right)_{T,\mathcal{H}} & \left(\frac{\partial S}{\partial \mathcal{H}}\right)_{T,P} \\ \left(\frac{\partial V}{\partial T}\right)_{P,\mathcal{H}} & \left(\frac{\partial V}{\partial P}\right)_{T,\mathcal{H}} & \left(\frac{\partial V}{\partial \mathcal{H}}\right)_{T,P} \\ \left(\frac{\partial \boldsymbol{M}}{\partial T}\right)_{P,\mathcal{H}} & \left(\frac{\partial \boldsymbol{M}}{\partial P}\right)_{T,\mathcal{H}} & \left(\frac{\partial \boldsymbol{M}}{\partial \mathcal{H}}\right)_{T,P} \end{pmatrix} \begin{pmatrix} dT \\ dP \\ d\mathcal{H} \end{pmatrix} \tag{5.52}$$

Each of the terms in the 3×3 matrix represents a property of the substance in question. The names of these properties are listed below as well as in Figure 5.8.

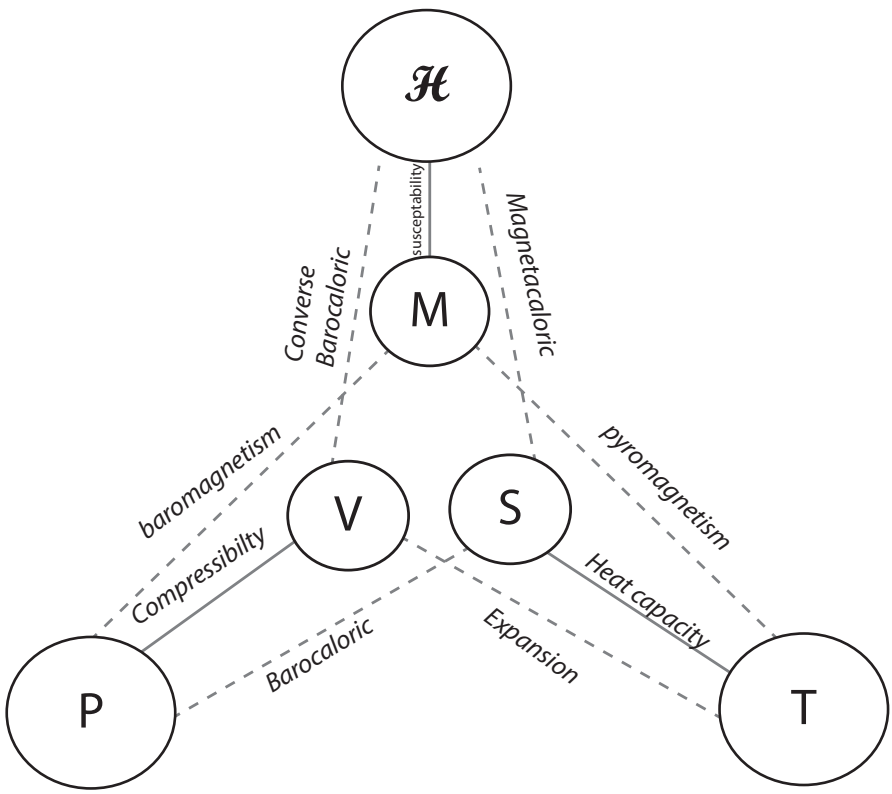

FIGURE 5.8 Diagram showing the intrinsic thermodynamic field variables T and P and $\mathcal{H}$ and their conjugate extrinsic thermodynamic variables, S, V, and $\boldsymbol{M}$. Also shown are the properties that relate the various thermodynamic variables.

Entropy related to the Temperature: heat capacity
Entropy related to the Pressure: barocaloric effect
Entropy related to the Magnetic Field: magnetocaloric effect
Volume related to the Temperature: thermal expansion
Volume related to the Pressure: the compressibility
Volume related to the Magnetic Field: converse baromagnetic effect
Magnetization related to the Temperature: pyromagnetism
Magnetization is related to the Pressure: baromagnetism
Magnetization is related to the Magnetic Field: susceptibility

It can be proved that the cross-diagonal terms are equal in absolute magnitude to each other (note that they are composed of Maxwell relations). As before the terms along the diagonal represent *direct effect properties* where the conjugate variables are involved (T/S, P/V and $\mathcal{H}/\boldsymbol{M}$). The off-diagonal terms measure the effect of variables on another that are not conjugate of each other and are sometimes called *indirect effects*.

The magnetocaloric effect will be discussed in more detail when we present the Third Law of Thermodynamics in Chapter 6. Now we will briefly introduce this important magnetic property.

Figure 5.9 shows Entropy *versus* Temperature plots for a paramagnetic material with and without an applied magnetic field, $\mathcal{H}$. The slope of the curves is positive $\left(\frac{\partial S}{\partial T}\right)_P = \frac{c_P}{T}$ and the curvature of the curves is positive as well. If we start at state R, where the spins in the paramagnet are *arrayed randomly*, and reversible and *isothermal* apply a magnetic field, $\mathcal{H}$, we end up at state A, where the spins are aligned and the entropy of the material is lower because of the decrease in its spin entropy.

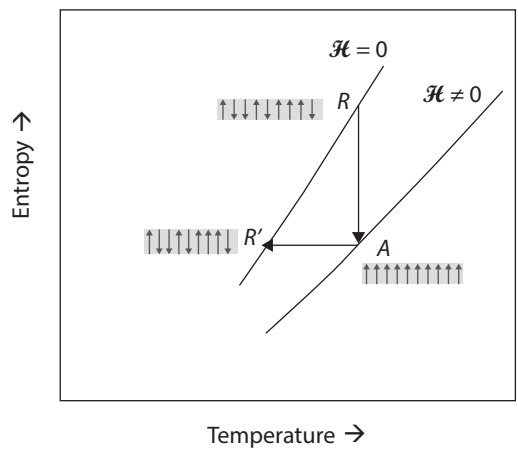

FIGURE 5.9 Entropy vs. temperature plots of a paramagnetic material with and without an applied magnetic field. A reversible isothermal process is shown as R to A, and a reversible adiabatic process is shown as A to R'.

During the application of the field, thermal energy left the material and was absorbed by the heat bath. Now, if the material is enclosed adiabatically, and the magnetic field is reversibly removed, the state goes from A to R′ where the spins are once again randomly arrayed. Since the process was reversible and adiabatic the total entropy of the material must stay constant. The spin entropy has increased however, necessitating a decrease in the thermal entropy of the material. The temperature of the paramagnet therefore decreases. This process is known as magnetocaloric cooling. It is another example of the importance of keeping the various aspects of entropy in mind when discussing changes of state.

Analogous processes can be performed by the pressure (barocaloric), by applied stress fields (mechanocaloric), or by electric fields (electrocaloric) in the case of nonconductors. Care must be taken to take into account the orientation of the sample with respect to the tensorial applied fields, as well as any internal anisotropies of the material.

5.11 AN ENERGY EQUATION (INTERNAL ENERGY)

Another use of the Maxwell's relations is as follows. For one mole of a closed system of fixed composition, Equation 3.12 gives

$$dU = TdS - PdV$$

Thus,

$$\left(\frac{\partial U}{\partial V}\right)_T = T\left(\frac{\partial S}{\partial V}\right)_T - P$$

Using a Maxwell relation (Equation 5.33) allows this to be written as

$$\left(\frac{\partial U}{\partial V}\right)_T = T\left(\frac{\partial P}{\partial T}\right)_V - P \tag{5.53}$$

which is an *equation of state* relating the internal energy, U, of a closed system of fixed composition to the measurable quantities T, V, and P. If the system is one mole of ideal gas, substitution of Equations 5.42 into 5.53 gives $\left(\partial U / \partial V\right)_T = 0$, which shows that the internal energy of an ideal gas is independent of the volume of the gas.

5.12 ANOTHER ENERGY EQUATION (ENTHALPY)

Similarly, for one mole of a closed system of fixed composition, Equation 5.10b gives $dH = TdS + VdP$, in which case

$$\left(\frac{\partial H}{\partial P}\right)_T = T\left(\frac{\partial S}{\partial P}\right)_T + V$$

Substituting a Maxwell relation (Equation 5.35) gives

$$\left(\frac{\partial H}{\partial P}\right)_T = -T\left(\frac{\partial V}{\partial T}\right)_P + V \tag{5.54}$$

which is another *equation of state* which gives the dependence of enthalpy on the measurable quantities *T*, *P*, and *V*. Again, if the system is one mole of an ideal gas, this equation of state shows that the enthalpy of an ideal gas is independent of its pressure.

5.13 GIBBS–HELMHOLTZ EQUATIONS

Starting with the definition of the Gibbs free energy for one mole of a substance,

$$G = H - TS$$

dividing by T and taking the derivative of both sides with respect to T at constant pressure, the following is obtained:

$$\left(\frac{\partial\left(\frac{G}{T}\right)}{\partial T}\right)_P = \frac{1}{T}\left(\frac{\partial H}{\partial T}\right)_P - \frac{H}{T^2} - \left(\frac{\partial S}{\partial T}\right)_P$$

But,

$$\frac{1}{T}\left(\frac{\partial H}{\partial T}\right)_P = \frac{C_P}{T} \quad \text{and} \quad \left(\frac{\partial S}{\partial T}\right)_P = \frac{C_P}{T}$$

Thus, we obtain

$$\left(\frac{\partial\left(\frac{G}{T}\right)}{\partial T}\right)_P = -\frac{H}{T^2} \tag{5.55}$$

which is a form of what is called the *Gibbs–Helmholtz equation*. It is applicable to a closed system undergoing processes at constant pressure. It is used to determine changes in the Gibbs energy as a function of temperature.

For an isobaric change of state of a closed system of fixed composition, Equation 5.55 gives the relation of the change in G to the change in H as

$$\left(\frac{\partial\left(\frac{\Delta G}{T}\right)}{\partial T}\right)_P = -\frac{\Delta H}{T^2} \tag{5.56}$$

This equation is of particular use in experimental thermodynamics, as it allows ΔG to be obtained from a measurement of ΔH, *or conversely* ΔH, the heat of a reaction, to be obtained from a measurement of the variation of ΔG, the free energy change for the reaction, with temperature. The usefulness of this equation will be developed and applied later in the text to the calculation of *partial molar heats of solution* as well as to the calculation of the temperature variation of the equilibrium constants of reactions in systems.

The corresponding relationship between the Helmholtz free energy and the internal energy is obtained as follows:

$$A = U - TS$$

Dividing by T and performing a similar procedure gives

$$\left(\frac{\partial \left(\frac{A}{T} \right)}{\partial T} \right)_V = -\frac{U}{T^2} \tag{5.57}$$

This equation is applicable to closed systems of fixed composition undergoing processes at constant volume. As before, for a change of state under these conditions:

$$\left(\frac{\partial \left(\frac{\Delta A}{T} \right)}{\partial T} \right)_V = -\frac{\Delta U}{T^2} \tag{5.58}$$

5.14 SUMMARY

1. The Helmholtz free energy, A, is defined by $A \equiv U - TS$. In a closed system held at constant T and V, the Helmholtz free energy can only
   - Decrease, for a spontaneous process
   - Remain constant if the system is in equilibrium

   Equilibrium at constant T and V is attained when the Helmholtz free energy achieves its minimum value.
2. The Gibbs free energy, G, is defined by $G \equiv H - TS$. In a closed system at constant pressure and temperature, the Gibbs free energy is a minimum at equilibrium. During an isothermal, isobaric process during which no form of work other than P-V work is performed (i.e., $w' = 0$), G can only
   - Decrease for a spontaneous process
   - Remain constant if the system is in equilibrium

   Equilibrium is attained at constant T and P when the Gibbs free energy reaches its minimum value.
3. For a change of state at constant pressure, $\Delta H' = q_p$.
4. The chemical potential, μ_i, of the ith component can be expressed as

$$\mu_i = \left(\frac{\partial G'}{\partial n_i}\right)_{T,P,n_j} = \left(\frac{\partial U'}{\partial n_i}\right)_{S,V,n_j} = \left(\frac{\partial H'}{\partial n_i}\right)_{S,P,n_j} = \left(\frac{\partial A'}{\partial n_i}\right)_{T,V,n_j}$$

5. The internal energy, U', varies with S', V', and composition as

$$dU' = TdS' - PdV' + \Sigma\mu_i dn_i$$

The enthalpy, H', varies with S', P, and composition as

$$dH' = TdS' + V'dP + \Sigma\mu_i dn_i$$

The Helmholtz free energy, A', varies with T, V', and composition as

$$dA' = -S'dT - PdV' + \Sigma\mu_i dn_i$$

The Gibbs free energy, G', varies with T, P, and composition as

$$dG' = -S'dT + V'dP + \Sigma\mu_i dn_i$$

6. For one mole of a closed system with magnetic terms, the following holds.

$$dG = -SdT + VdP - V\mu_0 MdH$$

7. The Maxwell relations for one mole of a closed simple system are

$$\left(\frac{\partial T}{dV}\right)_S = -\left(\frac{\partial P}{dS}\right)_V, \qquad \left(\frac{\partial T}{dP}\right)_S = \left(\frac{\partial V}{dS}\right)_P$$
$$\left(\frac{\partial S}{dV}\right)_T = \left(\frac{\partial P}{dT}\right)_V, \qquad \left(\frac{\partial S}{dP}\right)_T = -\left(\frac{\partial V}{dT}\right)_P$$

8. The Gibbs–Helmholtz equations are

$$\left[\frac{\partial\left(\frac{G}{T}\right)}{\partial T}\right]_P = -\frac{H}{T^2}$$

and

$$\left[\frac{\partial\left(\frac{A}{T}\right)}{\partial T}\right]_V = -\frac{U}{T^2}$$

5.15 CONCEPTS AND TERMS INTRODUCED IN THIS CHAPTER

The reader should write out brief definitions or descriptions of the following terms. Where appropriate, equations may be used.

Auxiliary functions
Barocaloric
Chemical potential
Chemical reaction
Chemical work
Energy equation of state
Enthalpy equation of state
Fundamental equations
Gibbs free energy
Gibbs–Helmholtz equation
Helmholtz free energy
Isentropic
Magnetic work
Magnetization as order parameter
Magnetocaloric
Maximum entropy criterion
Maxwell relations
Mechanocaloric
Minimum internal energy criterion
Property matrix
TdS equations
Thermodynamic potentials
Work function

5.16 QUALITATIVE EXAMPLE PROBLEMS

QUALITATIVE PROBLEM 1

Obtain the following expression:

$$c_p - c_v = \frac{VT\alpha_P^2}{\beta_T}$$

SOLUTION TO QUALITATIVE PROBLEM 1

Equation 2.8 gives the relationship between c_p and c_v as

$$c_p - c_v = \left(\frac{\partial V}{\partial T}\right)_P \left[P + \left(\frac{\partial U}{\partial V}\right)_T\right] \tag{2.8}$$

Since we know that $\alpha_P = 1/V\left(\partial V/\partial T\right)_P$, we obtain $\alpha_P V = \left(\partial V/\partial T\right)_P$

Also, $P = -\left(\partial A/\partial V\right)_T$, so combining this with $\alpha_P V = \left(\partial V/\partial T\right)_P$, we obtain

$$c_p - c_v = \alpha_P V\left[-\left(\frac{\partial A}{\partial V}\right)_T + \left(\frac{\partial U}{\partial V}\right)_T\right]$$

$$A = U - TS$$

$$\left(\frac{\partial A}{\partial V}\right)_T = \left(\frac{\partial U}{\partial V}\right)_T - T\left(\frac{\partial S}{\partial V}\right)_T$$

Rearranging, we get

$$-\left(\frac{\partial A}{\partial V}\right)_T = T\left(\frac{\partial S}{\partial V}\right)_T - \left(\frac{\partial U}{\partial V}\right)_T$$

$$c_p - c_v = \alpha_P V\left[T\left(\frac{\partial S}{\partial V}\right)_T\right] = T\alpha_P V\left(\frac{\partial P}{\partial T}\right)_V$$

From the equation $\left(\frac{\partial X}{\partial Y}\right)_Z\left(\frac{\partial Y}{\partial Z}\right)_X\left(\frac{\partial Z}{\partial X}\right)_Y = -1$ (see Appendix B)

The following is obtained

$$\left(\frac{\partial P}{\partial T}\right)_V = -\left(\frac{\partial P}{\partial V}\right)_T\left(\frac{\partial V}{\partial T}\right)_P$$

Finally,

$$c_p - c_v = (T\alpha_P V)\left(-\left(\frac{\partial P}{\partial V}\right)_T\left(\frac{\partial V}{\partial T}\right)_P\right) = (T\alpha_V)\cdot\left(\frac{1}{V\beta_T}\right)\cdot V\alpha_P = \frac{TV\alpha_P^2}{\beta_T}$$

Thus,

$$c_p - c_v = \frac{VT\alpha_P^2}{\beta_T} \tag{5.51}$$

and the right-hand side of this equation contains only experimentally measurable quantities. We see that $c_p - c_v > 0$ for all $T > 0$; $c_p = c_v = 0$ at $T = 0$.

QUALITATIVE PROBLEM 2

Joule and Thomson showed experimentally that when a steady stream of non-ideal gas is passed through a thermally insulated tube, in which is inserted a throttle valve, the temperature of the gas changes and the state of the gas is changed from P_1, T_1 to P_2, T_2.

a. Show that this process is isenthalpic.

b. The change in T is described in terms of the Joule-Thomson coefficient, μ_{J-T}, as $\mu_{J-T} = \left(\frac{\partial T}{\partial P}\right)_H$ Show that $\mu_{J-T} = \frac{V}{c_p}(\alpha_P T - 1)$

c. Show that the Joule-Thomson coefficient for an ideal gas is zero

SOLUTION QUALITATIVE PROBLEM 2

a. The process is adiabatic. Therefore, $\delta q = 0$

$\Delta H = \Delta U + \Delta(PV) = \delta q - \delta w + (P_2V_2 - P_1V_1)$

$\delta q = 0$ insulated tube, hence it is adiabatic

Work done by the gas entering the throttle $= P_1V_1$

Work done on the gas entering the throttle $= P_1V_1$

Thus: $\Delta H = (P_1V_1 - P_2V_2) + (P_2V_2 - P_1V_1) = 0$

b. $\mu_{J-T} = \left(\frac{\partial T}{\partial P}\right)_H$

$$\text{But} \quad \left(\frac{\partial T}{\partial P}\right)_H = -\frac{\left(\frac{\partial H}{\partial P}\right)_T}{\left(\frac{\partial H}{\partial T}\right)_P} = -\frac{1}{c_p}\left(\frac{\partial H}{\partial P}\right)_T$$

$$\text{And} \quad \left(\frac{\partial H}{\partial P}\right)_T = T\left(\frac{\partial S}{\partial P}\right)_T + V = -T\left(\frac{\partial V}{\partial T}\right)_P + V = -T\alpha_P V + V$$

$$\therefore \mu_{J-T} = -\frac{1}{c_p}(-\alpha_p TV + V) = \frac{V}{c_p}(\alpha_p T - 1)$$

c. For an ideal gas

$$\alpha_P = \frac{1}{T}, \text{ so } \alpha_P T = 1 \text{ and } \mu_{J-1} = 0$$

5.17 QUANTITATIVE EXAMPLE PROBLEMS

QUANTITATIVE PROBLEM 1

Determine the constant-volume heat capacity of aluminum at 20°C given the following data:

At 20°C, aluminum has the following properties:

$$c_p = 24.36 \text{ J/mole} \cdot \text{K}$$

$$\alpha_P = 7.05 \times 10^{-5}\ \mathrm{K}^{-1}$$

$$\beta_T = 1.20 \times 10^{-6}\ \mathrm{atm}^{-1}$$

$$\text{Density,}\quad \rho = 2.70\ \mathrm{g/cm}^3$$

SOLUTION TO QUANTITATIVE PROBLEM 1

The atomic weight of aluminum is 26.98, and thus, at 20°C, the molar volume of aluminum, *V*, is

$$V = \frac{26.98}{2.70 \times 1000} = 0.010\ \text{liters/mole}$$

and thus, the difference between c_p and c_v is (see Qualitative Problem 1):

$$c_p - c_v = \frac{VT\alpha_P{}^2}{\beta_T}$$

$$c_p - c_v = \frac{VT\alpha_P^2}{\beta_T}$$

$$\frac{0.010 \times 293 \times \left(7.05 \times 10^{-5}\right)^2}{1.20 \times 10^{-6}} = 0.0121\ \text{liter} \cdot \text{atm/mole} \cdot \text{K}$$

$$0.0121 \times \frac{8.3144}{0.08206} = 1.23\ \text{J/mole} \cdot \text{K}$$

The constant-volume molar heat capacity of aluminum at 20°C is thus

$$24.36 - 1.23 = 23.13\ \text{J/mole} \cdot \text{K}$$

QUANTITATIVE PROBLEM 2

The following example was provided by Dr. Bill Fahrenholtz, University of Missouri–Rolla.

The adiabatic thermoelastic effect describes the change in temperature with pressure for a brittle solid when it is loaded rapidly (i.e., the rate of loading is much more rapid than the rate of heat transfer). This effect has been used to measure the stresses that develop around defects in composite materials using cyclic loading and a high-speed thermal imaging camera. Using Maxwell relations, derive an expression for the adiabatic thermoelastic effect. Estimate the change in temperature for one mole of alumina that is loaded to 500 MPa.

Data:

Initial temperature = 298 K

$$\alpha_P = 2.2\times10^{-5}/\text{K}$$

$$c_P = 80\ \text{J/mole}\cdot\text{K}$$

SOLUTION TO QUANTITATIVE PROBLEM 2

The problem requires calculation of the variation in temperature with pressure at constant entropy—that is, $\left(\partial T / \partial P\right)_s$.

Start with the second *TdS* equation:

$$dS = \frac{c_P dT}{T} - \left(\frac{\partial V}{\partial T}\right)_P dP = \frac{c_P dT}{T} - \alpha_P V dP$$

At constant entropy:

$$dS = 0 = \frac{c_P dT}{T} - \alpha_P V dP$$

$$\frac{c_P dT}{T} = \alpha_P V dP$$

$$\left(\frac{\partial T}{\partial P}\right)_S = \frac{T\alpha_P V}{c_P}$$

It is reasonable to assume that Al_2O_3 is an incompressible solid and that its heat capacity does not vary significantly over small ranges of temperature and pressure. Thus, the variables can be separated for integration.

$$\left(\frac{\partial T}{\partial P}\right)_S = \frac{TV\alpha_P}{c_p}$$

$$\frac{dT}{T} = \frac{V\alpha_P dP}{c_p} \qquad \text{at constant } S\left(\text{an adiabatic process}\right)$$

$$\ln\frac{T_2}{T_1} = \left(\frac{V\alpha_P}{c_p}\right)\Delta P$$

$$\ln\left(\frac{T_2}{298}\right) = \left[\frac{\left(2.56\times10^{-5}\ \text{m}^3/\text{mole}\right)\left(2.2\times10^{-5}\ \text{K}^{-1}\right)}{80\ \text{J/mole}\cdot\text{K}}\right]\left(500\times10^{6}\ \text{N/m}^2\right)$$

$$= 0.00352$$

$$\therefore T_2 = 299\ \text{K} \quad \text{and} \quad \Delta T = 299 - 298\ \text{K} = 1.0\ \text{K}$$

PROBLEMS

5.1 Show that $\left(\frac{\partial S}{\partial V}\right)_P = \frac{c_p}{TV\alpha_P}$

5.2 Show that $\left(\frac{\partial S}{\partial P}\right)_V = \frac{c_p\beta_T}{T\alpha_P} - V\alpha_P$

5.3 Show that $\left(\frac{\partial A}{\partial P}\right)_V = -\frac{S\beta_T}{\alpha_P}$

5.4 Show that $\left(\frac{\partial A}{\partial V}\right)_P = -\left(\frac{S}{V\alpha_P} + P\right)$

5.5 Show that $\left(\frac{\partial H}{\partial S}\right)_V = T\left(1 + \frac{V\alpha_P}{c_v\beta_T}\right)$

5.6 Show that $\left(\frac{\partial H}{\partial V}\right)_S = -\frac{c_p}{c_v\beta_T}$

5.7 Show that $\left(\frac{\partial c_p}{\partial P}\right)_T = -TV\left(\alpha_P^2 + \frac{d\alpha_p}{dT}\right)$

5.8 Show that $\left(\frac{\partial T}{\partial P}\right)_S = \frac{T\alpha_P V}{c_p}$

5.9 Show that $\left(\frac{\partial P}{\partial V}\right)_S = -\frac{c_p}{c_v V\beta_T}$

5.10 Show that $\left(\frac{\partial^2 G}{\partial P^2}\right)_T = -\frac{1}{\left(\frac{\partial^2 A}{\partial V^2}\right)_T}$

5.11* Sometimes an ideal gas is defined as a gas which for one mole:

i. has an equation of state $PV = RT$

ii. has its internal energy U, only a function of temperature, T.

Show that if a gas obeys the ideal gas equation of state it **must** have $U = U(T)$, that is its internal energy is ONLY a function of temperature.

5.12 Determine the values of ΔU, ΔH, ΔS, ΔA, and ΔG for the following processes. (In (c), (d), and (e) show that an absolute value of the entropy is required).

a. The four processes in Problem 4.1.
b. One mole of an ideal gas at the pressure P and the temperature T expands into a vacuum to double its volume.
c. The adiabatic expansion of mole of an ideal gas from P_1, T_1 to P_2, T_2.
d. The expansion of mole of an ideal gas at constant pressure from V_1, T_1 to V_2, T_2.
e. The expansion of mole of an ideal gas at constant volume from P_1, T_1 to P_2, T_2.

5.13 Show that $\dfrac{\beta_T}{\beta_S} = \dfrac{c_P}{c_V} = \gamma$, where $\beta_T = \dfrac{1}{V}\left(\dfrac{\partial V}{\partial P}\right)_T$ and $\beta_S = \dfrac{1}{V}\left(\dfrac{\partial V}{\partial P}\right)_S$

Hint: use the *TdS* equations.

5.14 Starting from the following equation valid for a closed system, obtain the Maxwell relations.

$$dH = TdS + VdP - Vm_0 \mathcal{M} d\mathcal{H}$$

5.15 Starting from the following equation valid for a closed system, obtain Maxwell relations.

$$dA = -SdT - PdV + Vm_0 \mathcal{H} d\boldsymbol{M}$$

5.16 The cycle shown in Figure 5.10 consists of two isotherms (AB and CD) and two isobars (BC and DA). Use the *TdS* equations to draw the *T*-*S* diagram for this cycle.

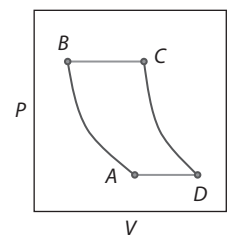

FIGURE 5.10 A pressure–volume diagram of two isothermals (AB and CD) and two isobaric changes (BC and DA), making up a cycle.

5.17* What energy potential is equal to the following expression:

$$-V^2 \frac{\partial}{\partial V}\left(\frac{G}{V}\right)_T$$

5.18* What energy potential is equal to the following expression:

$$-V^2 \frac{\partial}{\partial V}\left(\frac{A}{V}\right)_T$$

5.19* Determine the total differential of A, the Helmholtz free energy, when A is written as a function of pressure and temperature, that is when $A = A(T, P)$.

5.20* Sketch an enthalpy *versus* temperature plot at constant Pressure. Be sure that the slope and curvature of the plot are correctly drawn.

5.21* Use the equation $dH = C_P dT + (V - V\alpha_P T)dP$, derived in Problem 5.20 to plot Enthalpy versus Temperature and Enthalpy versus Pressure of an ideal monatomic gas.

5.22* An ideal gas (monatomic) is taken on a cycle from A to B to C to D as shown in Figure 5.11. Draw the cycle that it takes on the accompanying Temperature Entropy diagram,

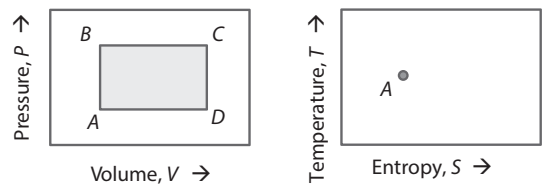

FIGURE 5.11 A cycle in a pressure vs. volume plot of an ideal monatomic gas.

For each segment of the plot obtain
Slope of *TS* plot.
Curvature of *TS* plot.

* New problem in this edition.

6 Heat Capacity, Enthalpy, Entropy, and the Third Law of Thermodynamics

6.1 INTRODUCTION

The heat capacity of a material of fixed composition is the ratio of the amount of thermal energy added to the material divided by the increase in temperature of the material (see Section 2.6). For simple systems, this gives rise to the following two expressions for heat capacity,namely:

the heat capacity at constant volume:

$$C_v = \left(\frac{\partial U'}{\partial T} \right)_V$$

and the heat capacity at constant pressure:

$$C_p = \left(\frac{\partial H'}{\partial T} \right)_P$$

both with units J/K.

Recall that in Chapter 5, another equation for the constant pressure heat capacity was derived, namely:

$$\left(\frac{\partial^2 G'}{\partial T^2} \right)_P = -\left(\frac{\partial S'}{\partial T} \right)_P = -\left(\frac{C_P}{T} \right) \tag{5.12}$$

It can also be shown (see Qualitative Problem 2 of Section 6.9) that the following holds for the constant volume heat capacity:

$$\left(\frac{\partial^2 A'}{\partial T^2} \right)_V = -\left(\frac{\partial S'}{\partial T} \right)_V = -\left(\frac{C_V}{T} \right)$$

DOI: 10.1201/9781003375388-7

There are other types of heat capacity. For example, for magnetic materials if only the magnetic work terms are considered (i.e., non-PdV work term), from Equation 5.11c and d:

$$C_{\mathcal{M}} = -T\left(\frac{\partial^2 A'}{\partial T^2}\right)_{\mathcal{M},V} = T\left(\frac{\partial S'}{\partial T}\right)_{\mathcal{M},V} = \left(\frac{\partial U'}{\partial T}\right)_{\mathcal{M},V}$$

and

$$C_{\mathcal{H}} = -T\left(\frac{\partial^2 G'}{\partial T^2}\right)_{\mathcal{H},P} = T\left(\frac{\partial S'}{\partial T}\right)_{\mathcal{H},P} = \left(\frac{\partial H'}{\partial T}\right)_{\mathcal{H},P}$$

In Chapter 2, the distinction between the heat capacity per mole of substance and the heat capacity of the entire substance was introduced as follows:

$$C_v dT = nc_v dT \quad \text{or} \quad dU = c_v dT \tag{2.6a}$$

$$C_p dT = nc_p dT \quad \text{or} \quad dH = c_p dT \tag{2.6b}$$

in which c_p and c_v are, respectively, the constant pressure and constant volume *molar heat capacities* (units J/mole K), and the internal energy and enthalpy are given for 1 mole of the substance.

Integration of Equation 2.6b between the states (T_1, P) and (T_2, P) gives the difference between the molar enthalpies of the two states as:

$$\Delta H = H(T_2, P) - H(T_1, P) = \int_{T_1}^{T_2} c_p dT \tag{6.1}$$

from which it is seen that knowledge of the variation of c_p with temperature is required for the determination of the temperature dependence of the enthalpy. Similarly, integration of Equation 2.6a between T_1 and T_2 at *constant volume* shows that knowledge of the variation of c_v with temperature is required for the determination of the temperature dependence of the internal energy. Later in this chapter, we will show that this is also the case for the determination of the temperature dependence of entropy. Thus, for a simple system, by knowing the temperature dependence at constant pressure (volume) of the heat capacity, we may find the Gibbs (Helmholtz) free energy change with temperature, which will enable us to determine the equilibrium state of the system in question.

6.2 TEMPERATURE DEPENDENCE OF THE HEAT CAPACITY

In 1819, Dulong (Pierre Louis Dulong, 1785–1838) and Petit (Alexis Thérèse Petit, 1791–1820) introduced an empirical rule which states that the constant volume molar heat capacities (c_v) of all solid *elements* have the value $3R$ (= 24.9 J/K). Later, in 1864,

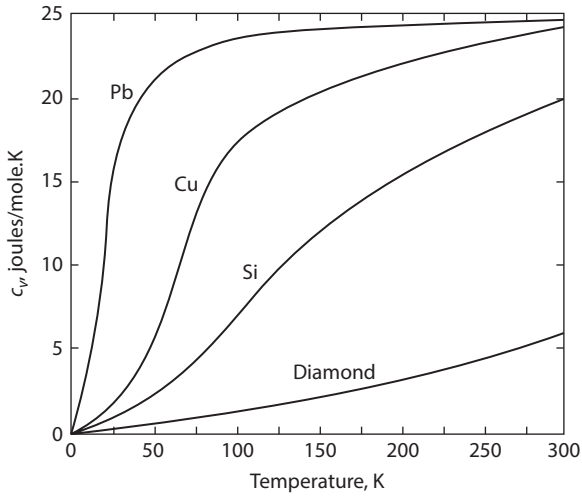

FIGURE 6.1 The constant-volume molar heat capacities of Pb, Cu, Si, and diamond as functions of temperature. (Adopted from DeHoff, *Thermodynamics in Materials Science*, CRC, 2006.)

Kopp (Emile Kopp, 1817–1875) introduced a rule which states that the constant volume molar heat capacity of a solid chemical compound approaches a value that is approximately equal to the sum of the molar heat capacities of its constituent chemical elements. Thus, for example, the constant volume molar heat capacity of an A_2B compound will be approximately $9R$ (i.e., $3 \times 3R$) at high temperatures.

Although the molar heat capacities of many elements at room temperature have values that are close to $3R$, some elements have values significantly lower than $3R$ at room temperature, and all elements at low temperatures show a decrease in their constant volume heat capacities. Figure 6.1 shows that although lead and copper closely obey Dulong and Petit's rule at room temperature, the constant volume heat capacities of silicon and diamond are significantly less than $3R$ at room temperature. Figure 6.1 also shows the significant decrease in the heat capacities at low temperatures of the heat capacities displayed.

As discussed in Chapter 4, Einstein applied the principles of quantum theory to show that the constant volume heat capacities of crystalline solids decrease below a material-specific temperature and eventually approach zero as the temperature approaches 0 K. However, finding equations that match well with experimentally determined values of heat capacity at larger temperatures has been elusive.

Thus, it has been a normal practice to fit the experimentally measured variation of the constant pressure molar heat capacity of a material (which is easier to measure in condensed materials than constant volume heat capacities) with temperature to empirical expressions. One such equation is of the form:

$$c_p = a + bT + \frac{c}{T^2}$$

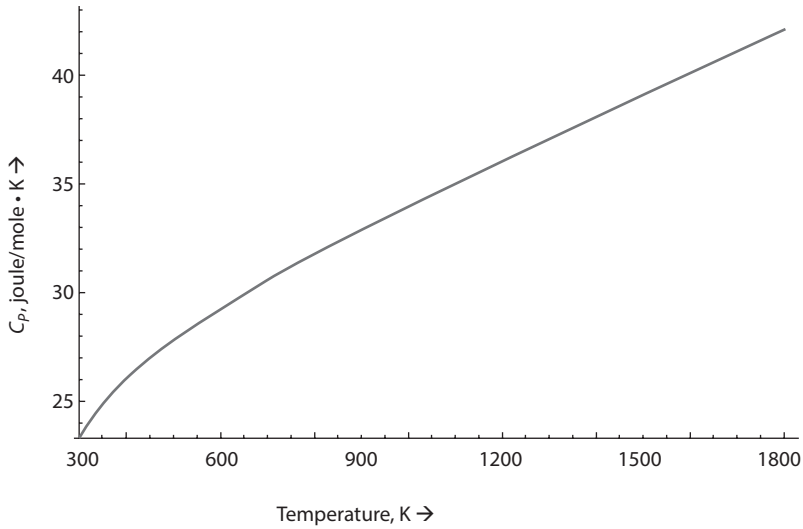

FIGURE 6.2 The variation with temperature, of the constant-pressure heat capacity of the transition metal Cr.

Such expressions are usually fitted to values of the heat capacity from room temperature to their melting temperature, which avoids the range where the heat capacities begin to decrease drastically. Such analytical expressions are only applicable in the stated temperature range over which the values of the heat capacity were measured and fit to the equation. For example, the transition metal Cr has been fitted to the following equation (see Table A.2, Appendix A)

$$\text{For Cr}: c_P = 24.43 + 9.87 \times 10^{-3} T - 3.68 \times 10^{5} T^{-2} \text{ J/mole} \cdot \text{K}$$

over the range of temperature 298–2130 K. Figure 6.2 plots this function. Note that at 298 K, the value of c_P is 23.3 J/mole K.

The variations, with temperature, of c_p for several elements and compounds that do not undergo phase transitions in the solid state are shown in Figure 6.3.

Zr is an element that has two crystalline phases, namely, α Zr (hcp, $P\frac{6_3}{m}mc$) and β Zr (bcc, $Im\bar{3}m$), which form above 863°C. Their heat capacities vary as follows:

$$\alpha\,\text{Zr}\; c_P = 21.97 + 11.63 \times 10^{-3} T \;\; \text{J/mole} \cdot \text{K} \qquad 300\ \text{K} < T < 1136\,\text{K}$$

$$\beta\ \text{Zr} \quad c_P = 23.22 + 4.64 \times 10^{-3} T \;\; \text{J/mole} \cdot \text{K} \qquad 1136\ \text{K} < T < 2100\,\text{K}$$

The heat capacity drops discontinuously at the transition temperature by about 6.7 J/K·mole as seen in Figure 6.4. At the transition temperature, both phases are stable, so adding thermal energy to the system would not change their temperature, and the molar heat capacity would have an apparent infinity.

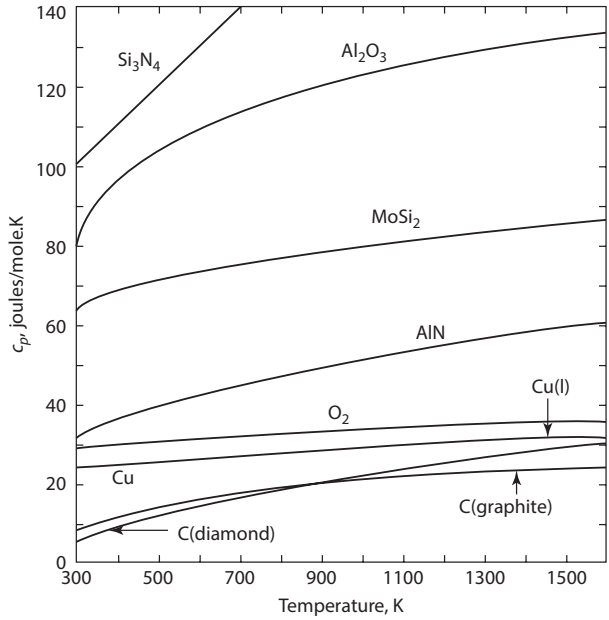

FIGURE 6.3 The variations, with temperature, of the constant-pressure heat capacities of several elements and compounds.

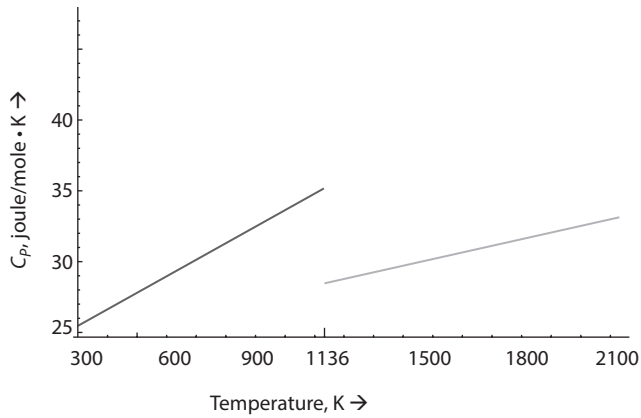

FIGURE 6.4 The variations, with temperature, of the constant-pressure molar heat capacity of Zr, which exhibits allotropy.

The variations for some elements, which exhibit allotropy, and compounds, which exhibit polymorphism, are shown in Figure 6.5. Other values for the coefficients of the analytical expressions for selected elements and compounds are found in Table A.2 of Appendix A.

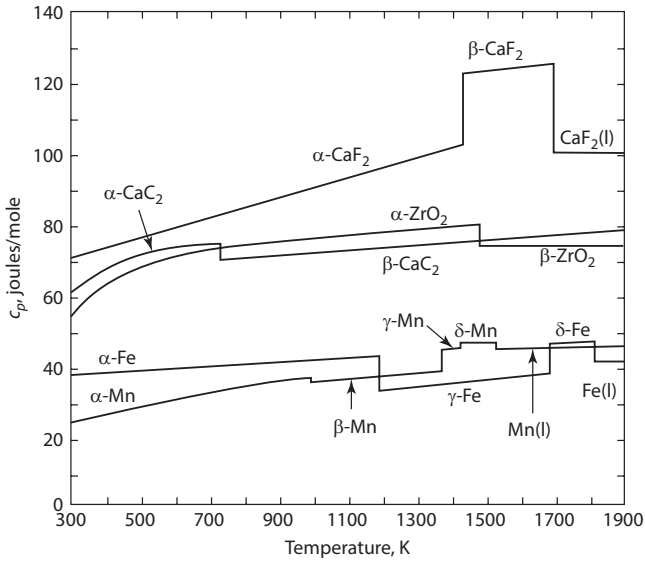

FIGURE 6.5 The variations, with temperature, of the constant-pressure molar heat capacities of some elements which exhibit allotropy and some compounds which exhibit polymorphism.

6.3 ENTHALPY AS A FUNCTION OF TEMPERATURE

In Section 6.1, it was shown that for a closed system of fixed composition undergoing a change in temperature from T_1 to T_2 at the constant pressure P, integration of Equation 2.6b gives Equation 6.1 for a change in the molar enthalpy:

$$\Delta H = H(T_2,P) - H(T_1,P) = \int_{T_1}^{T_2} c_p dT \tag{6.1}$$

ΔH is thus the area under a plot of c_p versus T between the limits T_1 and T_2. The change in enthalpy is $\Delta H = q_p$, which is simply the amount of thermal energy required to enter the system and to increase the temperature of 1 mole of the system from T_1 to T_2 at the constant pressure P.

When one mole of a system undergoes a chemical reaction or a phase transformation at constant temperature and pressure (e.g., the reaction $A + B = AB$), ΔH is the difference between the enthalpy of the products of the reaction (state 2) and the enthalpy of the reactants (state 1), that is,

$$\Delta H(T,P) = H_{AB}(T,P) - \left[H_A(T,P) + H_B(T,P)\right] \tag{6.2}$$

If ΔH is a positive quantity, the reaction causes the system to absorb thermal energy from its constant temperature heat bath, and the reaction is called *endothermic*. Conversely, if ΔH is a negative quantity, the reaction occurs with an evolution of

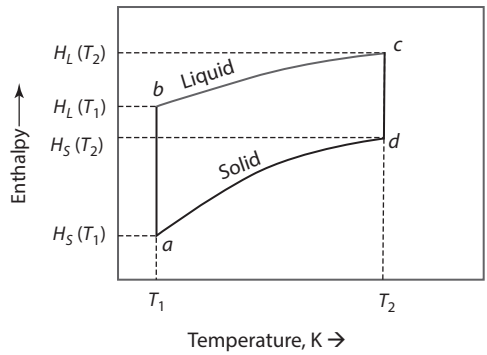

FIGURE 6.6 The variation, with temperature, of the molar enthalpies of the solid and liquid phases of a substance. T_2 is the equilibrium melting temperature of the solid at the pressure of one atmosphere.

thermal energy and is called an *exothermic* process. This convention is the same as that used in the First Law of Thermodynamics for the sign of q, the thermal energy entering or leaving the system. The changes in enthalpy caused by changes in temperature can be graphically represented on an enthalpy–temperature diagram (Figure 6.6).

Consider the change of state

$$A_{(l)} \rightarrow A_{(s)}$$

which represents the solidification of liquid A, whose equilibrium solidification temperature (which is also the equilibrium melting temperature) is T_2. The segment cd is the change in enthalpy at the equilibrium liquid-to-solid transformation; that is, it is the heat of solidification and can be seen to be $H_S(T_2) - H_L(T_2) < 0$ (exothermic). A supercooled liquid can transform to a solid at T_1. Since the enthalpy is a state function, the molar enthalpy of transformation of the liquid at this temperature can be determined. Thus,

$$\Delta H(b \rightarrow a) = \Delta H(b \rightarrow c) + \Delta H(c \rightarrow d) + \Delta H(d \rightarrow a) \tag{i}$$

- $\Delta H(b \rightarrow a) = \Delta H(l \rightarrow s, T_1)$ is the molar enthalpy of transformation of the supercooled liquid to the solid at the temperature T_1.
- $\Delta H(l \rightarrow s, T_1) = H(s, T_1) - H(l, T_1)$

This change in enthalpy (*ba)* in Figure 6.6 is negative (exothermic).

- $\Delta H(b \rightarrow c)$ is the thermal energy that needs to be supplied to 1 mole of liquid to increase its temperature from T_1 to T_2.

$$\int_{T_1}^{T_2} c_p(l)\,dT$$

in which $c_p(l)$ is the constant pressure molar heat capacity of liquid.

- $\Delta H(\mathrm{c} \rightarrow d) = \Delta H(l \rightarrow s, T_2) = H(s, T_2) - H(l, T_2)$ is the constant pressure molar enthalpy of transformation of the liquid at the equilibrium transition temperature T_2, represented in Figure 6.6 by *cd*.
- $\Delta H(d \rightarrow a)$ is the thermal energy required to leave the solid and decrease the temperature of 1 mole of solid from T_2 to T_1 at constant pressure.

$$\Delta H(d \rightarrow a) = \int_{T_2}^{T_1} c_p(s)\,dT$$

in which $c_p(s)$ is the constant pressure molar heat capacity of solid.

Substitution of the individual expressions into Equation (i) gives

$$\Delta H(l \rightarrow s, T_1) = \int_{T_1}^{T_2} c_p(l)\,dT + \Delta H(l \rightarrow s, T_2) + \int_{T_2}^{T_1} c_p(s)\,dT$$

$$\Delta H(l \rightarrow s, T_1) = \int_{T_2}^{T_1} \Delta c_p\,dT + \Delta H(l \rightarrow s, T_2) \tag{6.3}$$

where $\Delta c_p = c_p(l) - c_p(s)$.

The molar enthalpy of solidification (of fusion) at T_1 is seen to be more negative than at T_2 for the material shown in Figure 6.6.

Thus, if the molar enthalpy of fusion is known at one temperature and the constant pressure molar heat capacities of the products and the reactants are known (along with their dependencies on temperature), then the molar enthalpy of fusion at any other temperature can be calculated. It is to be noted that if $\Delta c_p = 0$, then $\Delta H_{T_2} = \Delta H_{T_1}$; that is, the thermal change of the reaction, ΔH, is independent of the temperature. In Figure 6.6, the slope of the line *ad*, which is $(\partial H / \partial T)_P$, is the molar heat capacity of the solid, c_p. It is a straight line only if the heat capacity is independent of temperature.

Since H does not have an absolute value (only changes in H can be measured), it is convenient to introduce a convention that will allow the comparison of different enthalpy–temperature diagrams. This convention assigns the value of zero to the enthalpy of *elements in their stable states at 298 K* (25°C) and $P = 1$ atm, that is, $\Delta H_{298} = 0$. Thus, the enthalpy of a compound at 298 K and $P = 1$ atm is simply the enthalpy of formation of one mole of the compound from its elements at 298 K and $P = 1$ atm. For example, for the oxidation reaction

$$\mathrm{M}_{(\mathrm{solid})} + \frac{1}{2}\mathrm{O}_{2(\mathrm{gas})} = \mathrm{MO}_{(\mathrm{solid})} \qquad \text{at 298 K and } P = 1 \text{ atm}$$

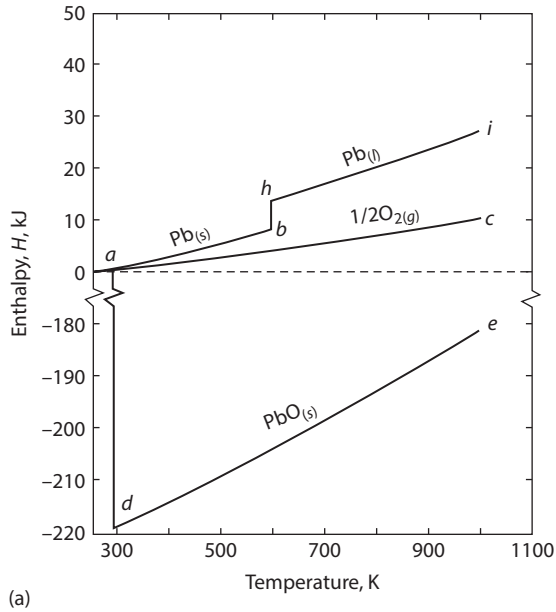

FIGURE 6.7a The variation, with temperature, of the enthalpies of $Pb_{(s)}$, $Pb_{(l)}$, $\frac{1}{2}O_{2(g)}$, and $PbO_{(s)}$.

$$\Delta H_{298} = H_{\mathrm{MO}(s)298} - H_{\mathrm{M}(s)298} - \frac{1}{2} H_{\mathrm{O}_2(g)298}$$

and, since $H_{\mathrm{M},298}$ and $H_{\mathrm{O}_2,298}$ are by convention set equal to zero, then

$$\Delta H_{298} = H_{\mathrm{MO},298}$$

The variation in heats of chemical reaction (or heats of formation) with temperature at constant pressure can be represented on an enthalpy–temperature diagram, such as those in Figures 6.7a and b, which are drawn for the oxidation reaction:

$$\mathrm{Pb} + \frac{1}{2}\mathrm{O}_2 = \mathrm{PbO}$$

The pertinent thermochemical data for this system are listed in Table 6.1.

In Figure 6.7a:

- *a* represents the enthalpy of 1/2 mole of oxygen gas and 1 mole of $Pb_{(s)}$ at 298 K (set = 0 by convention).
- *ab* represents the variation of $H_{\mathrm{Pb}(s)}$ with temperature in the range $298 \leq T \leq 600$ K, where $H_{\mathrm{Pb}(s)}$ at T is given by $\int_{298}^{T} c_{p,\mathrm{Pb}(s)} dT$.

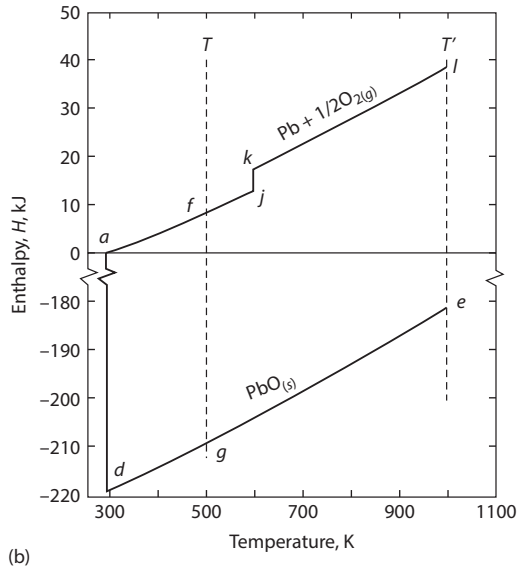

FIGURE 6.7b The variation, with temperature, of the enthalpies of the reactants ($Pb + \frac{1}{2}O_2$) and the product, PbO.

TABLE 6.1
Thermochemical Data for Pb, PbO, and O_2

$H_{\text{Pbo}(298)} = -219{,}000\,\text{J}$
$C_{p,\text{Pb}(s)} = 23.6 + 9.75 \times 10^{-3}\,T\,\text{J/K}$ from 298 K to $T_{m,\text{Pb}}$
$C_{p,\text{Pb}(l)} = 32.4 - 3.1 \times 10^{-3}\,T\,\text{J/K}$ from $T_{m,\text{Pb}}$ to 1200 K
$C_{p,\text{PbO}(s)} = 37.9 + 26.8 \times 10^{-3}\text{T J/K}$ from 298 K to $T_{m,\text{Pbo}}$
$C_{p,\text{O}_2(g)} = 29.96 + 4.18 \times 10^{-3}\,T - 1.67 \times 10^{5}\,T^{-2}\,\text{J/K}$ from 298 to 3000 K
$\Delta H_{m,\text{Pb}} = 4810\,\text{J}$ at $T_{m,\text{Pb}} = 600$ K
$T_{m,\text{PbO}} = 1159$ K

- *ac* represents the variation of $H_{\frac{1}{2}\text{O}_2(gf)}$ with temperature in the range $298 < T < 3000$ K, where $H_{\frac{1}{2}\text{O}_2(g)}$ is given by $\frac{1}{2}\int_{298}^{T} c_{p,\text{O}_2(g)}dT$.
- *ad* is $\Delta H_{\text{PbO}(s),\,298\text{ K}} = -219{,}000\,\text{J}$.
- *de* represents the variation of $H_{\text{PbO}(s)}$ with temperature in the range $298\text{ K} \leq T \leq 1159$ K, where $H_{\text{PbO}(s),T} = -219{,}000 + \int_{298}^{T} c_{p,\text{PbO}(s)}dT$ J.

In Figure 6.7b:

- a represents the enthalpy of 1/2 mole of $O_{2(g)}$ and 1 mole of $Pb_{(s)}$ at 298 K.
- f represents the enthalpy of 1/2 mole of $O_{2(g)}$ and 1 mole of $Pb_{(s)}$ at the temperature T.
- g represents the enthalpy of 1 mole of $PbO_{(s)}$ at the temperature T.

Therefore:

$$\Delta H_{\mathrm{PbO},298\,\mathrm{K}} = \Delta H\left(a \to f\right) + \Delta H\left(f \to g\right) + \Delta H\left(g \to d\right)$$

$$= \int_{298}^{T}\left(\frac{1}{2}c_{p,\mathrm{O_2}(g)} + c_{p,\mathrm{Pb}(s)}\right)dT + \Delta H_{\mathrm{PbO},T} + \int_{T}^{298} c_{p,\mathrm{PbO}(s)}dT$$

and therefore

$$\Delta H_{\mathrm{PbO},T} = \Delta H_{\mathrm{PbO},298\,\mathrm{K}} + \int_{298}^{T}\Delta c_p dT$$

where:

$$\Delta c_p = c_{p,\mathrm{PbO}(s)} - c_{p,\mathrm{Pb}(s)} - \frac{1}{2}c_{p,\mathrm{O_2}(g)}$$

From the data in Table 6.1,

$$\Delta c_p = -0.7 + 14.96\times10^{-3}T + 0.85\times10^{5}T^{-2}$$

and, thus, in the range of temperature from 298 to 600 K ($T_{m,\,\mathrm{Pb}}$):

$$\Delta H_T = -219{,}000 + \int_{298}^{T}\left(-0.7 + 14.96\times10^{-3}T + 0.85\times10^{5}T^{-2}\right)dT$$

$$= -219{,}000 - 0.7\left(T - 298\right) + 7.48\times10^{-3}\left(T^2 - 298^2\right)$$

$$-0.85\times10^{5}\left(\frac{1}{T} - \frac{1}{298}\right)$$

With $T = 500$ K, this gives $\Delta H_{500\,\mathrm{K}} = -217{,}800$ J, as can be seen in Figures 6.7b and 6.8.

If a phase change occurs in one or more of the reactants or products, between the two temperatures at which the reaction is being considered, then the enthalpies of

transformation of the phase changes must be considered. In Figure 6.7a, *h* represents the enthalpy of 1 mole of $Pb_{(l)}$ at the melting temperature of 600 K, given as

$$H_{\mathrm{Pb}(l),600\,\mathrm{K}} = \int_{298}^{600} c_{p,\mathrm{Pb}(s)}dT + \Delta H_{m,\mathrm{Pb}}$$

hb is the enthalpy of melting of Pb at the melting temperature of 600 K (= 4810 J).

The line *hi* represents the variation of the enthalpy of 1 mole of $Pb_{(l)}$ with temperature in the range 600–1000 K, and therefore, the enthalpy of the liquid phase at *T* is given as:

$$H_{\mathrm{Pb}(l),T} = \int_{298}^{600} c_{p,\mathrm{Pb}(s)}dT + \Delta H_{m,\mathrm{Pb}} + \int_{600}^{T} c_{p,\mathrm{Pb}(l)}dT$$

In Figure 6.7b, *ajkl* represents the variation of the enthalpy of 1 mole of Pb and 1/2 mole of $O_{2(g)}$, and hence, ΔH_T is calculated from the cycle

$$\Delta H_{298\,\mathrm{K}} = \Delta H(a \to d) = \Delta H(a \to j) + \Delta H(j \to k) + \Delta H(k \to l)$$
$$+\Delta H(l \to e) + \Delta H(e \to g) + \Delta H(g \to d)$$

where:

$$\Delta H(a \to j) = \int_{298}^{T_{m,\mathrm{Pb}}} \left(c_{p,\mathrm{Pb}(s)} + \frac{1}{2} c_{p\mathrm{O}_2(g)} \right) dT$$

$$\Delta H(j \to k) = \text{The latent heat of melting of Pb at } T_{m,\mathrm{Pb}} = 4810 \text{ J}$$

$$\Delta H(k \to l) = \int_{T_{m,\mathrm{Pb}}}^{T} \left(c_{p,\mathrm{Pb}(l)} + \frac{1}{2} c_{p,\mathrm{O}_2(g)} \right) dT$$

$$\Delta H(l \to e) = \Delta H_T$$

$$\Delta H(e \to g) = \int_{T}^{T_{m,\mathrm{Pb}}} c_{p,\mathrm{PbO}(s)}dT$$

$$\Delta H(g \to d) = \int_{T_{m,\mathrm{Pb}}}^{298} c_{p,\mathrm{PbO}(s)}dT$$

Thus,

$$\Delta H_T = \Delta H_{298\,\mathrm{K}} + \int_{298}^{T_{m,\mathrm{Pb}}} \left(c_{p,\mathrm{PbO}(s)} - c_{p,\mathrm{Pb}(s)} - \frac{1}{2} c_{p,\mathrm{O_2}(g)} \right) dT$$

$$-\Delta H_{m,\mathrm{Pb}} + \int_{T_{m,\mathrm{Pb}}}^{T} \left(c_{p,\mathrm{PbO}(s)} - c_{p,\mathrm{Pb}(l)} - \frac{1}{2} c_{p,\mathrm{O_2}(g)} \right) dT$$

$$= -219{,}000 + \int_{298}^{600} \left(-0.7 + 14.96 \times 10^{-3} T + 0.85 \times 10^{5} T^{-2} \right) dT$$

$$-4810 + \int_{600}^{T} \left(-9.3 + 27.8 \times 10^{-3} T + 0.85 \times 10^{5} T^{-2} \right) dT$$

This gives $\Delta H_{1000} = -216{,}700\,\mathrm{J}$ at $T' = 1000$ K, as is seen in Figures 6.7b and 6.8. Figure 6.8 shows the variation of $\Delta H_{\mathrm{PbO},T}$ with temperature in the range 298–1100 K.

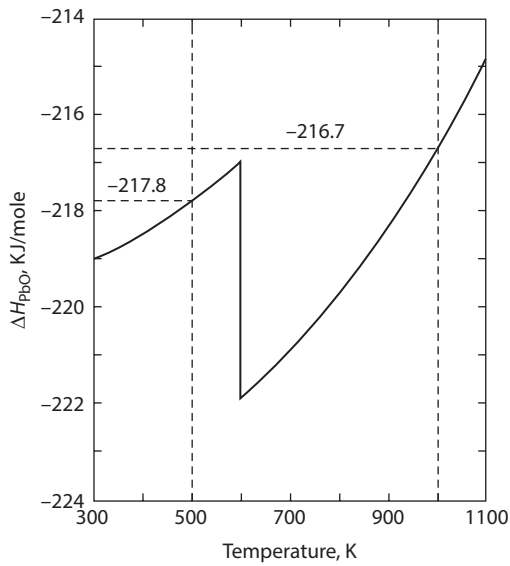

FIGURE 6.8 The variation, with temperature, of the enthalpy change for the reaction $\mathrm{Pb} + \frac{1}{2}\mathrm{O_2} = \mathrm{PbO}$.

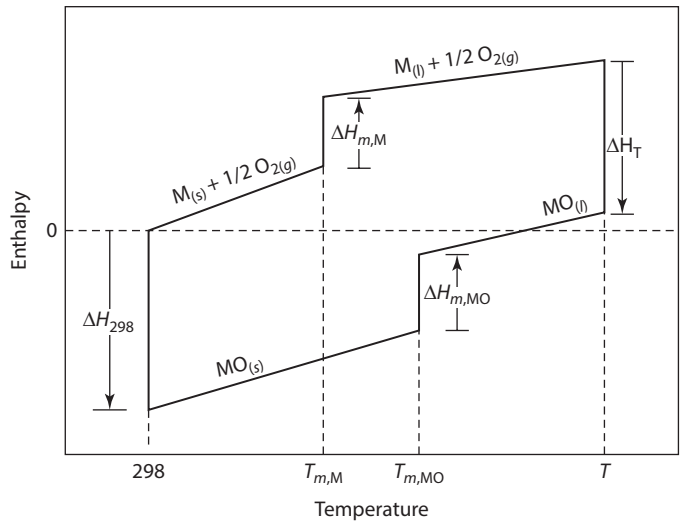

FIGURE 6.9 The variation with temperature of the enthalpies of the oxidation ΔH, of metal A over a range of temperature which includes the melting temperature of both the metal M and the oxide, MO.

If the temperature of interest is higher than the melting temperatures of both the metal and its oxide, then both enthalpies of melting must be considered. For example, with reference to Figure 6.9, which is drawn for the general oxidation,

$$\mathrm{M} + \frac{1}{2}\mathrm{O_2} = \mathrm{MO}$$

$$\Delta H_T = \Delta H_{298} + \int_{298}^{T_{m,\mathrm{M}}} \left(c_{p,\mathrm{MO}(s)} - c_{p,\mathrm{M}(s)} - \frac{1}{2} c_{p,\mathrm{O_2}(g)} \right) dT$$

$$-\Delta H_{m,\mathrm{M}} + \int_{T_{m,\mathrm{M}}}^{T_{m,\mathrm{MO}}} \left(c_{p,\mathrm{MO}(s)} - c_{p,\mathrm{M}(l)} - \frac{1}{2} c_{p,\mathrm{O_2}(g)} \right) dT$$

$$+\Delta H_{m,\mathrm{MO}} + \int_{T_{m,\mathrm{MO}}}^{T} \left(c_{p,\mathrm{MO}(l)} - c_{p,\mathrm{M}(l)} - \frac{1}{2} c_{p,\mathrm{O_2}(g)} \right) dT$$

When phase transformations of the reactants or products have to be considered, care must be taken with the signs of the changes in enthalpy. The signs can be obtained from a consideration of *Le Chatelier's principle* (Henry Louis Le Chatelier, 1850–1936), which can be stated as, "When a system, which is at equilibrium,

is subjected to an external influence, the system moves in that direction which nullifies the effects of the external influence." Thus, if the system contains a low-temperature phase in equilibrium with a high-temperature phase at the equilibrium phase transition temperature, such as a solid coexisting with a liquid at the equilibrium melting temperature, then the introduction of heat to the system (the external influence) would be expected to increase the temperature of the system (the effect). However, the system undergoes an endothermic change, which absorbs the heat introduced at constant temperature and hence nullifies the effect of the external influence. The endothermic process is the melting of some of the solid. A phase change from a low- to a high-temperature phase is always endothermic, and hence, ΔH for the change is always a positive quantity. Thus, ΔH_m, the molar enthalpy of melting, which is the difference between the enthalpy of a mole of liquid and the enthalpy of a mole of solid, is always positive.

Consider a phase transition between two allotropes, α and β, the β being the high-temperature allotrope.

$$\text{For } \alpha: \quad \left(\frac{\partial H_\alpha}{\partial T}\right)_P = c_p^\alpha$$

$$\text{For } \beta: \quad \left(\frac{\partial H_\beta}{\partial T}\right)_P = c_p^\beta$$

Subtraction gives

$$\left(\frac{\partial H_\beta}{\partial T}\right)_P - \left(\frac{\partial H_\alpha}{\partial T}\right)_P = c_p^\beta - c_p^\alpha$$

$$\left(\frac{\partial \left(H_\beta - H_\alpha\right)}{\partial T}\right)_P = \Delta c_p$$

or

$$\left(\frac{\partial \Delta H}{\partial T}\right)_P = \Delta c_p \tag{6.4}$$

and integrating from state 1 to state 2 gives

$$\Delta H_{T_2} - \Delta H_{T_1} = \int_{T_1}^{T_2} \Delta c_p dT \tag{6.5}$$

Equations 6.4 and 6.5 are expressions of *Kirchhoff's law.*

6.4 THE THIRD LAW OF THERMODYNAMICS

6.4.1 Historical Development of the Third Law of Thermodynamics[1]

The *Third Law of Thermodynamics* was enunciated and debated during the first three decades of the twentieth century. The Law has its roots in the desire of chemists to be able to calculate equilibrium constants of reactions based only on thermochemical data such as heat capacity and latent heats.

One of the forms of the Gibbs–Helmholtz equation:

$$\Delta G(T) = \Delta H(T) + T\left(\frac{\partial G}{\partial T}\right) \tag{6.6}$$

was the starting point for the quest to calculate the chemical affinity (driving force) for reactions.

Equation 6.6 can be more generally be rewritten as:

$$\Delta G(T) = \int_0^T \Delta c_P dT - T\left[\int_0^T \frac{c_p}{T} dT - \Delta S_0\right]$$

The term ΔS_0 is the constant of integration and is the change in the entropy for the reaction at 0 K, which was not known at the time. From the above equation, it can be seen that if this value could be determined, the thermodynamics of the reaction would be known if the heat capacities were known.

This was stated by Le Chatelier in 1888:

> It is highly probable that the constant of integration is a determinate function of certain physical properties of the substances in question. The determination of the nature of this function would lead to a complete knowledge of the laws of equilibrium. It would permit us to determine a priori independently of any new experimental data, the full conditions of equilibrium corresponding to a chemical reaction.[2]

In other words, if the value of ΔS_0 for a reaction could be determined, ΔG would be known as a function of temperature, and hence, the reaction thermodynamics would be known.

Consideration of the value of ΔS_0 in the late nineteenth and early twentieth century led to the statement of the Third Law of Thermodynamics. In 1902, Richards (Theodore William Richards, 1868–1928) collected data which showed that, for many reactions, the values of $\Delta G(T)$ and $\Delta H(T)$ asymptotically approached each other at low temperatures with slopes that approached zero, that is,

$$\left(\frac{\partial \Delta G}{\partial T}\right)_P = -\Delta S \tag{6.7}$$

---

[1] See D. E. Laughlin and W. A. Soffa, "The Third Law of Thermodynamics: Phase Equilibria and Phase Diagrams at Low Temperatures", *Acta Mat.* (2018), vol. 145, 49–61.

[2] H. Le Chatelier, *Ann. Mines* (1888), vol. 13, pp. 157ff. Translated by Lewis and Randall, *Thermodynamics and the Free Energy of Chemical Substances*, McGraw-Hill, New York, 1923, pp. 436ff.

and

$$\left(\frac{\partial \Delta H}{\partial T}\right)_P = T\left(\frac{\partial \Delta S}{\partial T}\right)_P = \Delta c_p \tag{6.8}$$

See Figures 6.10a and b.

In 1906, Nernst (Walther Hermann Nernst, 1864–1941) postulated that this was true for all reactions at 0 K involving liquids and solids. This would mean that the integration constant is zero for all reactions. This is what has become known as the *Nernst heat theorem*.

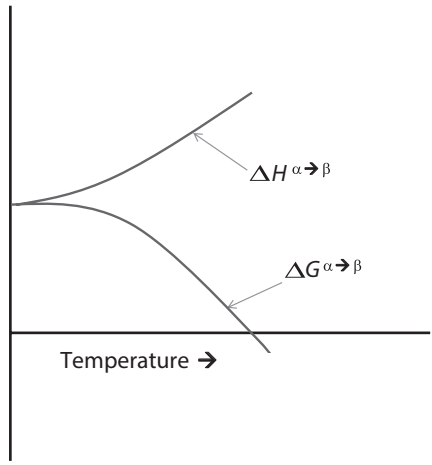

FIGURE 6.10a Schematic of the variation of the change in the Gibbs free energy and the enthalpy for a reaction with temperature. As the temperature approaches absolute zero, their values approach each other and their slopes approach 0.

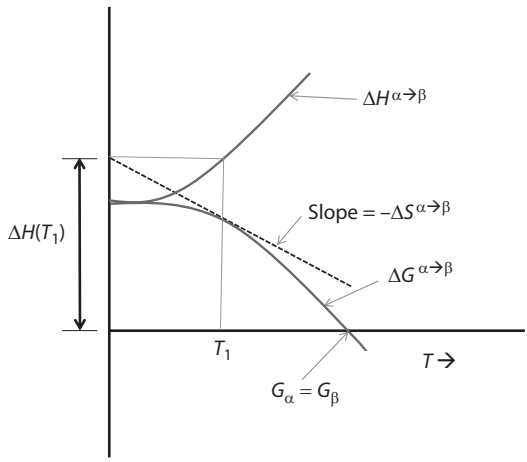

FIGURE 6.10b Schematic of the variation of the change in the Gibbs free energy and the enthalpy for a reaction with temperature. The value of $\Delta H(T_1)$ can be determined as the ordinate intercept of the tangent to $\Delta G(T_1)$.

For a more general reaction

$$A + B = AB$$

$\Delta S = S_{AB} - S_A - S_B = 0$ at $T = 0$, which indicates that the entropy of the product(s) minus the sum of the entropies of the reactants is also zero at 0 K.

Planck (Max Karl Ernst Ludwig Planck, 1858–1947) extended the Nernst's heat theorem by positing to the effect that the entropy of any homogeneous substance, which is in complete internal equilibrium, is zero at 0 K. This has become known as the *Nernst–Planck–Simon statement* (Francis Simon, 1893–1956) of the Third Law. Thus, in the aforementioned reaction, the entropy of *AB*, the entropy of *A*, and the entropy of *B* would all be zero at 0 K under the specifications of Planck.

This statement summarizes the Third Law of Thermodynamics. It is very important to remember that the substances must be *in internal equilibrium* (metastable or stable). The integration constant is not necessarily zero for substances *out of equilibrium*, such as those frozen in residual disorder (e.g., glasses).

The Third Law thus has ramifications on the types of phases that are stable at the absolute zero. Such phases should have zero configurational entropy. This concept will be utilized later in the text when *equilibrium phase diagrams* are discussed. Also, the finding that the value of Δc_P approaches zero as the T approaches zero is consistent with the low-temperature heat capacity models of Einstein and Debye in Chapter 4.

Finally, we see that the Third Law in Classical Thermodynamics is not merely a consequence of the first two laws. The experimental observations of the chemical reaction data collected by Richards (as $T \to 0, \left(\frac{\partial \Delta G}{\partial T}\right)_P \to 0$ and $\left(\frac{\partial \Delta H}{\partial T}\right)_P \to 0$) were necessary prior to Nernst's statement of the *heat theorem*.

6.4.1.1 Another Statement of the Third Law of Thermodynamics

As in the case of the First and Second Laws of Thermodynamics, there is a way of stating the Third Law as a negative declaration. This is the so-called unattainability statement. Essentially, it states that it is impossible to reach 0 K in a finite number of cooling steps. See Section 6.4.3.6 for further discussion.

6.4.2 Experimental Verification of the Third Law

The Third Law can be verified by considering the phase transition of one mole of an allotropic element, with α being the stable phase at low temperature.

$$\alpha \to \beta$$

In Figure 6.11, T_{trans} is the temperature, at atmospheric pressure, at which the α and β phases are in equilibrium with each other. Below T_{trans}, the α phase is the stable phase. For the cycle shown in Figure 6.11, since the entropy is a state function, we can write the change in entropy at 0 K, $\Delta S_0 = \Delta S_{\text{IV}}$

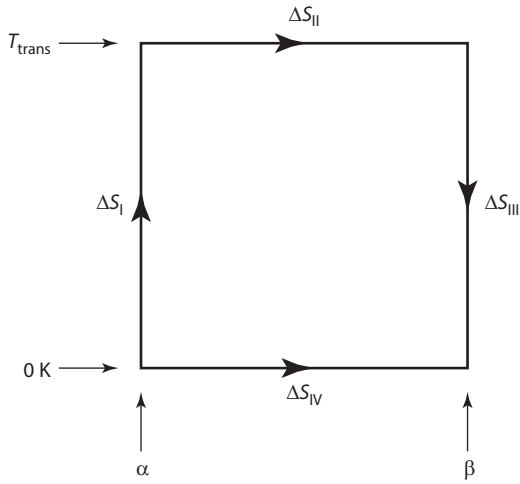

FIGURE 6.11 The cycle used for the experimental verification of the Third Law of thermodynamics.

$$\Delta S_{IV} = \Delta S_I + \Delta S_{II} + \Delta S_{III}$$

For the Third Law to be obeyed, $\Delta S_{IV} = 0$, which in turn requires that

$$\Delta S_{II} = -(\Delta S_I + \Delta S_{III})$$

where:

$$\Delta S_I = \int_0^{T_{trans}} \frac{c_{p(\alpha)}}{T} dT$$

$$\Delta S_{II} = \frac{\Delta H_{trans}}{T_{trans}} = H(\beta, T_{trans}) - H(\alpha, T_{trans})$$

$$\Delta S_{III} = \int_{T_{trans}}^{0} \frac{c_{p(\beta)}}{T} dT$$

ΔS_{II} is called the *experimental entropy change*, and $-(\Delta S_I + \Delta S_{III})$ is called the *Third Law entropy change*. If the Third Law is valid, $\Delta S_{II} = -(\Delta S_I + \Delta S_{III})$.

The cycle shown in Figure 6.11 has been examined for many allotropic elements and polymorphic compounds which have *metastable* high-temperature phases at 0 K. For example, in the case of sulfur, which has two allotropes: a monoclinic form that is stable above 368.5 K and an orthorhombic form that is stable below 368.5 K, with a molar enthalpy of transformation of 400 J/mole at the equilibrium transformation temperature of 368.5 K. Since monoclinic sulfur can be supercooled with relative

ease, the variations, with temperature, of the heat capacities of both allotropes have been measured experimentally at temperatures below 368.5 K. The measured heat capacities give

$$\Delta S_{\mathrm{I}} = \int_{0}^{368.5} \frac{c_{p(\mathrm{rhombic})}}{T} dT = 36.86 \text{ J/K}$$

$$\Delta S_{\mathrm{II}} = \frac{\Delta H_{\mathrm{trans}}}{T_{\mathrm{trans}}} = \frac{400}{368.5} = 1.09 \text{ J/K}$$

and

$$\Delta S_{\mathrm{III}} \int_{368.5}^{0} \frac{c_{p(\mathrm{monoclinic})}}{T} dT = -37.8 \text{ J/K}$$

Thus,

$$\left(\Delta S_{\mathrm{I}} + \Delta S_{\mathrm{III}}\right) = -\left(36.86 - 37.8\right) = 0.94 \text{ J/K}$$

This is the value of the Third Law entropy change. The value of the experimental entropy change ΔS_{II} was shown to be 1.09 J/K. Since the difference between the *experimental entropy change* and the *Third Law entropy change* (0.15 J/K) is less than the experimental error, their equality is taken as being an experimental verification of the premise that $\Delta S_{\mathrm{IV}} = 0$.

Thus, the entropies of the two phases are equal at 0 K. The same has been shown to be valid for many other allotropes such as SiC, Sn, and C.

6.4.3 Some Physical Consequences of the Third Law of Thermodynamics

The Third Law imposes interesting consequences on several material properties as the temperature approaches 0 K.

6.4.3.1 Thermal Expansion Coefficient

For a single component material, we write:

$$dG = -SdT + VdP$$

Since the Gibbs free energy is an exact function of P and T, we can

apply the Maxwell relation

$$-\left(\frac{\partial S}{\partial P}\right)_T = \left(\frac{\partial V}{\partial T}\right)_P = \alpha_P V$$

Thus, as the $T \to 0$ K, $\left(\frac{\partial S}{\partial P}\right)_T \to 0$ and therefore $\alpha_P \to 0$

Note that the entropy is not a function of pressure at 0 K.

6.4.3.2 The Thermal Coefficient of Pressure

For a single component material, we write:

$$dA = -SdT + PdV$$

Since the Helmholtz free energy is an exact function of V and T, we can write:

$$-\left(\frac{\partial S}{\partial V}\right)_T = \left(\frac{\partial P}{\partial T}\right)_V = P\gamma_V$$

Thus, as the $T \to 0$ K, $\left(\frac{\partial S}{\partial V}\right)_T \to 0$ and $\gamma_V \to 0$

Note that the entropy is not a function of volume at 0 K.

6.4.3.3 Heat Capacities

Figures 6.10a and b showed that $\Delta HT \to 0$ as $T \to 0$ K and therefore $\Delta c_P \to 0$ as $T \to 0$ K. This also follows from the models of the heat capacity discussed in Chapter 4.

6.4.3.4 Magnetization versus Temperature Plot

$$dG = -SdT + VdP - V_m\ \mu_0 \boldsymbol{M} d\boldsymbol{\mathcal{H}}$$

Since the Gibbs free energy is an exact function of $\boldsymbol{M}$ and T, at constant P we can write:

$$-\left(\frac{\partial S}{\partial \boldsymbol{\mathcal{H}}}\right)_T = V_m\ \mu_0 \left(\frac{\partial \boldsymbol{M}}{\partial T}\right)_{\boldsymbol{\mathcal{H}}} = 0$$

Thus, as the $T \to 0$ K, $\left(\frac{\partial S}{\partial \boldsymbol{\mathcal{H}}}\right)_T \to 0$ and $\left(\frac{\partial \boldsymbol{M}}{\partial T}\right)_{\boldsymbol{\mathcal{H}}} \to 0$

The slope of the magnetization versus temperature plot approaches 0 as $T \to 0$ K (see Figure 5.7). This is also true for the atomic order parameter versus temperature plot.

6.4.3.5 Energy Plots versus Entropy

In Chapter 3, a plot of the entropy *versus* internal energy for a simple system showed that the internal energy and entropy had their lowest values when the temperature was zero (see Figure 3.8). This is of course another way of presenting the Third Law of Thermodynamics. The slope of that plot was equal to the inverse of the absolute temperature. The related plot of internal energy *versus* entropy shows the same concepts (see Figure 6.12). In this plot, the slope of the curve is the absolute temperature, so that when the slope goes to zero, once again the values of the internal energy and entropy are at their lowest values. Figure 6.12 is similar to a plot that Gibbs presented in Figure 2 of his paper "Graphical Methods in the Thermodynamics of Fluids", *Transactions of the Connecticut Academy*, II, April/May 1873 and in Fig 3 in his

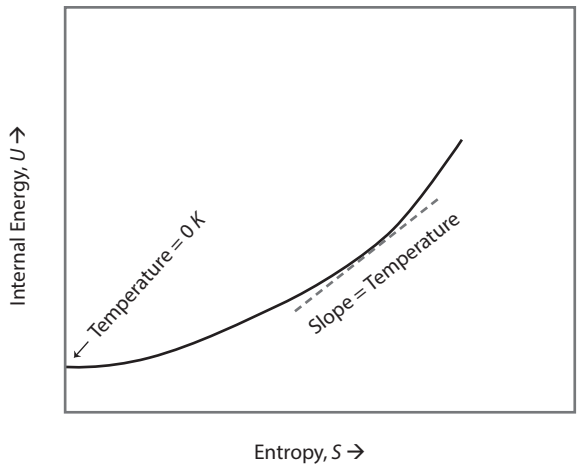

FIGURE 6.12 Internal energy *versus* entropy plot at constant volume for a simple system. The slope of the plot equals the absolute temperature. The zero in temperature corresponds to a minimum in energy and a zero entropy.

paper "A Method of Geometrical Representation of the Thermodynamic Properties of Substances by Means of Surfaces", *Transactions of the Connecticut Academy*, II, Dec 1873.

6.4.3.6 Stable Phases at 0 K

The Third Law of Thermodynamics imposes constraints on the ground state phases. For example, elements must exist in crystalline form, since their configurational entropy must be zero. Amorphous or glassy phases are not *ground state phases*. Also, compounds (or intermetallic phases) must have zero configurational entropy, which implies that at 0 K they must be stoichiometric and fully ordered. Any alloy must have zero configurational entropy when in internal equilibrium at 0 K, which means that the ground states of alloys must be composed of pure elements and/or stoichiometric compounds or intermetallic phases.

Simon introduced the term "aspects of entropy" in discussing the ground states of materials. For example, a random solid solution of an A-B alloy has two aspects of entropy, namely, its *thermal entropy* (i.e., vibrational entropy) and its *configurational entropy*. Both of these "aspects of entropy" should approach zero as the temperature approaches zero if the alloy is to approach its ground state. If the alloy is to obtain zero configurational entropy, it could do so by decomposing into a two-phase mixture of pure A and pure B, or it could form a compound in which the atoms are arrayed in an ordered configurational pattern (intermetallic alloy). Which of these options would depend on any interaction energies that exist in the alloy. See Chapter 15 for more on interaction energies and stable phases.

If the random solid solution of an A-B alloy is cooled to 0 K, and does not decompose as discussed above, it is still possible for its vibrational aspect of entropy to approach zero, and hence, its heat capacity would still go to zero at 0 K.

The situation can get even more complex, if a third "aspect of entropy" exists in the alloy, namely, a spin entropy (from magnetic moments). The spins could be randomly arrayed (a paramagnet) or aligned in an ordered fashion (e.g., the spins could be all parallel to each other, i.e., a ferromagnetic). For this alloy to attain its ground state, each of its aspects of entropy must approach zero as the temperature of the alloy approaches zero, i.e., the ground state could not have a random array of the atoms nor could it be paramagnetic.

These effects on equilibrium binary alloy phase equilibria are discussed further in Chapters 10 and 15.

6.4.3.7 Approaching 0 K

There are various methods that have been used to cool a system to very low temperatures. One of the first methods employed by investigators in the late nineteenth and early twentieth centuries is based on the barocaloric effect (see Section 5.10.5). This effect can be understood from Figure 6.13. The entropy *versus* temperature plots of a simple gaseous system at two different pressures are displayed in this figure. Starting at state A, the temperature of the gas is T_1 and the pressure is P_1. If the pressure is isothermally increased to P_2, the entropy of the gas is lowered to that of state B, because of its decrease in volume. The gas is then removed from contact with the heat bath and is isolated from the environment. The pressure is subsequently released and returned to its original pressure (P_1) and the state is now C. This state has a lower temperature than state A and state B. This is the case because the configurational entropy of the gas has increased in changing its state from B to C because its volume is larger than is as at state B. Since the system is isolated, its other degree of freedom, namely, its temperature, must decrease to keep the overall entropy of the system constant in this adiabatic process. This process can be repeated until the gas condenses.

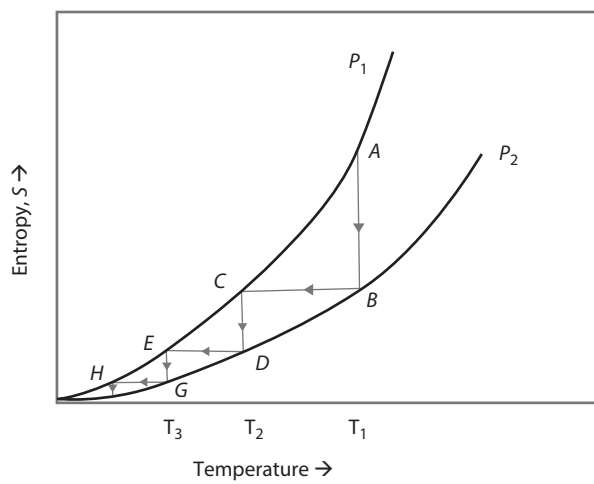

FIGURE 6.13 Entropy *versus* temperature plot for a system. At point A the temperature is T_1 and the pressure is P_1. When pressure is raised isothermally to P_2, and the entropy decreases. When the pressure is released adiabatically, the temperature decreases to T_2.

If one assumes that reversible isothermal and adiabatic processes are possible at lowest temperatures, one might be tempted to think that the absolute zero could be reached by such a method. However, one can see that as the temperature gets lower and lower, the two entropy *versus* temperature curves approach each other making it impossible to change the entropy of the system by changing the pressure. Thus, this technique of lowering the temperature will fail to reach the absolute zero.

Expanding on this, Simon (Sir Francis Simon, 1893–1956) stated that "it is impossible by any procedure, no matter how idealized, to reduce the temperature of any system to zero temperature in a finite number of finite operations."[3] This has been called the unattainability statement of the Third Law of Thermodynamics. See Section 6.4.1.1. This statement has been shown to be equivalent to the ones which state that the entropy of a substance approaches zero as the temperature approaches zero.

6.4.4 Apparent Contradictions to the Third Law of Thermodynamics

The requirement that the substance be in complete internal equilibrium is an important part of the statement of the Third Law of Thermodynamics. Proposed counterexamples of the Third Law that are often brought against it fail in some way to have the system in complete equilibrium. Several examples of such purported failings of the Third Law follow.

1. Glasses are noncrystalline solids that form from supercooled liquids in which the disordered atomic arrangements occurring in the liquid state have been "frozen" into the solid state. Substances that form glasses often have complex atomic, ionic, or molecular structures in the liquid state, and the structures would require extensive atomic reorganization in order to assume a periodic structure characteristic of its equilibrium crystalline state. In the absence of the ability of the glass-forming substance to undergo the necessary atomic rearrangement at its freezing temperature, the supercooled liquid simply becomes more and more viscous and eventually loses its rotational and translational degrees of freedom and forms a solid glass. If the solid glass were to crystallize, its enthalpy and entropy would decrease, and the decreases in the enthalpy and entropy would be, respectively, the enthalpy and entropy of crystallization at the temperature at which devitrification occurred. At temperatures below its equilibrium freezing temperature, the glassy state is not metastable with respect to the crystalline state, and thus, a glass, not being in internal equilibrium, has a non-zero configurational entropy at 0 K. The amount by which it is greater than zero is dependent on the cooling rate and the degree of atomic disorder in the glass.
2. Solutions are mixtures of atoms, ions, or molecules, and a contribution is made to their entropies by the fact that they are mixtures (see Equation 4.3). This contribution is called the *entropy of mixing* and is determined by the

[3] Quoted by Guggenheim (Edward Armand Guggenheim, 1901–1970) in *Thermodynamics: An Advanced Treatment for Chemists and Physicists*, North Holland, Amsterdam, 1985.

randomness with which the particles are mixed in the solution. The atomic randomness of a mixture determines its degree of order; for example, in a mixture containing 50 at% of A and 50 at% of B, complete ordering occurs when every atom of A is coordinated only by B atoms and vice versa, and complete randomness occurs when, on average, 50% of the neighbors of every atom are A atoms and 50% are B atoms. The degree of order in these two extreme configurations is, respectively, unity and zero. The equilibrium degree of order is temperature dependent and increases with decreasing temperature. However, the maintenance of the equilibrium degree of order is dependent on the abilities of the particles to change their positions in the solution, and, with ever-decreasing temperature, as atomic mobility decreases exponentially with decreasing temperature, the maintenance of internal equilibrium becomes increasingly difficult. Consequently, a nonequilibrium degree of order can be frozen into the solid solution, in which case the entropy will not decrease to zero at 0 K.

3. Even chemically pure elements are mixtures of isotopes, and because of the chemical similarity between isotopes, it is to be expected that random mixing of the isotopes occurs. Thus, an entropy of mixing exists, and consequently, the entropy does not decrease to zero at 0 K. For example, solid chlorine at 0 K is a solid solution of Cl^{35}–Cl^{35}, Cl^{35}–Cl^{37}, and Cl^{37}–Cl^{37} molecules. Thus, such substances are not in internal equilibrium and need not have a total entropy equal to zero at 0 K.
4. At any finite temperature, a pure crystalline solid contains an equilibrium number of vacant lattice sites, which, because of their random positioning in the crystal, give rise to an entropy of mixing which is similar to the entropy of mixing in a chemical solution. Both the equilibrium number of vacancies and the diffusivity of the atoms in the crystal decrease exponentially with decreasing temperature, and since the vacancies "disappear" by diffusing to the free surface of the crystal, nonequilibrium concentrations of vacancies can be frozen into the crystal at low temperatures if diffusion is limited, causing a nonzero entropy at 0 K.
5. Random crystallographic orientation of molecules in the crystalline state can also give rise to a nonzero entropy at 0 K. Such is the case with solid CO, in which a structure such as the following can occur.

CO CO OC CO OC CO CO
OC CO CO OC CO OC OC
OC CO CO OC OC CO CO

The entropy would have its maximum value if equal numbers of molecules were oriented in opposite directions and random mixing of the two orientations occurred. From Equation 4.3, the molar configurational entropy of mixing would be

$$\Delta S_{\text{conf}} = k_B \ln \frac{(N_O)!}{\left(\frac{1}{2}N_O\right)!\left(\frac{1}{2}N_O\right)!}$$

where N_O is Avogadro's Number, 6.0232×10^{23}. Thus, using Stirling's approximation,

$$\Delta S_{\text{conf}} = k_B\left[N_O \ln N_O - \frac{1}{2}N_O \ln\left(\frac{1}{2}N_O\right) - \frac{1}{2}N_O \ln\left(\frac{1}{2}N_O\right)\right]$$

$$= k_B \times 4.175 \times 10^{23}$$

$$= 1.38054 \times 10^{-23} \times 4.175 \times 10^{23}$$

$$= 5.76 \text{ J/mole} \cdot \text{K}$$

A comparison of this value with the measured value of 4.2 J/mole·K indicates that the actual molecular orientations in solid CO are not fully random.

In view of these considerations, it is once again clear that the statement of the Third Law of Thermodynamics requires the inclusion of the qualification that the system in question be in *complete internal equilibrium*.

6.5 TEMPERATURE DEPENDENCE OF ENTROPY AT HIGHER TEMPERATURES

Assigning a value of zero to the entropy at 0 K, S_0, allows the absolute value of the entropy of any material to be determined as

$$S_T = \int_0^T \frac{c_p}{T} dT \text{ J/K}$$

and molar entropies are normally tabulated at 298 K, where:

$$S_{298} = \int_0^{298} \frac{c_p}{T} dT \text{ J/K}$$

The variations, with temperature, of the molar entropies of several elements and compounds are shown in Figure 6.14.

With the constant pressure molar heat capacity of the solid expressed in the form

$$c_{p(s)} = a + bT + cT^{-2}$$

the molar entropy of the solid at the temperature T is obtained as

$$S_T = S_{298} + a\ln\left(\frac{T}{298}\right) + b(T - 298) - \frac{1}{2}c\left(\frac{1}{T^2} - \frac{1}{298^2}\right)$$

At temperatures higher than the melting temperature, T_m, the molar entropy of the liquid is obtained as

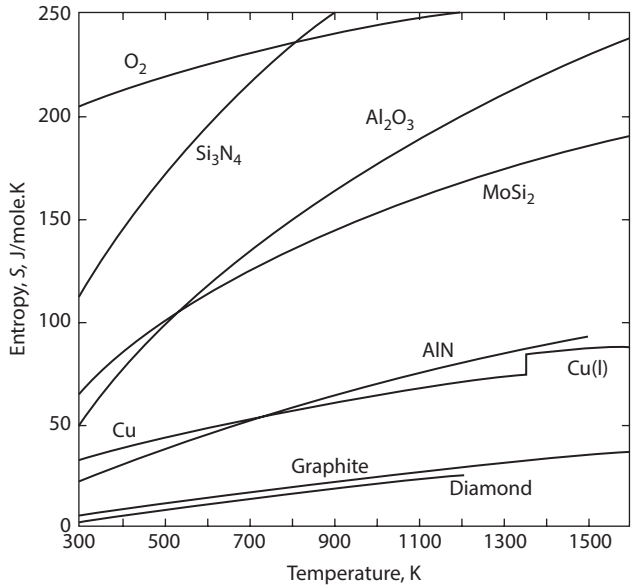

FIGURE 6.14 The variation, with temperature, of the molar entropies of several elements and compounds.

$$S_T = S_{298} + \int_{298}^{T_m} \frac{c_{p(s)}}{T} dT + \Delta S_m + \int_{T_m}^{T} \frac{c_{p(l)}}{T} dT \tag{6.9}$$

where the molar entropy of the melting, ΔS_m, is obtained as $\Delta H_m / T_m$.

6.5.1 Richard's Rule for Entropies of Melting

In 1897, Richards (Joseph W. Richards, 1864–1921) suggested that the molar entropies of fusion of metals should have approximately the same value, which would require that a plot of ΔH_m versus T_m be a straight line. Figure 6.15 is a plot of the molar enthalpies of fusion versus the melting temperatures of 11 face-centered cubic (FCC) metals (open circles) and 27 body-centered cubic (BCC) metals (closed circles) which have melting temperatures below 3000 K. A least-square analysis of the data for the face-centered cubic metals gives for the molar entropies of melting:

$$\Delta S_m^{\text{FCC}} = \frac{\Delta H_m^{\text{FCC}}}{T_m} = 9.6 \text{ J/K}$$

and for body-centered cubic metals:

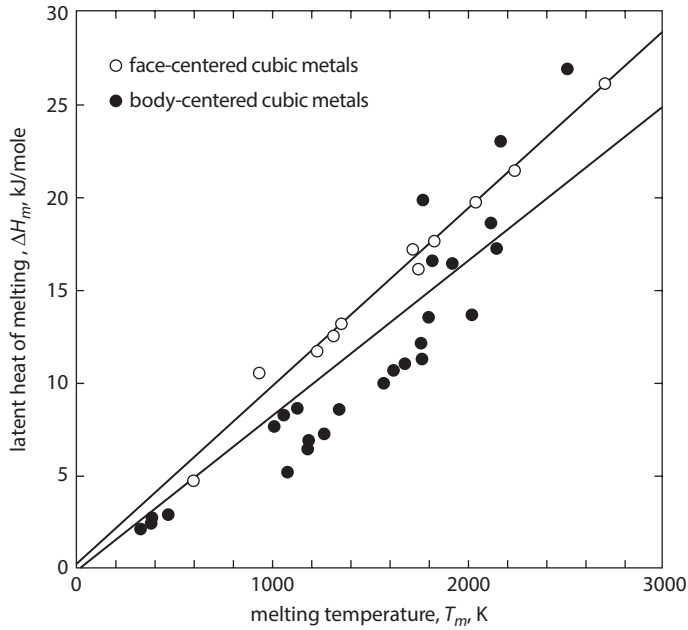

FIGURE 6.15 An illustration of Richards' rule.

$$\Delta S_m^{\text{BCC}} = \frac{\Delta H_m^{\text{BCC}}}{T_m} = 8.25 \text{ J/K}$$

This observation, which is known as *Richards' rule*, indicates that the difference between the degree of disorder in the liquid structure (due to configurational and thermal entropy) and that in both the FCC and BCC crystal structures are approximately the same for FCC and BCC metals. It also indicates that the more open (smaller number of near neighbors) BCC structure metals have a slightly smaller change in entropy in forming their liquid phase than do the FCC metals, which is consistent with the BCC structure being the more open structure.

6.5.2 Trouton's Rule for Entropies of Boiling

Trouton's rule (Frederick Thomas Trouton, 1863–1922) states that the molar entropy of boiling of a liquid metal is approximately constant. Figure 6.16 shows a plot of ΔH_b versus the boiling temperature, T_b, for 29 liquid metals with boiling temperatures below 4000 K. A least-squares fit of the data, shown as the full line, gives

$$\Delta H_b = 121 T_b - 43 \text{ J/K}$$

for an average value of 78 J/K;

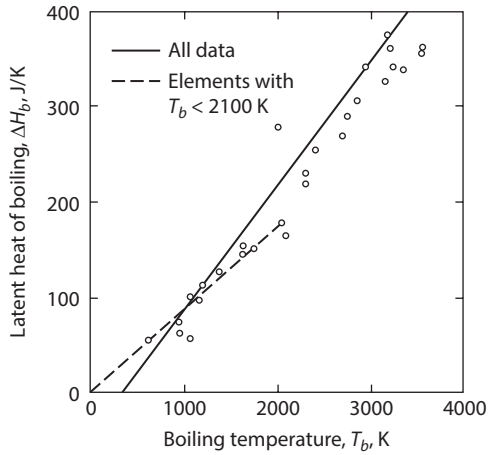

FIGURE 6.16 An illustration of Trouton's rule.

However, a least-squares fit of the data for the 13 metals with boiling temperatures below 2100 K, shown as the broken line, gives

$$\Delta H_b = 87T_b - 0.4 \text{ J/K}$$

which indicates a common molar entropy of boiling of approximately 87 J/K for these metals.

Figure 6.17 is the entropy–temperature diagram for the reaction

$$\text{Pb} + \frac{1}{2}\text{O}_2 = \text{PbO}$$

corresponding to the enthalpy–temperature diagram shown in Figure 6.7b.

Because of the similar magnitudes of the molar entropies of the condensed phases Pb and PbO, it is seen that the entropy change for the reaction

$$\Delta S_T = S_{T,\text{PbO}} - S_{T,\text{Pb}} - \frac{1}{2}S_{T,\text{O}_2}$$

is very nearly equal to $-\frac{1}{2}S_{T,\text{O}_2}$. For example, at 298 K,

$$\Delta S_{298} = S_{298,\text{PbO}} - S_{298,\text{Pb}} - \frac{1}{2}S_{298,\text{O}_2}$$

$$= 67.4 - 64.9 - \frac{1}{2} \times 205$$

$$= -100 \text{ J/K}$$

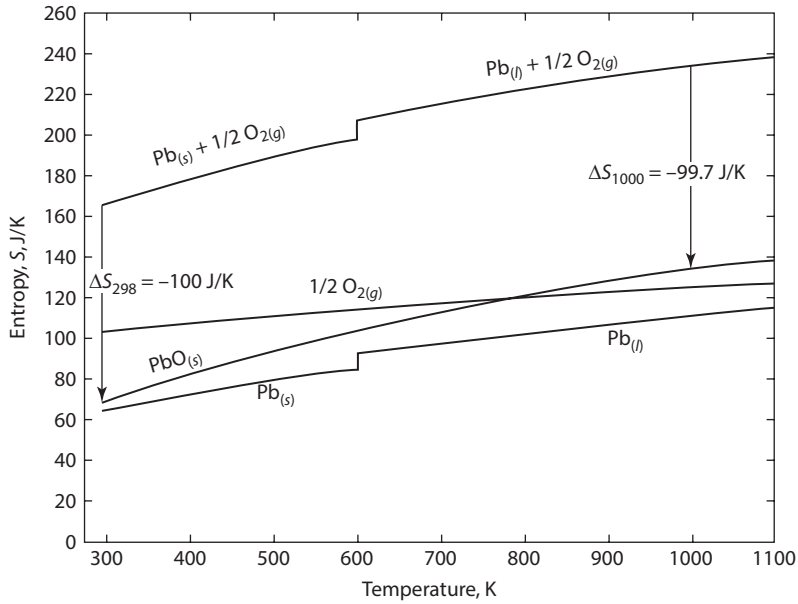

FIGURE 6.17 The variation, with temperature, of the entropies of $Pb_{(s)}$, $Pb_{(l)}$, $PbO_{(s)}$, and $\frac{1}{2}O_{2(g)}$, and the entropy change for the reaction $Pb + \frac{1}{2}O_2 = PbO$.

which is similar in magnitude to the decrease in entropy caused by the disappearance of 1/2 moles of oxygen gas. Such approximations are generally valid: that is, in reactions in which a gas reacts with a condensed phase to produce another condensed phase, the change in the entropy of the reaction is approximately equal to that caused by the disappearance of the gas.

6.6 THE INFLUENCE OF PRESSURE ON ENTHALPY AND ENTROPY

For one mole of a closed system of fixed composition undergoing a change of pressure at constant temperature,

$$dH = \left(\frac{\partial H}{\partial P}\right)_T dP$$

Equation 5.10b gives $dH = TdS + VdP$, and thus,

$$\left(\frac{\partial H}{\partial P}\right)_T = T\left(\frac{\partial S}{\partial P}\right)_T + V$$

A Maxwell relation (Equation 5.35) gives

$$\left(\frac{\partial S}{\partial P}\right)_T = -\left(\frac{\partial V}{\partial T}\right)_P$$

in which case

$$\left(\frac{\partial H}{\partial P}\right)_T = -T\left(\frac{\partial V}{\partial T}\right)_P + V$$

The isobaric coefficient of thermal expansion, α_P, is defined as

$$\alpha_P = \frac{1}{V}\left(\frac{\partial V}{\partial T}\right)_P$$

and thus,

$$\left(\frac{\partial H}{\partial P}\right)_T = -T\alpha_P V + V = V(1-\alpha_P T)$$

The change in molar enthalpy caused by the change in state from (P_1, T) to (P_2, T) is thus

$$\Delta H = H(P_2,T) - H(P_1,T) = \int_{P_1}^{P_2} V(1-\alpha_P T)\,dP \tag{6.10}$$

For an ideal gas, $\alpha_P = 1/T$, and thus, Equation 6.10 shows once again that the enthalpy of an ideal gas is independent of pressure, since the integral is exactly zero.

6.6.1 Example Calculations

The molar volume and expansion coefficient of Fe are, respectively, 7.1 cm^3 and 0.3 $\times$ 10^{-4} K^{-1}. Thus, an increase in the pressure exerted on Fe from 1 to 100 atm at 298 K causes the molar enthalpy to increase by

$$7.1\times10^{-3}\times\left(1-0.3\times10^{-4}\times298\right)\times(100-1) = 0.696 \text{ liter}\times\text{atm}$$

$$= 0.696\times101.3 = 71 \text{ J}$$

The same increase in molar enthalpy would be obtained by heating Fe from 298 to 301 K at 1 atm pressure, which is an example of the relative insensitivity of the effect of pressure on the enthalpy of a solid.

For a closed system of fixed composition undergoing a change of pressure at constant temperature,

$$dS = \left(\frac{\partial S}{\partial P}\right)_T dP$$

Maxwell's relation (Equation 5.34) is

$$\left(\frac{\partial S}{\partial P}\right)_T = -\left(\frac{\partial V}{\partial T}\right)_P$$

which, with the definition of α_P, gives

$$\left(\frac{\partial S}{\partial P}\right)_T = -\alpha_P V$$

Thus, for the change of state (P_1, T) to (P_2, T),

$$\Delta S = S(P_2,T) - S(P_1,T) = -\int_{P_1}^{P_2} \alpha_P V dP \tag{6.11}$$

For an ideal gas, since $\alpha = 1/T$, Equation 6.11 simplifies to

$$\Delta S = -\int_{P_1}^{P_2} R d\ln P = -R\ln\left(\frac{P_2}{P_1}\right) = R\ln\left(\frac{V_2}{V_1}\right)$$

as was obtained in Section 3.7.

An increase in the pressure exerted on Fe from 1 to 100 atm decreases the molar entropy by 0.0022 J/K, which is the same as is obtained by decreasing the temperature by 0.02 degrees from 298 K at 1 atm pressure. It is thus seen that the molar entropies of condensed phases are relatively insensitive to changes in pressure. In the majority of materials applications, in which the range of pressure is 0 to 1 atm, the influence of pressure on the enthalpies and entropies of condensed phases can be ignored.

For a closed system of fixed composition undergoing changes in both pressure and temperature, a combination of Equations 6.1 and 6.10 gives

$$\Delta H = H(P_2,T_2) - H(P_1,T_1) = \int_{T_1}^{T_2} c_p dT + \int_{P_1}^{P_2} V(1-\alpha_P T) dP \tag{6.12}$$

and Equation 6.11 gives

$$\Delta S = S(P_2,T_2) - S(P_1,T_1) = \int_{T_1}^{T_2} \frac{c_p}{T} dT - \int_{P_1}^{P_2} \alpha_P V dP \tag{6.13}$$

The pressure dependence of V and α_P must be known for the integration of Equations 6.10 and 6.11. However, for condensed phases being considered over small ranges of pressure, these pressure dependencies can be ignored.

6.7 SUMMARY

1. Knowledge of heat capacities and entropies of substances and heats of compound formation allows the enthalpy and entropy changes to be evaluated for any process—that is, for phase changes and chemical reactions.

2. Heat capacities can be fit to experimental data *via* an equation of the form

$$c_P = a + bT + \frac{c}{T^2}$$

3. Since enthalpy does not have an absolute value, it is conventional to assign the value of zero to the enthalpy of all elements in their stable states of existence at 298 K and to consider changes in enthalpy with respect to this reference state.
4. On the basis of thermochemical data compiled by *T.* W. Richards, Nernst formulated his Heat Theorem which states that as $T \rightarrow 0$ K, the difference between the reactants and products approaches 0. Thus, their entropies are the same, and the constant of integration of the Gibbs free energy is zero.
5. This was extended by Planck to say that the entropy of all substances which are in complete internal equilibrium is zero at 0 K. This is called the Nernst–Planck–Simon statement of the Third Law of Thermodynamics.
6. Simon has stated that it is impossible by any procedure, no matter how idealized, to reduce the temperature of any system to zero temperature in a finite number of finite operations.
7. Other properties (e.g. heat capacity, thermal expansion, etc.) also approach zero as the temperature approaches zero, and these can be shown to follow from the Third Law.
8. Both the enthalpy and entropy are dependent on pressure and temperature; however, the pressure dependence of the enthalpy and entropy of condensed phases is normally small enough to be ignored, especially when the pressure of interest is in the range 0–1 atm.
9. The variation of enthalpies of transformation with temperature and pressure can be calculated by the application of the First Law of Thermodynamics to the changes in enthalpy with temperature and pressure, as well as the temperature dependence of the heat capacities and expansion coefficients.
10. The enthalpies and entropies of transformation at the melting point and boiling point of metals can be estimated by the rules of Richards and Trouton.
11. The determination of ΔH_T and ΔS_T for any change of state at any temperature and pressure allows the all-important change in the Gibbs free energy for the change of state to be calculated as

$$\Delta G_T = \Delta H_T - T\Delta S_T$$

12. Since consideration of the Gibbs free energy in any isothermal, isobaric process provides the criterion for equilibrium, the equilibrium state of a system can be determined from knowledge of the thermochemical properties of the system.

6.8 CONCEPTS AND TERMS INTRODUCED IN THIS CHAPTER

The reader should write out brief definitions or descriptions of the following terms. Where appropriate, equations may be used.

Allotropy
Aspects of entropy
Endothermic process
Entropy of glass
Exothermic process
Heat capacity at constant magnetic field, $C_{\mathcal{H}}$.
Heat Capacity at constant magnetization, C_M.
Internal equilibrium
Kirchhoff's law
Kopp rule of the heat capacity of compounds
Law of Dulong and Petit
Le Chatelier's principle
Molar heat capacity, c_P and c_V.
Nernst heat theorem
Polymorphism
Richards' rule
Third Law of Thermodynamics
Trouton's rule

6.9 QUALITATIVE EXAMPLE PROBLEMS

QUALITATIVE PROBLEM 1

Estimate c_p, the molar heat capacity of the iron silicon spinel, Fe_2SiO_4, at temperatures >1400 K).

SOLUTION TO QUALITATIVE PROBLEM 1

Assume that this is in the range where the Dulong and Petit law is followed. There are seven atoms in the formula unit of the spinel. Thus, by Kopp's rule, we estimate c_v to be $7 \times 3R = 21R = 174.6$ J/mole·K; c_p would be larger than that number.

Actual c_p at 1400 K = 206 J/mole·K.

QUALITATIVE PROBLEM 2

Show that the following equation holds, relating the Helmholtz free energy to the constant-volume heat capacity of a material.

$$\left(\frac{\partial^2 A}{\partial T^2}\right)_V = -\left(\frac{\partial S}{\partial T}\right)_V = -\left(\frac{c_V}{T}\right)$$

SOLUTION TO QUALITATIVE PROBLEM 2

$$A = U - TS$$

$$-S = \left(\frac{\partial A}{\partial T}\right)_V = \left(\frac{\partial U}{\partial T}\right)_V - T\left(\frac{\partial S}{\partial T}\right)_V - S$$

$$\text{Thus,} \left(\frac{\partial U}{\partial T}\right)_V = T\left(\frac{\partial S}{\partial T}\right)_V = c_v$$

$$\text{We saw that } \left(\frac{\partial A}{\partial T}\right)_V = -S$$

$$\left(\frac{\partial^2 A}{\partial T^2}\right)_V = -\left(\frac{\partial S}{\partial T}\right)_V = -\frac{c_V}{T}$$

6.10 QUANTITATIVE EXAMPLE PROBLEMS

QUANTITATIVE PROBLEM 1

A mixture of Fe_2O_3 and Al, present in the molar ratio 1/2, is placed in an adiabatic container at 298 K, and the Thermit/themite reaction

$$2\ Al + Fe_2O_3 \rightarrow 2Fe + Al_2O_3$$

is allowed to proceed to completion. Calculate the state and the temperature of the reaction products.

SOLUTION TO QUANTITATIVE PROBLEM 1

From the thermochemical data

$$H_{Al_2O_3,298} = -1,675,700 \text{ J/mole}$$

and

$$H_{Fe_2O_3,298} = -823,400 \text{ J/mole}$$

the heat released by the Thermit reaction at 298 K is calculated as

$$\Delta H_{298} = -1,675,700 + 823,400 = -852,300 \text{ J}$$

and this heat raises the temperature of the reaction products. Assume, first, that the sensible heat raises the temperature of the products to the melting temperature of Fe, 1809 K, in which state the reactants occur as 2 moles of liquid Fe and 1 mole of solid Al_2O_3. The molar heat capacities and molar heats of transformation are

- $c_{p,Al_2O_3(s)} = 117.49 + 10.38 \times 10^{-3} T - 37.11 \times 10^5 T^{-2}$ in the range $298 - 2325$ K
- $c_{p,Fe(\alpha)} = 37.12 + 6.17 \times 10^{-3} T - 56.92 T^{-0.5}$ J/K in the range $298 - 1187$ K

- $c_{p,\mathrm{Fe}(\gamma)} = 24.48 + 8.45 \times 10^{-3} T$ in the range $1187 - 1664$ K
- $c_{p,\mathrm{Fe}(\delta)} = 37.12 + 6.17 \times 10^{-3} T - 56.92 T^{-0.5}$ J/K in the range $1667 - 1809$ K
- For $\mathrm{Fe}_{(\alpha)} \rightarrow \mathrm{Fe}_{(\gamma)}$, $\Delta H_{\mathrm{trans}} = 670$ J at 1187 K
- For $\mathrm{Fe}_{(\gamma)} \rightarrow \mathrm{Fe}_{(\delta)}$, $\Delta H_{\mathrm{trans}} = 840$ J at 1664 K
- For $\mathrm{Fe}_{(\delta)} \rightarrow \mathrm{Fe}_{(l)}$, $\Delta H_m = 13,770$ J at 1809 K

The heat required to raise the temperature of 1 mole of Al_2O_3 from 298 to 1809 K is

$$\begin{aligned}\Delta H_1 &= \left[117.48 \times (1809 - 298)\right] + \left[\frac{10.38}{2} \times 10^{-3}\left(1809^2 - 298^2\right)\right] \\ &\quad + 37.11 \times 10^5 \left(\frac{1}{1809} - \frac{1}{298}\right) \\ &= 183,649 \text{ J}\end{aligned}$$

and the heat required to raise the temperature of 2 moles of Fe from 298 to 1809 K and melt the 2 moles at 1809 K is

$$\begin{aligned}\Delta H_2 &= \left[2 \times 37.12 \times (1187 - 298)\right] + \left[\frac{2 \times 6.17}{2} \times 10^{-3}\left(1187^2 - 298^2\right)\right] \\ &\quad + \left[\frac{2 \times 56.92}{0.5}\left(1187^{0.5} - 298^{0.5}\right)\right] + (2 \times 670) \\ &\quad + \left[2 \times 24.28 \times (1664 - 1187)\right] + \left[\frac{2 \times 8.45}{2} \times 10^{-3}\left(1664^2 - 1187^2\right)\right] \\ &\quad + (2 \times 840) + \left[2 \times 37.12 \times (1809 - 1664)\right] \\ &\quad + \left[\frac{2 \times 6.17}{2} \times 10^{-3}\left(1809^2 - 1664^2\right)\right] + \left[\frac{2 \times 56.92}{0.5}\left(1809^{0.5} - 1664^{0.5}\right)\right] \\ &\quad + (2 \times 13,770) \\ &= (78,058 + 1340 + 34,654 + 1680 + 14,268 + 27,540) \\ &= 157,541 \text{ J}\end{aligned}$$

The total heat required is thus

$$\Delta H_1 + \Delta H_2 = 183,649 + 157,541 = 341,190 \text{ J}$$

The remaining available sensible heat is $852,300 - 341,190 = 511,110$ J.

Consider that the remaining sensible heat raises the temperature of the system to the melting temperature of Al_2O_3, 2325 K, and melts the mole of Al_2O_3. The heat required to increase the temperature of the mole of Al_2O_3 is

$$\Delta H_3 = \left[117.49 \times (2325 - 1809)\right] + \left[\frac{10.38}{2} \times 10^{-3}\left(2325^2 - 1809^2\right)\right]$$
$$+37.11 \times 10^5 \left[\frac{1}{2325} - \frac{1}{1809}\right]$$
$$= 71,240 \text{ J}$$

and, with $c_{p,\,\mathrm{Fe}(l)} = 41.84$ J/K, the heat required to increase the temperature of the 2 moles of liquid Fe is

$$\Delta H_4 = 2 \times 41.84 \times (2325 - 1809) = 43,178 \text{ J}$$

The molar latent heat of melting of Al_2O_3 at its melting temperature of 2325 K is 107,000 J, and thus, the sensible heat consumed is

$$71,240 + 43,178 + 107,000 = 221,418 \text{ J}$$

which still leaves 511, 110 − 221,418 = 289,692 J of sensible heat. Consider that this is sufficient to raise the temperature of the system to the boiling point of Fe, 3343 K. The constant-pressure molar heat capacity of liquid Al_2O_3 is 184.1 J/K, and thus, the heat required to increase the temperature of 1 mole of liquid Al_2O_3 and 2 moles of liquid Fe from 2325 to 3343 K is

$$(2 \times 41.84 + 184.1) \times (3343 - 2325) = 272,600 \text{ J}$$

which leaves 289,692 − 272,600 = 17,092 J. The molar heat of boiling of Fe at its boiling temperature of 3343 K is 340,159 J, and thus, the remaining 17,092 J of sensible heat is used to convert

$$\frac{17,092}{340,159} = 0.05$$

moles of liquid iron to iron vapor. The final state of the system is thus 1 mole of liquid Al_2O_3, 1.95 moles of liquid Fe, and 0.05 moles of iron vapor at 3343 K.

Suppose, now, that it is required that the increase in the temperature of the products of the Thermit reaction be limited to 1809 K to produce liquid Fe at its melting temperature. This could be achieved by including Fe in the reactants in an amount sufficient to absorb the excess sensible heat. The sensible heat remaining after the temperature of the mole of Al_2O_3 and the 2 moles of Fe has been increased to 1809 K has been calculated as 511,110 J, and the heat required to raise the temperature of 2 moles of Fe from 298 to 1809 K and melt the Fe has been calculated as $\Delta H_2 = 157,541$ J. The number of moles of Fe which must be added to the reaction of one mole of Fe_2O_3 and 2 moles of Al is thus

$$\frac{511,110}{0.5 \times 157,541} = 6.49$$

The required final state is thus achieved by starting with Fe, Al, and Fe_2O_3 at 298 K, occurring in the ratio 6.49/2/1. The Thermit reaction is used to weld steel in locations which are not amenable to conventional welding equipment.

QUANTITATIVE PROBLEM 2

A quantity of supercooled liquid tin is adiabatically contained at 495 K. Calculate the fraction of the tin which spontaneously freezes, given

$$\Delta H_{m,(\mathrm{Sn})} = 7070 \text{ J at } T_m = 505 \text{ K}$$
$$c_{p,\mathrm{Sn}(l)} = 34.7 - 9.2 \times 10^{-2} T \text{ J/K}$$
$$c_{p,\mathrm{Sn}(s)} = 18.5 + 26 \times 10^{-3} T \text{ J/K}$$

SOLUTION TO QUANTITATIVE PROBLEM 2

The equilibrium state of the adiabatically contained system is that in which the solid, which has formed spontaneously, and the remaining liquid coexist at 505 K. Thus, the fraction of the liquid which freezes is that which releases just enough heat to increase the temperature of the system from 495 to 505 K.

Consider 1 mole of tin and let the molar fraction which freezes be x. In Figure 6.18, the process is represented by a change of state from a to c, and, as the process is adiabatic, the enthalpy of the system remains constant; that is,

$$\Delta H = H_c - H_a = 0$$

Either of two paths can be considered.

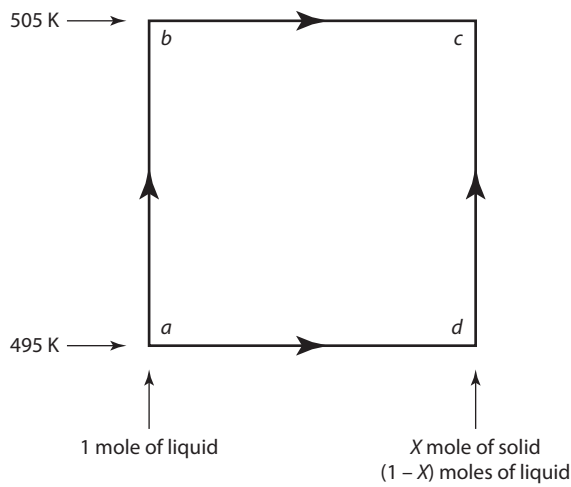

FIGURE 6.18 Changes in the state of Sn, considered in Quantitative Example 2.

Path 1: $a \rightarrow b \rightarrow c$, during which the temperature of the 1 mole of liquid is increased from 495 to 505 K and then x moles freeze. In this case,

$$\Delta H_{(a\rightarrow b)} = -\Delta H_{(b\rightarrow c)}$$

$$\Delta H_{(a\rightarrow b)} = \int_{495}^{505} c_{p,Sn(l)}dT = 34.7\times(505-495) - \frac{9.2}{2}\times 10^{-3}\left(505^2 - 495^2\right)$$

$$= 301 \text{ J}$$

$$\Delta H_{(b\rightarrow c)} = -7070x \text{ J}$$

and thus,

$$x = \frac{301}{7070} = 0.0426$$

That is, 4.26 mol% of the tin freezes.

Path 2: $a \rightarrow d \rightarrow c$; that is, the fraction x freezes at 495 K, and then, the temperature of the solid and the remaining liquid is increased from 495 to 505 K. In this case,

$$\Delta H_{(a\rightarrow d)} = -\Delta H_{(d\rightarrow c)}$$

$$\Delta H_{(a\rightarrow d)} = \text{The heat of freezing } x \text{ moles of tin at } 495\,\text{K}$$

$$= -x\Delta H_m\left(495\text{ K}\right)$$

But,

$$\Delta H_m\left(495\text{ K}\right) = \Delta H_m\left(505\text{ K}\right) + \int_{505}^{495}\Delta c_{p(s\rightarrow l)}dT$$

$$= 7070 + 16.2(495-505) - \frac{35.2}{2}\times 10^{-3}\left(495^2 - 505^2\right)$$

$$= 7084 \text{ J}$$

Thus,

$$\Delta H_{(a\rightarrow d)} = -7084x \text{ J}$$

$$\Delta H_{(d\rightarrow c)} = -x\int_{495}^{505} c_{p(s)}dT + (1-x)\int_{495}^{505} c_{p(l)}dT$$

$$= x\left[18.5(505-495) + \frac{26}{2}\times 10^{-3}\left(505^2 - 495^2\right)\right]$$

$$+(1-x)\left[34.7(505-495) - \frac{9.2}{2}\times 10^{-3}\left(505^2 - 495\right)\right]$$

$$= 301 + 14x$$

Thus,

$$-7084x = -14x - 301$$

which gives

$$x = \frac{301}{7070} = 0.0426$$

The actual path the process follows is intermediate between paths 1 and 2; that is, the process of freezing and increase in temperature occur simultaneously.

The entropy produced by the spontaneous freezing is

$$\Delta S_{(a\to b)} + \Delta S_{(b\to c)} = 34.7 \times \ln\left(\frac{505}{495}\right) - \left[9.2 \times 10^{-3}(505 - 495)\right]$$

$$-\left(0.0426 \times \frac{7070}{505}\right)$$

$$= 0.602 - 0.596 = 0.006 \text{ J/K} \cdot \text{mole}$$

QUANTITATIVE PROBLEM 3

The adiabatic flame temperature is that temperature reached when all of the sensible heat released by the combustion of a fuel is used to raise the temperature of the gaseous products of combustion. Consider the adiabatic flame temperature reached when acetylene, C_2H_2, is combusted at 298 K with (1) the stoichiometric amount of oxygen and (2) the number of moles of air containing the stoichiometric number of moles of oxygen. Air is, by mole or volume percent, 21% O_2 and 79% N_2.

The combustion reaction with stoichiometric oxygen is

$$C_2H_2 + 2.5\ O_2 = 2\ CO_2 + H_2O \qquad \text{(i)}$$

For C_2H_2: $\Delta H_{298} = +226{,}700$ J

For CO_2: $\Delta H_{298} = -393{,}500$ J

For H_2O: $\Delta H_{298} = -241{,}800$ J

SOLUTION TO QUANTITATIVE PROBLEM 3

Thus, for the reaction given by Equation (i):

$$\Delta H(\text{i})_{298} = (-2 \times 393{,}500) - 241{,}800 - 226{,}700 = -1{,}255{,}500 \text{ J}$$

The constant-pressure molar heat capacities of the products of reaction are

$$\text{For } H_2O: \quad c_p = 30.00 + 10.71 \times 10^{-3} T + 0.33 \times 10^5 T^{-2} \text{ J/K} \cdot \text{mole}$$

$$\text{For } CO_2: \quad c_p = 44.14 + 9.04 \times 10^{-3} T - 8.54 \times 10^5 T^{-2} \text{ J/K} \cdot \text{mole}$$

The adiabatic flame temperature, T, is then obtained from the requirement

$$\Delta H(\mathrm{i})_{298} + \int_{298}^{T} \left(2c_p, \mathrm{CO_2} + c_p, \mathrm{H_2O}\right) dT = 0$$

or

$$-1,255,500 + 118.28 \times (T - 298) + 14.40 \times 10^{-3} \times \left(T^2 - 298^2\right) + 16.75 \times 10^5 (1/T - 1/298) = 0$$

which has the solution $T = 6236$ K.

For combustion with the stoichiometric amount of air, the reaction is written as

$$\mathrm{C_2H_2} + 2.5\,\mathrm{O_2} + 2.5 \times (79/21)\,\mathrm{N_2} = 2\mathrm{CO_2} + \mathrm{H_2O} + 9.41\,\mathrm{N_2}$$

$$\text{For } \mathrm{N_2}: \quad c_p, \mathrm{N_2} = 27.87 + 4.27 \times 10^{-3} T \text{ J/mole} \cdot \mathrm{K}$$

and the adiabatic flame temperature, T, is obtained from

$$\Delta H(\mathrm{i})_{298} + \int_{298}^{T} \left(2c_p, \mathrm{CO_2} + c_p, \mathrm{H_2O} + 9.41 c_p, \mathrm{N_2}\right) dT = 0$$

or

$$-1,255,500 + 380.1 \times (T - 298) + 40.16 \times 10^{-3} \times \left(T^2 - 298^2\right) + 16.75 \times 10^5 (1/T - 1/298) = 0$$

as $T = 2{,}797$ K.

This high adiabatic flame temperature facilitates the use of acetylene for welding metals with high melting temperatures.

PROBLEMS

6.1 Calculate ΔH_{1600} and ΔS_{1600} for the reaction $\mathrm{Zr}(\beta) + \mathrm{O_2} = \mathrm{ZrO_2}(\beta)$.

6.2 Which of the following two reactions is the more exothermic?

a. $C_{(\text{graphite})} + 1/2\,\mathrm{O}_{2(g)} \rightarrow \mathrm{CO}_{(g)}$ at 1000 K

b. $C_{(\text{diamond})} + 1/2\,\mathrm{O}_{2(g)} \rightarrow \mathrm{CO}_{(g)}$ at 1000 K

6.3 Calculate the change in enthalpy and the change in entropy at 1000 K for the reaction $\mathrm{CaO}_{(s)} + \mathrm{TiO}_{2(s)} \rightarrow \mathrm{CaTiO}_{3(s)}$.

6.4 Copper exists in the state $T = 298$ K, $P = 1$ atm. Calculate the temperature to which the copper must be raised at 1 atm pressure to cause the same increase in molar enthalpy as is caused by increasing its pressure to 1000 atm at 298 K. The molar volume of Cu at 298 K is 7.09 $\mathrm{cm^3}$, and the

volumetric coefficient of thermal expansion is 0.501×10^{-4} K^{-1}. These values can be taken as being independent of pressure in the range 1–1000 atm.

6.5 Calculate ΔH_{298} and ΔS_{298} for the following reactions:

a. $2TiO + 1/2\,O_2 = Ti_2O_3$

b. $3Ti_2O_3 + 1/2\,O_2 = 2Ti_3O_5$

c. $Ti_3O_5 + 1/2\,O_2 = 3TiO_2$

6.6 An adiabatic vessel contains 1000 g of liquid aluminum at 700°C. Calculate the mass of Cr_2O_3 at room temperature, which, when added to the liquid aluminum (with which it reacts to form Cr and Al_2O_3), raises the temperature of the resulting mixture of Al_2O_3, Cr_2O_3, and Cr to 1600 K.

6.7 Calculate the adiabatic flame temperature attained when methane, at 298 K, is combusted with (a) oxygen in the molar ratio $O_2/CH_4 = 2.0$, and (b) air in the molar ratio air/$CH_4 = 9.524$. Assume that CO_2 and H_2O are the products of combustion. The adiabatic flame temperature is that temperature reached if all of the heat of the oxidation reaction is used to increase the temperature of the products of the reaction. Air is 21 mol% O_2 and 79 mol% N_2.

6.8 Calculate the value of ΔG for the reaction

$$Si_3N_4 + 3O_2 = 3SiO_{2(\alpha-\text{quartz})} + 2N_2$$

at 800 K. What percentage error occurs if it is assumed that Δc_p for the reaction is zero?

6.9 Determine the stoichiometric coefficients for the reaction

$$\left(3CaO \cdot Al_2O_3 \cdot 3SiO_2\right) + a\left(CaO \cdot Al_2O_3 \cdot SiO_2\right) = b\left(CaO \cdot Al_2O_3 \cdot 2SiO_2\right) + c\left(2CaO \cdot Al_2O_3 \cdot SiO_2\right)$$

and calculate ΔH_{298}, ΔS_{298}, and ΔG_{298} for the reaction.

6.10 How much heat is required to increase the temperature of 1 kg of cordierite, 2 MgO·2 Al_2O_3·5 SiO_2, from 298 K to its incongruent melting temperature of 1738 K?

6.11 A function $\Omega \equiv -A + \mu N$, has been defined, where A is the Helmholtz free energy, μ is the chemical potential and N is the number of particles in the system.

Obtain an expression for $d\Omega$ and thus determine the independent variables for this function.

6.12

a. Given that the Helmholtz energy can be written as:

$$A = -N_{\text{system}} k_B T \ln \mathcal{Z}$$

Obtain simplified expressions for both A and S of an Einstein solid.

b. Show that the entropy approaches 0 as the temperature approaches 0 in such a solid.

6.13* An amorphous material at temperature $T = 0$ K is heated to a temperature greater than the melting temperature of the material, T_M. In Figure 6.19 T_χ is the crystallization temperature and T_g is the glass transition temperature.

a. Starting at 0 K, sketch the entropy as a function of temperature.
b. Explain any features of interest (slopes, discontinuities etc.) and explain why they go in the direction that they do (e.g., up or down, etc.) (Figure 6.19).

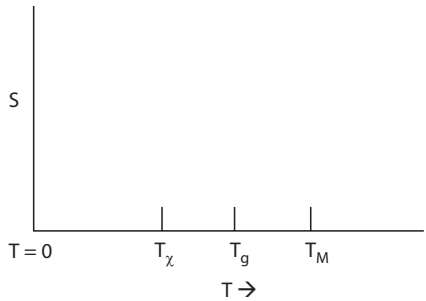

FIGURE 6.19 The axes of an entropy versus temperature plot for Problem 6.13*.

6.14*

i. Plot H versus S for a simple system that is held at constant pressure.
ii. What is the value of the slope of the curve as S goes to 0? Explain.
iii. What can be said about H as S goes to zero?

6.15* One mole of a certain system has been found to have the following equation of state:

$$S = c_V \ln T + R \ln V$$

a. Use this equation to find the value of $c_P - c_V$ for this system, in terms of T, R, and a thermodynamic property of the system.
b. If the system were an ideal gas, what is the value of $c_P - c_V$?

6.16* C_P is greater than C_V for all materials at all temperatures above 0 K.

i. Give a relationship for $C_{\mathcal{H}}$ and $C_{\mathcal{M}}$ (constant magnetic field heat capacity and constant magnetization heat capacity, respectively).
ii. Give an explanation for your equation in terms of the heat needed to raise the temperature of the material.

6.17* Consider the following four phases of an (AB) alloy (Figure 6.20).

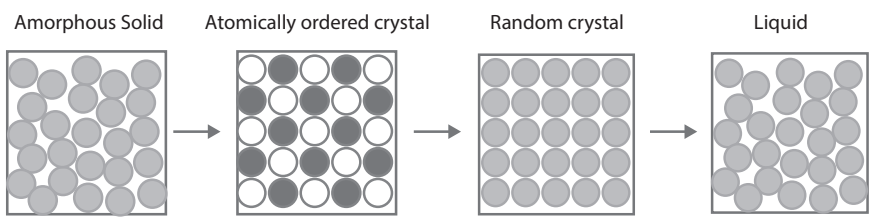

FIGURE 6.20 Schematic of the arrangement of atoms in four different states of an A-B

a. Give the sign of the change in enthalpy and entropy for the following changes:
   i. Amorphous solid to atomic ordered crystal.
   ii. Amorphous solid to random crystal.
   iii. Amorphous solid to liquid.
   iv. Random crystal to liquid.
b. Which of the above phases is most likely the equilibrium one at 0 K? Explain.

6.18* The magnetization vs. temperature and the c_P *vs*. temperature plots for a material are shown below. By X-ray diffraction, it is known that the material starts the process as an amorphous phase at $T = 0$ K (Figure 6.21).
a. Describe the state of the system at the positions A, B, C, and D.
b. Descriptors may include solid, liquid, vapor, amorphous, crystalline, ferromagnetic, and paramagntic. Include more than one descriptor for each state (phase).

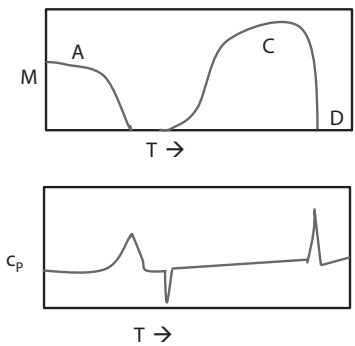

FIGURE 6.21 Magnetization versus temperature and heat capacity versus temperature plots of a material for Problem 6.18.

* New problem in this edition.

Part II

Phase Equilibria

Taylor & Francis
Taylor & Francis Group
http://taylorandfrancis.com

7 Phase Equilibrium in a One-Component System

7.1 INTRODUCTION

In Part II of the text, the fundamental thermodynamic laws, concepts, and relationships among the thermodynamic properties and functions are applied to material systems. In particular, we are interested in determining *equilibrium phase diagrams*, which describe the *constitution of materials* systems under given external and internal constraints. Materials are composed of regions called *phases*, so this chapter begins by defining this term and then moves on to determining relations among equilibrium phases in a variety of systems from the *fundamental equations*, laws, and concepts developed in the first six chapters.

A materials system is composed of one or more *phases*. A phase can be defined as:

> **…** a physically distinct homogeneous portion of a thermodynamic system delineated in space by a bounding surface, called an interphase interface, and distinguished by its state of aggregation (solid, liquid or gas), crystal structure, composition and its degree of order. Each phase in a material system generally exhibits a characteristic set of physical, mechanical, and chemical properties and is, in principle, mechanically separable from the whole.[1]

In systems that are called "simple systems", the thermodynamic variables that control equilibrium are often chosen to be the intensive thermodynamic variables of temperature and pressure. If more than one component is present in the system, the chemical potentials of the various *phases* that compose the system are needed to be included. At finite temperatures, the equilibrium state occurs at the minimum in its Gibbs free energy. After equilibrium is attained, the system is *stable* with respect to macroscopic change. If an outside influence imposes a gradient in any of the intensive thermodynamic variables, a *driving force* for change in the system arises.

The *temperature* of a system is a measure of the intensity of the thermal energy (heat) in the system. If the system is able to exchange energy with its surroundings, and if the surroundings are of a different temperature than the system, the gradient in temperature is a measure of the tendency for thermal energy (heat) to leave or enter the system. If, within an isolated system, a gradient in temperature exists, a driving force exists for the transport of thermal energy down the gradient from the part of the system at the higher temperature to the part of the system at the lower temperature. The spontaneous transfer of thermal energy (heat) occurs until the thermal energy gradient has been eliminated, in which state, the thermal energy is distributed at

[1] W. A. Soffa and D. E. Laughlin, "Diffusional Phase Transformations in the Solid State", in *Physical Metallurgy*, vol. I, edited by D. E. Laughlin and K. Hono, Elsevier, Amsterdam, Netherlands, 2014, pp. 851–1019.

DOI: 10.1201/9781003375388-9

uniform intensity (temperature) throughout the system. Thus, in an isolated system, thermal equilibrium is established when the temperature is uniform throughout the system. If the other potentials are at equilibrium values, the entropy of the system is maximized.

The *pressure* of a system is a measure of its potential for undergoing massive movement by expansion or contraction. If, in a system of fixed volume, the pressure exerted by one phase is greater than that exerted by another phase, then the tendency of the first phase to expand exceeds that of the second phase. The pressure gradient is the driving force for the expansion of the first phase, and this expansion decreases its pressure, hence decreasing its tendency for further expansion. The other phase contracts, which increases its pressure, and hence, its tendency to resist further contraction increases. Mechanical equilibrium is established when the massive movement of the two phases has occurred to the extent that the pressure gradient has been eliminated, in which state the pressure is uniform throughout the system.

The *chemical potential* of species i in a phase is a measure of the tendency of species i to leave the phase. It is thus a measure of the *chemical pressure* exerted by component i in the phase. If, at constant temperature and pressure, the chemical potential of i has different values in different phases of the system, then, as the escaping tendencies differ, the species i will tend to move from the phases in which it occurs at the higher chemical potential to the phases in which it occurs at the lower chemical potential. A gradient in chemical potential is the *driving force* for chemical diffusion. Equilibrium is attained when the various species i are distributed throughout all the phases in the system, such that the chemical potential of each species is the same in all the phases.

In a one-component simple system, at the temperature T and the pressure P, equilibrium occurs when the system exists in that state which has the *minimum* value of its total Gibbs free energy, G'. The equilibrium state can thus be determined by means of an examination of the dependence of G' (or the molar Gibbs free energy, G) on pressure and temperature. Unless otherwise noted in this chapter, we deal with the *molar properties* of one-component simple systems.

7.2 THE VARIATION OF GIBBS FREE ENERGY WITH TEMPERATURE AT CONSTANT PRESSURE

We have seen (Equation 5.10d) that the molar Gibbs free energy for a single-component closed system can be written as

$$dG = -SdT + VdP$$

At constant pressure, this reduces to

$$dG = -SdT$$

Using this equation, we can sketch the molar Gibbs free energy, G, versus the temperature T, for a crystalline solid phase, α, as shown in Figure 7.1. We now examine the features of this constant pressure plot of Gibbs free energy *versus* temperature.

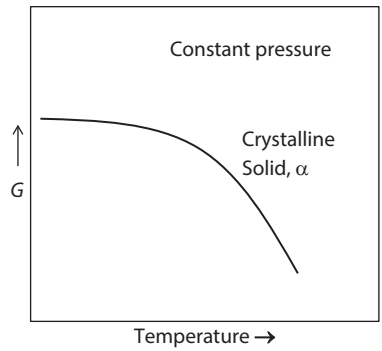

FIGURE 7.1 Schematic of the molar Gibbs free energy versus temperature plot at constant pressure of a single-component crystalline solid phase.

1. Since the slope of the plot is equal to minus that of the entropy of the crystalline solid, $\left(\frac{\partial G}{\partial T}\right)_P = -S$, and since the entropy must be positive, the slope of the curve must be negative for $T > 0$.
2. As T approaches zero, $S = -\left(\partial G / \partial T\right)_P$ approaches zero, as indicated by the Third Law of Thermodynamics (see Chapter 6).
3. The curvature of the plot is proportional to

$$\left(\frac{\partial^2 G}{\partial T^2}\right)_P = -\left(\frac{\partial S}{\partial T}\right)_P = -\frac{c_P}{T} \tag{7.1}$$

   and since c_p and T are positive ($T > 0$ K), the curvature is negative for $T > 0$ K.

4. As the temperature increases, the entropy of the system increases and the curvature of the plot decreases: $\left(\partial S / \partial T\right)_P = -\left(\partial^2 G / \partial T^2\right)_P$.

Now, consider the addition to the plot of the molar Gibbs free energy curve for the liquid phase of this one-component system (Figure 7.2). Once again, we examine the salient features of this plot.

1. We note that the Gibbs free energy of the liquid phase is greater than that of the crystalline solid at $T = 0$ and remains greater until the melting temperature. This follows since the crystalline solid phase is the stable phase below the system's melting point, T_m. If the liquid phase cannot be maintained at very low temperatures, it will transform to a crystalline solid or an amorphous phase.
2. The slope of the Gibbs free energy curve for the liquid, $\left(\partial G^L / \partial T\right)_P$, is more negative than the slope for the crystalline solid, at all temperatures >0 K, since the entropy of the liquid is greater than that of the crystalline solid at all temperatures >0 K.

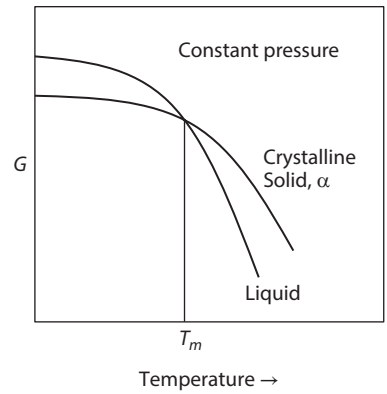

FIGURE 7.2 Schematic of the molar Gibbs free energy *versus* temperature plot of the crystalline solid phase shown in Figure 7.1 along with the plot of its liquid phase. T_M is the melting point of the solid.

3. At the temperature denoted as T_m, the Gibbs free energy of the solid equals that of the liquid: $G^S = G^L$. This is the equilibrium melting temperature of the solid. It is also the equilibrium freezing temperature of the liquid. The solid and liquid phases can coexist at T_M.
4. At T_m, since the slope of the liquid Gibbs free energy is more negative than that of the crystalline solid (since $S^L > S^S$), the Gibbs free energy of the liquid drops below that of the free energy of the crystalline solid, and hence, the liquid becomes the stable phase above T_m.
5. The curvature of the Gibbs free energy of the liquid is more negative than that of the solid, and hence, the heat capacity of the liquid is greater than that of the solid.

$$-\frac{c_P^L}{T} = \left(\frac{\partial^2 G^L}{\partial T^2}\right)_P < \left(\frac{\partial^2 G^S}{\partial T^2}\right)_P = -\frac{c_P^S}{T} < 0$$

$$\frac{c_P^L}{T} > \frac{c_P^S}{T}$$

This is a general feature of competing phases in a simple system: the phase with the largest heat capacity is the stable phase at high temperatures. This was first stated by van't Hoff (Jacobus Henricus van't Hoff, 1852–1911) and is sometimes called the *van't Hoff rule*.

These qualitative features of the molar Gibbs free energy plots of a crystalline solid phase and its liquid phase give insight into the underlying thermodynamic causes which bring about changes in the equilibrium of a system. For example, the liquid phase can only transform into the crystalline phase when its temperature is below T_M, since only below this temperature is the change of the Gibbs free energy for the transformation negative.

The result of reversibly adding thermal energy to the crystalline solid phase at constant pressure, starting at $T=0$ is now examined. As the temperature of the solid starts to increase, the molar heat capacity at constant pressure, c_P^S, which equals $\left(\partial H^S/\partial T\right)_P$, also increases. The crystalline phase remains solid until its equilibrium melting temperature T_m is reached. At this temperature (and pressure), the crystalline solid is able to exist in equilibrium with its liquid phase. If both phases are present at T_m and more thermal energy is added to the solid and liquid mixture, the temperature of the two-phase system *will not increase*. This is because the added thermal energy is utilized to melt the remaining solid until, eventually, only liquid at the melting temperature, T_m, remains. During the constant temperature process of melting, the amount of thermal energy added to the system is written as ΔH_m and is called the *molar enthalpy of melting* (sometimes the *latent heat of melting*). During the melting process, thermal energy is added to the system, but there is no change in temperature. The two-phase mixture of the solid and liquid effectively has an infinite heat capacity at the melting point. After the solid has completely melted, the continued addition of thermal energy increases the temperature of the liquid (see Figure 7.3b).

Since the transformation from solid to liquid occurs at constant temperature, the entropy change of the melting process can be calculated as follows:

$$\Delta S_{\text{melting}} = \frac{\Delta H_{\text{melting}}}{T_m} \tag{7.2}$$

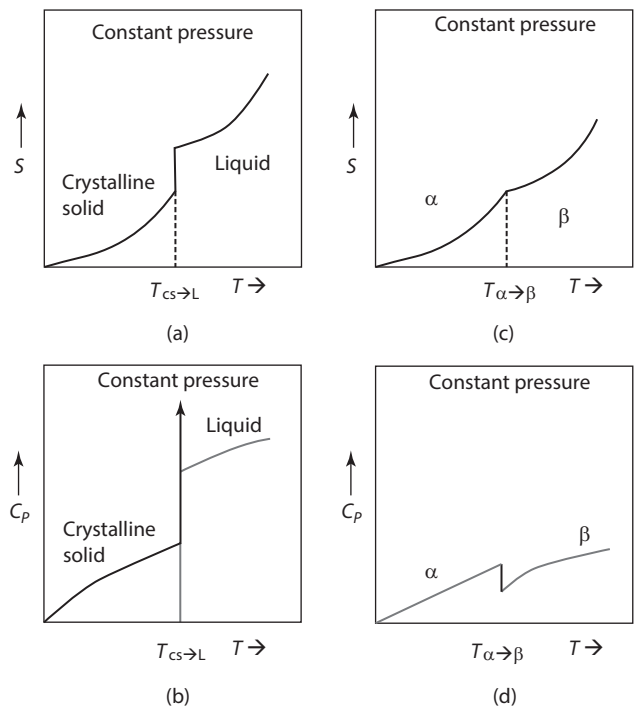

FIGURE 7.3 Schematic diagrams of entropy and heat capacity vs. temperature for First (a,b) and Second order (c,d) phase transformations.

This change in entropy is positive (thermal energy has entered the system), and therefore, as expected, the entropy of the liquid must be greater than that of the crystalline solid from which it is formed.

Above, it was noted that the slopes of the Gibbs free energy curves for the crystalline solid and the liquid phase are different at T_M. Thus, the entropy of the system changes *discontinuously*: the entropies of the two phases are different from one another at T_M. This is shown schematically in Figure 7.3a. This type of transformation is sometimes called a *discontinuous transformation*.

In Figure 7.3b the plot of the heat capacity of the system as a function of temperature is displayed. This plot shows what was described above during the process of heating the crystalline solid. The effective infinity in the heat capacity is denoted by the vertical arrow. The heat capacity of the liquid just above the melting temperature is shown to be larger than the heat capacity of the crystalline solid just before melting began because the curvature of its molar Gibbs free energy plot of a simple system is more negative than that of the crystalline solid.

Phase transformations such as the melting of a one-component crystalline solid are called *first-order phase transformations* (or transitions) after the designation developed by Ehrenfest (Paul Ehrenfest, 1880–1933). This terminology is based on the behavior of the derivative of the Gibbs free energy (or any other energy function of the system such as *U*, *H,* or *A*) in the vicinity of the phase change. The order of a phase transition in this classification is defined as the lowest derivative of the Gibbs free energy with respect to temperature (or pressure) which is *discontinuous* at the transformation temperature.

We have seen that the entropy, $S = -\left(\partial G/\partial T\right)_P$, is discontinuous at the melting temperature. Also, $\left(\partial G/\partial P\right)_T = V$ and $\left(\partial\left(G/T\right)/\partial\left(1/T\right)\right)_P = H$ are also discontinuous at the melting temperature. Each of these discontinuities in the derivatives shows that the variables derived (the molar entropy, *S*, the molar volume, *V*, and the molar enthalpy, *H*) have different values in the low-temperature phase and the high-temperature phase. The discontinuity in these thermodynamic state variables is a fundamental feature of *first-order phase transitions*. If they had the same values but different slopes, the transitions would be called *second-order transitions*, since it is the second derivative of the Gibbs free energy which is discontinuous in these cases (see Figure 7.3c and d). In a second-order transition, the heat capacity drops discontinuously at the transition temperature. Second-order transitions are rare, but cases where the extensive thermodynamic properties *S*, *H,* and *V* are continuous across the transition with apparent infinities in the heat capacity are not so rare. It is best to call these transitions "*higher order*" or continuous transitions (see Problem 7.15).

In Figure 7.4, the change in the enthalpy and the Gibbs free energy for transformation between the crystalline solid and liquid phases as a function of temperature is plotted. It can be seen that ΔG and ΔH approach the same value as the temperature approaches 0 K. This follows from the definition of the Gibbs free energy; that is,

$$\Delta G = \Delta H - T\Delta S$$

In addition, the slopes of the enthalpy and the Gibbs free energy for transformation, $\partial\Delta G/\partial T = -\Delta S$ and $\partial\Delta H/\partial T = \Delta C_P/T$ both approach zero as the temperature approaches 0 K. This was discussed in Chapter 6 when the *Third Law of Thermodynamics* was being considered.

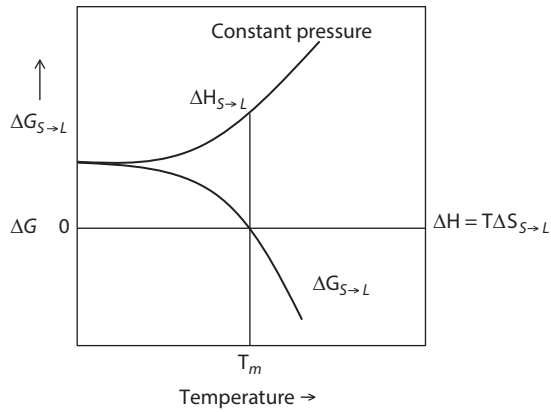

FIGURE 7.4 Schematic of the ΔH and ΔG plots of the crystalline solid-to-liquid transformation in the system depicted in Figures 7.1 and 7.2. At $T = 0$ K, $\Delta H = \Delta G$. At the equilibrium melting temperature, $\Delta G = 0$. Above T_m, $\Delta G_{S \to L} < 0$.

As the temperature increases, the difference between ΔG and ΔH becomes larger. The difference is the value of $T\Delta S_{S \to L}$. Below T_m, $\Delta G_{S \to L} = G_L - G_S > 0$, indicating that the crystalline solid phase will not transform into the liquid phase, since the crystalline solid phase is the stable phase. At T_m, the value of $\Delta G_{S \to L}$ goes to zero since the solid and liquid are in equilibrium at that temperature. Above T_m, $\Delta G_{S \to L} < 0$, indicating that the solid phase will transform into the equilibrium liquid phase.

7.3 THE VARIATION OF GIBBS FREE ENERGY WITH PRESSURE AT CONSTANT TEMPERATURE

From Equation 5.10d, it can be seen that the molar Gibbs free energy is a function of pressure as well as temperature. At constant temperature:

$$dG = VdP$$

A sketch of the molar Gibbs free energy versus pressure for the solid and liquid phases at a fixed temperature is shown in Figure 7.5. Since $\left(\partial G / \partial P\right)_T = V$, which is the molar volume of the phase, the slopes must be positive. The phase with the larger molar volume has a larger slope. Usually, this is the liquid phase, as shown in Figure 7.5. However, there are known examples to the contrary (e.g. water). The curvature of the plot of G versus P is proportional to $\left(\partial^2 G / \partial P^2\right)_T = \partial V / \partial P = -V\beta_T$, where β_T is the isothermal compressibility, which is inversely related to the elastic modulus in a solid phase. The compressibility is positive as defined, so the curvatures of the plots of Figure 7.5 are negative, as shown.

If the constant temperature of the phase shown in Figure 7.5 is the melting temperature of the solid, the pressure where the Gibbs free energies of the solid and liquid are equal is 1 atm, by definition. At this temperature and pressure, the solid and liquid phases are in equilibrium. If the pressure is increased (holding the temperature constant), it is readily seen that the liquid phase is not the stable phase and for the

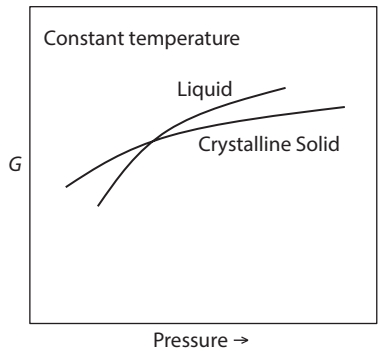

FIGURE 7.5 Schematic of the molar Gibbs free energy vs. pressure plot of the phases shown in Figures 7.1 and 7.2.

The role of pressure on the equilibrium of a solid and a liquid can be considered from the point of view of the *principle of Le Chatelier* which states that, when subjected to an external influence, the state of a system at equilibrium shifts in that direction which tends to nullify the effect of the external influence. Thus, when the pressure exerted on a system is increased, the state of the system shifts in the direction which causes a *decrease* in its volume. The material system depicted in Figure 7.5 shows a larger molar volume for the liquid phase ($\left(\partial G_L / \partial P\right)_T > \left(\partial G_S / \partial P\right)_T$). If the liquid and solid phases are in equilibrium in this system, and if the external pressure is increased, the system divests itself of the higher molar volume liquid phase and transforms to the solid phase. However, water has a smaller molar volume than ice at 0°C. Therefore, an increase in the pressure will cause the *melting* of ice.

7.4 THE GIBBS FREE ENERGY AS A FUNCTION OF TEMPERATURE AND PRESSURE

For a liquid and its crystalline solid phase to be in equilibrium, we know that their molar Gibbs free energies must be equal: $G^L = G^S$ (these are also the chemical potentials of this one component system, $\mu^L = \mu^S$, see Section 5.7). Thus, for a single-component system, we know that $dG^L = dG^S$. Consider Equation 5.10d applied to both the solid and liquid phases:

$$dG^S = -S^S dT + V^S dP$$

$$dG^L = -S^L dT + V^L dP$$

For equilibrium to be maintained between the liquid and solid phases,

$$-S^S dT + V^S dP = -S^L dT + V^L dP$$

or

$$\left(\frac{dP}{dT}\right)_{\text{eq}} = \frac{S^S - S^L}{V^S - V^L} = \frac{S^L - S^S}{V^L - V^S} = \frac{\Delta S}{\Delta V}$$

At equilibrium, $\Delta G = 0$, and hence, $\Delta H = T\Delta S$. When this is substituted into the preceding equation, we arrive at

$$\left(\frac{dP}{dT}\right)_{\text{eq}} = \frac{\Delta H}{T\Delta V} \tag{7.3}$$

This is known as the *Clapeyron equation* (Benoît Paul Émile Clapeyron, 1799–1864) and it gives the relationship between the variation of temperature and pressure, which is required for the maintenance of equilibrium between the solid and the liquid phases in a *first-order transformation*.

Consider again the equilibrium between a crystalline solid and its liquid phase. When thermal energy is added to this two-phase equilibrium ($\Delta H > 0$), the increase in heat causes the solid to melt and $\Delta H_{(S \to L)} > 0$ (endothermic). The sign of $(dP/dT)_{\text{eq}}$ is thus determined by the sign of $\Delta V_{(S \to L)}$. The value of $\Delta V_{(S \to L)}$ for H_2O is negative. Thus, $(dP/dT)_{\text{eq}}$ for H_2O is negative; that is, an increase in pressure decreases the equilibrium melting temperature, as discussed in Section 7.3. But for most materials, $\Delta V_{(S \to L)}$ is positive, which means that an increase in pressure at the melting temperature causes the solid to be in the stable phase, and thereby, the melting temperature increases.

The thermodynamic states of the solid and liquid phases in a one-component system can be represented in a three-dimensional diagram with the Gibbs free energy, *G*, the *temperature, T*, and the *pressure, P* as coordinates. A schematic of such a diagram for H_2O is shown in Figure 7.6. In this figure, the solid and liquid states of existence in *G-T-P* space, which are usually curved surfaces, are shown as planes for clarity. The line along which the planar surfaces intersect represents the variation

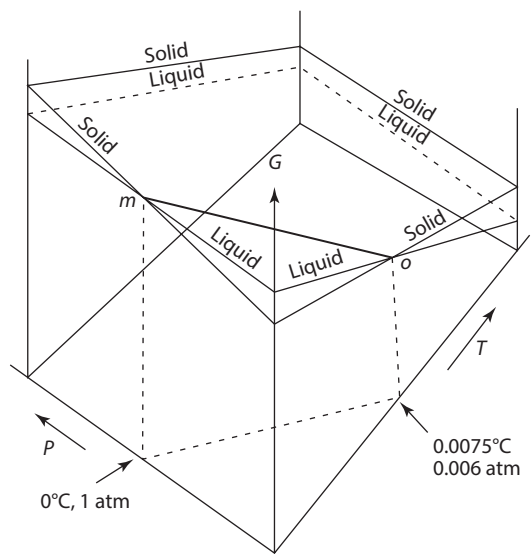

FIGURE 7.6 Schematic representation of the equilibrium surfaces of the solid and liquid phases of water in *G-T-P* space.

of P with T required for the maintenance of the equilibrium between the crystalline solid and liquid phases. At any state, which is determined by fixing the values of T and P, the equilibrium phase is that which has the lower value of Gibbs free energy.

If the *G-T-P* surface for the states of existence of the vapor phase were included in Figure 7.6, its planar surface would intersect with the crystalline solid-state planar surface along another line and would intersect with the liquid-state surface along yet another line. Projection of these curves, together with the curve of the intersection of the solid- and liquid-state surfaces, onto the two-dimensional *P-T* basal plane of Figure 7.6 would produce a plot such as that shown in Figure 7.7, which is a portion of the pressure–temperature phase diagram for water. The three planar surfaces representing the three phases, intersect at a point, the projection of which onto the *P-T* basal plane gives the invariant point *O*, known as the *triple point*. The dashed lines *OA′*, *OB′*, and *OC′* in Figure 7.7 represent, respectively, metastable crystalline solid–liquid, metastable vapor–liquid, and metastable vapor–crystalline solid equilibria of water. If a liquid in equilibrium with its vapor were to be cooled through the triple point the two-phase state may be able to be retained, in a metastable state. This state is at a local minimum in Gibbs free energy, but not at the global minimum. Eventually, it will transform to the single crystalline solid phase. Similarly, the solid–liquid equilibrium *OA′* is metastable with respect to the vapor phase, and the solid–vapor equilibrium *OC′* is metastable with respect to the liquid phase.

The curves *OA, OB,* and *OC* divide Figure 7.7 into three areas within each of which only one phase is stable. Within these areas, the pressure exerted on the phase and the temperature of the phase can be independently varied without changing the type of phase that is in equilibrium. In such cases, the equilibrium is said to have two *thermodynamic degrees of freedom*. The number of degrees of freedom that a system

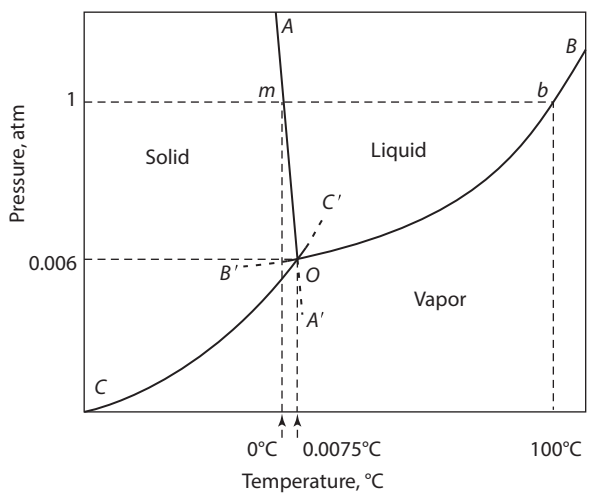

FIGURE 7.7 Schematic representation of part of the pressure–temperature phase diagram for H_2O, showing one, two, and three phase regions of stability. The metastable extensions of the two phase equilibrium curves are also shown.

in equilibrium has is the maximum number of thermodynamic variables which may be independently varied without changing the phase(s) which is (are) in equilibrium.

The single-phase areas meet at the lines *OA, OB,* and *OC* along which two phases coexist in equilibrium. For continued maintenance of any of these two-phase equilibria, only one variable (either P or T) can be independently varied. Two-phase equilibria in a one-component system thus have only one *thermodynamic degree of freedom*.

The three two-phase equilibria curves meet at the triple point, which is the invariant state at which solid, liquid, and vapor phases coexist in equilibrium. The three-phase equilibrium in a one-component system thus has no thermodynamic degrees of freedom. The maximum number of phases that can coexist at equilibrium in a one-component system is therefore three. The number of degrees of freedom, $\mathcal{F}$, that a system containing *one* component can have when ϕ phases are in equilibrium can be seen to be given by:

$$\mathcal{F} = 3 - \phi \tag{7.4}$$

This expression is the Equilibrium Gibbs Phase Rule for a single-component system. This is extended to C component systems in the appendix at the end of this chapter to be:

$$\mathcal{F} = C + 2 - \phi \tag{7.5}$$

From Figure 7.7 it can be seen that

$$S^S < S^L < S^V$$

Similarly, in Figure 7.8b, the slopes of the Gibbs free energy versus pressure plots in any isothermal section increase in the order liquid, solid, and vapor in accordance with the fact that, for H_2O,

$$V^L < V^S < V^V$$

Notice that the relative positions of the metastable extensions of the stable curves can be determined from these plots.

7.5 EQUILIBRIUM BETWEEN THE VAPOR PHASE AND A CONDENSED PHASE

If the Clapeyron equation is applied to the equilibrium between a vapor phase and a condensed phase, then ΔV is the change in the molar volume accompanying evaporation (liquid to vapor) or sublimation (solid to vapor), and ΔH is the corresponding change in the molar enthalpy—that is, the molar enthalpy of evaporation or sublimation.

Now, $\Delta V = V^{\text{vapor}} - V^{\text{condensed phase}}$, and since the molar volume of the vapor, V^{vapor}, is much larger than the molar volume of the condensed phase, $V^{\text{condensed phase}}$, then, with the introduction of an insignificant error,

$$\Delta V = V^{\text{vapor}}$$

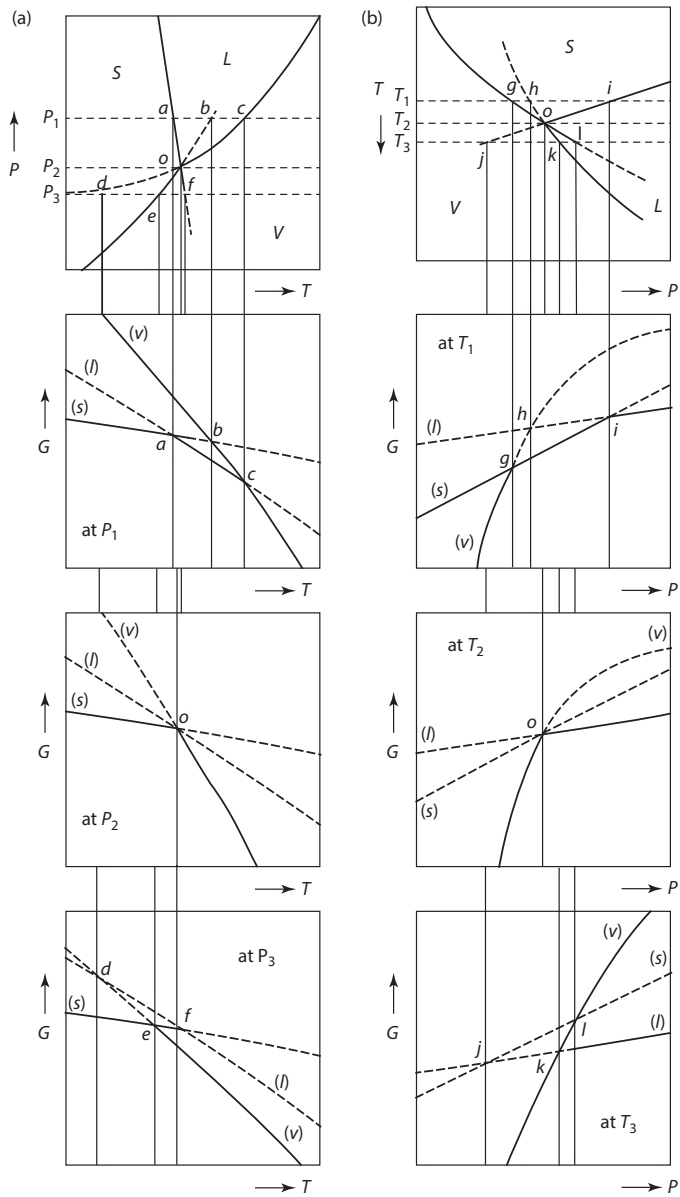

FIGURE 7.8 (a) Schematic of the constant pressure variations of the molar Gibbs free energies of solid, liquid, and vapor H_2O at pressures above, at, and below the triple-point pressure. (b) Schematic of the constant-temperature variations of the molar Gibbs free energies of solid, liquid, and vapor H_2O at temperatures above, at, and below the triple-point temperature.

Thus, for condensed phase–vapor equilibria, the Clapeyron equation can be written as

$$\left(\frac{dP}{dT}\right)_{\text{eq}} = \frac{\Delta H}{TV}$$

in which V^{vapor} is the molar volume of the vapor. If it is further assumed that the vapor in equilibrium with the condensed phase behaves ideally (i.e., $PV = RT$), then

$$\left(\frac{dP}{dT}\right)_{\text{eq}} = \frac{P\Delta H}{RT^2}$$

The rearrangement of which gives

$$\frac{dP}{P} = \frac{\Delta H}{RT^2}dT$$

or

$$d\ln P = \frac{\Delta H}{RT^2}dT \tag{7.6}$$

Equation 7.6 is known as the *Clausius–Clapeyron equation* (Rudolf Julius Emanuel Clausius, 1822–1888).

If ΔH is independent of temperature—that is, if c_p (vapor) $= c_p$ (condensed phase)—integration of Equation 7.6 gives

$$\ln\frac{P}{P_0} = \ln P = -\frac{\Delta H}{RT} + \text{constant} \tag{7.7}$$

where P_0 is the initial pressure.

Since equilibrium is maintained between the vapor phase and the condensed phase, the value of pressure at any temperature in Equation 7.7 is the saturated vapor pressure exerted by the condensed phase at the temperature T. This equation thus shows that the saturated vapor pressure exerted by a condensed phase increases exponentially with increasing temperature, as noted above in Section 5.3.

For this approximation, a plot of ln P versus $1/T$ is linear, with a slope of $-\Delta H/R$ (Figure 7.9). The change in slope in Figure 7.9 occurs at the melting point of the solid. The slope for the crystalline solid-to-vapor plot has a slightly more negative slope (and hence a larger heat of sublimation) than that of the liquid to vapor, consistent with the additional energy given off to form the bonds in the crystal. The saturated vapor pressure *versus* temperature of several of the more common elements is depicted in Figure 7.10.

If Δc_P for evaporation of condensation is not zero, but is independent of temperature, then from Equation 6.9 ΔH_T in Equation 7.6 is:

$$\Delta H_T = \Delta H_{298} + \Delta c_P\left(T - 298\right) \tag{7.8}$$

$$\Delta H_T = \left(\Delta H_{298} - 298\Delta c_P\right) + \Delta c_P T \tag{7.9}$$

In this case, integration of Equation 7.6 for $P_0 = 1$gives

$$\ln P = \left(\frac{298\Delta c_P - \Delta H_{298}}{R}\right)\frac{1}{T} + \frac{\Delta c_P}{R}\ln T + \text{constant}$$

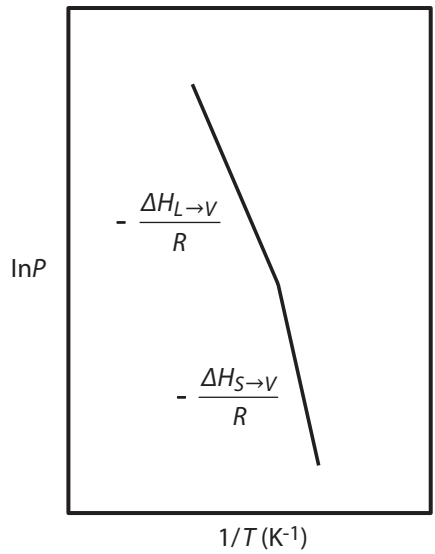

FIGURE 7.9 Schematic plot of ln P vs. 1/T. The slope of the plot is $-\Delta H/R$, where ΔH is the heat of vaporization for the solid or liquid phases divided by R. The slope changes at the melting point of the solid.

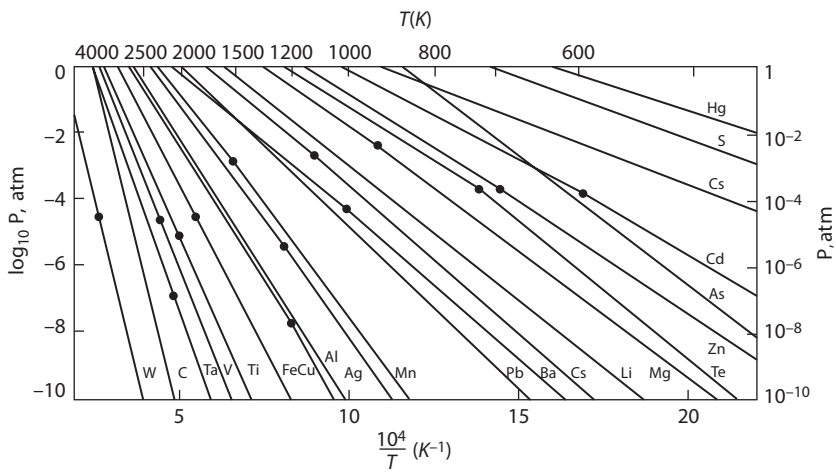

FIGURE 7.10 The vapor pressure vs. 1/T diagram of several elements as functions of temperature. The dots demark the melting points of the elements. (After R. DeHoff, *Thermodynamics in Materials Science*, second edition, CRC, Taylor & Francis (2006).)

and is often expressed in the form:

$$\ln P = -\frac{A}{T} + B\ln T + C \tag{7.10}$$

where $\Delta H_T = AR + BRT$. Table A.4 uses this expression for the vapor pressures of various substances.

7.6 GRAPHICAL REPRESENTATION OF VAPOR PHASE AND CONDENSED PHASE EQUILIBRIA ON PRESSURE TEMPERATURE PHASE DIAGRAMS

When a liquid and its vapor are in equilibrium, the normal *boiling temperature* of the liquid is defined as that temperature at which the *saturated vapor pressure* exerted by the liquid is 1 atm. Knowledge of the molar heat capacities of the liquid and vapor phases, the molar enthalpy of evaporation at any one temperature, $\Delta H_{\text{evap, } T}$, and the normal boiling temperature allows the saturated vapor pressure–temperature to be determined for any material.

The phase diagram of the one-component system depicted in Figure 7.7 has T and P as the independent thermodynamic coordinates. The curve AOA' is a graphical representation of the integral of Equation 7.3, which is the variation of pressure with temperature required for phase equilibrium between the solid and liquid phases. It was noted in Section 7.5 that if ΔH_m is independent of temperature, integration of Equation 7.3 gives an expression of the form

$$P = \frac{\Delta H}{\Delta V} \ln T + \text{constant} \tag{7.11}$$

By definition, the normal *melting temperature* of the material is the melting temperature at a pressure of 1 atm. In Figure 7.7, the normal melting point is designated as the point m. The curve BOB' is the curve for equilibrium between the vapor and the liquid given by Equation 7.7, in which ΔH_T is $\Delta H_{\text{evap, } T}$. In the case of water, the line BOB' represents the variation, with temperature, of the saturated vapor pressure of the liquid, or alternatively, the variation, with pressure, of the dew point of water vapor. The curve BOB' passes through the normal boiling point (represented by point b in the figure) and intersects the line AOA' at the *triple point*, O. The triple point is the state represented by the invariant values of P and T at which the solid, liquid, and vapor phases are in equilibrium with each other. Knowledge of the triple point, together with the value of $\Delta H_{\text{sublim, } T}$, allows the variation of the saturated vapor pressure of the solid with temperature to be determined. This equilibrium curve is drawn as COC' in Figure 7.7.

7.7 SOLID–SOLID EQUILIBRIA

Elements that can exist in more than one crystal form are said to exhibit *allotropy*, and chemical compounds or solid solutions that can exist in more than one solid form are said to exhibit *polymorphism*. The variation of pressure with temperature required to maintain equilibrium between two solids is given by Equation 7.3:

$$\left(\frac{dP}{dT}\right)_{\text{eq}} = \frac{\Delta H}{T\Delta V}$$

in which ΔH and ΔV are the changes in the molar enthalpy and the molar volume for the change of state solid I → solid II.

Figure 7.11a is a schematic of the *P-T* diagram of an element exhibiting two allotropes.

Figure 7.11b shows a schematic of the enthalpy of each of the phases as a function of temperature. Starting at low temperatures and atmospheric pressure, the stable phase is solid phase I. At $T_{I \rightarrow II}$, this phase transforms into the solid phase II. This transformation is shown to have an enthalpy of transformation and is therefore a *first-order transformation*. Phase II melts at T_m, and the liquid boils at T_b. These transformations also display enthalpies of transformation and are *thermodynamically first order.* The transformations are *endothermic* with increasing temperature. It can be seen that the heat of transformation from crystalline solid I to crystalline solid II is depicted as smaller than that of the crystalline solid II to the liquid phase. This is usually the case as the two crystalline solid phases have enthalpies that are more similar to each of than that of the enthalpy of a crystalline solid and its liquid.

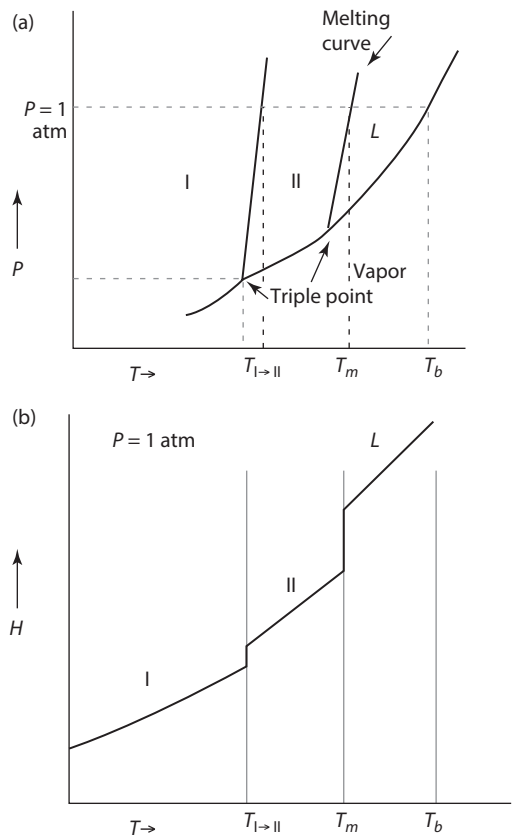

FIGURE 7.11 (a) Schematic pressure vs. temperature diagram of a system with two solid-state phases (I and II) and a liquid phase. (b) Schematic enthalpy vs. temperature diagram of the system in Figure 7.11a, showing the transformation temperature from I to II, the melting temperature, and the boiling temperature.

It can be seen that the presence of an allotropic transformation allows for the possibility of an additional equilibrium *triple point* on the pressure–temperature phase diagram. The new triple point is among the three phases crystalline solid I, crystalline solid II, and the vapor phase.

7.7.1 Solid–Solid Equilibria in Iron

A pressure–temperature phase diagram for iron at relatively low pressures is shown in Figure 7.12. Iron has the body-centered cubic crystal structures in the α and δ phases at, respectively, low and high temperatures and exhibits the face-centered cubic (FCC) crystal structure (γ phase) at intermediate temperatures. Figure 7.12 shows three triple points involving two condensed phases and the vapor phase.

It is of interest to consider the slope of the α–γ equilibrium curve. As was the case for the solid water–liquid water equilibrium curve, the slope is negative. For water, this was because of the *anomalous density* of liquid water, it being *greater* than that of solid water in the region of the equilibrium—that is $V_M\,(L) < V_M\,(S)$. This, combined with the greater entropy of liquid water, $S_M\,(L) > S_M\,(S)$, gives rise to a negative slope.

The negative slope of the *P-T* coexistence boundary for α and γ is also anomalous. The slope $dP/dT = \Delta S/\Delta V$ is usually positive in solids (considering only vibrational entropy), since the smaller molar volume phase usually has the smaller vibrational entropy. The volume change for the paramagnetic Fe transforming from α to γ is negative. Since $\Delta V^{\alpha \to \gamma}$ is negative, $\Delta S^{\alpha \to \gamma}$ must be positive in order for the curve to have a negative slope. This means that the entropy of the γ phase (FCC) is larger than that of α phase (body-centered cubic, BCC), which is unusual.

To explain this, recall that there are various *aspects of entropy*, and in a magnetic solid, the spin entropy must be considered. Thus, the important aspects of entropy here are

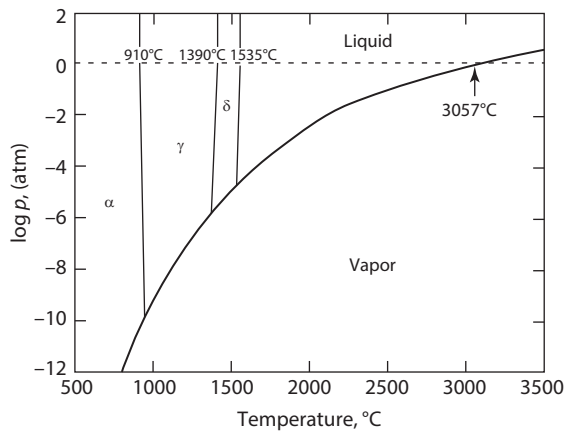

FIGURE 7.12 The pressure–temperature phase diagram for iron.

- Vibrational entropy (thermal)
- The spin entropy of the moments on each Fe atom

As stated above, the Clapeyron equation shows

$$S^{\gamma} > S^{\alpha}$$

Therefore,

$$S^{\gamma}_{\text{vibrational}} + S^{\gamma}_{\text{spin}} > S^{\alpha}_{\text{vibrational}} + S^{\alpha}_{\text{spin}}$$

The vibrational entropy for BCC metals is larger than that for FCC metals (see Chapter 6), so that it can be further concluded that

$$S^{\gamma}_{\text{spin}} > \left(S^{\alpha}_{\text{vibrational}} - S^{\gamma}_{\text{vibrational}}\right) + S^{\alpha}_{\text{spin}}$$

Since both terms on the right-hand side are positive, we conclude that

$$S^{\gamma}_{\text{spin}} > S^{\alpha}_{\text{spin}}$$

FCC γ iron must have larger spin entropy than BCC paramagnetic α iron does. The origin of the large c_p, and therefore, the entropy of the γ phase, is the disordering of the antiferromagnetic (AF) state of γ iron, which occurs at very low temperatures. It is this transition that gives the paramagnetic γ phase such a large spin entropy and stabilizes the γ phase at elevated temperatures. If γ iron were not antiferromagnetic at very low temperatures, where it is metastable, it would not have enough entropy to replace α iron at high temperatures. This would mean that martensite could not be formed in Fe-based alloys!

See T. B. Massalski and David E. Laughlin, *The Surprising Role of Magnetism on the Phase Stability of Fe (Ferro)*, CALPHAD, 2009, 33, pp. 3–7, for further discussion of this.

The curve for equilibrium between γ and δ has a positive slope. In this case, the high-temperature δ phase is BCC, so its vibrational entropy is greater than that of the FCC (γ) phase, and its molar volume is greater as well. At such high temperatures, the spin entropy differences are much smaller.

With increasing pressure, the slope of the γ–δ line being greater than that of the δ–liquid line, means the two lines meet at a triple point for the three-phase γ–δ liquid equilibrium at $P = 14{,}420$ atm and $T = 1590°\text{C}$ (not shown in Figure 7.12). The vapor pressure of liquid iron is given by:

$$\log p(\text{atm}) = -\frac{19{,}710}{T} - 1.27 \ln T + 10.39$$

This reaches 1 atm. at 3330 K (3057°C), which is thus the normal boiling temperature of iron.

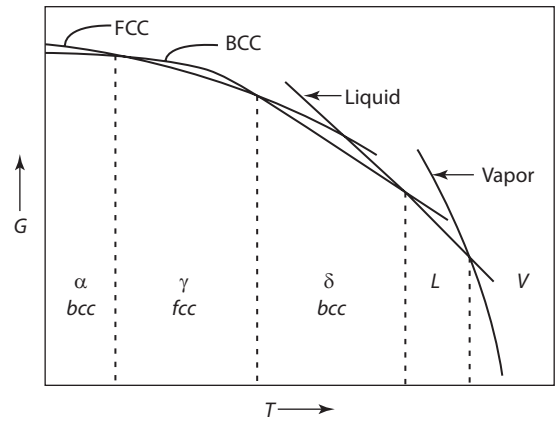

FIGURE 7.13 Schematic representation of the variation of the molar Gibbs free energies of the BCC, FCC, liquid, and vapor phases of iron with temperature at constant pressure.

Figure 7.13 is a schematic representation of the variation of the molar Gibbs free energies with temperature (at constant pressure) of the BCC, FCC, liquid, and vapor phases of iron. For iron, the less close-packed phase BCC (α) is stable at 0 K because its internal energy is lowered due to its *ferromagnetism*. The curvature of the BCC (α) iron Gibbs free energy *versus* temperature curve is more negative than that of the FCC (γ) curve, and hence, it can intersect the FCC iron curve twice, with the consequence that, at 1 atm pressure, BCC iron is stable relative to FCC iron at temperatures <910°C and at temperatures >1390°C. Since the curvature of the Gibbs free energy of the BCC iron is always more negative than that of FCC iron, the heat capacity of FCC (γ) iron is less than that of BCC (α) iron near the temperatures of transformation (See Figure 6.5).

7.7.2 Solid–Solid Equilibria in Zirconia

A schematic phase diagram for zirconia, ZrO_2, is shown in Figure 7.14. Zirconia has monoclinic, tetragonal, and cubic polymorphs. Note that the point group symmetry of the stable polymorph increases as the temperature increases (monoclinic to tetragonal to cubic). Including the liquid and vapor phases, zirconia exhibits five stable phases, and hence, the phase diagram may contain as many as $5!/3! = 20$ triple points (most of which are metastable), five of which are shown in Figure 7.14. The states *a*, *b*, and *c* are stable triple points for, respectively, the three-phase equilibria monoclinic–tetragonal–vapor, tetragonal–cubic–vapor, and cubic–liquid–vapor, and the states *d* and *e* are metastable triple points. The state *d* is that at which the extrapolated vapor pressure lines of the monoclinic and the cubic lines meet in the phase field of stable tetragonal zirconia. The state *d* is thus the metastable triple point for the equilibrium between vapor, monoclinic, and cubic zirconia, which occurs at a higher value of molar Gibbs free energy than that of tetragonal zirconia at the same

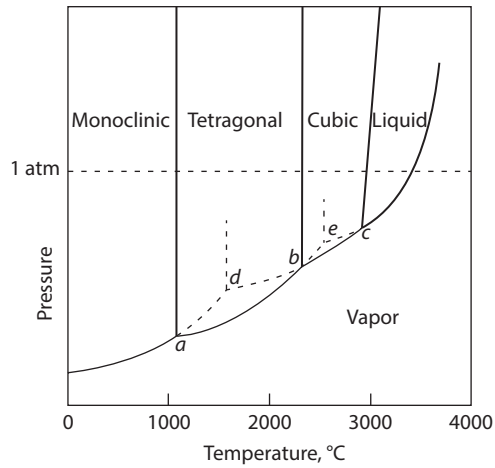

FIGURE 7.14 A schematic pressure–temperature phase diagram for zirconia, ZrO_2.

value of *P* and *T*. Similarly, the state *e*, which is that at which the extrapolated vapor pressures of tetragonal and liquid zirconia intersect in the phase field of stable cubic zirconia, is the metastable triple point for equilibrium between liquid, vapor, and tetragonal zirconia.

7.8 THE EFFECT OF AN APPLIED MAGNETIC FIELD ON THE *P-T* DIAGRAM

When a magnetic field is applied to a system in equilibrium, a change in the equilibrium state will occur. Consider the *P-T* diagram of Figure 7.15. The solid line represents the equilibrium between the β and γ phases when $\boldsymbol{\mathcal{H}} = 0$. If a magnetic field is now applied, there will be a change in the equilibrium state, indicated by the dotted line.

In Chapter 2, it was seen that when a magnetic field is applied to a material, the field does work on the material.

$$\delta w' = -V\mu_0 \overset{\text{true}\rightarrow}{\boldsymbol{\mathcal{H}}} \cdot d \overset{\text{true}\rightarrow}{\boldsymbol{\mathcal{M}}}$$

In Qualitative Problem 2 of Chapter 2, we saw that $\boldsymbol{\mathcal{H}} = \boldsymbol{\mathcal{M}}/\chi$ for the linear region of the $\boldsymbol{\mathcal{H}} - \boldsymbol{\mathcal{M}}$ plot, where χ is the *magnetic susceptibility* of the material. For equilibrium in a one-component system, we write the Gibbs free energy as

$$dG' = -S'dT + V'dP - V'\mu_0 \boldsymbol{\mathcal{M}} d\boldsymbol{\mathcal{H}}$$

and substituting $\chi\boldsymbol{\mathcal{H}}$ for $\boldsymbol{\mathcal{M}}$,

$$dG' = -S'dT + V'dP - V'\mu_0 \chi \boldsymbol{\mathcal{H}} d\boldsymbol{\mathcal{H}}$$

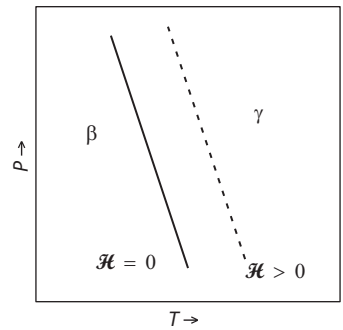

FIGURE 7.15 Schematic pressure vs. temperature diagram for two solid phases, β and γ. The β phase has a higher magnetic susceptibility. When a magnetic field is applied, the equilibrium curve shifts and expands the stability region of the phase with the higher magnetic susceptibility.

It can be seen from the preceding equations that the Gibbs free energy is lowered more for the phase with the larger *magnetic susceptibility* when an external magnetic field $\mathcal{H}$ is applied. The applied magnetic field thus stabilizes the phase with the larger magnetic susceptibility. For the example in Figure 7.15, the curve of β–γ equilibrium is shifted to higher temperatures. Thus, the β phase has a larger magnetic susceptibility than the γ phase; hence, the applied magnetic field increases the *stability field* of the material with a higher magnetic susceptibility. It must be pointed out that the dotted equilibrium line in Figure 7.15 is only valid while the external field is applied! When the field is removed, the solid line returns to being the boundary line for the β and γ equilibrium.

7.9 SUMMARY

1. The change in the Gibbs free energy of a system during changes in temperature can be determined from the changes in enthalpy and entropy, utilizing their dependency of heat capacity with temperature.
2. Since a closed one-component system has only two independent variables, the *Gibbs free energy* can be examined most simply by choosing the state variables *temperature* and *pressure* as the *independent variables*. These are the *natural independent variables* for the *Gibbs free energy* function. The phases in which the material can exist can thus be represented in a three-dimensional diagram using the state function *Gibbs free energy*, the independent state variables *pressure*, and *temperature* as coordinates.
3. If sections of these three-dimensional diagrams are taken at constant *pressure*, one obtains Gibbs free energy *versus temperature* plots for the phases. The phase that is in equilibrium at a given temperature is the one with the lowest *Gibbs* free energy. Intersections of the curves represent temperatures at which two (or three) phases are in equilibrium. The slope of the *Gibbs* free energy versus *temperature* plot is the negative of the entropy, and the negative curvature is related to the *heat capacity* of the phase delineated by the curve.
4. Sections of the three-dimensional diagrams may be taken at constant temperature. Such plots of *Gibbs* free energy versus *pressure* show which phase

are equal to the molar volume of the phases, and their negative curvatures are related to the *isothermal compressibility* of the phases.

5. In the three-dimensional diagrams, the various states in which the material can exist occur as surfaces. In any state, which is determined by the values of *pressure* and *temperature*, the stable phase is that which has the lowest Gibbs free energy. The surfaces in the diagram intersect with one another along curves, and these curves represent the variations of *pressure* with *temperature* required for equilibrium between the two phases.
6. The intersection of the surfaces for the solid and liquid phases gives the variation of the equilibrium melting temperature with pressure. The intersection of the surfaces for the liquid and vapor phases gives the variation of the boiling temperature with pressure. The normal melting and boiling points of the material occur on these intersections at *pressure* equal to one atmosphere. Three surfaces intersect at a point in the diagram, and the values of *pressure* and *temperature* at which this intersection occurs are those of the *invariant triple point* at which an equilibrium occurs among three phases. In a one-component system, no more than three phases can coexist in equilibrium with one another.
7. The three-dimensional *Gibbs free energy-temperature-pressure* diagram illustrates the differences between *stable*, *metastable*, and *unstable states* and, hence, shows the difference between *reversible* and *irreversible* process paths. At any value of P and T, the stable phase is that which has the lowest Gibbs free energy which lies on a state surface. Phases which have higher values of Gibbs free energy which lie on other surfaces at the same values of *pressure* and *temperature* are *metastable* with respect to the phase of lowest value of Gibbs free energy. States with a value of Gibbs free energy at any combination of *pressure* and *temperature* which do not *lie on a surface* in the diagram are *unstable*. A reversible process path involving a change in *pressure* and/or *temperature* lies on a *phase surface*, and the state of a phase is changed reversibly only when, during the change, the state of the system does not leave the surface of the phase. If the process path leaves the phase surface, then the change of state, which necessarily passes through nonequilibrium states, is irreversible.
8. In a three-dimensional perspective diagram, represented in two dimensions, is difficult to deal quantitatively with transition temperatures and pressures. Therefore it is normal practice to present the phase diagram for a one-component system as the basal plane of the *Gibbs free energy-temperature-pressure* diagram (i.e., a *pressure-temperature* diagram), onto which are projected the lines along which two surfaces intersect (equilibrium between two phases) and the points at which three surfaces intersect (equilibrium among three phases). Such a diagram contains areas in which a single phase is stable, which are separated by curves along which two phases exist at equilibrium, and points at the intersection of three curves at which three phases coexist in equilibrium. The curves for equilibrium between a condensed phase and the vapor phase are called *vapor pressure curves*, and they are exponential in form. In view of the fact that saturated vapor pressures can vary over several orders of magnitude, pressure–temperature

phase diagrams can often be presented in a more useful form as plots of ln P versus $1/T$ than as plots of P versus T.

9. The development of phase diagrams for one-component systems demonstrates the use of Gibbs free energy as a criterion for equilibrium when *temperature* and *pressure* are chosen as the *independent state variables*.
10. If the plots of entropy versus temperature show discontinuities at the transformation temperatures, the transformations are called *first-order transformations* or discontinuous transformations. These transformations allow for the coexistence of the phases at the transformation temperature. If the entropy versus temperature plots are continuous at the transformation temperature, the transformations are called higher order or continuous transformations, and no phase coexistence occurs at the transformation temperature.
11. The equilibrium Gibbs phase rule for a one-component simple system is

$$\mathcal{F} = 3 - \phi$$

where $\mathcal{F}$ is the number of degrees of freedom and the ϕ number of phases allowed to be present in equilibrium.

12. Thermodynamic equilibrium is affected by the application of external fields, such as a magnetic or electrical field.

7.10 CONCEPTS AND TERMS INTRODUCED IN THIS CHAPTER

The reader should write out brief definitions or descriptions of the following terms. Where appropriate, equations may be used.

Allotropy
Clapeyron equation
Clausius–Clapeyron equation
Constitution of materials
Constraints on the system
Continuous transition
Curvature of Gibbs free energy curves
Discontinuous transformation
Driving force
Enthalpy of melting
Entropy of melting
Entropy vs. temperature plots
Equilibrium phase diagrams
First-order phase transformation (transition)
Gibbs equilibrium phase rule
Higher-order phase transformation (transition)
Magnetic susceptibility
Melting temperature
Metastable extension
Phase

Polymorphism
Potential
Principle of Le Chatelier
Second-order phase transformation (transition)
Slope of Gibbs free energy curves
Spin entropy
Stable, metastable, and unstable phases
Thermodynamic degree of freedom
van't Hoff rule
Vibrational entropy

7.11 QUALITATIVE EXAMPLE PROBLEMS

QUALITATIVE PROBLEM 1

The pressure–temperature phase diagrams shown in Figure 7.16 of a single component system have appeared in publications.

i. Which (if any) show errors in their construction?

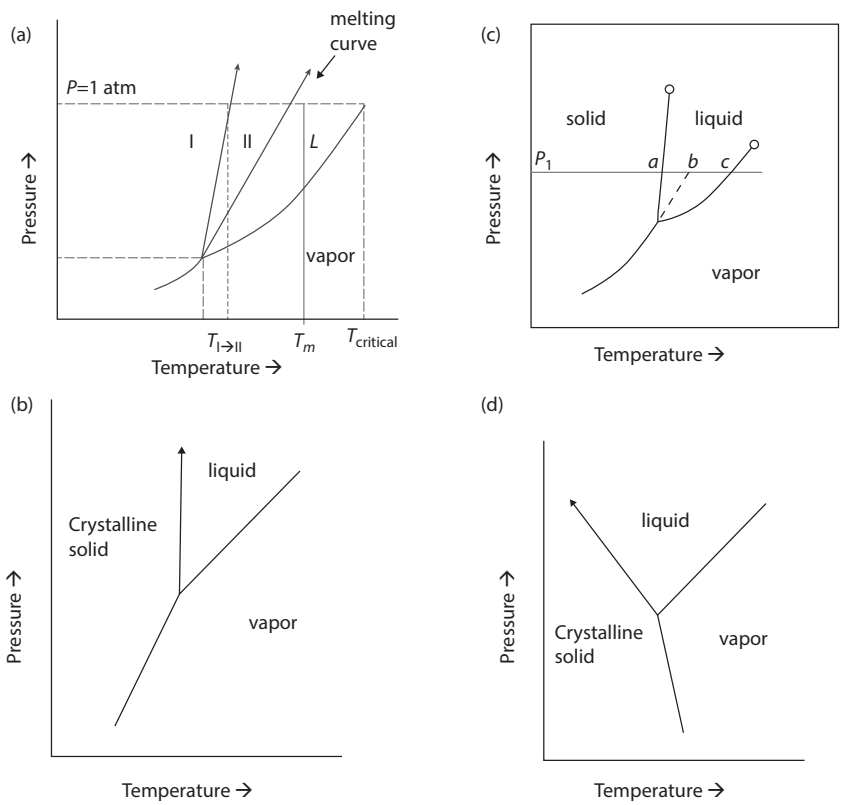

FIGURE 7.16 Four pressure–temperature phase diagrams of a single-component systems that may contain errors of construction.

ii. For those (if any) with errors, explain what is the thermodynamic principle that is violated?

SOLUTION TO QUALITATIVE PROBLEM 1

a. Has a point with four phases in equilibrium. This violates the Gibbs Equilibrium Phase Rule which limits the number of phases that can be in equilibrium to two more than the number of components.
b. No error here. A vertical solid/liquid curve is possible if the molar volumes of the two condensed phases are the same.
c. Has a critical point between a crystalline solid and a liquid, which is not possible. See Section 8.2 for critical points.
d. The slope of the crystalline solid/vapor phase must be positive, since the entropy and molar volume of the vapor must be greater than that of the solid.

QUALITATIVE PROBLEM 2

Part of the pressure versus temperature phase diagram of a system with three solid phases is shown in Figure 7.17.

i. Write an equation that relates the molar entropies of each of the phases.
ii. Write an equation that relates the molar volumes of each of the phases.

SOLUTION TO QUALITATIVE PROBLEM 2

i. By drawing a horizontal line at the pressure of the triple point, we see that:

$$S^{\gamma} < S^{\alpha} < S^{\beta}$$

ii. By drawing a vertical at a temperature of the triple point, we see that:

$$V^{\beta} > V^{\alpha} > V^{\gamma}$$

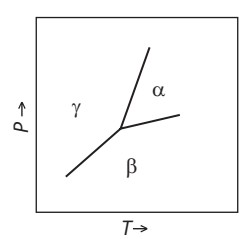

FIGURE 7.17 Pressure temperature phase diagram of a one-component system with three solid phases near a triple point.

7.12 QUANTITATIVE EXAMPLE PROBLEMS

QUANTITATIVE PROBLEM 1

The vapor pressure of solid NaF varies with temperature as

$$\ln p(\text{atm}) = \frac{-34,450}{T} - 2.01 \ln T + 33.74$$

and the vapor pressure of liquid NaF varies with temperature as

$$\ln p(\text{atm}) = \frac{-31,090}{T} - 2.52 \ln T + 34.66$$

Calculate

1. The normal boiling temperature of NaF
2. The temperature and pressure at the triple point
3. The molar enthalpy of evaporation of NaF at its normal boiling temperature
4. The molar enthalpy of melting of NaF at the triple point
5. The difference between the constant-pressure molar heat capacities of liquid and solid NaF

The phase diagram is shown *schematically* in Figure 7.18.

SOLUTION TO QUANTITATIVE PROBLEM 1

1. The normal boiling temperature, T_b, is defined as the temperature at which the saturated vapor pressure of the liquid is 1 atm. Thus, from the equation for the vapor pressure of the liquid, T_b is

$$\ln(1) = 0 = -\frac{31,090}{T_b} - 2.52 \ln T_b + 34.66$$

which has the solution $T_b = 2006$ K

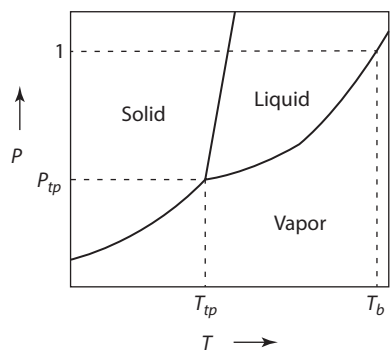

FIGURE 7.18 Schematic pressure–temperature phase diagram for a one-component system.

2. The saturated vapor pressures for the solid and liquid phases intersect at the triple point. Thus, at the temperature, T_{tp}, of the triple point

$$-\frac{34,450}{T_{tp}} - 2.01\ln T_{tp} + 33.74 = -\frac{31,090}{T_{tp}} - 2.52\ln T_{tp} + 34.66$$

which has the solution $T_{tp} = 1239$ K

The triple-point pressure is then calculated from the equation for the vapor pressure of the solid as

$$p = \exp\left(-\frac{34,450}{1239} - 2.01\ln 1239 + 33.74\right) = 2.29\times 10^{-4} \text{ atm}$$

or from the equation for the vapor pressure for the liquid as

$$p = \exp\left(-\frac{31,090}{1239} - 2.52\ln 1239 + 34.66\right) = 2.29\times 10^{-4} \text{ atm}$$

3. For vapor in equilibrium with the liquid:

$$\ln p(\text{atm}) = -\frac{31,090}{T} - 2.52\ln T + 34.66$$

$$\frac{d\ln p}{dT} = \frac{\Delta H}{RT^2} = \frac{31,090}{T^2} - \frac{2.52}{T}$$

Thus,

$$\Delta H_{(l\to v)} = (31,090\times 8.3144) - (2.52\times 8.3144)T = 258,500 - 20.95T$$

and, at the normal boiling temperature of 2006 K,

$$\Delta H_{(l\to v)} = 258,500 - 20.95\times 2006 = 216,500 \text{ J}$$

4. For vapor in equilibrium with the solid:

$$\ln p(\text{atm}) = -\frac{34,450}{T} - 2.01\ln T + 33.74$$

Thus,

$$\Delta H_{(s\to v)} = (34{,}450 \times 8.3144) - (2.01 \times 8.3144)T$$
$$= 286{,}400 - 16.71T \text{ J}$$

Near the triple point,

$$\Delta H_{(s\to l)} + \Delta H_{(l\to v)} = \Delta H_{(s\to v)}$$

and thus,

$$\Delta H_{(s\to l)} = 286{,}400 - 16.71T - 258{,}500 + 20.95T$$
$$= 27{,}900 + 4.24T$$

At the triple point,

$$\Delta H_{(s\to l)} = 27{,}900 + (4.24 \times 1239) = 33{,}150 \text{ J}$$

5. $\Delta H_{(s\to l)} = 27{,}900 + 4.24T$

$$\frac{d\Delta H}{dT} = \Delta c_p = 4.24 \text{ J/K}$$
$$= c_P^L - c_P^S > 0$$

QUANTITATIVE PROBLEM 2

Carbon has the following three allotropes: graphite, diamond, and a metallic form called solid III. Graphite is the stable form of 298 K and 1 atm pressure, and increasing the pressure on graphite at temperatures <1440 K causes the transformation of graphite to diamond and then the transformation of diamond to solid III. Calculate the pressure which, when applied to one mole graphite at 298 K, causes the transformation of graphite to diamond, given:

- $H_{298\text{ K, (graphite)}} - H_{298\text{ K, (diamond)}} = -1900\,\text{J}$.
- $S_{298\text{ K, (graphite)}} = 5.74\,\text{J/K}$.
- $S_{298\text{ K, (diamond)}} = 2.37\,\text{J/K}$.
- The density of graphite at 298 K is 2.22 g/cm^3.
- The density of diamond at 298 K is 3.515 g/cm^3.

SOLUTION TO QUANTITATIVE PROBLEM 2

For the transformation graphite → diamond at 298 K:

$$\Delta G = \Delta H - T\Delta S$$

$$= 1900 - 298(2.37 - 5.74) = 2904 \text{ J}$$

For the transformation of graphite to diamond at any temperature T:

$$\left(\frac{\partial \Delta G_{\text{graphite}\rightarrow\text{diamond}}}{\partial P}\right)_T = \Delta V_{\text{graphite}\rightarrow\text{diamond}}$$

$$V_{\text{graphite}} = \frac{12}{2.22} = 5.405 \text{ cm}^3/\text{mole}$$

and

$$V_{\text{diamond}} = \frac{12}{3.515} = 3.415 \text{ cm}^3/\text{mole}$$

Thus,

$$\Delta V = -1.99 \text{ cm}^3/\text{mole}$$

Equilibrium between graphite and diamond at 298 K requires that $\Delta G_{\text{graphite}\rightarrow\text{diamond}}$ be zero. Since

$$\left(\frac{\partial \Delta G}{\partial P}\right)_T = \Delta V$$

then

$$\Delta G(P, T = 298) = \Delta G(P = 1, T = 298) + \int_1^P \Delta V dP$$

If the difference between the isothermal compressibilities of the two phases is negligibly small (i.e., if the influence of pressure on ΔV can be ignored), then

$$1 \text{ cm}^3 \cdot \text{atm} = \frac{8.3144}{82.057} = 0.1013 \text{ J}$$

$$\Delta G(P, T = 298) = 2904 + (-1.99 \times 0.1013)(P - 1)$$

and thus,

$$(P-1) = P = \frac{2904}{1.99 \times 0.1013} = 14{,}400 \text{ atm}$$

Transformation of graphite to diamond at 298 K requires the application of a pressure >14,400 atm.

PROBLEMS

7.1 Using the vapor pressure–temperature relationships for $CaF_2(\alpha)$, $CaF_2(\beta)$, and liquid CaF_2, calculate
   a. The temperatures and pressures of the triple points for the equilibria $CaF_2(\alpha) - CaF_2(\beta) - CaF_2(v)$ and $CaF_2(\beta) - CaF_2(l) - CaF_2(v)$
   b. The normal boiling temperature of CaF_2
   c. The molar latent enthalpy of the transformation $CaF_2(\alpha) \rightarrow CaF_2(\beta)$
   d. The molar latent enthalpy of melting of $CaF_2(\beta)$

7.2 Calculate the approximate pressure required to distill mercury at 100°C.

7.3 One mole of $SiCl_4$ vapor is contained at 1 atm pressure and 350 K in a rigid container of fixed volume. The temperature of the container and its contents is cooled to 280 K. At what temperature does condensation of the $SiCl_4$ vapor begin, and what fraction of the vapor has condensed when the temperature is 280 K?

7.4 The vapor pressures of zinc have been written as

$$\ln p(\text{atm}) = -\frac{15{,}780}{T} - 0.755 \ln T + 19.25 \qquad \text{(i)}$$

and

$$\ln p(\text{atm}) = -\frac{15{,}250}{T} - 1.255 \ln T + 21.79 \qquad \text{(ii)}$$

Which of the two equations is for solid zinc?

7.5 At the normal boiling temperature of iron, $T_b = 3330$ K, the rate of change of the vapor pressure of liquid iron with temperature is 3.72×10^{-3} atm/K. Calculate the molar latent enthalpy of boiling of iron at 3330 K.

7.6 Below the triple point (–56.2°C), the vapor pressure of solid CO_2 is given as

$$\ln p(\text{atm}) = -\frac{3116}{T} + 16.01$$

The molar latent enthalpy of melting of CO_2 is 8330 J. Calculate the vapor pressure exerted by liquid CO_2 at 25°C and explain why solid CO_2 is referred to as "dry ice."

7.7 The molar volumes of solid and liquid lead at the normal melting temperature of lead are, respectively, 18.92 and 19.47 cm^3. Calculate the pressure that must be applied to lead in order to increase its melting temperature by 20°C.

7.8 Nitrogen has a triple point at $P = 4650$ atm and $T = 44.5$ K, at which state the allotropes α, β, and γ coexist in equilibrium with one another. At the triple point, $V_\beta - V_\alpha = 0.043\ cm^3$/mole and $V_\alpha - V_\gamma = 0.165\ cm^3$/mole. Also at the triple point, $S_\beta - S_\alpha = 4.59$ J/K and $S_\alpha - S_\gamma = 1.25$ J/K. The state of $P = 1$ atm, $T = 36$ K lies on the boundary between the fields of stability of the α and β phases, and at this state, for the transformation of α → β, $\Delta S = 6.52$ J/K and $\Delta V = 0.22\ cm^3$/mole. Sketch the phase diagram for nitrogen at low temperatures.

7.9 Measurements of the saturated vapor pressure of liquid $NdCl_5$ give 0.3045 atm at 478 K and 0.9310 atm at 520 K. Calculate the normal boiling temperature of $NdCl_5$.

7.10* Part of the pressure versus temperature phase diagram of a system with three solid phases is shown in Figure 7.19.

i. Write an equation that relates the molar entropies of each of the phases.

ii. Write an equation that relates the molar volumes of each of the phases.

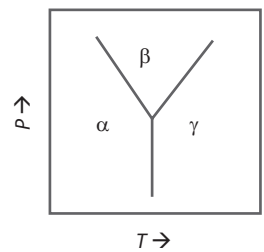

FIGURE 7.19 Schematic pressure–temperature phase diagram for a one-component system.

7.11 Figure 7.11 shows a pressure versus temperature phase diagram for a system exhibiting two solid-state phases. Sketch the Gibbs free energy curves versus temperature for the two solid phases and the liquid phase. Comment on the slopes of the curves.

7.12 Figure 7.20 is the Gibbs free energy *versus* pressure plot for three phases, solid (*S*), liquid (*L*), and gas, near the triple point for the system. It is known that the molar volume of the solid is greater than that of the liquid.

a. Label the three plots of *G* versus *P* as *S*, *L*, or Gas.

b. Draw the *T*-*P* plot for the material as shown in Figure 7.19. Label the *S*, *L*, and Gas fields and any other points of interest. Note that the temperature is increasing in the downward direction.

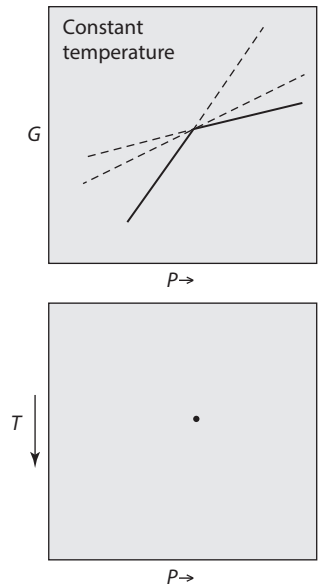

FIGURE 7.20 Schematic Gibbs free energy vs. temperature diagram for a one-component system and a template of the plot to be used in answering the problem.

7.13 The pressure–temperature phase diagram of a certain material is shown in Figure 7.21. Construct the volume–temperature diagram for this substance using the arrangement shown in the figure and label all phase fields.

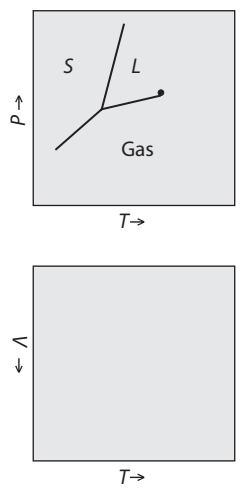

FIGURE 7.21 The pressure–temperature phase diagram of the system discussed in Problem 7.13 along with the volume vs. temperature template to be used in the answer.

7.14 It can be seen from Figure 7.7 that the metastable extensions of the two-phase equilibria go into single-phase fields. At the triple point, it can be seen that the stable and metastable equilibrium curves alternate as one goes around the triple point. Show that the metastable extensions must alternate with stable two-phase curves.

7.15* The heat capacity versus temperature plots for the first- and second-order phase transformations are shown in Figure 7.3b and d. Figure 7.22 is a schematic plot of the heat capacity versus temperature for a ferromagnetic to paramagnetic transformation in a metal. For convenience, the thermal heat capacity curve has been subtracted and the so-called spin heat capacity versus temperature plot is displayed.

i. Is this a *first-order* transformation?
ii. Is this a *second-order* transformation?

Explain your answers.

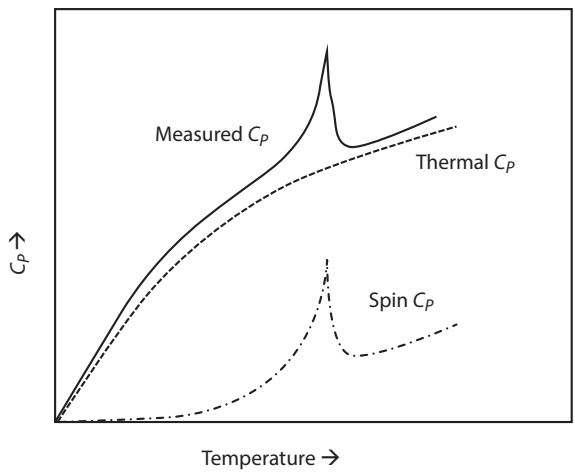

FIGURE 7.22 A schematic heat capacity versus temperature plot for a ferromagnetic to paramagnetic transformation.

7.16*

a. Use the data displayed in Figure 7.7 to plot the ln (P) versus $1/T$ for the liquid/vapor equilibrium co-existence of water.
b. Now use Equation 7.7 to obtain the enthalpy change during the vaporization of liquid water.

7.17* A portion of a pressure–temperature diagram showing the vapor/liquid equilibrium and the critical point is shown in Figure 7.23. Sketch the corresponding equilibria in the Pressure Entropy and the Volume Temperature diagrams.

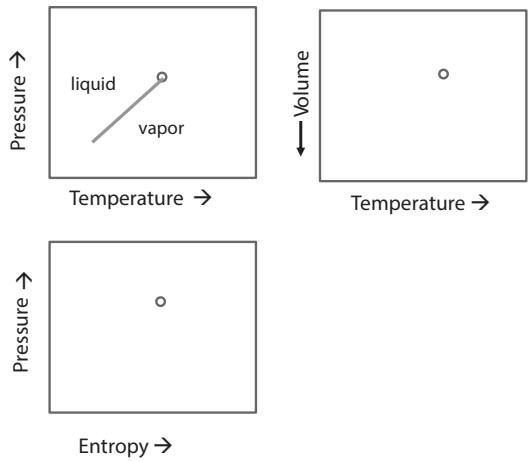

FIGURE 7.23 Various phase diagrams that depict liquid-vapor equilibrium. The pressure/entropy and the volume/temperature diagrams are to be completed. The critical points are shown in the figures.

APPENDIX 7A: DERIVATION OF THE GIBBS EQUILIBRIUM PHASE RULE

7A.1 One Component System

Consider a one-component system with ϕ phases. Each phase has two thermodynamic state variables, namely, its temperature, T, and its pressure, P. Thus, the total number of thermodynamic variables in this system is 2ϕ.

If the system is in equilibrium the following constraints are present:

$$T^{\alpha} = T^{\beta} = \cdots \phi - 1$$

$$P^{\alpha} = P^{\beta} = \cdots \phi - 1$$

$$\mu^{\alpha} = \mu^{\beta} = \cdots \phi - 1$$

where μ is, the chemical potential or molar Gibbs free energy for each phase.

These $3(\phi - 1)$ equations are constraints on the system.

The degrees of freedom, $\mathcal{F}$, is given by the number of thermodynamic variables minus the number of constraints on the system.

$$\mathcal{F} = 2\phi - 3(\phi - 1)$$

$$\phi + \mathcal{F} = 3$$

$$\mathcal{F} = 3 - \phi$$

This shows that a one-component system can have *at most three phases* in equilibrium with each other.

---

* New problem in this edition.

7A.2 System with *C* Components

Consider a C component system with no reactions occurring in it, and having ϕ phases.

Each phase has the thermodynamic state variables, T, P, and $C-1$ composition variables Thus, the total number of thermodynamic variables in this system is $2\phi + C - 1$.

If the system is in equilibrium the following constraints are present:

$$T^{\alpha} = T^{\beta} = \cdots \phi - 1$$

$$P^{\alpha} = P^{\beta} = \cdots \phi - 1$$

$$\mu^{\alpha} = \mu^{\beta} = \cdots \phi - 1$$

The total number of constraints on the system is thus $3(\phi - 1)$.

The degrees of freedom, $\mathcal{F}$, is given by the number of thermodynamic variables minus the number of constraints on the system.

$$\mathcal{F} = (2\phi + C - 1) - 3(\phi - 1)$$

$$\mathcal{F} = C + 2 - \phi$$

This shows that a C component system can have at most $C+2$ phases in equilibrium with each other.

8 The Behavior of Gases

8.1 INTRODUCTION

Up to this point, frequent use has been made of the *ideal gas* to illustrate the nature of changes in the thermodynamic state of a gaseous system. In this chapter, the behavior of *real gases* is compared with ideal behavior. The differences between the two are related mainly to the atomic or molecular interactions of real gases. Although knowledge of the physical interactions of a real gas is not required in a thermodynamic examination of the gas, an appreciation of the origin of the physical properties derived from molecular considerations provides a better understanding of the thermodynamic behavior.

8.2 THE *P-V-T* RELATIONSHIPS OF GASES

Experimental observation has shown that, for 1 mole of all real gases,

$$\text{limit} \quad P \to 0 \frac{PV}{RT} \to 1 \tag{8.1}$$

where:

P is the pressure of the gas
V is the molar volume of the gas
R is the universal gas constant
T is the absolute temperature of the gas

Thus, as the pressure of the gas approaches zero, isotherms plotted on a P-V diagram approach the form of a rectangular hyperbola (Figure 1.3a), given by the equation

$$PV = RT \tag{8.2}$$

Equation 8.2 is the equation of state for 1 mole of an ideal gas and is sometimes called the *ideal gas equation or law.* A gas that obeys this law over a range of states is said to behave ideally in this range of states, and a gas that obeys this law in *all states* is called a *perfect gas.* The perfect gas is a convenient model with which the behavior of real gases can be compared.

8.3 THE THERMODYNAMIC PROPERTIES OF IDEAL GASES AND MIXTURES OF IDEAL GASES

The variation of the molar Gibbs free energy with the pressure of a closed system of fixed composition and at constant temperature is found from the *fundamental equation* (Equation 5.25) to be

$$dG = VdP \tag{8.3}$$

For 1 mole of an ideal gas, this can be written as

$$dG = \frac{RT}{P}dP = RTd\ln P \tag{8.4}$$

and thus, for an isothermal change of pressure from P_1 to P_2 at T,

$$G(P_2,T) - G(P_1,T) = RT\ln\frac{P_2}{P_1} \tag{8.5}$$

It can be seen that increasing the pressure of an ideal gas *increases* its Gibbs free energy. This means the gas can do work of expansion when the pressure is returned to its original value.

Since Gibbs free energies do not have absolute values (only changes in G can be measured), it is convenient to choose an arbitrary reference state from which the changes in Gibbs free energy can be measured. This reference state is called the *standard state* and is chosen as being the state of 1 mole of pure gas at 1 atm pressure and the temperature of interest. The Gibbs free energy of 1 mole of gas in the standard state $G(P=1, T)$ is designated $G^\circ(T)$, and thus, from Equation 8.5, the Gibbs free energy of 1 mole of gas at any other pressure P is given as

$$G(P,T) = G^\circ(T) + RT\ln\frac{P}{P^0} \tag{8.6}$$

or simply,

$$G(P,T) = G^\circ(T) + RT\ln P \tag{8.7}$$

since P^0 equals one atm and P has the same units. Thus, the argument of the *natural logarithm term* is the ratio $\frac{P}{P^0}$ which is a dimensionless number.

Before discussing the thermodynamic properties of mixtures of ideal gases, it is necessary to introduce the concepts of *mole fraction*, *partial pressure*, and *partial molar quantities*.

8.3.1 Mole Fraction

When a system contains more than one component (i.e., when the composition of the system is variable), it is necessary to devise a means of expressing the composition. In this text, the mole fraction, X_i, of the component i is used. The mole fraction is

defined as the ratio of the number of moles of i in the system to the total number of moles of all of the components in the system. For example, if the system contains n_A moles of A, n_B moles of B, and n_C moles of C, then

$$X_A = \frac{n_A}{n_A + n_B + n_C} \tag{8.8}$$

$$X_B = \frac{n_B}{n_A + n_B + n_C} \tag{8.9}$$

$$X_C = \frac{n_C}{n_A + n_B + n_C} \tag{8.10}$$

The sum of the mole fractions of all of the components in a system is unity ($X_A + X_B + X_C = 1$). Thus, there are only two *independent mole fraction composition variables* in a three-component system.

8.3.2 Dalton's Law of Partial Pressures

The pressure P exerted by a mixture of ideal gases is equal to the sum of the pressures exerted by each of the individual component gases. The contribution made to the total pressure, P, by each individual gas is called the *partial pressure* of that gas. The partial pressure exerted by a component gas, p_i, is thus the pressure that it would exert if it alone were present. In a mixture of the ideal gases A, B, and C,

$$P = p_A + p_B + p_C$$

Consider a fixed volume V' at the temperature T which contains n_A moles of an ideal gas A. The pressure exerted is thus

$$p_A = \frac{n_A RT}{V'} \tag{8.11}$$

If n_B moles of ideal gas B are added to this constant volume containing n_A moles of gas A, the pressure increases to

$$P = p_A + p_B = (n_A + n_B)\frac{RT}{V'} \tag{8.12}$$

Division of Equations 8.11 by 8.12 gives

$$\frac{p_A}{p_A + p_B} = \frac{n_A}{n_A + n_B}$$

which, for the gas A in the mixture, can be written as

$$\frac{p_A}{P} = X_A$$

or

$$p_A = X_A P \tag{8.13}$$

Thus, in a mixture of ideal gases, the partial pressure of a component gas is the product of its mole fraction and the total pressure of the gas mixture. Equation 8.13 is called *Dalton's law of partial pressures* (John Dalton, 1766–1844).

8.3.3 Partial Molar Quantities

The partial molar value[1] of an *extensive thermodynamic variable* Q' is the rate of change of Q' with respect to the addition of n_i moles of component i at constant temperature, pressure, and composition. This can be written as

$$\bar{Q}_i = \left(\frac{\partial Q'}{\partial n_i} \right)_{T,p,n_j,n_k,\ldots} \tag{8.14}$$

where Q' is the value of the *extensive* thermodynamic variable for an arbitrary quantity of the mixture (see Figure 8.1).

The definition of $\bar{Q}_i$ can also be made as follows. If 1 mole of i is added, at constant temperature and pressure, to a *quantity of a solution* that is sufficiently large that the addition causes *virtually no change* in the composition of the *solution*, the consequent increase in the value of Q' equals the value of $\bar{Q}_i$ in the solution.

In the case of the extensive variable being the Gibbs free energy,

$$\bar{G}_i = \left(\frac{\partial G'}{\partial n_i} \right)_{T,P,n_j,n_k,\ldots}$$

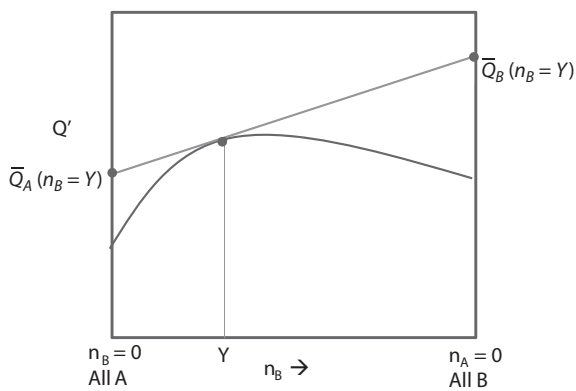

FIGURE 8.1 Schematic of a general extensive property, Q', of a binary solution showing the values of the partial molar quantities for a solution of composition $n_B = Y$.

[1] Some texts call this the partial *molal* property, which emphasizes that the intensive variables of T and P are held constant for all the partial quantities.

and, from Equation 5.21, it is seen that

$$\bar{G}_i = \mu_i$$

That is, the partial molar Gibbs free energy of a component in a solution equals the *chemical potential* of the component in the solution. Remember from Chapter 7, for equilibrium in a multi-phase system, the chemical potential of the species i must be the same in all the phases in the system. If not, there will be driving forces for diffusion.

The relationships among the various state variables developed in the preceding chapters are applicable to the *partial molar properties* of the components of a system. For example, the fundamental equation at constant T and composition (Equation 5.25) gives

$$\left(\frac{\partial G'}{\partial P}\right)_{T,\text{comp}} = V'$$

where G' is the Gibbs free energy of the system and V' is the volume of the system. For a variation in n_i, the number of moles of component i in the system, at constant T, P, and n_j,

$$\left[\frac{\partial}{\partial n_i}\left(\frac{\partial G'}{\partial P}\right)_{T,\text{comp}}\right]_{T,P,n_j} = \left(\frac{\partial V'}{\partial n_i}\right)_{T,P,n_j}$$

But, by definition,

$$\left(\frac{\partial V'}{\partial n_i}\right)_{T,P,n_j} = \bar{V}_i$$

and since the Gibbs free energy is a thermodynamic *state variable*, in which case the order of partial differentiation has no influence on the result,

$$\left[\frac{\partial}{\partial n_i}\left(\frac{\partial G'}{\partial P}\right)_{T,\text{comp}}\right]_{T,P,n_j} = \left[\frac{\partial}{\partial P}\left(\frac{\partial G'}{\partial n_i}\right)_{T,P,n_j}\right]_{T,\text{comp}}$$

$$= \left(\frac{\partial \bar{G}_i}{\partial P}\right)_{T,\text{comp}}$$

Hence,

$$\left(\frac{\partial \bar{G}_i}{\partial P}\right)_{T,\text{comp}} = \bar{V}_i$$

which is simply the application of Equation 5.25 to the component i in the system.

For the ideal gas A in a mixture of ideal gases,

$$d\bar{G}_A = \bar{V}_A dP$$

the partial molar volume, $\bar{V}_A$, in a gas mixture is

$$\bar{V}_A = \left(\frac{n_A}{\sum n_i} \right) \left(\frac{RT}{p_A} \right) = \frac{X_A RT}{p_A}$$

Taking the differential of Equation 8.13 at constant T and composition gives $dp_A = X_A\, dP$, and hence,

$$d\bar{G}_A = \bar{V}_A dP = \frac{X_A RT}{p_A} \frac{dp_A}{X_A} = RTd\left(\ln p_A\right)$$

Integration from $p_A = 1$ to $p_A = p_A$ gives

$$\begin{aligned} \bar{G}_A &= G_A^\circ + RT \ln p_A \\ &= G_A^\circ + RT \ln X_A + RT \ln P \end{aligned} \tag{8.15}$$

Equation 8.15 could also have been obtained by integrating Equation 8.4 (in the form of a partial molar Gibbs free energy) from the standard state $p_A = P_A = 1$, $X_A = 1$, T to the state p_A, X_A, T.

8.4 MIXING OF IDEAL GASES

Each of the values of the extensive thermodynamic functions for the mixing of ideal gases will now be derived.

8.4.1 The Internal Energy of Mixing of Ideal Gases

The internal energy of an ideal gas depends only on its temperature. Also, since the internal energy of mixing of ideal gases is a constant temperature process be zero, $\Delta U'^{\text{mix}} = 0$.

8.4.2 The Enthalpy of Mixing of Ideal Gases

For each component gas in a mixture of ideal gases:

$$\bar{G}_i = G_i^\circ + RT \ln X_i + RT \ln P$$

where P is the total pressure of the gas mixture at the temperature T. Dividing by T and differentiating with respect to T at constant pressure and composition gives

$$\left(\frac{\partial\left(\frac{\bar{G}_i}{T}\right)}{\partial T}\right)_{P,n_i} = \left(\frac{\partial\left(\frac{G_i^\circ}{T}\right)}{\partial T}\right)_{P,n_i} \tag{8.16}$$

From Equation 5.55,

$$\left(\frac{\partial\left(\frac{G_i^\circ}{T}\right)}{\partial T}\right)_{P,n_i} = -\frac{H_i^\circ}{T^2} \quad \text{and} \quad \left(\frac{\partial\left(\frac{\bar{G}_i}{T}\right)}{\partial T}\right)_{P,n_i} = -\frac{\bar{H}_i}{T^2} \tag{8.17}$$

and thus,

$$\bar{H}_i = H_i^\circ \tag{8.18}$$

That is, the partial molar enthalpy of ideal gas *i* in a mixture of ideal gases equals the molar enthalpy of pure *i*, and thus, the enthalpy of the gas mixture equals the sum of the enthalpies of the component gases before mixing; that is,

$$\Delta H'^{\text{mix}} = \sum_i n_i \bar{H}_i - \sum_i n_i H_i^\circ = 0 \tag{8.19}$$

where $\Delta H'^{(\text{mix})}$ is the change in the enthalpy caused by the process of mixing. Thus, the enthalpy change of mixing (the heat of mixing) of an ideal gas is zero. The zero heat of mixing of ideal gases is a consequence of the fact that the particles of an ideal gas do not interact with one another.

Since G_i° is, by definition, a function only of temperature, then, from Equations 8.16 and 8.17, it is seen that $\bar{H}_i$ is a function only of temperature. Thus, in addition to being independent of composition, the partial molar enthalpy of an ideal gas, $\bar{H}_i$, is independent of pressure. Thus, $\bar{H}_i = \bar{H}_i(T)$.

8.4.3 The Gibbs Free Energy of Mixing of Ideal Gases

For each component gas *i* in a mixture of ideal gases,

$$\bar{G}_i = G_i^\circ + RT \ln p_i$$

and for each component gas before mixing,

$$G_i = G_i^\circ + RT \ln P_i$$

where:

p_i is the partial pressure of *i* in the gas mixture

P_i is the pressure of the pure gas *i* before mixing

The mixing process, being a change of state, can be written as

$$\text{Unmixed components}\left(\text{state 1}\right) \rightarrow \text{Mixed components}\left(\text{state 2}\right)$$

and

$$\begin{aligned}\Delta G'(1 \rightarrow 2) &= G'(\text{mixture}) - G'\left(\text{unmixed components}\right) \\ &= \Delta G'^{\text{mix}} \\ &= \sum_i n_i \bar{G}_i - \sum_i n_i G_i \\ &= \sum_i n_i RT \ln\left(\frac{p_i}{P_i}\right)\end{aligned} \tag{8.20}$$

Thus, the value of $\Delta G'^{\text{mix}}$ depends on the value of p_i and P_i for each gas. If, before mixing, the gases are all at the same pressure (i.e., if $P_i = P_j = P_k = \cdots$) and mixing is carried out at total constant volume such that the total pressure of the mixture, P_{mix}, equals the initial pressures of the gases before mixing, then, since $p_i/P_i = X_i$,

$$\Delta G'^{\text{mix}} = \sum_i n_i RT \ln X_i \tag{8.21}$$

Since the values of X_i are less than unity, $\Delta G'^{\text{mix}}$ is a negative quantity, which corresponds with the fact that the mixing of ideal gases is a *spontaneous process*. Hence the mixing of ideal gases is an irreversible process as well.

8.4.4 The Entropy of Mixing of Ideal Gases

Since $\Delta H'^{\text{mix}} = 0$ (Equation 8.19) and $\Delta G'^{\text{mix}} = \sum_i n_i RT \ln X_i$ (Equation 8.21)

$$\text{Then, since} \quad \Delta G'^{\text{mix}} = \Delta H'^{\text{mix}} - T\Delta S'^{\text{mix}} \tag{8.22}$$

$$S'^{\text{mix}} = -R\sum_i n_i \ln X_i \tag{8.23}$$

The entropy of mixing is seen to be positive, in accord with the fact that the mixing of ideal gases is a spontaneous process (i.e., the entropy increases).

Any interaction among the particles of the gas would *decrease* the entropy of mixing of such gases from that of the value of mixing of ideal gases.

8.5 DEVIATION FROM IDEALITY AND EQUATIONS OF STATE FOR REAL GASES

The variation of V with P at several temperatures for a typical real gas is shown in Figure 8.2. The figure shows that, as the temperature of the gas is decreased

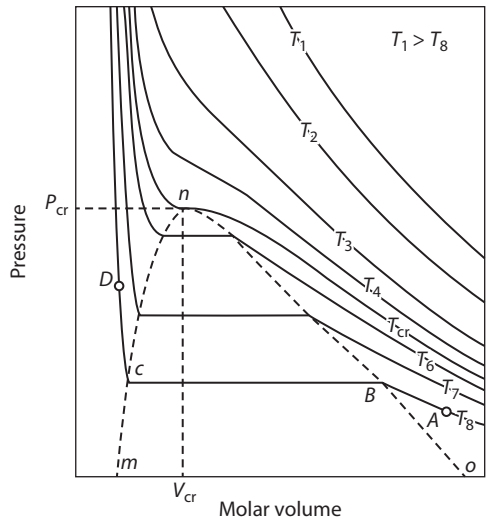

FIGURE 8.2 Schematic of *P-V* isotherms for a typical real gas. At temperatures below the critical temperature, equilibrium state is two phase, liquid and vapor.

from the high-temperature T_1, the shape of the *P-V* isotherms changes, and, eventually, a critical value of $T = T_{cr}$ is reached at which, at some fixed critical pressure, P_{cr}, and fixed molar volume, V_{cr}, a horizontal inflection occurs on the isotherm; that is,

$$\left(\frac{\partial P}{\partial V}\right)_{T_{cr}} = 0 \quad \text{and} \quad \left(\frac{\partial^2 P}{\partial V^2}\right)_{T_{cr}} = 0$$

At temperatures less than T_{cr}, two phases exist in equilibrium: a vapor phase and a liquid phase. For example, if 1 mole of vapor, initially in the state *A* (Figure 8.2), is isothermally compressed at T_8, the state of the vapor moves along the isotherm toward the state *B*. At *B*, the pressure of the vapor is the saturated vapor pressure of the liquid at T_8, and further compression of the system causes condensation of the vapor and the consequent appearance of the liquid phase. The liquid phase, which is in equilibrium with the vapor phase, first appears when the vapor reaches *B on the* T_8 *isotherm*. V_C is the molar volume of the liquid at P_C and T_8. Further compression causes further condensation, during which the states of the liquid and vapor phases remain fixed at *C* and *B*, respectively, and the total volume of the system, which is determined by the relative proportions of the liquid and vapor phases, moves along the horizontal line from *B* to *C*. Eventually, condensation is complete, and the system exists as 100% liquid in the state *C*. Further increase in pressure moves the state of the system along the isotherm toward the state *D*. The large value of $-(\partial P / \partial V)_T$ in the range of liquid states and the smaller value of $-(\partial P / \partial V)_T$ in the range of vapor states indicate the low compressibility of the

liquid phase and the high compressibility of the vapor phase. Recall that the isothermal compressibility equals:

$$\beta_T = -\frac{1}{V}\left(\frac{\partial V}{\partial P}\right)_T$$

Figure 8.2 also shows that, as the temperature is increased from T_8 to T_{cr}, the molar volume of the liquid in equilibrium with the vapor (corresponding to the point C at T_8) progressively increases and the molar volume of the vapor in equilibrium with the liquid (corresponding to the point B at T_8) progressively decreases. Thus, as the temperature is increased toward T_{cr}, the vapor in equilibrium with the liquid becomes more dense, and the liquid in equilibrium with the vapor becomes less dense. Eventually, when T_{cr} is reached, the molar volumes of the coexisting phases coincide at the state P_{cr}, T_{cr}. Thus, the critical point coincides with the equilibrium state in which the molar volume of the liquid equals the molar volume of the vapor.

At temperatures greater than T_{cr}, distinct two-phase equilibria involving two phases separated by a boundary, across which the properties of the system change abruptly, do not occur. Thus, the gaseous state cannot be liquefied by isothermal compression at temperatures greater than T_{cr}. Since the vapor can be condensed by isothermal compression at temperatures lower than T_{cr}, the critical isotherm provides a distinction between the gaseous and vapor states and defines the gaseous state phase field. The phase fields are shown in Figure 8.3. Note, however, that along the critical isotherm, there is no physical distinction between the vapor and gaseous phase and hence no phase transformation.

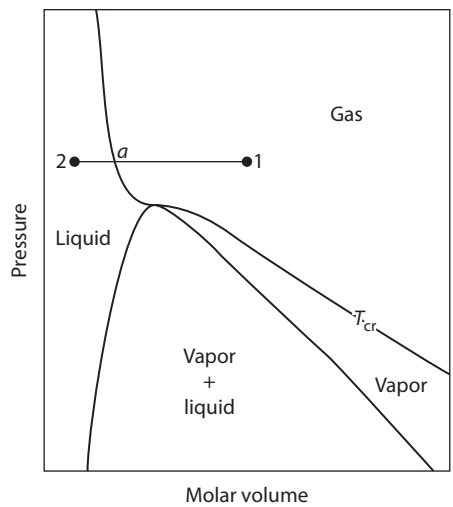

FIGURE 8.3 Schematic *P-V* diagram showing the fields of phase stability of a typical real gas.

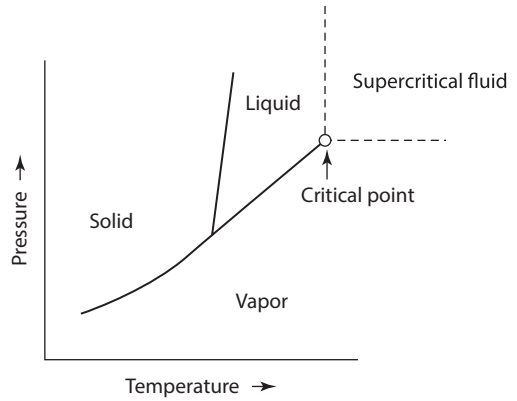

FIGURE 8.4 Schematic *P-T* diagram showing the critical point at the end of the liquid–vapor equilibrium curve and the supercritical fluid region.

Liquefaction of a *gas* requires that the gas be cooled. Consider the isobaric process path 1 → 2 in Figure 8.3. According to this path, which represents the cooling of the gas at constant pressure, the phase change gas → liquid occurs at the point *a*, at which the temperature falls below T_{cr}. In fact, at pressures greater than P_{cr}, the critical-temperature isotherm has no physical significance. In passing from the state 1 to the state 2, the molar volume of the system progressively decreases, and hence, the density of the system progressively increases. No phase separation occurs between the states 1 and 2, and the system in state 2 can equivalently be regarded as being a liquid of normal density or a gas of high density and in state 1 can be regarded as being a gas of normal density or a liquid of low density. Physically, no distinction can be made between the liquid and gaseous states at pressures greater than P_{cr}, and consequently, the system existing in these states is called a *supercritical fluid*. In the *P-T* phase diagram for the system shown in Figure 8.4, the critical point exists at the termination of the liquid–vapor coexistence equilibrium curve, where $P = P_{cr}$ and $T = T_{cr}$.

The deviation of a real gas from ideal behavior can be measured as the deviation of the compressibility factor from unity. The compressibility factor, Z, is defined as

$$Z = \frac{PV}{RT} \tag{8.24}$$

which has the value of 1 for a perfect gas in all states of existence. Z itself is a function of state of the system and, thus, is dependent on any two chosen dependent variables; for example, $Z = Z(P, T)$. Figure 8.5 shows the variation of Z with P at constant temperature for several gases.

If Figure 8.5 is replotted as Z versus the reduced pressure, P_R (where $P_R = P / P_{cr}$), for fixed values of the reduced temperature, T_R (= T/T_{cr}), it is found that all gases lie on a single curve. Figure 8.6 shows a series of such plots. The behavior shown in Figure 8.6 gives rise to the *law of corresponding states*, which states that all gases

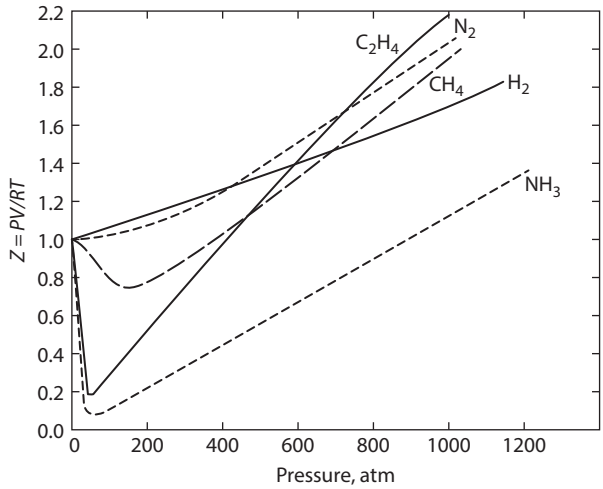

FIGURE 8.5 The variations, with pressure, of the compressibility factors of several gases at 0°C.

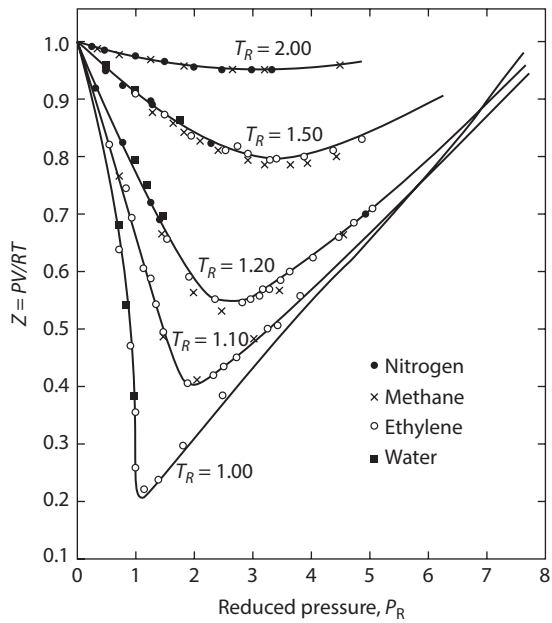

FIGURE 8.6 The variations of the compressibility factors of several gases with reduced pressure at several reduced temperatures, displaying the law of corresponding states.

obey the same equation of state when expressed in terms of the reduced variables P_R, T_R, and V_R instead of P, T, and V. If the values of two reduced variables are identical for two gases, then the gases have approximately equal values of the third reduced variable and are then said to be in corresponding states. The compressibility factor

is the same function of the reduced variables for all gases (see Problem 8.1). From the figure, it can be noted that at temperatures greater than twice that of the critical temperature, the gases behave ideally.

8.6 THE VAN DER WAALS FLUID

Recall that an ideal gas obeys the ideal gas law and has an internal energy, U, which is a function only of temperature. An ideal gas is considered to consist of volumeless particles that do not interact with one another, the energy of which is entirely the translational energy of motion of the constituent particles. Attempts to derive equations of state for *real* gases have modified the ideal gas equation by taking into account two considerations:

- The particles of a real gas occupy a finite volume.
- The particles of a real gas interact with one another.

The magnitude of the importance of these two considerations depends on the state of the gas. For example, if the molar volume of the gas is large, then the volume fraction occupied by the particles themselves is small, and the magnitude of this effect on the behavior of the gas will be correspondingly small. Similarly, as the molar volume increases, the average distance between the particles increases, and thus, the effect of interactions between particles on the behavior of the gas decreases. For a fixed number of moles of gas, an increase in the molar volume corresponds to a decrease in the density, n / V'. These states of existence occur at low pressure and high temperature, as can be seen from the ideal gas equation; that is,

$$\frac{n}{V'} = \frac{P}{RT}$$

Thus, the approach toward ideal behavior is to be expected as the pressure is decreased and the temperature is increased.

The most celebrated equation of state for nonideal gases, which was derived from considerations 1 and 2, is the van der Waals equation (Johannes Diderik van der Waals, 1837–1923), which, for 1 mole of gas, is written as

$$\left(P + \frac{a}{V^2}\right)(V - b) = RT \tag{8.25}$$

where:

a and b are constants
P is the measured pressure of the gas
a/V^2 is a correction term for the interactions that occur among the particles of the gas
V is the measured volume of the gas
b is a correction term for the finite volume of the particles[2]

[2] For n moles of a van der Waals fluid, the equation of state is $\left(P + \frac{n^2 a}{V'^2}\right)(V' - nb) = nRT$, where $V' = nV$.

The expression $\left(P+\frac{a}{V^2}\right)$ is the pressure that the gas would exert if it were ideal. The value of a for a specific gas can also be evaluated from the critical values of its temperature, pressure, and volume.

The constant b in Equation 8.25 arises because of the finite volume of all real atoms or molecules. The effective volume of real gaseous systems is less than the volume of its container by the amount excluded. Thus, for one mole of a gas, $(V-b)$ is that volume which is available for the motion of the particles, and hence, $(V-b)$ is the volume the gas would have were it ideal. The value of b varies from gas to gas and can be determined from the critical values of its temperature, pressure, and volume.

The van der Waals equation (Equation 8.25) can be written as

$$PV^3-(Pb+RT)V^2+aV-ab=0$$

Since this equation is cubic in V, there are three roots. Plotting V as a function of P for different values of T gives the family of isotherms shown in Figure 8.7. As the temperature is increased from T_1, the minimum and the maximum approach one another until, at a temperature designated as T_{cr}, they coincide and produce a horizontal inflection on the P-V curve. This is the critical point, $T=T_{cr}$, $P=P_{cr}$, and $V=V_{cr}$, and the van der Waals equation gives

$$P=\frac{RT}{(V-b)}-\frac{a}{V^2}$$

$$\left(\frac{\partial P}{\partial V}\right)_T=\frac{-RT}{(V-b)^2}+\frac{2a}{V^3}$$

$$\left(\frac{\partial^2 P}{\partial V^2}\right)_T=\frac{2RT}{(V-b)^3}-\frac{6a}{V^4}$$

Setting the last two equations equal to zero and solving these equations gives

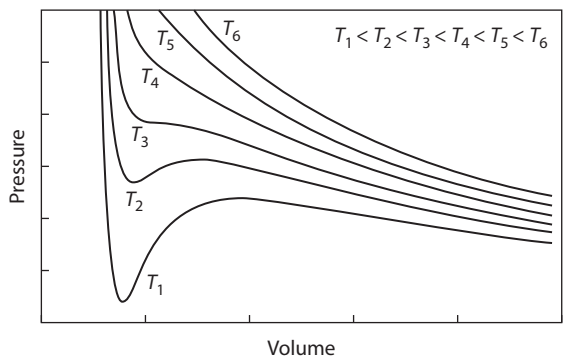

FIGURE 8.7 The isothermal variation of V with P for a van der Waals fluid at several temperatures.

$$T_{cr} = \frac{8a}{27bR}, \quad V_{cr} = 3b, \quad P_{cr} = \frac{a}{27b^2} \tag{8.26}$$

Thus, the constants a and b for any gas can be evaluated from knowledge of the values of T_{cr} and P_{cr}. Alternatively, the values of a and b can be obtained by fitting the van der Waals equation to experimentally measured variations of V with T and P for real gases. The critical states, van der Waal constants, and values of Z, the compressibility factor, at the critical point for several gases are listed in Table 8.1.

The value of the compressibility factor for the van der Walls fluid is at the critical point:

$$Z = \frac{P_{cr}V_{cr}}{RT_{cr}} = 0.375$$

Consider the isothermal variation of V with P given by the van der Waals equation and shown in Figure 8.8. Any increase in the pressure exerted on a system must cause a decrease in the volume of the system, $\left(\partial P / \partial V\right)_T < 0$. This is a condition of *intrinsic stability*. In Figure 8.8, this condition is *violated* over the portion *JIHGF*, which means that this portion of the curve is a region of instability. No state along *JIHGF* is stable or metastable. All states of fluids with positive values of $\left(\partial P / \partial V\right)_T$ are unstable.

The equilibrium states of the system at this temperature can be obtained from a consideration of the variation of the Gibbs free energy with P along the isotherm. Equation 5.25 gives the variation of G with P at constant T as $dG = VdP$, and integration of this equation between the state (P, T) and (P_A, T) gives

$$G(P,T) - G(P_A,T) = \int_{P_A}^{P} VdP$$

TABLE 8.1
The Critical States, van der Waals Constants, and Values of *Z* at the Critical Points for Several Gases

Gas	T_{cr}, K	P_{cr}, atm	V_{cr}, cm³/mole	a, $\frac{\text{liters}^2 \cdot \text{atm}}{\text{mole}^2}$	b, liters/mole	Z_{cr}
He	5.3	2.26	57.6	0.0341	0.0237	0.299
H_2	33.3	12.8	65.0	0.2461	0.0267	0.304
N_2	126.1	33.5	90.0	1.39	0.0391	0.292
CO	134.0	35.0	90.0	1.49	0.0399	0.295
O_2	153.4	49.7	74.4	1.36	0.0318	0.293
CO_2	304.2	73.0	95.7	3.59	0.0427	0.280
NH_3	405.6	111.5	72.4	4.17	0.0371	0.243
H_2O	647.2	217.7	45.0	5.46	0.0305	0.184

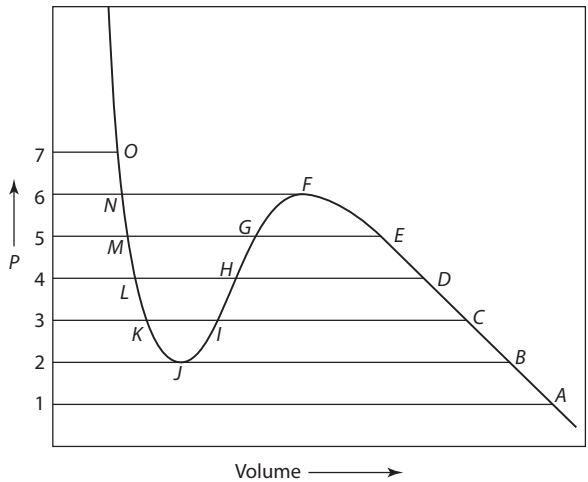

FIGURE 8.8 The isothermal variation, with pressure, of the volume of a van der Waals fluid at a temperature below the critical temperature.

TABLE 8.2
Graphical Integration of Figure 8.8

$G_B = G_A + \int_{P_A}^{P_B} V dP$	$= G_A +$ area 1AB2
G_C	$= G_A +$ area $1AC3$
G_D	$= G_A +$ area $1AD4$
G_E	$= G_A +$ area $1AE5$
G_F	$= G_A +$ area $1AF6$
G_G	$= G_A +$ area $1AE5 +$ area EFG
G_H	$= G_A +$ area $1AD4 +$ area DFH
G_I	$= G_A +$ area $1AC3 +$ area CFI
G_J	$= G_A +$ area $1AB2 +$ area BFJ
G_K	$= G_A +$ area $1AC3 +$ area $CFI -$ area IJK
G_L	$= G_A +$ area $1AD4 +$ area $DFH -$ area HJL
G_M	$= G_A +$ area $1AE6 +$ area $EFG -$ area GJM
G_N	$= G_A +$ area $1AF6 -$ area FJN
G_O	$= G_A +$ area $1AF6 -$ area $FJN +$ area $6NO7$

or

$$G = G_A + \int_{P_A}^{P} V dP \tag{8.27}$$

If an arbitrary value is assigned to G_A, then graphical integration of the integral from Figure 8.8 allows the variation of G with P, to be plotted corresponding to the variation of V with P in Figure 8.8. The values of the integrals are listed in Table 8.2, and the variation of G with P

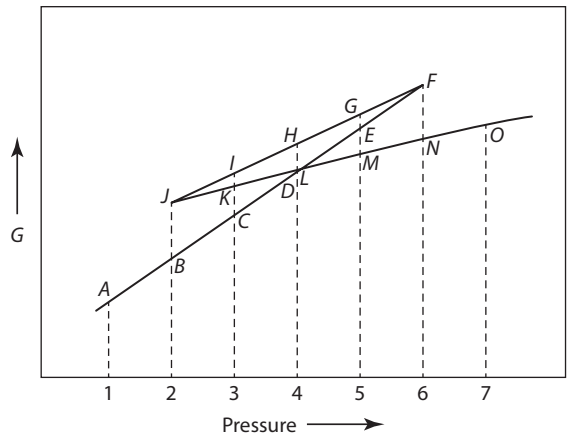

FIGURE 8.9 Schematic representation of the variation, with pressure, of the molar Gibbs free energy of a van der Waals fluid at a constant temperature lower than the critical temperature. Region *FGHIJ* is an instability region. *F* and *J* demark the limits of phase stability, sometimes called the *spinodals*.

Figure 8.9 is the Gibbs free energy versus pressure for the van der Waals gas whose *P V* plot is displayed in Figure 8.8. It shows that, as the pressure is increased from P_1, the value of *G* increases. At pressures greater than P_2, three states of existence become available to the system. For example, at P_3, the three states are given by the points *I*, *K*, and *C*. The stable, or equilibrium, state is that with the lowest Gibbs free energy, and hence, over the range of pressure from P_2 to P_4, the stable states lie on the line *BCD* as seen in Figure 8.9. As the pressure is increased above P_4, the state with the lowest Gibbs free energy no longer lies on the original line (the continuation of the curve *BCD*) but lies on the curve *LMN*. The change of stability at P_4 corresponds to a *change of phase* at this point; that is, at pressures less than P_4, one phase is stable (vapor), and at pressures greater than P_4, another phase is stable (liquid). At low pressures ($P < P_4$), the system exists as a vapor, and at high pressures ($P > P_4$), it exists as a liquid. At P_4, G_D, which is the molar Gibbs free energy of the vapor phase, equals G_L, which is the molar Gibbs free energy of the liquid phase, and thus, vapor and liquid coexist in equilibrium with one another at the state P_4. The transition from the vapor phase to the liquid phase is a *first-order phase transition* (see Chapter 7).

In Figure 8.8, a tie-line connects the points *D* and *L* across a two-phase region. In Figure 8.9, line *DF* represents the metastable vapor phase, and the line *LJ* represents the metastable liquid states. Thus, in the absence of the formation of the liquid phase from the vapor phase at the state *D*, a supersaturated vapor would exist along the curve *DEF*, and, in the absence of the formation of the vapor phase from the liquid phase at the state *L*, supersaturated liquid would exist along the line *LKJ*. In view of the violation of the criterion for intrinsic stability over the states' path *JHF*, the states represented by this line in both Figures 8.8 and 8.9 are *unstable*, and a transformation will occur spontaneously (i.e., without an energy barrier) to a two-phase equilibrium.

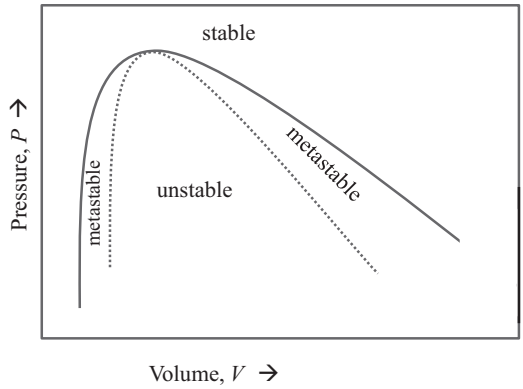

FIGURE 8.10 *P-V* diagram showing the locus of *spinodal* points and regions of metastability and instability.

The points *F* and *J* represent the limits of metastability of the vapor and liquid phases, respectively. These were called *spina* by van der Waals in his *Lehrbuch der Thermodynamik* (1908).[3] The spina or *spinodes* occur where the value of $\left(\partial P / \partial V\right)_T = 0$, which, for an isotherm of the van der Waals fluid, yields two points the minimum and the maximum in Figure 8.8). Between *JIHGF*, a single-phase absolute equilibrium does not exist. This region is a "gap" in the *P-V* diagram. Like all regions of instability, they are delineated by points where the second derivative of an energy state function with respect to variable (in this case, $\left(\partial^2 G / \partial V^2\right)_T$) equals zero. Figure 8.10 shows a typical *P-V* diagram of a van der Waal fluid in which the regions have been delineated: the region of *stability*, regions of *metastability*, and a region of *absolute instability*. We will encounter such gaps when we study *equilibrium binary phase diagrams* in Chapters 9, and 10, where we call them *miscibility gaps*. Within the gap, the equilibrium state is a two-phase state.

It is thus seen that the van der Waals equation predicts the phase change that occurs in the system at temperatures less than T_{cr}. At any temperature below T_{cr}, the value of *P* for equilibrium between the vapor and liquid phases (e.g., P_4 in Figures 8.8 and 8.9) is that whereby the area *HFD* equals the area *LJH* in Figure 8.8. This is called the *Maxwell construction*. See for example Figure 8.11.

8.6.1 The van der Waals Equation for CO_2

The measured values of T_{cr} and P_{cr} for CO_2 are, respectively, 31°C and 72.9 atm. Thus, from Equation 8.26,

$$b = \frac{RT_{cr}}{8P_{cr}} = 0.0427 \text{ liters/mole}$$

[3] "This singular point is located on the curve, the curve possesses a point (node) of return. From this form of its intersection which resembles a thorn (spina, in Latin) the curve obtains its name." Translated by A. H. Cahn, in J. W. Cahn, "Spinodal Decomposition," Appendix B, *Trans. Met. Soc. AIME* (1967), vol. 242, pp. 166–180.

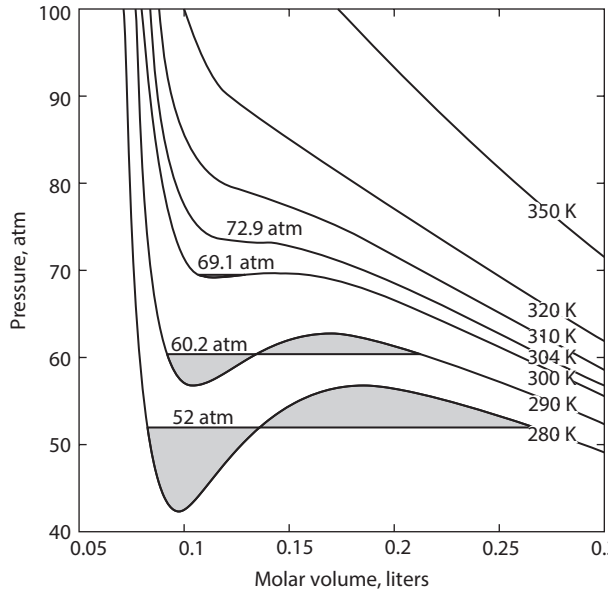

FIGURE 8.11 *P-V* isotherms for CO_2 modeled as a van der Waals gas.

and

$$a = 27b^2P_{cr} = 3.59 \text{ liters}^2 \cdot \text{atm/mole}^2$$

in which case the van der Waals equation for CO_2 is given as

$$\left(P + \frac{3.59}{V^2}\right)(V - 0.0427) = RT$$

The variation of P with V given by this equation is shown for several temperatures in Figure 8.11, in which it is seen that the 304 K isotherm exhibits a horizontal inflection at the critical point. At temperatures lower than 304 K, the isotherms show the expected maximum and minimum. The variation, with temperature, of the saturated vapor pressure of van der Waals liquid CO_2 can be determined by finding the tie-line on each isotherm which gives equal areas *DFH* and *LJH*, as explained with reference to Figure 8.8. Alternatively, the variation of the molar Gibbs free energy with pressure can be determined along each isotherm by graphical integration of the variation of V with P. These relationships are shown for several temperatures in Figure 8.12, which shows the variation of the saturated vapor pressure of liquid CO_2 (the points P) with temperature. Figure 8.12 also shows that, as the temperature increases toward the critical point, the range of unstable states (J to F in Figure 8.9) diminishes and finally disappears at T_{cr}. At temperatures greater than T_{cr}, the full line indicates that only one phase is stable over the entire range of pressure. Since G_A in Equation 8.27 is a function of temperature, the values of G in Figure 8.12 are arbitrary; only the P-axis is quantitatively significant.

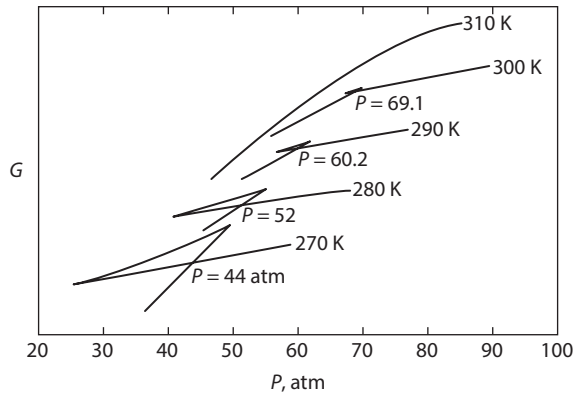

FIGURE 8.12 The variations of G with P for van der Waals CO_2 at several temperatures.

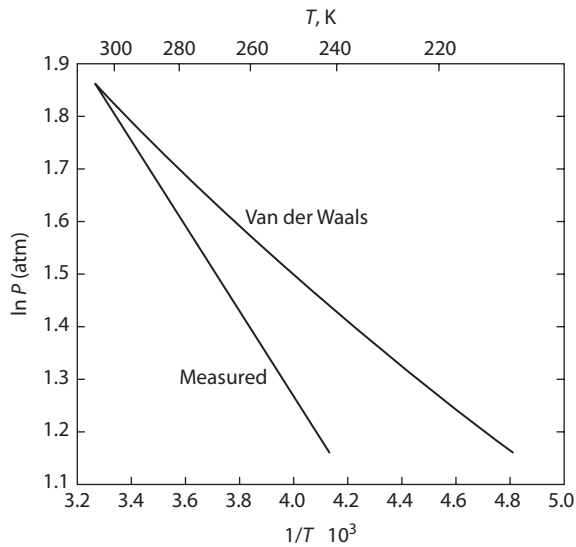

FIGURE 8.13 Comparison of the variation, with temperature, of the vapor pressure of van der Waals liquid CO_2 with the measured vapor pressures.

The variation of the saturated vapor pressure of liquid CO_2 with temperature, obtained from the van der Waals equation and plotted as the logarithm of P versus the reciprocal of the absolute temperature, is shown in Figure 8.13. This figure also shows the variation of the measured saturated vapor pressure with temperature. Comparison shows that the van der Waals equation predicts values of vapor pressure which are higher than the measured values, although the difference between the

two values decreases with increasing temperature. Consequently, the van der Waals equation predicts a value of the *molar latent heat of evaporation* of liquid CO_2 which is less than the measured value, with ΔH_{evap} being obtained as $-2.303\ R\times$(the slope of the line) in Figure 8.13 (cf. Figures 7.9 and 7.10). The molar latent heat of evaporation of a liquefied van der Waals fluid can be calculated as follows:

$$\Delta H_{\text{evap}} = H_v - H_l = U_v - U_l + P\left(V_v - V_l\right) \tag{8.28}$$

where:

V_v and V_l are, respectively, the molar volumes of the coexisting vapor and liquid phases

P is the saturated vapor pressure at the temperature T

From Equations 3.12 and 5.33,

$$\left(\frac{\partial U}{\partial V}\right)_T = T\left(\frac{\partial P}{\partial T}\right)_V - P$$

which, applied to the van der Waals fluid, gives

$$\left(\frac{\partial U}{\partial V}\right)_T = T\left(\frac{R}{V-b}\right) - P = \frac{a}{V^2}$$

Integration gives

$$U = -\frac{a}{V} + \text{constant}$$

in which the integration constant is a function of temperature, so that, unlike the ideal gas, the internal energy of a van der Waal fluid is a function of both V and T.

From Equation 8.28

$$\begin{aligned}\Delta H_{\text{evap}} &= -\frac{a}{V_v} + \frac{a}{V_l} + P\left(V_v - V_l\right) \\ &= -a\left(\frac{1}{V_v} - \frac{1}{V_l}\right) + P\left(V_v - V_l\right)\end{aligned} \tag{8.29}$$

Equation 8.29 thus correctly predicts that ΔH_{evap} for a van der Waals fluid rapidly falls to zero as the temperature approaches T_{cr}, in which state, $V_v = V_l$. There is no heat of vaporization at and above the critical point.

8.6.2 Summarizing Remarks on the van der Waals Equation

Although van der Waals developed his equation from a consideration of the physical factors causing nonideal behavior, the requirement that the pressure, volume,

and temperature at the critical point be known for the calculation of the constants a and b means that the equation is *empirical*. This, however, does not detract from the usefulness of the equation in representing the behavior of a gas which exhibits a relatively small departure from ideality. The van der Waals equation correctly predicts a discontinuous, first-order transformation for the vapor-to-liquid transformation. It also predicts a critical point in the pressure–temperature phase diagram above which the first-order transformation becomes a continuous transformation. Finally, it also predicts the limits of stability of the metastable extensions of the phase at points on the pressure–volume curve denoted as spinodal points.

8.7 OTHER EQUATIONS OF STATE FOR NONIDEAL GASES

Other examples of derived equations of state for nonideal gases include the *Dieterici equation* (Conrad Dieterici, 1858–1929):

$$P\left(V - b'\right)e^{a'/RTV} = RT$$

and the *Berthelot equation* (Pierre Eugène Marcellin Berthelot, 1827–1907):

$$\left(P + \frac{A}{TV^2}\right)(V - B) = RT$$

Neither of these equations has a fundamental basis.

Other general empirical equations include the *Beattie–Bridgeman equation* (James A. Beattie, 1895–1981; Oscar C. Bridgeman), which contains five constants in addition to R and fits the *P-V-T* relationships over wide ranges of temperature and pressure, and the *Kamerlingh Onnes* or *virial equation of state* (Heike Kamerlingh Onnes, 1853–1926). In the latter equation, it is assumed that PV/RT is a power series of either P or of $1/V$; that is,

$$\frac{PV}{RT} = 1 + BP + CP^2 + \cdots$$

or

$$\frac{PV}{RT} = 1 + \frac{B'}{V} + \frac{C'}{V^2} + \cdots$$

The product PV is called the *virial*, B or B' is called the *first virial coefficient*, C or C' is called the *second virial coefficient*, and so on, and the virial coefficients are functions of temperature. In both equations, as pressure approaches zero and volume approaches infinity, $PV/RT \to 1$. The virial equation converges rapidly in the gas phase, and thus, the equation of state can be represented by the virial expansion over the entire range of densities and pressures. In practice, however, the virial equation is used only when the first few terms need to be retained. At low pressures or densities,

$$\frac{PV}{RT} = 1 + BP$$

or

$$\frac{PV}{RT} = 1 + \frac{B'}{V}$$

8.8 FURTHER THERMODYNAMIC TREATMENT OF NONIDEAL GASES

Equation 8.7 showed that, at any temperature, the molar Gibbs free energy of an ideal gas is a linear function of the logarithm of the pressure of the gas.

$$G = G^{\circ}(T) + RT \ln P \tag{8.7}$$

This property arises from the ideal gas law, which was used in the derivation of this equation. If the gas is not ideal, then the relationship between the logarithm of the pressure of the gas and its molar Gibbs free energy *is not linear.* However, in view of the simple form of Equation 8.7, a function has been *defined* which, when used in place of pressure in Equation 8.7, gives a linear relationship between the molar Gibbs free energy of a nonideal gas and the logarithm of the function. This function is called the *fugacity*, *f*, and is partially defined by the equation

$$dG = RTd \ln f$$

The integration constant is chosen such that the fugacity approaches the pressure as the pressure approaches zero; that is,

$$\frac{f}{P} \to 1 \quad \text{as} \quad P \to 0$$

in which case

$$G = G^{\circ} + RT \ln f \tag{8.30}$$

where G° is the molar Gibbs free energy of the gas in its standard state, which is now defined as that state in which $f = 1$ at the temperature T; that is, $G^{\circ} = G(f = 1, T)$. The standard state for an ideal gas was defined as being $P = 1$, T.

Consider a gas that obeys the equation of state

$$V = \frac{RT}{P} - \alpha$$

where α is a function only of temperature and is a measure of the deviation of the gas from ideality. Equation 5.25 gives $dG = VdP$ at constant T, and Equation 8.30 gives

$$dG = RTd\ln f \quad \text{at constant } T.$$

Thus, at constant T,

$$VdP = RTd\ln f$$

and hence,

$$d\ln\left(\frac{f}{P}\right) = -\frac{\alpha}{RT}dP \tag{8.31}$$

Integration between the states $P = P$ and $P = 0$, at constant T gives

$$\ln\left(\frac{f}{P}\right)_{P=P} - \ln\left(\frac{f}{P}\right)_{P=0} = -\frac{\alpha P}{RT} \tag{8.32}$$

Since $(f/P) = 1$ when $P = 0$, then $\ln(f/P) = 0$ when $P = 0$, and hence,

$$\ln\left(\frac{f}{P}\right) = -\frac{\alpha P}{RT} \quad \text{or} \quad \frac{f}{P} = e^{-\alpha P/RT}$$

In order that α can be taken as being independent of pressure, the deviation of the gas from ideality must be small, in which case α is a small number. Thus,

$$e^{-\frac{\alpha P}{RT}} = 1 - \frac{\alpha P}{RT}$$

and hence,

$$\frac{f}{P} = 1 - \frac{\alpha P}{RT} = 1 - \left(\frac{RT}{P} - V\right)\frac{P}{RT} = \frac{PV}{RT}$$

If the gas behaved ideally, then the ideal pressure, P_{id}, would be given as RT/V. Thus,

$$\frac{f}{P} = \frac{P}{P_{id}} \tag{8.33}$$

which shows that the actual pressure of the gas is the *geometric mean* of its fugacity and the pressure which it would exert if it behaved ideally. It is also

seen that the percentage error involved in assuming that the fugacity is equal to the pressure is the same as the percentage departure from the ideal gas law.

Alternatively, the fugacity can be considered in terms of the compressibility factor Z. From Equation 8.31,

$$d\ln\left(\frac{f}{P}\right) = -\frac{\alpha}{RT}dP = \left(\frac{V}{RT} - \frac{1}{P}\right)dP$$

But $Z = PV / RT$, and hence,

$$d\ln\left(\frac{f}{P}\right) = \frac{Z-1}{P}dP$$

and

$$\ln\left(\frac{f}{P}\right)_{P=P} = \int_{P=0}^{P=P} \frac{Z-1}{P}dP \tag{8.34}$$

This can be evaluated either by graphical integration of a plot of $(Z-1)/P$ *versus* P at constant T, or by direct integration if Z is known as a function of P—that is, if the virial equation of state of the gas is known.

8.8.1 Numerical Examples Using Fugacity

For example, the variation of PV (cm^3·atm) with P in the range 0–200 atm for nitrogen gas at 0°C is represented by the equation

$$PV = 22{,}414.6 - 10.281P + 0.065189P^2 + 5.1955\times10^{-7}P^4 - 1.3156\times10^{-11}P^6 + 1.009\times10^{-16}P^8$$

Thus, dividing by $RT = 22{,}414.6$ at 0°C gives

$$\frac{PV}{RT} = Z = 1 - 4.5867\times10^{-4}P + 2.9083\times10^{-6}P^2 + 2.3179\times10^{-11}P^4 - 5.8694\times10^{-15}P^6 + 4.5015\times10^{-21}P^8$$

This variation of Z with P is shown graphically in Figure 8.4. From the integration of Equation 8.34, ln (f/P) is obtained as

$$\ln\left(\frac{f}{P}\right) = -4.5867\times10^{-4}P + 1.4542\times10^{-6}P^2 + 5.794\times10^{-12}P^4$$

$$-0.9782\times10^{-16}P^6 + 5.627\times10^{-22}P^8$$

This variation of f/P with P is shown in Figure 8.14. Note that as the pressure approaches one atmosphere, the fugacity approaches unity.
The change in the molar Gibbs free energy of a nonideal gas caused by an isothermal change in pressure can be calculated from either

$$dG = VdP$$

or

$$dG = RTd\ln f$$

The correspondence between these two approaches is illustrated as follows. The virial equation of the state of the gas is

$$\frac{PV}{RT} = Z = 1 + BP + CP^2 + DP^3 + \cdots$$

Then,

$$V = RT\left(\frac{1}{P} + B + CP + DP^2 + \cdots\right)$$

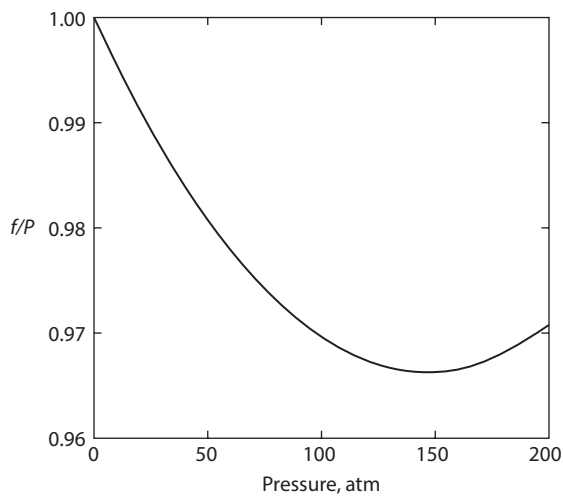

FIGURE 8.14 The variation of f/P with pressure for nitrogen gas at 0°C.

and so, for the change of state of 1 mole of gas from (P_1, T) to (P_2, T),

$$\Delta G = \int_{P_1}^{P_2} V dP = RT \int_{P_1}^{P_2} \left(\frac{1}{P} + B + CP + DP^2 + \cdots \right) dP$$

$$= RT \left[\ln \frac{P_2}{P_1} + B(P_2 - P_1) + \frac{C}{2}\left(P_2^2 - P_1^2\right) + \frac{D}{3}\left(P_2^3 - P_1^3\right) + \cdots \right]$$

If the gas had been ideal, then

$$\Delta G = RT \ln \left(\frac{P_2}{P_1} \right)$$

and so, the contribution to change in the molar Gibbs free energy arising from the nonideality of the gas is

$$RT \left[B(P_2 - P_1) + \frac{C}{2}\left(P_2^2 - P_1^2\right) + \frac{D}{3}\left(P_2^3 - P_1^3\right) + \cdots \right]$$

Alternatively, $dG = RT\, d \ln f$, where, from Equation 8.34,

$$\ln \left(\frac{f}{P} \right) = \int_0^P \frac{Z-1}{P} dP$$

$$= \int_0^P \left(B + CB + DP^2 + \cdots \right) dP$$

$$= BP + \frac{CP^2}{2} + \frac{DP^3}{3} + \cdots$$

Now,

$$dG = RTd \ln f = RTd \ln \left(\frac{f}{P} \right) + RTd \ln P$$

and so,

$$\Delta G = RT \left[B(P_2 - P_1) + \frac{C}{2}\left(P_2^2 - P_1^2\right) + \frac{D}{3}\left(P_2^3 - P_1^3 + \cdots\right) \right] + RT \ln \left(\frac{P_2}{P_1} \right)$$

in agreement with the preceding equations.

Thus, for 1 mole of nitrogen at 0°C, the difference between the Gibbs free energy at $P = 150$ atm and that at $P = 1$ atm is

$$\Delta G = RT\left[\ln\left(\frac{f}{P}\right)_{150} - \ln\left(\frac{f}{P}\right)_{1}\right] + RT\ln 150$$

$$= 8.3144 \times 273(-0.034117 + 0.000457) + 8.3144 \times 273 \times 5.011 \text{ J}$$

$$= -76 + 11,373$$

$$= 11,297 \text{ J}$$

The contribution due to the nonideality of nitrogen is seen to be only 76 J in almost 11,300 J.

The number of terms that must be retained in the virial equation depends on the magnitude of the range of pressure over which it must be applied. For example, in the virial equation for nitrogen at 0°C, only the first term is needed up to 6 atm and only the first two terms are needed up to 20 atm. When only the first term is needed, the expression is

$$\frac{PV}{RT} = 1 + BP$$

or

$$V = \frac{RT}{P} + BRT$$

and hence, $-BRT = \alpha$ in Equation 8.31, and α is a function only of temperature.

Consider a nonideal gas that obeys the equation of state $PV = RT(1 + BP)$. The work done by this nonideal gas in a reversible, isothermal expansion from P_1 to P_2 is the same as that done when an ideal gas is reversibly and isothermally expanded from P_1 to P_2 at the same temperature. However, the work done by the nonideal gas in a reversible, isothermal expansion from V_1 to V_2 is greater than that done when an ideal gas is reversibly and isothermally expanded from V_1 to V_2 at the same temperature. Consider why this is so.

For the ideal gas $V = RT/P$, and for the nonideal gas $V = RT/P + BRT$. Thus, on a *P-V* diagram, any isotherm for the nonideal gas is displaced from the isotherm for the ideal gas by the constant increment in volume *BRT*, as shown in Figure 8.15. Because of the constant displacement, the area under the isotherm for the ideal gas between P_1 and P_2 (the area *abcd*) is the same as the area under the isotherm for the nonideal gas between the same pressures (the area *efgh*). Thus, the same amount of work is done by both gases in expanding isothermally from P_1 to P_2.

For the ideal gas,

$$w_{\text{ideal gas}} = \int_{V_1}^{V_2} P dV = RT\ln\left(\frac{V_2}{V_1}\right) = RT\ln\left(\frac{P_1}{P_2}\right)$$

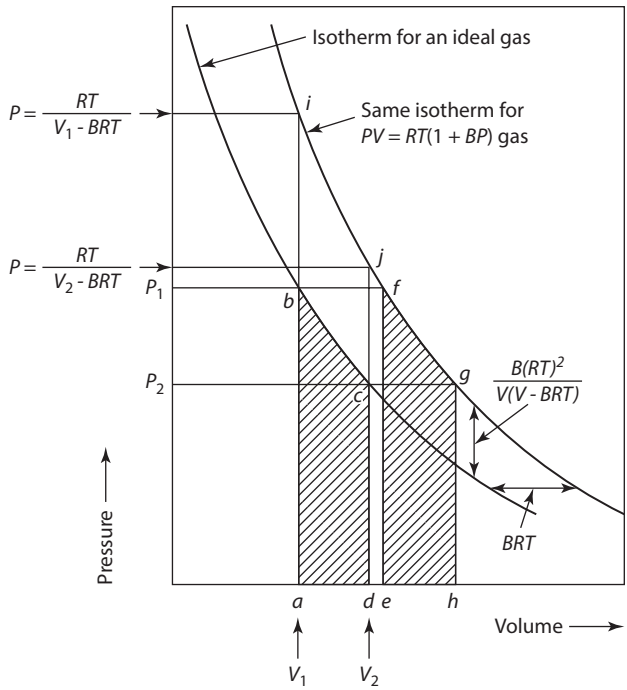

FIGURE 8.15 Isotherms for an ideal gas and a nonideal gas.

and for the nonideal gas,

$$w_{\text{nonideal gas}} = \int_{V_1}^{V_2} P\,dV$$

but, since $V = RT/P + BRT$, and hence, at constant T, $dV = -\mathrm{RT}(dP/P^2)$, then

$$w_{\text{nonideal gas}} = -\int_{P_1}^{P_2} RT\left(\frac{dP}{P}\right) = RT\ln\left(\frac{P_1}{P_2}\right) = w_{\text{ideal gas}}$$

However, since any isotherm for the nonideal gas also lies above the isotherm for the ideal gas (for a positive value of B), the work done by the nonideal gas in expanding isothermally and reversibly from V_1 to V_2 (the area *aijd*) is greater than that done by the ideal gas in isothermally and reversibly expanding between V_1 and V_2 (the area *abcd*). The vertical separation between the two isotherms is

$$P_{\text{nonideal gas}} - P_{\text{ideal gas}} = \frac{RT}{V - BRT} - \frac{RT}{V} = \frac{B(RT)^2}{V(V - BRT)}$$

For the ideal gas, $w_{\text{ideal gas}} = RT \ln (V_2/V_1)$, and for the nonideal gas,

$$w = \int_{V_1}^{V_2} P dV$$

where

$$P = \frac{RT}{V - BRT}$$

such that

$$w_{\text{nonideal gas}} = RT \ln\left(\frac{V_2 - BRT}{V_1 - BRT}\right) > w_{\text{ideal gas}}$$

Consider the comparison of the behavior of hydrogen gas, for which $PV = RT(1 + 0.00064P)$, with that of an ideal gas in reversible isothermal expansions of 1 mole between $P_1 = 100$ atm and $P_2 = 50$ atm at 298 K:

$$V_{1(\text{ideal, } P_1=100 \text{ atm, } T=298 \text{ K})} = \frac{RT}{P_1} = \frac{0.08206 \times 298}{100} = 0.2445 \text{ liters}$$

$$V_{1(\text{H}_2 \ P_1=100 \text{ atm, } T=298 \text{ K})} = \frac{RT}{P_1} + RTB = 0.2445 + 0.08206 \times 298 \times 6.4 \times 10^{-4}$$

$$= 0.2445 + 0.0157 = 0.2602 \text{ liters}$$

$$V_{2(\text{ideal, } P_2=50 \text{ atm, } T=298 \text{ K})} = \frac{0.08206 \times 298}{50} = 0.4890 \text{ liters}$$

$$V_{2(\text{H}_2 \ P_1=50 \text{ atm, } T=298 \text{ K})} = 0.4890 + 0.0157 = 0.5047 \text{ liters}$$

Thus, for the change of state

$$(V_1 = 0.2445, \ T = 298 \text{ K}) \rightarrow (V_2 = 0.4890, \ T = 298 \text{ K})$$

$$w_{\text{ideal gas}} = RT \ln\left(\frac{V_2}{V_1}\right) = 8.3144 \times 298 \times \ln\left(\frac{0.4890}{0.2445}\right)$$

$$= 1717 \text{ J}$$

and

$$w_{\text{H}_2} = RT \ln\left(\frac{V_2 - RTB}{V_1 - RTB}\right) = 8.3144 \times 298 \times \ln\left(\frac{0.4890 - 0.0157}{0.2445 - 0.0157}\right)$$

$$= 1801 \text{ J}$$

Thus, 84 more Joules of work is performed by the expansion of the nonideal gas than by that of the ideal gas. The expansion of the gas lowered the interaction between the molecules and some of that energy was converted to work.

The following calculations are for the above example of Hydrogen gas. The values at the points *b, c, i,* and *j* on the schematic plot of Figure 8.15 are evaluated.

For the ideal gas:

$$V_1 = 0.2445 \text{ liters}, \; T = 298 \text{ K}, \quad P_{1\ \text{ideal gas}} = 100 \text{ atm.} \; (\text{point } b)$$

$$V_2 = 0.489 \text{ liters}, \; T = 298 \text{ K}, \quad P_{2\ \text{ideal gas}} = 50 \text{ atm.} \; (\text{point } c)$$

For the H_2 gas:

$$V_1 = 0.2445 \text{ liters}, \quad T = 298 \text{ K}, \text{ and } P_{H_2} = \frac{RT}{V - RTB}$$

$$= \frac{0.08206 \times 298}{0.2445 - 0.0157}$$

$$= 106.4 \text{ atm} \; (\text{point } i)$$

$$V_2 = 0.489 \text{ liters}, \; T = 298 \text{ K}, \; P_{H_2} = \frac{0.08206 \times 298}{0.4890 - 0.0157} = 51.7 \text{ atm} \; (\text{point } j)$$

8.9 SUMMARY

1. An ideal gas is an assemblage of volumeless noninteracting particles which obeys the ideal gas law, $PV = RT$. The internal energy of an ideal gas arises solely from the translational motions of the gas particles and, hence, is a function only of temperature. The enthalpy of an ideal gas is also a function only of temperature.
2. A consequence of the ideal gas law is that, at constant temperature, the Gibbs free energy of an ideal gas is a linear function of the logarithm of the pressure of the gas.
3. Since Gibbs free energies do not have absolute magnitudes, it is convenient to measure changes in Gibbs free energy from some arbitrary state. This state is chosen as $P = 1$ atm at the temperature of interest and is called the standard state. Thus, the difference between the molar Gibbs free energy in the state (P, T) and that in the standard state ($P = 1$ atm, T) is $\Delta G = RT \ln P$.

4. The composition of a mixture of gases is most conveniently expressed in terms of the mole fractions of its component gases, and if the mixture is ideal, the partial pressures exerted by the component gases are related to the total pressure P and the mole fraction X_i by $p_i = X_i P$. This equation is called Dalton's law of partial pressures. In a mixture of ideal gases, the partial molar Gibbs free energy of a component gas is a linear function of the logarithm of its partial pressure, and in a mixture of nonideal gases, it is a linear function of the logarithm of its fugacity.
5. Since the atoms in an ideal gas do not interact with one another, no change in enthalpy occurs when different ideal gases are mixed; that is, the enthalpy change of mixing of ideal gases, $\Delta H'^{\text{mix}}$, is zero. The entropy change occurring when ideal gases are mixed arises solely from the complete randomization of the different types of atoms in the available volume, and thus, as $\Delta H^{\text{mix}} = 0$, $\Delta G^{\text{mix}} = -\text{T}\Delta\text{S}^{\text{mix}}$.
6. The deviations of real gases from ideal behavior are caused by the atoms or molecules of real gases having finite volumes and by the interactions that occur among the atoms.
7. Various attempts have been made to correct the ideal gas law for these effects, and the best-known derived equation is the van der Waals equation of state, which can be applied to gases that show small deviations from ideality. This equation predicts the condensation of vapor caused by compression at temperatures below the critical temperature, but does not give the correct dependence on the temperature of the saturated vapor pressure of the liquid phase. This equation also predicts the limits of stability of the vapor phase and the vapor–liquid equilibrium can be determined.
8. Generally, measured variations of the molar volumes of gases with P and T are fitted to power series equations, in P or $1/V$, of the function PV. Such equations are called virial equations.
9. The compressibility factor, $Z = PV/RT$, of all real gases at constant reduced temperature, $T_R = T / T_{\text{cr}}$, is the same function of the reduced pressure, $P_R = P / P_{\text{cr}}$. This gives rise to the law of corresponding states, which states that when two gases have identical values of two reduced variables, they have almost identical values of the third reduced variable.
10. Consideration of the thermodynamic behavior of nonideal gases is facilitated by the introduction of the fugacity, f, which is defined by the equation $dG = RT\, d \ln f$ and by the condition $f / P \to 1$ as $P \to 0$. Thus, the standard state for a nonideal gas is that in which the fugacity is unity at the temperature of interest. For small deviations from ideality, the pressure of the gas is the geometric mean of its fugacity and P_{id}, the pressure which the gas would exert if it were ideal.

8.10 CONCEPTS AND TERMS INTRODUCED IN THIS CHAPTER

The reader should write out brief definitions or descriptions of the following terms. Where appropriate, equations may be used.

Compressibility factor, Z
Critical point
Dalton's law of partial pressure
Enthalpy of mixing
Entropy of mixing
Fugacity
Gas
Gibbs free energy of mixing
Ideal/perfect gas
Law of corresponding states
Liquid/vapor equilibrium
Maxwell construction
Mixtures of gases
Mole fraction
Partial molar quantity
Partial pressure
Real gas
Reference state
Region of instability
Stable/unstable/metastable states
Standard state
Supercritical fluid
van der Waals fluid
Vapor
Virial equation

8.11 QUALITATIVE EXAMPLE PROBLEMS

QUALITATIVE PROBLEM 1

Obtain simplified expressions for the three total derivatives, dP, dT, and dV for one mole of an ideal gas.

SOLUTION TO QUALITATIVE PROBLEM 1

$$dP = \left(\frac{\partial P}{\partial T}\right)_V dT + \left(\frac{\partial P}{\partial V}\right)_T dV$$

For an ideal gas : $\left(\frac{\partial P}{\partial T}\right)_V = \frac{R}{V} = \frac{P}{T}$

$$\left(\frac{\partial P}{\partial V}\right)_T = -\frac{P}{V},$$

Thus, $dP = \frac{P}{T}dT - \frac{P}{V}dV \qquad \frac{dP}{P} = \frac{dT}{T} - \frac{dV}{V}$

$$dT = \left(\frac{\partial T}{\partial P}\right)_V dP + \left(\frac{\partial T}{\partial V}\right)_P dV$$

For an ideal gas : $\left(\frac{\partial T}{\partial P}\right)_V = \frac{V}{R} = \frac{T}{P}$

$$\left(\frac{\partial T}{\partial V}\right)_P = \frac{P}{R} = \frac{T}{V}$$

Thus, $dT = \frac{T}{P}dP + \frac{T}{V}dV \qquad \frac{dT}{T} = \frac{dP}{P} + \frac{dV}{V}$

$$dV = \left(\frac{\partial V}{\partial P}\right)_T dP + \left(\frac{\partial V}{\partial T}\right)_P dT$$

For an ideal gas : $\left(\frac{\partial V}{\partial P}\right)_T = -\frac{V}{P}$

$$\left(\frac{\partial V}{\partial T}\right)_P = \frac{V}{T}$$

Thus, $dV = -\frac{V}{P}dP + \frac{V}{T}dT \qquad \frac{dV}{V} = -\frac{dP}{P} + \frac{dT}{T}$

QUALITATIVE PROBLEM 2

Obtain an expression for $\left(\frac{\partial H}{\partial V}\right)_T$ for a van der Waals gas.

SOLUTION TO QUALITATIVE PROBLEM 2

$$dH = TdS + VdP$$

$$\left(\frac{\partial H}{\partial V}\right)_T = T\left(\frac{\partial S}{\partial V}\right)_T + V\left(\frac{\partial P}{\partial V}\right)_T = T\left(\frac{\partial P}{\partial T}\right)_V + V\left(\frac{\partial P}{\partial V}\right)_T$$

$$P = \frac{RT}{V-b} - \frac{a}{V^2}$$

$$\left(\frac{\partial P}{\partial T}\right)_V = \frac{R}{V-b} \qquad \left(\frac{\partial P}{\partial V}\right)_T = -\frac{RT}{(V-b)^2} + \frac{2a}{V^3}$$

$$\left(\frac{\partial H}{\partial V}\right)_T = T\left(\frac{\partial P}{\partial T}\right)_V + V\left(\frac{\partial P}{\partial V}\right)_T$$

$$\left(\frac{\partial H}{\partial V}\right)_T = T\left(\frac{R}{V-b}\right) + V\left(-\frac{RT}{(V-b)^2} + \frac{2a}{V^3}\right)$$

$$\left(\frac{\partial H}{\partial V}\right)_T = -\frac{RTb}{(V-b)^2} + \frac{2a}{V^2}$$

This shows that the enthalpy is a function of V in the van der Waal gas. For an ideal gas, this reduces to $\left(\frac{\partial H}{\partial V}\right)_T = 0$ since $a = b = 0$, since the enthalpy is not a function of V in an ideal gas.

8.12 QUANTITATIVE EXAMPLE PROBLEMS

QUANTITATIVE PROBLEM 1

Assuming that nitrogen behaves as a van der Waals gas with $a = 1.39$ (liter)^2·atm/mole^2 and $b = 39.1$ cm^3/mole, calculate the change in the Gibbs free energy and the change in entropy when the volume of 1 mole of nitrogen is increased from 1 to 2 liters at 400 K.

SOLUTION TO QUANTITATIVE PROBLEM 1

For a van der Waals fluid

$$P = \frac{RT}{V-b} - \frac{a}{V^2}$$

and thus

$$dP = -\frac{RT}{(V-b)^2}dV + \frac{R}{(V-b)}dT + \frac{2a}{V^3}dV$$

$$dP = \frac{R}{V-b}dT + \left[\frac{2a(V-b)^2 - RTV^3}{V^3(V-b)^2}\right]dV \quad \text{(i)}$$

$$dP = \frac{R}{V-b}dT + \left[\frac{2a(V-b)^2 - RTV^3}{V^3(V-b)}\right]dV \quad \text{(ii)}$$

At constant temperature

$$dG = VdP$$

which, from Equation (i), gives

$$dG = \left[\frac{2a}{V^2} - \frac{RTV}{(V-b)^2}\right]dV$$

Integrating between V_2 and V_1 gives

$$\Delta G = \int_{V_1}^{V_2}\left[\frac{2a}{V^2} - \frac{RTV}{(V-b)^2}\right]dV$$

$$= \left[-\frac{2a}{V} + \frac{RTb}{V-b} - RT\ln(V-b)\right]_{V_1}^{V_2}$$

$$= RTb\left(\frac{1}{V_2-b} - \frac{1}{V_1-b}\right) - RT\ln\frac{V_2-b}{V_1-b} - 2a\left(\frac{1}{V_2} - \frac{1}{V_1}\right)$$

$$= 0.08206 \times 400 \times 0.0391\left(\frac{1}{2-0.0391} - \frac{1}{1-0.0391}\right)$$

$$-0.08206 \times 400 \times \ln\frac{2-0.0391}{1-0.0391} - 2 \times 1.39\left(\frac{1}{2} - \frac{1}{1}\right)$$

$$= -0.68 - 23.41 + 1.39$$

$$= -22.70 \text{ atm}$$

$$= -\frac{22.70 \times 8.3144}{0.08206} \text{ J}$$

$$= -2300.4 \text{ J}$$

From Equation 6.13, at constant temperature,

$$dS = -\alpha_p VdP$$

where

$$\alpha_p = \frac{1}{V}\left(\frac{\partial V}{\partial T}\right)_P$$

From Equation (ii), at constant pressure

$$\frac{dV}{dT} = \frac{-R}{(V-b)} \frac{V^3(V-b)^2}{\left[2a(V-b)^2 - RTV^3\right]}$$

and thus, for a van der Waals fluid

$$\alpha_p = \frac{-RV^2(V-b)}{2a(V-b)^2 - RTV^3}$$

and

$$dS = -\left[\frac{-RV^2(V-b)}{2a(V-b)^2 - RTV^3}\right] V \left[\frac{2a(V-b)^2 - RTV^3}{V^3(V-b)^2}\right] dV$$

$$= \frac{RdV}{V-b}$$

Therefore,

$$\Delta S = R \ln \frac{V_2 - b}{V_1 - b}$$

$$= 8.3144 \ln \frac{2 - 0.0391}{1 - 0.0391}$$

$$= 5.93 \text{ J/K}$$

If the nitrogen had behaved as an ideal gas, the changes in Gibbs free energy and entropy would have been

$$\Delta G = RT \ln \frac{V_1}{V_2}$$

$$= 8.3144 \times 400 \times \ln \frac{1}{2}$$

$$= -2305 \text{ J}$$

and

$$\Delta S = R \ln \frac{V_2}{V_1}$$

$$= 8.3144 \times \ln 2$$

$$= 5.76 \text{ J/K}$$

QUANTITATIVE PROBLEM 2

The virial equation of state for *n*-butane at 460 K is $Z = 1 + A/V + B/V^2$, in which $A = -265\,\text{cm}^3/\text{g·mole}$ and $B = 30{,}250\,\text{cm}^6/\text{g·mole}^2$. Calculate the change in the Gibbs free energy when the volume of 1 mole of *n*-butane is decreased from 400 to 200 cm^3 at 460 K.

SOLUTION TO QUANTITATIVE PROBLEM 2

The equation of state is

$$PV = RT\left(1 - \frac{265}{V} + \frac{30{,}250}{V^2}\right)$$

$$\therefore P = RT\left(\frac{1}{V} - \frac{265}{V^2} + \frac{30{,}250}{V^3}\right)$$

and, at constant temperature,

$$dP = RT\left(-\frac{1}{V^2} + \frac{2\times 265}{V^3} - \frac{3\times 30{,}250}{V^4}\right)dV$$

Thus,

$$dG = VdP = RT\left(-\frac{1}{V} + \frac{530}{V^2} - \frac{90{,}750}{V^3}\right)dV$$

and

$$\Delta G = RT\left[-\ln\frac{V_2}{V_1} - 530\left(\frac{1}{V_2} - \frac{1}{V_1}\right) + \frac{90{,}750}{2}\left(\frac{1}{V_2^2} - \frac{1}{V_1^2}\right)\right]$$

$$= 8.3144\times 460\left[-\ln\frac{1}{2} - 530\left(\frac{1}{200} - \frac{1}{400}\right) + 45{,}375\left(\frac{1}{200^2} - \frac{1}{400^2}\right)\right]$$

$$= 8.3144\times 460(0.693 - 1.325 + 0.851)$$

$$= 838\ \text{J}$$

PROBLEMS

8.1 Demonstrate the law of corresponding states by writing the van der Waals equation in terms of the reduced variables. Calculate the compressibility factor for a van der Waals fluid at its critical point and compare the result with the values obtained for real gases at their critical points listed in Table 8.1. Calculate the value of $(\partial U/\partial V)_T$ for a van der Waals fluid.

8.2 *n* moles of an ideal gas *A* and $(1 - n)$ moles of an ideal gas *B*, each at 1 atm pressure, are mixed at total constant pressure. What ratio of *A* to *B* in the mixture maximizes the decrease in the Gibbs free energy of the system?

If the decrease in the Gibbs free energy is ΔG^M, to what value must the pressure be increased in order to increase the Gibbs free energy of the gas mixture by $1/2\Delta G^M$?

8.3 You are responsible for the purchase of oxygen gas which, before use, will be stored at a pressure of 200 atm at 300 K in a cylindrical vessel of diameter 0.2 m and height 2 m. Would you prefer that the gas behaved ideally or as a van der Waals fluid? The van der Waals constants for oxygen are $a = 1.36$ liters^2 atm/mole^2 and $b = 0.0318$ liters/mole.

8.4 The virial equation of state for *n*-butane at 460 K is $Z = 1 + A/V + B/V^2$, in which $A = -265$ cm^3/g·mole and $B = 30{,}250$ cm^6/g·mole^2. Calculate the work required to reversibly compress 1 mole of *n*-butane from 50 to 100 atm at 460 K.

8.5 For sulfur dioxide, $T_{cr} = 430.7$ K and $P_{cr} = 77.8$ atm. Calculate

a. The critical van der Waals constants for the gas
b. The critical volume of van der Waals SO_2
c. The pressure exerted by 1 mole of SO_2 occupying a volume of 500 cm^3 at 500 K. Compare this with the pressure that would be exerted by an ideal gas occupying the same molar volume at the same temperature.

8.6 One hundred moles of hydrogen gas at 298 K are reversibly and isothermally compressed from 30 to 10 liters. The van der Waals constants for hydrogen are $a = 0.2461$ liters^2·atm/mole^2 and $b = 0.02668$ liters/mole, and in the range of pressure 0–1500 atm, the virial equation for hydrogen is $PV = RT\ (1 + 6.4 \times 10^{-4}\ P)$. Calculate the work that must be done on the system to effect the required change in volume and compare this with the values that would be calculated assuming that (a) hydrogen behaves as a van der Waals fluid and (b) hydrogen behaves as an ideal gas.

8.7 Using the virial equation of state for hydrogen at 298 K given in Problem 8.6, calculate

a. The fugacity of hydrogen at 500 atm and 298 K
b. The pressure at which the fugacity is twice the pressure
c. The change in the Gibbs free energy caused by a compression of 1 mole of hydrogen at 298 K from 1 to 500 atm

What is the magnitude of the contribution to (c) caused by the nonideality of hydrogen?

8.8 Show that the truncated Kamerlingh Onnes virial equation

$$\frac{PV}{RT} = 1 + \frac{B(T)}{V}$$

reduces to $P(V - b') = RT$, and find the expression for b'.

8.9 Figure 8.8 shows an isothermal variation, with pressure, of the volume of a van der Waals fluid at a temperature below its critical temperature. Redraw this figure and below it sketch the Helmholtz free energy versus volume plot. Be sure to indicate important points on the A versus V plot.

8.10 Obtain a simplified expression for the total derivative of the pressure for a van der Waals gas.

8.11* Obtain a simplified expression for the total derivative of the pressure for a gas that obeys the truncated Kammerlingh Onnes virial equation:

$$\frac{PV}{RT} = 1 + \frac{B'(T)}{V}$$

8.12 Derive an expression for Z_{cr} of a van der Waals fluid.

$$Z_{cr} = \frac{P_{cr}V_{cr}}{RT_{cr}}$$

8.13* Use the general equation $\left(\frac{\partial U}{\partial V}\right)_T = T\left(\frac{\partial P}{\partial T}\right)_V - P$, to demonstrate that c_V is independent of volume for a van der Waal gas.

8.14* The van der Waals' equation of state for n moles of a gas is given as:

$$\left(P + \frac{n^2 a}{V^2}\right)(V - nb) = nRT$$

a. Derive an expression for the work performed by or on the gas when it is isothermally compressed from V_1 to V_2.
b. Is the work positive or negative? Explain.

8.15*

a. Obtain the expression for $\left(\frac{\partial V}{\partial T}\right)_P$ for one mole of a van der Waal's gas.
b. Use the expressions of the critical values of P and T to obtain the value of $\left(\frac{\partial V}{\partial T}\right)_P$ at the critical point for a van der Waals' gas.

8.16* The equation of state of a nonideal gas is given as

$$\left(P + aV^m\right)(V - b) = RT$$

a. Calculate the critical value of the volume in terms of the constants b and m:
b. Show that the value you get for this gas reduces to the critical pressure of a van der Waals gas ($V_{cr} = 3b$).

8.17* Demonstrate that the Dieterici equation of state reduces to that of the van der Waals equation of state at low densities.

* New problem in this edition.

9 The Behavior of Solutions

9.1 INTRODUCTION

In the previous chapters, it was shown that gases may be considered to be ideal when there is no interaction among their constituent atoms or molecules. This lack of interaction allows the gas to exist in a state in which its configurational entropy has its highest possible value. Gases that can be considered to be ideal all have the same thermodynamic mixing properties. Any interaction, such as is present in a van der Waals gas, lowers the entropy of the gas, and with decreasing temperature, the interactions eventually lead to the gas condensing to a liquid or a solid, depending on its pressure.

Condensed phases do have interactions existing among their constituent atoms, molecules, or ions. The nature and magnitudes of these interactions have a significant influence on the thermodynamic behavior of the solution. The interactions are determined by such factors as atomic size, electronegativity, and electron-to-atom ratio, and these determine the extent to which a component is soluble in a solution and whether or not two or more components will react chemically to form a new species. *Solution thermodynamics* is concerned with the vapor pressure–temperature–composition relationships of the components of a solution. An initial examination of solution thermodynamics is made in this chapter.

9.2 RAOULT'S LAW AND HENRY'S LAW

If a quantity of pure liquid A is placed in a closed, initially evacuated vessel at the temperature T, some of the liquid will spontaneously evaporate until the pressure in the vessel reaches the saturated vapor pressure of liquid A, p_A°, at the temperature T. In this state, a *dynamic equilibrium* is established in which the rate of *evaporation* of liquid A equals the rate of *condensation* of vapor A. The rate of evaporation, $r_{e(A)}$, is determined by the magnitude of the energy of the bonds between the atoms of A at the surface of the liquid. The forces exerted between the atoms are such that each surface atom is located near the bottom of a potential energy well. For an atom to leave the surface of the liquid and enter the vapor phase, it must acquire an activation energy, E^*. The intrinsic rate of evaporation, $r_{e(A)}$, is determined by the depth of the potential energy well—that is, by the magnitude of E^*—and by the temperature T. On the other hand, the rate of condensation, $r_{c(A)}$, is proportional to the number of A atoms in the vapor phase which strike the surface of the liquid in a unit time. For a given temperature, this is proportional to the pressure of the vapor. Thus, $r_{c(A)} = k^A p_A^\circ$, and at equilibrium, $r_{e(A)} = r_{c(A)}$ Thus,

$$r_{e(A)} = k^A p_A^\circ \tag{9.1}$$

The energies of the atoms at the surface are quantized, and the distribution of the surface atoms among the available quantized energy levels is given by Equation 4.17 as

$$n_i = \frac{n \exp\left(-\frac{E_i}{k_B T}\right)}{\mathcal{Z}}$$

where n_i / n is the fraction of the atoms in the E_ith energy level, and $\mathcal{Z}$, the partition function, is given by

$$\mathcal{Z} = \sum_0^\infty \exp\left(-\frac{E_i}{k_B T}\right)$$

If the quantized energy levels are spaced closely enough that the summation can be replaced by an integral, then

$$\mathcal{Z} = \int_0^\infty \exp\left(-\frac{E_i}{k_B T}\right) dE = k_B T$$

which is the average energy per atom. Thus, the fraction of surface atoms that have energies greater than the activation energy for evaporation, E^*, is

$$\frac{n_i^*}{n} = \frac{1}{k_B T} \int_{E^*}^\infty \exp\left(-\frac{E_i}{k_B T}\right) dE = \exp\left(-\frac{E^*}{k_B T}\right)$$

The evaporation rate, $r_{e(A)}$, is proportional to n_i^* / n, and thus, it increases exponentially with increasing temperature and decreases exponentially with the increasing value of E^*. This equation illustrates why the *saturated vapor pressures* of liquids are exponential functions of temperature.

Similarly, when pure liquid B is placed in an initially evacuated vessel at the temperature T, equilibrium between the liquid and its vapor phase occurs when:

$$r_{e(B)} = k^B p_B^\circ \tag{9.2}$$

Consider the effect of the addition of a small quantity of liquid B to liquid A. If the mole fraction of A in the solution is X_A and the atomic diameters of A and B are similar, then, assuming that the composition of the surface of the liquid is the same as that of the bulk liquid, the fraction of the surface sites occupied by A atoms is X_A. Since A can only evaporate from surface sites occupied by A atoms, the rate of evaporation of A is *decreased* by the factor X_A. Since the rates of evaporation and condensation are equal to one another at equilibrium, the equilibrium vapor pressure of A exerted by the A–B solution is decreased from p_A° to p_A, where:

$$r_{e(A)} X_A = k^A p_A \tag{9.3}$$

Similarly, for liquid B containing a small amount of A,

$$r_{e(B)}X_B = k^B p_B \tag{9.4}$$

Combination of Equations 9.1 and 9.3 gives

$$p_A = X_A p_A^\circ \tag{9.5}$$

and combination of Equations 9.2 and 9.4 gives

$$p_B = X_B p_B^\circ \tag{9.6}$$

Equations 9.5 and 9.6 are expressions of *Raoult's law* (François-Marie Raoult, 1830–1901), which states that the vapor pressure exerted by a component i in a solution is equal to the product of the mole fraction of i in the solution and the saturated vapor pressure of pure liquid i at the temperature of the solution. Raoult's law is shown in Figure 9.1; the components of a solution that obeys Raoult's law are said to exhibit *Raoultian* behavior.

The derivations of Equations 9.3 and 9.4 require the assumption that the *intrinsic rates of evaporation* of A and B are *independent* of the composition of the solution. This requires that the magnitudes of the A–A, B–B, and A–B bond energies in the solution be identical, in which case the depth of the potential energy well of an atom at the surface is independent of the types of atoms which it has as its nearest neighbors. When this happens, the arrangement of the atoms does not depend on the bond energies, and hence, they will take a configuration that *maximizes* the configurational entropy of the solution.

Consider the case in which the A–B bond energy is considerably more negative than the A–A and B–B bond energies, and consider a solution of B in A which is sufficiently dilute that every B atom on the surface of the liquid is surrounded only by A

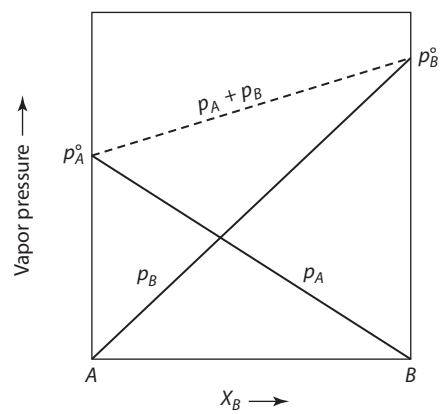

FIGURE 9.1 The vapor pressures exerted by the components of a binary solution as a function of composition. Both components of this solution obey Raoult's law at all compositions.

atoms. In this case, the B atoms at the surface are each located in a *deeper potential energy* well than are the B atoms at the surface of pure B. Thus, in order to leave the surface and enter the vapor phase, the B atoms have to overcome *larger energy barriers*, and, consequently, the intrinsic rate of evaporation of B is *decreased* from $r_{e(B)}$ to $r'_{e(B)}$. Equilibrium between the condensed solution and the vapor phase occurs when

$$r'_{e(B)} X_B = k'^{,B} p_B \tag{9.7}$$

Combination of Equation 9.1 and 9.7 then gives

$$p_B = \frac{r'_{e(B)}}{r_{ef(B)}} X_B p_B^{\circ} \tag{9.8}$$

and since $r'_{e(B)} < r_{e(B)}$, p_B in Equation 9.8 is a smaller quantity than p_B in Equation 9.5. Equation 9.8 can be written as

$$p_B = k'^{,B} X_B \tag{9.9}$$

where $k'^{,B} < 1$.

As the mole fraction of B in the A–B solution is increased, the probability that all of the B atoms on the surface of the liquid are surrounded only by A atoms decreases. The occurrence of a pair of neighboring B atoms on the surface decreases the depth of the potential wells in which they are located and, hence, increases the value of $r'_{e(B)}$. Beyond some critical mole fraction of A, $r'_{e(B)}$ varies with composition, and hence, Equation 9.9 is no longer obeyed by B in solution. Consequently, Equation 9.9 is obeyed only over an initial range of concentration of B in A, the extent of which is dependent on the temperature of the solution and on the relative magnitudes of the A–A, B–B, and A–B bond energies. A similar consideration of dilute solutions of A in B gives

$$p_A = k'^{,A} X_A \tag{9.10}$$

which is obeyed over an initial range of concentration. Equations 9.9 and 9.10 are known as *Henry's law* (William Henry, 1774–1836), and, in the ranges of composition in which Henry's law is obeyed, the solutes are said to exhibit *Henrian* behavior.

If the A–B bond energy is *less negative* than the A–A and B–B bond energies, then, since $r'_{e(B)} > r_{e(B)}$, the Henry's law line lies above the Raoult's law line (Figure 9.2a). The solutes in such solutions are said to exhibit *positive deviations* from *Raoultian behavior.* Conversely, if the A–B bond energy is more negative than the A–B and B–B bond energies, the solute atom, surrounded only by solvent atoms, is located in a deeper potential energy well than that which occurs in the pure solute. In this case, $r'_{e(B)} < r_{e(B)}$, and hence, the Henry's law line for the solute lies below the Raoult's law line (Figure 9.2b). The solute in these solutions is said to exhibit *negative deviations* from Raoultian behavior, and $k'^{,B} < 1$. This is the case described previously and summarized in Equation 9.9.

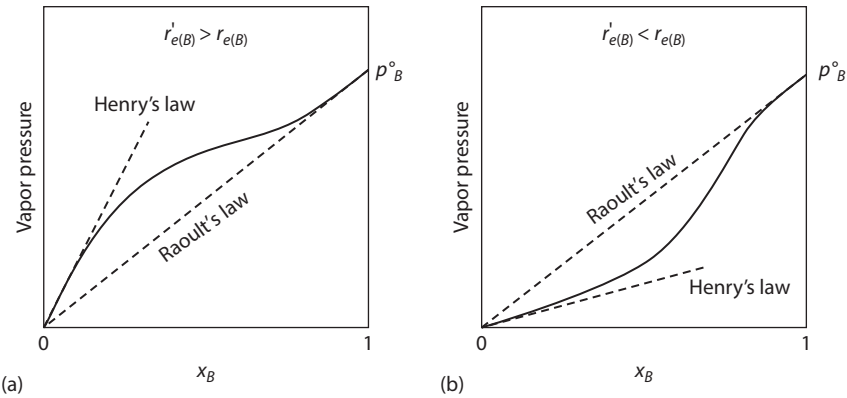

FIGURE 9.2 (a) The vapor pressure of a solute of a binary solution that exhibits positive deviation from Raoultian behavior. (b) The vapor pressure of a solute of a binary solution that exhibits negative deviation from Raoultian behavior. Henry's law is obeyed in the linear regions of the plots.

9.3 THE THERMODYNAMIC ACTIVITY OF A COMPONENT IN SOLUTION

The thermodynamic *activity* of a component in any state at the temperature T is formally defined as being the ratio of the fugacity (see Section 8.8) of the substance in that state to its *fugacity* in its standard state. For the species or substance i,

$$\text{Activity of } i \equiv a_i \equiv \frac{f_i}{f_i^\circ} \tag{9.11}$$

In a condensed solution, f_i is the fugacity of the component i in the solution at the temperature T, and f_i° is the fugacity of pure i (the standard state) at the temperature T.

If the vapor in equilibrium with the condensed solution is *ideal*, then $f_i = p_i$, in which case

$$a_i = \frac{p_i}{p_i^\circ} \tag{9.12}$$

That is, the activity of i in a solution, with respect to pure i, is the ratio of the partial pressure of i exerted by the solution to the saturated vapor pressure of pure i at the same temperature.

If the component i exhibits Raoultian behavior, then Equations 9.5 and 9.12 give

$$a_i = X_i \tag{9.13}$$

which is an alternative expression of Raoult's law (cf. Equations 9.5 and 9.6).

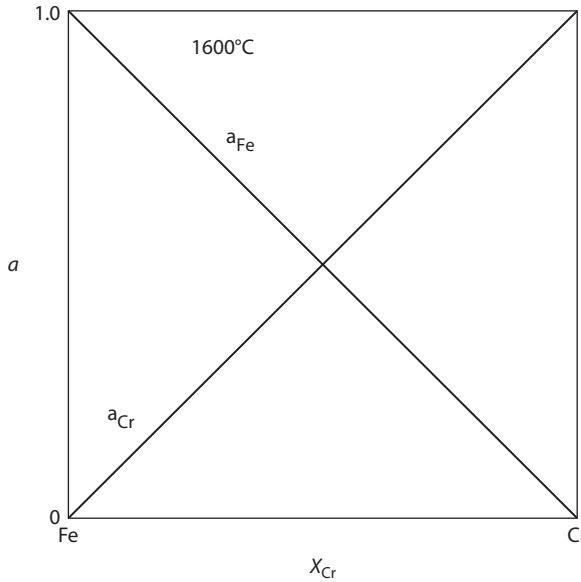

FIGURE 9.3 Activities in the liquid binary system iron–chromium at 1600°C.

Figure 9.3 shows Raoultian behavior over all compositions in a liquid binary solution of Fe and Cr, in terms of the activities of the two components. The definition of activity normalizes the vapor pressure–composition relationship with respect to the saturated vapor pressure exerted in the standard state. In an *equilibrium state*, the activity of a solution can never exceed unity.

Over the composition range in which Henry's law is obeyed by the solute *i*, Equations 9.9 and 9.12 give

$$p_B = k'^{,i} X_B$$

$$a_i = \frac{k'^{,i} X_i}{p_i^{\circ}} = k_{(i)} X_i \tag{9.14}$$

which is an alternative expression of Henry's law (cf. Equations 9.9 and 9.10).

Henrian behavior, in terms of the activity of a component of the binary solution Fe and Ni, is shown in Figure 9.4. It can be seen that at $X_{Ni} = 0.5$, the Ni atoms in a liquid solution of Fe–Ni are less "active" than they would be if such a solution were a Raoultian one. This implies that the Ni atoms are bonded more tightly to Fe atoms than they are to other Ni atoms; that is, $E_{Ni–Fe} < E_{Ni–Ni}$. Thus, the liquid Fe–Ni system exhibits *negative deviation from ideality*. It is of interest to note that in the solid state, the Fe–Ni system has an *atomically ordered phase* in which the Fe atoms have all Ni near neighbors (e.g., $FeNi_3$, $L1_2$, $Pm\bar{3}m$, $cP4$).

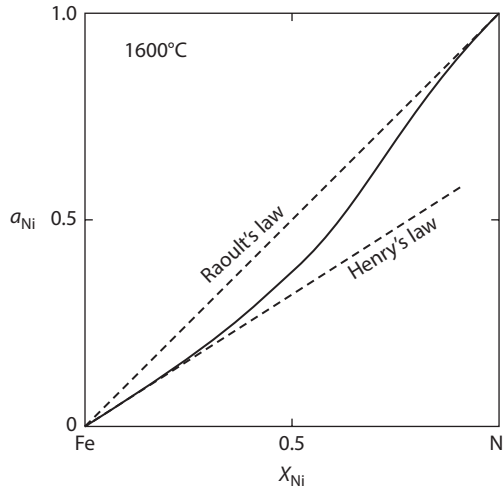

FIGURE 9.4 The activity of nickel in the liquid iron–nickel system at 1600°C displaying negative deviation from Raoultian behavior.

9.4 THE GIBBS–DUHEM EQUATION

It is frequently found that the *extensive thermodynamic variables* of only one component of a binary (or multicomponent) solution are amenable to experimental measurement. In such cases, the corresponding extensive variables of the other component can be obtained from a general relationship between the values of the properties of both components. This relationship, which is known as the Gibbs–Duhem relationship, is introduced in this section, and some of its applications are discussed in Section 9.8.

The value of an extensive thermodynamic variable (state function) of a solution is a function of the temperature, the pressure, and the numbers of moles of the components of the solution. If Q is an extensive molar property then the total value of, Q' in a solution is given as:

$$Q' = Q'\left(T, P, n_i, n_j, n_k, \ldots\right)$$

At constant T and P, the variation of Q' with the composition of the solution is given as

$$dQ' = \left(\frac{\partial Q'}{\partial n_i}\right)_{T,P,n_j,n_k,\ldots} dn_i + \left(\frac{\partial Q'}{\partial n_j}\right)_{T,P,n_i,n_k,\ldots} dn_j + \left(\frac{\partial Q'}{\partial n_k}\right)_{T,P,n_i,n_j,\ldots} dn_k + \cdots \quad (9.15)$$

In Chapter 8, the *partial molar value* of an extensive property of a component was defined as

$$\bar{Q}_i = \left(\frac{\partial Q'}{\partial n_i}\right)_{T,P,n_j,n_k,\ldots}$$

In this case, Equation 9.15 can be written as

$$dQ' = \bar{Q}_i dn_i + \bar{Q}_j dn_j + \bar{Q}_k dn_k + \cdots \tag{9.16}$$

Also in Chapter 8, it was seen that $\bar{Q}_i$ is the increase in the value of Q' for the mixture or solution when 1 mole of i is added to a large quantity of the solution at constant T and P. (The stipulation that the quantity of solution be large is necessitated by the requirement that the addition of 1 mole of i to the solution should not cause a measurable change in its composition.) Thus, if $\bar{Q}_i$ is the value of Q per mole of i in the solution, then the value of Q' for the solution itself is

$$Q' = n_i \bar{Q}_i + n_j \bar{Q}_j + n_k \bar{Q}_k + \cdots \tag{9.17}$$

differentiation of which gives

$$dQ' = n_i d\bar{Q}_i + n_j d\bar{Q}_j + n_k d\bar{Q}_k + \cdots + \bar{Q}_i dn_i + \bar{Q}_j dn_j + \bar{Q}_k dn_k + \cdots \tag{9.18}$$

Comparison of Equations 9.16 and 9.18 shows that, at constant T and P,

$$n_i d\bar{Q}_i + n_j d\bar{Q}_j + n_k d\bar{Q}_k + \cdots = 0$$

or, generally,

$$\sum_i n_i d\bar{Q}_i = 0 \tag{9.19}$$

Division of Equation 9.19 by n, the total number of moles of all the components of the solution, gives

$$\sum_i X_i d\bar{Q}_i = 0 \tag{9.20}$$

Equations 9.19 and 9.20 are equivalent expressions of the generalized *Gibbs–Duhem equation*.

For example, at constant temperature and pressure, the partial molar Gibbs free energies (chemical potentials, μ_i) in a binary system are related as

$$X_A d\bar{G}_A + X_B d\bar{G}_B = 0 \tag{9.21}$$

$$X_A \mu_A + X_B \mu_B = 0 \tag{9.22}$$

9.5 THE GIBBS FREE ENERGY OF FORMATION OF A SOLUTION

9.5.1 The Molar Gibbs Free Energy of a Solution and the Partial Molar Gibbs Free Energies of the Components of the Solution

Applying Equation 9.17 to a binary solution, the Gibbs free energy (an extensive thermodynamic state function) at fixed temperature and pressure is

$$G' = n_A\bar{G}_A + n_B\bar{G}_B \tag{9.23}$$

where:

$\bar{G}_A$ and $\bar{G}_B$ are, respectively, the partial molar Gibbs free energies of A and B in the solution

G' is the total Gibbs free energy of the solution

Dividing both sides of Equation 9.23 by $n_A + n_B$ gives the molar Gibbs free energy of the solution as

$$G(X_B) = X_A\bar{G}_A + X_B\bar{G}_B \tag{9.24}$$

$$G(X_B) = (1 - X_B)\bar{G}_A + X_B\bar{G}_B \tag{9.25}$$

Figure 9.5a is a plot of the molar Gibbs free energy of a binary solution. The tangent to the curve at X_B intersects the ordinates of the plot at the partial molar values $\bar{G}_A$ and $\bar{G}_B$.

Since the partial molar Gibbs free energies are equal to their chemical potentials:

$$\bar{G}_i = \mu_i = RT\ln a_i(X_B). \tag{9.26}$$

From Figure 9.5a:

$$\frac{dG(X_B)}{dX_B} = \bar{G}_B - \bar{G}_A$$

Thus,

$$\bar{G}_A(X_B) = G(X_B) - X_B\frac{dG(X_B)}{dX_B} \tag{9.27a}$$

$$\bar{G}_B(X_B) = G(X_B) + X_A\frac{dG(X_B)}{dX_B} \tag{9.27b}$$

These expressions relate the dependence on composition of the partial molar Gibbs free energies, $\bar{G}_i$, (chemical potentials, μ_i) of the components of a binary solution and the molar Gibbs free energy, G, of the solution.

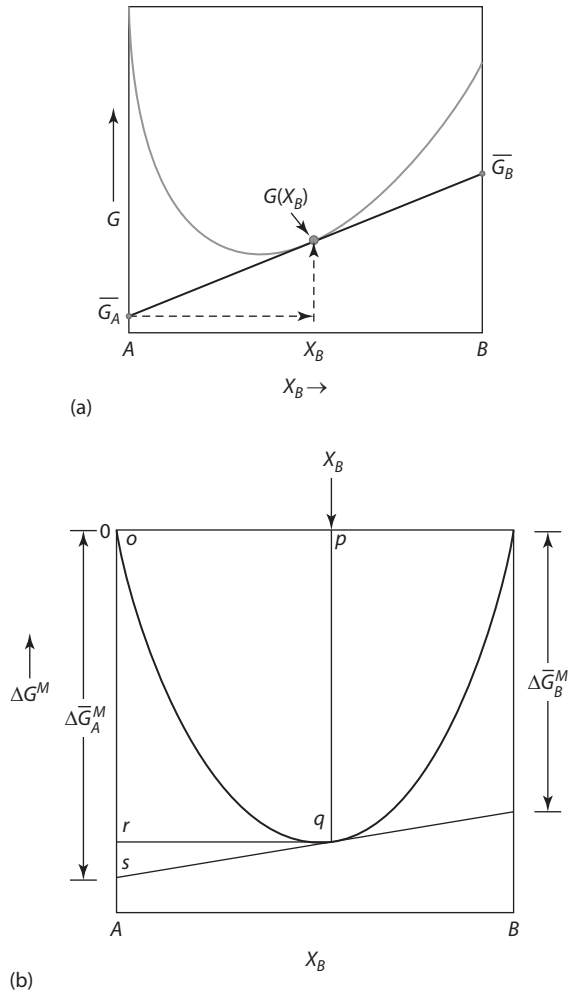

FIGURE 9.5 (a) The variation of the molar Gibbs free energy with composition, showing the partial molar Gibbs free energies of components *A* and *B* for the solution of composition X_B; (b) The variation, with composition, of the molar Gibbs free energy of formation (mixing) of a binary solution at a temperature, *T*. The partial molar values for the alloy $X_B = q$ are shown by the tangent intercepts with ordinate axes. At this temperature, there is complete solubility of *A* in *B* and *B* in *A*.

9.5.2 The Change in Gibbs Free Energy due to the Formation of a Solution (Mixing)

The variation, with composition, of the molar Gibbs free energy of formation (mixing) of a solution from its pure components at a temperature, *T* is shown in Figure 9.5b. The values of Gibbs free energy of formation at $X_B = 0$ and $X_B = 1$ are zero.

The intercepts of the tangent with ordinate axes are the partial molar values of mixing. At this temperature, there is complete solubility of A in B and B in A.

The quantity designated $\Delta\bar{G}_i^M$ is the partial molar Gibbs free energy of mixing of the solution of component i and equals:

$$\Delta\bar{G}_i^M = \bar{G}_i - G_i^\circ = RT \ln a_i \tag{9.28}$$

If n_A moles of A and n_B moles of B are mixed to form a solution at constant temperature and pressure,

$$\text{The Gibbs free energy before mixing} = n_A G_A^\circ + n_B G_B^\circ$$

and

$$\text{The Gibbs free energy after mixing} = n_A \bar{G}_A + n_B \bar{G}_B$$

The change in the *total* Gibbs free energy caused by the mixing process, $\Delta G'^{\mathrm{M}}$, sometimes referred to as the *integral* Gibbs free energy of mixing (*total* Gibbs free energy of mixing), is the difference between these quantities; that is,

$$\begin{aligned}\Delta G'^M &= \left(n_A \bar{G}_A + n_B \bar{G}_B\right) - \left(n_A G_A^\circ + n_B G_B^\circ\right) \\ &= n_A\left(\bar{G}_A - G_A^\circ\right) + n_B\left(\bar{G}_B - G_B^\circ\right)\end{aligned}$$

Substitution from Equation 9.28 gives

$$\Delta G'^M = n_A \Delta\bar{G}_A^M + n_B \Delta\bar{G}_B^M \tag{9.29}$$

or

$$\Delta G'^M = RT\left(n_A \ln a_A + n_B \ln a_B\right) \tag{9.30}$$

For 1 mole of solution, Equations 9.29 and 9.30, respectively, become

$$\Delta G^M = X_A \Delta\bar{G}_A^M + X_B \Delta\bar{G}_B^M \tag{9.31}$$

and

$$\Delta G^M = RT\left(X_A \ln a_A + X_B \ln a_B\right) \tag{9.32}$$

The variation of ΔG^M with composition, given by Equation 9.32, is shown in Figure 9.5b. $\Delta G^M\left(X_B = q\right)$ is given by the segment $\overline{pq}$ and the segment $\overline{or}$.

9.5.3 The Method of Tangential Intercepts

From Figure 9.5b and by analogy with Equations 9.27a and b, it can be seen that

$$\Delta\bar{G}_A^M = \Delta G^M - X_B \frac{d\Delta G^M}{dX_B} \tag{9.33a}$$

and

$$\Delta\bar{G}_B^M = \Delta G^M + X_A \frac{d\Delta G^M}{dX_B} \tag{9.33b}$$

Here, the partial molar Gibbs free energy of mixing of the components A and B can be read directly from the tangential intercepts at $X_B = 0$ and $X_B = 1$, respectively, just as the partial molar Gibbs free energies of X_B and X_A (their chemical potentials) can be read directly from Figure 9.5a.

9.6 THE PROPERTIES OF IDEAL SOLUTIONS

The components of a Raoultian solution obey the relation $a_i = X_i$. An ideal solution is a solution that obeys Raoult's law at *all temperatures, pressures*, and *compositions*. Thus, for an ideal binary A–B solution, the molar Gibbs free energy of mixing from Equation 9.32 becomes

$$\Delta G^{M,\text{id}} = RT\left(X_A \ln X_A + X_B \ln X_B\right) \tag{9.34}$$

with the partial molar Gibbs free energy of mixing of the components A and B given as

$$\Delta\bar{G}_A^{M,\text{id}} = RT \ln X_A \quad \text{and} \quad \Delta\bar{G}_B^{M,\text{id}} = RT \ln X_B$$

It is seen that $\Delta G^{M,\text{id}}$ is less than zero for all $T > 0$.

9.6.1 The Change in Volume Accompanying the Formation of an Ideal Solution

As discussed in Chapter 8, the general thermodynamic relationships between the state properties of a system are applicable to the partial molar properties of the components of a system. Thus, for the species i occurring in a solution,

$$\left(\frac{\partial\bar{G}_i}{\partial P}\right)_{T,\text{comp}} = \bar{V}_i \tag{9.35}$$

and, for pure i,

$$\left(\frac{\partial G_i^\circ}{\partial P}\right)_T = V_i^\circ \tag{9.36}$$

Subtraction of Equations 9.36 from 9.35 gives

$$\left[\frac{\partial\left(\overline{G}_i - G_i^\circ\right)}{\partial P}\right]_{T,\text{comp}} = \left(\overline{V}_i - V_i^\circ\right)$$

or

$$\left(\frac{\partial \Delta \overline{G}_i^M}{\partial P}\right)_{T,\text{comp}} = \Delta \overline{V}_i^M \tag{9.37}$$

The change in volume due to mixing, $\Delta V'^{\text{M}}$, is the difference between the volumes of the components in the solution and the volumes of the pure components; that is, for a binary A–B solution containing n_A moles of A and n_B moles of B,

$$\begin{aligned}\Delta V'^M &= \left(n_A\overline{V}_A + n_B\overline{V}_B\right) - \left(n_A V_A^\circ + n_B V_B^\circ\right)\\ &= n_A\left(\overline{V}_A - V_A^\circ\right) + n_B\left(\overline{V}_B - V_B^\circ\right)\\ &= n_A\Delta\overline{V}_A^M + n_B\Delta\overline{V}_B^M\end{aligned}$$

In an ideal solution, $\Delta\overline{G}_i^{M,\text{id}} = RT\ln X_i$, and since this term is not a function of pressure, $\left(\frac{\partial\Delta\overline{G}_i^{M,\text{id}}}{\partial P}\right)_{T,\text{comp}} = \Delta\overline{V}_i^{M,\text{id}} = 0$. Thus, it is seen that the change in volume accompanying an ideal solution is zero; that is,

$$\Delta V'^{M,\text{id}} = 0 \tag{9.38}$$

The volume of an ideal solution is thus equal to the sum of the volumes of the pure components. The variation, with composition, of the molar volume of an ideal binary solution is shown in Figure 9.6. At any composition, the values of the partial molar

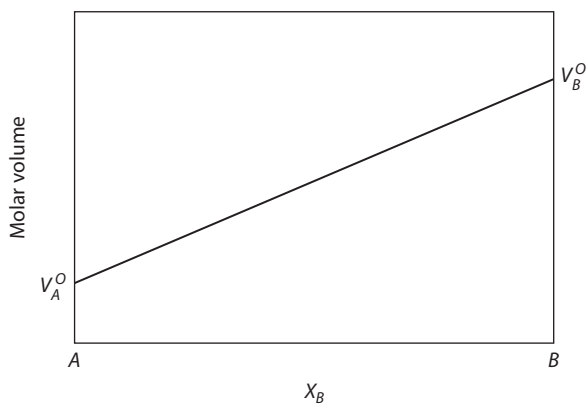

FIGURE 9.6 The variation, with composition, of the molar volume of a binary ideal solution.

volumes $\overline{V}_A^M$ and $\overline{V}_B^M$ are obtained as the intercepts of the tangents to the volume–composition line with the respective axes. Since the molar volume of an ideal solution is a linear function of composition (i.e., it follows the rule of mixtures), the tangent at any point coincides with the straight line, such that

$$\overline{V}_A = V_A^\circ \quad \text{and} \quad \overline{V}_B = V_B^\circ$$

For crystalline solids, this plot is similar to the case where the lattice parameter of a cubic phase *versus* composition is linear (called *Vegard's law*, after Lars Vegard, 1880–1963).

9.6.2 The Enthalpy of Formation of an Ideal Solution

For a component in a solution, the Gibbs–Helmholtz equation (Equation 5.55), can be used to obtain

$$\left[\frac{\partial \dfrac{\overline{G}_i}{T}}{\partial T}\right]_{P,\text{comp}} = -\frac{\overline{H}_i}{T^2} \tag{9.39}$$

and, for the pure component,

$$\left[\frac{\partial \dfrac{G_i^\circ}{T}}{\partial T}\right]_{P,\text{comp}} = -\frac{H_i^\circ}{T^2} \tag{9.40}$$

where $\overline{H}_i$ and H_i° are, respectively, the partial molar enthalpy of i in the solution and the standard molar enthalpy of i.

Subtraction of Equation 9.40 from Equation 9.39 gives

$$\left[\frac{\partial\left(\dfrac{\overline{G}_i - G_i^\circ}{T}\right)}{\partial T}\right]_{P,\text{comp}} = -\frac{\left(\overline{H}_i - H_i^\circ\right)}{T^2}$$

or

$$\left[\frac{\partial\left(\dfrac{\Delta\overline{G}_i^M}{T}\right)}{\partial T}\right]_{P,\text{comp}} = -\frac{\Delta\overline{H}_i^M}{T^2} \tag{9.41}$$

where $\Delta\bar{H}_i^M$ is the partial molar enthalpy of mixing of solution of *i*.

In an ideal solution, $\Delta\bar{G}_i^{M,\text{id}} = RT\ln X_i$, substitution of which into Equation 9.41 gives

$$\frac{d\left(R\ln X_i\right)}{dT} = -\frac{\Delta\bar{H}_i^M}{T^2}$$

and, since the first term is not a function of temperature, it is seen that, for a component of an ideal solution,

$$\Delta\bar{H}_i^{M,\text{id}} = \bar{H}_i - H_i^\circ = 0 \tag{9.42}$$

or

$$\bar{H}_i = H_i^\circ$$

The enthalpy of formation of a solution (or the enthalpy of mixing of the components) is the difference between the enthalpies of the components in solution and the enthalpies of the pure components before mixing. Thus, for a mixture of n_A moles of *A* and n_B moles of *B*,

$$\begin{aligned}\Delta H'^M &= \left(n_A\bar{H}_A + n_B\bar{H}_B\right) - \left(n_A H_A^\circ + n_B H_B^\circ\right)\\ &= n_A\left(\bar{H}_A - H_A^\circ\right) + n_B\left(\bar{H}_B - H_B^\circ\right)\\ &= n_A\Delta\bar{H}_A^M + n_B\Delta\bar{H}_B^M\end{aligned}$$

and

$$\Delta H^M = X_A\Delta\bar{H}_A^M + X_B\Delta\bar{H}_B^M$$

For an ideal solution, $\Delta\bar{H}_i^M = 0$, (Equation 9.42) and thus, it is seen that the enthalpy of formation (or the enthalpy of mixing) of an ideal solution is zero; that is,

$$\Delta H^{M,\text{id}} = 0 \tag{9.43}$$

9.6.3 The Entropy of Formation of an Ideal Solution

The fundamental equation (Equation 5.25), gives

$$\left(\frac{\partial G}{\partial T}\right)_{P,\text{comp}} = -S$$

Thus, for the formation of one mole of a solution,

$$\left(\frac{\partial \Delta G^M}{\partial T}\right)_{P,\text{comp}} = -\Delta S^M$$

For an ideal solution, Equation 9.34 showed that

$$\Delta G^{M,\mathrm{id}} = RT\left(X_A \ln X_A + X_B \ln X_B\right)$$

and hence,

$$\Delta S^{M,\mathrm{id}} = -\left(\frac{\partial \Delta G^{M,\mathrm{id}}}{\partial T}\right)_{P,\mathrm{comp}}$$

$$= -R\left(X_A \ln X_A + X_B \ln X_B\right) \tag{9.44}$$

Equation 9.44 shows that the entropy of formation of an ideal binary solution is independent of temperature and is positive.

Equation 4.3 for total change in configurational entropy gives, for the mixing of N_A particles of A with N_B particles of B,

$$\Delta S'^{M} = k_B \ln \frac{(N_A + N_B)!}{N_A!\,N_B!}$$

$$= k_B\left[\ln(N_A + N_B)! - \ln N_A! - \ln N_B!\right]$$

Application of *Stirling's approximation*[1] (after James *Stirling*, 1692–1770) gives

$$\Delta S'^{M} = k_B\left[(N_A + N_B)\ln(N_A + N_B)\right.$$

$$\left.-(N_A + N_B) - N_A \ln N_A + N_A - N_B \ln N_B + N_B\right]$$

$$= -k_B\left[N_A \ln\left(\frac{N_A}{N_A + N_B}\right) + N_B\left(\frac{N_B}{N_A + N_B}\right)\right]$$

Now,

$$\frac{N_A}{N_A + N_B} = \frac{n_A}{n_A + n_B} = X_A$$

and, similarly,

$$\frac{N_B}{N_A + N_B} = X_B$$

Also,

$$N_A \text{ particles of } A = \frac{N_A}{N_O} \text{ moles of } A = n_A \text{ moles of A}$$

and

$$N_B \text{ particles of } B = \frac{N_B}{N_O} \text{ moles of } B = n_B \text{ moles of } B$$

[1] Stirling's approximation comes from $m! = \sqrt{2\pi m}\; m^m e^m$; and thus, $\ln m! = \tfrac{1}{2}\ln(2\pi m) + m \ln m - m$, which, for large values of m, can be written as $\ln m! =$

where N_O is Avogadro's number. Thus,

$$\Delta S'^{M} = -k_B N_O \left(n_A \ln X_A + n_B \ln X_B\right)$$

But, since Boltzmann's constant, k_B, times Avogadro's number, N_O, equals the gas constant, R,

$$\Delta S'^{M} = -R\left(n_A \ln X_A + n_B \ln X_B\right)$$

Division by the total number of moles, $n_A + n_B$, gives

$$\Delta S^{M} = -R\left(X_A \ln X_A + X_B \ln X_B\right) \tag{9.45}$$

which is identical to Equation 9.44.

The increase in entropy accompanying the formation of 1 mole of an ideal solution is a measure of the increase in the number of *spatial configurations* that become available to the system as a result of the mixing process. This is dependent only on the numbers of moles of the components in the solution and is *independent of temperature*. The variation of $\Delta S^{M,id}$ with composition in a binary A–B solution is shown in Figure 9.7. Note that this is symmetric about $X_B = 0.5$ and has a maximum value of R ln 2. The function has infinite slopes at $X_B = 0$ and $X_B = 1$.

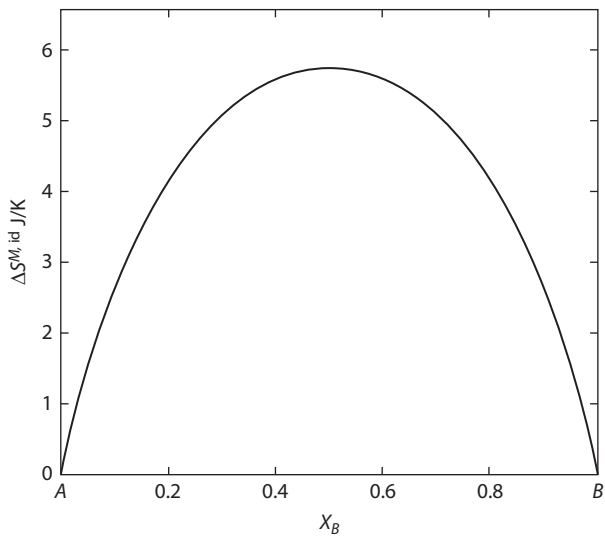

FIGURE 9.7 The variation, with composition, of the molar entropy of formation of a binary ideal solution. The maximum value is R ln 2. The initial slopes at both ends of the plot are infinite.

9.6.4 The Gibbs Free Energy of Formation of an Ideal Solution

Since

$$\Delta S^M = X_A \Delta \bar{S}_A^M + X_B \Delta \bar{S}_B^M$$

it is seen that, in an ideal solution,

$$\Delta \bar{S}_A^{M,\text{id}} = -R\ln X_A \quad \text{and} \quad \Delta \bar{S}_B^{M,\text{id}} = -R\ln X_B$$

For any solution,

$$\Delta G^M = \Delta H^M - T\Delta S^M$$

and, for an ideal solution, since $\Delta H^{M,\text{id}} = 0$, then

$$\Delta G^{M,\text{id}} = -T\Delta S^{M,\text{id}} < 0$$

9.7 NONIDEAL SOLUTIONS

A nonideal solution is one in which the *activities* of the components are not equal to their mole fractions at all compositions or temperatures. However, in view of the convenience of the concept of activity and the simplicity of Raoult's law, it is convenient to define an additional thermodynamic function called the *activity coefficient*, γ. The activity coefficient of a component of a solution is defined as the ratio of the activity of the component to its mole fraction; that is, for the component *i*,

$$\gamma_i = \frac{a_i}{X_i} \tag{9.46}$$

The value of γ_i can be greater or less than unity ($\gamma_i = 1$ gives Raoultian behavior). This coefficient varies over the composition range of the solution. In the region of a solution obeying Henry' law, γ_i is constant (see Equation 9.14).

If $\gamma_i > 1$, then the component *i* is said to exhibit a *positive deviation* from Raoultian behavior, and, if $\gamma_i < 1$, then the component *i* is said to exhibit a *negative deviation* from Raoult's law.

Figure 9.8 shows the variation of a_i with X_i for a component *i* that exhibits negative deviations. Figure 9.9 shows a system that exhibits positive deviations. Note that in both of these figures in the composition range where Henry's law is followed by the solute, Raoult's law is followed by the solvent. This is discussed in Section 9.8.1.

If γ_i varies with temperature, then $\Delta \bar{H}_i^M$ has a nonzero value; that is, from Equation 9.41,

$$\frac{\partial\left(\frac{\Delta \bar{G}_i^M}{T}\right)}{\partial T} = -\frac{\Delta \bar{H}_i^M}{T^2}$$

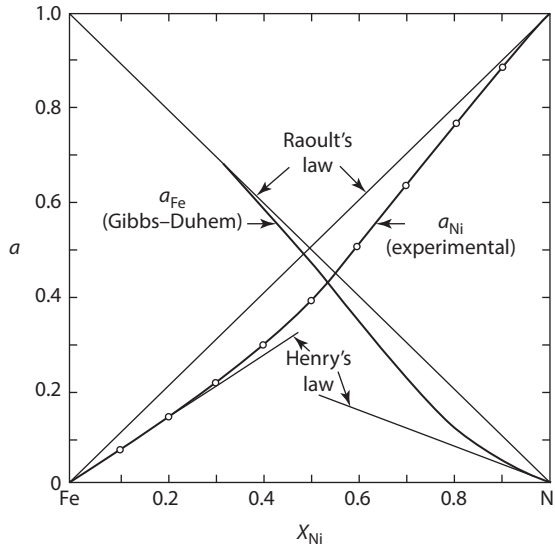

FIGURE 9.8 Activities in the liquid system iron–nickel at 1600°C which display negative deviation from ideality. (From G. R. Zellars, S. L. Payne, J. P. Morris, and R. L. Kipp, "The Activities of Iron and Nickel in Liquid Fe–Ni Alloys," *Trans. AIME* (1959), vol. 215, p. 181.)

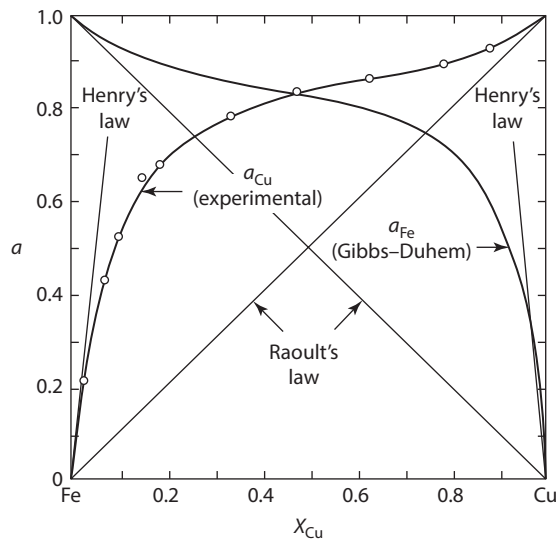

FIGURE 9.9 Activities in the liquid system iron–copper at 1550°C which display positive deviation from ideality. (From J. P. Morris and G. R. Zellars, "Vapor Pressure of Liquid Copper and Activities in Liquid Fe–Cu Alloys," *Trans. AIME* (1956), vol. 206, p. 1086.)

and

$$\Delta\bar{G}_i^M = RT\ln a_i = RT\ln\gamma_i + RT\ln X_i$$

Thus,

$$\frac{\partial\left(\dfrac{\Delta\bar{G}_i^M}{T}\right)}{\partial T} = \frac{\partial\left(R\ln\gamma_i\right)}{\partial T} = -\frac{\Delta\bar{H}_i^M}{T^2}$$

and since

$$d\left(\frac{1}{T}\right) = -\frac{dT}{T^2}$$

then

$$\frac{\partial\left(R\ln\gamma_i\right)}{\partial\left(\dfrac{1}{T}\right)} = \Delta\bar{H}_i^M \tag{9.47}$$

In general, increasing the temperature of a nonideal solution causes a decrease in the extent to which its components deviate from ideal behavior. At any temperature where $\gamma_i > 1$, an increase in temperature causes γ_i to decrease toward unity. Likewise, at any temperature where $\gamma_i < 1$, an increase in temperature causes γ_i to increase toward unity. Thus, in a solution, the components of which exhibit positive deviations from ideality, the values of the activity coefficients decrease with increasing temperature, and from Equation 9.47, it is seen that the partial molar enthalpies of formation of the components are *positive* quantities. This means that the molar enthalpy of formation (mixing) of the solution, ΔH^M, is a positive quantity, which indicates that the mixing process is endothermic. ΔH^M is the quantity of thermal energy absorbed from the thermal reservoir surrounding the solution per mole of solution formed at the temperature T.

Conversely, in a solution, the components of which exhibit negative deviations from ideality, the activity coefficients increase with increasing temperature, and hence, the partial molar enthalpies of mixing and the molar enthalpy of mixing are negative. Such a solution forms *exothermically*, and ΔH^M is the enthalpy absorbed by the constant-temperature thermal reservoir, per mole of solution formed, at the temperature T.

These trends can be understood for liquid solutions by assuming that the interactions among particles decrease as the temperature rises, because the particles have greater movement with increasing temperature and therefore less chance of interacting with each other.

Exothermic mixing in an *A–B* binary condensed system occurs when the *A–B* bond energy is more negative than both the *A–A* and *B–B* bond energies, and this causes a tendency toward atomic *ordering*. In a solution with only nearest neighbor interactions, the *A* atoms (*B* atoms) attempt to have as many *B* atoms (*A* atoms)

as the nearest neighbors as is possible for the overall composition of the solution. Exothermic mixing thus indicates a tendency toward the formation of an atomically ordered phase or compound between the two components (e.g., the Fe–Ni system).

Conversely, *endothermic* mixing occurs when the *A*–*B* bond energy is less negative than both the *A*–*A* and *B*–*B* bond energies, and this causes a tendency toward phase separation or *clustering* in the solution (e.g., the Fe–Cu system). The *A* atoms attempt to be coordinated only by *A* atoms, and the *B* atoms attempt to be coordinated only by *B* atoms.

In both of these cases (exothermic and endothermic), the equilibrium configuration of the solution is reached as a compromise between the *enthalpy* and *entropy* factors. The enthalpy, being determined by the relative magnitudes of the bond energies, attempts to either order (negative deviation from ideality) or unmix (positive deviation from ideality) the solution. At finite temperatures, the entropy factor attempts to maximize the randomness of mixing of the atoms in the solution. For the clustering case, as the temperature approaches 0 K, the equilibrium state approaches a *two phase state*, one of pure solid *A* and one of pure solid *B*. Thus, as the temperature approaches 0 K, the configurational entropy of the alloy approaches zero. For the ordering case, the situation is more complex and will be discussed later in Chapter 10. However, it too predicts zero configurational entropy for the crystalline alloy as the temperature approaches 0 K. These are Third Law constraints on the ground state (0 K) equilibrium entropy of alloys.

9.8 APPLICATION OF THE GIBBS–DUHEM RELATION TO THE DETERMINATION OF ACTIVITY

Equation 9.20 applied to a binary *A*–*B* solution and using the partial molar Gibbs free energy of mixing (Equation 9.31) as the extensive property become

$$X_A d\Delta\bar{G}_A^M + X_B d\Delta\bar{G}_B^M = 0 \tag{9.48}$$

and, since $\Delta\bar{G}_i^M = RT \ln a_i$, then

$$X_A d \ln a_A + X_B d \ln a_B = 0 \tag{9.49a}$$

$$X_A d \log a_A + X_B d \log a_B = 0 \tag{9.49b}$$

or

$$d \ln a_A = -\frac{X_B}{X_A} d \ln a_B \tag{9.50a}$$

$$d \log a_A = -\frac{X_B}{X_A} d \log a_B \tag{9.50b}$$

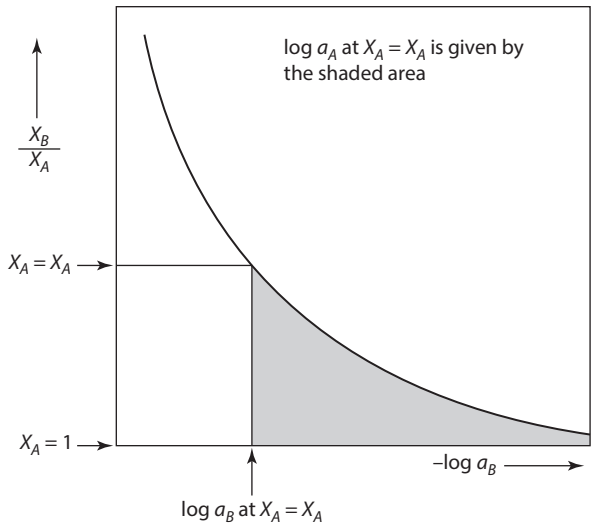

FIGURE 9.10 A schematic representation of the variation of log a_B with X_B/X_A in a binary solution, illustrating the application of the Gibbs–Duhem equation to the calculation of the activity of component A.

If the variation of a_B with composition is known, then the integration of Equation 9.50b from $X_A = 1$ to X_A gives the value of log a_A at X_A as

$$\log a_A \text{ at } X_A = -\int_{\log a_B \text{ at } X_A = 1}^{\log a_B \text{ at } X_A = X_A} \left(\frac{X_B}{X_A}\right) d \log a_B \tag{9.51}$$

Since an analytical expression for the variation of the activity of B is not usually computed, Equation 9.51 is solved by graphical integration.

Figure 9.10 shows a typical variation of log a_B with composition, and the value of log a_A at $X_A = X_A$ is equal to the shaded area under the curve. Two points are to be noticed in Figure 9.10.

1. $X_B \to 1$, $a_B \to 1$, log $a_B \to 0$, and $X_B/X_A \to \infty$. Thus, the curve exhibits a tail to infinity as $X_B \to 1$.
2. $X_B \to 0$, $a_B \to 0$, and log $a_B \to -\infty$. Thus, the curve exhibits a tail to minus infinity as $X_B \to 0$.

These points have been addressed by Darken and Gurry,[2] and methods of integrating with better accuracy are presented in their text. See also the fifth edition of this text, pages 230–235.

[2] L. S. Darken and R. W. Gurry, *Physical Chemistry of Metals*, McGraw-Hill, New York, 1953, pp. 258–266.

9.8.1 The Relationship between Henry's and Raoult's Laws

Henry's law for the solute B in a binary A–B solution (Equation 9.14) can be written as

$$a_B = \gamma_B X_B$$

or, in terms of logarithms,

$$\ln a_B = \ln \gamma_B + \ln X_B$$

differentiation of which gives

$$d \ln a_B = d \ln X_B$$

since γ_B is constant in the range of composition over which the solute B obeys Henry's law. Inserting this into the Gibbs–Duhem equation gives

$$d \ln a_A = -\frac{X_B}{X_A} d \ln X_B = -\frac{X_B}{X_A}\frac{dX_B}{X_B} = -\frac{dX_B}{X_A}$$

$$d \ln a_A = \frac{dX_A}{X_A} = d \ln X_A$$

Integration gives

$$\ln a_A = \ln X_A + \ln (\text{constant})$$

or

$$a_A = \text{constant} \times X_A$$

But, by definition, $a_i = 1$ when $X_i = 1$, and thus, the integration constant equals unity. Consequently, in the range of composition over which the solute B obeys Henry's law, the solvent A obeys Raoult's law.

As an example of this, see Figure 9.8, where Henry's law holds for the solute Ni up to about $X_{Ni} = 0.3$ and Raoult's law holds for the solvent Fe for $X_{Ni} < 0.3$. Also, Figure 9.9 shows that Henry's law holds for the solute Cu up to about $X_{Cu} = 0.04$ and Raoult's law holds for the solvent Fe for $X_{Cu} < 0.04$.

9.8.2 Direct Calculation of the Total Molar Gibbs Free Energy of Mixing

Equation 9.33a gave

$$\Delta \bar{G}_A^M = \Delta G^M + X_B \frac{d\Delta G^M}{dX_A}$$

Rearranging and dividing by X_B^2 gives

$$\frac{\Delta\bar{G}_A^M dX_A}{X_B^2} = \frac{X_B d\Delta G^M - \Delta G^M dX_B}{X_B^2} = d\left(\frac{\Delta G^M}{X_B}\right)$$

or

$$d\left(\frac{\Delta G^M}{X_B}\right) = \frac{\Delta\bar{G}_A^M}{X_B^2} dX_A$$

Integrating between $X_A = X_A$ and $X_A = 0$ gives

$$\Delta G^M = X_B \int_0^{X_A} \frac{\Delta\bar{G}_A^M}{X_B^2} dX_A \tag{9.52a}$$

Since $\Delta\bar{G}_A^M = RT \ln a_A$, the integral molar Gibbs free energy of mixing of A and B can be obtained directly from the variation of a_A with composition as

$$\Delta G^M = RTX_B \int_0^{X_A} \frac{\ln a_A}{X_B^2} dX_A \tag{9.52b}$$

The measured activities of Ni in Fe and Cu in Fe shown in Figures 9.8 and 9.9 can be used to obtain

$$\Delta G^M \left(\text{in the system Fe} - \text{Ni}\right) = RTX_{\text{Fe}} \int_0^{X_{\text{Ni}}} \frac{\ln a_{\text{Ni}}}{X_{\text{Fe}}^2} dX_{\text{Ni}} \tag{9.53a}$$

and

$$\Delta G^M \left(\text{in the system Cu} - \text{Fe}\right) = RTX_{\text{Fe}} \int_0^{X_{\text{Cu}}} \frac{\ln a_{\text{Cu}}}{X_{\text{Fe}}^2} dX_{\text{Cu}} \tag{9.53b}$$

Figure 9.11 shows the plots of $(\ln a_{\text{Cu}})/X_{\text{Fe}}^2$ versus X_{Cu}(a) and $(\ln a_{\text{Ni}})/X_{\text{Fe}}^2$ versus X_{Ni}(c). Also shown is the variation of $(\ln X_i)/(1 - X_i)^2$ with X_i, which is the variation of the function for a component i which exhibits Raoultian behavior. In Figure 9.11, the shaded area (which is the value of the integral between $X_{\text{Cu}} = 0.5$ and $X_{\text{Cu}} = 0$) multiplied by the factor $(2.303 \times 8.3144 \times 1823 \times 0.5)$ gives the value of ΔG^M at $X_{\text{Fe}} = 0.5$. Some uncertainty is introduced into the integration by virtue of the fact that the function $(\ln a_i)/(1 - X_i)^2 \to -\infty$, as $X_i \to 0$. Such integration can also be done for the Ni-Fe system by integrating Equation 9.53a.

In Figure 9.12, ΔG^M of the ideal solution model at the temperatures 1550°C and 1600°C is shown as dotted curves. The graphically determined plot of ΔG^M of Cu-Fe at 1550°C lies above that of the ideal solution plot, showing the Cu-Fe solution to have a *positive deviation* from ideality. This is due to the positive value of ΔH^M for Cu-Fe. The graphically determined plot of ΔG^M of Ni-Fe at 1600°C lies below that

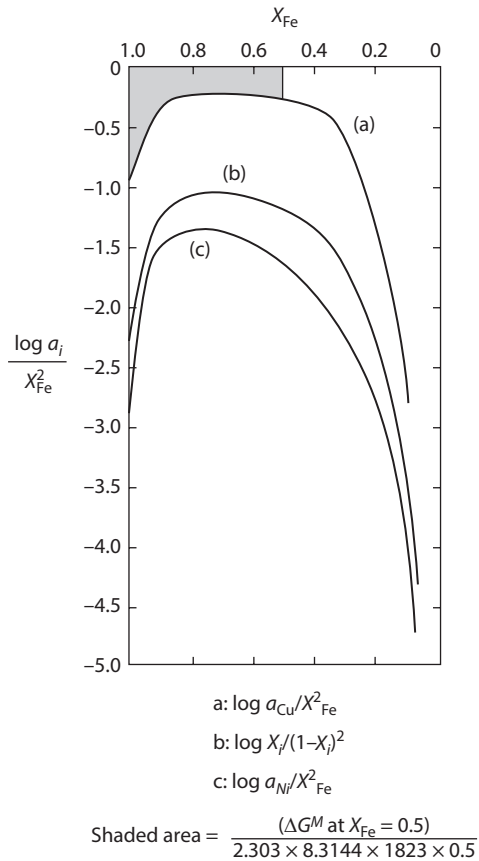

FIGURE 9.11 Illustration of the direct calculation of the molar Gibbs free energies of mixing in the liquid systems iron–copper at 1550°C and iron–nickel at 1600°C.

of that of the ideal solution plot, showing that solution to have a *negative deviation* from ideality. This is due to the negative value of ΔH^M for Fe-Ni. At the temperatures denoted, both plots show that the solutions are single phase over the entire composition range.

In both cases, it is seen that the solutions are non-ideal. However, the ΔG^M plots do have a similar shape as that of an ideal solution (for example, both are symmetric about the 50%-atomic mixture). They are vertically displaced from the ideal mixing plot in the direction of the sign of their deviation from ideality.

9.9 REGULAR SOLUTIONS

Up to this point, two classes of solutions have been identified. The first is the *ideal solution*, in which

$$a_i = X_i$$

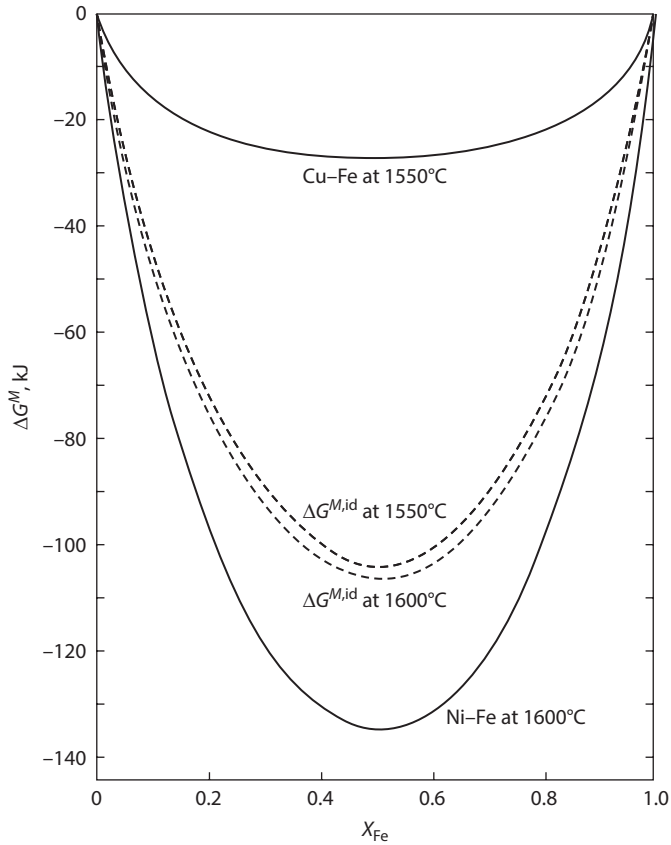

FIGURE 9.12 The molar Gibbs free energies of mixing in the liquid systems iron–copper at 1550°C and iron–nickel at 1600°C. Iron nickel displays negative deviations from ideality and iron copper displays positive deviations from ideality.

$$\Delta \bar{H}_i^M = 0$$

$$\Delta \bar{V}_i^M = 0$$

$$\Delta \bar{S}_i^M = -R \ln X_i$$

for all X_i, all temperatures, and all pressures.

All other solutions can be classified as *nonideal solutions* in which the relationships $a_i = X_i$ and $\Delta \bar{H}_i^M = 0$ are not valid.

Attempts to classify nonideal solutions have involved the development of equations that describe the behavior of hypothetical solutions. The simplest of these mathematical formalisms is that which generates what is now known as *regular solution behavior.*

A regular solution is one in which

$$\Delta H^M = \alpha X_A X_B \tag{9.54}$$

and

$$\Delta S^M = \Delta S^{M,\text{ideal}} \tag{9.55}$$

where α is a constant with the same sign and units as ΔH^M. The value of α is positive, for solutions exhibiting positive deviations from ideality, or negative for those solutions exhibiting negative deviations from ideality. See Section 9.7 and Figure 9.12.

For a regular solution:

$$\Delta G^M = \alpha X_A X_B - T\Delta S^{M,\text{ideal}} \tag{9.56}$$

It is common to define excess functions as the value of the state function minus that of the ideal value of the state function.

$$G^{\text{XS}} = G - G^{\text{id}} \tag{9.57}$$

Thus, for a regular solution, the excess molar Gibbs free energy of mixing is

$$G^{\text{XS}} = \Delta G^M - \Delta G^{M,\text{ideal}} = \Delta H^M = \alpha X_A X_B \tag{9.58}$$

Also, for a regular solution,

$$\frac{\partial G^{\text{XS}}}{\partial T} = -S^{\text{XS}} = 0$$

At any composition,

$$\bar{G}_A^{\text{XS}} = RT \ln \gamma_A$$

Thus the excess value of the Gibbs free energy of mixing is positive for $\gamma > 1$ and negative for $\gamma < 1$. See Figure 9.12.

Also note that $\bar{G}_A^{\text{XS}}$is independent of temperature in this regular solution model. Thus,

$$\bar{G}_A^{\text{XS}} = RT_1 \ln \gamma_A(T_1) = RT_2 \ln \gamma_A(T_2)$$

from which:

$$\frac{\ln \gamma_A(T_2)}{\ln \gamma_A(T_1)} = \frac{T_1}{T_2} \tag{9.59}$$

Equation 9.59 is of considerable practical use in converting activity data for a regular solution at one temperature to activity data at another temperature. We also see that as T_2 becomes very large, $\gamma_A\,(T_2)$ approaches unity (see also the discussion in Section 9.7 concerning Equation 9.47).

It can be seen that:

$$\Delta\bar{H}_B = \Delta H^M + (1 - X_B)\frac{d\Delta H^M}{dX_B}$$

and since $\Delta H^M = \alpha X_A X_B$, this yields

$$\Delta\bar{H}_B = \alpha X_A^2 \tag{9.60}$$

Since all the state functions of a regular solution are symmetric with respect to the interchanging of X_A and X_B:

$$\Delta\bar{H}_A = \alpha X_B^2 \tag{9.61}$$

Now,

$$\Delta\bar{G}_A^M = RT\ln a_A = \Delta\bar{H}_A^M - T\Delta\bar{S}_A^M$$

$$RT\ln a_A + T\Delta\bar{S}_A^M = \Delta\bar{H}_A^M$$

$$RT\ln\gamma_A + RT\ln X_A - RT\ln X_A = \Delta\bar{H}_A^M$$

$$\therefore RT\ln\gamma_A = \Delta\bar{H}_A^M = \alpha X_B^2 \tag{9.62}$$

Finally, this gives

$$\gamma_A = \exp\left(\frac{\alpha X_B^2}{RT}\right) \tag{9.63}$$

$$\gamma_B = \exp\left(\frac{\alpha X_A^2}{RT}\right) \tag{9.64}$$

Equation 9.63 shows once again that as the temperature increases to very large values, the activity coefficient approaches unity.

Also since $\bar{G}_A^{XS} = RT\ln\gamma_A$, $\bar{G}_A^{XS} = \alpha X_B^2$ and $\bar{G}_B^{XS} = \alpha X_A^2$. (See Equations 9.60 and 9.61 and remember that in a regular solution $\bar{G}_i^{XS} = \bar{H}_i^{XS}$).

The following relationships are valid for a regular solution.

$$\text{As } X_A \to 1,\ \gamma_A = \exp\left(\frac{\alpha \cdot 0}{RT}\right) \to 1,\ A \text{ is a Raultian solution.}$$

$$\text{As } X_A \to 0,\ \gamma_A = \exp\left(\frac{\alpha \cdot 1}{RT}\right) \to \text{a constant},\ A \text{ is a Henrian solution.}$$

$$\text{As } X_B \to 1,\ \gamma_B = \exp\left(\frac{\alpha \cdot 0}{RT}\right) \to 1,\ B \text{ is a Raultian solution.}$$

$$\text{As } X_B \to 0,\ \gamma_B = \exp\left(\frac{\alpha \cdot 1}{RT}\right) \to \text{a constant},\ B \text{ is a Henrian solution.}$$

Figures 9.13 and 9.14, respectively, show the variation, with composition, of the activities and activity coefficients in the liquid system tin–thallium measured by Hildebrand and Sharma[3] at three temperatures. The values of the activities of Sn in the solution were calculated from the Gibbs–Duhem equation. Figure 9.15 shows the linear variations of log γ_{Tl} with X_{Sn}^2, the slopes of which equal α at the given temperatures.

The variation of γ_i with X_i is that of a regular solution, but Figure 9.16 shows that αT, which for strict adherence to regular behavior should be independent of T,

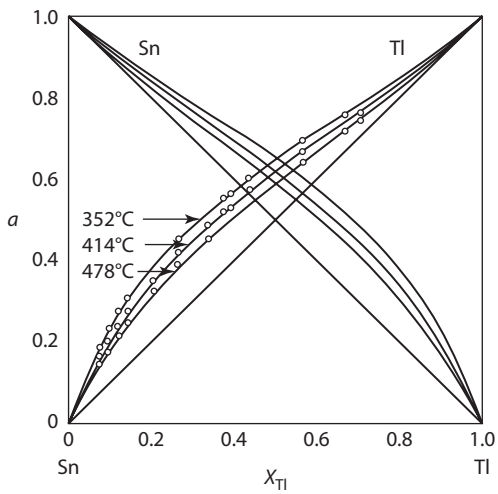

FIGURE 9.13 Activities in the liquid system tin–thallium. (From J. H. Hildebrand and J. N. Sharma, "The Activities of Molten Alloys of Thallium with Tin and Lead," *J. Am. Chem. Soc.* (1929), vol. 51, p. 462.)

[3] J. H. Hildebrand and J. N. Sharma, "The Activities of Molten Alloys of Thallium with Tin and Lead," *J. Am. Chem. Soc.* (1929), vol. 51, p. 462.

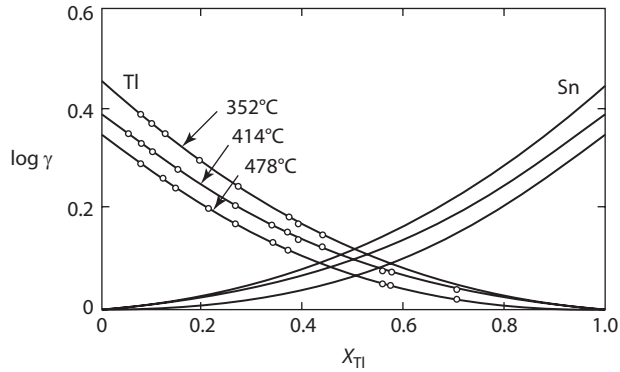

FIGURE 9.14 Activity coefficients in the liquid system tin–thallium. (From J. H. Hildebrand and J. N. Sharma, "The Activities of Molten Alloys of Thallium with Tin and Lead," *J. Am. Chem Soc.* (1929), vol. 51, p. 462.)

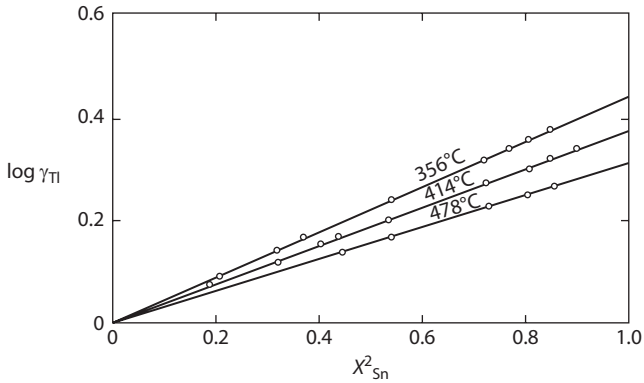

FIGURE 9.15 Log γ_{T1} vs. X^2_{Sn} in the system tin–thallium. (From J. H. Hildebrand and J. N. Sharma, "The Activities of Molten Alloys of Thallium with Tin and Lead," *J. Am. Chem. Soc.* (1929), vol. 51, p. 462.)

decreases slowly with increasing temperature. Figure 9.17 shows the variations, with composition, of ΔG^M, ΔH^M, and $-T\Delta S^{\text{M}}$ for the liquid system Sn–Tl at 414°C. It is to be noted that a parabolic form for ΔH^M or G^{XS} should not be taken as being a demonstration that the solution is regular, as it is frequently found that ΔH^M or G^{XS} can be adequately expressed by means of the relations.

$$\Delta H^M = bX_AX_B \quad \text{or} \quad G^{\text{XS}} = b'X_AX_B$$

where b and b' are unequal, in which case

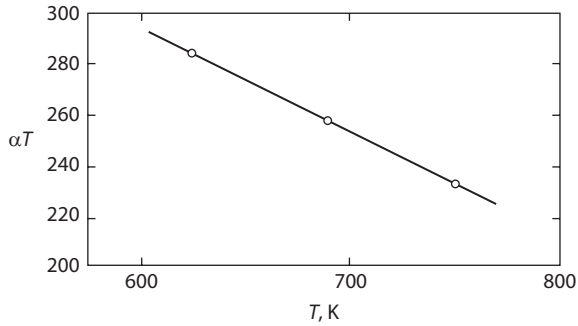

FIGURE 9.16 The variation of the product αT with T in the system Sn–Tl, showing that the system does not conform to a regular solution, since αT depends on T.

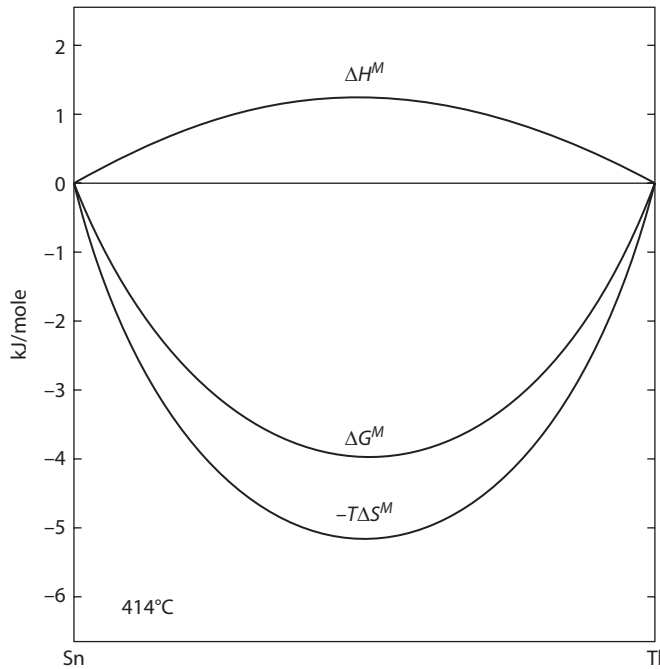

FIGURE 9.17 The molar enthalpy, entropy, and Gibbs free energy of mixing of liquid tin and thallium at 414°C. The system exhibits positive deviations from ideality.

$$\Delta S^M \neq \Delta S^{M,\text{id}}$$

If only configurational entropy is considered, then $\Delta S^M < \Delta S^{M,\text{id}}$. If, however, other *aspects* of entropy exist in the alloy (e.g., magnetic spins, defects, volume effects), ΔS^M may be greater than $\Delta S^{M,\text{id}}$.

9.10 THE GIBBS FREE ENERGY OF FORMATION OF REGULAR SOLUTIONS

Figure 9.12 shows that the plots of the molar Gibbs free energy of mixing of non-ideal solutions may be either above or below that of the plots of the ideal Gibbs free energy of mixing at the same temperature. If the solution is a regular solution, than at any temperature, the difference in their values for the 50% solution is equal to the enthalpy of mixing of the regular solution, which is equal to the excess Gibbs free energy of mixing:

$$\Delta G^M - \Delta G^{M,\text{id}} \equiv G^{\text{XS}} = \Delta H^M = \alpha X_A X_B \tag{9.65}$$

For the Cu-Fe solution, $\Delta G^M > \Delta G^{M,\text{id}}$, and thus, ΔH^M of the solution and α are positive quantities (see Figure 9.12).

It is of interest to consider the effect of increasingly positive values of α on the shape of the Gibbs free energy of mixing curve for a regular solution. In Figure 9.18, curve I is drawn as $-\Delta S^{M,\text{id}}/R = X_A \ln X_A + X_B \ln X_B$. This curve represents $\Delta G^{M,\text{id}}$. Curves for $\Delta H^M/RT = \alpha X_A X_B / RT$ are drawn for $\alpha/RT = 0, +1.0, +2.0$, and $+3.0$,

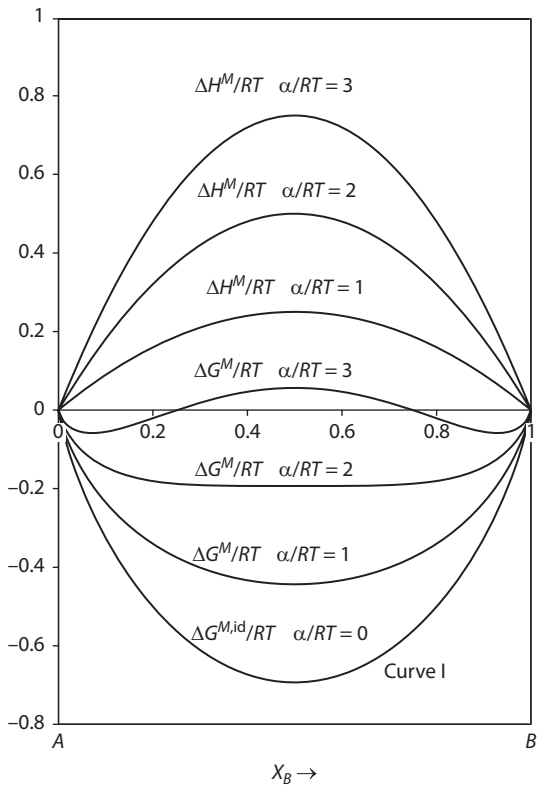

FIGURE 9.18 The effect of the magnitude of α / RT on the reduced enthalpies and integral molar Gibbs free energies of formation of a binary regular solution.

and the corresponding $\Delta G^M / RT$ curves are drawn as the sum of the particular $\Delta H^M / RT$ and $-\left(\Delta S^{M,\text{id}} / R\right)$ curves. As the magnitude of α / RT is increased, it is seen that the shape of the $\Delta G^M / RT$ curve continuously changes from a shape typified by $\alpha = 0$ to a form typified by $\alpha / RT = 3$.

Before discussing the consequences of this change of shape on the behavior of the solutions, it is pertinent to examine the significance of the shape of the curve (Figure 9.19a).

This curve has positive curvature at all compositions. Thus, the homogeneous solution formed from any mixture of *A* and *B* is the stable state at the temperature in question, since this state has the lowest possible Gibbs free energy of mixing. Consider, further, two separate solutions—say, *a* and *b* in Figure 9.19a. Before the mixing of these two solutions, the Gibbs free energy of the two-solution system, with respect to pure *A* and pure *B*, lies on the straight line joining *a* and *b*, with the exact position being determined, via the lever rule, by the relative proportions of the separate solutions. If the solutions *a* and *b* are present in equal amounts, then the molar Gibbs free energy of the system (before mixing) is given by the point *c*. When mixed,

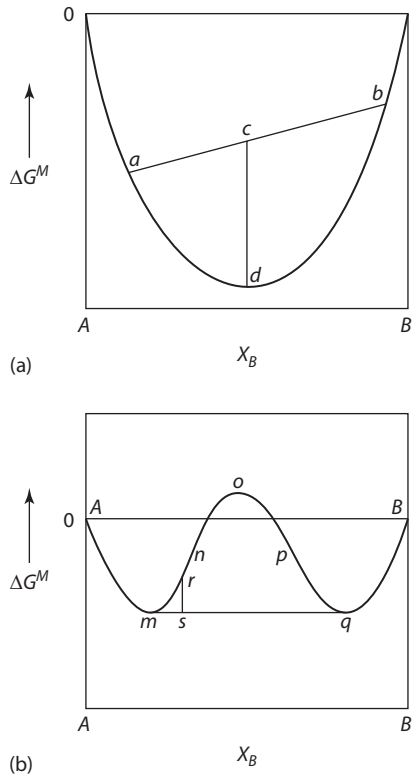

FIGURE 9.19 (a) The molar Gibbs free energies of mixing of binary components at a temperature that forms a complete range of solutions. (b) The molar Gibbs free energies of mixing of binary components at a temperature in a system that exhibits a miscibility gap (two-phase region).

the two solutions form a new *homogeneous solution*, since the Gibbs free energy of mixing of the system is thereby decreased from *c* to *d*, the minimum Gibbs free energy of mixing it can have.

Consider now Figure 9.19b, in which the $\Delta G^M / RT$ curve for $\alpha / RT > 2$ is shown. This curve has positive curvature between *A* and *n* and between *p* and *B*, and it has negative curvature between *n* and *p*. The Gibbs free energy of mixing of a system of composition between *m* and *q* is minimized when the system occurs as two solutions, one of composition *m* and the other of composition *q*. The homogeneous solution of composition *r* is not stable and separates into the two coexisting solutions *m* and *q*, and the Gibbs free energy of mixing of the system is decreased from *r* to *s*. The equilibrium coexistence of two separate solutions at the temperature *T* and pressure *P* requires that

$$\bar{G}_A\left(\text{in solution } m\right) = \bar{G}_A\left(\text{in solution } q\right) \tag{i}$$

and

$$\bar{G}_B\left(\text{in solution } m\right) = \bar{G}_B\left(\text{in solution } q\right) \tag{ii}$$

Subtracting G_A° from both sides of Equation (i) gives

$$RT \ln a_{A(\text{in solution } m)} = RT \ln a_{A(\text{in solution } q)}$$

or

$$a_{A(\text{in solution } m)} = a_{A(\text{in solution } q)} \tag{iii}$$

Similarly,

$$a_{B(\text{in solution } m)} = a_{B(\text{in solution } q)} \tag{iv}$$

Equations (iii) and (iv) are the criteria for equilibrium coexistence of two solutions (or phases) at constant *T* and *P*.

Since

$$\Delta\bar{G}_A^M\left(\text{in solution } m\right) = \Delta\bar{G}_A^M\left(\text{in solution } q\right), \text{ and}$$

$$\Delta\bar{G}_B^M\left(\text{in solution } m\right) = \Delta\bar{G}_B^M\left(\text{in solution } q\right)$$

it is seen that the tangent to the curve at the point *m* is also the tangent to the curve at the point *q*. The positioning of this common tangent defines the positions of the points *m* and *q* on the Gibbs free energy of the mixing curve.

The *A–B* system, as represented in Figure 9.19b, is one in which, at the temperature *T*, the value of α / RT is sufficiently positive that the consequent tendency toward *clustering of like atoms* is great enough to cause *phase separation*.

Consider the addition of *B* atoms to an initial solution of pure A. A homogeneous solution (phase I) is formed when *B* is initially added to *A* and the saturation of phase I with *B* occurs at the composition *m*. Further addition of *B* causes the appearance of a second solution (phase II) of composition *q* (which is phase II saturated with *A*). Continued addition of *B* causes an increase in the ratio of phase II to phase I occurring until the overall composition of the two-phase system reaches *q*, at which point phase I disappears. A homogeneous solution (phase II) occurs between the compositions *q* and *B*. The curve *mn* represents the Gibbs free energy of mixing of phase I supersaturated (and therefore *metastable*) with *B*, and the curve *qp* represents the Gibbs free energy of mixing of phase II supersaturated (and therefore *metastable)* with *A*. The points on *AmqB* represent the stable equilibrium states of the system. Between the compositions *nop*, the homogeneous solution is *unstable*.

9.11 CRITERIA FOR PHASE STABILITY IN REGULAR SOLUTIONS

If we consider Figure 9.18, for a given temperature, it is obvious that a critical value of α / RT occurs, below which a homogeneous solution is *stable* over the entire range of composition and above which phase separation occurs. The criteria used to determine this critical value are illustrated in Figure 9.20. In Figure 9.20a–c shows how ΔG^M, $\partial \Delta G^M / \partial X_B$, $\partial^2 \Delta G^M / \partial X_B^2$, and $\partial^3 \Delta G^M / \partial X_B^3$ vary with composition for $\alpha / RT < \alpha_{\text{critical}} / RT$, $\alpha / RT = \alpha_{\text{critical}} / RT$, and $\alpha / RT > \alpha_{\text{critical}} / RT$, respectively. The critical value of α/RT is seen to be that which makes $\partial^2 \Delta G^M / \partial X_B^2$ and $\partial^3 \Delta G^M / \partial X_B^3$ simultaneously equal to zero at that composition at which immiscibility (the breakup into two phases) becomes imminent.

For a regular solution,

$$\Delta G^M = RT\left(X_A \ln X_A + X_B \ln X_B\right) + \alpha X_A X_B \tag{9.66}$$

$$\frac{\partial \Delta G^M}{\partial X_B} = RT\left[\ln \frac{X_B}{X_A}\right] + \alpha\left(1 - 2X_B\right) \tag{9.67}$$

$$\frac{\partial^2 \Delta G^M}{\partial X_B^2} = RT\left(\frac{1}{X_A} + \frac{1}{X_B}\right) - 2\alpha \tag{9.68}$$

and

$$\frac{\partial^3 \Delta G^M}{\partial X_B^3} = RT\left(\frac{1}{X_A^2} - \frac{1}{X_B^2}\right) \tag{9.69}$$

The second derivative , $\partial^2 \Delta G^M / \partial X_B^2 = 0$ at $X_A = 0.5$, equals zero when $\alpha / RT = 2$, which is thus the *critical value* of α / RT above which *phase separation* occurs Figure 9.20b.

Thus, if $\alpha / RT > 0$, the critical temperature of the *miscibility gap* is

$$T_{cr} = \frac{\alpha}{2R} \tag{9.70}$$

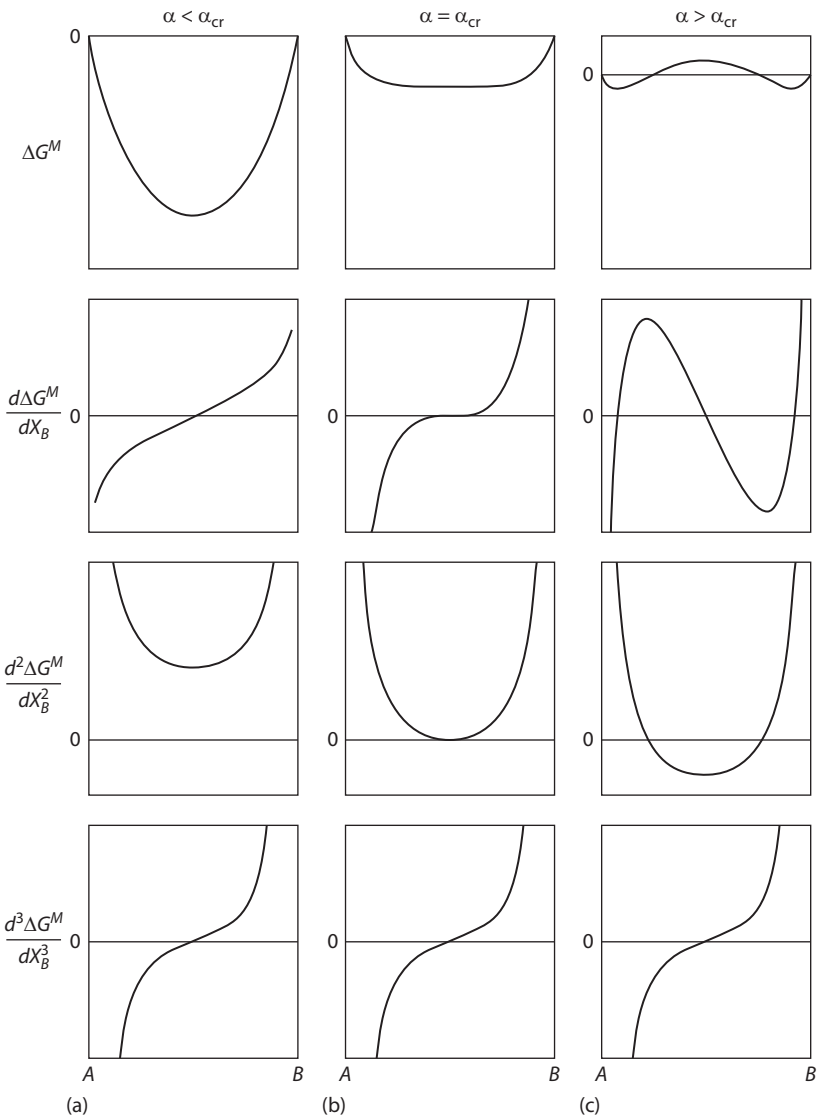

FIGURE 9.20 The effect of the magnitude of α on the first (a), second (b), and third (c) derivatives of the integral Gibbs free energy of mixing with respect to composition.

Figure 9.21a shows the variation, with temperature, of the Gibbs free energy of mixing curve for a regular solution which has a positive molar heat of mixing ($\alpha = 16{,}630\,\text{J}$) and a critical temperature of $T_{cr} = 16{,}630/2R = 1000\,\text{K}$. The Gibbs free energy of mixing expression contains a negative logarithmic term, the magnitude of which is proportional to temperature, and a positive parabolic term which is independent of temperature. At high enough temperature, the logarithmic contribution predominates and the Gibbs free energy of mixing has positive curvature at all compositions. However, with decreasing temperature, the contribution of the logarithmic term decreases, and eventually, the *positive parabolic* term predominates and produces a range of composition centered on $X_B = 0.5$, over which the Gibbs free energy curve has negative curvature. The logarithmic term still requires that the tangents to the curve at $X_A = 1$ and $X_B = 1$ be vertical.

Figure 9.21b shows the binary equilibrium phase diagram for the system, in which the miscibility curve bounding the two-phase region is simply the locus of the common tangent compositions in Figure 9.21a. The influence of temperature on the variations of the activity of component B with composition is shown in Figure 9.21c. The activities are obtained from the intercepts, with the $X_B = 1$ axis, of tangents drawn to the free energy curves as $\Delta\bar{G}_B^M = RT \ln a_B$. At T_{cr}, the activity exhibits a horizontal inflection at $X_B = 0.5$, as is seen from the following. From Equation 9.33b,

$$\Delta\bar{G}_B^M = \Delta G^M + X_A\left(\frac{\partial \Delta G^M}{\partial X_B}\right) = RT \ln a_B \tag{9.71}$$

Thus,

$$\frac{\partial \Delta\bar{G}_B^M}{\partial X_B} = X_A \frac{\partial^2 \Delta G^M}{\partial X_B^2} = \frac{RT}{a_B}\frac{\partial a_B}{\partial X_B} \tag{9.72}$$

and

$$\frac{\partial^2 \Delta\bar{G}_B^M}{\partial X_B^2} = X_A\left(\frac{\partial^3 \Delta G^M}{\partial X_B^3}\right) - \left(\frac{\partial^2 \Delta G^M}{\partial X_B^2}\right) = \frac{RT}{a_B}\frac{\partial^2 a_B}{\partial X_B^2} - \frac{RT}{a_B^2}\left(\frac{\partial a_B}{\partial X_B}\right)^2 \tag{9.73}$$

At T_{cr} and $X_B = 0.5$, both the second and third derivatives of ΔG^M with respect to X_B are zero, and thus, from Equations 9.72 and 9.73, the first and second derivatives of a_B with respect to X_B are zero, which produces a horizontal inflection point on the activity curve at $X_B = 0.5$ and T_{cr}.

For $T < T_{cr}$, the activity curve has a maximum and a minimum, which occur at the *spinodal compositions* (where $\partial^2 \Delta G^M / \partial X_B^2$ and hence $\partial a_B / \partial X_B$ are zero)—for example, the points n and p in Figure 9.19b and the points b and c on the activity curve at 800 K are shown in Figure 9.22. The portion of the curve given by ab in Figure 9.22 represents the activity of B in phase I which is supersaturated with B, and the portion of the activity curve given by cd represents the activity of B in phase II which is supersaturated with A. The value of $\partial a_B / \partial X_B$ is negative between b and c, and this violates an *intrinsic criterion for stability*, which requires that $\partial a_i / \partial X_i$ always be positive [cf. $\left(\partial P / \partial V\right)_T > 0$ over the portion JHF in Figure 8.8]. Thus, the

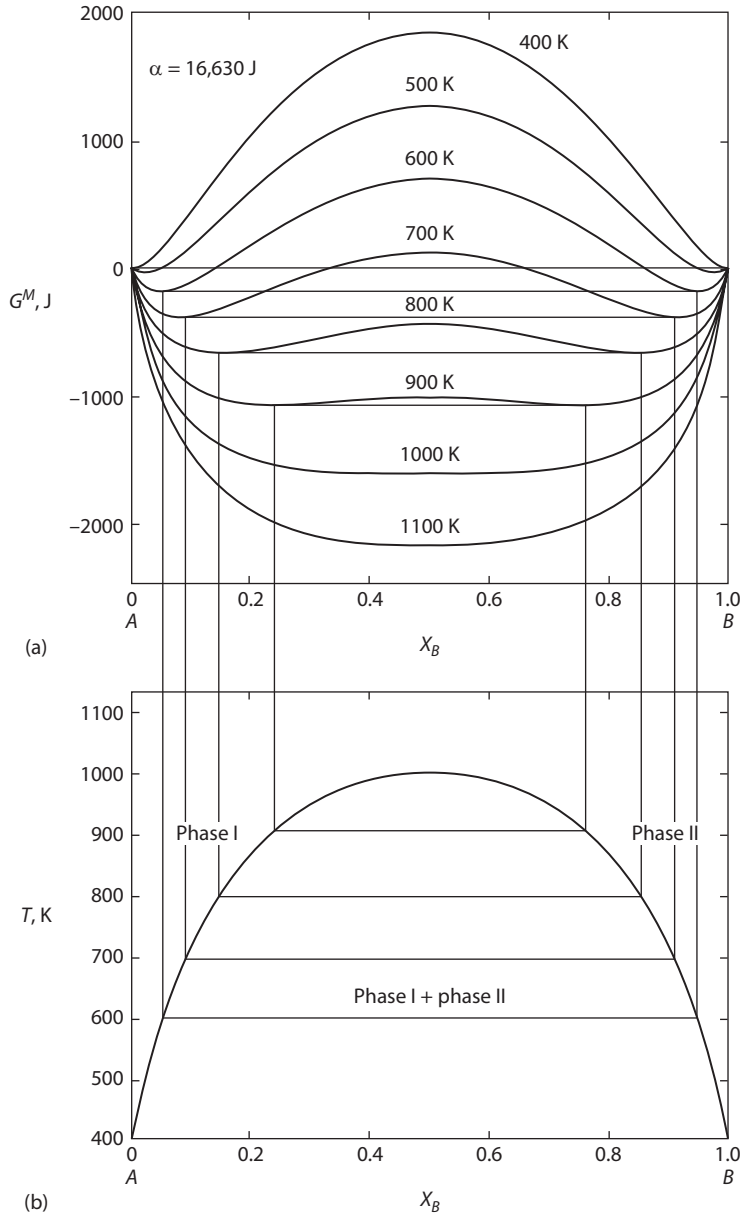

FIGURE 9.21 (a) The effect of temperature on the molar Gibbs free energy of mixing a binary regular solution for which $\alpha = 16{,}630$ J. (b) The loci of the common tangent points in (a), which generate the phase diagram for the system. (c) The activities of component *B* derived from (a).

(*Continued*)

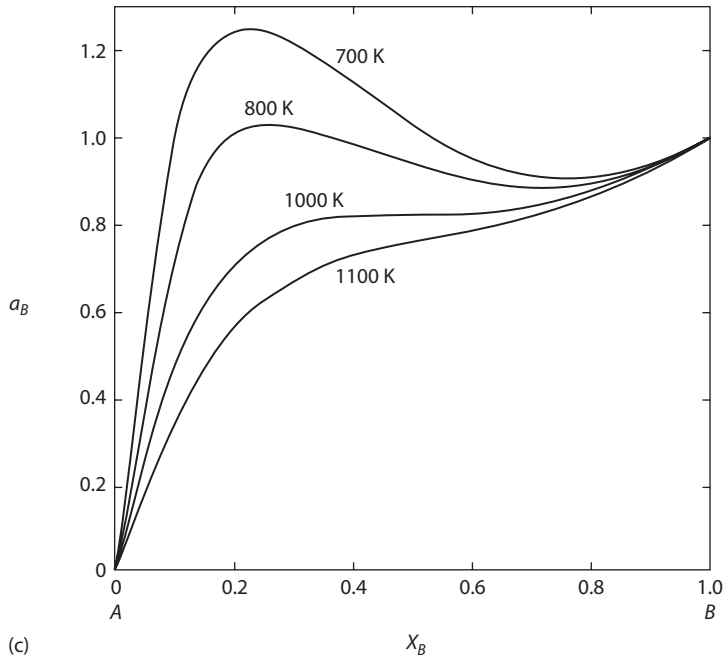

FIGURE 9.21 (*Continued*) (a) The effect of temperature on the molar Gibbs free energy of mixing a binary regular solution for which $\alpha = 16{,}630$ J. (b) The loci of the common tangent points in (a), which generate the phase diagram for the system. (c) The activities of component *B* derived from (a).

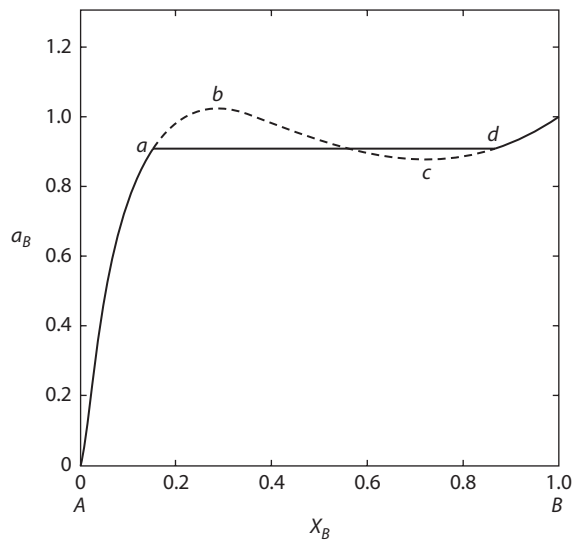

FIGURE 9.22 The activity of *B* at 800 K derived from Figure 9.21.

derived activity curve between b and c, and, consequently, the Gibbs free energy of mixing curve between the spinodal compositions, are regions of *absolute instability*. The horizontal line drawn between a and d in Figure 9.22 represents the actual constant activity of B in the equilibrium two-phase region, and the compositions a and d are those of the double tangents to the Gibbs free energy of mixing curve.

Thus, the regular solution under discussion has the following different regions of stability at 800 K (see Figure 9.22):

- $X_B = 0$ to $X_B = a$, the single-phase solution I is *stable*.
- $X_B = a$ to $X_B = d$, the stable state is a two-phase mixture of solution I and II.
- $X_B = a$ to $X_B = b$, the single-phase solution of I is *metastable* (it will decompose into solution I of composition a and solution II of composition d).
- $X_B = b$ to $X_B = c$, any homogeneous solution is absolutely *unstable*.
- $X_B = c$ to $X_B = d$, the single-phase solution of II is *metastable*.
- $X_B = d$ to $X_B = 1$, the solid solution II is the phase.

The phase diagram of a generalized regular solution with critical temperature T_{cr} can be determined as a function of temperature and composition X_B. The equation for the phase boundary of the miscibility gap known as the binodal, is given as:

$$T^{\text{Binodal}} = \left(\frac{2T_{cr}}{\ln\left(\frac{X_B}{X_A}\right)} \right)\left(X_B - X_A\right) \tag{9.74}$$

The equation for the spinodal is given as

$$T^{\text{spinodal}} = 4T_{cr}X_AX_B$$

See Qualitative Problem 2.

The phase diagram shown in Figure 9.23 is the plot of the function of Equation 9.74. Included in the plot is the locus of the spinodal curve for this binary regular solution. See Problem 9.13. The regions of stability, metastability and instability of the single phase α are denoted on the phase diagram. Compare this with Figure 8.10.

9.12 THE FLORY–HUGGINS REGULAR SOLUTION MODEL FOR APPLICATION TO POLYMERS

In 1942, Flory (Paul John Flory (1910–1985) and Huggins (Maurice Loyal Huggins, (1897–1981) independently modified the regular solution model to account for some of the differences that polymers present to the modeling of the thermodynamics of the mixing of polymers.

The main difference lies in the entropy of mixing term for polymers, which in modern notation is written as

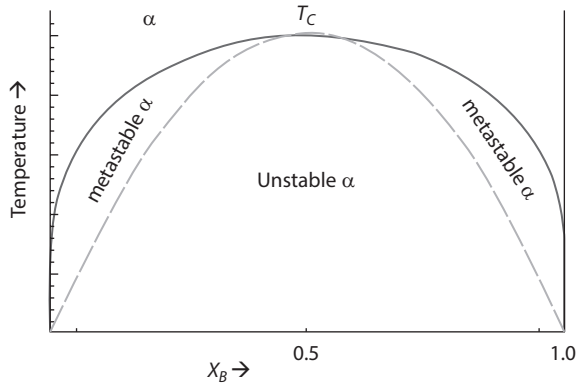

FIGURE 9.23 A regular solution phase diagram and its corresponding spinodal curve (dotted). Regions of stability, metastability and instability denoted.

$$\Delta S^{\text{mix}} = -R\left(\frac{\phi_A}{N_A}\ln\phi_A + \frac{\phi_B}{N_B}\ln\phi_B\right)$$

where ϕ_i is the volume fraction of the *i*th monomers which make up the polymer and N_i is the average number of *monomers* in the length of the molecule (the degree of polymerization). For polymers, the entity which is randomly located in the solution is not a single atom or molecule but rather a long chain consisting of the many *-mers* of the polymer. This lowers the number of ways that the polymer can be arranged in a given volume, and it is accounted for by the N_i terms in the expression for the entropy of mixing. This greatly lowers the role of entropic mixing in large polymers.

The enthalpy of mixing term was written as

$$\Delta H^{\text{mix}} = RT\phi_A\phi_B\chi$$

where χ accounts for the increase (decrease) in the enthalpy of the solution due to interactions between the polymers.

This term, combined with the entropy of mixing term, gave rise to the Gibbs free energy of mixing term[4]:

$$\Delta G^{\text{mix}} = RT\left(\frac{\phi_A}{N_A}\ln\phi_A + \frac{\phi_B}{N_B}\ln\phi_B + \phi_A\phi_B\chi\right)$$

It can be seen for polymers of long length (N_i large), the entropy of mixing term is not as large as that for solutions of single atoms or small molecules. Since most polymers have positive enthalpies of mixing, this accounts for the limited miscibility of many polymers.

[4] The regular solution "constant" in the Flory–Huggins model is thus $RT\chi$.

The expression shows that if one of the polymers is not very long, it can act as the solvent and the long-chained polymer as the solute (a polymer blend). This enables much more miscibility for the polymer solutions, as the entropy term becomes more significant to the polymer thermodynamics.

9.13 SUMMARY

1. Raoult's law is $p_i = X_i p_i^\circ$, and a component of a solution that conforms with this law is said to exhibit Raoultian behavior. In all solutions, the behavior of the component i approaches Raoult's law as $X_i \to 1$.
2. Henry's law is $p_i = k' X_i$, and a component of a solution that conforms with this equation is said to exhibit Henrian behavior. In all solutions, the behavior of the component i approaches Henry's law as $X_i \to 0$. In a binary solution, Henry's law is obeyed by the solute in that composition range over which Raoult's law is obeyed by the solvent.
3. The activity of the component i in a solution, with respect to a given standard state, is the ratio of the vapor pressure (strictly, the fugacity) of i exerted by the solution to the vapor pressure (the fugacity) of i in the given standard state. If the standard state is chosen as being pure i, then $a_i = p_i / p_i^\circ$. An activity is thus a ratio, and its introduction effects a normalization of the vapor pressure exerted by the component i in the solution. In terms of activity, Raoult's law is $a_i = X_i$, and Henry's law is $a_i = k^I, {}^B X_i$.
4. The difference between the value of an extensive thermodynamic property per mole of i in a solution and the value of the property per mole of i in its standard state is called the partial molar property change of i for the solution process; that is, if Q is any extensive thermodynamic property, the change in the property due to the solution of 1 mole of i is $\Delta\bar{Q}_i^M = \bar{Q}_i - Q_i^\circ$. In the case of the Gibbs free energy, $\Delta\bar{G}_i^M = \bar{G}_i - G_i^\circ$. This difference in the molar Gibbs free energy is related to the activity of i in solution, with respect to the standard state, as $\Delta\bar{G}_i^M = RT \ln a$, and $\Delta\bar{G}_i^M$ is called the partial molar Gibbs free energy of solution of i.

   The change in the Gibbs free energy accompanying the formation of 1 mole of solution from the pure components i (called the integral Gibbs free energy change) is $\Delta G^M = \sum_i X_i \Delta\bar{G}_i^M$, so that, for the binary A–B, $\Delta G^M = X_A \Delta\bar{G}_A^M + X_B \Delta\bar{G}_B^M$. Since $\Delta\bar{G}_A^M = RT \ln a_A$, then

$$\Delta G^M = RT\left(X_A \ln a_A + X_B \ln a_B\right)$$

   In a Raoultian solution, since $a_i = X_i$, then

$$\Delta G^M = RT\left(X_A \ln X_A + X_B \ln X_B\right)$$

   For any general extensive thermodynamic property, Q,

$$\Delta Q^M = \sum_i X_i \Delta\bar{Q}_i^M$$

5. An ideal solution has the following properties:

$$a_i = X_i$$

$\bar{V}_i = V_i^\circ$ (i.e., there is no change in volume when the components are mixed)
$\bar{H}_i^M = H_i^\circ$ (i.e., there is zero heat of mixing)
$\Delta G^{M,\text{id}} = RT\left(X_A \ln X_A + X_B \ln X_B\right)$
Since $\Delta S^{M,\text{id}} = -(\partial \Delta G^{M,\text{Bid}}/\partial T)$, $\Delta S^{M,\text{id}} = -\text{R}\sum X_i \ln X_i$, in an ideal solution, $\Delta \bar{S}_i^M = -R \ln X_i$. $\Delta S^{M,\text{id}}$ is thus independent of temperature and is simply an expression for the maximum number of spatial configurations available to the system.

6. The thermodynamic behavior of non-Raoultian solutions is dealt with by introducing the activity coefficient, γ, which for the component *i* is defined as $\gamma_i = a_i / X_i$. The coefficient γ_i, which can have values of greater or less than unity, thus quantifies the deviation of *i* from Raoultian behavior. Since $\ln a_i = \ln X_i + \ln \gamma_i$,

$$\frac{d \ln a_i}{d\left(\frac{1}{T}\right)} = \frac{\Delta \bar{H}_i^M}{R} = \frac{d \ln \gamma_i}{d\left(\frac{1}{T}\right)}$$

Thus, if $d\gamma_i / dT$ is positive, $\Delta \bar{H}_i^M$ is negative, and if $d\gamma_i / dT$ is negative, $\Delta \bar{H}_i^M$ is positive. The magnitude of the heat of formation of a nonideal solution is determined by the magnitudes of the deviations of the components of the solution from ideal behavior. Nonideal components approach Raoultian behavior with increasing temperature. Thus, if $\gamma_i < 1$, then $d\gamma_i / dT$ is positive, and if $\gamma_i > 1$, $d\gamma_i / dT$ is negative. Solutions, the components of which exhibit negative deviations from Raoult's law, form exothermically; that is, $\Delta H^M < 0$, and those that exhibit positive deviations form endothermically.

7. The Gibbs–Duhem relationship is $\sum_i X_i d\bar{Q}_i = 0$ at constant temperature and pressure, where $\bar{Q}_i$ is the partial molar value of the extensive thermodynamic function *Q* of the solution component *i*. The excess value of an extensive thermodynamic property of a solution is the difference between the actual value and the value that the property would have if the components obeyed Raoult's law. Thus, for the general function *Q*, $Q^{\text{XS}} = Q - Q^{\text{id}}$, or for the Gibbs free energy, $G^{\text{XS}} = G - G^{\text{id}}$, or $G^{\text{XS}} = \Delta G^M - \Delta G^{M,\text{id}}$. Since $\gamma_i = a_i / X_i$, then

$$G^{\text{XS}} = RT \sum X_i \ln \gamma_i$$

8. A regular solution is one which has an ideal entropy of formation and a non-zero heat of formation from its pure components. The activity coefficients of the components of a regular binary solution are given by the expression

$$RT \ln \gamma_i = \alpha(1 - X_i)^2$$

where α is a temperature-independent constant, the value of which is characteristic of the particular solution. Thus, $\ln \gamma_i$ varies inversely with temperature, and, since $\bar{G}_i^{XS} = RT \ln \gamma_i$, then $\bar{G}_i^{XS} = \Delta \bar{H}_i^M$ is independent of temperature. Furthermore, the heat of formation of a regular solution, being equal to G^{XS}, is a parabolic function of composition, given by

$$\Delta H^M = G^{XS} = \alpha X_A X_B$$

9. Immiscibility becomes imminent in a regular solution at the critical value of $\alpha = 2$. The critical temperature, below which immiscibility occurs in a regular system, is given by $T_{cr} = \alpha/2R$.
10. The equations for the miscibility gap (binodal) and the spinodal curves of a regular solution are:

$$T^{\text{Binodal}} = \left(\frac{2T_{cr}}{\ln\left(\frac{X_B}{X_A}\right)} \right)(X_B - X_A) \quad \text{and} \quad T^{\text{spinodal}} = 4T_{cr} X_A X_B$$

11. Polymer solutions can be modelled as regular solutions with a different equation,

$$\Delta G^{\text{mix}} = RT\left(\frac{\phi_A}{N_A} \ln \phi_A + \frac{\phi_B}{N_B} \ln \phi_B + \phi_A \phi_A \chi \right)$$

where ϕ_i is the volume fraction of the ith monomers which make up the polymer and N_i is the average number of *monomers* in the length of the molecule (the degree of polymerization).

9.14 CONCEPTS AND TERMS INTRODUCED IN THIS CHAPTER

The reader should write out brief definitions or descriptions of the following terms. Where appropriate, equations may be used.

Activation energy
Activity
Activity coefficient
Binodal curve

Bond energy
Chemical potential
Condensation/sublimation
Condensed phases
Deviations from ideality
Dynamic equilibrium
Endothermic
Energy barrier
Evaporation
Exothermic
Flory–Huggins regular solution model
Gibbs free energy of mixing (solution)
Henry's law
Ideal solution
Interactions among particles
Nonideal solution
Phase separation
Polymer
Raoult's law
Regular solution
Saturated Solution
Solution Thermodynamics
Spinodal curve
Stable, metastable, unstable solution

9.15 QUALITATIVE EXAMPLE PROBLEMS

QUALITATIVE PROBLEM 1

The activities of liquid iron-nickel solutions at 1600°C as a function of composition are shown in Figure 9.8. Sketch the activity coefficients as a function of composition at this temperature.

SOLUTION TO QUALITATIVE PROBLEM 1

Figure 9.24 shows the actual plot of the activity coefficients γ_{Fe} and γ_{Ni} as a function of composition. Your plot should show the following:

1. γ_{Fe} starts at $\gamma_{Fe} = 1$ and drops off after Henrys' law no longer holds ($\sim X_{Fe} = 0.7$).
2. γ_{Ni} starts at less than one and begins to rise and approach one after $\sim X_{Ni} = 0.3$).
3. $\gamma_{Fe} = 1$ at pure Fe and $\gamma_{Ni} =$ one at pure Ni.

QUALITATIVE PROBLEM 2

Derive the equation for the phase boundary

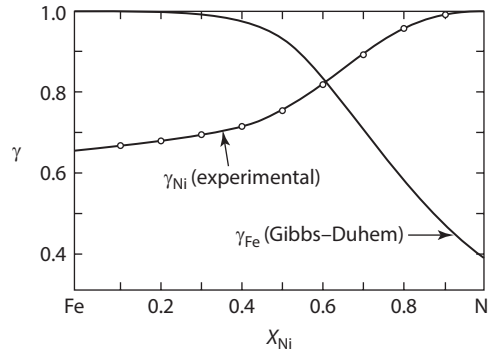

FIGURE 9.24 Activity coefficients in the liquid system iron–nickel at 1600°C (also see Figure 9.8).

$$T^{\text{Binodal}} = \left(\frac{2T_{\text{cr}}}{\ln\left(\frac{X_B}{X_A}\right)} \right)(X_B - X_A)$$

of the miscibility gap (the binodal) of a regular solution in the form $T = T(T_C, X_B)$ starting from Equation 9.67.

SOLUTION TO QUALITATIVE PROBLEM 2

$$\frac{\partial \Delta G^M}{X_B} = RT \ln\left(\frac{X_B}{X_A}\right) + \alpha(1 - 2X_B)$$

Setting this equation equal to zero gives us its extreme values

which will be the Binodal values.

$$RT \ln\left(\frac{X_B}{X_A}\right) = \alpha(2X_B - 1)$$

But : $\alpha = 2RT_{\text{cr}}$

$$\therefore RT \ln\left(\frac{X_B}{X_A}\right) = 2RT_{cr}(2X_B - 1)$$

also $2X_B - 1 = 2X_B - (X_A + X_B) = (X_B - X_A)$

Finally $T^{\text{Binodal}} = \dfrac{2T_{\text{cr}}}{\ln\left(\frac{X_B}{X_A}\right)}(X_B - X_A)$

9.16 QUANTITATIVE EXAMPLE PROBLEMS

QUANTITATIVE PROBLEM 1

Copper and gold form the complete range of solid solution at temperatures between 410°C and 889°C, and, at 600°C, the excess molar Gibbs free energy of formation of the solid solutions is given by

$$G^{XS} = -28,280 X_{Au} X_{Cu} \text{ J}$$

Calculate the partial pressures of Au and Cu exerted by the solid solution of $X_{Cu} = 0.6$ at 600°C.

The saturated vapor pressure of solid copper is given by

$$\ln p^{\circ}_{Cu}(\text{atm}) = -\frac{40,920}{T} - 0.86 \ln T + 21.67$$

and the saturated vapor pressure of solid gold is given by

$$\ln p^{\circ}_{Au}(\text{atm}) = -\frac{44,538}{T} - 0.7479 \ln T + 10.81$$

SOLUTION TO QUANTITATIVE PROBLEM 1

The solid solutions are regular with $\alpha = -28,280$ J. Therefore, from Equation 9.63,

$$\ln \gamma_{Cu} = \frac{\alpha}{RT} X^2_{Au} = -\frac{28,280 \times 0.4^2}{8.3144 \times 873} = -0.624$$

Thus,

$$\gamma_{Cu} = 0.536 \quad \text{and} \quad a_{Cu} = \gamma_{Cu} X_{Cu} = 0.536 \times 0.6 = 0.322$$

Similarly,

$$\ln \gamma_{Au} = \frac{28,280 \times 0.6^2}{8.3144 \times 873} = -1.403$$

Thus,

$$\gamma_{Au} = 0.246 \quad \text{and} \quad a_{Au} = 0.246 \times 0.4 = 0.098$$

Therefore, at 873 K,

$$p^{\circ}_{Cu} = 3.35 \times 10^{-14} \text{ atm}$$

and

$$p^{\circ}_{Au} = 1.46 \times 10^{-15} \text{ atm}$$

From Equation 9.12, $a_i = p_i / p_i^\circ$, and thus, the partial pressures exerted by the alloy are

$$p_{\mathrm{Cu}} = 0.322 \times 3.35 \times 10^{-14} = 1.08 \times 10^{-14} \text{ atm}$$

and

$$p_{\mathrm{Au}} = 0.098 \times 1.46 \times 10^{-15} = 1.43 \times 10^{-16} \text{ atm}$$

QUANTITATIVE PROBLEM 2

At 700 K, the activity of Ga in a liquid Ga–Cd solution of composition $X_{\mathrm{Ga}} = 0.5$ has the value 0.79. On the assumption that liquid solutions of Ga and Cd exhibit regular solution behavior, estimate the energy of the Ga–Cd bond in the solution. The molar enthalpies of evaporation of liquid Ga and liquid Cd at their melting temperatures are, respectively, 270,000 and 100,000 J.

At their melting temperatures, the coordination numbers of liquid Cd and liquid Ga are, respectively, 8 and 11. It will thus be assumed that the coordination number in the 50:50 solution is the average of 8 and 11—namely, 9.5.

SOLUTION TO QUANTITATIVE PROBLEM 2

With $a_{\mathrm{Ga}} = 0.79$ at $X_{\mathrm{Ga}} = 0.5$,

$$\gamma_{\mathrm{Ga}} = \frac{a_{\mathrm{Ga}}}{X_{\mathrm{Ga}}} = \frac{0.79}{0.5} = 1.59$$

Therefore, from Equation 9.63,

$$\ln 1.59 = \frac{\alpha \times 0.5^2}{8.3144 \times 700}$$

which gives

$$\alpha = \frac{0.464 \times 8.3144 \times 700}{0.5^2} = 10,795 \text{ J}$$

The bond energy, $E_{\mathrm{Ga–Ga}}$, is obtained from the molar enthalpy of evaporation, ΔH_{evap}, according to

$$\Delta H_{\mathrm{evap,Ga-Ga}} = -\frac{1}{2} z N_{\mathrm{O}} E_{\mathrm{Ga-Ga}}$$

The negative sign is required to conform with the convention that bond energies are negative quantities. Thus,

$$E_{\text{Ga–Ga}} = -\frac{270,000 \times 2}{11 \times 6.023 \times 10^{23}} = -8.15 \times 10^{-20}\,\text{J}$$

and similarly,

$$E_{\text{Cd–Cd}} = -\frac{100,000 \times 2}{8 \times 6.023 \times 10^{23}} = -4.15 \times 10^{-20}\ \text{J}$$

The bond energy, $E_{\text{Cd–Ga}}$, is obtained from

$$\alpha = zN_{\text{O}}\left[E_{\text{Cd-Ga}} - \frac{1}{2}\left(E_{\text{Cd-Cd}} + E_{\text{Ga-Ga}}\right)\right]$$

That is,

$$10,795 = 9.5 \times 6.023 \times 10^{23}\left[E_{\text{Cd-Ga}} - \frac{1}{2}\left(-4.15 \times 10^{-20} - 8.15 \times 10^{-20}\right)\right]$$

Thus, $E_{\text{Cd–Ga}} = -5.96 \times 10^{-20}\,\text{J}$.

PROBLEMS

For some of these problems, the tables in the Appendix A may be needed.

9.1 One mole of solid Cr_2O_3 at 2500 K is dissolved in a large volume of a liquid Raoultian solution of Al_2O_3 and Cr_2O_3, in which $X_{Cr_2O_3} = 0.2$ and which is also at 2500 K. Calculate the changes in enthalpy and entropy caused by the addition. The normal melting temperature of Cr_2O_3 is 2538 K, and it can be assumed that $\Delta S_{m,Al_2O_3} = \Delta S_{m,Cr_2O_3}$.

9.2 When 1 mole of argon gas is bubbled through a large volume of an Fe–Mn melt of $X_{\text{Mn}} = 0.5$ at 1863 K, the evaporation of Mn into the Ar causes the mass of the melt to decrease by 1.5 g. The gas leaves the melt at a pressure of 1 atm. Calculate the activity coefficient of Mn in the liquid alloy.

9.3 The variation, with composition, of G^{XS} for liquid Fe–Mn alloys at 1863 K is as follows:

X_{Mn}	0.1	0.2	0.3	0.4	0.5	0.6	0.7	0.8	0.9
G^{XS} J	395	703	925	1054	1100	1054	925	703	395

a. Does the system exhibit regular solution behavior?
b. Calculate $\bar{G}_{\text{Fe}}^{\text{XS}}$ and $\bar{G}_{\text{Mn}}^{\text{XS}}$ at $X_{\text{Mn}} = 0.6$.
c. Calculate ΔG^M at $X_{\text{Mn}} = 0.4$.
d. Calculate the partial pressures of Mn and Fe exerted by the alloy of $X_{\text{Mn}} = 0.2$.

9.4 Calculate the heat required to form a liquid solution at 1356 K, starting with 1 mole of Cu and 1 mole of Ag at 298 K. At 1356 K, the molar heat of mixing of liquid Cu and liquid Ag is given by $\Delta H^M = -20{,}590 X_{Cu} X_{Ag}$.

9.5 Melts in the system Pb–Sn exhibit regular solution behavior. At 473°C, $a_{Pb} = 0.055$ in a liquid solution of $X_{Pb} = 0.1$. Calculate the value of α for the system and calculate the activity of Sn in the liquid solution of $X_{Sn} = 0.5$ at 500°C.

9.6

a. Calculate the values of $\Delta\overline{G}_B$ and a_B for an alloy of $X_B = 0.5$ at 1000 K, assuming the solution is ideal.

b. Calculate the values of $\Delta\overline{G}_B$ and a_B for an alloy of $X_B = 0.5$ at 1000 K that is a regular solution with $\Delta H_{mixing} = 16{,}628\ \text{J} \cdot X_A \cdot X_B$.

9.7 A regular solution exhibits a miscibility gap. Sketch the activity of B vs. X_B at a temperature within the miscibility gap.

Denote regions where Henry's law is obeyed and where Raoult's law is obeyed if applicable.

9.8 Tin obeys Henry's law in dilute liquid solutions of Sn and Cd, and the Henrian activity coefficient of Sn, γ°_{Sn}, varies with temperature as

$$\ln \gamma^{\circ}_{Sn} = -\frac{840}{T} + 1.58$$

Calculate the change in temperature when 1 mole of liquid Sn and 99 moles of liquid Cd are mixed in an adiabatic enclosure. The molar constant-pressure heat capacity of the alloy formed is 29.5 J/K.

9.9 Use the Gibbs–Duhem equation to show that, if the activity coefficients of the components of a binary solution can be expressed as

$$\ln \gamma_A = \alpha_1 X_B + \frac{1}{2}\alpha_2 X_B^2 + \frac{1}{3}\alpha_3 X_B^3 + \cdots$$

and

$$\ln \gamma_B = \beta_1 X_A + \frac{1}{2}\beta_2 X_A^2 + \frac{1}{3}\beta_3 X_A^3 + \cdots$$

over the entire range of composition, then $\alpha_1 = \beta_1 = 0$, and that, if the variation can be represented by the quadratic terms alone, then $\alpha_2 = \beta_2$.

9.10 The activity coefficient of Zn in liquid Zn–Cd alloys at 435°C can be represented as

$$\ln \gamma_{Zn} = 0.875 X_{Cd}^2 - 0.30 X_{Cd}^3$$

Derive the corresponding expression for the dependence of $\ln \gamma_{Cd}$ on composition and calculate the activity of cadmium in the alloy of $X_{Cd} = 0.5$ at 435°C.

9.11 The molar excess Gibbs free energy of formation of solid solutions in the system Au–Ni can be represented by

$$G^{XS} = X_{Ni}X_{Au}\left(24{,}140X_{Au} + 38{,}280X_{Ni} - 14{,}230X_{Au}X_{Ni}\right)\left(1 - \frac{T}{2660}\right)\text{J}$$

Calculate the activities of Au and Ni in the alloy of $X_{Au} = 0.5$ at 1100 K.

9.12 The activities of liquid iron–copper solutions at 1550°C as a function of composition are shown in Figure 9.9. Sketch the activity coefficients as a function of composition at this temperature.

9.13* Derive the equation for the spinodal curve of the miscibility gap of a regular solution, in the form $T_S = T_S(T_C, X_B)$ starting from Equation 9.68.

9.14 It has been found that in a certain solution, the activity $a_A = X_A$ over a certain range of composition. Determine the relationship between a_B and X_B over the same range of composition.

9.15 All regular solutions with positive heats of mixing have the same value of the activity of its components (*A* or *B*) at the critical point of the miscibility gap.

a. Calculate this activity.

b. Plot temperature versus a_B for a regular solution miscibility gap.

9.16 At a certain temperature, *T*, the *A*–*B* system exhibits regular solution behavior. The activity coefficient of *A* is given by

$$\ln\left(\gamma_A\right) = -b\left(1 - X_A\right)^2$$

where *b* is a constant at the given *T*.

Compute the corresponding equation for the variation of γ_B with composition at the same temperature. Be sure to state the justification for the steps of your solution.

9.17* Determine the value of the slopes of the miscibility gap of a regular solution at $T = 0$ on both sides of the phase diagram.

9.18* Determine the value of the slopes of the spinodal curves of a regular solution at $T = 0$ on both sides of the phase diagram. See Problem 9.13*

9.19* Determine the ratio of Y_2/Y_1 of the segments shown in Figure 9.25.

9.20 The free energy of mixing of a regular solution is given by:

$$\Delta G_{mix} = a_0 X_A X_B + RT\left(X_A \ln X_A + X_B \ln X_B\right)$$

$$\text{and} \quad a_0 = 24{,}943 \text{ Joules/mole}$$

a. Plot ΔG_{mix} vs. X_B at 1400, 1500 and 1600 K.

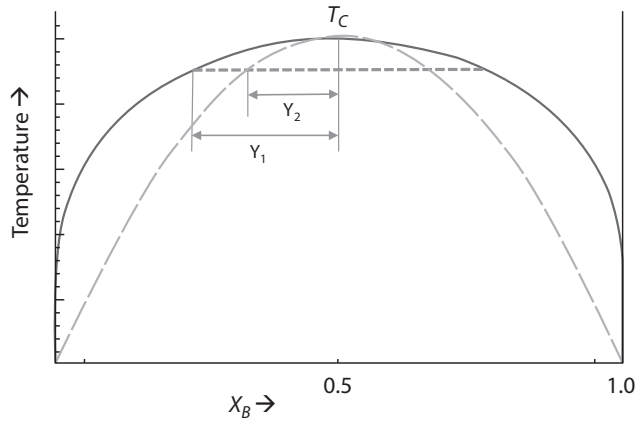

FIGURE 9.25 The figure for Problem 9.19, showing the segments whose ratio, Y_2/Y_1, is to be determined.

b. Plot $\dfrac{\partial \Delta G_{\text{mix}}}{\partial X_B}$ vs. X_B at the same temperatures as (a).

c. Determine the critical temperature for this alloy. Show work.

* New problem in this edition.

10 Gibbs Free Energy Composition and Phase Diagrams of Binary Systems

10.1 INTRODUCTION

It was shown in Chapter 7 that when temperature and pressure are the independent variables of a one-component system, the phase(s) with the lowest Gibbs free energy is (are) the stable phase(s). Likewise, in a two-component (binary) system at constant temperature and pressure, the stable state of existence at each composition of a system is that which has the lowest possible value of Gibbs free energy. This was discussed in detail in Chapter 9 for the regular solution model with positive α. Thus, phase stability, in a system presented on an *isobaric* temperature *versus* composition binary phase diagram, can be determined from knowledge of the variations of the Gibbs free energies of the various possible phases with composition and temperature.

When a binary liquid solution is cooled, a *liquidus temperature* is eventually reached, at which point a solid phase begins to separate from the liquid solution. This solid phase could be a virtually pure component, a solid solution of the same or different composition from the liquid, a chemical compound formed by a reaction between two or more of the components, or an atomically ordered solution phase. In each of these cases, the composition of the solid phase which is in equilibrium with the liquid solution is that which minimizes the Gibbs free energy of the system. If liquid solutions are stable over the entire range of composition, then the Gibbs free energies of the liquid states are lower than those of any possible solid-state phase. Conversely, if the temperature of the system is lower than the lowest *solidus* temperature, then the Gibbs free energies of the solid states are everywhere lower than those of liquid-state phases. At intermediate temperatures, the variation of Gibbs free energy with composition will consist of ranges of composition over which liquid states are stable, ranges over which solid states are stable, and intermediate ranges in which solid and liquid phases coexist in equilibrium with one another. Thus, there must exist a quantitative correspondence between Gibbs free energy–composition diagrams and the equilibrium temperature-composition phase diagrams by virtue of the following facts:

1. The state of lowest Gibbs free energy is the stable state.
2. When phases coexist in equilibrium, the *partial molar Gibbs free energy* of component i, $\overline{G}_i$, (that is, the *chemical potential of i*) has the same value in all of the coexisting phases.

This correspondence is examined in this chapter, in which it will be seen that isobaric temperature–composition phase diagrams are generated by, and are representations of, isobaric Gibbs free energy–composition–temperature diagrams.

10.2 GIBBS FREE ENERGY AND THERMODYNAMIC ACTIVITY

The Gibbs free energy of mixing of the components A and B to form a mole of solution is given by Equation 9.32,

$$\Delta G^M = RT\left(X_A \ln a_A + X_B \ln a_B\right)$$

where ΔG^M is the difference between the Gibbs free energy of a mole of the homogeneous solution and the Gibbs free energy of the corresponding numbers of moles of the unmixed components. Since only changes in Gibbs free energy can be measured, the Gibbs free energies of the pure unmixed components are assigned the value of zero. If the solution is ideal (i.e., if $a_i = X_i$), then the molar ideal Gibbs free energy of mixing is given by Equation 9.34

$$\Delta G^{M,\mathrm{id}} = RT\left(X_A \ln X_A + X_B \ln X_B\right)$$

and has the characteristic shape shown, at the temperature T, as curve I in Figure 10.1. Since $\Delta H^{M,\mathrm{id}} = 0$, then $\Delta G^{M,\mathrm{id}} = -T\Delta S^{M,\mathrm{id}}$. The curve I in Figure 10.1 is obtained by inverting the ideal entropy of mixing curve (Figure 9.7) and multiplying it by the temperature in question. It is thus seen that the *shape* of the variation of $\Delta G^{M,\mathrm{id}}$ with composition depends only on the temperature of the solution.

If the solution exhibits a small positive deviation from ideal mixing (i.e., if $\gamma_i > 1$ and $a_i > X_i$), then, at the temperature T, the Gibbs free energy of mixing curve is typically as shown by curve II in Figure 10.1, that is, the curve is displaced upward in the figure.

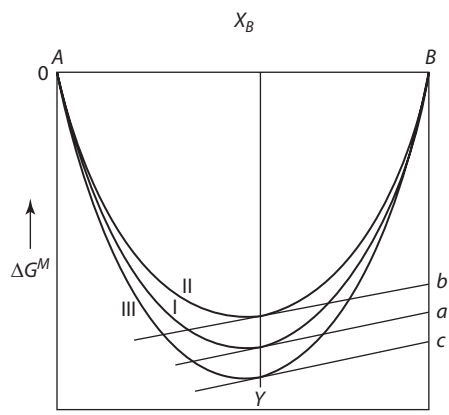

FIGURE 10.1 The molar Gibbs free energies of mixing in binary systems exhibiting ideal behavior (I), positive deviation from ideal behavior (II), and negative deviation from ideal behavior (III).

If the solution shows a slight negative deviation from ideal mixing (i.e., if $\gamma_i < 1$ and $a_i < X_i$), the Gibbs free energy of mixing curve is typically as shown by curve III in Figure 10.1, it is displaced downward in the figure. From the discussion of Equation 9.33a and b the tangent drawn to the ΔG^M curve at any composition intersects the $X_A = 1$ and $X_B = 1$ axes at $\Delta\bar{G}_A^M$ and $\Delta\bar{G}_B^M$, respectively. Also, since $\Delta\bar{G}_i^M = RT \ln a_i$, there is a relationship between the ΔG^M –composition and the activity–composition plots.

In Figure 10.1, at the composition *Y, which is slightly larger than 50% B*, tangents drawn to curves I, II, and III intersect the $X_B = 1$ axis at *a*, *b*, and *c*, respectively. Thus,

$$Bb = \Delta\bar{G}_B^M = RT \ln a_B \left(\text{in solution II}\right) < Ba = \Delta\bar{G}_B^M = RT \ln X_B$$

$$< Bc = \Delta\bar{G}_B^M = RT \ln a_B \left(\text{in solution III}\right)$$

from which it is seen that

$$\gamma_B \text{ in solution II} > \gamma_B \text{ in solution I} > \gamma_B \text{ in solution III}$$

The variation, with composition, of the tangential intercepts generates the variations of *activity* with composition shown in Figure 10.2. It can be seen from Figure 10.2 that solutions II and III follow Henry's law for $X_B \to 0$ and Raoult's law for $X_B \to 1$.

As $X_i \to 0$, the tangent to $\Delta G^M \to -\infty$ and the tangential intercept $\Delta\bar{G}_i^M = RT \ln a_i \to -\infty$ (see Figure 10.1). The Gibbs free energy of mixing curves has vertical tangents at their extremities, indicating that the first atom of *B* added to pure *A* (and the first atom of *A* added to pure *B*) *decreases* the Gibbs free energy! This also can be seen from the ideal entropy of the mixing curve in Figure 9.7, which by virtue of being logarithmic, has vertical tangents at its extremities. This thermodynamic principle thus implies that pure elemental components are highly unlikely in these solutions for $T > 0$ K.

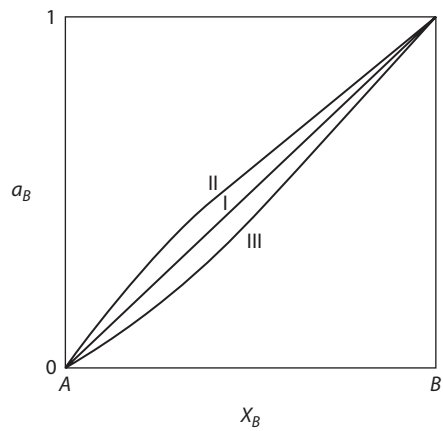

FIGURE 10.2 The activities of component *B* obtained from lines I, II, and III in Figure 10.1. Solution II exhibits positive deviation from ideality, and solution III exhibits negative deviation from ideality.

10.3 LIQUID AND SOLID STANDARD STATES

The choice of the standard state of a component of a condensed system is often that of the pure component in its stable state at the particular temperature and pressure of interest. At 1 atm pressure (the pressure normally considered), the stable state is determined by whether or not the temperature of interest is above or below the normal melting temperature of the component. It is often assumed that the temperature of interest is either above or below the melting temperatures of both components. An activity *versus* composition curve could be drawn for liquid immiscibility, in which case the standard states are the two pure liquids, or it could be drawn for solid immiscibility, in which case the standard states are the two pure solids. Since the standard state of a component is simply a reference state with which the component in any other state is compared, it follows that any state can be chosen as the standard state, and the choice is normally made purely on the *basis of convenience*.

10.3.1 Analysis of the Development of Solidus and Liquidus Curves for Ideal Solutions

Consider the isobaric binary system A–B at the temperature T, which is below the melting temperature of B, $T_{m(B)}$, and above the melting temperature of A, $T_{m(A)}$. Consider, further, that this system forms *Raoultian ideal liquid* solutions and *Raoultian ideal solid* solutions. The phase diagram for the system is shown in Figure 10.3a. Figure 10.3b shows the two Gibbs free energy of mixing curves at the temperature of interest. Curve I is drawn for liquid solutions and curve II is drawn for solid solutions. At the temperature T, the stable states of pure A and B are located at $\Delta G^M = 0$, with pure liquid A located at $X_A = 1$ (the point a) and pure solid B located at $X_B = 1$ (the point b). The point c represents the molar Gibbs free energy of solid A relative to that of liquid A at the temperature T, and $T > T_{m(A)}$. Thus, $G^\circ_{A(s)} - G^\circ_{A(l)}$ is a positive quantity which is equal to the negative of the molar Gibbs free energy of *melting* of A at the temperature T. That is,

$$G^\circ_{A(s)} - G^\circ_{A(l)} = -\Delta G^\circ_{m(A)} = -\left(\Delta H^\circ_{m(A)} - T\Delta S^\circ_{m(A)}\right)$$

and if $c_{p,\,A(s)} = c_{p,\,A(l)}$ (i.e., if $\Delta H^\circ_{m(A)}$ and $\Delta S^\circ_{m(A)}$ are *independent of temperature*), then

$$\Delta G^\circ_{m(A)} = \Delta H^\circ_{m(A)}\left(\frac{T_{m(A)} - T}{T_{m(A)}}\right) \tag{10.1}$$

As the temperature decreases and approaches the melting point of A, $\Delta G^\circ_{m(A)}$ (T) approaches zero.

Similarly, point d in Figure 10.3 represents the molar Gibbs free energy of liquid B relative to that of solid B at the temperature T, and, since $T < T_{m(B)}$, then $G^\circ_{B(l)} - G^\circ_{B(s)}$ is a positive quantity equal to $\Delta G^\circ_{m(B)}$.

The line in Figure 10.3b joining a and d represents the Gibbs free energy of unmixed liquid A and liquid B relative to that of the standard state of unmixed

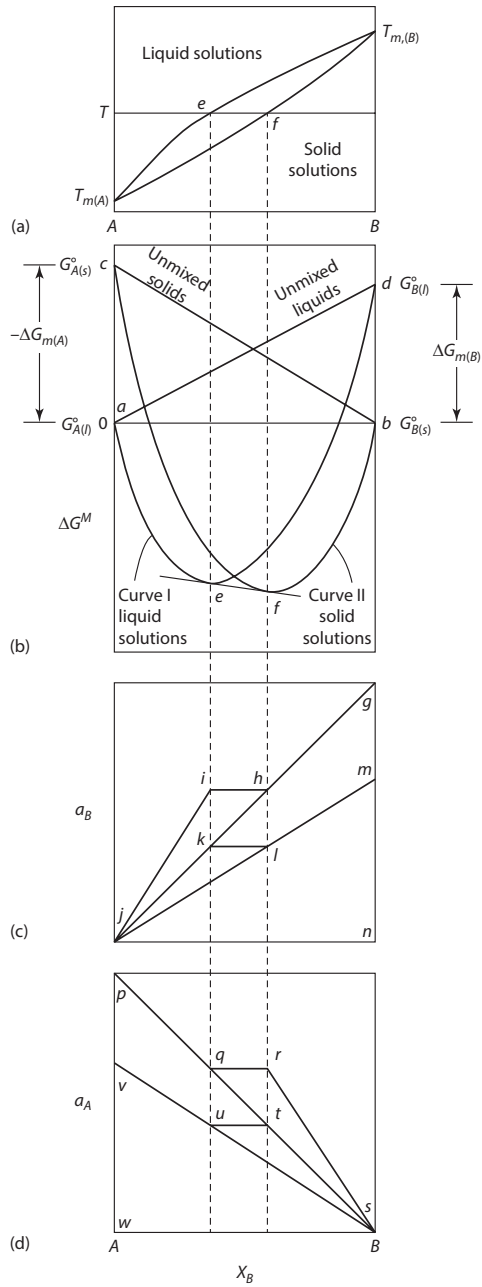

FIGURE 10.3 (a) The lens phase diagram for the system *A*–*B*. (b) The Gibbs free energies of mixing in the system *A*–*B* at the temperature *T*. (c) The activities of *B* at the temperature *T* and comparison of the solid and liquid standard states. (d) The activities of *A* at the temperature *T* and comparison of the solid and liquid standard states.

liquid *A* and solid *B*, and the line joining *c* and *b* represents the Gibbs free energy of unmixed solid *A* and solid *B* relative to that of the standard state. The line *cb* can be represented by the equation

$$\Delta G = -X_A \Delta G^{\circ}_{m(A)}$$

and the equation for the line *ad* is

$$\Delta G = X_B \Delta G^{\circ}_{m(B)}$$

At any composition, the formation of a homogeneous liquid solution from pure liquid *A* and pure solid *B* can be considered as being a two-step process involving

1. The melting of X_B moles of *B*, which involves the change in Gibbs free energy

$$\Delta G = X_B \Delta G^{\circ}_{m(B)}$$

2. The mixing of X_B moles of liquid *B* and X_A moles of liquid *A* to form an ideal liquid solution, which involves the change in Gibbs free energy

$$\Delta G = \Delta G^{M,\text{id}} = RT\left(X_A \ln X_A + X_B \ln X_B\right)$$

Thus, the *molar Gibbs free energy of mixing* (which can also be called the *molar Gibbs free energy of formation*) of an ideal liquid solution, $\Delta G^{M}_{(l)}$, from liquid *A* and solid *B* is given by

$$\Delta G^{M}_{(l)} = RT\left(X_A \ln X_A + X_B \ln X_B\right) + X_B \Delta G^{\circ}_{m(B)} \tag{10.2}$$

which is the equation of curve I in Figure 10.3b.

Similarly, at any composition, the formation of an ideal solid solution from liquid *A* and solid *B* involves a change in Gibbs free energy of

$$\Delta G^{M}_{(s)} = RT\left(X_A \ln X_A + X_B \ln X_B\right) - X_A \Delta G^{\circ}_{m(A)} \tag{10.3}$$

which is the equation of curve II in Figure 10.3b.

At the composition *e*, of Figure 10.3b, the tangent to the free energy of mixing curve for the liquid solution is also the tangent to the free energy of mixing curve of the solid solution at the composition *f*. At this temperature, the chemical potentials of each of the components in both phases are equal as are their activities. Thus, at the temperature *T*, the liquid of composition *e* is in *equilibrium* with the solid of composition *f*; that is, *e* is the liquidus composition and *f* is the solidus composition, as seen in Figure 10.3a.

As the temperature is lowered, the magnitude of *ca* decreases until, at the melting point of *A*, the length of *ca* equals zero. With decreasing temperature, the magnitude of *db* increases. The consequent movement of the positions of curves I and II relative to one another is such that the positions *e* and *f* of the double tangent to the

curves shift to the left. Correspondingly, if the temperature is increased, the relative movement of the Gibbs free energy curves is such that *e* and *f* shift to the right. The loci of *e* and *f* with change in temperature trace out the *liquidus* and *solidus* curves, respectively.

The equations for the solidus and liquidus curves of this system are derived in Appendix 10A of this chapter. There, the equations are found to be

$$X_{A(s)} = \frac{1 - \exp\left(-\dfrac{\Delta G^{\circ}_{m(B)}}{RT}\right)}{\exp\left(-\dfrac{\Delta G^{\circ}_{m(A)}}{RT}\right) - \exp\left(-\dfrac{\Delta G^{\circ}_{m(B)}}{RT}\right)} \tag{10.4}$$

and

$$X_{A(l)} = \frac{\left[1 - \exp\left(-\dfrac{\Delta G^{\circ}_{m(B)}}{RT}\right)\right]\exp\left(-\dfrac{\Delta G^{\circ}_{m(A)}}{RT}\right)}{\exp\left(-\dfrac{\Delta G^{\circ}_{m(A)}}{RT}\right) - \exp\left(-\dfrac{\Delta G^{\circ}_{m(B)}}{RT}\right)} \tag{10.5}$$

Thus, the phase diagram for a system that forms *ideal solid and liquid solutions* is determined only by the *melting temperatures* and the *molar heats of melting* of the components. See Equation 10.1.

Figure 10.4 shows the Gibbs free energy of mixing curves for a binary system *A*–*B* which forms ideal solid solutions and ideal liquid solutions, drawn at a temperature of 500 K, which is lower than $T_{m,(B)}$ and higher than $T_{m,(A)}$. At 500 K, $\Delta G^{\circ}_{m,A} = -1500$ J and $\Delta G^{\circ}_{m,B} = 1000$ J. Figure 10.4a shows the curves when liquid *A* and solid *B* are chosen as the standard states, located at $\Delta G^{M} = 0$. Figure 10.4b shows the curves when liquid *A* and liquid *B* are chosen as the standard states, and Figure 10.4c shows the curves when solid *A* and solid *B* are chosen as the standard states. Comparison among the three Figure 10.3a–c shows that, because of the logarithmic nature of the Gibbs free energy curves, the positions of the compositions of common tangency are not influenced by the choice of standard state. Rather, the compositions of common tangency are determined *only* by the temperature *T* and by the magnitude of the difference between $G^{\circ}_{(l)}$ and $G^{\circ}_{(s)}$ for both components at the temperature *T*.

The activity–composition relationships for component *B* are shown in Figure 10.3c. There are two possible standard states (Figure 10.3b). The point *b* for solid *B* and the point *d* for liquid *B* could be chosen as standard states. The lengths of the tangential intercepts with the $X_B = 1$ axis can be measured from *b*, in which case the activities of *B* are obtained with respect to solid *B* as the standard state, or the lengths can be measured from *d*, which gives the activities with respect to liquid *B* as the standard state.

If pure solid *B* is chosen as the standard state and is located at point *g* in Figure 10.3c, then the length *gn* is, by definition, unity, and this defines the solid standard-state activity scale. The line *ghij* then represents a_B in the solutions, with respect to solid *B* having unit activity at *g*. The line is obtained from the variation

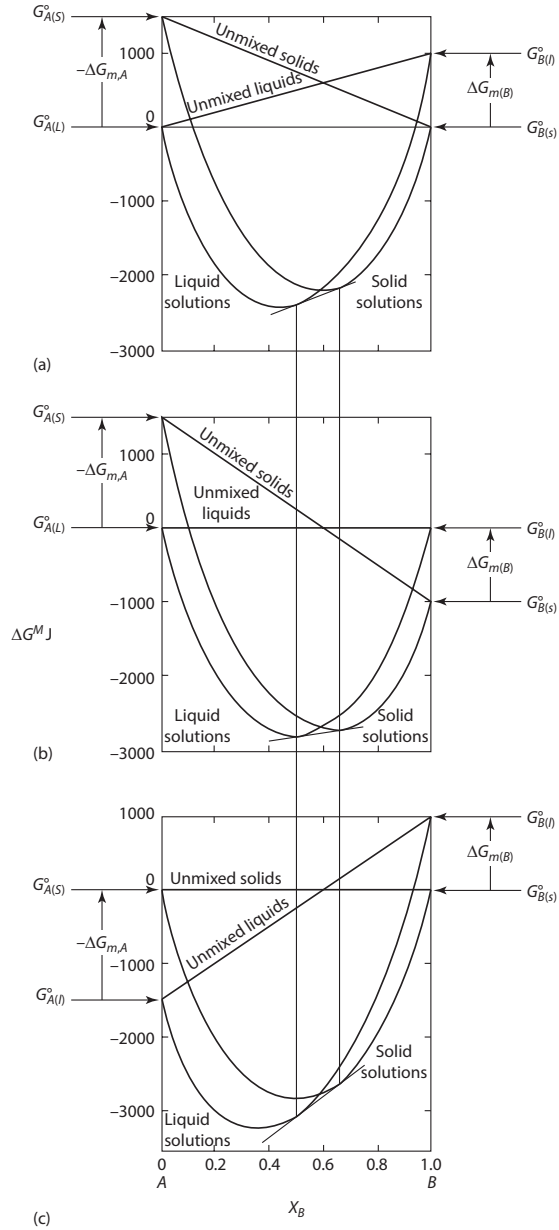

FIGURE 10.4 The Gibbs free energy of mixing curves for a binary system *A*–*B* which forms ideal solid solutions and ideal liquid solutions, at a temperature that is higher than $T_{m(A)}$ and lower than $T_{M(B)}$. (a) Liquid *A* and solid *B* were chosen as standard states located at $\Delta G^M = 0$. (b) Liquid *A* and liquid *B* were chosen as standard states located at $\Delta G^M = 0$. (c) Solid *A* and solid *B* were chosen as standard states located at $\Delta G^M = 0$. The positions of the points of double tangency are not influenced by the choice of standard state.

of the tangential intercepts from the curve *aefb* to the $X_B = 1$ axis, measured from the point *b*. On this activity scale, Raoult's law is given by *jg*, and the points *i* and *h* represent, respectively, the activity of *B* in the coexisting liquid solution *e* and solid solution *f*.

Point *m* represents the activity of pure liquid *B* measured on the solid standard-state activity scale of *B*. This activity is less than unity, being given by the ratio *mn*/*gn*. For *B* in any state along the *aefb* Gibbs free energy of mixing curve, in which state the partial molar Gibbs free energy of *B* is $\bar{G}_B$, the following relations hold.

$$\bar{G}_B = G^{\circ}_{B(l)} + RT \ln\left(a_B \text{ with respect to liquid } B\right)$$

and

$$\bar{G}_B = G^{\circ}_{B(s)} + RT \ln\left(a_B \text{ with respect to solid } B\right)$$

Thus,

$$G^{\circ}_{B(l)} - G^{\circ}_{B(s)} = \Delta G^{\circ}_{m(B)} = RT \ln\left(\frac{a_B \text{ with respect to solid } B}{a_B \text{ with respect to liquid } B}\right) \tag{10.6}$$

Since $T < T_{m(B)}, \Delta G^{\circ}_{m(B)}$ is a positive quantity, the activity of *B* in any solution with respect to solid *B* as the standard state is greater than the activity of *B* with respect to liquid *B* as the standard state, where both activities are measured on the same (solid or liquid) activity scale. For pure *B*, $a_{B(s)} > a_{B(l)}$ (i.e., $gn > mn$ in Figure 10.3c), and, if $gn = 1$, then $mn = \exp\left(-\Delta G^{\circ}_{m(B)}/RT\right)$. Equation 10.6 simply states that the length of the tangential intercept from any point on the curve *aefb*, measured from *b* added to the length *bd* equals the length of the tangential intercept from the same point on the curve measured from *d*.

If pure liquid *B* is chosen as the standard state and is located at the point *m*, then the length *mn* is, by definition, unity, and this defines the liquid standard-state activity scale. Raoult's law on this scale is given by the line *jm*, and the activities of *B* in solution, with respect to pure liquid *B* having unit activity, are represented by the line *mlkj*. The activity of solid *B*, located at *g*, is greater than unity on the liquid standard-state activity scale, being equal to $\exp\left(\Delta G^{\circ}_{m(B)}/RT\right)$. When measured on one or the other of the two activity scales, the lines *jihg* and *jklm* vary in the constant ratio $\exp\left(\Delta G^{\circ}_{m(B)}/RT\right)$, but *jihg* measured on the solid standard-state activity scale is identical with *jklm* measured on the liquid standard-state activity scale.

The variation of a_A with composition is shown in Figure 10.3d. In this case, since $T > T_{m(A)}$, $\Delta G^{\circ}_{m(A)}$ is a negative quantity, and hence,

$$a_A\left(\text{with respect to liquid } A\right) > a_A\left(\text{with respect to solid } A\right)$$

when measured on the same activity scale. If pure liquid *A* is chosen as the standard state and is located at the point *p*, then the length of *pw* is, by definition, unity, and the line *pqrs* represents the activity of *A* in the solution with respect to the liquid

standard state. On the liquid standard-state activity scale, the activity of pure solid A, located at the point v, has the value $\exp\left(\Delta G^{\circ}_{m(A)}/RT\right)$. If, on the other hand, pure solid A is chosen as the standard state, then the length of vw is, by definition, unity, and Raoult's law is given by the line vs. The line $vuts$ represents the activities of A in the solutions with respect to pure solid A. On the solid standard-state activity scale, liquid A, located at the point p, has the value $\exp\left(-\Delta G^{\circ}_{m(A)}/RT\right)$. Again, the two lines, measured on one or the other of the two activity scales, vary in the constant ratio $\exp\left(\Delta G^{\circ}_{m(A)}/RT\right)$, and when measured on their respective scales, they are identical.

If the temperature of the system is decreased to a value less than T indicated in Figure 10.3a, then the length of ac, being equal to $\left|\Delta G^{\circ}_{m(A)}\right|$ at the temperature of interest, decreases; correspondingly, the magnitude of $\left|\Delta G^{\circ}_{m(B)}\right|$, and hence the length of bd, increases. The consequent change in the positions of the Gibbs free energy of mixing curves I and II in Figure 10.3b causes the double tangent points e and f to shift to the left toward A. The effect on the activities is as follows. In the case of both components,

$$\frac{a_i \text{ with respect to solid } i}{a_i \text{ with respect to liquid } i} = \exp\left(\frac{\Delta G^{\circ}_{m(i)}}{RT}\right)$$

which, from Equation 10.1,

$$= \exp\left[\Delta H^{\circ}_{m(i)}\left(\frac{T_{m(i)} - T}{RTT_{m(i)}}\right)\right] \tag{10.7}$$

With respect to component B, if the temperature, which is less than $T_{m(B)}$, is decreased, the ratio $a_{B(\text{solid})}/a_{B(\text{liquid})}$, which is greater than unity, increases. Thus, in Figure 10.3c, the ratio gn/mn increases. With respect to component A, if the temperature, which is higher than $T_{m(A)}$, is decreased, then the ratio $a_{A(\text{solid})}/a_{A(\text{liquid})}$, which is less than unity, increases. Thus, the ratio vw/pw in Figure 10.3d increases. At the temperature $T_{m(A)}$, solid and liquid A coexist in equilibrium, $\Delta G^{\circ}_{m(A)} = 0$, and the points p and v coincide. Similarly, at the temperature $T^{\circ}_{m(B)}$, the points m and g coincide.

10.4 PHASE DIAGRAMS, GIBBS FREE ENERGY, AND THERMODYNAMIC ACTIVITY

Complete mutual solid state solubility of the components A and B requires that A and B have the *same crystal structures*, that they are of comparable atomic size, and that they have similar electronegativities and valencies. These are commonly called the Hume-Rothery (William Hume-Rothery, 1899–1968) Rules.[1] If any one of these conditions is not met, then one or more two-phase regions will occur in the solid state.

Consider the *eutectic* A–B binary system, the phase diagram of which is shown in Figure 10.5a, in which A and B have different crystal structures. Two terminal

[1] W. Hume Rothery and G. V. Raynor, *The Structure of Metals and Alloys*, Institute of Metals, London, 1954.

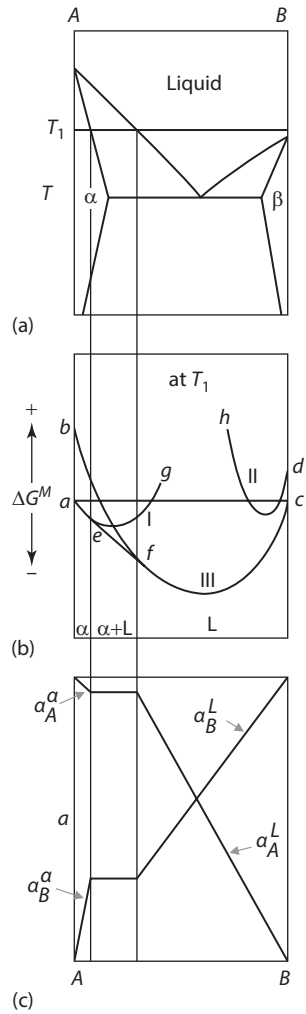

FIGURE 10.5 (a) An eutectic phase diagram where the solid phases have different crystal structures. (b) The molar Gibbs free energy of mixing diagrams of the three phases at $T = T_1$. (c) Activity diagrams of the phases at T_1.

solid solutions, α and β, occur. The molar Gibbs free energy of mixing curves, at the temperature T_1, are shown in Figure 10.5b. In this figure, *a* and *c*, located at $\Delta G^M = 0$, represent, respectively, the molar Gibbs free energies of pure solid *A* and pure liquid *B*. The points *b* and *d* represent, respectively, the molar Gibbs free energies of pure liquid *A* and pure solid *B*. The curve *aeg* (curve I) is the Gibbs free energy of mixing of solid *A* and solid *B* to form homogeneous α solid solutions, which have the same crystal structure as has *A*. This curve intersects the $X_B = 1$ axis at the molar Gibbs free energy which solid *B would have* if it had the same crystal structure as *A*. Similarly, the curve *dh* (curve II) represents the Gibbs free energy of mixing of solid *B* and solid *A* to form homogeneous β solid solutions which have the same crystal

structure as has *B*. This curve would intersect the $X_A = 1$ axis at the molar Gibbs free energy which *A* would have if it had the same crystal structure as *B*. The curve *bfc* (curve III) represents the molar Gibbs free energy of mixing of liquid *A* and liquid *B* to form a homogeneous liquid solution. Since curve II lies everywhere above curve III, solid β solutions are not stable at the temperature T_1. The common tangent to the curves I and III identifies the α *solidus* composition at the temperature T_1 as *e* and the *liquidus* composition as *f*.

Figure 10.5c shows the activity–composition relationships of the components at the temperature T_1, drawn with respect to solid as the standard state for *A* and liquid as the standard state for *B*. These relationships are drawn in accordance with the assumption that the liquid solutions exhibit Raoultian ideality and the solid solutions of α, show positive deviations from Raoult's law, that is $a_B^a > 1$ for $0 < X_B < f$.

As the temperature decreases below T_1, the length of *ab* increases and the length of *cd* decreases until, at $T = T_{m(B)}$, the points *c* and *d* coincide at $\Delta G^M = 0$. See Figure 10.6. For $T_2 < T_{m(B)}$, point *c* (liquid *B*) lies above *d* in Figure 10.6b, and since curve II lies partially below curve III, two common tangents can be drawn: one to the curves I and III, which defines the compositions of the solidus α and its conjugate liquidus, and one to the curves II and III, which defines the compositions of the solidus β and its conjugate liquidus. The activity-composition curves at T_2 are shown in Figure 10.6c, in which the solid is the standard state for both components.

With the further decrease in temperature, the two liquidus compositions *m* and *n* in Figure 10.6b approach one another and, at the unique temperature T_E (the eutectic temperature), they coincide. See Figure 10.7. This means that the two common tangents merge to form the "triple" common tangent to the three curves shown in Figure 10.7b. At compositions between *o* and *p* in Figure 10.7b, a doubly saturated eutectic liquid coexists in equilibrium with the α and β solid solutions. From the Gibbs phase rule discussed in Section 7.4, this three-phase equilibrium has one degree of freedom, which is used to specify the pressure of the system. Thus, at the specified pressure, the three-phase equilibrium is *invariant* (the compositions of the three phases are fixed and the temperature is fixed). Figure 10.7c shows the activities of *A* and *B* at T_E. At $T_3 < T_E$ (see Figure 10.8), curve III lies above the common tangent to curves I and II, and thus, the liquid phase is not stable. This behavior and the corresponding activity–composition relationships are shown, respectively, in Figure 10.8b and c.

As mentioned above, this diagram is called an eutectic binary phase diagram. Eutectic derives from the Greek phrase meaning *easy melting.* The temperature at which solution with compositions between *o* and *p* begins to melt *well* below the melting temperatures of the component elements. Note that the two-phase fields in the diagram ($\alpha + L$, $\beta + L$, and $\alpha + \beta$) lie between their respective single-phase fields. Also the three-phase field (a line in this case) lies between their corresponding two-phase fields. These phase field configurations are a result of the *Gibbs Equilibrium Phase Rule* (see Chapter 7).

10.5 CALCULATIONS OF PORTIONS OF PHASE DIAGRAMS

If the ranges of solid state solubility in the α and β phases are immeasurably small, then, as a reasonable *approximation,* it can be said that *A* and *B* are insoluble in one another in the solid state. The phase diagram for such a system is shown in

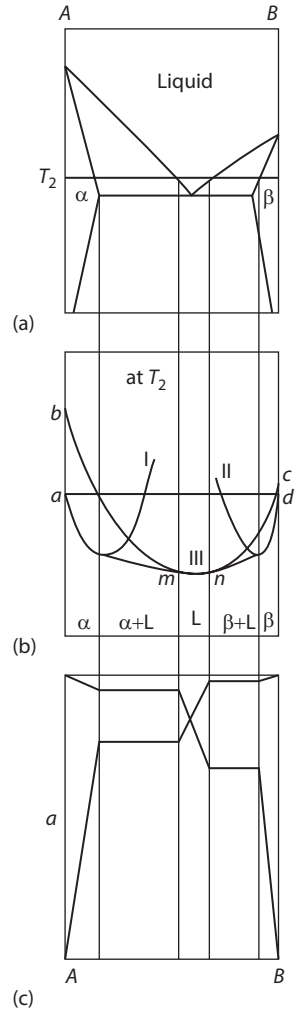

FIGURE 10.6 (a) The same eutectic phase diagram as Figure 10.5. (b) The molar Gibbs free energy of mixing diagrams of the three phases at $T = T_2$. (c) Activity diagrams of the phases at T_2.

Figure 10.9a. Since the range of solid solubility in Figure 10.9a is so small that it may be neglected on the scale of the figure, then the molar Gibbs free energy of mixing curves for the formation of α and β (curves I and II in Figures 10.5–10.8) are also compressed toward the $X_A = 1$ and $X_B = 1$ axes, respectively. On the scale of Figures 10.5–10.8, they coincide with the vertical axes. The sequence in Figure 10.10 shows how, as the solubility of B in α decreases, the molar Gibbs free energy curve for α is compressed against the $X_A = 1$ axis. The molar Gibbs free energy of formation of the liquid solutions in the system A–B at the temperature T is shown in Figure 10.9b. The common tangent to the α solid solution and liquid solution curves is reduced to a tangent drawn from the point on the $X_A = 1$ axis which represents pure solid A to the

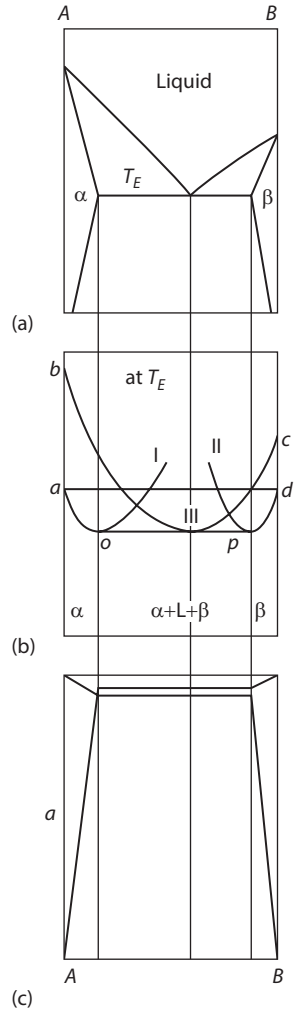

FIGURE 10.7 (b) The molar Gibbs free energy curves and (c) the activity plots for the eutectic diagram shown in (a) at temperature T_E, the eutectic temperature.

liquid solutions curve. The corresponding activity–composition relations are shown in Figure 10.9c. Again, these are drawn in accordance with the supposition that the liquid solutions are ideal.

In Figure 10.9c:

- *pqr* is the activity of *A* with respect to pure solid *A* at *p*
- *s* is the activity of pure liquid *A* with respect to solid *A* at *p*
- *str* is the activity of *A* with respect to liquid *A* having unit activity at *s*
- *Auvw* is the activity of *B* with respect to liquid *B* having unit activity at *w*

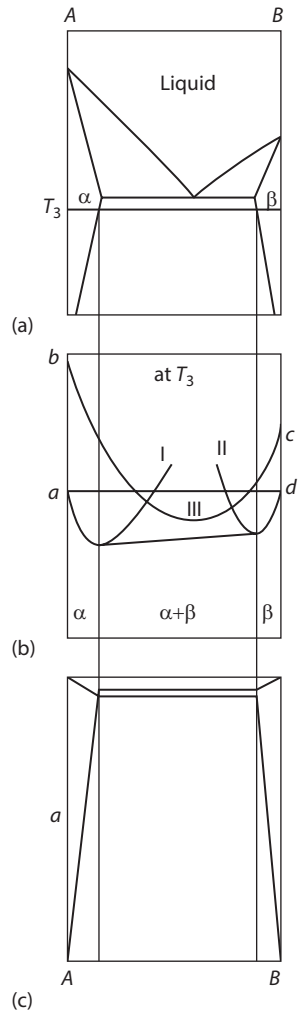

FIGURE 10.8 (b) The molar Gibbs free energy curves and (c) the activity plots for the eutectic diagram shown in (a) at temperature T_3, which is below the eutectic temperature.

In a binary system that exhibits complete miscibility in the liquid state and virtually complete immiscibility in the solid state (e.g., Figure 10.9a), the variations of the activities of the components of the liquid solutions can be obtained from consideration of the liquidus curves. At any temperature T (Figure 10.9a), the system with a composition between pure A and the liquidus composition exists as virtually pure solid A in equilibrium with a liquid solution of the liquidus composition. Thus, at T,

$$G^{\circ}_{A(s)} = \overline{G}^{A}_{(l)}$$

$$= G^{\circ}_{A(l)} + RT \ln a_A$$

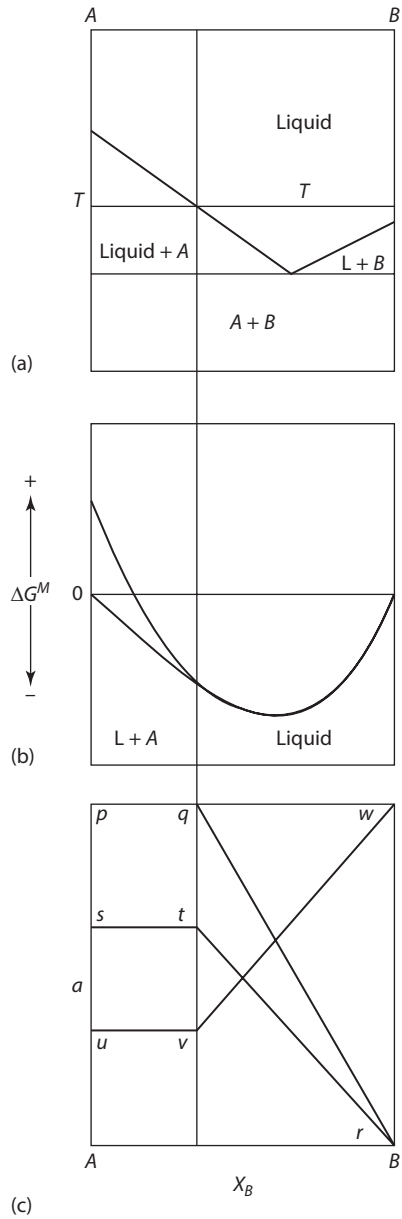

FIGURE 10.9 The molar Gibbs free energy of mixing (b) and the activities (c) in a binary eutectic system (a) that exhibits complete liquid miscibility and virtually complete solid immiscibility.

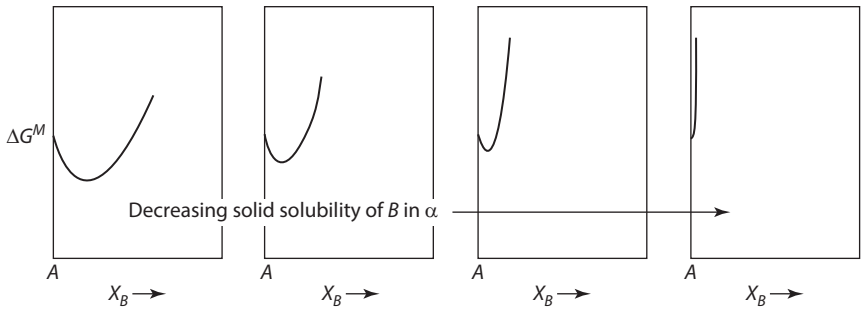

FIGURE 10.10 The effect of decreasing solid solubility on the molar Gibbs free energy of the mixing curve.

in which a_A is with respect to liquid A as the standard state. Thus,

$$\Delta G^{\circ}_{m(A)} = -RT \ln a_A \tag{10.8a}$$

or, if the liquid solutions are Raoultian,

$$\Delta G^{\circ}_{m(A)} = -RT \ln X_A \tag{10.8b}$$

10.5.1 Calculations of a Portion of the Bi-Cd Phase Diagram

Now, consider an alloy system that approximates the solution thermodynamics just discussed. Figure 10.11 shows the binary temperature–composition phase diagram for the Bi–Cd system. This system shows the limited solubility of Bi in Cd and virtually zero solubility of Cd in Bi. In Appendix 10B to this chapter, the liquidus lines are calculated using Equations 10B.1 and 10B.2 and ancillary thermodynamic information. The calculated liquidus curves as well as the eutectic composition and temperature are plotted as dashed lines in Figure 10.11 is seen to be good. The deviations come from the departure from ideality of the liquid solution.

10.5.2 Calculations of Liquidus Lines with Varying Positive Deviations from Ideality

It is of interest to examine what happens to the liquidus line as the magnitude of the positive deviation from Raoultian behavior in the liquids increases—that is, as G^{XS} becomes increasingly positive.

Assuming regular solution behavior, Equation 10.8a, written in the form

$$-\Delta G^{\circ}_{m(A)} = RT \ln X_A + RT \ln \gamma_A$$

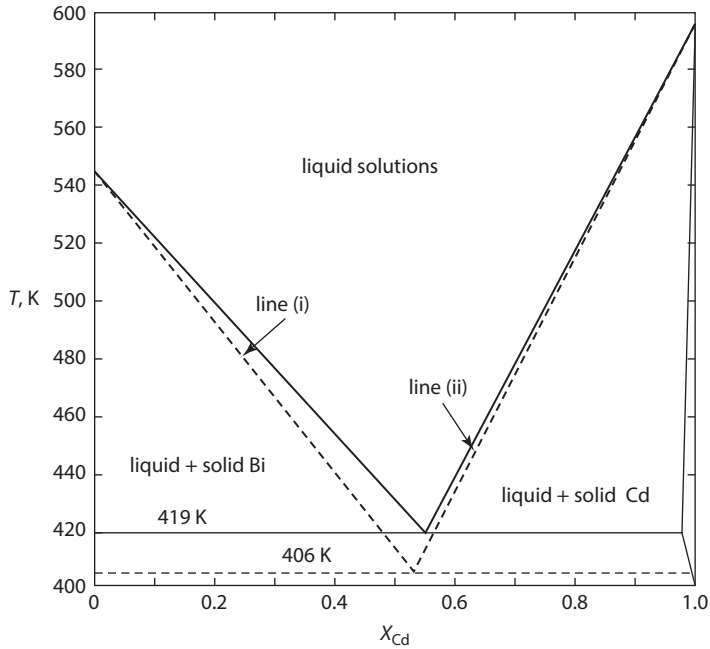

FIGURE 10.11 The phase diagram for the system Bi–Cd. The full lines are the measured liquidus lines, and the broken lines are calculated assuming no solid solution and ideal mixing in the liquid solutions. Details of the calculations are in Appendix 10B.

becomes

$$-\Delta G^{\circ}_{m(A)} = RT \ln X_A + \alpha(1 - X_A)^2 \tag{10.9}$$

Consider a hypothetical system *A*–*B* in which $\Delta H^{\circ}_{m(A)} = 10$ kJ at $T_{m,A} = 2000$ K. Thus, for this system,

$$\Delta S^{\circ}_{m(A)} = \frac{\Delta H^{\circ}_{m(A)}}{T_{m(A)}} = \left(\frac{10{,}000J}{2000K}\right)$$

$$-\Delta G^{\circ}_{m(A)} - 10{,}000 + 5T = RT \ln X_A + \alpha(1 - X_A)^2$$

where X_A is the composition of the *A* liquidus at the temperature *T*. The *A* liquidus lines, drawn for $\alpha = 0.0$, 10.0, 20.0, 25.3, 30.0, 40.0, and 50.0 kJ, are shown in Figure 10.12. As α exceeds some critical value (which is 25.3 kJ in this case), the form of the liquidus curve changes from a monotonic decrease in liquidus temperature with decreasing X_A to a form that contains a maximum and a minimum (e.g., the liquidus for $\alpha = 30$ kJ). At the critical value of α, the maximum and minimum coincide at $X_A = 0.5$ to produce a *horizontal inflection* in the liquidus curve. It is apparent that, when α exceeds the critical value, isothermal tie-lines cannot be drawn between

pure solid A and all points on the liquidus lines, which, necessarily, means that the calculated liquidus lines are impossible.

From Equation 10.6 and remembering that $\Delta S^{\circ}_{m(A)} = \dfrac{\Delta H^{\circ}_{m(A)}}{T_{m(A)}}$

$$\ln a_A = \frac{-\Delta H^{\circ}_{m(A)}}{RT} + \frac{\Delta H^{\circ}_{m(A)}}{RT_{m(A)}}$$

Thus,

$$d \ln a_A = \frac{da_A}{a_A} = \frac{\Delta H^{\circ}_{m(A)}}{RT^2} dT$$

or

$$\frac{dT}{dX_A} = \frac{RT^2}{\Delta H^{\circ}_{m(A)} a_A} \frac{da_A}{dX_A} \tag{10.10}$$

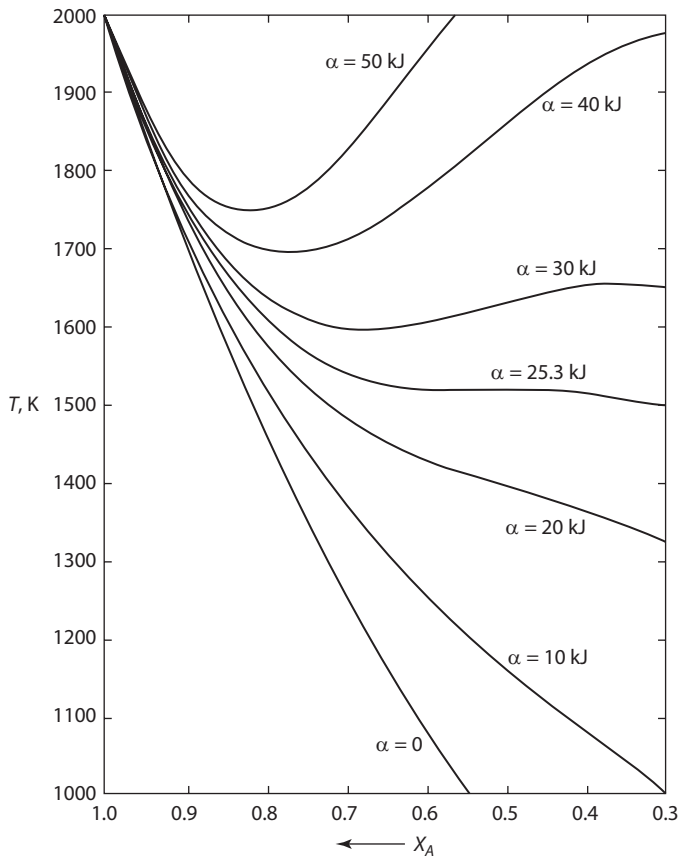

FIGURE 10.12 Calculated liquidus lines assuming regular solution behavior in the liquid solutions and no solid solubility.

and also,

$$\frac{d^2T}{dX_A^2} = \frac{2RT}{\Delta H^{\circ}_{m(A)} a_A} \frac{da_A}{dX_A} \frac{dT}{dX_A} - \frac{RT^2}{\Delta H^{\circ}_{m(A)} a_A^2} \left(\frac{da_A}{dX_A} \right)^2 + \frac{RT^2}{\Delta H^{\circ}_{m(A)} a_A} \frac{d^2 a_A}{dX_A^2} \quad (10.11)$$

In Equations 9.72 and 9.73, it was seen that $da_A/dX_A = d^2a_A/dX_A^2 = 0$ at the state of imminent immiscibility. Thus, in Equations 10.10 and 10.11, $dT/dX_A = d^2T/dX_A^2 = 0$ at the state of imminent immiscibility. In Figure 10.12, $\alpha_{cr} = 25.3$ kJ, and the horizontal inflection in the critical liquidus curve occurs at $X_A = 0.5$, $T = 1413$ K. Thus,

$$\frac{\alpha_{cr}}{RT_{cr}} = \frac{25,390}{8.3144 \times 1413} = 2$$

which is in accord with Equation 9.70.

The phase equilibria generated when $\alpha > \alpha_{cr}$ are shown in Figure 10.13, which shows the immiscibility in regular liquid solutions with $\alpha = 30,000$ J and the *A*-liquidus

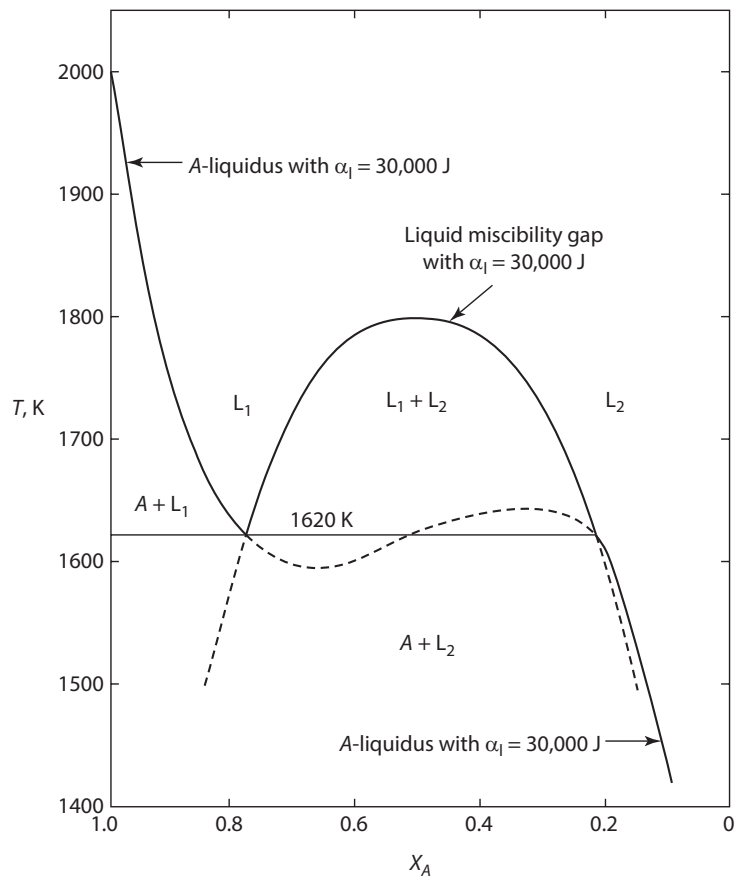

FIGURE 10.13 The monotectic equilibrium in a binary system in which the liquid solutions exhibit regular solution behavior with $\alpha = 30,000$

for $\alpha = 30{,}000\,\text{J}$ shown in Figure 10.12. The liquid immiscibility curve is symmetric about $X_A = 0.5$ as should be the case for regular solution miscibility gaps (see Chapter 9). The *A*-liquidus curve intersects the liquid miscibility gap at 1620 K to produce a three-phase *monotectic equilibrium* between solid *A* and liquidus L_1 and L_2. The liquid miscibility gap is metastable at temperatures <1620 K, and the calculated *A*-liquidus is physically impossible between the compositions of L_1 and L_2 at 1620 K.

At 1620 K the alloy when at equilibrium is composed of three phases, namely A, L_1 and L_2. Just below this temperature, the equilibrium is between the phases A and L_2, which have nearly the same composition as they did at 1620 K. The L_1 phase has decomposed into A and L_2. This gives rise to very interesting microstructures!

10.6 THE PHASE DIAGRAMS OF BINARY SYSTEMS THAT EXHIBIT REGULAR SOLUTION BEHAVIOR IN BOTH THE LIQUID AND SOLID STATES

In Sections 10.6.1–10.6.3, the binary equilibrium phase diagrams in three systems *A–B* which form *regular **liquid** solutions* and *regular **solid** solutions* are developed. The melting temperatures of *A* and B in each of the systems are respectively, 800 and 1200 K, and their molar Gibbs free energies of melting in J are

$$\Delta G_{m,(A)} = 8000 - 10T$$

$$\Delta G_{m,(B)} = 12{,}000 - 10T$$

10.6.1 Solution with $\alpha_l = -20{,}000\,\text{J}$ and $\alpha_s = 0$

Consider the system in which $\alpha_l = -20{,}000\,\text{J}$ in the liquid solutions and $\alpha_s = 0$ in the solid solutions. The Gibbs free energy of mixing curves at 1000 K are shown in Figure 10.14a. Since $T_{m,(A)} < 1000\ \text{K} < T_{m,(B)}$, the liquid is chosen as the standard state for *A*, and the solid is chosen as the standard state for *B*. With reference to these standard states, the molar Gibbs free energies of mixing are

$$\Delta G_l^M = X_B \Delta G^\circ_{m,(B)} + RT\left(X_A \ln X_A + X_B \ln X_B\right) + \alpha_l X_A X_B$$

for the liquid solutions and

$$\Delta G_s^M = -X_A \Delta G^\circ_{m,(A)} + RT\left(X_A \ln X_A + X_B \ln X_B\right) + \alpha_s X_A X_B$$

for the solid solutions. Inserting the numerical data gives

$$\Delta G_l^M = (12{,}000 - 10T) X_B + 8.3144T\left(X_A \ln X_A + X_B \ln X_B\right) - 20{,}000 X_A X_B$$

and

$$\Delta G_s^M = -(8000 - 10T) X_A + 8.3144T\left(X_A \ln X_A + X_B \ln X_B\right)$$

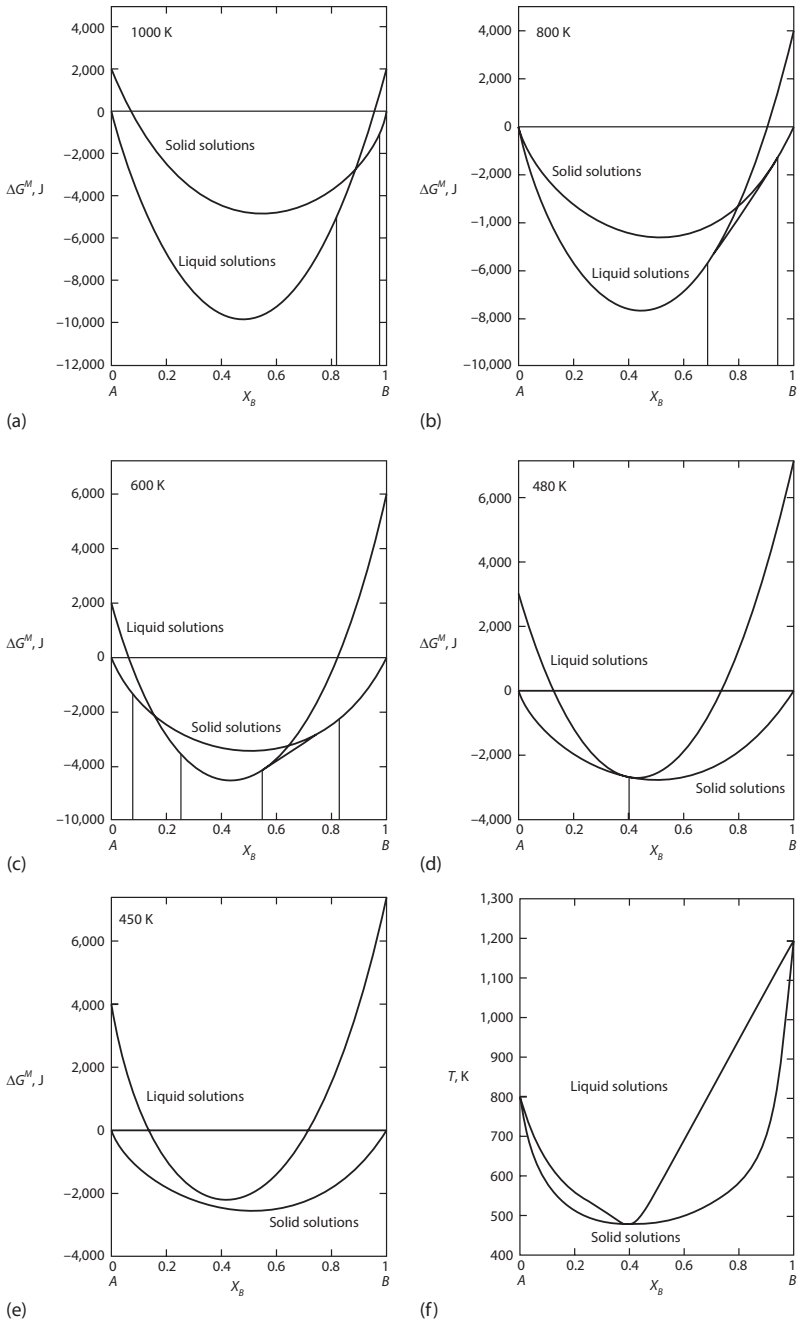

FIGURE 10.14 The molar Gibbs free energy of mixing curves at various temperatures, and the phase diagram for a binary system that forms regular solid solutions in which $\alpha_s = 0$ and regular liquid solutions in which $\alpha_l = -20{,}000\,\text{J}$.

The common tangent to the curves in Figure 10.14a gives the liquidus composition of $X_B = 0.82$ and the solidus composition of $X_B = 0.97$. Decreasing the temperature causes the Gibbs free energies of the liquids to increase relative to those of the solids. As shown in Figure 10.14b, the Gibbs free energies of pure solid A and pure liquid B are equal at the melting temperature of A, and the common tangent gives liquidus and solidus compositions of $X_B = 0.69$ and $X_B = 0.94$, respectively. At temperatures lower than $T_{m,(A)}$ and $T_{m,(B)}$, solid is chosen as the standard state for both components and the Gibbs free energies of mixing are written as

$$\Delta G_l^M = (12{,}000 - 10T)X_B + (8000 - 10T)X_A + 8.3144T(X_A \ln X_A + X_B \ln X_B) - 20{,}000X_A X_B$$

and

$$\Delta G_s^M = RT(X_A \ln X_A + X_B \ln X_B)$$

(See Equations 10.2 and 10.3)

The curves at 600 K, shown in Figure 10.14c, contain two common tangents, and as the temperature is further decreased, the curve for the liquids is raised relative to the curve for the solids until, at 480 K, the two double tangents collapse to a single point of contact between the curves at $X_B = 0.41$. At temperatures <480 K, the curve for the liquids lies above that for the solids, and thus, solid solutions are stable over the entire range of composition. The variations, with temperature, of the compositions of the double tangents give the phase diagram shown in Figure 10.14f. The minima in the liquidus and solidus curve coincide at 480 K. Thus a liquid of composition $X_B = 0.41$ will solidify to a single phase solid just below 480 K. Such a point in the diagram is sometimes called a congruent point and the solidification process is called congruent solidification.

Note that at 0 K the phase diagram would display a *solid solution* of the two elements A and B as being the equilibrium phase, in violation of the Third Law. This is so because the solid phase was set as being *ideal*, meaning there are *no interactions* among the components. Such interactions are necessary for a solution to comply with the Third Law constraint. See Section 10.8.

10.6.2 Solution with $\alpha_l = -20{,}000$ J and $\alpha_s = +10{,}000$ J

Consider now the binary system A–B which forms a *regular liquid solution* and a *regular solid solution*. The melting temperatures of A and B and the molar Gibbs free energies of melting are the same as in 10.6.1. Here however the system has $\alpha_l = -2000$ J and $\alpha_s = 10{,}000$ J. This system is shown in Figure 10.15.

As seen in Figure 10.15a–c, the behavior is similar to that shown in Figure 10.14. However, with a positive value of α_s, a critical temperature exists below which immiscibility occurs in the solid state. With $\alpha_s = 10{,}000$ J, the critical temperature is $10{,}000/2R = 601$ K, and the mixing curves at 601 K are shown in Figure 10.15d. The phase diagram is shown in Figure 10.15f. With increasingly negative values of α_l and increasingly positive values of α_s, the temperature of the point of contact of

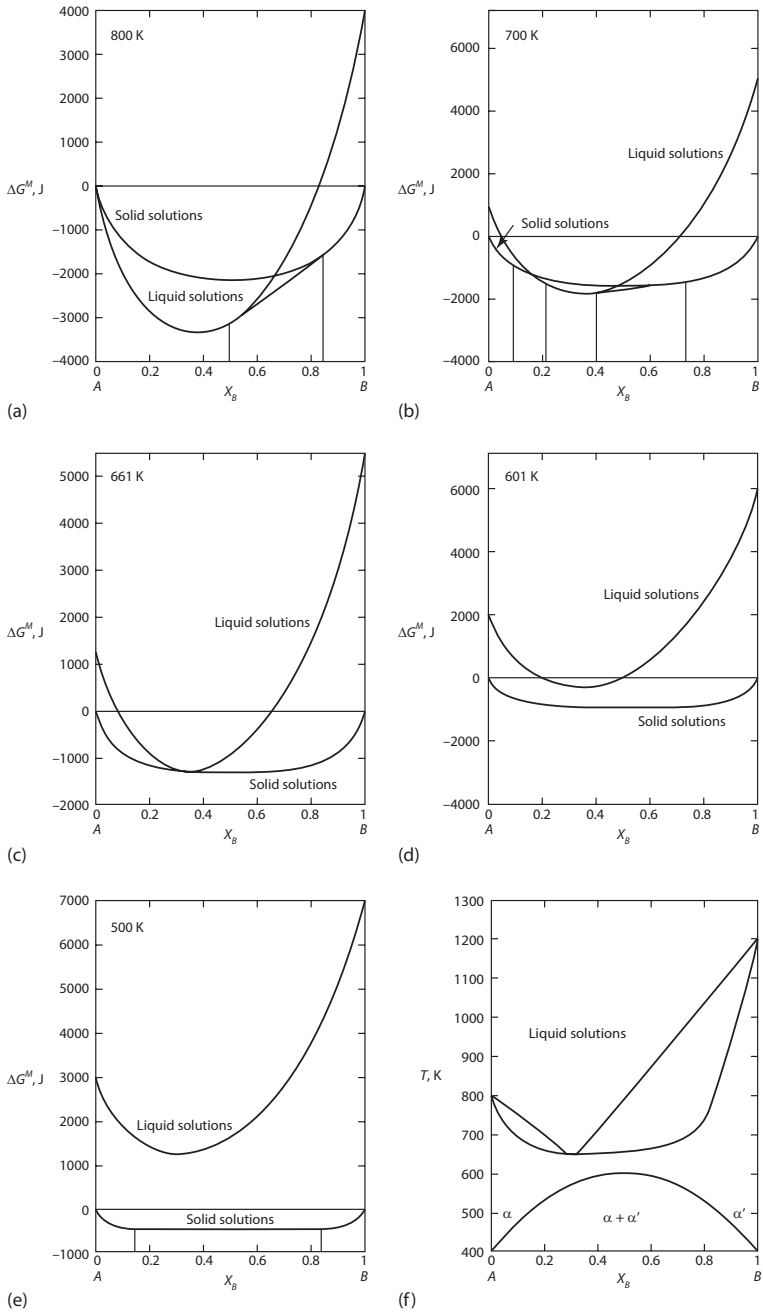

FIGURE 10.15 The molar Gibbs free energy of mixing curves at various temperatures, and the phase diagram for a binary system that forms regular solid solutions in which $\alpha_s = 10{,}000\,\text{J}$ and regular liquid solutions in which $\alpha_l = -2000\,\text{J}$.

the liquidus curve with the solidus curve decreases and the critical temperature in the solid-state increases, which eventually produces a eutectic system. Note that at 0 K the phase diagram displays the two pure components *A* and *B* as being in equilibrium, thus satisfying the Third Law constraint (see Section 10.8).

10.6.3 Solution with $\alpha_l = +20{,}000\,J$ and $\alpha_s = +30{,}000\,J$

The behavior of a system in which $\alpha_l = 20{,}000\,J$ and $\alpha_s = 30{,}000\,J$ is shown in Figure 10.16. The critical temperatures for the liquid and solid solutions are, respectively, 1203 and 1804 K, and the Gibbs free energy of mixing curves at 1203 K are shown in Figure 10.16a. At $T \geq 1203$ K, homogeneous liquids are the stable state, and at temperatures lower than 1203 K, immiscibility occurs in the liquid state. The curves shown in Figure 10.16b at 1150 K contain two common tangents, one joining the conjugate liquid solutions L_1 and L_2 and one connecting the liquidus L_2 with the solidus α'. With decreasing temperature, the compositions of the conjugate liquid L_2 and the liquidus L_2 approach one another until, at 1090 K, the two common tangents merge to form a *triple tangent* to liquid compositions at $X_B = 0.23$ and 0.77 and α' at $X_B = 0.98$. This is a monotectic equilibrium (see also Figure 10.13). Further cooling produces a common tangent between L_1 and α', as shown in Figure 10.16d, and at 789 K another "triple" common tangent occurs between α at $X_B = 0.01$, L_1 at $X_B = 0.03$, and $\alpha' = 0.99$. At temperatures lower than the eutectic temperature of 789 K, the liquid phase is not stable, and, depending on its composition, the system exists as α, $\alpha + \alpha'$, or α'. The monotectic and eutectic equilibria are shown in the phase diagram in Figure 10.16f. Note that at 0 K the diagram displays the two pure components *A* and *B* as being in equilibrium, thus satisfying the Third Law constraint.

The influence of systematic changes in the values of α_l and α_s on the phase relationships that occur in the binary system *A*–*B* which forms regular solid and liquid solutions is shown in Figure 10.17.[2] The values of the melting temperatures and the entropies of melting are the same as those solutions in Figures 10.14–10.16.

- In moving from the bottom of any column to the top, the value of α_s becomes more positive at constant α_l eventually giving rise to miscibility in the solid state.
- In moving from left to right along any row, the value of α_l becomes more positive at constant α_s giving rise to either miscibility in the liquid or a maximum in the melting temperature of solutions.
- In the sequence Figure 10.17a–e, the liquid solutions become increasingly less stable relative to the solid phases, with the consequence that the eutectic temperature is increased.
- In the transition Figure 10.17d–e, the *A*-liquidus becomes unstable and a monotectic equilibrium occurs.
- In the sequence Figure 10.17h–i, the temperature at which the three-phase equilibrium occurs is increased from 633 to 799 K, with the consequence that the eutectic equilibrium in Figure 10.17h becomes a peritectic equilibrium in Figure 10.17i.

[2] A. D. Pelton and W. T. Thompson, *Prog. Solid State Chem.* (1975), vol. 10(3), p. 119.

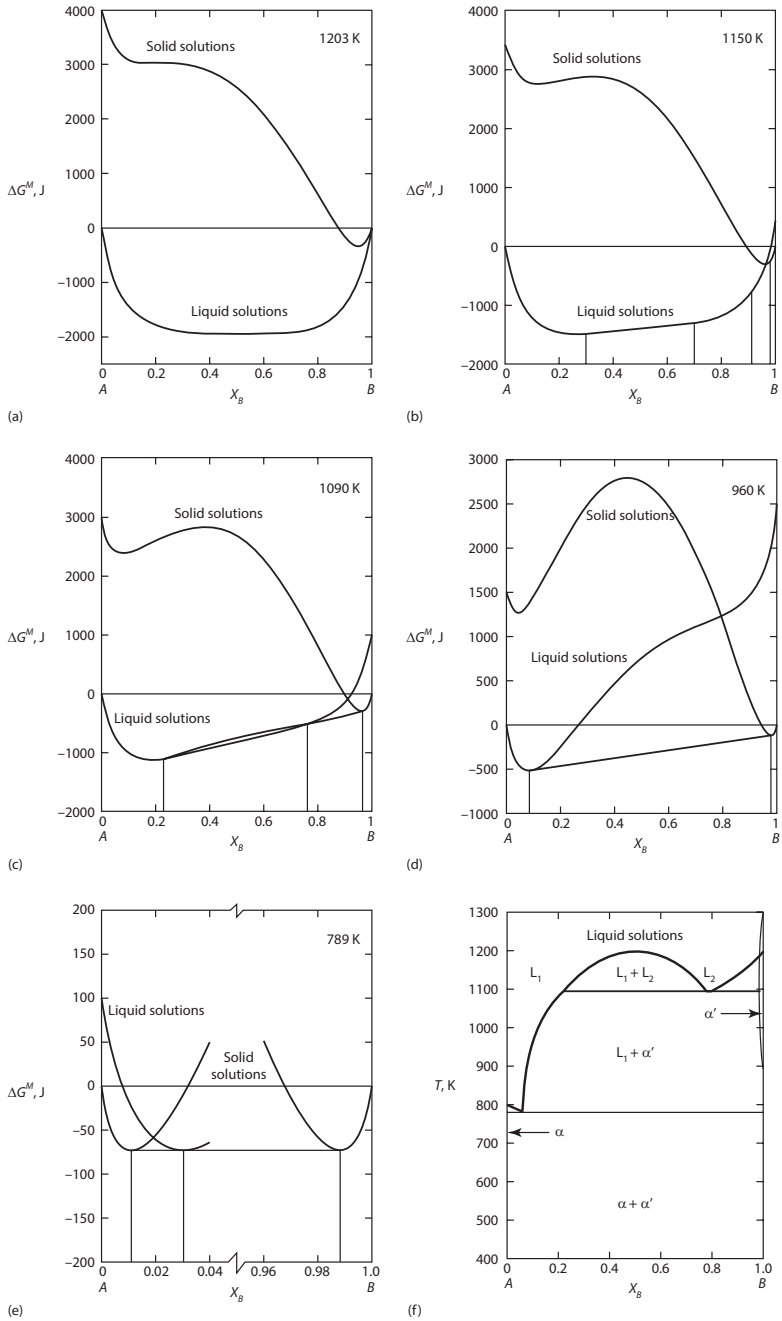

FIGURE 10.16 The molar Gibbs free energy of mixing curves at various temperatures, and the phase diagram for a binary system that forms regular solid solutions in which $\alpha_s = 30{,}000\,\text{J}$ and regular liquid solutions in which $\alpha_l = 20{,}000\,\text{J}$.

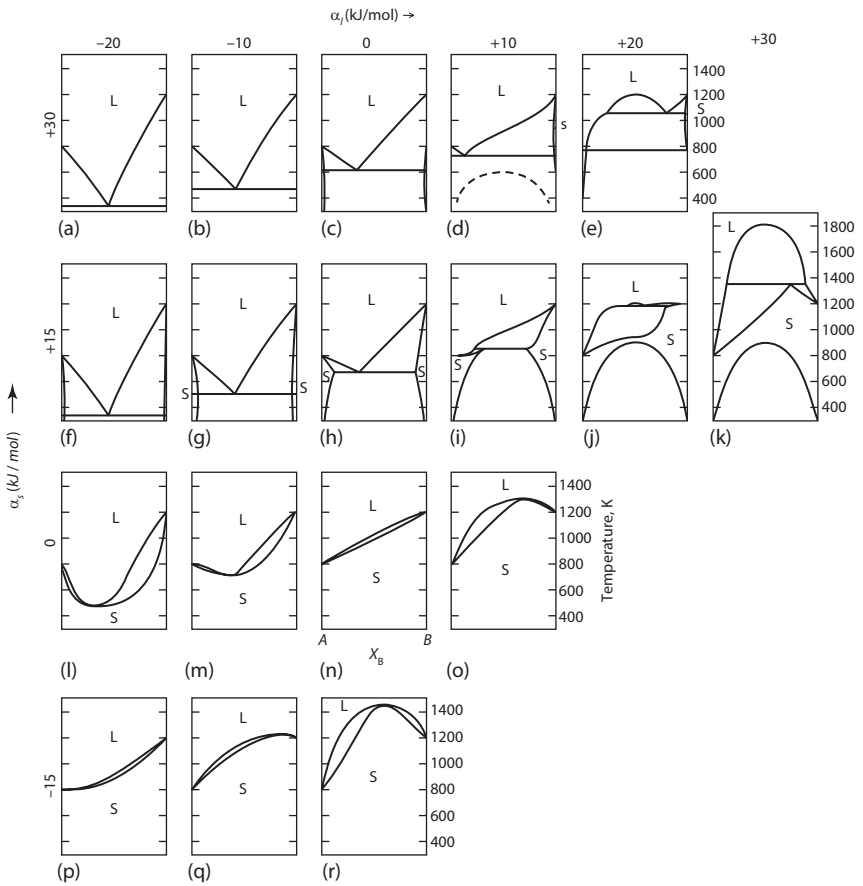

FIGURE 10.17 Topological changes in the phase diagram for a system *A*–*B* with regular solid and liquid solutions, brought about by systematic changes in the values of α_s and α_l. The melting temperatures of *A* and *B* are, respectively, 800 and 1200 K, and the molar entropies of melting of both components are 10 J/K. See text for a full explanation. (From A. D. Pelton and W. T. Thompson, *Prog. Solid State Chem.* (1975), vol. 10, part 3, p. 119.)

- In Figure 10.17i, the critical point of the miscibility gap disappears at a temperature above that at which peritectic equilibrium could occur.
- With $\alpha_l = 20$ kJ in Figure 10.17j, liquid immiscibility occurs at temperatures lower than $20{,}000/(2 \times 8.3144) = 1202$ K, and hence, a monotectic equilibrium occurs at 1190 K.
- In Figure 10.17k, the three-phase L_1–L_2–α equilibrium occurs at 1360 K, which, being higher than $T_{m,(B)}$, produces a *syntectic* equilibrium in which the composition of the α phase lies between the compositions of the two liquids.
- In the sequence $p \rightarrow l \rightarrow f$ in Figure 10.17, the solid phase becomes increasingly less stable than the liquid phase, which deepens the depression of the liquidus and solidus curves and eventually forms a eutectic.

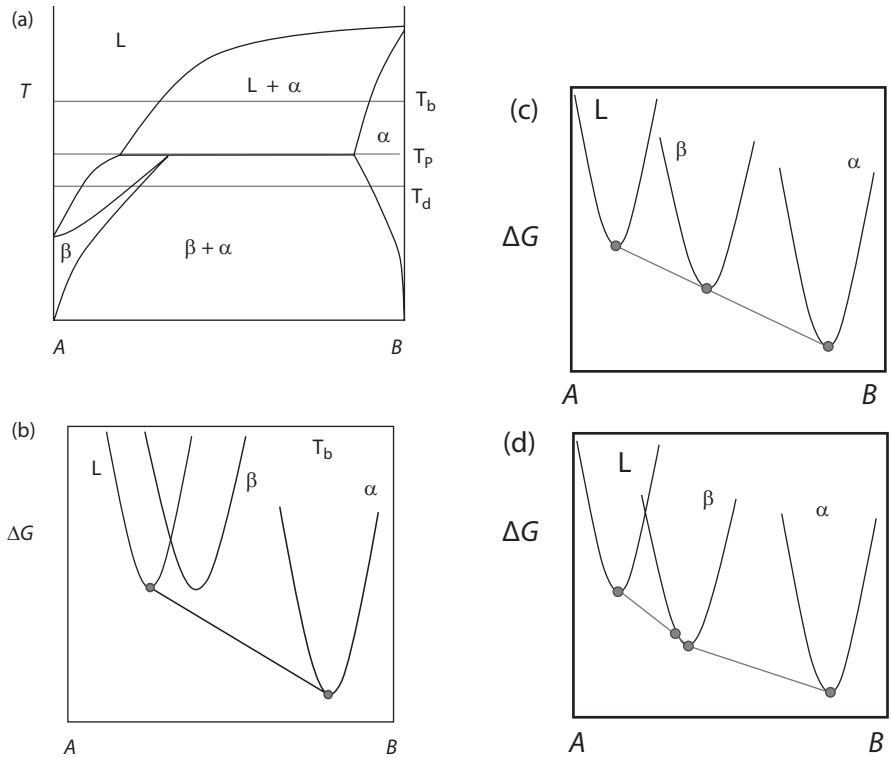

FIGURE 10.18 (a) A peritectic binary phase diagram displaying two solid phases (α and β) and one liquid phase. (b) Gibbs free energy of mixing curves of the three phases at a temperature above the peritectic invariant temperature. Note that the free energy of mixing curve of the liquid phase is to the BA rich side of both free energy curves of the solid phases. (c) Gibbs free energy of mixing curves of the three phases at the peritectic temperature T_P. (d) Gibbs free energy of mixing curves of the three phases at the temperature T_d.

- Figures 10.14 and 10.16, respectively, show the Gibbs free energy relations in Figure 10.17l and e.
- Figure 10.15 shows the phase equilibria occurring between those in Figure 10.17l and those in Figure 10.17f.

A peritectic phase diagram like the one shown in Figure 10.17i can be obtained from Gibbs free energy curves as shown in Figure 10.18.

10.6.4 Concluding Remarks on Section 10.6

Even though the calculations performed in this Section (10.6) used regular solution models, the trends of changing the regular solution constants α_l and α_s do shed light on the way in which various experimentally determined diagrams vary with respect to each other.

In this section, we have seen the following invariant three-phase equilibria in binary alloy systems that occur on cooling:

Eutectic: $\text{Liquid} \rightarrow \text{Solid}_1 + \text{Solid}_2$
Monotectic: $\text{Liquid}_1 \rightarrow \text{Solid}_1 + \text{Liquid}_2$
Peritectic: $\text{Liquid}_1 + \text{Solid}_1 \rightarrow \text{Solid}_2$

If the liquid phases are replaced with solid phases, we get the related invariant phase equilibria for binary alloys, where the suffix *oid* (like) replaces the suffix *ic*:

Eutectoid: $\text{Solid} \rightarrow \text{Solid}_1 + \text{Solid}_2$
Monotectoid: $\text{Solid} \rightarrow \text{Solid}_1 + \text{Solid}_2$ (special case of eutectoid)
Peritectoid: $\text{Solid} + \text{Solid}_1 \rightarrow \text{Solid}_2$

In the *eutectic* phase diagrams, the high-temperature liquid phase has a composition between that of the two low-temperature solid phases at the invariant temperature. See for example Figure 10.5a. In *peritectic* diagrams, the liquid phase is the richest in solute (or solvent) at the invariant temperature. See Figure 10.18a, where the invariant reaction is written as:

$$\alpha + \text{L} \rightarrow \beta$$

This is followed by the reaction

$$\beta \rightarrow \alpha + \beta$$

There are two other invariant reactions that may occur involving three phases in the peritectic system: namely, the hypo-peritectic reaction:

$$\alpha + \text{L} \rightarrow \alpha + \beta$$

And the hyper-peritectic reaction:

$$\alpha + \text{L} \rightarrow \beta + \text{L}$$

10.7 SLOPES OF THE TEMPERATURE COMPOSITION CURVES INVOLVING FIRST-ORDER TRANSFORMATIONS

The following two equations adopted from Wagner[3] (Carl Wilhelm Wagner, 1901–1977) represent the slopes of coexistence curves in binary temperature-composition phase diagrams:

$$\left(\frac{dT}{dX_B^{\alpha}}\right) = -\frac{\left(X_B^{\beta} - X_B^{\alpha}\right) T \left(\dfrac{\partial^2 G^{M,\alpha}}{\partial \left(X_B^{\alpha}\right)^2}\right)}{\left\{X_A^{\beta} \Delta H_A^{0(\alpha \rightarrow \beta)} + X_B^{\beta} \Delta H_B^{0(\alpha \rightarrow \beta)}\right\}} \tag{10.12}$$

[3] C. Wagner, *Thermodynamics of Alloys*

$$\left(\frac{dT}{dX_B^{\beta}}\right) = -\frac{\left(X_B^{\beta} - X_B^{\alpha}\right) T \left(\frac{\partial^2 G^{M,\beta}}{\partial\left(X_B^{\beta}\right)^2}\right)}{\left\{X_A^{\alpha}\Delta H_A^{0(\alpha\rightarrow\beta)} + X_B^{\alpha}\Delta H_B^{0(\alpha\rightarrow\beta)}\right\}} \tag{10.13}$$

where:

$\left(\frac{dT}{dX_B^{\alpha}}\right)$ and $\left(\frac{dT}{dX_B^{\beta}}\right)$ are the slopes of the two curves, respectively,

X_B^{α} and X_B^{β} are the B compositions of the α and β phases,

T is the temperature of the system

$\left(\frac{\partial^2 G^{M,\alpha}}{\partial\left(X_B^{\alpha}\right)^2}\right)$ and $\left(\frac{\partial^2 G^{M,\beta}}{\partial\left(X_B^{\beta}\right)^2}\right)$ are the second derivatives of the

Gibbs free Energy of mixing of the α and β phases

$\Delta H_A^{0(\alpha\rightarrow\beta)}$ and $\Delta H_B^{0(\alpha\rightarrow\beta)}$ are the enthalpies of transition of the α to β phase.

Goodman et al.[4] have also discussed these equations and denoted them as the Gibbs-Konovalov equations (Dmitry Petrovich Konovalov, 1856–1929).

Consider the coexistence curves for the α and β phases shown in Figure 10.19a. From Equations 10.12 and 10.13, we see the following:

- Since the denominators of both of these equations are related to the heats of formation of the high temperature α phase to the low temperature β phase, they are negative (exothermic).
- The numerators of the equations are positive, since $\left(X_B^{\beta} - X_B^{\alpha} > 0\right)$
- The curvatures of the Gibbs free energy curves are positive since they represent equilibrium phases.

Thus, the slopes must be positive as shown in the figure.

If the coexistence curves intersect, $X_B^{\beta} = X_B^{\alpha}$. It can be seen from the equations that this would yield a zero slope for both of the solvi at their intersection. That is, the curves should intersect with zero slope at a maximum in the temperature–composition phase diagram with the configuration shown in Figure 10.19b. Such points are often called congruent points because the compositions of the phases that are involved in the transformation *are the same*. On heating, the β phase transforms to the α phase at such a temperature without a change in composition.

The same arguments apply to the minima curves in the solidus and liquidus curves shown in Figures 10.14f and 10.15f. These are called congruent melting points and their transformations are termed congruent.

[4] D. A. Goodman, J. W. Cahn, and L. H. Bennett, "The Centennial of the Gibbs-Konovalov Rule for Congruent Points", *Bull Alloy Phase Diagr*

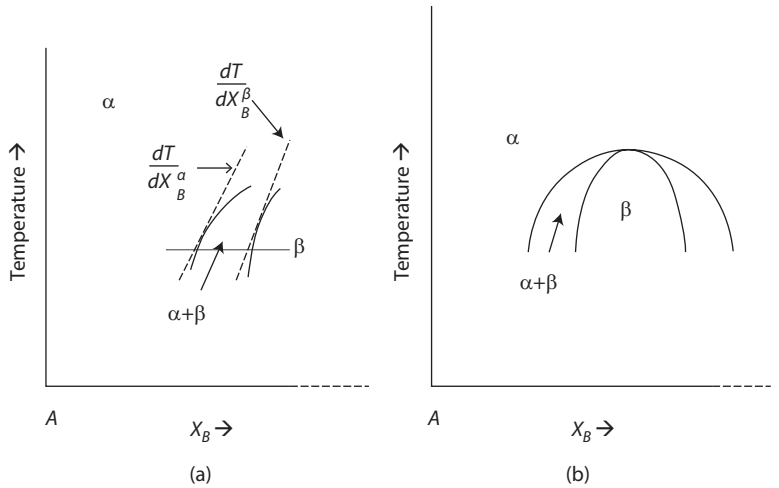

FIGURE 10.19 (a) A partial temperature/composition phase diagram at constant pressure which displays the solvi of a and b phases that are in equilibrium. The slopes of the solvi can be determined by Equations 10.12 and 10.13. (b) A correct completion of the equilibrium diagram shown in (a) showing that at their intersection both solvi have zero slope.

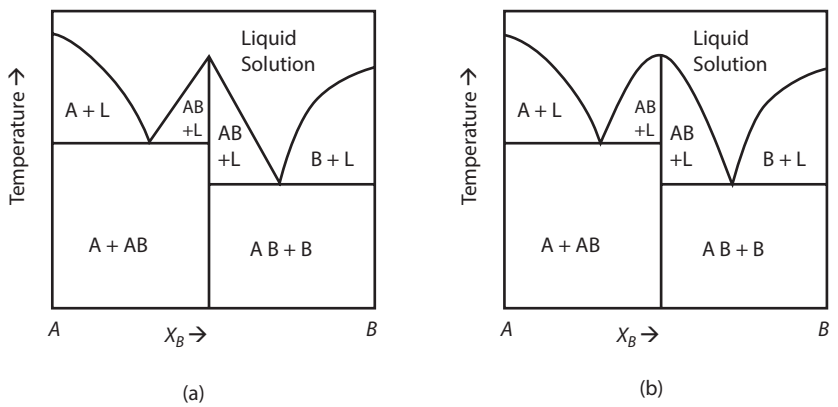

FIGURE 10.20 (a) A constant pressure temperature/composition phase diagram that displays the equilibria near the congruent melting of the AB compound incorrectly. (b) Corrected version of the phase diagram showing the liquidus curves with a maximum with zero slope. In these diagrams, it is the solubility of B in either the liquid or solid phase of A and the solubility of A in either the liquid or solid phase B is very small and cannot be depicted on the diagram.

10.8 EXAMPLES OF INCORRECT BINARY PHASE DIAGRAM CONFIGURATIONS

A phase diagram that incorrectly displays a congruently melting intermediate compound phase is shown in Figure 10.20a. The two liquid/compound phase boundaries must meet at *zero slope* and be drawn as shown in Figure 10.20b, in accord

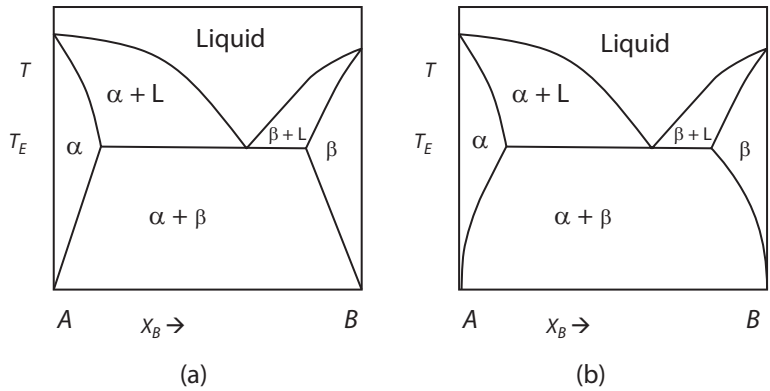

FIGURE 10.21 (a) A binary eutectic phase diagram (a) which displays the α and β solvi boundaries which do not have slopes approaching + or − infinity at *d* and *e,* respectively at 0 K. (b) Corrected eutectic phase diagram.

with the Gibbs-Konovalov rule. Such incorrect drawings of phase diagrams can lead to drastic misunderstandings of the phase equilibria in these systems. Care must be made of conclusions based on such misunderstandings.

A temperature composition phase diagram displaying an eutectic is shown in Figure 10.21a. It correctly shows that the composition of the α phase approaches $X_B = 0$ and that of the β phase approaches 1 as the temperature approaches 0 K, this being a Third Law constraint on the phase diagram. However, the slope of the T X_B plot at $X_B = 0$ and 1 should be $+\infty$ and $-\infty$, respectively. This can be seen from Equation 9.74 and was the subject of Problem 9.17* if we assume that the α + β phase field is a miscibility gap.

There are many other kinds of errors in construction that appear in published phase diagrams. Some of these are discussed in *Construction of equilibrium phase diagrams: some errors to be avoided*, David E Laughlin, T.B. Massalski - *Progress in Materials Science*, 2021.

10.9 MAGNETIC TRANSFORMATIONS AND THE PHASE DIAGRAM

Figure 10.22 shows a portion of the Fe-C (metastable) phase diagram. In the diagram, the paramagnetic BCC phase is denoted as the β phase, and its *ferromagnetic* conjugate phase is denoted as the α phase. It can be seen that as carbon is added to Fe, the transformation temperature between the paramagnetic β phase and the ferromagnetic α phase (the Curie temperature) is lowed. The line of transformation eventually intersects the boundary of the two-phase β + γ region, after which the Curie temperature is shown to be horizontal. (At these temperatures, the γ phase of Fe is paramagnetic). Along and above the *dot-dash* line, the β and γ phases are in equilibrium, and below the line, the α and γ phases are in equilibrium. Note that in this case the horizontal line is not an invariant three phase region, as only two phases exist on the line, namely the *paramagnetic* β BCC phase and the γ phase.

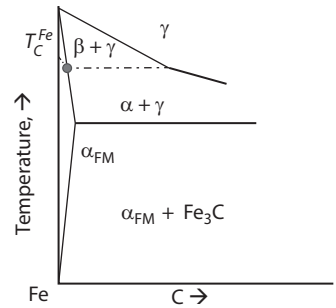

FIGURE 10.22 Schematic of a portion of the metastable Fe-C constant pressure temperature/composition phase diagram showing the intersection of the Curie line with a two phase region. This line produces two phase regions separated by a horizontal line (*dot-dash*) which corresponds to the Curie temperature of the α_{FM} phase which is saturated with C.

The intersection of the horizontal line with the phase boundaries brings with it a subtle change in the slope of the phase boundaries since the boundaries represent different but related phase equilibria.

10.10 SUMMARY

1. The molar Gibbs free energy of formation of binary solution *A–B* is given by

$$\Delta G^M = RT\left(X_A \ln a_A + X_B \ln a_B\right)$$

2. For a regular solution, the *excess Gibbs free energy* is defined as:

$$\Delta G^M - \Delta G^{M,\text{id}} = G^{\text{xs}} = \alpha X_A X_B = \Delta H^M$$

3. The criteria for equilibrium between the phases α and β in the binary system *A–B* are

$$a_A\left(\text{in } \alpha\right) = a_A\left(\text{in } \beta\right)$$

and

$$a_B\left(\text{in } \alpha\right) = a_B\left(\text{in } \beta\right)$$

4. Binary phase diagrams displaying invariant reactions include eutectic, eutectoid, peritectic, peritectoid, monotectic, monotectoid, and metatectic.
5. Immiscibility becomes imminent in a regular solution at the critical value of $\alpha/RT = 2$. The critical temperature, below which immiscibility occurs in a regular system, is given by $T_{\text{cr}} = \alpha/2R$.
6. In a binary system *A–B* which forms ideal liquid solutions and ideal solid solutions, the solidus is given by

$$X_{A(s)} = \frac{1 - \exp\left(-\Delta G^{\circ}_{m(B)}/RT\right)}{\exp\left(-\Delta G^{\circ}_{m(A)}/RT\right) - \exp\left(-\Delta G^{\circ}_{m(B)}/RT\right)}$$

and the liquidus line is given by

$$X_{A(l)} = \frac{\left[1 - \exp\left(-\Delta G^{\circ}_{m(B)}/RT\right)\right]\exp\left(-\Delta G^{\circ}_{m(A)}/RT\right)}{\exp\left(-\Delta G^{\circ}_{m(A)}/RT\right) - \exp\left(-\Delta G^{\circ}_{m(B)}/RT\right)}$$

7. In a binary system *A*–*B* which contains a eutectic equilibrium and in which the extent of solid solution is negligibly small, the liquidus lines are determined by the conditions

$$\Delta G^{\circ}_{m(A)} = -RT \ln a_A \left(\text{in the } A\text{ - liquidus melt}\right)$$

and

$$\Delta G^{\circ}_{m(B)} = -RT \ln a_B \left(\text{in the } B\text{ - liquidus melt}\right)$$

8. Thus, if the liquid solutions are ideal, the *A*-liquidus compositions are given by

$$-\Delta G^{\circ}_{m(A)} = RT \ln X_A$$

and if the liquid solutions are regular, the *A*-liquidus compositions are given by

$$-\Delta G^{\circ}_{m(A)} = RT \ln X_A + \alpha\left(1 - X_A\right)^2$$

9. The slopes of the phase boundaries temperature composition binary phase diagrams can be expressed in terms of thermodynamic parameters such as heats of transformation, curvatures of Gibbs free energy *versus* composition plots and entropies of transformation.
10. In constructing phase diagrams, various thermodynamic relationships place constraints on the way the phase boundaries are topologically related to each other.
11. Higher-order phase transition temperatures such as Curie temperatures of ferromagnetic phases can be displayed on phase diagrams, but they do not follow the same thermodynamic constraints as first-order phase transformations. In particular, the Gibbs Equilibrium Phase Rule is not valid for such transformations.

10.11 CONCEPTS AND TERMS INTRODUCED IN THIS CHAPTER

The reader should write out brief definitions or descriptions of the following terms. Where appropriate, equations may be used.

Common tangent
Congruent temperature
Congruent transformation
Constituent

Eutectic phase diagram
Eutectoid phase diagram
Gibbs free energy versus composition curves
Gibbs–Konovalov rule
Horizontal inflection point
Hypereutectic reaction
Hypoeutectic reaction
Invariant transformation temperatures
Lens phase diagram
Liquidus curve
Metatectic phase diagram
Molar free energy of melting
Monotectic phase diagram
Monotectoid phase diagram
Peritectic phase diagram
Peritectoid phase diagram
Solidus curve
Standard state
Syntectic phase diagram
Temperature versus composition phase diagram
Third Law constraints

10.12 QUALITATIVE EXAMPLE PROBLEMS

QUALITATIVE PROBLEM 1

Part of the binary phase diagram is shown in Figure 10.23a. When a magnetic field is applied, the solubility of the β phase decreases, as shown by the dotted line. Using Gibbs free energy plots of the α and β phases, determine which phase has the larger magnetic susceptibility.

SOLUTION TO QUALITATIVE PROBLEM 1

The Gibbs free energy plots for the α and β phases are shown in Figure 10.23b. Since the solubility of β has decreased, its free energy curve must have decreased more than that of the α phase in order for the common tangent to move to the left. Hence, the β phase must have the larger magnetic susceptibility. As in the case discussed in Section 7.8, applying a magnetic field enlarges the *region of stability* of the phase with the higher *magnetic susceptibility.*

QUALITATIVE PROBLEM 2

All regular solutions with positive enthalpies of mixing have the same value of the activity of its components (*A* or *B*) at the critical point of the miscibility gap that is at $X_B = 0.5$. Calculate the activity a_A and a_B at T_C for a regular solution with regular solution constant α.

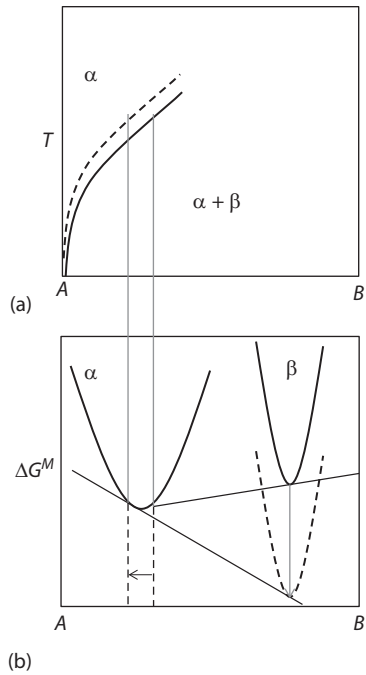

FIGURE 10.23 (a) The *A*-rich section of a binary phase diagram showing the shift in the β solvus when an external magnetic field is applied. (b) The corresponding Gibbs free energy curves for the phases displayed in (a). In this case $\chi_\beta > \chi_\alpha$.

SOLUTION TO QUALITATIVE PROBLEM 2

At the critical temperature,

$$RT_c \ln a_B = \bar{G}_B(0.5) = \Delta G^M(0.5) = \Delta H^M(0.5) - T_c \Delta S^M(0.5$$

$$RT_c \ln a_B(0.5) = \Delta H^M(0.5) - T_c \Delta S^M(0.5)$$

$$R\left(\frac{\alpha}{2R}\right)\ln a_B(0.5) = \frac{\alpha}{4} - \left(\frac{\alpha}{2R}\right)R\ln 2$$

$$a_B(0.5) = 0.824$$

10.13 QUANTITATIVE EXAMPLE PROBLEMS

QUANTITATIVE PROBLEM 1

The phase diagram for the system Cs–Rb is shown in Figure 10.24. Examine the extent to which the phase diagram can be reproduced, assuming that the liquid solutions are ideal and that the solid solutions are regular.

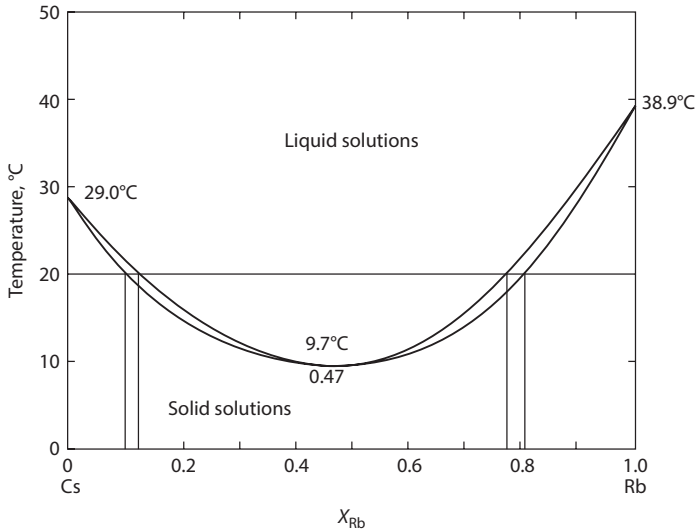

FIGURE 10.24 The phase diagram for the system Cs–Rb.

For Cs:

$$\Delta G^{\circ}_{m,\mathrm{Cs}} = 2100 - 6.95T \text{ J}$$

and for Rb:

$$\Delta G^{\circ}_{m,\mathrm{Rb}} = 2200 - 7.05T$$

SOLUTION TO QUANTITATIVE PROBLEM 1

Initially, draw the Gibbs free energy of mixing curves for the solid and liquid solutions at 9.7°C (282.7 K) and determine if some value of α gives Gibbs free energy of mixing curves similar to those shown in Figure 10.15c; that is, the curve for the liquid solutions lies above the curve for the solid solutions, except at a single composition where the two curves touch one another.

Relative to the pure solids as standard states at the temperature T,

$$\begin{aligned}\Delta G^{M}\left(\text{liquid solutions}\right) = {} & X_{Rb}\Delta G^{\circ}_{m,Rb} + X_{Cs}\Delta G^{\circ}_{m,Cs} \\ & + RT\left(X_{Rb}\ln X_{Rb} + X_{Cs}\ln X_{Cs}\right)\end{aligned} \tag{i}$$

which, at 282.7 K, becomes

$$\begin{aligned}\Delta G^{M}\left(\text{liquid solutions}\right) = {} & 205X_{Rb} + 133\left(1 - X_{Rb}\right) + 8.3144 \times 282.7 \\ & \times\left[X_{Rb}\ln X_{Rb} + \left(1 - X_{Rb}\right)\ln\left(1 - X_{Rb}\right)\right]\end{aligned}$$

Also,

$$\Delta G^M\left(\text{solid solutions}\right) = RT\left(X_{Rb}\ln X_{Rb} + X_{Cs}\ln X_{Cs}\right) + \alpha X_{Rb}X_{Cs} \qquad \text{(ii)}$$

Which at 282.7 K becomes

$$\Delta G^M\left(\text{solid solutions}\right) = 8.3144 \times 282.7 \times \left(X_{Rb}\ln X_{Rb} + X_{Cs}\ln X_{Cs}\right) + \alpha X_{Rb}X_{Cs}$$

The Gibbs free energy of mixing curves, drawn with $\alpha = 668$ J, are shown in Figure 10.25, which shows that the curves touch one another at $X_{\text{Rb}} = 0.47$, in exact agreement with Figure 10.24.

The Gibbs free energies of mixing, given by Equations (i) and (ii), with = 668 J and $T = 293$ K, are shown in Figure 10.25b. The common tangent at the Cs-rich side of the diagram gives the solidus composition as $X_{\text{Rb}} = 0.10$ and the liquidus composition as $X_{\text{Rb}} = 0.13$, which is in excellent agreement with the phase diagram. At the Rb-rich side of the diagram, the double tangent gives the solidus and liquidus compositions as, respectively, $X_{\text{Rb}} = 0.81$, and $X_{\text{Rb}} = 0.75$, which are in good agreement with the phase diagram values of 0.80 and 0.77.

It is thus seen that the phase diagram is reproduced by assuming that the liquid solutions are ideal and the solid solutions are regular with $\alpha = 668$ J.

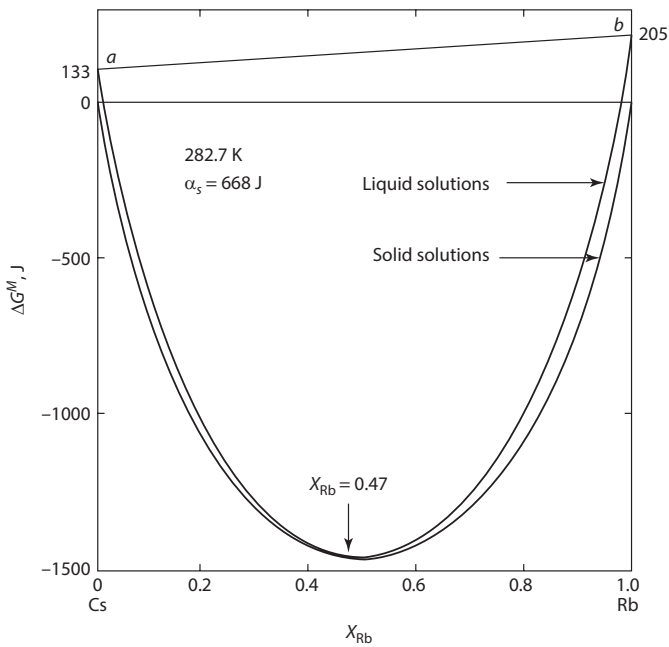

FIGURE 10.25a The molar Gibbs free energy of mixing curves for ideal liquid solutions and regular solid solutions (with $\alpha_S = 668$ J) at 282.7 K, drawn using the Gibbs free energies of melting of Cs and Rb.

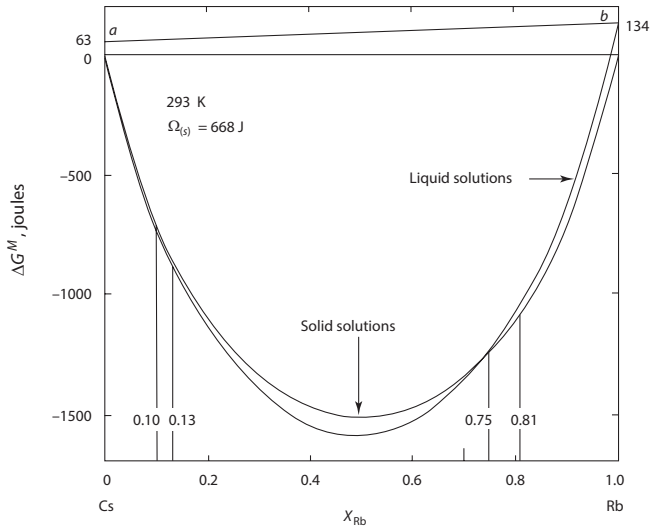

FIGURE 10.25b The molar Gibbs free energy of mixing curves for ideal liquid solutions and regular solid solutions (with $\alpha_S = 668$ J) at 293 K, drawn using the Gibbs free energies of melting of Cs and Rb.

QUANTITATIVE PROBLEM 2

The Ge–Si System

The system Ge–Si exhibits the complete ranges of liquid and solid solutions.

a. Calculate the phase diagram for the system assuming that the solid and liquid solutions are Raoultian in their behavior.
b. Calculate the temperature at which the liquidus (and hence the solidus) composition exerts its maximum vapor pressure.

Given:
Silicon melts at 1685 K, and its standard Gibbs free energy change on melting is

$$\Delta G^{\circ}_{m,\mathrm{Si}} = 50,200 - 29.8T \text{ J}$$

The saturated vapor pressure of solid Si is

$$\log p^{\circ}_{\mathrm{Si}(s)}(\mathrm{atm}) = -\frac{23,550}{T} - 0.565 \log T + 9.47$$

Germanium melts at 1213 K and its standard Gibbs free energy change on melting is

$$\Delta G^{\circ}_{m,\mathrm{Ge}} = 36,800 - 30.3T \text{ J}$$

The saturated vapor pressure of liquid Ge is

$$\log p^{\circ}_{\mathrm{Ge}(l)}\,(\mathrm{atm}) = -\frac{18,700}{T} - 0.565\log T + 9.99$$

SOLUTION TO QUANTITATIVE PROBLEM 2a

The equation of the liquidus curve is obtained from Equation 10.5 as

$$X_{\mathrm{Ge},(\mathrm{liquidus}),T} = \frac{\exp\left(\dfrac{-\Delta G^{\circ}_{m,\mathrm{Ge}}}{RT}\right)\left[1-\exp\left(\dfrac{-\Delta G^{\circ}_{m,\mathrm{Si}}}{RT}\right)\right]}{\exp\left(\dfrac{-\Delta G^{\circ}_{m,\mathrm{Ge}}}{RT}\right)-\exp\left(\dfrac{-\Delta G^{\circ}_{m,\mathrm{Si}}}{RT}\right)}$$

and the equation of the solidus curve is obtained from Equation 10.4 as

$$X_{\mathrm{Ge},(\mathrm{solidus}),T} = \frac{1-\exp\left(\dfrac{-\Delta G^{\circ}_{m,\mathrm{Si}}}{RT}\right)}{\exp\left(\dfrac{-\Delta G^{\circ}_{m,\mathrm{Ge}}}{RT}\right)-\exp\left(\dfrac{-\Delta G^{\circ}_{m,\mathrm{Si}}}{RT}\right)}$$

The calculated liquidus and solidus curves are shown in comparison with the measured lines in Figure 10.26a.

SOLUTION TO QUANTITATIVE PROBLEM 2b

The partial pressure of Si exerted by the solidus composition (and hence by the corresponding liquidus melt) at the temperature T is

$$p_{\mathrm{Si},T} = X_{\mathrm{Si},(\mathrm{solidus}),T} \times p^{\circ}_{\mathrm{Si},(s),T} \tag{i}$$

and the partial pressure of Ge exerted by the liquidus melt composition (and hence by the corresponding solidus) is

$$p_{\mathrm{Ge},T} = X_{\mathrm{Ge},(\mathrm{liquidus}),T} \times p^{\circ}_{\mathrm{Ge},(l),T} \tag{ii}$$

Equations (i) and (ii), together with the sum of the partial pressures, are shown in Figure 10.26b. In Equation (i) the values of both $X_{\mathrm{Si},(\mathrm{solidus}),\,T}$ and $p^{\circ}_{\mathrm{Si},(s),T}$ increase with increasing liquidus temperature, and thus, the partial pressure of Si exerted by the liquidus composition increases from zero at 1213 K to the saturated vapor pressure of pure solid Si $\left(\log p^{\circ}_{\mathrm{Si},(s),1683\,\mathrm{K}} = -6.33\right)$ at 1683 K. In contrast, in Equation (ii), increasing the liquidus temperature causes an increase in $p^{\circ}_{\mathrm{Ge},(l),T}$ and a decrease in $X_{\mathrm{Ge},(\mathrm{liquidus}),T}$, and Figure 10.26b shows that, at lower liquidus temperatures, the influence of $p^{\circ}_{\mathrm{Ge},(l),T}$ on the partial pressure of Ge predominates and the partial pressure

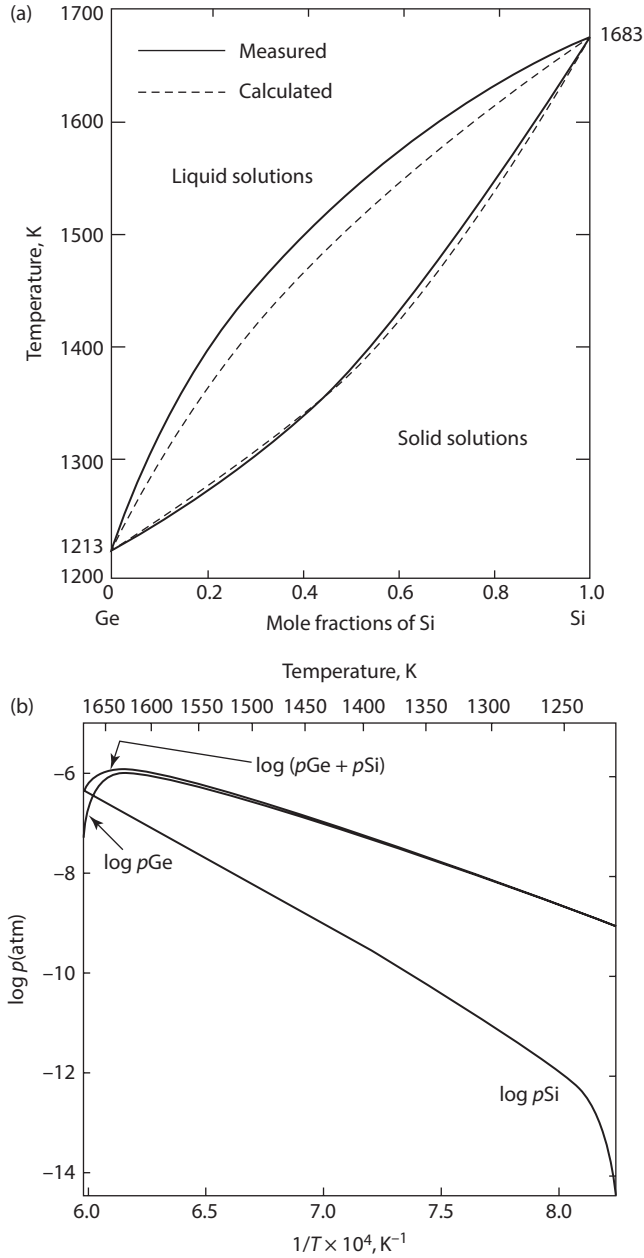

FIGURE 10.26 (a) The calculated phase diagram for the system Ge–Si assuming Raoultian behavior of the solid and liquid solutions. (b) The variations, with temperature, of the partial pressures of Ge and Si (and their sum) with composition along the liquidus line.

initially increases with increasing liquidus temperature. However, with the continued increase in temperature along the liquidus line, the relative influence of the dilution of Ge increases, and the partial pressure of Ge passes through a maximum at the liquidus state $X_{Ge} = 0.193$, $T = 1621$ K before decreasing rapidly to zero at 1683 K. The maximum in the partial pressure of Ge causes a maximum in the total vapor pressure to occur at the liquidus state $X_{Ge} = 0.165$, $T = 1630$ K.

PROBLEMS

10.1 CaF_2 and MgF_2 are mutually insoluble in the solid state and form a simple binary eutectic system. Calculate the composition and temperature of the eutectic melt assuming that the liquid solutions are Raoultian. The actual eutectic occurs at $X_{CaF_2} = 0.45$ and $T = 1243$ K.

10.2 Gold and silicon are mutually insoluble in the solid state and form a eutectic system with a eutectic temperature of 636 K and a eutectic composition of $X_{Si} = 0.186$. Calculate the Gibbs free energy of the eutectic melt relative to (a) unmixed liquid Au and liquid Si, and (b) unmixed solid Au and solid Si.

$$\text{At 636 K } \Delta G^{\circ}_{m,\text{Au}} = 12{,}600\left[\frac{1338-636}{1338}\right] = 6{,}611 \text{ J}$$

$$\text{and } \Delta G^{\circ}_{m,\text{Si}} = 50{,}200\left[\frac{1685-636}{1685}\right] = 30{,}943 \text{ J}$$

10.3 Al_2O_3, which melts at 2324 K, and Cr_2O_3, which melts at 2538 K, form complete ranges of solid and liquid solutions. Assuming that $\Delta S^{\circ}_{m,Cr_2O_3} = \Delta S^{\circ}_{m,Al_2O_3}$ and that the solid and liquid solutions in the system Al_2O_3–Cr_2O_3 behave ideally, calculate

a. The temperature at which equilibrium melting begins when an alloy of $X_{Al_2O_3} = 0.5$ is heated
b. The composition of the melt which first forms
c. The temperature at which equilibrium melting is complete
d. The composition of the last-formed solid

10.4 $Na_2O{\cdot}B_2O_3$ and $K_2O{\cdot}B_2O_3$ form complete ranges of solid and liquid solutions and the solidus and liquidus show a common minimum at the equimolar composition and $T = 1123$ K. Calculate the molar Gibbs free energy of formation of the equimolar solid solution from solid $Na_2O{\cdot}B_2O_3$ at 1123 K, assuming that the liquid solutions are ideal.

10.5 SiO_2, which melts at 1723°C, and TiO_2, which melts at 1842°C, are immiscible in the solid state, and the SiO_2–TiO_2 binary system contains a monotectic equilibrium at 1794°C, at which temperature virtually pure TiO_2 is in equilibrium with two liquids containing mole fractions of SiO_2 of 0.04 and 0.76. If, for the purpose of simple calculation, it is assumed that the compositions of the two liquids are $X_{SiO_2} = 0.24$ and $X_{SiO_2} = 0.76$ and that the liquid solutions are regular in their behavior, what is the value of α_l and at what temperature does the liquid immiscibility gap disappear?

10.6 The binary system Ge–Si contains complete solid and liquid solutions. The melting temperatures are $T_{m,\mathrm{Si}} = 1685$ K and $T_{m,\mathrm{Ge}} = 1210$ K, and $\Delta H^{\circ}_{m,\mathrm{Si}} = 50,200$ J. At 1200°C, the liquidus and solidus compositions are, respectively, $X_{\mathrm{Si}} = 0.32$ and $X_{\mathrm{Si}} = 0.665$. Calculate the value of $\Delta H^{\circ}_{m,\mathrm{Ge}}$, assuming that

a. The liquid solutions are ideal.
b. The solid solutions are ideal.

Which assumption gives the better estimate? The actual value of $\Delta H^{\circ}_{m,\mathrm{Ge}}$ at $T_{m,\mathrm{Ge}}$ is 36,900 J.

10.7 CaO and MgO form a simple eutectic system with limited ranges of solid solubility. The eutectic temperature is 2370°C. Assuming that the solutes in the two solid solutions obey Henry's law with $\gamma^{\circ}_{\mathrm{CaO}}$ in MgO = 12.88 and $\gamma^{\circ}_{\mathrm{MgO}}$ in CaO = 6.23 at 2300°C, calculate the solubility of CaO in MgO and the solubility of MgO in CaO at 2300°C.

10.8 A metatectic binary phase diagram displays the following invariant transformation on cooling:

$$\beta \rightarrow \alpha + \mathrm{L}$$

Sketch such a phase diagram and then draw free energy curves of mixing just below, at, and just above the invariant temperature.

10.9* Consider a binary phase diagram in the vicinity of the melting temperature of component *A*. See Figure 10.27.

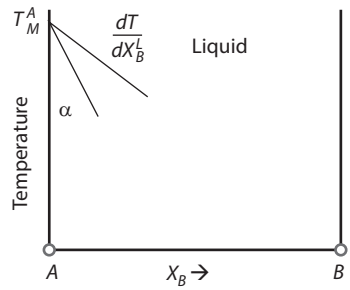

FIGURE 10.27 Portion of a constant pressure, temperature composition binary phase diagram, showing the solidus and liquidus of the phases a and *L*.

Show that if the solubility *B* in the solid α is negligible, the slope of the liquidus is:

$$\frac{dT}{dX_B^{\mathrm{L}}} = -\frac{RT_M}{\Delta S_A^{0(\alpha \rightarrow \mathrm{L})}}$$

This is a version of the van't Hoff relationship.

Hint: Start with Equations 10.12 and 10.13.

10.10* Use the van't Hoff relationship derived in Problem 10.9 to show that the initial slope of the liquidus projects to between 100% and 115%B at 0 K for BCC and FCC systems.

Hint: Use the findings of Richard's shown in Figure 6.15 of the text.

10.11 The phase diagram of an alloy that has a eutectoid transformation is shown in Figure 10.28 (below).
a. Sketch the Gibbs free energy curves for this alloy at $T = T'$.
b. Show that the α/γ solvus must enter the α/β two phase field (as shown by the arrow).

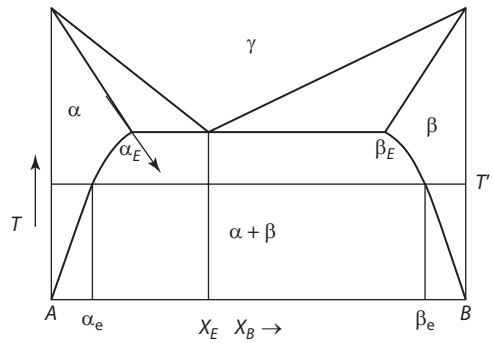

FIGURE 10.28 A eutectoid phase diagram showing the extension of the α/γ equilibrium curve into the α/β solvus.

10.12 An eutectoid phase diagram is shown in Figure 10.28. Draw the phase diagram that would result if for some reason it were impossible to form the α phase.

10.13* An A-B alloy has a liquid miscibility gap at high temperatures and a eutectic "gap" at low temperatures. Sketch a possible temperature/composition phase diagram for this alloy.

10.14* The phase diagram shown in Figure 10.29 was found in a textbook.
a. Circle regions of the phase diagram that have been drawn incorrectly and state what thermodynamic principle is violated.
b. Redraw the phase diagram without any of the errors noted.

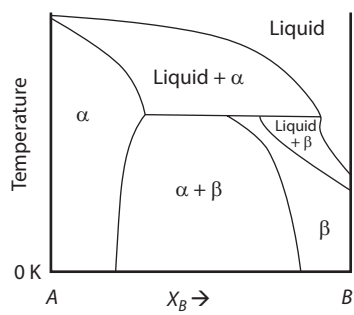

FIGURE 10.29 A constant pressure binary phase diagram that displays several errors of construction.

10.15* A pressure *vs. activity* plot of binary system at constant temperature is shown in Figure 10.30. Plot the corresponding Pressure vs. X_B plot keeping in mind invariant reactions, which are delineated by the dashed lines.

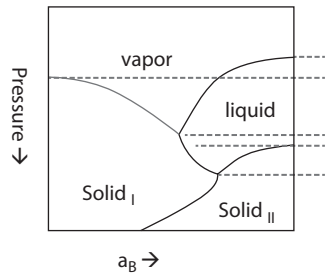

FIGURE 10.30 A constant temperature, pressure vs. activity binary phase diagram.

10.16* At 0 K three phases exist in an AB alloy: pure A, an FCC phase (α), a pure B, a FCC phase (β) and an intermediate ordered phase, $L1_0$ 50% B. The liquid phase of less than 50% B decomposes eutectically to α plus $L1_0$. When the liquid phase is greater than 50% B it decomposes to $L1_0$ plus the β phase. At 50% B the liquid phase freezes congruently to the $L1_0$ phase.

i. Sketch the phase diagram with the above information.
ii. Discuss what the slopes of the phase boundaries must be as the *T* approaches 0 K.

APPENDIX 10A

The equations for the phase diagram of a system that consists of ideal solid and ideal liquid solutions are derived in this appendix.

For equilibrium between the solid and liquid phases,

$$\Delta\bar{G}_A^M\left(\text{in the solid solution}\right) = \Delta\bar{G}_A^M\left(\text{in the liquid solution}\right) \tag{10A.1}$$

and

$$\Delta\bar{G}_B^M\left(\text{in the liquid solution}\right) = \Delta\bar{G}_B^M\left(\text{in the solid solution}\right) \tag{10A.2}$$

At any temperature *T*, these two conditions fix the solidus and liquidus compositions—that is, the position of the points of common tangency. From Equation 10.2:

$$\frac{\partial\Delta G_{(l)}^M}{\partial X_{A(l)}} = RT\left(\ln X_{A(l)} - \ln X_{B(l)}\right) - \Delta G^\circ_{m(B)}$$

* New problem in this edition.

Thus,

$$X_{B(l)}\frac{\partial \Delta G^{M}_{(l)}}{\partial X_{A(l)}} = RT\left(X_{B(l)}\ln X_{A(l)} - X_{B(l)}\ln X_{B(l)}\right) - X_{B(l)}\Delta G^{\circ}_{m(B)} \qquad (10A.3)$$

From Equation 9.33a:

$$\Delta \bar{G}^{M}_{A}\left(\text{in liquid solutions}\right) = \Delta G^{M}_{(l)} + X_{B(l)}\frac{\partial \Delta G^{M}_{(l)}}{\partial X_{A(l)}}$$

Thus, adding Equations 10.2 and 10A.3 gives

$$\Delta \bar{G}^{M}_{A}\left(\text{in liquid solutions}\right) = RT\ln X_{A(l)} \qquad (10A.4)$$

From Equation 10.3:

$$\frac{\partial \Delta G^{M}_{(s)}}{\partial X_{A(s)}} = RT\left(\ln X_{A(s)} - \ln X_{B(s)}\right) - \Delta G^{\circ}_{m(A)}$$

Thus,

$$X_{B(s)}\frac{\partial \Delta G^{M}_{(s)}}{\partial X_{A(s)}} = RT\left(X_{B(s)}\ln X_{A(s)} - X_{B(s)}\ln X_{B(s)}\right) - X_{B(s)}\Delta G^{\circ}_{m(A)} \qquad (10A.5)$$

Adding Equations 10.3 and 10A.5 gives

$$\Delta \bar{G}^{M}_{A}\left(\text{in solid solutions}\right) = \Delta G^{M}_{(s)} + X_{B(s)}\frac{\partial \Delta G^{M}_{(s)}}{\partial X_{A(s)}} = RT\ln X_{A(s)} - \Delta G^{\circ}_{m(A)} \qquad (10A.6)$$

Thus, from Equations 10A.1, 10A.4 and 10A.6:

$$RT\ln X_{A(l)} = RT\ln X_{A(s)} - \Delta G^{\circ}_{m(A)} \qquad (10A.7)$$

Similarly, from Equations 10.2 and 9.33b:

$$\Delta \bar{G}^{M}_{B}\left(\text{in liquid solutions}\right) = \Delta G^{M}_{(l)} + X_{A(l)}\frac{\partial \Delta G^{M}_{(l)}}{\partial X_{B(l)}} = RT\ln X_{B(l)} + \Delta G^{\circ}_{m(B)} \qquad (10A.8)$$

and from Equations 10.3 and 9.33b:

$$\Delta \bar{G}^{M}_{B}\left(\text{in solid solutions}\right) = \Delta G^{M}_{(s)} + X_{A(s)}\frac{\partial \Delta G_{(s)}}{\partial X_{B(s)}} = RT\ln X_{B(s)} \qquad (10A.9)$$

Thus, from Equations 10A.2, 10A.8, and 10A.9:

$$RT\ln X_{B(l)} + \Delta G^{\circ}_{m(B)} = RT\ln X_{B(s)} \qquad (10A.10)$$

The solidus and liquidus compositions are thus determined by Equations 10A.7 and 10A.10 as follows. Equation 10A.7 can be written as

$$X_{A(l)} = X_{A(s)} \exp\left(\frac{-\Delta G^{\circ}_{m(A)}}{RT}\right) \tag{10A.11}$$

and, noting that $X_B = 1 - X_A$, Equation 10A.10 can be written as

$$\left(1 - X_{A(l)}\right) = \left(1 - X_{A(s)}\right) \exp\left(\frac{-\Delta G^{\circ}_{m(B)}}{RT}\right) \tag{10A.12}$$

Combination of Equations 10A.11 and 10A.12 gives

$$X_{A(s)} = \frac{1 - \exp\left(-\dfrac{\Delta G^{\circ}_{m(B)}}{RT}\right)}{\exp\left(-\dfrac{\Delta G^{\circ}_{m(A)}}{RT}\right) - \exp\left(-\dfrac{\Delta G^{\circ}_{m(B)}}{RT}\right)} \tag{10A.13}$$

and

$$X_{A(l)} = \frac{\left[1 - \exp\left(-\dfrac{\Delta G^{\circ}_{m(B)}}{RT}\right)\right] \exp\left(-\dfrac{\Delta G^{\circ}_{m(A)}}{RT}\right)}{\exp\left(-\dfrac{\Delta G^{\circ}_{m(A)}}{RT}\right) - \exp\left(-\dfrac{\Delta G^{\circ}_{m(B)}}{RT}\right)} \tag{10A.14}$$

If $c_{p,i(s)} = c_{p,i(l)}$, we get from Equation 10.1, for $i = A$ and B,

$$\Delta G^{\circ}_{m(i)} = \Delta H^{\circ}_{m(i)} \left[\frac{T_{m(i)} - T}{T_{m(i)}}\right]$$

Thus, the phase diagram for a system that forms ideal solid and liquid solutions is determined only by the melting temperatures and the molar heats of melting of the components.

APPENDIX 10B

Consider the application of Equation 10.12 to the calculation of the liquidus lines in a binary eutectic system. In the system Cd–Bi, the phase diagram for which is shown in Figure 10.11, cadmium is virtually insoluble in solid bismuth, and the maximum solubility of bismuth in solid cadmium is 2.75 mole percent at the eutectic temperature of 419 K. If the liquidus solutions are ideal, the Bi liquidus is obtained from Equation 10.8a as

$$\Delta G^{\circ}_{m(\mathrm{Bi})} = -RT \ln X_{\mathrm{Bi(liquidus)}}$$

$$\Delta H^{\circ}_{m(\mathrm{Bi})} = 10{,}900 \text{ J at } T_{m(\mathrm{Bi})} = 544 \text{ K, and thus,}$$

$$\Delta S^{\circ}_{m(\mathrm{Bi})} = \frac{10{,}900}{544} = 20.0 \text{J/K at } 544\text{K}$$

The molar constant pressure heat capacities of solid and liquid bismuth vary with temperature as

$$c_{p,\mathrm{Bi}(s)} = 18.8 + 22.6\times10^{-3}T \text{ J/K}$$

$$c_{p,\mathrm{Bi}(l)} = 20 + 6.15\times10^{-3}T + 21.1\times10^{5}T^{-2} \text{ J/K}$$

Thus,

$$c_{p,\mathrm{Bi}(l)} - c_{p,\mathrm{Bi}(s)} = \Delta c_{p,\mathrm{Bi}} = 1.2 - 16.45\times10^{-3}T + 21.1\times10^{5}T^{-2} \text{ J/K}$$

and

$$\Delta G^{\circ}_{m(\mathrm{Bi})} = \Delta H^{\circ}_{m(\mathrm{Bi}),544} + \int_{544}^{T} \Delta c_{p,\mathrm{Bi}}\,dT - T\left(\Delta S^{\circ}_{m(\mathrm{Bi}),544} + \int_{544}^{T} \frac{\Delta c_{p,Bi}}{T}\,dT\right)$$

$$= 16{,}560 - 23.79T - 1.2T\ln T + 8.225\times10^{-3}T^{2} - 10.22\times10^{5}T^{-1} \qquad (10\text{B.1})$$

$$= -RT\ln X_{\mathrm{Bi(liquidus)}}$$

or

$$\ln X_{\mathrm{Bi(liquidus)}} = -\frac{1992}{T} + 2.861 + 0.144\ln T - 9.892\times10^{-4}T + 1.269\times\frac{10^{5}}{T^{2}}$$

This equation is drawn as the broken line (i) in Figure 10.11.

Similarly, if the small solid solubility of Bi in Cd is ignored,

$$\Delta G^{\circ}_{m(\mathrm{Cd})} = -RT\ln X_{\mathrm{Cd(liquidus)}}$$

$\Delta H^{\circ}_{m(\mathrm{Cd})} = 6400$ J at $T_{m,\mathrm{Cd}} = 594$ K, and thus, $\Delta S^{\circ}_{m(\mathrm{Cd})} = 6400/594 = 10.77$ J/K at 594 K. The constant-pressure molar heat capacities are

$$c_{p,\mathrm{Cd}(s)} = 22.2 + 12.3\times10^{-3}T \text{ J/K}$$

and

$$c_{p,\mathrm{Cd}(l)} = 29.7 \text{ J/K}$$

Thus,

$$c_{p,\mathrm{Cd}(l)} - c_{p,\mathrm{Cd}(s)} = \Delta c_{p,\mathrm{Cd}} = 7.5 - 12.3\times10^{-3}T \text{ J/K}$$

$$\Delta G^{\circ}_{m(\mathrm{Cd})} = \Delta H^{\circ}_{m(\mathrm{Cd}),594} + \int_{594}^{T} \Delta c_{p,\mathrm{Cd}}\, dT - T\left(\Delta S^{\circ}_{m(\mathrm{Cd}),594} + \int_{594}^{T} \frac{\Delta c_{p,\mathrm{Cd}}}{T}\, dT \right)$$

$$= 4155 + 37.32T - 7.5T \ln T + 6.15 \times 10^{-3} T^2 \text{ J} \qquad \text{(10B.2)}$$

$$= -RT \ln X_{\mathrm{Cd(liquidus)}}$$

or

$$\ln X_{\mathrm{Cd(liquidus)}} = -\frac{495}{T} - 4.489 + 0.90 \ln T - 7.397 \times 10^{-4} T$$

which is drawn as the broken line (ii) in Figure 10.11. Lines (i) and (ii) intersect at the composition of the Raoultian liquid which is simultaneously saturated with Cd and Bi and at 406 K, which would be the eutectic temperature if the liquids were ideal. The actual liquidus lines lie above those calculated, and the actual eutectic temperature is 419 K. From Equation 10B.1, $\Delta G^{\circ}_{m(\mathrm{Bi}),419\,\mathrm{K}} = 2482$ J, and from Equation 10B.2, $\Delta G^{\circ}_{m(\mathrm{Cd}),419\,\mathrm{K}} = 1898$ J. Thus, from Equation 10.8a, in the actual eutectic melt,

$$a_{\mathrm{Bi}} = \exp\left(-\frac{2482}{8.3144 \times 419} \right) = 0.49$$

and

$$a_{\mathrm{Cd}} = \exp\left(-\frac{1898}{8.3144 \times 419} \right) = 0.58$$

The actual eutectic composition is $X_{\mathrm{Cd}} = 0.55$, $X_{\mathrm{Bi}} = 0.45$, and thus, the activity coefficients are

$$\gamma_{\mathrm{Bi}} = \frac{0.49}{0.45} = 1.09$$

and

$$\gamma_{\mathrm{Cd}} = \frac{0.58}{0.55} = 1.05$$

Thus, positive deviations from Raoultian ideality cause an increase in the liquidus temperatures.

Part III

Reactions and Transformations of Phases

Taylor & Francis
Taylor & Francis Group
http://taylorandfrancis.com

11 Reactions Involving Gases

11.1 INTRODUCTION

In Chapter 8, it was stated that the absence of interatomic forces between the atoms of ideal gases causes the enthalpy of the mixing of ideal gases to be zero. This situation represents one extreme of a range of possible situations. Toward the other extreme of this range is the situation in which gases are mixed which exhibit marked chemical affinity for one another. For example, when gaseous hydrogen and oxygen are mixed in the presence of a catalyst, considerable heat is released. The thermodynamics of such a system can be treated in either of two ways:

1. The mixture can be considered to be a highly *nonideal* mixture of H_2 and O_2, the thermodynamic equilibrium state of which, at a given temperature and pressure, can be defined in terms of the fugacities of the components H_2 and O_2.
2. It can be considered that the H_2 and O_2 have reacted with one another to some extent to produce the product species H_2O.

In the latter case, if the pressure of the system is low enough, the equilibrium state at the given temperature can be defined in terms of the partial pressures exerted by the three species, H_2, O_2, and H_2O, occurring in the system. Although both treatments are thermodynamically equivalent, the latter is the more *convenient* and practical.

As with any constant-pressure, constant-temperature system, the equilibrium state is that in which the Gibbs free energy of the system has its minimum possible value. If the gases that are present initially in the system react to form distinct product species, the total change in the Gibbs free energy of the system comprises a contribution arising from the following:

- The change in Gibbs free energy due to the *chemical reaction*
- The change in Gibbs free energy due to the *mixing* of the appearing product gases with the remaining reactant gases

Knowledge of the variation of this total change in the Gibbs free energy with composition (which ranges from the pure unmixed reactant gases to the pure unmixed product gases) allows for the determination of the equilibrium state in any system of reactive gases. This determination is facilitated by the introduction of the *equilibrium constant* for the reaction, and it will be seen that the relation between this constant and the *standard Gibbs free energy* change for the reaction is one of the more important relationships in reaction equilibrium thermodynamics.

DOI: 10.1201/9781003375388-14

11.2 REACTION EQUILIBRIUM IN A GAS MIXTURE AND THE EQUILIBRIUM CONSTANT

Consider the reaction

$$A_{(g)} + B_{(g)} = 2C_{(g)}$$

occurring at constant temperature T and constant pressure P. At any instant during the reaction, the total Gibbs free energy of the system is

$$G' = n_A\overline{G}_A + n_B\overline{G}_B + n_C\overline{G}_C \tag{11.1}$$

where n_A, n_B, and n_C are, respectively, the numbers of moles of A, B, and C present in the reaction system at that instant, and $\overline{G}_A, \overline{G}_B$, and $\overline{G}_C$ are, respectively, the partial molar Gibbs free energies (chemical potentials) of A, B, and C in the gas mixture which occurs at that instant. It is of interest to determine the values of n_A, n_B, and n_C which *minimize* the value of G' in Equation 11.1, since this state of minimum Gibbs free energy is the equilibrium state of the system at the given temperature and pressure. That is, once the chemical reaction between A and B has proceeded to the extent that the Gibbs free energy of the system has been minimized, the reaction at the *macroscopic level* appears to stop. On the *microscopic level*, however, reaction equilibrium occurs when the rate of the chemical reaction proceeding from right to left equals that of the reaction proceeding from left to right. This is a *dynamic equilibrium*: that is, reactions still occur when the system is at equilibrium.

The stoichiometry of the reaction allows the numbers of moles of all the species present at any instant to be expressed in terms of the number of moles of any one of the species. Starting with 1 mole of A and 1 mole of B (i.e., 2 moles of gas), as 1 atom of A reacts with 1 atom of B to produce 2 molecules of C, then, at any time during the reaction,

$$n_A = n_B$$

and

$$n_C = 2 - n_A - n_B = 2(1 - n_A)$$

Equation 11.1 can thus be written as

$$G' = n_A\overline{G}_A + n_A\overline{G}_B + 2(1 - n_A)\overline{G}_C$$

From Equation 8.15:

$$\overline{G}_i = G_i^\circ + RT \ln P + RT \ln X_i$$

and

$$X_A = \frac{n_A}{2}, \quad X_B = \frac{n_A}{2}, \quad X_C = \frac{2(1-n_A)}{2} = (1-n_A)$$

substitution of which gives

$$G' = n_A\left(G_A^\circ + G_B^\circ - 2G_C^\circ\right) + 2G_C^\circ + 2RT\ln P$$
$$+2RT\left[n_A \ln\left(\frac{n_A}{2}\right) + (1-n_A)\ln(1-n_A)\right]$$

or

$$G' - 2G_C^\circ = n_A\left(-\Delta G^\circ\right) + 2RT\ln P$$
$$+2RT\left[n_A \ln\left(\frac{n_A}{2}\right) + (1-n_A)\ln(1-n_A)\right] \tag{11.2}$$

The term $\Delta G^\circ = 2G_C^\circ - G_A^\circ - G_B^\circ$ is the *standard Gibbs free energy change* for the chemical reaction at the temperature *T*. Table A.1 lists the values of ΔG°, as a function of temperature for selected reactions.

The standard Gibbs free energy change for any reaction is the difference between the sum of the Gibbs free energies of the reaction products in their standard states and the sum of the Gibbs free energies of the reactants in their standard states. In the present case, ΔG° is the difference between the Gibbs free energy of 2 moles of *C* at 1 atm pressure and the temperature *T*, and 1 mole of *A* and 1 mole of *B*, each at 1 atm pressure and the temperature *T*. If the total pressure of the system is 1 atm, then Equation 11.2 simplifies to

$$G' - 2G_C^\circ = n_A\left(-\Delta G^\circ\right) + 2RT\left[n_A \ln\left(\frac{n_A}{2}\right) + (1-n_A)\ln(1-n_A)\right] \tag{11.3}$$

The left-hand side of Equation 11.3 is the difference between the Gibbs free energy of the 2-mole system when $n_A = n_B$ and the Gibbs free energy of the system when it consists of 2 moles of *C*. This difference is determined by two factors:

1. The *change* in the Gibbs free energy due to the chemical reaction—that is, due to the disappearance of the reactants and the appearance of the products, given by the first term on the right-hand side of Equation 11.3
2. The *decrease* in the Gibbs free energy caused by the mixing of the gases, given by the second term on the right-hand side of Equation 11.3

Figure 11.1 is drawn for the reaction.

$$A_{(g)} + B_{(g)} = 2C_{(g)}$$

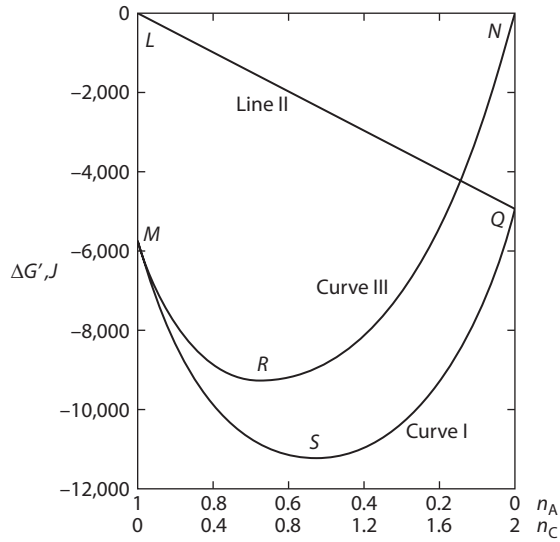

FIGURE 11.1 The variations of the contributions to the decrease in the Gibbs free energy due to chemical reaction (curve II), the contribution to the decrease in the Gibbs free energy due to gas mixing (curve III), with the extent of the reaction $A_{(g)}+B_{(g)}=2C_{(g)}$, for which $\Delta G^\circ=-5000\,\text{J}$ at 500 K. Curve I is the sum of curves II and III.

at 500 K and 1 atm pressure. ΔG°_{500} for the reaction is taken as −5000 J. If the reference for the Gibbs free energy is arbitrarily chosen as $\left(G^\circ_A+G^\circ_B\right)=0$, then $2G^\circ_C=-5000\,\text{J}$. In Figure 11.1, the ordinate $\Delta G'$ is plotted as the difference between the Gibbs free energy of the system containing n_A moles of A and the Gibbs free energy of the system comprising 1 mole of A and 1 mole of B before the mixing of A and B occurs. Thus, the point L ($n_A=1$, $n_B=1$ before mixing) is located at $\Delta G'=0$, and the point Q ($n_C=2$) is located at $\Delta G'=-5000\,\text{J}$.

The point M represents the decrease in the Gibbs free energy due to mixing of 1 mole of A and 1 mole of B before any chemical reaction between the two occurs; that is, from Equation 8.20:

$$\Delta G'(L\rightarrow M)=\sum_i n_i RT\ln\left(\frac{p_i}{P_i}\right)$$

$$=RT\left[n_A\ln\left(\frac{p_A}{P_A}\right)+n_B\ln\left(\frac{p_B}{P_B}\right)\right]$$

But $n_A=n_B=1$, and

$$P_A+P_B=P_{\text{mixture}}=1$$

in which case

$$p_A = p_B = \frac{1}{2}$$

Thus,

$$\Delta G'(L \rightarrow M) = 8.3144 \times 500 \times 2 \times \ln 0.5$$

$$= -5763 \text{ J}$$

Substituting this into Equation 11.3, we obtain

$$G' + 5000 = (1 \times 5000) - 5763 \text{ J}$$

and hence,

$$G' = -5763 \text{ J}$$

Thus, at M,

$$\Delta G' = G' - \left(G_A^\circ + G_B^\circ\right) = -5763 \text{ J}$$

Curve I represents the variation of $\Delta G'$ with n_A. It is obtained as the sum of line II (given by the first term on the right-hand side of Equation 11.3, the decrease in Gibbs free energy due to chemical reaction) and curve III (given by the second term on the right-hand side of Equation 11.3, the decrease in Gibbs free energy due to gas mixing). It can be seen that the magnitude of the chemical reaction contribution to the decrease in the Gibbs free energy of the system increases linearly with increasing n_C, but the magnitude of the *contribution to the change* in the total Gibbs free energy due to gas mixing is greatest at the composition R. R occurs at that composition of the gas mixture which permits maximum randomization of the system. Further chemical reaction, which takes the composition of the system beyond R, decreases the magnitude of the gas-mixing contribution, since further increase in n_C, at the expense of n_A and n_B, decreases the randomness of the system. Eventually, the composition S is reached, in which state the sum of the two contributions to the *decrease* in the Gibbs free energy is a *maximum*. If the chemical reaction continued beyond S, then, since the decrease in line II is smaller than the increase in curve III, the total Gibbs free energy of the system would increase. The composition S is thus that at which the Gibbs free energy of the system has its minimum value and is hence the equilibrium state at 500 K and 1 atm pressure.

The position of the minimum in curve I is fixed by the criterion that, at the minimum,

$$\left(\frac{\partial G'}{\partial n_A}\right)_{T,P} = 0$$

and since

$$G' = n_A\bar{G}_A + n_A\bar{G}_B + 2(1-n_A)\bar{G}_C$$

and including the use of the Gibbs–Duhem equation,[1]

$$\left(\frac{\partial G'}{\partial n_A}\right) = \bar{G}_A + \bar{G}_B - 2\bar{G}_C = 0$$

That is, the criterion for reaction equilibrium is

$$\bar{G}_A + \bar{G}_B = 2\bar{G}_C \tag{11.4}$$

Or, the chemical potential of the reactants equals the chemical potential of the products.

Equation 11.4 can be written as

$$G_A^\circ + RT\ln p_A + G_B^\circ + RT\ln p_B = 2G_C^\circ + 2RT\ln p_C \tag{11.5}$$

where p_A, p_B, and p_C are, respectively, the partial pressures of A, B, and C *which occur at reaction equilibrium*. Rearrangement of Equation 11.5 gives

$$2G_C^\circ - G_A^\circ - G_B^\circ = -RT\ln\frac{p_C^2}{p_A p_B}$$

or

$$\Delta G^\circ = -RT\ln\left(\frac{p_C^2}{p_A p_B}\right) \tag{11.6}$$

The quotient of the equilibrium partial pressure of the reactants and products occurring as the logarithmic term in Equation 11.6 is called the *equilibrium constant for the reaction*, K_P; that is,

$$\left(\frac{p_C^2}{p_A p_B}\right)_{\text{eq}} = K_P \tag{11.7}$$

and hence,

$$\Delta G^\circ = -RT\ln K_P \tag{11.8}$$

Since ΔG° is a function only of temperature, it follows from Equation 11.8 that K_P is a function only of temperature.

[1] Equation 9.19: $n_A d\bar{G}_A + n_B d\bar{G}_B + n_C d\bar{G}_C = 0$.

For the example used in Figure 11.1,

$$\ln K_P = -\frac{\Delta G^\circ}{RT} = \frac{5000}{8.3144 \times 500} = 1.203$$

Therefore,

$$K_P = 3.329$$

Now,

$$K_P = \frac{p_C^2}{p_A p_B} = \frac{X_C^2 P^2}{X_A P X_B P} = \frac{X_C^2}{X_A X_B}$$

and since $X_A = X_B = n_A / 2$ and $X_C = (1 - n_A)$,

$$K_P = \frac{(1 - n_A)^2}{\left(\frac{n_A^2}{4}\right)} = 3.329$$

Thus,

$$n_A = 0.523 \left(\text{the other solution, } n_A = 11.4, \text{ is nonphysical}\right)$$

The minimum in curve I in Figure 11.1 occurs at

$$n_A = n_B = 0.523 \text{ and}$$

$$n_C = 2 - 2(0.523) = 0.954$$

The chemical reaction $A + B = 2C$ has proceeded to 47.7% completion.

If the temperature T was such that ΔG° for the reaction was zero, there would be no chemical reaction *contribution* to $\Delta G'$, and the variation of $\Delta G'$ with n_A would be given by curve III in Figure 11.1. That is, the criterion for reaction equilibrium would be the maximization of the configurational entropy of the system, which occurs at the composition R on the curve. From Equation 11.8, if $\Delta G^\circ = 0$, then $K_P = 1$, and thus,

$$1 = \frac{4(1 - n_A)^2}{n_A^2} \quad \text{and} \quad n_A = \frac{2}{3}$$

The minimum in curve III occurs at $n_A = n_B = n_C = ⅔$, and thus, the maximum entropy in the system occurs when all three species are present in equal amounts.

It is important to note that the minimum in curve I in Figure 11.1, representing the equilibrium state of the system at $P = 1$ atm and 500 K, is the only point on curve I that has any significance within the scope of *classical equilibrium thermodynamics*. Point S is the only state on curve I which lies *on the equilibrium surface* in P-T–composition space for the fixed values of $P = 1$ atm and $T = 500$ K. Any change in P and/or T changes the curves II and III, which in turn produces a "new" curve I. This new curve I has a different minimum and hence represents a new equilibrium state. This is discussed further in the following section.

11.3 THE EFFECT OF TEMPERATURE ON THE EQUILIBRIUM CONSTANT

The position of the minimum in curve I in Figure 11.1 is determined by the difference between the lengths of *LM* and *NQ*. The length *LM* is the decrease in the Gibbs free energy caused by the mixing of the gases *before the reaction begins*. The length *NQ* is the standard Gibbs free energy change, ΔG°, for the reaction at the temperature in question. The lengths of both of these lines are dependent on temperature.

$$LM = 2RT \ln 0.5$$

$$NQ = \Delta G^\circ = f(T)$$

The effect of temperature on the composition at which the minimum occurs in curve I (and hence on the value of K_P) thus depends on the relative effects of temperature on the lengths of *LM* and *NQ*. For given reactants, the length of *LM* increases linearly with temperature. The variation of the length *NQ* with temperature is determined by the sign and magnitude of the standard entropy change for the reaction according to

$$\left(\frac{\partial \Delta G^\circ}{\partial T}\right)_P = -\Delta S^\circ$$

Increasing the temperature increases the length of *LM*, and if ΔS° is negative, increasing T must increase ΔG°, hence decreasing the length of *NQ*. Thus, the position of the minimum in the curve I shifts to the left, which indicates that K_P *decreases* with increasing temperature.

The exact variation of K_P with temperature is obtained from consideration of the Gibbs–Helmholtz equation (Equation 5.55):

$$\left[\frac{\partial(\Delta G^\circ/T)}{\partial T}\right]_P = -\frac{\Delta H^\circ}{T^2}$$

From Equation 11.8, $\Delta G^\circ = -RT \ln K_P$, and *since* ΔG° *is only a function of T*,

$$\frac{d \ln K_P}{dT} = \frac{\Delta H^\circ}{RT^2} \tag{11.9}$$

or

$$\frac{d \ln K_P}{d(1/T)} = -\frac{\Delta H^\circ}{R} \tag{11.10}$$

Equation 11.10 is known as the *van't Hoff equation* (Jacobus Henricus van't Hoff, 1852–1911). The equation shows that the effect of temperature on K_P is determined by the *sign* and *magnitude* of ΔH° for the reaction. The van't Hoff equation enables

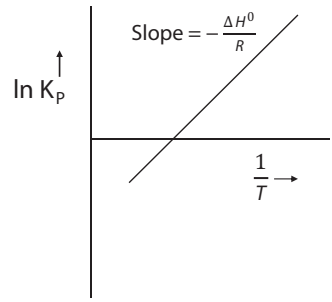

FIGURE 11.2 The variation of the ln (K_P) versus 1/T of an exothermic reaction (a van't Hoff plot).

the determination of ΔH° from a plot of ln K_P versus the inverse of absolute temperature. The slope of the plot is $-\left(\Delta H^\circ / R\right)$ (Figure 11.2).

The van't Hoff equation can also be obtained as follows:

We know that

$$\Delta G^\circ = -RT \ln K_P$$

$$\text{and that } \Delta G^\circ = \Delta H^\circ - T\Delta S^\circ$$

Equating the two expressions we

$$\ln K_P = -\frac{\Delta H^\circ}{RT} + \frac{\Delta S^\circ}{R}$$

Thus a plot of ln K_P vs $\frac{1}{T}$ gives rise to a line of slope $-\frac{\Delta H^\circ}{R}$. The intercept along the ordinate equals $\frac{\Delta S^\circ}{R}$. This assumes that $\Delta C_P = 0$.

The following cases are possible:

- If ΔH° is positive (endothermic) the slope of the plot is negative, and K_P increases with increasing temperature.
- If ΔH° is negative (exothermic) the slope of the plot is positive, and K_P decreases with increasing temperature.
- If ΔS° is positive (increase in entropy) the intercept of the plot along the ordinate is positive.
- If ΔS° is negative (decrease in entropy) intercept of the plot along the ordinate is negative.

Integration of Equation 11.10 requires knowledge of the temperature dependence of ΔH°, which, as was seen in Chapter 6, depends on the value of Δc_p for the reaction.

The direction of the variation of K_P with temperature also can be obtained from the application of Le Chatelier's principle (Henry Louis Le Chatelier, 1850–1936). If thermal energy is added to a system at reaction equilibrium, then the equilibrium is displaced in that direction which involves the *absorption of heat*.

Consider the simple gaseous reaction

$$Cl_2 = 2Cl$$

This reaction is endothermic and hence has a positive value of ΔH°. Thus, the equilibrium constant, $K_P = p_{Cl}^2/p_{Cl_2}$, increases with increasing temperature; that is, the equilibrium shifts in that direction which involves the absorption of thermal energy. Conversely, if the reaction were written as

$$2Cl = Cl_2$$

then, since the reaction has a negative value of ΔH°, $K_P = p_{Cl_2}/p_{Cl}^2$ decreases with increasing temperature; that is, the equilibrium shifts in that direction which involves the *absorption* of thermal energy. In both cases, an increase in temperature increases p_{Cl} and decreases p_{Cl_2}.

11.4 THE EFFECT OF PRESSURE ON THE EQUILIBRIUM CONSTANT

The equilibrium constant, K_P, as defined by Equation 11.7, is independent of pressure. This is a consequence of the fact that ΔG° is the difference between the Gibbs free energies of the pure products (each at unit pressure) and the Gibbs free energies of the pure reactants (each at unit pressure), which is, by definition, independent of pressure. However, if reaction equilibrium is expressed in terms of the *number of moles of species* present rather than in terms of the partial pressures of the species present, the constant is *dependent* on the *total pressure* if the chemical reaction involves a *change* in the total number of moles present.

Consider again the reaction $Cl_2 = 2Cl$. Completion of this reaction causes a doubling of the number of moles present, and the effect of a change in pressure can again be obtained by the application of Le Chatelier's principle. If the pressure exerted on a system at reaction equilibrium is increased, then the equilibrium shifts in that direction which tends to *decrease* the pressure exerted by the system; that is, it shifts in that direction which *decreases* the number of moles present. Thus, if the pressure exerted on the Cl–Cl_2 system is increased, the equilibrium will shift toward the Cl_2 side, as, thereby, the total number of moles present will be decreased to accommodate the increased pressure. Specifically, the effect of pressure on the reaction equilibrium expressed in terms of the number of moles present (or in terms of mole fractions) can be seen as follows:

$$K_p = \frac{p_{Cl}^2}{p_{Cl_2}}, \quad \text{which is independent of pressure}$$

$$= \frac{X_{Cl}^2 P^2}{X_{Cl_2} P} = \frac{X_{Cl}^2 P}{X_{Cl_2}} = K_x P$$

where K_x is the equilibrium constant expressed in terms of the mole fractions. Thus, if the pressure is increased, then K_x decreases in order to maintain K_P constant, and the decrease in K_x is achieved by the reaction equilibrium shifting toward the Cl_2 side such that X_{Cl} decreases and X_{Cl_2} increases.

In the case of the reaction $A + B = 2C$, the system at all times contains two moles of gas, and thus, the reaction equilibrium, expressed in terms of the mole fractions, is independent of pressure; that is,

$$K_P = \frac{p_C^2}{p_A p_B} = \frac{X_C^2 P^2}{(X_A P)(X_B P)} = \frac{X_C^2}{X_A X_B} = K_x$$

This can also be seen from Equation 11.2, since, if $P \neq 1$, then the effect of the non-zero term $2RT \ln P$ is the raising or lowering of curve I in Figure 11.1 without affecting the position of the minimum with respect to the composition axis.

The magnitude of the effect of a change in pressure on the value of K_x depends on the magnitude of the change in the number of moles present in the system, occurring as a result of the chemical reaction. For the general reaction

$$aA + bB = cC + dD$$

$$K_P = \frac{p_C^c p_D^d}{p_A^a p_B^b} = \frac{X_C^c X_D^d}{X_A^a X_B^b} \frac{P^c P^d}{P^a P^b} = K_x P^{(c+d-a-b)}$$

which shows that K_x is independent of the total pressure only if $c + d = a + b$.

11.5 REACTION EQUILIBRIUM AS A COMPROMISE BETWEEN ENTHALPY AND ENTROPY

Since the Gibbs free energy of a system is defined as

$$G' = H' - TS'$$

low values of G' are obtained with low values of H' and large values of S'. It was seen in the discussion of one-component systems in Chapter 7 that equilibrium occurs as the result of a compromise between *enthalpy* and *entropy* considerations. A similar discussion is now made concerning chemical reaction equilibria.

Consider again the reaction $Cl_2 = 2Cl$. This reaction has a positive value of ΔH° (ΔH° is the thermal energy required to break Avogadro's number of Cl–Cl bonds) and has a positive value of ΔS° (2 moles of chlorine atoms are produced from 1 mole of chlorine molecules). Thus,

- The system occurring as Cl atoms has a high value of H and a high value of S.
- The system occurring as Cl_2 molecules has a low value of H and a low value of S.

The minimum value of G thus occurs somewhere between the two extreme states. This compromise between the enthalpy and the entropy is analogous to the compromise between the contributions of the chemical reaction and the mixing of gases to the decrease in Gibbs free energy shown in Figure 11.1.

For the reaction $A + B = 2C$, Equation 11.3 can be written as

$$G' - 2G_C^\circ = n_A\left(-\Delta H^\circ\right) + n_A\left(T\Delta S^\circ\right) + 2RT\left[n_A \ln\left(\frac{n_A}{2}\right) + (1-n_A)\ln(1-n_A)\right]$$

$$= \left[n_A\left(-\Delta H^\circ\right)\right] + T\left\{n_A\Delta S^\circ + 2R\left[n_A \ln\left(\frac{n_A}{2}\right) + (1-n_A)\ln(1-n_A)\right]\right\} \tag{11.11}$$

The first term on the right-hand side is the enthalpy contribution to the change in the Gibbs free energy. The second term on the right-hand side of the equation is the entropy contribution, with $n_A\ \Delta S^\circ$ being the entropy change caused by the chemical reaction and $2R[n_A \ln (n_A/2) + (1 - n_A) \ln (1 - n_A)]$ being the entropy change caused by gas mixing. In the example in Section 11.2, ΔG° was equal to -5000 J at 500 K. Let it be that $\Delta H^\circ = -2500$ J and $\Delta S^\circ = 5$ J/K, in which case Figure 11.3 can be drawn from Figure 11.1. In Figure 11.3, the $\Delta H'$ line is the first term on the right-hand side of Equation 11.11 and the $T\Delta S'$ curve is the second term. The sum of these two gives $G' - 2G_C^\circ$, the scale of which is given on the left-hand ordinate of Figure 11.3. The scale on the right-hand ordinate of the figure is $\Delta G'$, where, as before, the reference

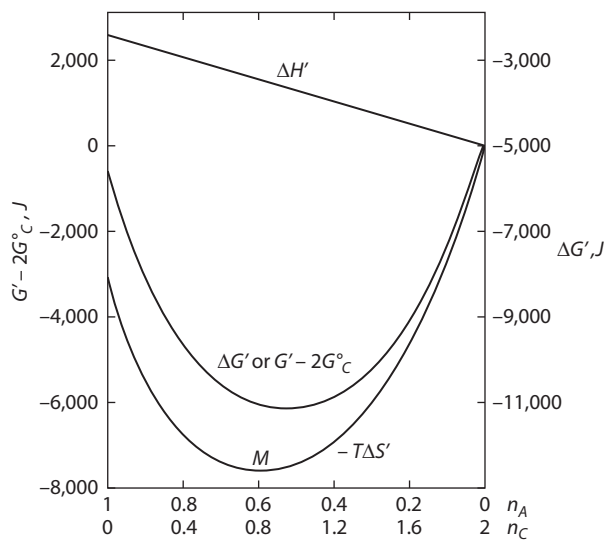

FIGURE 11.3 The variations at 500 K of $\Delta H'$, $-T\Delta S'$, and $\Delta G'$ with the extent of reaction $A_{(g)} + B_{(g)} = 2C_{(g)}$, for which $\Delta G^\circ = -2500 - 5T$.

zero of Gibbs free energy is chosen as $G_A^\circ + G_B^\circ = 0$, such that $\Delta G' = G'$ (i.e., the scale is displaced by $2G_C^\circ = -5000$ J). On this scale, the $\Delta G'$ curve in Figure 11.3 is identical with curve I in Figure 11.1. It can be seen that the minimum in the $\Delta G'$ curve is determined as a compromise between the minimum value of $\Delta H'$ at $n_A = 0$ and the maximum value of $T\Delta S'$ at $n_A = 0.597$ (the point M in Figure 11.3). If the temperature is increased, then the $T\Delta S'$ term becomes relatively more important, and hence the equilibrium value of n_A increases (the minimum in the $\Delta G'$ curve shifts to the left). Thus, K_P decreases with increasing temperature in accordance with Equation 11.9 for negative ΔH°.

The effect of temperature on the $\Delta G'$ curve is illustrated in Figure 11.4, in which curves are drawn for the reaction $A + B = 2C$ at 500, 1000, and 1500 K. It is assumed that Δc_p for the reaction is zero, in which case ΔH° and ΔS° are independent of temperature. Since $\Delta G^\circ = \Delta H^\circ - T\Delta S^\circ$,

$$\Delta G_{500}^\circ = -2{,}500 - (500 \times 5) = -5{,}000 \text{ J} \quad K_{P,500} = 3.329$$

$$\Delta G_{1000}^\circ = -2{,}500 - (1{,}000 \times 5) = -7{,}500 \text{ J} \quad K_{P,1000} = 2.465$$

$$\Delta G_{1500}^\circ = -2{,}500 - (1{,}500 \times 5) = -10{,}000 \text{ J} \quad K_{P,1500} = 2.229$$

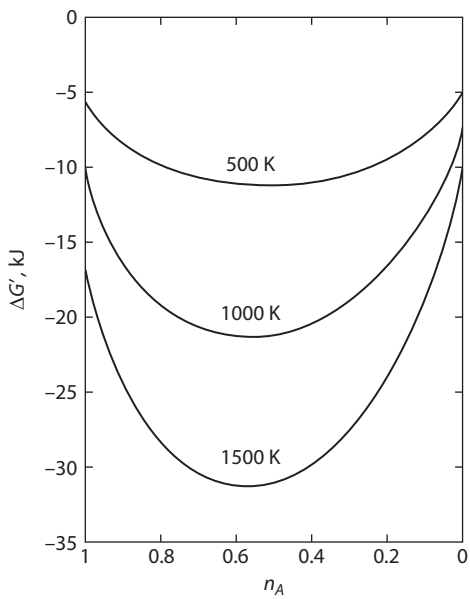

FIGURE 11.4 The effect of temperature on the equilibrium state of the reaction $A_{(g)} + B_{(g)} = 2C_{(g)}$, for which $\Delta G^\circ = -2500 - 5T$ J.

The equilibrium values of n_A at 500, 1000, and 1500 K are thus, respectively, 0.523, 0.560, and 0.572. Thus, increasing the temperature, *shifts the minimum to the left,* thereby increasing the amount of *A* and *B* in equilibrium.

Although K_P is constant at a constant temperature, note that an infinite set of partial pressures of reactants and products correspond to the fixed value of K_P. If the reaction involves three species, then an arbitrary choice of the partial pressures of two of the species uniquely fixes the equilibrium partial pressure of the third. This can also be shown by Gibbs' equilibrium phase rule (see Qualitative Problem 2 in Section 11.10).

11.6 REACTION EQUILIBRIUM IN THE SYSTEM $SO_{2(G)}$–$SO_{3(G)}$–$O_{2(G)}$

Consider the equilibrium reaction of the oxidation of sulfur dioxide to sulfur trioxide:

$$SO_{2(g)} + \frac{1}{2}O_{2(g)} = SO_3(g) \tag{11.12}$$

The standard Gibbs free energy change for this reaction is

$$\Delta G^\circ = -94,600 + 89.37T \text{ J}$$

Thus, at 1000 K,

$$\Delta G^\circ_{1000} = -5230 \text{ J}$$

$$\ln K_P = \frac{5230}{8.3144 \times 1000} = 0.629$$

and

$$K_P = 1.876 = \frac{p_{SO_3}}{p_{SO_2} p_{O_2}^{1/2}}$$

Now consider the reaction between 1 mole of SO_2 gas at 1 atm pressure and ½ mole of O_2 gas at 1 atm pressure to form an equilibrium mixture of SO_2, SO_3, and O_2 at 1 atm pressure and 1000 K. From the stoichiometry of the chemical reaction given by Equation 11.12, *x* moles of SO_3 are formed from the reaction of *x* moles of SO_2 and ½x moles of O_2. Thus, any reacting mixture contains *x* moles of SO_3, $(1-x)$ moles of SO_2, and ½$(1-x)$ moles of O_2; that is,

	SO_2	+	$\frac{1}{2}O_2$	→	SO_3
Initially,	1		$\frac{1}{2}$		0
Upon reaction,	$1-x$		$\frac{1}{2}-\frac{1}{2}x$		x

The total number of moles in the system, n_T, is

$$n_T = 1 - x + \frac{1}{2} - \frac{1}{2}x + x = \frac{1}{2}(3 - x)$$

and, since

$$p_i = \frac{n_i}{n_T} P$$

then

$$p_{SO_2} = \frac{2(1-x)P}{(3-x)}, \quad p_{O_2} = \frac{(1-x)P}{(3-x)}, \quad p_{SO_3} = \frac{2xP}{(3-x)}$$

Thus,

$$K_P^2 = \frac{p_{SO_3}^2}{p_{SO_2}^2 p_{O_2}} = \frac{(3-x)x^2}{(1-x)^3 P}$$

or

$$\left(1 - PK_P^2\right)x^3 + \left(3PK_P^2 - 3\right)x^2 - 3PK_P^2 x + PK_P^2 = 0 \tag{11.13}$$

which, with $P = 1$ and $K_P = 1.876$, gives $x = 0.463$. Thus, at equilibrium, there are 0.537 moles of SO_2, 0.269 moles of O_2, and 0.463 moles of SO_3, such that

$$p_{SO_2} = \frac{2(1-0.463)}{(3-0.463)} = 0.365 \text{ atm}$$

$$p_{O_2} = \frac{(1-0.463)}{(3-0.463)} = 0.212 \text{ atm}$$

and

$$p_{SO_3} = \frac{2 \times 0.463}{(3-0.463)} = 0.365 \text{ atm}$$

As a check,

$$K_P = \frac{0.365}{0.423 \times 0.212^{1/2}} = 1.874$$

The composition of the equilibrium gas is thus 42.3% SO_2, 21.2% O_2, and 36.5% SO_3.

11.6.1 The Effect of Temperature in the System $SO_{2(G)}$–$SO_{3(G)}$–$O_{2(G)}$

Since ΔH° for the reaction given by Equation 11.12 is negative (–94,600 J), and Le Chatelier's principle predicts that a decrease in temperature at constant pressure shifts the equilibrium in that direction which involves an evolution of thermal energy

(heat), decreasing the temperature at constant pressure causes the equilibrium to shift toward the SO_3 side. At 900 K,

$$\Delta G^{\circ}_{900} = -14{,}167 \text{ J}$$

$$\ln K_P = \frac{14{,}167}{8.3144 \times 900} = 1.893$$

and thus,

$$K_P = 6.64$$

Substituting $K_P = 6.64$ and $P = 1$ atm into Equation 11.13 gives $x = 0.704$, and thus,

$$p_{SO_2} = 0.258 \text{ atm}, \quad p_{O_2} = 0.129 \text{ atm}, \quad p_{SO_3} = 0.613 \text{ atm}$$

As a check,

$$K_P = \frac{0.613}{0.258 \times 0.129^{1/2}} = 6.64$$

Thus, of the total number of moles present,

- SO_2 constitutes 25.8%, which is a decrease from 42.3% at 1000 K.
- O_2 constitutes 12.9%, which is a decrease from 21.2% at 1000 K.
- SO_3 constitutes 61.3%, which is an increase from 36.5% at 1000 K.

It is seen that a decrease in temperature has shifted the equilibrium toward the SO_3 side.

11.6.2 The Effect of Pressure in the System $SO_{2(G)}$–$SO_{3(G)}$–$O_{2(G)}$

Although K_P is independent of pressure, Le Chatelier's principle predicts that an increase in total pressure at constant temperature shifts the equilibrium in that direction which involves a decrease in the number of moles in the system—that is, toward the SO_3 side. Consider the equilibrium mixture at $P = 10$ atm and $T = 1000$ K. Substituting $P = 10$ and $K_P = 1.876$ into Equation 11.13 gives $x = 0.686$, in which case $n_{SO_2} = 0.314$, $n_{O_2} = 0.157$, $n_{SO_3} = 0.686$. Thus,

$$p_{SO_2} = \frac{2(1-0.686) \times 10}{(3-0.686)} = 2.714 \text{ atm}$$

$$p_{O_2} = \frac{(1-0.686) \times 10}{(3-0.686)} = 1.357 \text{ atm}$$

and

$$p_{SO_3} = \frac{2 \times 0.686 \times 10}{(3 - 0.686)} = 5.929 \text{ atm}$$

As a check,

$$K_P = \frac{5.929}{2.714 \times 1.357^{1/2}} = 1.875$$

Of the total number of moles present

- SO_2 constitutes 27.1%, which is a decrease from 42.3% at $P = 1$ atm.
- O_2 constitutes 13.75%, which is a decrease from 21.2% at $P = 1$ atm.
- SO_3 constitutes 59.29%, which is an increase from 36.5% at $P = 1$ atm.

Thus, it is seen that an increase in pressure has shifted the equilibrium toward the SO_3 side.

11.6.3 The Combined Effect of Temperature and Pressure Changes in the System $SO_{2(G)}$–$SO_{3(G)}$–$O_{2(G)}$

In order to simultaneously vary the temperature and the pressure in such a manner that the numbers of moles of the three gaseous species present remain constant, Equation 11.13 indicates that the variation must be such that the term PK_P^2 remains constant, where

$$K_P = \exp\left(-\frac{\Delta G^\circ}{RT}\right) = \exp\left(\frac{94{,}600}{8.3144 \cdot T}\right) \cdot \exp\left(\frac{-89.37}{8.3144}\right)$$

It is apparent that, by mixing SO_2 gas and SO_3 gas, an equilibrium mixture with a known partial pressure of O_2 can be produced. For example, consider that it was required to have an SO_3–SO_2–O_2 mixture at 1 atm total pressure in which $p_{O_2} = 0.1$ atm. To obtain this gas mixture, SO_3 and SO_2, both at 1 atm pressure, would be mixed in the molar ratio $SO_2/SO_3 = a$ and allowed to equilibrate. If a moles of SO_2 and 1 mole of SO_3 are mixed, then from the stoichiometry of Equation 11.12, x moles of SO_3 would decompose to form x moles of SO_2 and ½x moles of O_2, such that, at equilibrium, the number of moles present would be

	SO_2	+	$\frac{1}{2}O_2$	→	SO_3
Initially,	a		0		1
Upon reaction,	$a + x$		$\frac{1}{2}x$		$1 - x$

with

$$n_T = a + x + \frac{1}{2}x + 1 - x = \frac{1}{2}(2a + 2 + x)$$

In this gas mixture,

$$p_{O_2} = \frac{n_{O_2}}{n_T} = \frac{x}{2a + 2 + x} P$$

which, for $P = 1$ and $p_{O_2} = 0.1$, gives $a = 4.5x - 1$. Also,

$$K_P^2 = \frac{p_{SO_3}^2}{p_{SO_2}^2 p_{O_2}} = \frac{(1 - x)^2 (2a + 2 + x)}{(a + x)^2 xP}$$

At 1000 K, $K_P = 1.876$. Thus, substituting for a in terms of x and taking $K_P^2 = 3.519$ gives

$$96.45x^3 - 18.709x^2 - 6.481x = 0$$

or, since $x \neq 0$,

$$96.45x^2 - 18.709x - 6.481 = 0$$

which has the solution $x = 0.374$. Thus,

$$a = (4.5 \times 0.374) - 1 = 0.683$$

$$p_{O_2} = \frac{xP}{2a + 2 + x} = \frac{0.374}{(2 \times 0.683) + 2 + 0.374} = 0.1 \text{ atm}$$

$$p_{SO_3} = \frac{2(1 - x)}{2a + 2 + x} = \frac{2(1 - 0.374)}{(2 \times 0.683) + 2 + 0.374} = 0.335 \text{ atm}$$

and

$$p_{SO_2} = \frac{2(a + x)}{2a + 2 + x} = \frac{2(0.683 + 0.374)}{(2 \times 0.683) + 2 + 0.374} = 0.565 \text{ atm}$$

In the equilibrium mixture, $p_{SO_2} / p_{SO_3} = 1.7$ compared with $p_{SO_2} / p_{SO_3} = a = 0.683$ in the initial mixture. As a check,

$$K_P = \frac{0.355}{0.565 \times 0.1^{1/2}} = 1.875$$

If it had been required to have $p_{O_2} = 0.212$ atm (the equilibrium value of p_{O_2} in an equilibrated gas at 1 atm pressure of initial composition 1 mole of $SO_2 + ½$ mole of O_2), then the solution of the stoichiometric condition would have given $a = 0$, which indicates that pure SO_3 at 1000 K and 1 atm pressure decomposes to the same equilibrium gas mixture as that formed from an initial mixture of 1 mole of $SO_2 + ½$ mole of O_2 at 1 atm. Thus, 0.212 atm is the maximum value of p_{O_2} which can be produced in an SO_2–SO_3 mixture at 1000 K and 1 atm total pressure.

11.7 EQUILIBRIUM IN H_2O–H_2 AND CO_2–CO MIXTURES

H_2O–H_2 and CO_2–CO gas mixtures are used when it is required that the partial pressure of oxygen in a gas phase be fixed at a very low value. For example, if it were required to have a gaseous atmosphere containing a partial pressure of oxygen of 10^{-10} atm, then such an oxygen potential can be obtained with relative ease by establishing the equilibrium

$$H_2 + \frac{1}{2}O_2 = H_2O$$

for which

$$\Delta G^\circ = -247{,}500 + 55.85T \text{ J}$$

From Equation 11.8,

$$\ln K_P = \frac{247{,}500}{8{,}3144 \cdot T} - \frac{55.85}{8.3144}$$

If it is required to have an atmosphere containing $p_{O_2} = 10^{-10}$ atm at $T = 2000$ K, then, at this temperature,

$$\ln K_P = \frac{247{,}500}{8.3144 \cdot 2000} - \frac{55.85}{8.3144}$$
$$= 8.167$$

Therefore,

$$K_P = 3.521 \times 10^3 = \frac{p_{H_2O}}{p_{H_2} p_{O_2}^{1/2}}$$

and with $p_{O_2} = 10^{-10}$ atm,

$$\frac{p_{H_2O}}{p_{H_2}} = 3.521 \times 10^3 \times 10^{-5} = 3.521 \times 10^{-2}$$

Thus, in the H_2–H_2O gas mixture, if $p_{H_2} = 1$ atm, then p_{H_2O} must be 0.0352 atm.

The saturated vapor pressure of liquid water at 27.0°C is found from

$$\log p(\text{atm}) = -\frac{2900}{T} - 4.65 \cdot \log T + 19.732$$

to be 0.0352. Thus, the required gas mixture can be produced by bubbling hydrogen gas at 1 atm pressure through pure liquid water at 27.0°C to saturate it with water vapor. The establishment of reaction equilibrium at 2000 K gives $p_{O_2} = 10^{-10}$ atm in the gas.

Similarly, the partial pressure of oxygen in a gaseous atmosphere can be determined by establishing the reaction

$$CO + \frac{1}{2}O_2 = CO_2$$

The standard Gibbs free energy change for the reaction

$$CO_{(g)} = \frac{1}{2}O_{2(g)} + C_{(s)}$$

is

$$\Delta G^\circ = 111{,}700 + 87.65T \text{ J, in the range 298-2000 K}$$

and that for the reaction

$$C_{(s)} + O_{2(g)} = CO_{2(g)}$$

is

$$\Delta G^\circ = -394{,}100 - 0.84T \text{ J}$$

Summation of the standard Gibbs free energy changes gives

$$\Delta G^\circ = -282{,}400 + 86.81T \text{ J}$$

for the reaction

$$CO_{(g)} + \frac{1}{2}O_{2(g)} = CO_{2(g)}$$

Thus,

$$\ln K_P = \frac{282{,}400}{8.3144 \cdot T} - \frac{86.81}{8.3144}$$

If it were required to have $p_{O_2} = 10^{-20}$ atm at 1000 K, then

$$\ln K_p = \frac{282,400}{8.3144 \cdot 1000} - \frac{86.81}{8.3144} = 23.52$$

Therefore,

$$K_P = 1.646 \times 10^{10} = \frac{p_{CO_2}}{p_{CO} p_{O_2}^{1/2}} = \frac{p_{CO_2}}{p_{CO} \cdot 10^{-10}}$$

and so

$$\frac{p_{CO_2}}{p_{CO}} = 1.646$$

If the total pressure $P = 1$ atm, then, since $p_{CO_2} + p_{CO} = 1$, the partial pressure, $p_{CO_2} = 1.646(1 - p_{CO_2}) = 0.622\,\text{atm}$ and $p_{CO} = 0.378$. The required mixture is produced by mixing CO_2 and CO in the volume ratio 1.561/1—that is, 62.2 volume percent CO_2 and 37.8 volume percent CO.

In both of the preceding equilibria, the oxygen pressure in the equilibrated gas is so small that the p_{H_2}/p_{H_2O} and p_{CO_2}/p_{CO} ratios in the equilibrated gases are negligibly different from the corresponding ratios in the initial mixtures. The equality of the ratio of the volume percentages with the ratio of the partial pressures in a gas mixture can be demonstrated as follows. Consider a cm^3 of gas A at 1 atm pressure and b cm^3 of gas B at 1 atm pressure being mixed at constant pressure (and hence at constant total volume, $a + b$). The number of moles of $A = n_A = (1 \times a)/RT = a/RT$, and the number of moles of $B = n_B = (1 \times b)/RT = b/RT$. Therefore, in the mixture,

$$p_A = \frac{n_A RT}{V'} = \frac{n_A RT}{(a+b)}$$

and

$$p_B = \frac{n_B RT}{(a+b)}$$

Thus,

$$\frac{p_A}{p_B} = \frac{n_A}{n_B} = \frac{a}{b} = \frac{\text{Volume percentage of } A}{\text{Volume percentage of } B}$$

11.8 SUMMARY

1. The equilibrium state of the reaction $aA + bB = cC + dD$ is that in which $a\bar{G}_A + b\bar{G}_B = c\bar{G}_C + d\bar{G}_D$. The equilibrium state of the reaction is thus determined by the value of ΔG° for the reaction and is quantified by the equilibrium constant K_P, where $K_P = \left(p_C^c p_D^d / p_A^a p_B^b\right)_{eq}$ and the standard state for each reactant and product gas is the pure gas at 1 atm pressure.

2. ΔG° and K_P are related by $\Delta G^\circ = -\mathrm{RT} \ln K_P$. This relation is one of the more powerful equations in chemical thermodynamics and will be used extensively in subsequent chapters. For increasingly negative values of ΔG°, K_P becomes increasingly greater than unity, and, conversely, for increasingly positive values of ΔG°, K_P becomes increasingly less than unity.
3. Since ΔG° is a function only of temperature, K_P is a function only of temperature, and the dependence of K_P on temperature is determined by the value of ΔH° for the reaction; that is,

$$\Delta G^\circ = \Delta H^\circ - T\Delta S^\circ = -RT \ln K_P$$

and hence,

$$\ln K_P = -\frac{\Delta H^\circ}{RT} + \frac{\Delta S^\circ}{R}$$

or

$$\frac{d \ln K_P}{dT} = \frac{\Delta H^\circ}{RT^2}$$

or

$$\frac{d \ln K_P}{d(1/T)} = -\frac{\Delta H^\circ}{R}$$

Thus, for an exothermic reaction, K_P decreases with increasing temperature, and for an endothermic reaction, K_P increases with increasing temperature.

4. Since $p_i = X_i P$ in an ideal gas mixture, the equilibrium constant can be written in terms of the mole fractions; that is,

$$K_P = \frac{p_C^c p_D^d}{p_A^a p_B^b} = \frac{X_C^c X_D^d}{X_A^a X_B^b} P^{(c+d-a-b)} = K_x P^{(c+d-a-b)}$$

Although K_P is, by definition, independent of pressure, K_x is independent of pressure only if $(c + d - a - \mathrm{b}) = 0$—that is, if the gas mixture contains a constant number of moles in all states along the reaction coordinate. If the forward progression of the reaction decreases the number of moles present (i.e., if $[c + d - a - b] < 0$), then an increase in pressure increases the value of K_x; conversely, if $(c + d - a - b) > 0$, an increase in pressure decreases the value of K_x. The dependence of K_x on pressure and the dependence of K_P on temperature are examples of Le Chatelier's principle.

5. If ΔH° and ΔS° are known for the reaction, the following can be stated.
   - If $\Delta H^\circ > 0$ and $\Delta S^\circ > 0$, the reaction will occur spontaneously at high temperatures.
   - If $\Delta H^\circ < 0$ and $\Delta S^\circ < 0$, the reaction will occur spontaneously at low temperatures.
   - If $\Delta H^\circ > 0$ and $\Delta S^\circ < 0$, the reaction will not occur spontaneously.
   - If $\Delta H^\circ < 0$ and $\Delta S^\circ > 0$, the reaction will occur spontaneously at all temperatures.

11.9 CONCEPTS AND TERMS INTRODUCED IN THIS CHAPTER

The reader should write out brief definitions or descriptions of the following terms. Where appropriate, equations may be used.

Catalyst
Chemical affinity
Constant pressure equilibrium constant K_P
Dynamic equilibrium
Equilibrium constant K_x
Gaseous reaction
Gibbs free energy change due to chemical reaction
Le Chatelier's principle
Reactants and products
Standard Gibbs free energy change
Stoichiometry

11.10 QUALITATIVE EXAMPLE PROBLEMS

QUALITATIVE PROBLEM 1

Sketch the natural log of K_P vs. $1/T$ for the cases:

a. $\Delta H^\circ < 0 \quad \Delta S^\circ < 0$
b. $\Delta H^\circ < 0 \quad \Delta S^\circ > 0$
c. $\Delta H^\circ > 0 \quad \Delta S^\circ > 0$
d. $\Delta H^\circ > 0 \quad \Delta S^\circ < 0$

SOLUTION TO QUALITATIVE PROBLEM 1

QUALITATIVE PROBLEM 2 (SEE FIGURE 11.5)

Use the Gibbs equilibrium phase rule to show that the gaseous reaction

$$A + B = 2C$$

has only 2 degrees of freedom at a fixed temperature.

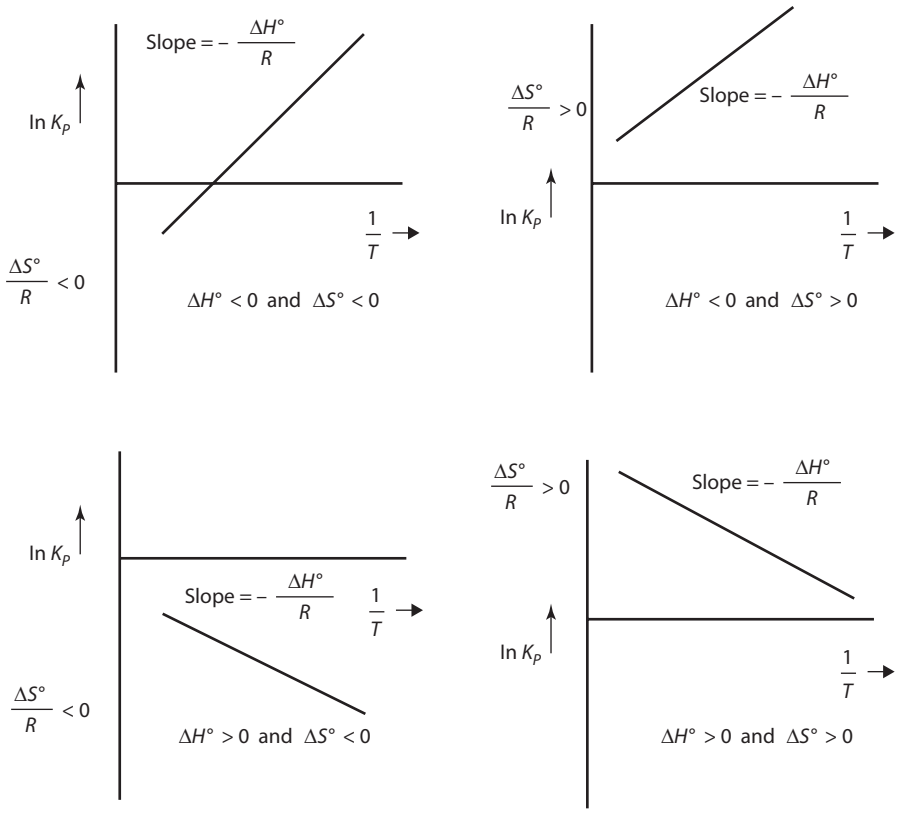

FIGURE 11.5 Plots of ln K_P vs. $1/T$ for the four cases described in Qualitative Problem 1.

SOLUTION TO QUALITATIVE PROBLEM 2

The Gibbs equilibrium phase rule is written as

$$\Phi + \mathcal{F} = C + 2$$

For $\Phi = 1$ (a mixture of gases is still one phase) and fixed temperature, we get

$$\mathcal{F} = C$$

However, in this case, the number of independent components, C, is reduced by one since there is one equation of the chemical reaction that exists among the components.

Thus, $\mathcal{F} = C - 1 = 2$. Only two partial pressures can be chosen arbitrarily.

11.11 QUANTITATIVE EXAMPLE PROBLEMS

QUANTITATIVE PROBLEM 1

Consider the partial decomposition of gaseous P_4 according to

$$P_{4(g)} = 2P_{2(g)}$$

Calculate

a. The temperature at which $X_{P_4} = X_{P_2} = 0.5$ at a total pressure of 1 atm
b. The total pressure at which $X_{P_4} = X_{P_2} = 0.5$ at 2000 K
given that, for the reaction $P_{4(g)} = 2P_{2(g)}$,

$$\Delta G^\circ = 225{,}400 + 7.90T \ln T - 209.4T \text{ J}$$

SOLUTION TO QUANTITATIVE PROBLEM 1

a. Since $\Delta G^\circ = 225{,}400 + 7.90T \ln T - 209.4T$ J,

$$\ln K_P = \frac{-27{,}109}{T} - 0.95 \ln T + 25.18 \tag{i}$$

Partial decomposition of 1 mole of P_4 produces $(1 - x)$ moles of P_4 and $2x$ moles of P_2. Thus, for $X_{P_4} = (1 - x)/(1 + x) = 0.5$, $x = 1/3$, and we can write

$$p_{P_4} = \left(\frac{1 - \frac{1}{3}}{1 + \frac{1}{3}} \right) P = 0.5P$$

and

$$p_{P_2} = \left(\frac{2 \times \frac{1}{3}}{1 + \frac{1}{3}} \right) P = 0.5P$$

Thus, with $X_{P_4} = X_{P_2} = 0.5$ and the pressure P,

$$K_P = \frac{p_{P_2}^2}{p_{P_4}} = 0.5P \tag{ii}$$

With $P = 1$ atm, Equation (i) gives

$$\ln K_p = \ln(0.5) = \frac{-27{,}109}{T} - 0.95 \ln T + 25.18$$

which has the solution $T = 1429$ K. Thus, at $P = 1$ atm and $T = 1429$ K, $X_{P_2} = X_{P_4} = 0.5$ in a P_4–P_2 mixture.

b. From Equations (i) and (ii):

$$K_{P,2000\,\mathrm{K}} = 81.83 = 0.5P$$

which gives $P = 163.6$ atm. Thus, at $P = 163.6$ atm and $T = 2000$ K, $X_{P_4} = X_{P_2} = 0.5$ in the mixture.

The variations of X_{P_4} and X_{P_2} with temperature in an equilibrated P_4–P_2 mixture at $P = 1$ atm and at $P = 163.6$ atm are shown in Figure 11.6. Since the dissociation of P_4 is endothermic, increasing the temperature at constant pressure shifts the equilibrium toward P_2, and since the dissociation increases the number of moles present, increasing the pressure at constant temperature shifts the equilibrium toward P_4.

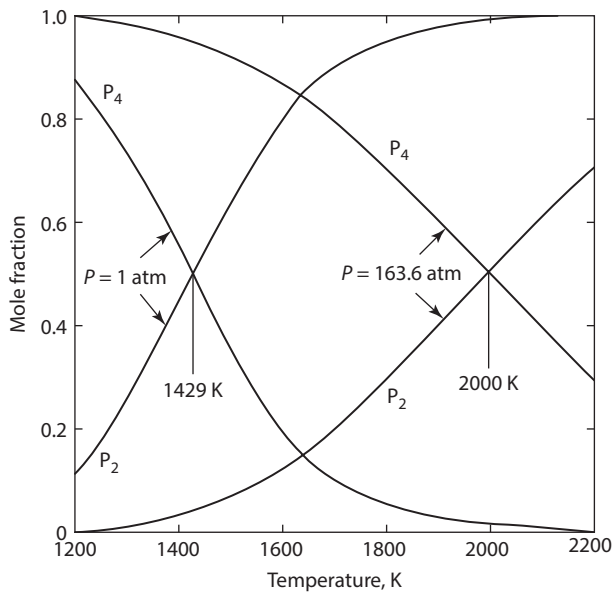

FIGURE 11.6 The variations of the mole fractions of P_2 and P_4 with temperature in an equilibrated P_2–P_4 mixture at $P = 1$ atm and at $P = 163.6$ atm.

QUANTITATIVE PROBLEM 2

Consider the cracking of gaseous ammonia according to the reaction

$$2NH_{3(g)} = N_{2(g)} + 3H_{2(g)} \tag{i}$$

under the following conditions:

a. Constant total pressure
b. Constant volume at 400°C

SOLUTION TO QUANTITATIVE PROBLEM 2

a. The standard Gibbs free energy change for the reaction given by Equation (i) is

$$\Delta G^\circ = 87{,}030 - 25.8T \ln T - 31.7T \text{ J}$$

Therefore,

$$\Delta G^\circ_{673\,\text{K}} = -47{,}370 \text{ J} \quad \text{and} \quad K_{P,673\text{K}} = 4748$$

From the stoichiometry of the reaction, partial decomposition of 1 mole of NH_3 produces $3x$ moles of H_2, x moles of N_2, and $(1-2x)$ moles of NH_3. Thus, for

	$2NH_3$	$\rightarrow$	N_2	+	$3H_2$
Initially,	1		0		0
Upon decomposition,	$1-2x$		x		$3x$

and $n_T = 1-2x+x+3x = 1+2x$ moles. Thus,

$$p_{H_2} = \frac{3x}{1+2x}P, \quad p_{N_2} = \frac{x}{1+2x}P, \quad \text{and} \quad p_{NH_3} = \frac{1-2x}{1+2x}P$$

such that

$$K_{P,673\text{K}} = \frac{p_{H_2}^3 p_{N_2}}{p_{NH_3}^2} = \frac{27x^4P^2}{(1+2x)^2(1-2x)^2} \tag{ii}$$

See Figure 11.5, Using the identity $(1-y)(1+y) = 1-y^2$, Equation (ii) can be written as

$$K_P = \frac{27x^4P^2}{\left[1-(2x)^2\right]^2}$$

or

$$K_P^{1/2} = \frac{5.196x^2P}{\left(1-4x^2\right)}$$

Thus, for a constant total pressure of 1 atm,

$$(4748)^{1/2}\left(1-4x^2\right)=5.196x^2$$

which has the solution $x=0.4954$. Thus, at equilibrium,

$$p_{H_2}=\frac{3x}{1+2x}=0.7465 \text{ atm}$$

$$p_{N_2}=\frac{x}{1+2x}=0.2488 \text{ atm}$$

and

$$p_{NH_3}=\frac{1-2x}{1+2x}=0.0047 \text{ atm}$$

in which state, 99.53% of the NH_3 has decomposed.

An alternative approach to the problem is as follows. From the stoichiometry of the reaction, at all times

$$p_{H_2}=3p_{N_2} \tag{iii}$$

and

$$P=p_{NH_3}+p_{N_2}+p_{H_2} \tag{iv}$$

Eliminating p_{NH_3} and p_{H_2} from Equations (iii) and (iv) and substituting into Equation (ii) gives

$$K_P=\frac{27p_{N_2}^4}{\left(P-4p_{N_2}\right)^2}$$

or

$$K_P^{1/2}=\frac{(27)^{1/2}\,p_{N_2}^2}{\left(P-4p_{N_2}\right)}$$

with $P=1$ atm,

$$(4784)^{1/2}\left(1-4p_{N_2}\right)=(27)^{1/2}\,p_{N_2}^2$$

which gives

$$p_{N_2}=0.2488 \text{ atm}$$

$$p_{H_2}=3p_{N_2}=0.7464 \text{ atm}$$

and

$$p_{NH_3}=1-p_{H_2}-p_{N_2}=0.0048 \text{ atm}$$

b. Now consider that the decomposition occurs at constant volume. As the decomposition reaction increases the number of moles of gas from 1 to $(1+2x)$, the reaction at constant P increases the volume of the gas by the factor $(1+2x)$. From Le Chatelier's principle, an increase in pressure shifts the equilibrium in that direction which decreases the number of moles of gas present—that is, in the direction $3H_2+N_2 \rightarrow 2NH_3$. Thus, the extent of equilibrium decomposition of ammonia at constant volume will be less than that occurring at constant pressure and will cause an increase in pressure.

As before,

$$p_{H_2} = \frac{3x}{1+2x} P'$$

$$p_{N_2} = \frac{x}{1+2x} P'$$

and

$$p_{NH_3} = \frac{1-2x}{1+2x} P' \tag{v}$$

where P' is the pressure of the reacting mixture. Before decomposition begins, the 1 mole of NH_3 obeys the relation $PV=RT$. The decomposition reaction, at constant V and T, increases the number of moles of gas to $(1+2x)$ and hence increases the total pressure of the gas to P', where

$$P'V = (1+2x)RT$$

Therefore,

$$V = \text{constant} = \frac{RT}{P} = \frac{(1+2x)RT}{P'}$$

such that, in Equation (v), the original pressure of NH_3 at volume V before decomposition started is equal to $P'/(1+2x)$. Thus, for an original pressure of $P=1$ atm, at equilibrium,

$$p_{H_2} = 3x$$

$$p_{N_2} = x$$

and

$$p_{NH_3} = 1-2x$$

Hence,

$$K_P = \frac{27x^4}{(1-2x)^2}$$

or

$$K_P^{1/2} = (4784)^{1/2} = \frac{(27)^{1/2}\, x^2}{(1-2x)}$$

which has the solution $x = 0.4909$. Thus,

$$p_{H_2} = 3x = 1.4727 \text{ atm}$$

$$p_{N_2} = x = 0.4909 \text{ atm}$$

$$p_{NH_3} = 1 - 2x = 0.0182 \text{ atm}$$

$$P = \sum_i p_i = 1.9819 = 1 + 2x$$

in which state, 98.18% of the NH_3 has decomposed.

It can be shown that the yield of NH_3 formed by the reaction between H_2 and N_2 is maximized when the reactants H_2 and N_2 are mixed in the molar ratio 3/1. In the mixture, $P = p_{H_2} + p_{N_2} + p_{NH_3}$, and, at reaction equilibrium, let it be that

$$p_{H_2} = a p_{N_2}$$

Thus,

$$p_{NH_3} = P - (a+1)\, p_{N_2}$$

or

$$p_{N_2} = \frac{P - p_{NH_3}}{a+1} \quad \text{and} \quad p_{H_2} = \frac{a\left(P - p_{NH_3}\right)}{(a+1)}$$

and hence,

$$\begin{aligned} K_P &= \frac{p_{NH_3}^2}{p_{H_2}^3\, p_{N_2}} \\ &= \frac{p_{NH_3}^2}{\left[a\left(P - p_{NH_3}\right)/(a+1)^3\right]\left[\left(P - p_{NH_3}\right)/(a+1)\right]} \\ &= \frac{p_{NH_3}^2\,(a+1)^4}{a^3\left(P - p_{NH_3}\right)^4} \end{aligned} \tag{vi}$$

It now must be shown that p_{NH_3} has its maximum value when $a = 3$; that is,

$$\frac{dp_{NH_3}}{da} = 0 \quad \text{when} \quad a = 3$$

The derivative is most easily obtained by taking the logarithms of Equation (vi):

$$\ln K_P + 3\ln a + 4\ln\left(P - p_{NH_3}\right) = 2\ln p_{NH_3} + 4\ln(a+1)$$

and differentiating to obtain

$$\left[\frac{3}{a} - \frac{4}{(1+a)}\right]da = \left[\frac{2}{p_{NH_3}} + \frac{4}{\left(P - p_{NH_3}\right)}\right]dp_{NH_3}$$

Thus, $dp_{NH_3}/da = 0$ requires that $3/a = 4/(1+a)$, or $a = 3$.

The stoichiometry of the reaction shows that, for the ratio p_{H_2}/p_{N_2} to have the value 3 in the equilibrium mixture, the reactants H_2 and N_2 must be mixed in the ratio 3/1.

PROBLEMS

11.1 A gas mixture of 50% CO, 25% CO_2, and 25% H_2 (by volume) is fed to a furnace at 900°C. Determine the composition of the equilibrium CO–CO_2–H_2–H_2O gas if the total pressure of the gas in the furnace is 1 atm.

11.2 How much heat is evolved when 1 mole of SO_2 and ½ mole of O_2, each at 1 atm pressure, react to form the equilibrium SO_3–SO_2–O_2 mixture at 1000 K and 1 atm pressure?

11.3 A CO_2–CO–H_2O–H_2 gas mixture at a total pressure of 1 atm exerts a partial pressure of oxygen of 10^{-7} atm at 1600°C. In what ratio were the CO_2 and H_2 mixed to produce the gas with this oxygen pressure?

11.4 Lithium bromide vapor dissociates according to $LiBr_{(g)} \rightarrow Li_{(g)} + \frac{1}{2}Br_{2,(g)}$. At what temperature does the partial pressure of Li reach the value of 10^{-5} atm when the gas is heated at a constant total pressure of 1 atm?

11.5 When SO_3 is decomposed at the constant pressure P and $T = 1000$ K, the partial pressure of O_2 in the equilibrium gas is 0.05 atm. What is the pressure P? If the pressure of this equilibrated gas is increased to 1 atm, to what value must the temperature be decreased to produce a gas mixture in which $p_{O_2} = 0.05$ atm?

11.6 For the dissociation of nitrogen according to

$$N_2 = 2N$$

$$\Delta G^\circ = 945{,}000 - 114.9T \text{ J}$$

calculate

a. The equilibrium partial pressure of N in nitrogen gas at 3000 K and a total pressure of 1 atm
b. The total pressure of the gas, at 3000 K, at which the partial pressure of N_2 is 90% of the total pressure

11.7 Ammonia gas is heated to 300°C. At what total pressure is the mole fraction of N_2 in the equilibrium gas mixture equal to 0.2? Calculate the standard enthalpy change and the standard entropy change for the reaction

$$\frac{3}{2}H_{2(g)} + \frac{1}{2}N_{2(g)} = NH_{3(g)}$$

at 300°C.

11.8 By establishing the equilibrium

$$PCl_{5(g)} = PCl_{3(g)} + Cl_{2(g)}$$

at 500 K in a mixture of PCl_5 and PCl_3, a gas is obtained at 1 atm total pressure in which the partial pressure of Cl_2 is 0.1 atm. In what ratio were PCl_5 and PCl_3 mixed to obtain this equilibrium gas?

11.9 Air and hydrogen are mixed in the ratio 4:1 and are heated to 1200 K. Calculate the partial pressures of H_2 and O_2 in the equilibrium gas at 1 atm pressure and at 10 atm pressure. Air contains 21 volume percent O_2.

11.10 One mole of each of hydrogen, iodine vapor, and HI gas are allowed to react at 1500 K and $P = 1$ atm. Calculate the mole fractions of H_2, I_2, and HI in the equilibrium mixture. The temperature is then changed to that value at which p_{HI} in the equilibrated gas is five times p_{H_2}. What is this temperature?

11.11 Consider the reduction of magnetite by CO to form pure iron:

$$Fe_3O_{4(s)} + 4CO_{(g)} = 3Fe_{(s)} + 4CO_{2(g)}$$

Calculate the partial pressure of CO and CO_2 in terms of the equilibrium constant K_P for the reaction.

11.12 It is known that at 300 K, the value of K_P for a certain reaction is 10^{12}. For the reaction, ΔH° is 100 kJ/mole.

a. Determine if this reaction is favorable at 800 K and estimate K_P(800 K). Explain.
b. The actual value of K_P (800 K) is 35. Explain any discrepancy from your estimate.

11.13* Calculate the partial pressure of monatomic hydrogen gas at 2000 K and 1 atm. pressure. For ½ $H_{2(g)} = H_{(g)}$
$\Delta H^\circ_{298} = 217{,}990$ J and $\Delta S^\circ_{298} = 49.35$ joules/degree

11.14*

i. Calculate ΔG°_{1000} for the reaction

$$CH_{4(g)} + H_2O_{(g)} = CO_{(g)} + 3H_{2(g)}$$

ii. At what temperature does $K_P = 1$?

iii. In which direction does the equilibrium shift when:
   a. The temperature of an equilibrated CH_4–H_2O–CO–H_2 gas mixture is increased?
   b. The total pressure is decreased?

11.15* Sketch qualitatively (no numbers) the natural log of K_P versus $1/T$ for the reaction: $2Cl = Cl_2$. Of importance is the *sign* of the *slope* and the *intercept on the ordinate*, whether it be plus or minus.

* New problem in this edition.

12 Reactions Involving Pure Condensed Phases and a Gaseous Phase

12.1 INTRODUCTION

The criterion for equilibrium in a gaseous reaction system was discussed in Chapter 11. We now investigate how the situation is changed when one or more of the reactants or products of the reaction occurs as a *condensed phase*. In this chapter, we consider condensed phases that are of *pure species*—that is, are of fixed composition. Many practical systems occur in this category: for example, the reaction of pure metals with gaseous elements to form pure metal oxides, sulfides, halides, and so on. Questions of interest include the following:

1. What is the maximum oxygen pressure that can be tolerated in a gaseous atmosphere without oxidation of a given metal occurring at a given temperature?
2. To what temperature must a given carbonate, for example, be heated in a gaseous atmosphere of a given partial pressure of carbon dioxide to cause the decomposition of the carbonate?

The first question is of interest in any of the many annealing processes that are performed in the laboratory or industrial plants. The second is of interest in, for example, the production of lime from limestone.

In such systems, complete equilibrium entails the establishment of the following:

- *Phase equilibrium* among the individual condensed phases and the gas phase
- *Reaction equilibrium* among the various species present in the gas phase

Since phase equilibrium is established when the pure condensed phases exert their saturated vapor pressures, which are uniquely fixed when the temperature of the system is fixed, then the only pressures that can be varied at constant temperature are those of the species that exist only in the gas phase. The unique variations, with temperature, of the saturated vapor pressures of pure condensed-phase species and the relative insensitivity of the Gibbs free energies of condensed phases to changes in pressure considerably simplify the thermodynamic treatment of reaction equilibria in systems containing both gaseous and pure condensed phases.

12.2 REACTION EQUILIBRIUM IN A SYSTEM CONTAINING PURE CONDENSED PHASES AND A GAS PHASE

Consider the reaction equilibrium between a pure solid metal M, its pure oxide[1] MO, and oxygen gas at the temperature T and the pressure P:

$$\mathrm{M}_{(s)} + \frac{1}{2}\mathrm{O}_{2(g)} = \mathrm{MO}_{(s)}$$

Here we assume that the oxygen is insoluble in the solid metal and that MO is stoichiometric. They are pure species.

Both the metal M and the oxide MO are in equilibrium with their *vapor species* in the gas phase, as is required by the criterion for phase equilibrium, that is, their chemical potentials must be equal:

$$\bar{G}_{\mathrm{M}}\left(\text{in the gas phase}\right) = G_{\mathrm{M}}\left(\text{in the solid metal phase}\right)$$

and

$$\bar{G}_{\mathrm{MO}}\left(\text{in the gas phase}\right) = G_{\mathrm{MO}}\left(\text{in the solid oxide phase}\right)$$

Thus, the reaction equilibrium

$$\mathrm{M}_{(g)} + \frac{1}{2}\mathrm{O}_{2(g)} = \mathrm{MO}_{(g)}$$

is established in the gas phase. From Equation 11.6, the criterion for this reaction equilibrium to occur at the temperature T is

$$\Delta G^{\circ} = G^{\circ}_{\mathrm{MO}(g)} - \frac{1}{2}G^{\circ}_{\mathrm{O}_2(g)} - G^{\circ}_{\mathrm{M}(g)} = -RT\ln\frac{p_{\mathrm{MO}}}{p_{\mathrm{M}}p_{\mathrm{O}_2}^{1/2}} \tag{12.1}$$

or

$$\Delta G^{\circ} = -RT\ln\frac{p_{\mathrm{MO}}}{p_{\mathrm{M}}p_{\mathrm{O}_2}^{1/2}}.$$

where ΔG° is the difference between the Gibbs free energy of 1 mole of *gaseous* MO *at 1 atm pressure* and the sum of the Gibbs free energies of ½ mole of oxygen gas at 1 atm pressure and 1 mole of *gaseous* M *at 1 atm pressure*, all at the temperature T. Since M and MO are present in the system as *pure solids*, phase equilibrium requires that p_{MO} in Equation 12.1 be the saturated vapor pressure of solid MO at the temperature T, and that p_{M} be the saturated vapor pressure of solid M at the temperature T.

[1] By *pure oxide*, it is meant that there is no third element dissolved in it. It acts as a single component.

Thus, the values of p_{MO} and p_M in the gas phase are uniquely fixed by the temperature T. Thus, the value of p_{O_2} in Equation 12.1, at which reaction equilibrium is established, is fixed at the temperature T.

As stated previously, phase equilibrium in the system requires that

$$\bar{G}_M\left(\text{in the gas}\right) = G_M\left(\text{in the solid metal phase}\right) \tag{12.2}$$

and

$$\bar{G}_{MO}\left(\text{in the gas phase}\right) = G_{MO}\left(\text{in the solid oxide phase}\right) \tag{12.3}$$

Equation 12.2 can be written as

$$G^{\circ}_{M(g)} + RT \ln p_{M(g)} = G^{\circ}_{M(s)} + \int_{P=1}^{P=p_{M(g)}} V_{M(s)} dP \tag{12.4a}$$

and Equation 12.3 can be written as

$$G^{\circ}_{MO(g)} + RT \ln p_{MO(g)} = G^{\circ}_{MO(s)} + \int_{P=1}^{P=p_{MO(g)}} V_{MO(s)} dP \tag{12.5a}$$

Consider Equation 12.4.

- $G^{\circ}_{M(s)}$ is the molar Gibbs free energy of solid M under a pressure of 1 atm at the temperature T.
- The integral $\int_{P=1}^{P=p_{M(g)}} V_{M(s)} dP$ is the effect of a change in pressure from $P = 1$ atm to $P = P$ on the value of the molar Gibbs free energy of solid M at the temperature T (where $V_{M(s)}$ is the molar volume of the solid metal at the pressure P and temperature T).

In the following, it is shown that the value of the integral is negligible compared with the other values in Equation 12.4a, and hence, Equation 12.4a can be written as

$$G^{\circ}_{M(g)} + RT \ln p_{M(g)} = G^{\circ}_{M(s)} \tag{12.4b}$$

As an example to show that this is the case, consider iron as a typical metal at a temperature of 1000°C. The saturated vapor pressure of solid iron at 1000°C is 6×10^{-10} atm, and thus, the term $RT \ln p_{M(g)}$ has the value $8.3144 \times 1273 \times \ln (6 \times 10^{-10}) = -224{,}750$ J. The molar volume of solid iron at 1000°C is 7.34 cm^3, which in the range 0–1 atm is independent of pressure. The value of the integral for $P = 6 \times 10^{-10}$ atm is

$$\int_{P=1}^{P=p_{M(g)}} 7.24 dP \approx 7.24 \text{ cm}^3 \cdot \text{atm} \times 101.325 \text{ KPa/atm} \times (-1) = -0.74 \text{ J}$$

It is thus seen that $G^{\circ}_{\mathrm{Fe}(g)}$ at 1000°C is much larger in value than $G^{\circ}_{\mathrm{Fe}(s)}$ at 1000°C, which is to be expected in view of the large metastability of the iron vapor at 1 atm pressure and a temperature of 1000°C with respect to the solid. Since the value of the integral (−0.74 J), is small compared with −224,750 J, Equation 12.4a can be written as Equation 12.4b.

As a consequence of the negligible effect of pressure on the Gibbs free energy of a condensed phase (when the pressure is in the range 0–1 atm), the standard state of a species occurring as a condensed phase can be defined as being the *pure species at the temperature T*. Thus, the specification that the pressure be 1 atm is no longer required. $G^{\circ}_{\mathrm{M}(s)}$ is now simply the molar Gibbs free energy of pure solid M at the temperature *T*.

Similarly, Equation 12.5a can be written as

$$G^{\circ}_{\mathrm{MO}(g)} + RT \ln p_{\mathrm{MO}(g)} = G^{\circ}_{\mathrm{MO}(s)} \tag{12.5b}$$

and thus, Equation 12.1 can be written as

$$\Delta G^{\circ} = G^{\circ}_{\mathrm{MO}(s)} - \frac{1}{2} G^{\circ}_{\mathrm{O}_2(g)} - G^{\circ}_{\mathrm{M}(s)} = -RT \ln \left(\frac{1}{p^{1/2}_{\mathrm{O}_2}} \right)$$

or

$$\Delta G^{\circ} = -RT \ln K \tag{12.6}$$

where $K = 1/p^{1/2}_{\mathrm{O}_2}$, and ΔG° is the *standard Gibbs free energy change* for the reaction

$$\mathrm{M}_{(s)} + \frac{1}{2}\mathrm{O}_{2(g)} = \mathrm{MO}_{(s)}$$

Thus, in the case of a reaction equilibrium involving only pure condensed phases and a gas phase, the equilibrium constant *K* can be written solely in terms of those species that occur *only* in the gas phase. Again, since ΔG° is a function only of temperature, then *K is a function only of temperature*. Thus, at any fixed temperature, the establishment of reaction equilibrium occurs at a unique value of $p_{\mathrm{O}_2} = p_{\mathrm{O}_2(\mathrm{eq}.T)}$.

For *reactive systems*, it is best to consider the number of components to be the number of distinct molecular species present, *N* (called herein *component species*), and then to reduce this number by the *number of independent reactions* involved in the equilibrium, *R*. Thus for the case under discussion, the Gibbs Equilibrium Phase Rule is written as:

$$\mathcal{F} = (N - R) + 2 - \Phi$$

$\Phi = 3$ (two pure solids and a gas phase)
$N = 3$ component species (M, O_2, and MO)
$R = 1$ reaction

$$\mathcal{F} = (N - R) + 2 - \Phi = \ 2 + 2 - 3 = 1$$

Thus the reaction can be at equilibrium at many temperatures (one degree of freedom), but at each temperature, the vapor pressure of the species is of specific values that are fixed by the chosen temperature.

If, at any temperature T, the actual partial pressure of oxygen in a closed metal–metal oxide–oxygen system is greater than $p_{O_2(\text{eq.}T)}$, spontaneous oxidation of the metal will occur, consuming oxygen and decreasing the oxygen pressure in the gas phase. When the actual oxygen pressure has thus been decreased to $p_{O_2(\text{eq.}T)}$, then, provided that both solid phases are still present, the oxidation ceases and reaction equilibrium is re-established. Similarly, if the oxygen pressure in the closed vessel was originally less than $p_{O_2(\text{eq.}T)}$, spontaneous *reduction* of the oxide would occur until $p_{O_2(\text{eq.}T)}$ was reached.

Extraction metallurgical processes involving the reduction of oxide ores depend on the achievement and maintenance of an oxygen pressure less than $p_{O_2(\text{eq.}T)}$ in the reaction vessel.

For example, the standard Gibbs free energy change for the reaction

$$4Cu_{(s)} + O_{2(g)} = 2Cu_2O_{(s)}$$

is

$$\Delta G^\circ = -324,400 + 138.5T \text{ J}$$

in the temperature range 298–1200 K. Thus,

$$-\ln K = \ln p_{O_2(\text{eq.}T)} = \frac{\Delta G^\circ}{RT}$$

or

$$\log p_{O_2(\text{eq.}T)} = -\frac{324,400}{2.303 \times 8.3144T} + \frac{138.5}{2.303 \times 8.3144}$$
$$= -\frac{16,940}{T} + 7.23$$

This variation of $\log p_{O_2(\text{eq.}T)}$ with $1/T$ is drawn as the line *ab* in Figure 12.1. All points on the line represent the unique oxygen pressure, $p_{O_2(\text{eq.}T)}$, required for equilibrium among solid Cu, solid Cu_2O, and oxygen gas at the particular temperature T for the system (there is only one degree of freedom, $\mathcal{F}$, on the line). Thus, the line *ab* divides the diagram into two regions. Above the line *ab* (where $p_{O_2} > p_{O_2(\text{eq.}T)}$), the metal phase is not stable, and thus, the system exists as $Cu_2O_{(s)} + O_{2(g)}$. Below the line *ab* (where $p_{O_2} < p_{O_2(\text{eq.}T)}$), the oxide is not stable, and hence the system exists as $Cu_{(s)} + O_{2(g)}$.

Other equilibria among two condensed pure phases and a gas phase include the formation of *hydroxides* and *carbonates*.

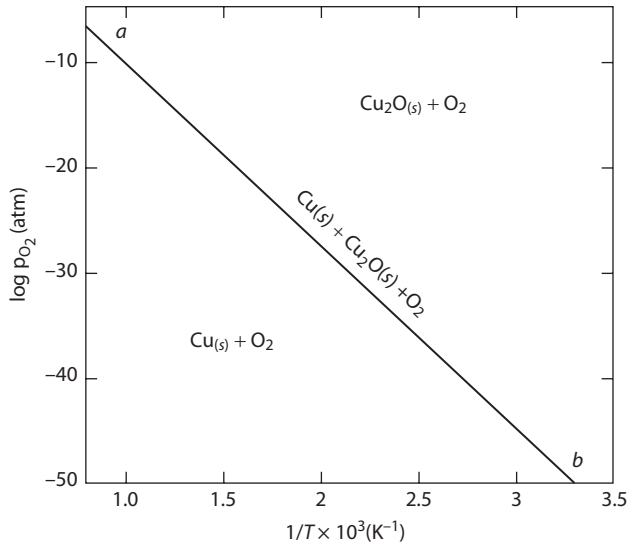

FIGURE 12.1 The variation, with temperature, of the oxygen pressure required for maintenance of the equilibrium $4Cu_{(s)} + O_2 = 2Cu_2O$.

For example, at the temperature T, the equilibrium

$$MO_{(s)} + H_2O_{(g)} = M(OH)_{2(s)}$$

occurs when

$$G^\circ_{MO(s)} + G^\circ_{H_2O(g)} + RT \ln p_{H_2O} = G^\circ_{M(OH)_{2(s)}}$$

that is, when

$$\Delta G^\circ = -RT \ln K = RT \ln p_{H_2O(eq.T)}$$

Similarly, the equilibrium

$$MO_{(s)} + CO_{2(g)} = MCO_{3(s)}$$

occurs when

$$G^\circ_{MO(s)} + G^\circ_{CO_2(g)} + RT \ln p_{CO_2(eq.T)} = G^\circ_{MCO_3(s)}$$

that is, when

$$\Delta G^\circ = -RT \ln K = RT \ln p_{CO_2(eq.T)}$$

12.3 THE VARIATION OF THE STANDARD GIBBS FREE ENERGY CHANGE WITH TEMPERATURE

For any chemical reaction, ΔG° for the reaction as a function of temperature can be written as:

$$\begin{aligned}\Delta G_T^\circ &= \Delta H_T^\circ - T\Delta S_T^\circ \\ &= \Delta H_{298}^\circ + \int_{298}^{T} \Delta c_p dT - T\Delta S_{298}^\circ - T\int_{298}^{T} \frac{\Delta c_p}{T} dT\end{aligned} \tag{12.7}$$

from which it is seen that the deviation from linearity between ΔG° and T depends on the sign and the magnitude of Δc_p for the reaction.

Generally, however, the variation of ΔG° with T is considered as follows. For each of the individual reactants and products of the reaction, the molar heat capacity, c_p, is expressed, over a stated range of temperature, in the form

$$c_p = a + bT + cT^{-2}$$

Hence, for the reaction, again within the stated range of temperature,

$$\Delta c_p = \Delta a + \Delta bT + \Delta cT^{-2}$$

From Kirchhoff's law: (Equation 6.4)

$$\left(\frac{\partial \Delta H^\circ}{\partial T}\right)_P = \Delta c_p = \Delta a + \Delta bT + \Delta cT^{-2}$$

where ΔH° is the standard enthalpy change for the reaction.

Integration gives

$$\Delta H_T^\circ = \Delta H_0 + \Delta aT + \frac{\Delta bT^2}{2} - \frac{\Delta c}{T} \tag{12.8}$$

where ΔH_0 is an integration constant which would be equal to the standard enthalpy of the reaction at 0 K only if the analytical expression for Δc_p as a function of T was valid down to 0 K. ΔH_0 is normally evaluated by substituting a known value of ΔH_T° into Equation 12.8.

The Gibbs–Helmholtz equation for the reaction is

$$\frac{\partial\left(\frac{\Delta G^\circ}{T}\right)}{\partial T} = -\frac{\Delta H^\circ}{T^2} = -\frac{\Delta H_0}{T^2} - \frac{\Delta a}{T} - \frac{\Delta b}{2} + \frac{\Delta c}{T^3}$$

integration of which gives

$$\frac{\Delta G^\circ}{T} = I + \frac{\Delta H_0}{T} - \Delta a \ln T - \frac{\Delta bT}{2} - \frac{\Delta c}{2T^2}$$

or

$$\Delta G^\circ = IT + \Delta H_0 - \Delta aT \ln T - \frac{\Delta bT^2}{2} - \frac{\Delta c}{2T} \tag{12.9}$$

where I is an integration constant.

Since $\Delta G^\circ = -RT \ln K$, then Equation 12.9 gives

$$\ln K = -\frac{\Delta H_0}{RT} - \frac{I}{R} + \frac{\Delta a \ln T}{R} + \frac{\Delta bT}{2R} + \frac{\Delta c}{2RT^2} \tag{12.10}$$

In Appendix 12A we show how I can be calculated for the reaction $4Cu_{(s)} + O_{2(g)} + 2Cu_2O_{(s)}$. The variation of ΔG°_T, as calculated from the experimentally measured variation of $p_{O_2(\text{eq.}T)}$ with temperature, can be fitted to an equation of the form

$$\Delta G^\circ = A + BT \ln T + CT$$

For the oxidation of $4Cu_{(s)}$ to $2Cu_2O_{(s)}$, this gives

$$\Delta G^\circ = -338,900 - 14.2T \ln T + 247T \text{ J} \tag{i}$$

which can be approximated in linear form by

$$\Delta G^\circ = -333,000 + 141.3T \text{ J} \tag{ii}$$

in the temperature range 298–1200 K.

At 300 K, Equations (12A.1), (i), and (ii) give, respectively, the values of: −282.8, −289.1, and −290.6 kJ for ΔG° and, at 1200 K, these give −169.7, −163.3, and −163.4 kJ for ΔG°. This shows that the various approximations are not too far off the mark.

12.4 ELLINGHAM DIAGRAMS

Ellingham[2] (Harold Johann Thomas Ellingham, 1897–1975) plotted the experimentally determined variations of ΔG° with T for the oxidation and sulfidation of a series of metals. He found that, in spite of the terms involving T, $T \ln T$, T^2, and T^{-1} in Equation 12.9, the relationship approximated to straight lines over ranges of temperature in which no change of state occurred. The relations could be expressed by means of the simple equation

$$\Delta G^\circ = A + BT \tag{12.11}$$

[2] H. J. T. Ellingham, "Reducibility of Oxides and Sulfides in Metallurgical Processes," *J. Soc. Chem. Ind.* (1944), vol. 63, p. 125.

in which the constant A is identified with the *temperature-independent* standard enthalpy change for the reaction, ΔH°, and the constant B is identified with the negative of the temperature-independent standard entropy change for the reaction, $-\Delta S^\circ$.

12.4.1 Ellingham Diagram of the Oxidation of Silver

The variation of ΔG° with T for the oxidation reaction

$$4Ag_{(s)} + O_{2(g)} = 2Ag_2O_{(s)}$$

is shown in Figure 12.2, which is known as an *Ellingham diagram*. From Equation 12.11, the length of the intercept of the line with the $T=0$ K axis gives ΔH°, and ΔS° is given by the negative of the slope of the line. Since ΔS° is a negative quantity (the reaction involves the disappearance of a mole of gas), the line has a positive slope. $\Delta G^\circ = 0$ at $T = 462$ K, and thus, at this temperature, pure solid silver and oxygen gas at 1 atm pressure are in equilibrium with pure solid silver oxide. From Equation 12.6, $\Delta G^\circ = -RT \ln K = RT \ln p_{O_2(\text{eq.}T)} = 0$ at 462 K, and, therefore, $p_{O_2(\text{eq.462K})} = 1$. If the temperature of the system (pure $Ag_2O_{(s)}$, pure $Ag_{(s)}$, and gaseous oxygen at 1 atm pressure) is decreased to T_1, then, since ΔG° for the oxidation reaction becomes negative, the metal phase becomes unstable relative to silver oxide and gaseous oxygen at 1 atm pressure and is hence spontaneously oxidized. At this temperature, the value of $p_{O_2(\text{eq.}T_1)}$ is calculated from $\Delta G^\circ_{T_1} = RT_1 \ln p_{O_2(\text{eq.}T_1)}$, and, since $\Delta G^\circ_{T_1}$ is a negative quantity, $p_{O_2(\text{eq.}T_1)} < 1$ atm, that is, some of the pure oxygen is used to oxidize the Ag.

Similarly, if the temperature of the system is increased from 462 K to T_2, then, since ΔG° for the oxidation becomes positive, the oxide phase becomes unstable

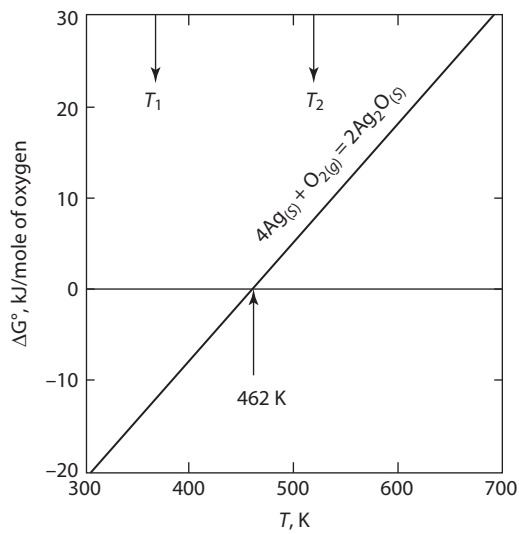

FIGURE 12.2 The Ellingham *line* for the oxidation of silver.

relative to silver metal and gaseous oxygen at 1 atm and spontaneously dissociates. Since $\Delta G^\circ_{T_2}$ is a positive quantity, $p_{O_2(\text{eq.}T_2)}$ is greater than 1 atm, since oxygen was released from the Ag oxide.

The value of ΔG° for oxidation is thus a measure of the *chemical affinity* (attraction) of the metal for oxygen, and the more negative the value of ΔG° at any temperature, the more *stable is the oxide*.

12.4.2 Some General Features of Ellingham Diagrams

For the oxidation reaction $A_{(s)} + O_{2(g)} = AO_{2(s)}$,

$$\Delta S^\circ = S^\circ_{AO_2(s)} - S^\circ_{O_2(g)} - S^\circ_{A(s)}$$

and since, generally, in the temperature range in which A and AO_2 are solid, $S^\circ_{O_2}$ is considerably greater than both S°_A and $S^\circ_{AO_2}$ (see, for example, Figure 6.14), then

$$\Delta S^\circ \approx -S^\circ_{O_2}$$

Thus, the standard entropy changes for oxidation reactions involving solid phases have nearly the same values, which correspond to the disappearance of 1 mole of oxygen gas initially at 1 atm pressure. Since the slopes of the lines in an Ellingham diagram are equal to $-\Delta S^\circ$, the lines for various metals are more or less parallel to one another, as will later be seen in the full Ellingham diagram shown in Figure 12.13.

ΔG° at any temperature is the sum of the enthalpy contribution ΔH° (which is independent of T if $\Delta c_p = 0$) and the entropy contribution $-T\Delta S$ (which, if $\Delta c_p = 0$, is a linear function of temperature). The two contributions are illustrated in Figure 12.3 for the oxidation reaction of cobalt:

$$2Co_{(s)} + O_{2(g)} = 2CoO_{(s)}$$

for which

$$\Delta G^\circ = -467{,}800 + 143.7T \text{ J}$$

in the temperature range 298–1763 K, and for the oxidation reaction of manganese,

$$2Mn_{(s)} + O_{2(g)} = 2MnO_{(s)}$$

for which

$$\Delta G^\circ = -777{,}800 + 152.6T \text{ J}$$

in the temperature range 298–1517 K.

Since the values of ΔS° for these two reactions are virtually equal to one another, Figure 12.3 shows that the relative stabilities of the oxides CoO and MnO are

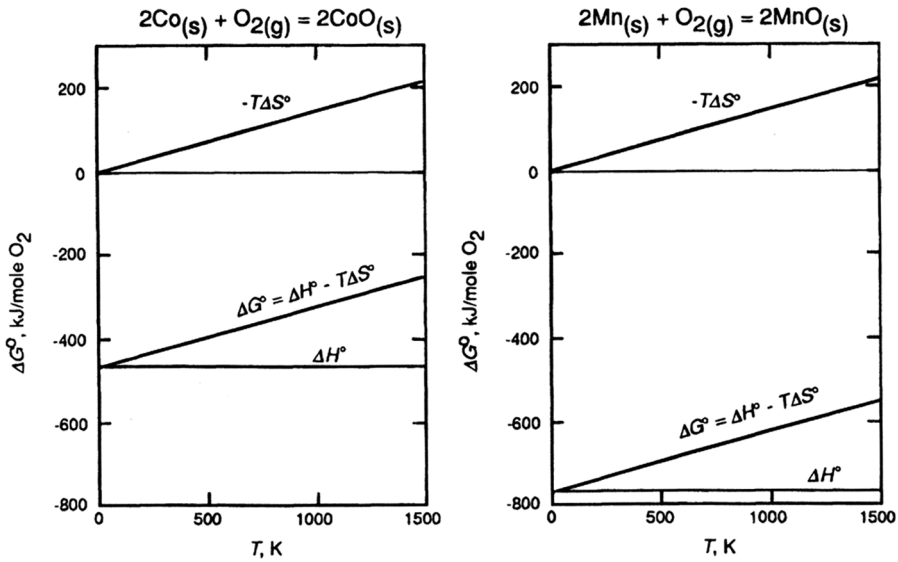

FIGURE 12.3 Illustration of the effect of the magnitude of ΔH° on the $\Delta G^\circ - T$ relationships for the oxidation of (a) Co and (b) Mn, both of the type $2M_{(s)} + O_{2(g)} = 2MO_{(s)}$.

determined by their values of ΔH°, in that the more negative the value of ΔH°, the more negative the value of ΔG°, and hence the more stable the oxide. Since

$$\ln K = -\frac{\Delta H^\circ}{RT} + \frac{\Delta S^\circ}{R} = \ln\left(\frac{1}{p_{O_2(\text{eq}.T)}}\right)$$

then

$$p_{O_2(\text{eq}.T)} = \exp\frac{\Delta H^\circ}{RT}\exp\frac{-\Delta S^\circ}{R} = \text{constant} \times \exp\frac{\Delta H^\circ}{RT}$$

Since ΔH° is a negative quantity:

- $p_{O_2(\text{eq}.T)}$ increases exponentially with increasing temperature
- at any temperature, $p_{O_2(\text{eq}.T)}$ decreases as ΔH° becomes more negative.

12.4.3 Ellingham Diagrams with Intersecting Stability Lines

Consider two oxidation reactions, the Ellingham lines of which intersect each other; for example,

$$2A + O_2 = 2AO \qquad \text{(i)}$$

and

$$B + O_2 = BO_2 \qquad \text{(ii)}$$

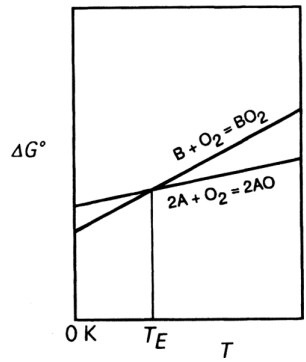

FIGURE 12.4 Intersecting Ellingham lines for two hypothetical oxidation reactions.

which are shown in Figure 12.4. From Figure 12.4 it is seen that $\Delta H^{\circ}_{(ii)}$ is more negative than $\Delta H^{\circ}_{(i)}$ and that $\Delta S^{\circ}_{(ii)}$ is more negative than $\Delta S^{\circ}_{(i)}$. Subtracting reaction (i) from reaction (ii) gives

$$B + 2AO = 2A + BO_2 \qquad \text{(iii)}$$

for which the variation of ΔG° with T is as shown in Figure 12.5. At temperatures less than T_E, A and BO_2 are stable with respect to B and AO, and at temperatures higher than T_E, the reverse is the case. At T_E, A, B, AO, and BO_2, occurring in their standard states, are in equilibrium with one another. The equilibrium at T_E (as with any equilibrium) occurs as the result of a compromise between enthalpy and entropy considerations. Since $\Delta H^{\circ}_{(iii)} = \Delta H^{\circ}_{(ii)} - \Delta H^{\circ}_{(i)} < 0$ and $\Delta S^{\circ}_{(iii)} = \Delta S^{\circ}_{(ii)} - \Delta S^{\circ}_{(i)} < 0$, the system $A + B + O_2$ has

- A minimum enthalpy when the system occurs as $A + BO_2$
- A maximum entropy when the system occurs as $B + AO$

At T_E, $\Delta H^{\circ}_{(iii)}$ equals $-T_E \Delta S^{\circ}_{(iii)}$, and thus, $\Delta G^{\circ}_{(iii)} = 0$. At temperatures less than T_E, the enthalpy contribution to $\Delta G^{\circ}_{(iii)}$ outweighs the entropy contribution, and thus, $\Delta G^{\circ}_{(iii)}$ is negative and $A + BO_2$ is the stable state. At temperatures greater than T_E, the reverse is the case: $\Delta G^{\circ}_{(iii)}$ is positive and $B + AO$ is the stable state.

Figure 12.5 thus shows that if pure A were to be used as a reducing agent to reduce pure BO_2, to form pure B and pure AO, then the reduction would have to be conducted at temperatures greater than T_E. The foregoing discussion also illustrates that, in order to compare the stabilities of different oxides, the Ellingham diagrams must be drawn for oxidation reactions involving the consumption of the *same number of moles of oxygen*. Thus, the unit of ΔG° for the oxidation reaction must be one of energy (e.g., joules) per mole of oxygen.

In order to avoid having to calculate the value of $p_{O_2(eq.T)}$ for any oxidation reaction, Richardson[3] (Frederick Denys Richardson 1913–1983) added a *nomographic* scale to the Ellingham diagram. This scale is constructed as follows. At any temperature T,

[3] F. D. Richardson and J. H. E. Jeffes, "The Thermodynamics of Substances of Interest in Iron and Steel Making from 0°C to 2400°C: I—Oxides," *J. Iron Steel Inst.* (1948), vol. 160, p. 261.

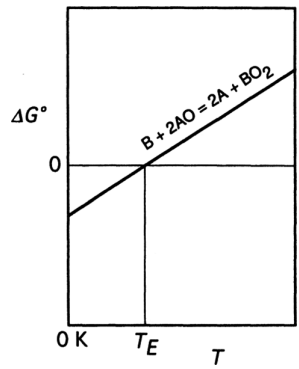

FIGURE 12.5 The variation of ΔG° with T for $B + 2AO = 2A + BO_2$ from Figure 12.4.

the standard Gibbs free energy change for an oxidation reaction, ΔG°_T, is given by Equation 12.6 as $RT \ln p_{O_2(\text{eq}.T)}$. However, from Equation 8.7,

$$G = G^\circ + RT \ln P$$

ΔG°_T is seen to be numerically equal to the decrease in the Gibbs free energy of 1 mole of oxygen gas when its pressure is decreased from 1 atm to $p_{O_2(\text{eq}.T)}$ atm at the temperature T. Consider the variation of ΔG with T in Equation 8.7. For a decrease in the pressure of 1 mole of ideal gas from 1 atm to P atm, ΔG versus T is a straight line with a slope of $R \ln P$, and, since $P < 1$, the line has a negative slope. Similarly, for an increase in the pressure of 1 mole of ideal gas from 1 to P atm, the variation of ΔG with T is linear with a positive slope of $R \ln P$. Thus, a series of lines can be drawn for given pressure changes (from 1 to P atm) as a function of temperature. These lines radiate from the point $\Delta G = 0$, $T = 0$, as shown in Figure 12.6. The superimposition of Figure 12.6 with a typical Ellingham diagram is shown in Figure 12.7.

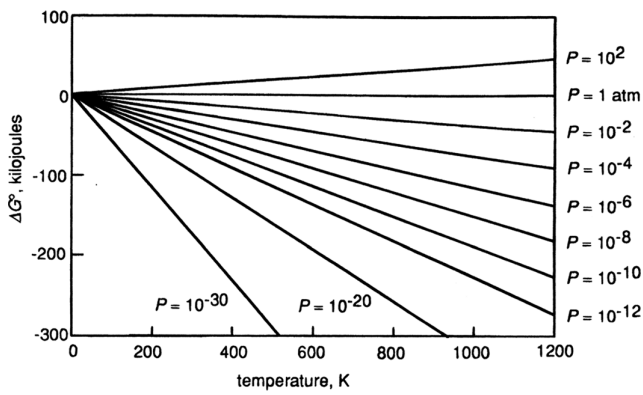

FIGURE 12.6 The variation, with temperature, of the difference between the Gibbs free energy of 1 mole of ideal gas in the state ($P = P$ atm, T) and the Gibbs free energy of 1 mole of ideal gas in the state ($P = 1$ atm, T).

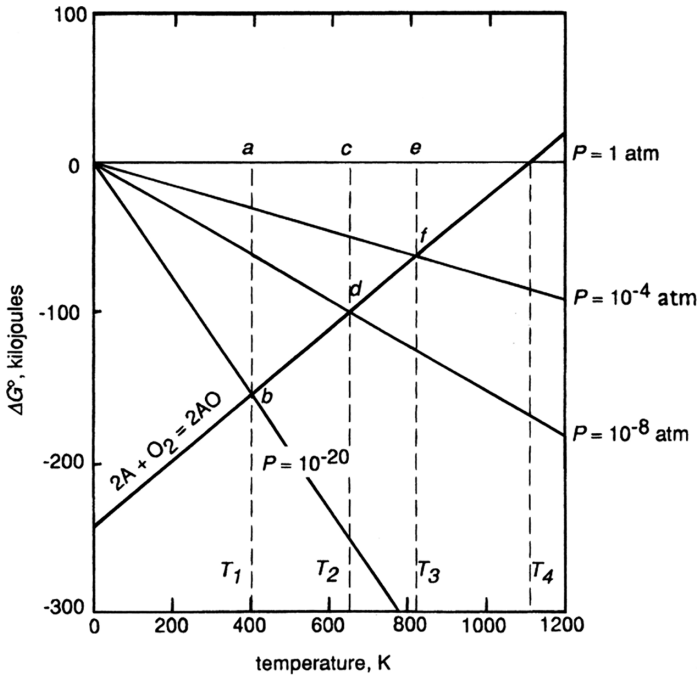

FIGURE 12.7 The superimposition of an Ellingham line onto Figure 12.6.

In Figure 12.7,

- At T_1, $\Delta G^\circ_{T_1} = ab$ = the decrease in Gibbs free energy when p_{O_2} is decreased from 1 atm to 10^{-20} atm at T_1.
- At T_2, $\Delta G^\circ_{T_2} = cd$ = the decrease in Gibbs free energy when p_{O_2} is decreased from 1 atm to 10^{-8} atm at T_2.
- At T_3, $\Delta G^\circ_{T_3} = ef$ = the decrease in Gibbs free energy when p_{O_2} is decreased from 1 atm to 10^{-4} atm at T_3.
- At T_4, $\Delta G = 0$, which corresponds to no change of p_{O_2} from 1 atm. Thus, $p_{O_2(\text{eq.}T_4)} = 1$ atm.

The $p_{O_2(\text{eq.}T)}$ nomographic scale is thus added to the Ellingham diagram along the right-hand edge and along the bottom edge. The value of $p_{O_2(\text{eq.}T)}$ for any metal–metal oxide equilibrium is read off the graph as that value on the scale which is collinear with the points $\Delta G^\circ = 0$, $T = 0$, and ΔG°_T, $T = T$. Thus, for the pressure = 10^{-20} atm, the metal A is stable for temperatures above 400 K.

The reactions (i) and (ii) shown in Figure 12.4 can be reexamined using the $p_{O_2(\text{eq.}T)}$ nomographic scale. Figure 12.4 is reproduced with a nomographic oxygen pressure scale in Figure 12.8. At any temperature lower than T_E (say, T_1), it is seen that

$$p_{O_2} \text{ (equation for reaction (ii) at } T_1) < p_{O_2} \text{ (equation for reaction (i) at } T_1)$$

If, therefore, metal A and metal B are placed in a *closed system* in an atmosphere of oxygen at $P = 1$ atm, both metals spontaneously oxidize. As a consequence of the consumption of oxygen to form the oxides, the pressure of oxygen decreases.

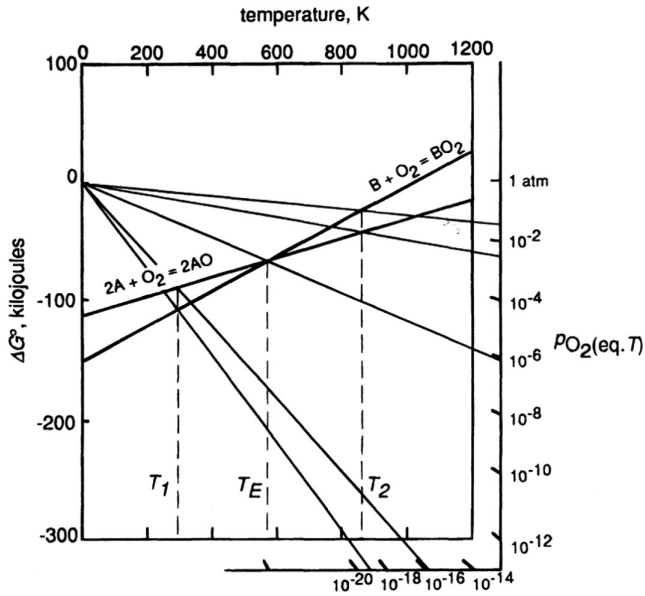

FIGURE 12.8 Illustration of the addition of the Richardson oxygen pressure nomographic scale to an Ellingham diagram.

Oxidation of both metals continues until the oxygen pressure is decreased to the value p_{O_2} (equation for reaction (i) at T_1), at which point the oxidation of A ceases. However, since $B + O_2$ at p_{O_2} (equation for reaction (i) at T_1) is still unstable with respect to BO_2, the oxidation of B continues until the oxygen pressure has been decreased to p_{O_2} (equation for reaction (ii) at T_1). Since the oxygen pressure is decreased below p_{O_2} (equation from reaction (i) at T_1), then AO becomes unstable with respect to A and O_2 at the prevailing pressure, and hence AO decomposes. When complete equilibrium is attained, the state of the system is $A + BO_2 + O_2$ at p_{O_2} (equation for reaction (ii) at T_1).

At any temperature higher than T_E (say, T_2),

$$p_{O_2}\left(\text{equation for reaction (i) at } T_2\right) < p_{O_2}\left(\text{equation for reaction (ii) at } T_2\right)$$

and an argument similar to this shows that the equilibrium state of the closed system containing, initially, $A + B + O_2$ at 1 atm pressure, is $B + AO + O_2$ at p_{O_2} (equation for reaction (i) at T_2). It is thus obvious that A, B, AO, BO_2, and an oxygen atmosphere are in equilibrium only at that temperature T at which

$$p_{O_2\,(\text{eq.}[\text{i}]T)} = p_{O_2\,(\text{eq.}[\text{ii}]T)}$$

Figure 12.9 shows that this unique temperature is T_E, the temperature at which the Ellingham lines intersect one another. The system has no degrees of freedom. The reader should verify this *via* the Gibbs Equilibrium Phase Rule.

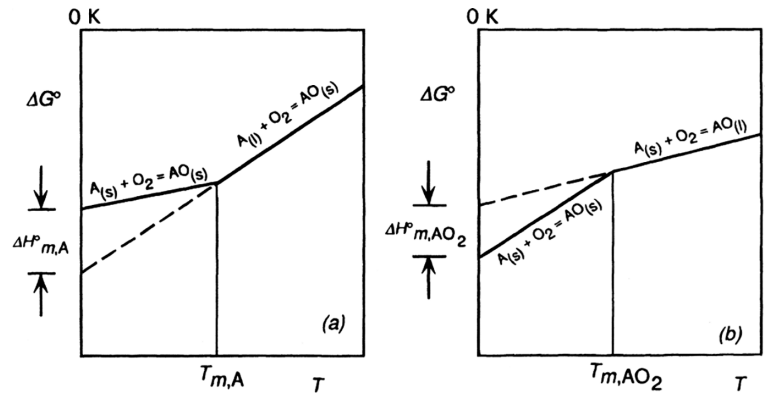

FIGURE 12.9 (a) The effect of melting of the metal on the Ellingham line for the oxidation of the metal. (b) The effect of melting of the metal oxide on the Ellingham line for the oxidation of the metal.

12.5 THE EFFECT OF PHASE TRANSFORMATIONS

In the previous section, it was stated that the variation of ΔG° with temperature can be approximated by a straight line only over ranges of temperature in which no change of phase of a reactant or product occurs. However, the enthalpy of a high-temperature phase (e.g., the liquid phase) exceeds that of a low-temperature phase (e.g., the solid phase) by the latent enthalpy of the phase change. Similarly, the entropy of the higher-temperature phase exceeds that of the lower-temperature phase. Thus, a change in the slope of the ΔG° line (an *elbow*) occurs on an Ellingham line at the temperature of a phase change in either a reactant phase or product phase of the reaction.

Consider the reaction

$$\mathrm{A}_{(s)} + \mathrm{O}_{2(g)} = \mathrm{AO}_{2(s)}$$

for which ΔH° is the standard enthalpy change and ΔS° is the standard entropy change. At $T_{m,\mathrm{A}}$, the melting temperature of A, the change of phase

$$\mathrm{A}_{(s)} \rightarrow \mathrm{A}_{(l)}$$

occurs, for which the standard enthalpy change (the enthalpy of melting) is $\Delta H^\circ_{m,\mathrm{A}}$ and the corresponding change in entropy is $\Delta S^\circ_{m,\mathrm{A}}$.

Thus, for the reaction

$$\mathrm{A}_{(l)} + \mathrm{O}_{2(g)} = \mathrm{AO}_{2(s)}$$

the standard enthalpy change is $\Delta H^\circ - \Delta H^\circ_{m,\mathrm{A}}$ and the standard entropy change is $\Delta S^\circ - \Delta S^\circ_{m,\mathrm{A}}$. Since $\Delta H^\circ_{m,\mathrm{A}}$ and $\Delta S^\circ_{m,\mathrm{A}}$ are positive quantities (melting is an endothermic process), then $\Delta H^\circ - \Delta H^\circ_{m,\mathrm{A}}$ is a larger negative quantity than is ΔH° and $\Delta S^\circ - \Delta S^\circ_{m,\mathrm{A}}$ is a larger negative quantity than is ΔS°. Consequently, the Ellingham

line for the oxidation of liquid A to form solid AO_2 has a greater slope than the corresponding line for the oxidation of solid A, and the line contains an *elbow upward* at $T_{m,A}$. This is shown in Figure 12.9a. The line does not contain a discontinuity, since, at $T_{m,A}$, $G^\circ_{A(s)} = G^\circ_{A(l)}$.

If the melting temperature of the oxide, T_{m,AO_2}, is lower than the melting temperature of the metal, then, at T_{m,AO_2}, the change of phase

$$AO_{2(s)} \rightarrow AO_{2(l)}$$

occurs, for which the standard enthalpy and entropy changes are, respectively, $\Delta H^\circ_{m,AO_2}$ and $\Delta S^\circ_{m,AO_2}$. Thus, for the reaction

$$A_{(s)} + O_{2(g)} = AO_{2(l)}$$

the standard enthalpy change is $\Delta H^\circ + \Delta H^\circ_{m,AO_2}$ and the standard entropy change is $\Delta S^\circ + \Delta S^\circ_{m,AO_2}$, both of which are less than the corresponding quantities ΔH° and ΔS°. In this case, the Ellingham line for oxidation of the solid metal to produce the liquid oxide has a lower slope than the line for oxidation of the solid metal to the solid oxide, and thus, as shown in Figure 12.9b, the Ellingham line has an *elbow downward* at T_{m,AO_2}.

In brief, if $T_{m,A} < T_{m,AO_2}$, the Ellingham line is as shown in Figure 12.10a, and, if $T_{m,A} > T_{m,AO_2}$, the line is as shown in Figure 12.10b.

12.5.1 Example of the Oxidation of Copper

Copper is a metal that melts at a lower temperature than its lowest oxide Cu_2O. The standard Gibbs free energy change for the oxidation of solid copper to form solid cuprous oxide in the range of temperature 298 K to $T_{m,Cu}$ is

$$\Delta G^\circ = -338{,}900 - 14.2T \ln T + 247T \text{ J} \qquad \text{(i)}$$

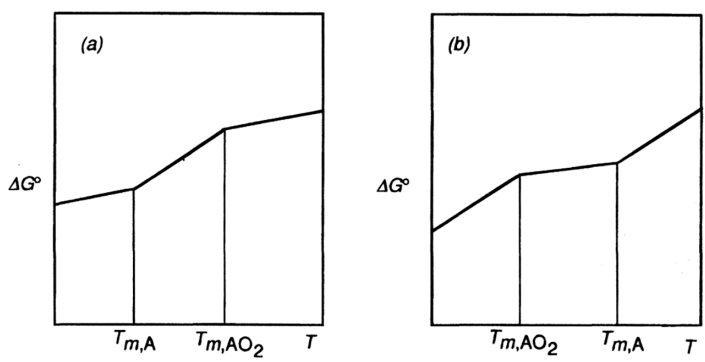

FIGURE 12.10 Illustration of the effects of phase changes of the reactants and products of the reactions on the Ellingham line for the reactions exhibited in Figure 12.9*a* and *b*.

and for the oxidation of liquid copper to form solid cuprous oxide in the range of temperature $T_{m,\mathrm{Cu}}$ to 1503 K,

$$\Delta G^\circ = -390{,}800 - 14.2T \ln T + 285.3T \text{ J} \qquad \text{(ii)}$$

These two lines, which are drawn in Figure 12.11, intersect at 1356 K, which is the melting temperature of copper. $\Delta G^\circ_{(\mathrm{i})} - \Delta G^\circ_{(\mathrm{ii})}$ gives

$$\Delta G = 51{,}900 - 38.3T \text{ J}$$

for the phase change

$$4\mathrm{Cu}_{(s)} = 4\mathrm{Cu}_{(l)}$$

or, for the melting of 1 mole of Cu,

$$\Delta G^\circ_{m,\mathrm{Cu}} = 12{,}970 - 9.58T \text{ J}$$

from which

$$\Delta H^\circ_{m,\mathrm{Cu}} = 12{,}970 \text{ J}$$

and

$$\Delta S^\circ_{m,\mathrm{Cu}} = 9.58 \text{ J/K}$$

Thus, at $T_{m,\mathrm{Cu}}$, the slope of the Ellingham line for the oxidation of Cu increases by 9.58 J/K.

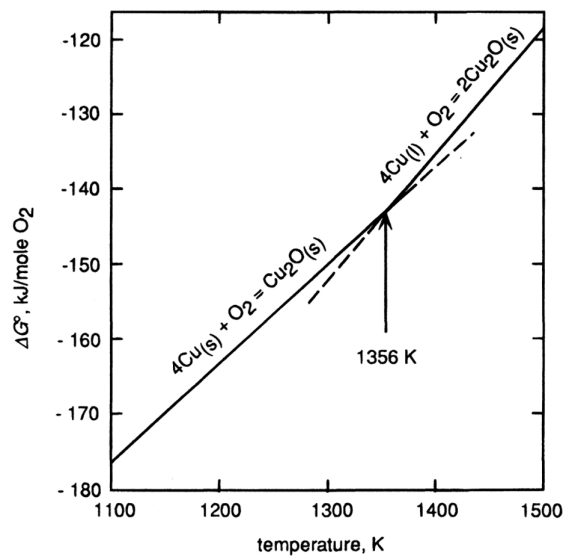

FIGURE 12.11 The Ellingham line for the oxidation of copper.

12.6 THE OXIDES OF CARBON

Carbon forms two gaseous oxides, CO and CO_2, according to

$$C_{(gr)} + O_{2(g)} = CO_{2(g)} \tag{i}$$

for which $\Delta G^\circ_{(i)} = -394{,}100 - 0.84T$ J, and

$$2C_{(gr)} + O_{2(g)} = 2CO_{(g)} \tag{ii}$$

for which $\Delta G^\circ_{(ii)} = -223{,}400 - 175.3T$ J.

Combining reactions (i) and (ii) gives

$$2CO_{(g)} + O_{2(g)} = 2CO_{2(g)} \tag{iii}$$

for which $\Delta G^\circ_{(iii)} = 2\Delta G^\circ_{(i)} - \Delta G^\circ_{(ii)} = -564{,}800 + 173.62T$ J.

The Ellingham lines for reactions (i), (ii), and (iii) are plotted in Figure 12.12, in which it is seen that

- The line for reaction (iii) has a positive slope (2 moles of gas produced from 3 moles of gas, $\Delta S^\circ_{(iii)} = -173.62$ J/K).
- The line for reaction (i) has virtually zero slope (1 mole of gas produced from 1 mole of gas, $\Delta S^\circ_{(i)} = 0.84$ J/K).
- The line for reaction (ii) has a negative slope (2 moles of gas produced from 1 mole of gas, $\Delta S^\circ_{(ii)} = 175.3$ J/K).

Consider the equilibrium

$$C_{(gr)} + CO_{2(g)} = 2CO_{(g)} \tag{iv}$$

for which $\Delta G^\circ_{(iv)} = \Delta G^\circ_{(ii)} - \Delta G^\circ_{(i)} = 170{,}700 - 174.5T$. Reaction (iv) is known as the *Boudouard reaction* (Octave Leopold Boudouard, 1872–1923) and is important in the reduction of the oxides of iron in the blast furnace.

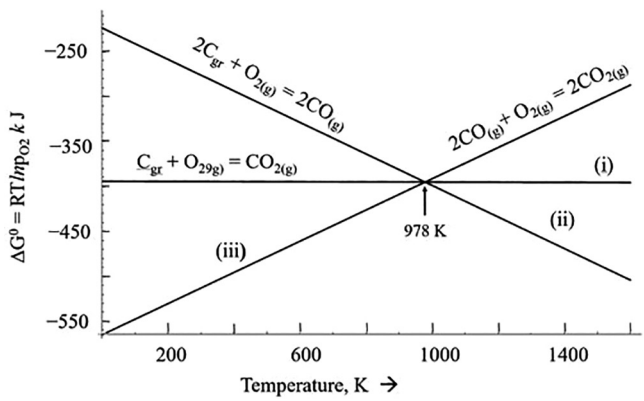

FIGURE 12.12 The Ellingham diagram for the oxides of carbon.

12.6.1 The Effect of Pressure on the Oxidation of Carbon

The value of $\Delta G^{\circ}_{(\mathrm{iv})} = 0$ at $T = 978$ K (705°C), the temperature at which the Ellingham lines for reactions (i) and (ii) intersect one another. At this temperature, CO and CO_2, in their standard states (i.e., both at 1 atm pressure), are in equilibrium with solid graphite, and the total pressure of the system is 2 atm. Since reaction equilibria are normally considered for systems under a total pressure of 1 atm, it is instructive to calculate the temperature at which CO and CO_2, each at a pressure of 0.5 atm, are in equilibrium with solid C. Consideration of Le Chatelier's principle indicates whether this temperature is higher or lower than 978 K. For reaction (iv), $\Delta G^{\circ}_{978\,\mathrm{K}} = 0 = -RT \ln K_p = -RT \ln\left(p^2_{\mathrm{CO}}/p_{\mathrm{CO_2}}\right)$; that is, at 978 K, $K_p = 1$, and hence $p_{\mathrm{CO_2}} = p_{\mathrm{CO}} = 1$ and $P_{\mathrm{total}} = 2$ atm. If the pressure of the system is decreased to 1 atm, then, as K_p is independent of pressure (remaining equal to unity) p_{CO} becomes greater than $p_{\mathrm{CO_2}}$; that is, the equilibrium shifts toward the CO side, as is predicted by Le Chatelier's principle. Since $\Delta H^{\circ}_{(\mathrm{iv})} = +170{,}700$ J, reaction (iv) is endothermic, and thus, from Le Chatelier's principle, as a decrease in temperature shifts the equilibrium in that direction which involves an evolution of heat, a decrease in temperature shifts the equilibrium toward the $C + CO_2$ side. Thus, if it is required to decrease the pressure of the system from 2 to 1 atm and, at the same time, maintain $p_{\mathrm{CO}} = p_{\mathrm{CO_2}}$, the temperature of the system must be decreased.

The temperature required for $p_{\mathrm{CO}} = p_{\mathrm{CO_2}}$ is calculated as follows. For reaction (i):

$$\mathrm{C} + \mathrm{O_2} = \mathrm{CO_2} \quad \Delta G^{\circ}_{(\mathrm{i})} = -394{,}100 - 0.84T \text{ J}$$

If the pressure of the CO_2, which is produced at 1 atm, is decreased to 0.5 atm, then, for the change of state

$$\mathrm{CO_2}\left(T, P = 1\text{ atm}\right) \rightarrow \mathrm{CO_2}\left(T, P = 0.5\,\text{atm}\right) \tag{v}$$

the decrease in Gibbs free energy is $\Delta G_{(\mathrm{v})} = RT \ln 0.5$, and hence, for the reaction

$$\mathrm{C}_{(gr)} + \mathrm{O}_{2\left(g, P=1\,\text{atm}\right)} = \mathrm{CO}_{2\left(\mathrm{g}, P=0.5\,\text{atm}\right)}$$

$$\begin{aligned} \Delta G_{(\mathrm{iv})} &= \Delta G^{\circ}_{(\mathrm{i})} + \Delta G_{(\mathrm{v})} \\ &= -394{,}100 - 0.84T + RT \ln 0.5 \text{ J} \end{aligned} \tag{vi}$$

This line is obtained on the Ellingham diagram by rotating the line for reaction (i) clockwise about its point of intersection with the $T = 0$ axis until, at the temperature T, the vertical separation between line (i) and line (vi) is $RT \ln 0.5$. This is illustrated in Figure 12.14.

Similarly, the Ellingham line for the reaction

$$2\mathrm{C}_{(gr)} + \mathrm{O}_{2\left(g, P=1\,\text{atm}\right)} = 2\mathrm{CO}_{\left(g, P=0.5\,\text{atm}\right)} \tag{vii}$$

is obtained as the sum of $\Delta G^{\circ}_{(\mathrm{ii})}$ and ΔG for the change of state

$$2\mathrm{CO}\left(T, P = 1\,\text{atm}\right) \rightarrow 2\mathrm{CO}\left(T, P = 0.5\,\text{atm}\right)$$

That is,

$$\Delta G_{(\text{vii})} = -223,400 - 175.3T + 2RT\ln 0.5 \text{ J}$$

This line is obtained by rotating the line for reaction (ii) clockwise about its point of intersection with the $T = 0$ axis until, at any temperature T, the vertical separation between line (ii) and line (vi) is $2RT$ ln 0.5.

Combination of reactions (vi) and (vii) gives

$$C_{(gr)} + CO_{2(g,0.5\text{atm})} = 2CO_{(g,0.5\text{ atm})} \qquad \text{(viii)}$$

for which

$$\Delta G_{(\text{viii})} = \Delta G^{\circ}_{(\text{iv})} + RT \ln 0.5$$

Thus, CO_2 and CO, each at 0.5 atm pressure, are in equilibrium with solid C at that temperature at which $\Delta G_{(\text{viii})} = 0$, the temperature of intersection of the lines (vi) and (vii) in Figure 12.14 (point *c*).

The temperature at which CO (at 0.25 atm) and CO_2 (at 0.75 atm) are in equilibrium with solid C is obtained in a similar manner as the intersection of line (i) rotated clockwise until, at T, it has been displaced a vertical distance RT ln 0.75 and line (ii) rotated clockwise until, at T, it has been displaced a vertical distance $2RT$ (ln 0.25). This is the point *b* in Figure 12.14. Similarly, the point *d* in Figure 12.14 is the temperature at which CO at 0.75 atm pressure and CO_2 at 0.25 atm pressure are in equilibrium with solid C. For a mixture of CO and CO_2 at 1 atm pressure in equilibrium with solid C, the variation of percent CO by volume in the gas with temperature is shown in Figure 12.15. Figure 12.15 includes the points *a*, *b*, *c*, *d*, and *e* drawn in Figure 12.14.

Figure 12.15 shows that, at temperatures <600 K, the equilibrium gas is virtually CO_2 at 1 atm pressure, and at temperatures >1400 K, the equilibrium gas is virtually CO at 1 atm pressure. These points are, respectively, the points *a* and *e* in Figure 12.14. Thus, in Figure 12.14, the variation, with temperature, of the Gibbs free energy change for oxidation of solid C to produce a CO–CO_2 mixture at 1 atm pressure which is in equilibrium with solid C is given by line (i) up to the point *a*, then by the line *abcde*, and then by the line (ii) beyond the point *e*.

At any temperature T, the CO–CO_2 mixture in equilibrium with C exerts an equilibrium oxygen pressure *via* the equilibrium

$$2CO + O_2 = 2CO_2$$

for which

$$\Delta G^{\circ}_{(\text{iii})} = -564,800 + 173.62T \text{ J} = -\text{RT} \ln\left(\frac{p^2_{CO_2}}{p^2_{CO}\, p_{O_2}}\right)$$

$$= 2RT \ln\left(\frac{p_{CO}}{p_{CO_2}}\right)_{\text{eq. with C}} + RT \ln p_{O_2(\text{eq.})}$$

Thus,

$$\ln p_{O_2(\text{eq}.T)} = -\frac{564{,}800}{8.3144T} + \frac{173.62}{8.3144} + 2\ln\left(\frac{p_{CO_2}}{p_{CO}}\right)_{\text{eq. with C}} \tag{12.12}$$

If it is required that solid carbon be used as a reducing agent to reduce a metal oxide MO_2 at the temperature T, then $p_{O_2(\text{eq}.T)}$ in Equation 12.12 must be lower than $p_{O_2(\text{eq}.T)}$ for the equilibrium $M + O_2 = MO_2$ (see Section 12.7).

12.6.2 The Effect of P_{CO_2}/P_{CO} on the Equilibrium Reaction $2CO + O_2 = 2CO_2$

The Ellingham line for the reaction $2CO + O_2 = 2CO_2$ is shown in Figure 12.16 as the line *cs*. Since it is the variation, with temperature, of the standard Gibbs free energy of formation, ΔG°, this line is for the reaction that produces CO_2 at 1 atm pressure from CO at 1 atm pressure and O_2 at 1 atm pressure. The effect of producing the CO_2 at any pressure, P, other than 1 atm (from CO and O_2 each at 1 atm) is the rotation of the Ellingham line *cs* about the point *c*, clockwise if $P < 1$ atm and anticlockwise if $P > 1$ atm. For the given value of P the rotation is such that, as before, at the temperature T, the vertical displacement of *cs* is $2RT \ln P$. A series of lines, radiating from the point *c*, can thus be drawn for different pressures of CO_2 produced from CO and O_2, each at 1 atm. Figure 12.16 shows four of these lines:

- Line *cq* for CO_2 produced at 10^2 atm
- Line *cr* for CO_2 produced at 10 atm
- Line *cu* for CO_2 produced at 0.1 atm
- Line *cv* for CO_2 produced at 10^{-2} atm

The significance of this series of lines, with respect to the possibility of using CO–CO_2 gas mixtures as reducing agents for the metal oxide MO_2, is illustrated as follows. The Ellingham line for the reaction $M + O_2 = MO_2$ is drawn in Figure 12.16. This intersects the line *cs* at the temperature T_s, which is thus the temperature at which the standard Gibbs free energy change for reaction

$$MO_2 + 2CO = M + 2CO_2 \tag{ix}$$

is zero; that is,

$$\Delta G^\circ_{(\text{ix})} \text{ at } T_s = 0 = -RT \ln\left(\frac{p_{CO_2}}{p_{CO}}\right)^2$$

and thus,

$$\frac{p_{CO_2}}{p_{CO}} = 1$$

At temperatures higher than T_s, a CO–CO_2 mixture of $p_{CO}/p_{CO_2} = 1$ is reducing with respect to MO_2, and at temperatures lower than T_s, it is oxidizing with respect to the metal M. Compare this with the previous discussion of Figure 12.2.

If it is required that a CO–CO_2 mixture be made to be reducing with respect to MO_2 at temperatures lower than T_s, then the ratio p_{CO}/p_{CO_2} must be *increased* to a value greater than unity. The Ellingham line for the reaction $M + O_2 = MO_2$ intersects the line *cu* at the temperature T_u, and T_u is thus the temperature at which the reaction

$$MO_2 + 2CO\left(1\text{ atm}\right) = M + 2CO_2\left(0.1\text{ atm}\right) \tag{x}$$

is at equilibrium; that is,

$$\Delta G_{(x)} \text{ at } T_u = \Delta G^\circ_{(ix)} + 2RT \ln 0.1$$

But, by definition,

$$\Delta G^\circ_{(ix)} = -RT \ln \left(\frac{p_{CO_2}}{p_{CO}} \right)^2_{eq}$$

and thus,

$$\Delta G_{(x)} = 0 = -2RT \ln \left(\frac{p_{CO_2}}{p_{CO}} \right)_{eq} + 2RT \ln 0.1$$

Thus, $\left(p_{CO}/p_{CO_2}\right)_{eq} = 10$ at T_u, and hence, by decreasing the temperature from T_s to T_u, the CO/CO_2 ratio must be increased from 1 to 10 in order to maintain reaction equilibrium.

Similarly, at T_v the equilibrium CO/CO_2 ratio is 100, at T_r the equilibrium CO/CO_2 ratio is 0.1, and at T_q the equilibrium ratio is 0.01. Thus, a CO/CO_2 nomographic scale can be added to the Ellingham diagram, and for any reaction

$$MO_2 + 2CO = M + 2CO_2$$

the equilibrium CO/CO_2 ratio at any temperature T is read off the nomographic scale as that point which is collinear with the point C and the point ΔG°_T, $T = T$, for the reaction $M + O_2 = MO_2$. This scale is included in Figure 12.13.

Figure 12.15 was generated by reading off the equilibrium CO/CO_2 ratios for the reaction $C + O_2 = CO_2$ up to the point *a* in Figure 12.14, then the CO/CO_2 ratios along the line *abcde*, and finally the CO/CO_2 ratios for the reaction $2C + O_2 = 2CO$ beyond the point *e*.

In exactly the same manner, the H_2/H_2O nomographic scale is added to Figure 12.3 by considering the effect of the variation of the pressure of H_2O on the reaction equilibrium

$$2H_2 + O_2 = 2H_2O$$

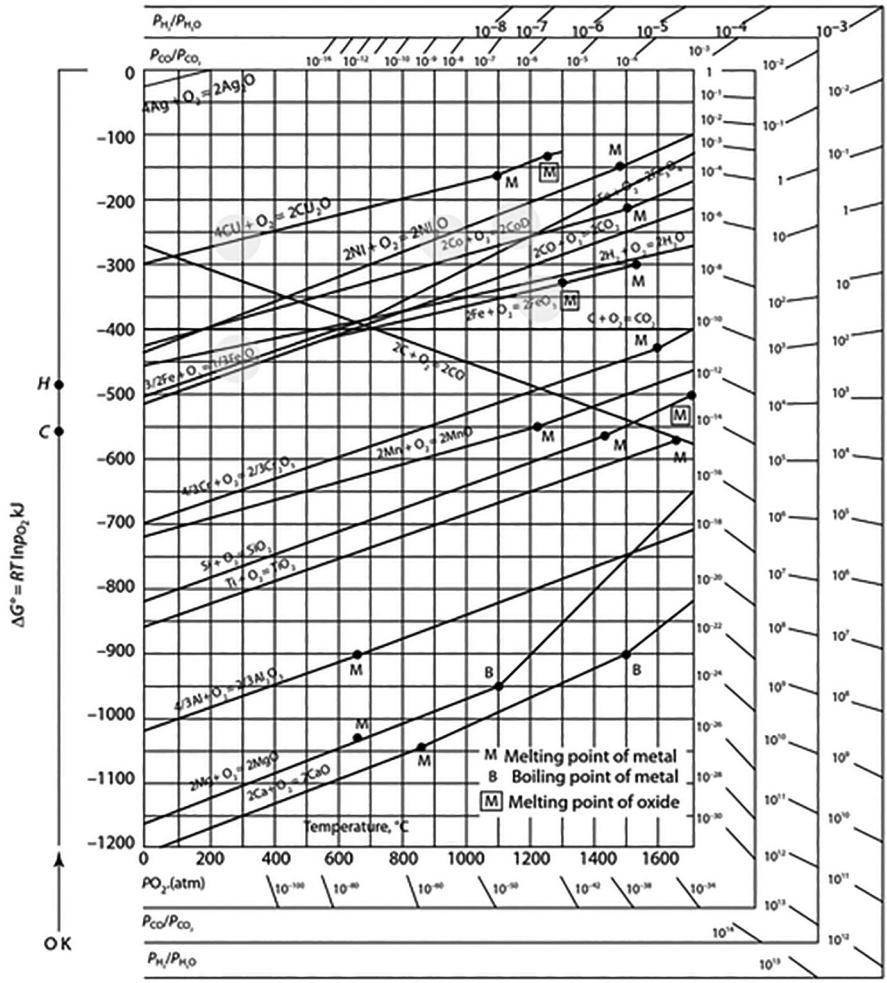

FIGURE 12.13 The Ellingham diagram for selected oxides.

The equilibrium H_2/H_2O ratio at the temperature T for the reaction

$$MO_2 + 2H_2 = M + 2H_2O$$

is read off the H_2/H_2O scale as the point which is collinear with the points H and ΔG°_T, $T = T$ for the reaction $M + O_2 = MO_2$.

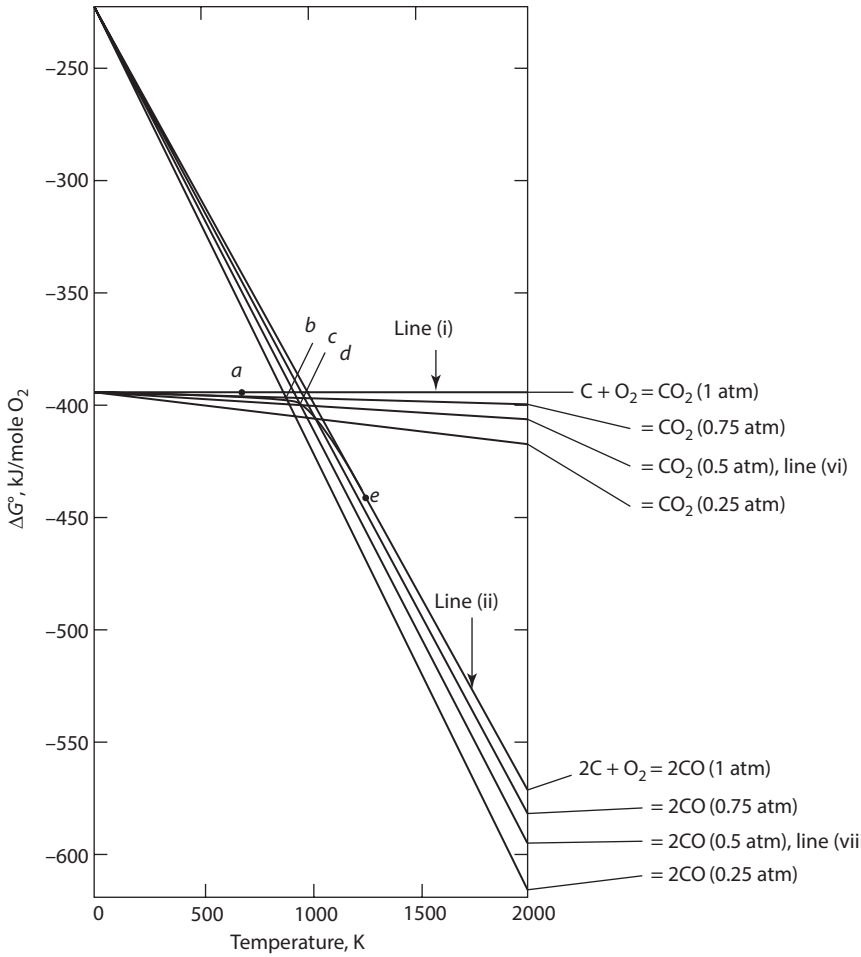

FIGURE 12.14 The effect of varying the pressures of the product gases of the reactions $C_{(gr)} + O_{2(g,\ p = 1\ atm)} = CO_{2(g)}$ and $2C_{(gr)} + O_{2(g,\ p = 1\ atm)} = 2CO_{(g)}$ on the variations of ΔG with T for the two reactions.

12.7 GRAPHICAL REPRESENTATION OF EQUILIBRIA IN THE SYSTEM METAL–CARBON–OXYGEN

The main criteria for graphical representation of equilibria in a system are

- The amount of information provided
- Clarity

Both of these considerations are dependent on the coordinates chosen for use in the graphical representation. Since the nomographic scale for the ratio CO/CO_2 in Figure 12.13 shows that the range of interest of values of p_{CO} / p_{CO_2} is 10^{-14} to 10^{14}, it is convenient to present this ratio on a logarithmic scale. Figure 12.17, which uses the

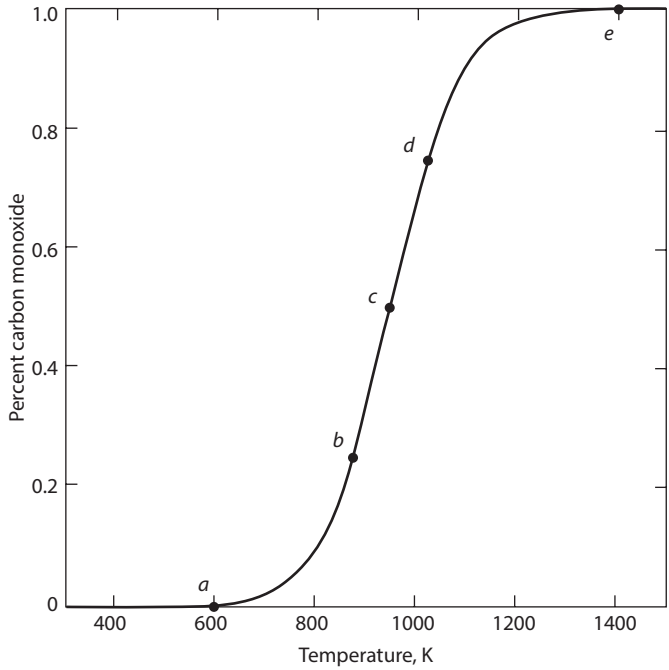

FIGURE 12.15 The variation, with temperature, of the composition of the CO–CO_2 gas mixture in equilibrium with solid graphite at $P_{\text{total}} = 1$ atm.

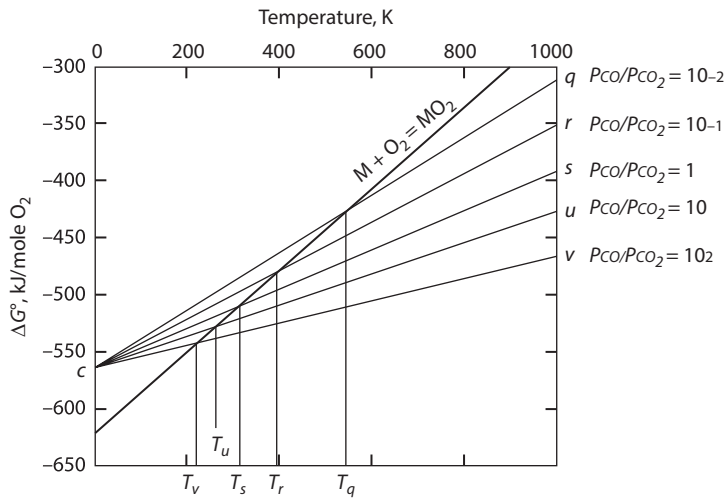

FIGURE 12.16 Illustration of the effect of the ratio $\boldsymbol{P_{CO_2}/P_{CO}}$ in a CO_2–CO gas mixture on the temperature at which the equilibrium $M + CO_2 = MO + CO$ is established.

coordinates $\log\left(p_{CO_2} / p_{CO}\right)$, and T represents a convenient method of clearly presenting the reaction equilibrium in the carbon–oxygen and carbon–oxygen–metal systems.

From Equation (iii), for

$$2CO_{(g)} + O_{2(g)} = 2CO_{2(g)}$$

$$\Delta G^{\circ}_{(iii)} = -546{,}800 + 173.62T \text{ J}$$

$$= -RT \ln\left(\frac{p^2_{CO_2}}{p^2_{CO} p_{O_2}} \right)$$

and thus,

$$\log\left(\frac{p_{CO_2}}{p_{CO}} \right) = \frac{1}{2} \log p_{O_2} + \frac{564{,}800}{2 \times 2.303 \times 8.3144T} - \frac{173.62}{2 \times 2.303 \times 8.3144} \qquad \text{(xi)}$$

For any given value of p_{O_2}, this gives the variation of the given oxygen isobar with $\log\left(p_{CO_2}/p_{CO}\right)$ and temperature. The oxygen isobars in the range 10^{-29} to 10^{-4} atm are drawn as a function of $\log\left(p_{CO_2}/p_{CO}\right)$ and T in Figure 12.17.

The equilibrium

$$C_{(gr)} + CO_{2(g)} = 2CO_{(g)} \qquad \text{(iv)}$$

sets a lower limit on the CO_2/CO ratio which can be obtained at any temperature:

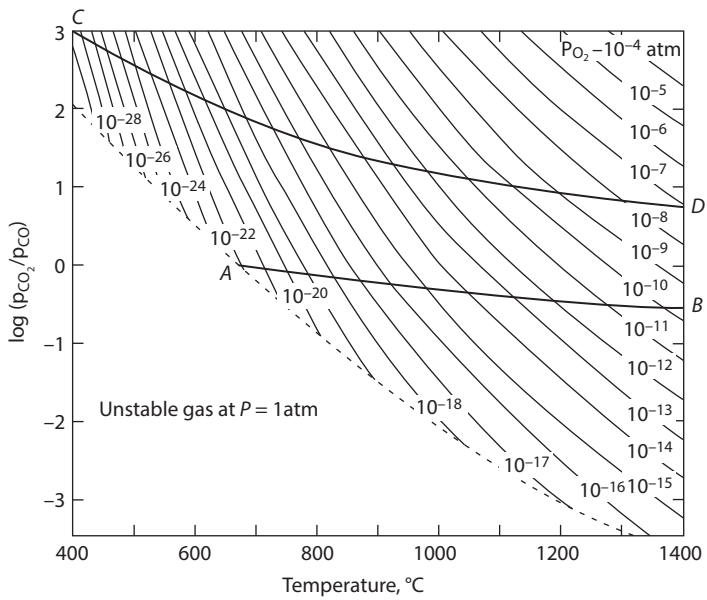

FIGURE 12.17 The relationship between the partial pressure of oxygen in a CO_2–CO gas mixture and temperature. The broken line is the variation, with temperature, of the composition of the gas which is in equilibrium with graphite at 1 atm pressure. The lines *AB* and *CD* represent, respectively, the equilibria $Fe + CO_2 = FeO + CO$ and $Co + CO_2 = CoO + CO$.

$$\Delta G^{\circ}_{(\mathrm{iv})} = 170,700 - 174.5T \text{ J} = -RT \ln\left(\frac{p^2_{\mathrm{CO}}}{p_{\mathrm{CO_2}}}\right)$$

and thus, at a total pressure of 1 atm (i.e., when $p_{\mathrm{CO_2}} = 1 - p_{\mathrm{CO}}$),

$$\frac{p^2_{\mathrm{CO}}}{1 - p_{\mathrm{CO}}} = \exp\left(\frac{-170,700}{8.3144T}\right)\exp\left(\frac{174.5}{8.3144}\right) = x$$

or

$$p^2_{\mathrm{CO}} + p_{\mathrm{CO}}x - x = 0$$

solution of which gives

$$p_{\mathrm{CO}} = \frac{-x + \sqrt{x^2 + 4x}}{2}$$

$$p_{\mathrm{CO_2}} = \frac{2 + x - \sqrt{x^2 + 4x}}{2}$$

And

$$\frac{p_{\mathrm{CO_2}}}{p_{\mathrm{CO}}} = \frac{2 + x - \sqrt{x^2 + 4x}}{-x + \sqrt{x^2 + 4x}} \qquad \text{(xii)}$$

The value of $p_{\mathrm{CO_2}}/p_{\mathrm{CO}}$ given by Equation (xii) is the minimum obtainable value at the temperature *T*. If an attempt is made to mix CO and CO_2 (at $P_{\mathrm{total}} = 1$ atm) in a ratio $p_{\mathrm{CO_2}}/p_{\mathrm{CO}}$ lower than that given by Equation (xii), carbon will not precipitate until, thereby, the ratio is increased to the unique value required for equilibrium with carbon at the temperature *T*. The variation of $\log\left(p_{\mathrm{CO_2}}/p_{\mathrm{CO}}\right)_{\mathrm{eq.C/CO/CO_2}}$ with temperature is shown as the broken line in Figure 12.17. The variation of the corresponding minimum values of $p_{\mathrm{O_2}}$ with temperature in Figure 12.17 is given by the intersections of the oxygen isobars with the carbon deposition line.

Equilibria such as

$$\mathrm{MO} + \mathrm{CO} = \mathrm{M} + \mathrm{CO_2}$$

can readily be presented on plots such as that in Figure 12.17. For example, for

$$\mathrm{FeO}_{(s)} + \mathrm{CO}_{(g)} = \mathrm{Fe}_{(s)} + \mathrm{CO}_{2(g)}$$

$$\Delta G^{\circ} = -22,800 + 24.26T \text{ J}$$

and thus, the variation of the equilibrium ratio CO_2/CO with temperature is given by

$$\log\left(\frac{p_{\mathrm{CO_2}}}{p_{\mathrm{CO}}}\right)_{\mathrm{eq.FeO/Fe}} = \frac{22,800}{2.303 \times 8.3144T} - \frac{24.26}{2.303 \times 8.3144}$$

This variation is drawn as the line *AB* in Figure 12.17, and thus, any gas, the state of which lies above the line *AB*, is oxidizing with respect to Fe, and states below *AB* are reducing with respect to FeO. The variation of $\log p_{O_2\,(\text{eq.T,Fe/FeO})}$ with temperature is given by the intersections of the oxygen isobars with the line *AB*. The temperature at which *AB* intersects the carbon deposition line is the minimum temperature at which solid FeO can be reduced to solid Fe by graphite, and this is the temperature at which $Fe_{(s)}$, $FeO_{(s)}$, $C_{(s)}$, and the $CO–CO_2$ atmosphere at 1 atm pressure coexist in equilibrium; that is, it is the temperature at which

$$p_{O_2\,(\text{eq.C/CO/CO}_2)} = p_{O_2\,(\text{eq.Fe/FeO})}$$

The line *CD* in Figure 12.17 represents the variation of $\log\left(p_{CO_2}/p_{CO}\right)$ with *T* for the equilibrium

$$CoO_{(s)} + CO_{(g)} = Co_{(s)} + CO_{2(g)}$$

for which

$$\Delta G^\circ = -48{,}500 + 14.9T \text{ J}$$

and

$$\log\left(\frac{p_{CO_2}}{p_{CO}}\right)_{\text{eq.Co/CoO}} = \frac{48{,}500}{2.303\times 8.3144T} - \frac{14.9}{2.303\times 8.3144}$$

Since the equilibrium constant *K* for the reaction

$$MO + CO = M + CO_2$$

is given by $p_{CO_2}/p_{CO(\text{eq.}T,\text{M/MO})}$, a plot of $\log p_{CO_2}/p_{CO(\text{eq.}T,\text{M/MO})}$ versus $1/T$ is a plot of $\log K$ versus $1/T$. Figure 12.18 shows the information given in Figure 12.17 as such a plot. With respect to the amount of information that can be obtained from a graphical representation of equilibria in a system, Figure 12.18 is a better representation than is Figure 12.17.

Since

$$\left[\frac{d\ln K}{d\left(\frac{1}{T}\right)}\right] = -\frac{\Delta H^\circ}{R}$$

the slope of a tangent to an equilibrium line at the temperature *T* gives the value of $-\Delta H^\circ/R$. If $\Delta c_p = 0$, $\log K$ is a linear function of $1/T$. Thus, the slope of line *AB* in Figure 12.18 equals $-\Delta H^\circ/R$ for the reaction $FeO + CO = Fe + CO_2$, and the slope of line *CD* equals $-\Delta H^\circ/R$ for the reaction $CoO + CO = Co + CO_2$. Also, if they are linear, the intercepts of the lines themselves with the $1/T = 0$ axis give the corresponding values of $\Delta S^\circ/R$ for the reactions. From Equation (xi), the slope of any oxygen

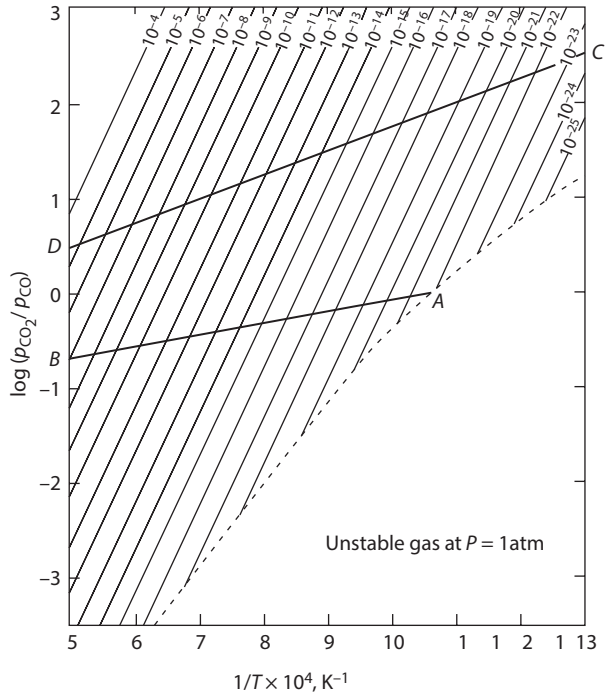

FIGURE 12.18 Figure 12.17 reproduced as log $\boldsymbol{P_{CO_2}/P_{CO}}$ vs. $1/T$.

isobar equals $-\Delta H^{\circ}/2R$ for the reaction $2CO + O_2 = 2CO_2$, and thus, the oxygen isobars in Figure 12.18 are parallel lines.

12.8 SUMMARY

1. The following two facts facilitate a convenient definition of the standard state of species occurring as condensed phases.
   - A pure species occurring as a condensed phase exerts a unique saturated vapor pressure at the temperature T.
   - The dependence of the Gibbs free energy of a condensed phase on pressure (at low pressure) is negligibly small.

   This standard state is simply the pure species in its stable condensed state at the temperature T.
2. Using this standard state, the equilibrium constant for a reaction involving pure condensed phases and a gas phase can be written in terms of the partial pressures of those species that occur only in the gas phase. For example, for the oxidation of a pure metal to its pure stoichiometric oxide, the equilibrium constant is given by $1/p_{O_2(\text{eq.}T)}$, where $p_{O_2(\text{eq.}T)}$ is the unique partial pressure of oxygen required for equilibrium between the metal, its oxide, and the gas phase at the temperature T. This pressure is such that

$$G^{\circ}_{M} + G^{\circ}_{O_2} + RT \ln p_{O_2(}$$

or

$$\Delta G_T^\circ = -RT \ln K = -RT \ln \left(\frac{1}{p_{O_2(\text{eq}.T)}} \right)$$

3. Determination of the equilibrium state of a chemical reaction system requires knowledge of the variation, with temperature, of the standard Gibbs free energy change for the reaction. This relationship can be obtained from thermochemical data—that is, from knowledge of the standard enthalpy and entropy changes at a single temperature (usually ΔH_{298}° and ΔS_{298}°) and the variations, with temperature, of the constant-pressure molar heat capacities of the reactants and products, or it can be determined from knowledge of the variation, with temperature, of the equilibrium constant for the reaction.
4. The Gibbs Equilibrium Phase Rule for systems undergoing reactions is written as:

$$\mathcal{F} = (N - R) + 2 - \Phi$$

Where N is the number of component species present, R is the number of reactions.

5. For the oxidation of a pure metal to its pure oxide, experimental measurement of the variation of $p_{O_2(\text{eq}.T)}$ with temperature gives the variation of ΔG° with temperature as

$$\ln \left(\frac{1}{p_{O_2(\text{eq}.T)}} \right) = -\frac{\Delta H^\circ}{RT} + \frac{\Delta S^\circ}{R} = -\frac{\Delta G^\circ}{RT}$$

If ΔH° and ΔS° are independent of temperature (i.e., if $\Delta c_p = 0$), ln K is a linear function of $1/T$.

6. The fitting of the variation of ΔG° with T to a line produces the so-called Ellingham line for the reaction, and a plot of ΔG° versus T is known as an Ellingham diagram. Ellingham lines plotted on a single diagram for a series of similar reactions (e.g., for the formation of oxides, sulfides, etc.) provide a convenient representation of the relative stabilities of the compounds.
7. The addition of $p_{O_2}, p_{CO}/p_{CO_2}$ and p_{H_2}/p_{H_2O} nomographic scales to these diagrams facilitates the geometric determination of $p_{O_2(\text{eq}.T)}, p_{CO}/p_{CO_2(\text{eq}.T)}$, and $p_{H_2}/p_{H_2O(\text{eq}.T)}$ for, respectively, the equilibria $2M + O_2 = 2MO$, $M + CO_2 = MO + CO$, and $M + H_2O = MO + H_2$.

12.9 CONCEPTS AND TERMS INTRODUCED IN THIS CHAPTER

The reader should write out brief definitions or descriptions of the following terms. Where appropriate, equations may be used.

Blast furnace
Boudouard reaction
Carbonates
Carbon–oxygen reactions

Chemical affinity
Component species
Condensed-phase reactions with gases
Decomposition of a solid phase
Ellingham diagrams
Gibbs equilibrium phase rule
Hydroxides
Log pressure versus 1/*T* phase diagram
Metal–carbon–oxygen equilibria
Oxidation of pure solid phase
Phase Equilibrium
Phase transformations and the Ellingham diagram
Pure species
Reaction Equilibrium
Reduction of an oxide
Richardson nomographic scale
Temperature dependence of the standard free energy change

12.10 QUALITATIVE EXAMPLE PROBLEMS

QUALITATIVE PROBLEM 1

Apply the Gibbs equilibrium phase rule to the oxidation of Cu to form cuprous oxide (Figure 12.1).

SOLUTION TO QUALITATIVE PROBLEM 1

$$4\mathrm{Cu}_{(s)} + \mathrm{O}_{2(g)} = 2\mathrm{Cu}_2\mathrm{O}_{(s)}$$

The Gibbs Equilibrium Phase Rule for reactions is given by the equation

$$\Phi + \mathcal{F} = (N - R) + 2$$

where:
Φ is the number of phases in equilibrium
$\mathcal{F}$ is the thermodynamic degrees of freedom
N is the number of component species
R is the number of Chemical Reactions needed to specify equilibrium
2 accounts for the intensive variables pressure and temperature
For this case:
$R = 1$
$N = 3$
$\Phi = 3$ (2 solids and one gaseous)

$$3 + \mathcal{F} = (3 - 1) + 2 \quad \text{or} \quad \mathcal{F} = 1$$

We can see from Figure 12.1 that when the temperature is specified, there is only one possible partial pressure of oxygen gas that allows for the equilibrium of the given reaction. Or, if a specific pressure is desired, it can be found at but one temperature.

QUALITATIVE PROBLEM 2

Apply the Gibbs equilibrium phase rule to the reduction of cupric oxide by ammonia and determine the number of degrees of freedom that exist for the reaction.

SOLUTION TO QUALITATIVE PROBLEM 2

$$3CuO_{(s)} + 2NH_{3(g)} = 3Cu_{(s)} + 3H_2O_{(g)} + N_{2(g)}$$

We use the equation

$$\Phi + \mathcal{F} = (N - R) + 2$$

Where:

Φ is the number of phases in equilibrium
$\mathcal{F}$ is the thermodynamic degrees of freedom
N is the number of component species
R is the number of Chemical Reactions needed to specify equilibrium
2 accounts for the intensive variables pressure and temperature
For this case:
$R = 1$
$\Phi = 3$ (2 solids and one gaseous)
$N = 5$

$$3 + \mathcal{F} = (5 - 1) + 2 \quad \text{or} \quad \mathcal{F} = 3$$

Thus at a given temperature, only two of the partial pressures of the gaseous components can be varied.

This can also be seen by writing the equilibrium constant for the reaction and noting that at a *fixed temperature* the equilibrium constant, $K = \dfrac{p_{N_2}\, p^3_{H_2O}}{p^2_{NH_3}}$. Thus only two of the partial pressures of the gaseous component species can be varied.

12.11 QUANTITATIVE EXAMPLE PROBLEMS

QUANTITATIVE PROBLEM 1

Compare the relative efficiencies of H_2 and CO as reducing agents for metal oxides.

For $CO + \frac{1}{2} O_2 = CO_2$,

$$\Delta G^\circ_{(i)} = -282,400 + 86.81T \text{ J} \tag{i}$$

and for $H_2 + \frac{1}{2} O_2 = H_2O$,

$$\Delta G^\circ_{(ii)} = -247{,}500 + 55.85T \text{ J} \quad \text{(ii)}$$

SOLUTION TO QUANTITATIVE PROBLEM 1

The values of ΔH° and ΔS° for these two reactions cause their Ellingham lines to intersect at 1127 K, as shown in Figure 12.12, with $\Delta G^\circ_{(ii)}$ being more negative than $\Delta G^\circ_{(i)}$ at temperatures higher than 1127 K and $\Delta G^\circ_{(i)}$ being more negative than $\Delta G^\circ_{(ii)}$ at temperatures lower than 1127 K. This indicates that H_2 is the more efficient reducing agent at higher temperatures and that CO is the more efficient reducing agent at lower temperatures.

Consider the reduction of CoO by each of H_2 and CO at 1673 K and at 873 K.

For $CoO(s) = Co_{(s)} + \frac{1}{2} O_{2(g)}$:

$$\Delta G^\circ_{(iii)} = +233{,}900 - 71.85T \text{ J} \quad \text{(iii)}$$

Combination of $\Delta G^\circ_{(i)}$ and $\Delta G^\circ_{(iii)}$ gives

$$\Delta G^\circ_{(iv)} = -48{,}500 + 14.96T \quad \text{(iv)}$$

for $CoO + CO = Co + CO_2$, and combination of $\Delta G^\circ_{(iii)}$ and $\Delta G^\circ_{(ii)}$ gives

$$\Delta G^\circ_{(v)} = -12{,}500 - 17.05T \text{ J} \quad \text{(v)}$$

for $CoO + H_2 = Co + H_2O$.

The positive value of $\Delta S^\circ_{(v)}$ causes $\Delta G^\circ_{(v)}$ to become more negative with increasing temperature and the negative value of $\Delta S^\circ_{(iv)}$ causes $\Delta G^\circ_{(iv)}$ to become less negative with increasing temperature. At 1673 K $\Delta G^\circ_{(v)} = -41{,}024$ J, and thus,

$$K_{(v),1673K} = \exp\left(\frac{41{,}024}{8.3144 \times 1673}\right) = 19.1 = \left(\frac{p_{H_2O}}{p_{H_2}}\right)_{eq.}$$

Thus, if H_2 at 1673 K is passed through a column of CoO, which is long enough that reaction equilibrium is achieved before the gas leaves the column, the fraction of H_2 which is consumed before equilibrium is reached is 19.1/20.1 = 0.95, and thus, 1 mole of H_2 is required to reduce 0.95 moles of CoO.

At 1673 K, $\Delta G^\circ_{(iv)} = -23{,}470$ J, and thus,

$$K_{(iv),1673} = 5.40 = \left(\frac{P_{CO_2}}{p_{CO}}\right)_{eq.}$$

and thus, the fraction of CO which is consumed by the reduction reaction at 1673 K before equilibrium is reached is 5.40/6.40 = 0.844. Thus, 1 mole of CO is required to reduce 0.844 moles of CoO.

At 873 K, $\Delta G^{\circ}_{(v)} = -27,384$ J, which gives

$$K_{(v),873} = 43.5 = \left(\frac{p_{H_2O}}{p_{H_2}} \right)_{eq.}$$

and thus, the fraction of H_2 consumed is 43.5/44.5 = 0.978 and 1 mole of H_2 reduces 0.978 moles of CoO.

At 873, $\Delta G^{\circ}_{(iv)} = -35,440$ J, which gives

$$K_{(iv),873} = 132 = \left(\frac{p_{CO_2}}{p_{CO}} \right)_{eq.}$$

Thus, the fraction of CO consumed is 132/133 = 0.992, and 1 mole of CO reduces 0.992 moles of CoO. Thus, H_2 is the more efficient reducing agent at higher temperatures and CO is the more efficient at lower temperatures. Also, decreasing the temperature at which the reduction reaction is conducted increases the efficiencies of both reductants.

QUANTITATIVE PROBLEM 2

Consider the reduction of solid ZnO by CO to form Zn vapor and CO_2 according to

$$ZnO_{(s)} + CO_{(g)} = Zn_{(v)} + CO_{2(g)} \tag{i}$$

For $ZnO_{(s)} = Zn_{(v)} + ½O2_{(g)}$:

$$\Delta G^{\circ}_{(ii)} = 460,200 - 198T \text{ J} \tag{ii}$$

For $CO_{(g)} + ½\ O_{2(g)} = CO_{2(g)}$:

$$\Delta G^{\circ}_{(iii)} = -282,400 + 86.81T \text{ J} \tag{iii}$$

Summing $\Delta G^{\circ}_{(ii)}$ and $\Delta G^{\circ}_{(iii)}$ gives

$$\Delta G^{\circ}_{(i)} = -177,800 - 111.2T \text{ J}$$

The equilibrium involves four component species (ZnO, $CO_{(g)}$, $Zn_{(v)}$ and $CO_{2(g)}$) and two phases (a solid and a gas), and thus, from the Gibbs Equilibrium Phase Rule

$$\mathcal{F} = (N - 1) + 2 - \Phi = 3 + 2 - 2 = 3 \text{ degrees of freedom}$$

However, the stoichiometric requirement that $p_{Zn} = p_{CO_2}$ uses one of the degrees of freedom, and thus, the equilibrium is fixed when the temperature and total pressure are fixed.

a. Calculate the composition of the gas phase at 950°C and $P = 1$ atm.
b. To what value must the total pressure of the gas mixture be increased in order to cause condensation of the zinc vapor at 1223 K?

c. Calculate the composition of the gas phase if the total pressure is increased to 150 atm at 1223 K.

SOLUTION TO QUANTITATIVE PROBLEM 2

a. At 1223 K,

$$\Delta G^{\circ}_{(\mathrm{i})} = 177{,}800 - (111.2 \times 1223) = 41{,}800 \text{ J}$$

and thus,

$$K_{(\mathrm{i})1223\,\mathrm{K}} = \exp\left(\frac{-41{,}800}{8.3144 \times 1223}\right) = 0.0164 = \frac{p_{\mathrm{Zn}} p_{\mathrm{CO_2}}}{p_{\mathrm{CO}}}$$

From the stoichiometry, $p_{\mathrm{Zn}} = p_{\mathrm{CO_2}}$ and the total pressure P is

$$P = p_{\mathrm{CO}} + p_{\mathrm{Zn}} + p_{\mathrm{CO_2}} \tag{iv}$$

Thus, with $P = 1$ atm, $p_{\mathrm{CO}} = 1 - 2p_{\mathrm{Zn}}$ and

$$0.0164 = \frac{p^2_{\mathrm{Zn}}}{1 - 2p_{\mathrm{Zn}}} \tag{v}$$

which has the solution $p_{\mathrm{Zn}} = 0.113$ atm. Therefore, $p_{\mathrm{CO_2}} = 0.113$ atm and $p_{\mathrm{CO}} = 1 - (2 \times 0.113) = 0.775$ atm. At $P = 1$ atm, the mole fractions of the species in the gas phase are equal to their partial pressures.

b. Condensation occurs when the partial pressure of Zn reaches the value of the saturated vapor pressure of liquid zinc at 1223 K. The saturated vapor pressure of liquid zinc is given by

$$\ln p^{\circ}_{\mathrm{Zn},(l)}(\mathrm{atm}) = \frac{-15{,}250}{T} - 1.255 \ln T + 21.79$$

which gives $p^{\circ}_{\mathrm{Zn},(l)} = 1.49$ atm at 1223 K. Therefore,

$$K_{(\mathrm{i})1223\,\mathrm{K}} = 0.0164 = \frac{1.49^2}{P - (2 \times 1.49)}$$

which has the solution $P = 138$ atm.

Thus, $p_{\mathrm{Zn}} = p_{\mathrm{CO_2}} = 1.49$ atm and $p_{\mathrm{CO}} = 138 - (2 \times 1.49) = 135$ atm.

At the point of condensation of zinc, the mole fractions of the species in the gas phase are $X_{\mathrm{Zn}} = X_{\mathrm{CO_2}} = 1.49/138 = 0.011$ and $X_{\mathrm{CO}} = 135/138 = 0.978$.

c. The system now contains three phases and the equilibrium thus has 2 degrees of freedom. Condensation of the zinc eliminates the stoichiometric requirement that $p_{\mathrm{Zn}} = p_{\mathrm{CO_2}}$, but phase equilibrium between liquid zinc and zinc vapor at 1223 K requires that the partial pressure of zinc be the saturated value of 1.49 atm. Thus,

$$K_{1223\,\mathrm{K}} = 0.0164 = \frac{1.49 \times p_{\mathrm{CO_2}}}{p_{\mathrm{CO}}} \tag{vi}$$

and

$$P = 150 = 1.49 + p_{CO} + p_{CO_2} \tag{vii}$$

Simultaneous solution of Equation (vi) and (vii) gives $p_{CO} = 146.9$ atm and $p_{CO_2} = 1.61$ atm. The mole fractions of the species in the gas phase are thus $X_{Zn} = 1.49/150 = 0.01$, $X_{CO_2} = 1.61/150 = 0.011$, and $X_{CO} = 146.9/150 = 0.98$.

Further Considerations:

i. Consider, now, the reduction of ZnO by graphite to form zinc vapor, CO, and CO_2 according to

$$ZnO_{(s)} + C_{(gr)} = Zn_{(v)} + CO_{(g)} \tag{viii}$$

and

$$2ZnO_{(s)} + C_{(gr)} = 2Zn_{(v)} + CO_{2(g)} \tag{ix}$$

For $2C + O_2 = 2CO$:

$$\Delta G^\circ_{(x)} = -223,400 - 175.3T \text{ J} \tag{x}$$

For $C + O_2 = CO_2$:

$$\Delta G^\circ_{(xi)} = -394,100 - 0.84T \text{ J} \tag{xi}$$

Combination of $\Delta G^\circ_{(ii)}$ and $\Delta G^\circ_{(x)}/2$ gives

$$\Delta G^\circ_{(viii)} = 348,500 - 285.7T \text{ J}$$

for $ZnO + C = Zn + CO$, and combination of $2\Delta G^\circ_{(ii)}$ and $\Delta G^\circ_{(xi)}$ gives

$$\Delta G^\circ_{(ix)} = 526,300 - 396.8T \text{ J}$$

for $2ZnO + C = 2Zn + CO_2$.

ii. The equilibrium involves three component species and three phases (ZnO, graphite, and a gas phase) and thus, according to the phase rule, has two degrees of freedom. However, as stoichiometric ZnO is the only source of oxygen and zinc in the gas phase, one of the degrees of freedom is used by the requirement that equal numbers of moles of Zn and O occur in the gas phase. Alternatively, as ZnO has a fixed composition, the system can be considered to be the quasi-binary ZnO–C, in which case the phase rule gives one degree of freedom to the equilibrium. Thus, fixing either (1) the temperature, (2) the total pressure, (3) p_{Zn}, (4) p_{CO}, or (5) p_{CO_2} fixes the equilibrium. Determine the equilibrium state at 1223 K.

At 1223 K, $\Delta G^\circ_{(viii)1223K} = -850$ J and thus,

$$K_{(\text{viii})1223\,\text{K}} = \exp\left(\frac{850}{8.3144\times 1223}\right) = 1.087 = p_{\text{Zn}}p_{\text{CO}} \tag{xii}$$

and $\Delta G^{\circ}_{(\text{ix})1223\,\text{K}} = 40{,}960$ J, in which case

$$K_{(\text{ix})1223\,\text{K}} = \exp\left(\frac{-40{,}960}{8.3144\times 1223}\right) = 0.018 = p^2_{\text{Zn}}p_{\text{CO}_2} \tag{xiii}$$

The requirement that $n_{\text{Zn}}/n_{\text{O}} = 1$ in the gas phase leads to

$$\frac{n_{\text{Zn}}}{n_{\text{O}}} = 1 = \frac{n_{\text{Zn}}}{n_{\text{CO}} + 2n_{\text{CO}_2}} = \frac{p_{\text{Zn}}}{p_{\text{CO}} + 2p_{\text{CO}_2}}$$

Thus,

$$p_{\text{Zn}} = p_{\text{CO}} + 2p_{\text{CO}_2} \tag{xiv}$$

Substitution of Equations (xiv) into (xii) gives

$$\left(p_{\text{CO}} + 2p_{\text{CO}_2}\right)p_{\text{CO}} = 1.08 \tag{xv}$$

and substitution of Equations (xiv) into (xiii) gives

$$\left(p_{\text{CO}} + 2p_{\text{CO}_2}\right)^2 p_{\text{CO}_2} = 0.018 \tag{xvi}$$

Simultaneous solution of Equations (xv) and (xvi) gives $p_{\text{CO}} = 1.023$ atm and $p_{\text{CO}_2} = 0.016$ atm, and Equation (xiv) gives $p_{\text{Zn}} = 1.023 + (2\times 0.016) = 1.055$ atm. The total pressure at which the equilibrium exists at 1223 K is thus $1.055 + 1.023 + 0.016 = 2.094$ atm.

iii. Consider now the temperature at which the total pressure is 1 atm. Rewriting Equations (xii) and (xiii) to include temperature as a variable gives

$$K_{(\text{viii}),T} = \exp\left(\frac{-\Delta G^{\circ}_{(\text{viii})}}{RT}\right) = p_{\text{Zn}}p_{\text{CO}}$$

or, substituting for $\Delta G^{\circ}_{(\text{viii})}$ and p_{Zn},

$$\exp\left(\frac{-348{,}500}{8.3144T}\right)\exp\left(\frac{285.7}{8.3144}\right) = \left(p_{\text{CO}} + 2p_{\text{CO}_2}\right)p_{\text{CO}} \tag{xvii}$$

and

$$K_{(\text{ix}),T} = \exp\left(\frac{-\Delta G^{\circ}_{(\text{ix})}}{RT}\right) = \text{p}^2_{\text{Zn}}p_{\text{CO}_2}$$

or, substituting for $\Delta G^{\circ}_{(\text{ix})}$ and p_{Zn},

$$K_{(\text{ix}),T} = \exp\left(\frac{-526{,}300}{8.3144T}\right)\exp\left(\frac{396.8}{8.3144}\right) = \left(p_{\text{CO}} + 2p_{\text{CO}_2}\right)^2 p_{\text{CO}_2} \tag{xviii}$$

The third equation is

$$P = 1 = p_{Zn} + p_{CO} + p_{CO_2}$$

or

$$1 = \left(p_{CO} + 2p_{CO_2}\right) + p_{CO} + p_{CO_2} \qquad \text{(xix)}$$

Simultaneous solution of Equations (xvii), (xviii), and (xix) gives

$$T = 1172 \text{ K}$$

$$p_{CO} = 0.489 \text{ atm}$$

and

$$p_{CO_2} = 0.007 \text{ atm}$$

Thus, $p_{Zn} = 0.489 + (2 \times 0.007) = 0.503$ atm, and the total pressure is $0.489 + 0.503 + 0.007 = 1$ atm.

QUANTITATIVE PROBLEM 3

During the chlorination of NiO in a reactor at 900 K, it is required that 90% conversion of the chlorine gas be achieved during a single pass through the reactor. Calculate the required total gas pressure.

SOLUTION TO QUANTITATIVE PROBLEM 3

The reaction is

$$NiO_{(s)} + Cl_{2(g)} = NiCl_{2(s)} + \frac{1}{2}O_{2(g)}$$

for which $\Delta G^{\circ}_{900\text{K}} = -15{,}490$ J. Thus,

$$K_{900\text{K}} = \exp\left(\frac{15{,}490}{8.3144 \times 900}\right) = 7.925$$

From the stoichiometry of the reaction,

$$NiO_{(s)} + Cl_{2(g)} = NiCl_{2(s)} + \frac{1}{2}O_{2(g)}$$

	$NiO_{(s)} + Cl_{2(g)}$		$= NiCl_{2(s)}$	$+ \frac{1}{2}O_{2(g)}$
Moles before reaction	1	1	0	0
Moles after reaction	$(1-x)$	$(1-x)$	x	$\frac{1}{2}x$

For 90% conversion of the Cl_2, $x = 0.9$, and thus, $n_{Cl_2} = 0.1, n_{O_2} = 0.45$, and $n_T = 0.55$. In a Cl_2–O_2 mixture at the pressure P, the partial pressures of chlorine and oxygen are thus

$$p_{Cl_2} = \frac{0.1}{0.55} P = 0.182P \quad \text{and} \quad p_{O_2} = \frac{0.45}{0.55} P = 0.818P$$

Thus,

$$K_{900\,K} = 7.925 = \frac{p_{O_2}^{1/2}}{p_{Cl_2}} = \frac{(0.818P)^{1/2}}{0.182P} = \frac{4.969}{P^{1/2}}$$

which has the solution $P = 0.393$ atm.

PROBLEMS

12.1 To what temperature must $MgCO_3$ be heated in an atmosphere containing a partial pressure of CO_2 of 10^{-2} atm to cause the decomposition of the carbonate?

12.2 Using the standard Gibbs free energies of formation of NiO from solid Ni and liquid Ni, calculate the melting temperature, molar heat of melting, and the molar entropy of melting of nickel.

12.3 Calculate the temperature at which pure Ag_2O decomposes to Ag metal and O_2 gas when heated in (a) pure oxygen at 1 atm pressure, and (b) air.

12.4 Determine the maximum pressure of water vapor in wet hydrogen at 1 atm pressure in which chromium can be heated without oxidation occurring at 1500 K. Is the oxidation of Cr by water vapor exothermic or endothermic?

12.5 A mixture of argon gas and hydrogen gas at 1 atm total pressure is passed through a reaction vessel containing a mixture of liquid Sn and liquid $SnCl_2$ at 900 K. The composition of the gas leaving the vessel is 50% H_2, 7% HCl, and 43% Ar. Has equilibrium been attained between the gas phase and the liquid phases in the vessel?

12.6 Fe and FeO are in equilibrium with a gas mixture of composition 71.8% CO–28.2% CO_2 at 1273 K. Which of the two solid phases disappears if the composition of the gas is held constant and the temperature of the system is decreased?

12.7 Calculate the vapor pressure of Mg exerted at 1400°C by the system in which the following reaction equilibrium is established.

$$MgO_{(s)} + Si_{(s)} = 2Mg_{(g)} + Mg_2SiO_{4(s)}$$

12.8 One gram of $CaCO_3$ is placed in an evacuated rigid vessel of volume 1 liter at room temperature, and the system is heated. Calculate (a) the highest temperature at which the $CaCO_3$ phase is present, (b) the pressure in the vessel at 1000 K, and (c) the pressure in the vessel at 1500 K. The molecular weight of $CaCO_3$ is 100.

12.9 Calculate the total pressure $\left(p_{SO_3} + p_{SO_2} + p_{O_2}\right)$ exerted by equilibrated CoO and $CoSO_4$ at 1223 K.

12.10 A gas mixture initially containing 90% CO, 0.4% COS, and 9.6% inert constituents (by volume) is passed over sponge iron at 1000 K to remove sulfur by the following reaction:

$$COS_{(g)} + Fe_{(s)} = CO_{(g)} + FeS_{(s)}$$

a. Assuming that the effluent gas is in equilibrium with Fe and FeS, calculate the percentage of sulfur removed from the gas by reaction with the sponge iron.
b. Calculate the partial pressure of S_2 in the effluent gas.

12.11 An Ar–H_2O gas mixture of $p_{H_2O} = 0.9$ atm ($P_{total} = 1$ atm) is passed over solid CaF_2, as a result of which CaO forms according to

$$CaF_{2(s)} + H_2O_{(g)} = CaO_{(s)} + 2HF_{(g)}$$

The reaction proceeds to equilibrium and solid CaO and solid CaF_2 are mutually immiscible. When the gas flow rate (measured at 298 K and 1 atm pressure) over the sample is 1 liter per minute, the measured rates of weight loss of the sample are 2.69×10^{-4} and 8.30×10^{-3} grams per hour at 900 and 1100 K, respectively. Use these data to calculate the variation of ΔG° for the preceding reaction with temperature. The atomic weights are

$$O = 16,\ F = 19,\ \text{and } Ca = 40.08$$

12.12 Magnetite (Fe_3O_4) is reduced to sponge iron (Fe) in a continuous reactor operating at 800 K using methane gas (CH_4) as the reducing agent. The gaseous reaction product leaving the reactor at a total pressure of 1 atm is a mixture of CO, CO_2, H_2, and H_2O with a negligible methane content. The gas is at equilibrium with the Fe–Fe_3O_4 mixture in the reactor. Calculate the consumption of methane as moles of methane used per mole of sponge iron produced.

12.13 Three equations for the oxidation of Mg according to $Mg + ½O2_{(g)} = MgO_{(s)}$ are

$$\Delta G^\circ = -604{,}000 - 5.36T \ln T + 142.0T \text{ J} \quad \text{(i)}$$

$$\Delta G^\circ = -759{,}800 - 13.4T \ln T + 317T \text{ J} \quad \text{(ii)}$$

$$\Delta G^\circ = -608{,}100 - 0.44T \ln T + 112.8T \text{ J} \quad \text{(iii)}$$

One of these expressions is for the oxidation of solid Mg, one is for the oxidation of liquid Mg, and one is for the oxidation of gaseous Mg. Determine which equation is for which oxidation and calculate the melting and normal boiling temperature of Mg.

12.14 Two hundred grams of liquid zinc are placed in a crucible at 1030 K. Two moles of air are bubbled through the liquid zinc, and the gas comes to equilibrium with the liquid before leaving the system. If the total pressure of the gas remains constant at 0.8 atm throughout the process, how many grams of *metallic* zinc are left in the crucible? The atomic weights of Zn and O are, respectively, 65.38 and 16.

12.15 Methane gas is burned with twice the amount of stoichiometric air (i.e., the initial ratio of CH_4 and O_2 in the mixture is 0.25), and the combustion gas produced, in which the concentration of methane is negligible, is used to calcine $CaCO_3$ in an isothermal furnace. The gas and the solids are at 1080 K and the pressure of the gas is maintained constant at 1 atm. How many moles of $CaCO_3$ are decomposed per mole of CH_4 burned?

12.16 Mercuric oxide (HgO) is placed in a vessel which is then evacuated, filled with nitrogen, and heated to 600 K, at which temperature it is observed that the total pressure in the vessel is 2 atm. Calculate the mole fractions of O_2 and Hg vapor in the gas phase.

12.17 In Figure 12.17 the line *AB*, which represents the equilibrium

$$FeO_{(s)} + CO_{(g)} = Fe_{(s)} + CO_{2(g)}$$

intersects the carbon deposition line at the point *A* ($T = 972$ K, $p_{CO(s)} = 0.595$ atm, $p_{CO_2} = 0.405$ atm, $P = 1.000$ atm). At what total pressure does the point of intersection of the lines occur at 1000 K, and what are the values of the partial pressures of CO and CO_2 in this state?

12.18* Sketch the $\log p_{CO_2}$ vs. $\frac{1}{T}$ plot for the reaction:

$$MgO_{(s)} + CO_{2(g)} = MgCO_{3(s)}$$

See Table A.1

12.19* Apply the Gibbs Equilibrium Phase Rule to the hypothetical system depicted in Figure 12.5 and discuss the significance of the value of the degree of freedom.

APPENDIX 12A: DETERMINATION OF I IN EQUATION 12.10

The value of *I* in Equation 12.10 can be determined if *K* is known at any temperature *T*. For the reaction

$$4Cu_{(s)} + O_{2(g)} = 2Cu_2O_{(s)}$$

We have

---

* New problem in this edition.

$$\Delta H^{\circ}_{298} = -324,400 \text{ J}$$
$$\Delta S^{\circ}_{298} = -138.5 \text{ J/K}$$

and thus,

$$\Delta G^{\circ}_{298} = -324,400 + (298 \times 138.5) = -283,100 \text{ J}$$

which is $K = K(T)$ with no unknown constants.

In the range 298–1356 K,

$$c_{p,\text{Cu}(s)} = 22.6 + 6.3 \times 10^{-3} T \text{ J/K}$$

In the range 298–1200 K,

$$c_{p,\text{Cu}_2\text{O}(s)} = 62.34 + 24 \times 10^{-3} T \text{ J/K}$$

and in the range 298–3000 K,

$$c_{p,\text{O}_2(g)} = 30 + 4.2 \times 10^{-3} T - 1.7 \times 10^{5} T^{-2} \text{ J/K}$$

such that in the temperature range 298–1200 K,

$$\Delta c_p = 2c_{p,\text{Cu}_2\text{O}(s)} - 4c_{p,\text{Cu}(s)} - c_{p,\text{O}_2(g)}$$
$$= 4.28 + 18.6 \times 10^{-3} T + 1.7 \times 10^{5} T^{-2} \text{ J/K}$$

Thus,

$$\Delta H^{\circ}_T = \Delta H_0 + 4.28T + 9.3 \times 10^{-3} T^2 - 1.7 \times 10^{5} T^{-1} \text{ J}$$

Substitution of $\Delta H^{\circ}_{298} = -324,400$ J gives $\Delta H_0 = -325,900$ J. Dividing by $-T^2$, integrating with respect to T, and multiplying through by T gives

$$\Delta G^{\circ}_T = -325,900 - 4.28T \ln T - 9.3 \times 10^{-3} T^2 - 0.85 \times 10^{5} T^{-1} + IT$$

Substitution of $\Delta G^{\circ}_{298} = -283,100$ J gives $I = 171.7$, and hence,

$$\Delta G^{\circ}_T = -325,900 - 4.28T \ln T - 9.3 \times 10^{-3} T^2 - 0.85 \times 10^{5} T^{-1} + 171.7T \qquad (12A.1)$$

and

$$-\ln K = \frac{\Delta G^{\circ}_T}{RT} = \ln p_{\text{O}_2(eq.T)}$$
$$= -\frac{39,200}{T} - 0.515 \ln T - 1.1 \times 10^{-3} T - \frac{1.0 \times 10^{4}}{T^2} + 20.65$$

13 Reaction Equilibria in Systems Containing Components in Condensed Solution

13.1 INTRODUCTION

Dissolving the pure component i in a condensed solution which is in contact with a vapor phase causes a decrease in the vapor pressure exerted by i from the value p_i° (exerted by pure i) to p_i (exerted by i when it occurs in solution). This decrease in the equilibrium vapor pressure corresponds, via Equation 8.5, to a decrease of $RT \ln\left(p_i/p_i^\circ\right)$ in the value of the partial molar Gibbs free energy of i in the vapor phase. Since phase equilibrium is maintained between the vapor phase and the condensed solution, the partial molar Gibbs free energy of i (*chemical potential*) in the solution is $RT \ln\left(p_i/p_i^\circ\right)$ lower than the molar Gibbs free energy of pure condensed i at the temperature T. Since the activity, a_i, of i in the solution with respect to pure i is defined by $\left(p_i/p_i^\circ\right)$, the partial molar Gibbs free energy of i in the condensed solution is lower than the molar Gibbs free energy of pure i by the amount $RT \ln a_i$. The value of p_i, and hence a_i, depends on the composition and the nature of the components of the solution and on temperature, and inasmuch as the solution of i affects the value of $\overline{G}_i$, it necessarily affects the equilibrium state of any chemical reaction system in which the component i is involved.

As an example, consider the equilibrium between silica, silicon, and oxygen gas:

$$SiO_{2(s)} = Si_{(s)} + O_{2(g)}$$

By analogy with Equation 11.4, the equality

$$\overline{G}_{SiO_2} = \overline{G}_{Si} + \overline{G}_{O_2}$$

is the criterion for reaction equilibrium at any temperature and total pressure; that is, equal chemical potentials of the reactants and products must be present in a reacting system at equilibrium. If the SiO_2 and the Si present in the system are both "pure", and the pure solids are chosen as the standard states, then

$$G^\circ_{SiO_2} = G^\circ_{Si} + \overline{G}_{O_2}$$

DOI: 10.1201/9781003375388-16

or

$$G^{\circ}_{SiO_2} = G^{\circ}_{Si} + G^{\circ}_{O_2} + RT \ln p_{O_2(eq.T)}$$

It has been seen in Chapter 11 that the values of G°_i are dependent only on temperature. Thus, at the temperature T there exists a *unique partial pressure* of oxygen, $p_{O_2(eq.T)}$, at which equilibrium occurs in the system. This unique oxygen pressure is calculated as

$$p_{O_2(eq.T)} = \exp\left[\frac{1}{RT}\left(G^{\circ}_{SiO_2} - G^{\circ}_{Si} - G^{\circ}_{O_2}\right)\right]$$

and, if it is required to *reduce pure silica* at the temperature T, the oxygen pressure in the system must be lower than $p_{O_2(eq.T)}$.

Suppose now that the silica occurs at the activity a_{SiO_2} in an Al_2O_3–SiO_2 solution. The criterion for equilibrium among SiO_2, Si, and O_2 is still

$$\bar{G}_{SiO_2} = \bar{G}_{Si} + \bar{G}_{O_2}$$

but now

$$\bar{G}_{SiO_2} = G^{\circ}_{SiO_2} + RT \ln a_{SiO_2}$$

and thus, in terms of standard Gibbs free energies,

$$G^{\circ}_{SiO_2} + RT \ln a_{SiO_2} = G^{\circ}_{Si} + G^{\circ}_{O_2} + RT \ln p'_{O_2(eq.T)}$$

Thus, for a given value of a_{SiO_2}, there now exists a new unique equilibrium oxygen pressure, $p'_{O_2(eq.T)}$, which is given by

$$p'_{O_2(eq.T)} = p_{O_2(eq.T)} a_{SiO_2}$$

and so, if it is required to reduce SiO_2 from an Al_2O_3 solution to form pure Si, the oxygen pressure in the system must be lower than $p'_{O_2(eq.T)}$.

Thus the possibility of reducing SiO_2 from an Al_2O_3–SiO_2 solution to produce pure Si with a gas of given partial pressure of oxygen at a given temperature is determined by *the solution thermodynamics* of the system Al_2O_3–SiO_2. Generally, the calculation of the equilibrium state of any reaction involving components in condensed solution requires knowledge of the thermodynamic properties of the various solutions present in the system. The influence of *solution thermodynamics* on reaction equilibria is examined in this chapter.

13.2 THE CRITERIA FOR REACTION EQUILIBRIUM IN SYSTEMS CONTAINING COMPONENTS IN CONDENSED SOLUTION

Consider the general reaction

$$aA + bB = cC + dD$$

occurring at the temperature T and the pressure P. If none of the reactants or products of the reaction occurs in its standard state, the change in the Gibbs free energy for the reaction is

$$\Delta G' = c\bar{G}_C + d\bar{G}_D - a\bar{G}_A - b\bar{G}_B \tag{13.1}$$

If, however, all of the reaction and products occur in their standard states, the change in the Gibbs free energy is the standard Gibbs free energy change, ΔG°, given by

$$\Delta G^\circ = cG_C^\circ + dG_D^\circ - aG_A^\circ - bG_B^\circ \tag{13.2}$$

Subtraction of Equation 13.2 from Equation 13.1 gives

$$\Delta G' - \Delta G^\circ = c\left(\bar{G}_C - G_C^\circ\right) + d\left(\bar{G}_D - G_D^\circ\right) - a\left(\bar{G}_A - G_A^\circ\right) - b\left(\bar{G}_B - G_B^\circ\right) \tag{13.3}$$

For a component i occurring in some state other than its standard state, Equation 9.28 gives

$$\bar{G}_i = G_i^\circ + RT \ln a_i$$

where a_i is the activity of i with respect to the standard state, and thus, Equation 13.3 can be written as

$$\begin{aligned} \Delta G' - \Delta G^\circ &= c\left(RT \ln a_C\right) + d\left(RT \ln a_D\right) - a\left(RT \ln a_A\right) - b\left(RT \ln a_B\right) \\ &= RT \ln\left(\frac{a_C^c a_D^d}{a_A^a a_B^b}\right) = RT \ln Q \end{aligned} \tag{13.4}$$

where $Q = a_C^c a_D^d / a_A^a a_B^b$ is called the *activity quotient* at any stage of the reaction.

Reaction equilibrium is established when the reaction has proceeded to such an extent that

$$a\bar{G}_A + b\bar{G}_B = c\bar{G}_C + d\bar{G}_D$$

that is, that the Gibbs free energy of the system at the fixed temperature and pressure has been minimized, or that $\Delta G'$, for the reaction is zero. Thus, at equilibrium,

$$\Delta G^\circ = -RT \ln Q^{\text{eq}} \tag{13.5}$$

where Q^{eq} is the value of the *activity quotient* at equilibrium. From Equation 11.8,

$$\Delta G^\circ = -RT \ln K$$

and thus,

$$Q^{\text{eq}} = K$$

That is, at reaction *equilibrium*, the *activity quotient* is numerically equal to the equilibrium constant K.

Consider the oxidation of the pure solid metal M by gaseous oxygen to form the pure solid metal oxide MO_2:

$$M_{(s)} + O_{2(g)} = MO_{2(s)} \tag{i}$$

at the temperature T and the pressure P. For this reaction,

$$Q = \frac{a_{MO_2}}{a_M a_{O_2}}$$

Since M and MO_2 are pure (i.e., occur in their *standard states*), then $a_M = a_{MO_2} = 1$, and, from the formal definition of activity, the activity of oxygen gas is given as

$$a_{O_2} = \frac{\text{The pressure of oxygen in the gas phase}}{\text{The pressure of oxygen in its standard state}}$$

Since the standard state for gaseous species has been chosen to be the gas at 1 atm pressure and the temperature of interest, then the activity of oxygen in the gas phase is equal to its partial pressure (assuming ideal behavior of the gas). Thus,

$$Q = \frac{1}{p_{O_2}} \quad \text{and} \quad Q^{eq} = \frac{1}{p_{O_2(eq.T)}} = K$$

Now consider that the metal in equilibrium with its pure oxide and oxygen in a gaseous atmosphere occurs at the activity a_M in a solution. In this case,

$$Q^{eq} = \frac{1}{a_M p_{O_2(eq.T)}} = K$$

and, since K is dependent only on temperature and $a_M < 1$, it is seen that the oxygen pressure required to maintain equilibrium between M in solution and pure MO_2 is larger than that required for equilibrium between pure M and pure MO_2 at the same temperature.

Similarly, if the pure metal M is in equilibrium with MO_2 occurring at the activity a_{MO_2} in solution and oxygen in a gas phase, then

$$Q^{eq} = \frac{a_{MO_2}}{p_{O_2(eq.T)}} = K$$

in which case the oxygen pressure required for the equilibrium between pure M and its oxide in solution is lower than that for the equilibrium between pure M and pure MO_2.

In Figure 13.1, the line *ab* is drawn as the variation of the standard Gibbs free energy change, with temperature for the oxidation

$$M_{(s)} + O_{2(g,1\,atm)} = MO_{2(s)} \tag{i}$$

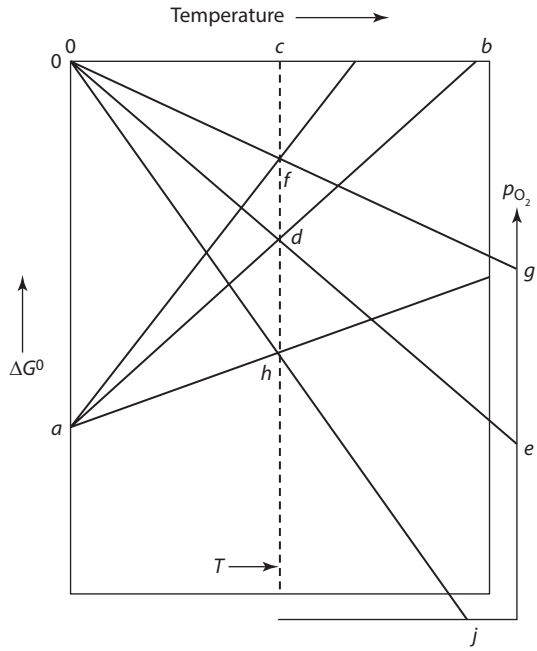

FIGURE 13.1 The influence of non-unit activities of the reactants and products of a reaction on the ΔG°–T relationship for the reaction $M_{(s)} + O_{2(g)} = MO_{2(s)}$

At the temperature T, $\Delta G^\circ = cd$, and the oxygen pressure for equilibrium between pure solid M and pure solid MO_2 is drawn as the point e on the oxygen pressure *nomographic* scale.

Now consider the reaction

$$M_{(\text{in solid solution at } a_M)} + O_{2(g,1\text{ atm})} = MO_{2(s)} \qquad \text{(ii)}$$

for which, at the temperature T, the Gibbs free energy change is $\Delta G_{(ii)}$. Reaction (ii) can be written as the sum of

$$M_{(\text{in solid solution at } a_M)} \rightarrow M_{(s,\text{pure})} \qquad \text{(iii)}$$

for which

$$\Delta G_{(iii)} = G^\circ_M - \bar{G}_M = -RT \ln a_M$$

and

$$M_{(s)} + O_{2(g,1\text{atm})} = MO_{2(s)} \qquad \text{(i)}$$

for which

$$\Delta G_{(i)} = \Delta G^\circ \text{ at the temperature } T$$

Thus,

$$\Delta G_{(\text{ii})} = \Delta G_{(\text{i})} + \Delta G_{(\text{iii})}$$

$$= \Delta G^{\circ} - RT \ln a_{\text{M}}$$

At the temperature T, ΔG° is a negative quantity, and, since $a_{\text{M}} < 1$, then $\Delta G_{(\text{ii})}$ is a less negative quantity, drawn in Figure 13.1 as *cf*. The effect of the solution of M on its oxidation is thus an *anticlockwise rotation* of the standard Gibbs free energy line about the point a (ΔG° at $T = 0$), with the extent of this rotation being such that, at the temperature T, the vertical separation from the standard line equals $RT \ln a_{\text{M}}$. The extent of the rotation is determined by the value of a_{M}. The oxygen pressure required for equilibrium between M in solution and pure MO_2 is increased from e to g in accordance with

$$K_T = \frac{1}{p_{\text{O}_2\left(T,\text{eq M}_{(s)}\right)}}$$

$$= \frac{1}{a_{\text{M}}\, p_{\text{O}_2\left(T,\text{eqM}_{(\text{at } a_{\text{M}})}/\text{MO}_{2(s)}\right)}}$$

Consider the reaction

$$\text{M}_{(s,\text{ pure})} + \text{O}_{2(g,1\text{ atm})} = \text{MO}_{2(\text{in solid solution at } a_{\text{MO}_2})} \qquad \text{(iv)}$$

for which, at the temperature T, the Gibbs free energy change is $\Delta G_{(\text{iv})}$. Reaction (iv) can be written as the sum of

$$\text{MO}_{2(s,\text{pure})} \rightarrow \text{MO}_{2(\text{in solution at } a_{\text{MO}_2})} \qquad \text{(v)}$$

and reaction (i); that is,

$$\Delta G_{(\text{iv})} = \Delta G^{\circ} + RT \ln a_{\text{MO}_2}$$

At the temperature T, ΔG° is a negative quantity, and, since $a_{\text{MO}_2} < 1$, then $\Delta G_{(\text{iv})}$ is a more negative quantity, drawn in Figure 13.1 as *ch*. The effect of the solution of MO_2 on the oxidation of M is thus seen to be a clockwise rotation of the Gibbs free energy line about the point a with the extent of the rotation being such that, at the temperature T, the vertical separation from the standard Gibbs free energy line equals $RT \ln a_{\text{MO}_2}$. The extent of the rotation is determined by the value of a_{MO_2}, and the oxygen pressure required for equilibrium between pure M and MO_2 in solution is decreased from e to j in accordance with

$$K_T = \frac{1}{p_{\text{O}_2\left(T,\text{eqM}_{(s)}/\text{MO}_{2(s)}\right)}}$$

$$= \frac{a_{\text{MO}_2}}{p_{\text{O}_2[T,\text{eqM}_{(s)}/\text{MO}\ (\quad)}}$$

In the general case,

$$M_{(\text{in solution at } a_M)} + O_{2(g,\text{at } p_{O_2})} = MO_{2(\text{in solution at } a_{MO_2})} \tag{vi}$$

for which, at the temperature T, the free energy change is $\Delta G_{(vi)}$:

$$\begin{aligned}\Delta G_{(vi)} &= \Delta G^\circ - RT \ln a_M - RT \ln p_{O_2} + RT \ln a_{MO_2} \\ &= \Delta G^\circ + RT \ln \frac{a_{MO_2}}{a_M p_{O_2}} \\ &= \Delta G^\circ + RT \ln Q\end{aligned}$$

At equilibrium, the values of a_M, a_{MO_2}, and p_{O_2} are such that $\Delta G_{(vi)} = 0$, and thus,

$$\Delta G^\circ = -RT \ln Q^{eq} = -RT \ln K$$

as in Equation 13.5.

Example 13.1

Examine the conditions under which a liquid Fe–Mn alloy can be in equilibrium with an FeO–MnO liquid solution in an atmosphere containing oxygen at 1800°C. For

$$\begin{aligned}Mn_{(l)} + \frac{1}{2}O_{2(g)} &= MnO_{(l)} \\ \Delta G^\circ_{(i)} &= -344{,}800 + 55.90T \text{ J}\end{aligned} \tag{i}$$

and for

$$\begin{aligned}Fe_{(l)} + \frac{1}{2}O_{2(g)} &= FeO_{(l)} \\ \Delta G^\circ_{(ii)} &= -232{,}700 + 45.13T \text{ J}\end{aligned} \tag{ii}$$

Solution

The pertinent equilibrium is

$$FeO_{(l)} + Mn_{(l)} = MnO_{(l)} + Fe_{(l)} \tag{iii}$$

for which

$$\begin{aligned}\Delta G^\circ_{(iii),2073\,K} &= \Delta G^\circ_{(i),2073\,K} - \Delta G^\circ_{(ii),2073\,K} \\ &= -228{,}900 + 138{,}800 = -90{,}100 \text{ J} \\ &= -8.3144 \times 2073 \ln K_{(iii),2073\,K} \text{ J}\end{aligned}$$

Therefore,

$$K_{(\text{iii}),2073\,\text{K}} = 186 = \frac{(a_{\text{MnO}})[a_{\text{Fe}}]}{(a_{\text{FeO}})[a_{\text{Mn}}]}$$

where:

(a_{MnO}) = the activity of MnO in the liquid oxide phase with respect to pure MnO

(a_{FeO}) = the activity of FeO in the liquid oxide phase with respect to iron-saturated liquid iron oxide

$[a_{\text{Mn}}]$ = the activity of Mn in the liquid metal phase with respect to pure liquid Mn

$[a_{\text{Fe}}]$ = the activity of Fe in the liquid metal phase with respect to pure liquid Fe.

Since both the liquid metal solution and the liquid oxide solution exhibit Raoultian behavior, the condition for phase equilibrium between the two is

$$\frac{(X_{\text{MnO}})[X_{\text{Fe}}]}{(X_{\text{FeO}})[X_{\text{Mn}}]} = 186 \qquad \text{(iv)}$$

or

$$\frac{[X_{\text{Fe}}]}{[X_{\text{Mn}}]} = 186\frac{(X_{\text{FeO}})}{(X_{\text{MnO}})}$$

A series of tie-lines joining the compositions of equilibrated metal and oxide solutions is shown in Figure 13.2. Consider the metallic alloy of composition $X_{\text{Fe}} = 0.5$. Equation (iv) gives

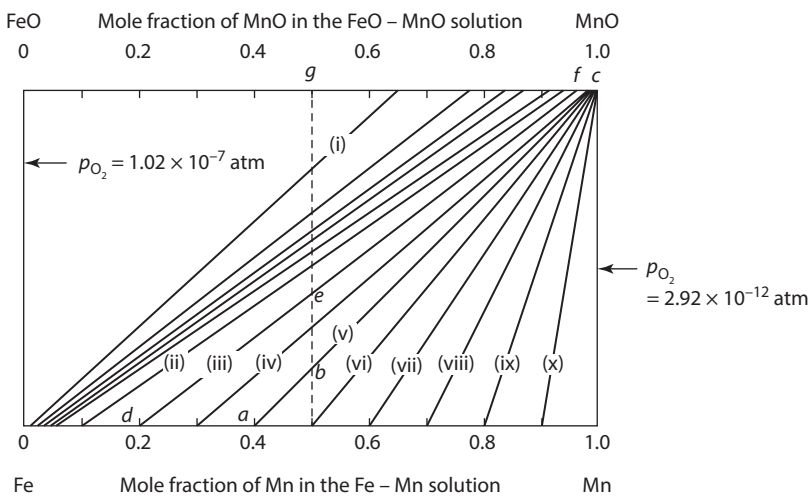

FIGURE 13.2 Tie-lines between the compositions of equilibrated metallic and oxide alloys in the system Fe–Mn–O. The tie-lines are also oxygen isobars with oxygen pressures as follows: (i) 1.24×10^{-8} atm, (ii) 2.65×10^{-10} atm, (iii) 7.0×10^{-11} atm, (iv) 3.14×10^{-11} atm, (v) 1.79×10^{-11} atm, (vi) 1.15×10^{-11} atm, (vii) 8.04×10^{-12} atm, (viii) 5.92×10^{-12} atm, (ix) 4.46×10^{-12} atm, and (x) 3.58×10^{-12} atm.

$$1 = 186\frac{(X_{\mathrm{FeO}})}{1-(X_{\mathrm{FeO}})}$$

or

$$(X_{\mathrm{FeO}}) = 0.00535$$

and thus, when a metallic alloy of composition $X_{\mathrm{Fe}} = 0.5$ is equilibrated with an oxide solution, the composition of the latter is $X_{\mathrm{FeO}} = 0.00535$.

Consider now the influence of the partial pressure of oxygen in the gaseous atmosphere:

$$\Delta G^{\circ}_{(\mathrm{i})} = -RT\ln K_{(\mathrm{i})} = -RT\ln\frac{(a_{\mathrm{MnO}})}{[a_{\mathrm{Mn}}]p_{\mathrm{O_2}}^{1/2}}$$

Thus, since

$$\Delta G^{\circ}_{(\mathrm{i}),2073\,\mathrm{K}} = -228{,}900\ \mathrm{J}$$

$$K_{(\mathrm{i}),2073\,\mathrm{K}} = 5.856\times10^{5} = \frac{(a_{\mathrm{MnO}})}{[a_{\mathrm{Mn}}]p_{\mathrm{O_2}}^{1/2}}$$

or, since the metallic and oxide solutions are ideal,

$$\frac{(X_{\mathrm{MnO}})}{[X_{\mathrm{Mn}}]} = 5.856\times10^{5}\,p_{\mathrm{O_2}}^{1/2} \qquad \text{(v)}$$

Similarly,

$$\Delta G^{\circ}_{(\mathrm{ii})} = -RT\ln\frac{(a_{\mathrm{FeO}})}{[a_{\mathrm{Fe}}]p_{\mathrm{O_2}}^{1/2}}$$

and since

$$\Delta G^{\circ}_{(\mathrm{ii}),2073\mathrm{K}} = -138{,}800\mathrm{J}$$

then

$$K_{(\mathrm{ii}),2073\,\mathrm{K}} = 3143 = \frac{(a_{\mathrm{FeO}})}{[a_{\mathrm{Fe}}]p_{\mathrm{O_2}}^{1/2}}$$

or

$$\frac{(a_{\mathrm{FeO}})}{[a_{\mathrm{Fe}}]} = 3143\,p_{\mathrm{O_2}}^{1/2} \qquad \text{(vi)}$$

The ideal Raoultian behavior of the two solutions allows Equation (vi) to be written as

$$\frac{(X_{\mathrm{FeO}})}{[X_{\mathrm{Fe}}]} = 3143 p_{\mathrm{O_2}}^{1/2}$$

Consider the equilibrium between the metallic alloy of $X_{\mathrm{Fe}} = 0.5$ and the oxide solution of $X_{\mathrm{FeO}} = 0.00535$. From Equation (v),

$$p_{\mathrm{O_2}} = \left(\frac{0.99465}{0.5} \times \frac{1}{5.856 \times 10^5} \right)^2 = 1.15 \times 10^{-11} \text{ atm}$$

and from Equation (vi)

$$p_{\mathrm{O_2}} = \left(\frac{0.00535}{0.5} \times \frac{1}{3143} \right)^2 = 1.15 \times 10^{-11} \text{ atm}$$

Thus, the tie-line connecting the compositions of the equilibrated metallic and oxide alloy is also the oxygen isobar in Figure 13.2. Thus, at any fixed oxygen pressure, the individual ratios

$$\frac{(a_{\mathrm{FeO}})}{[a_{\mathrm{Fe}}]} \left(= \frac{(X_{\mathrm{FeO}})}{[X_{\mathrm{Fe}}]} \right) \quad \text{and} \quad \frac{(a_{\mathrm{MnO}})}{[a_{\mathrm{Mn}}]} \left(= \frac{(X_{\mathrm{MnO}})}{[X_{\mathrm{Mn}}]} \right)$$

are fixed by Equations (v) and (vi), combination of which gives

$$\frac{(X_{\mathrm{MnO}})[X_{\mathrm{Fe}}]}{(X_{\mathrm{FeO}})[X_{\mathrm{Mn}}]} = \frac{5.856 \times 10^5}{3143} = 186$$

in accordance with Equation (iv).

Consider the oxidation of a finite quantity of a liquid metallic alloy of composition $X_{\mathrm{Fe}} = 0.5$ by an infinite oxygen-containing gaseous atmosphere in which the partial pressure of oxygen is slowly increased. From Figure 13.2, the metal phase is stable when the partial pressure of oxygen is less than 1.15×10^{-11} atm. At $p_{\mathrm{O_2}} = 1.15 \times 10^{-11}$ atm, the metallic alloy is in equilibrium with an oxide solution of $X_{\mathrm{FeO}} = 0.00535$. Increasing the partial pressure of oxygen to 1.79×10^{-11} atm moves the state of the system to the state *b* on the (v) isobar in Figure 13.2. In this state, a metallic alloy of $X_{\mathrm{Fe}} = 0.6$ (at *a*) is in equilibrium with an oxide solution of $X_{\mathrm{FeO}} = 0.0053$ (at *c*), and the relative quantities of the two phases are given by application of the lever rule to the tie-line (v); that is, the fraction of the system occurring as the metallic alloy in state *a* is *bc*/*ac*, and the fraction occurring as the oxide solution in state *c* is *ab*/*ac*. Increasing the oxygen pressure to 7.0×10^{-11} atm moves the system to the state *e* on the (iii) isobar, where a metallic alloy of $X_{\mathrm{Fe}} = 0.8$ (at *d*) is in equilibrium with an oxide solution of $X_{\mathrm{FeO}} = 0.021$ (at *f*). The ratio of metallic alloy to oxide solution occurring is *ef*/*de*. Continued increase in the partial pressure of oxygen moves the state of the system upward along the broken line in Figure 13.2, during which the ratio of oxide-to-metal phase increases and the mole fraction of Fe in the metal phase and the mole fraction of FeO in the oxide phase

increase. When the composition of the oxide reaches $X_{FeO} = 0.5$ (at *g*), the infinitesimal amount of equilibrium metal phase has the composition $X_{Mn} = 0.00535$ and the oxygen pressure is 2.55×10^{-8} atm. The oxidation of Fe–Mn alloys at 2073 K occurs between the limits of oxygen pressure 2.92×10^{-12} atm for the equilibrium between pure Mn and pure MnO, and 1.02×10^{-7} atm for the equilibrium between pure Fe and pure FeO.

The establishment of equilibrium (iii) requires that the $\Delta G - T$ lines for the oxidation of Fe and Mn intersect at 2073 K—that is, that $\Delta G_{(iii),2073\ K} = 0$. For any oxidation $2M + O_2 = 2MO$, clockwise rotation of the $\Delta G - T$ line (e.g., the line *ab* in Figure 13.1) about its point of intersection with the $T = 0$ axis occurs when the ratio a_{MO}/a_M is decreased to a value less than unity, and, conversely, anticlockwise rotation of the line occurs when the ratio a_{MO}/a_M is increased to a value greater than unity. Also, since the equilibrium constant K is a function only of temperature, then, at any oxygen pressure p_{O_2} in the system M–MO–O_2 at the temperature T, the equilibrium ratio a_{MO}/a_M must be

$$\frac{a_{MO}}{a_M} = \frac{p_{O_2}^{1/2}}{p_{O_2(\text{eq.}T,\ \text{pure M/pure MO})}^{1/2}}$$

where $p_{O_2(\text{eq.}T\ \text{pure M/pure MO})}$ is that unique oxygen pressure at the temperature T required for equilibrium between pure M and pure MO. Thus, for any oxygen pressure within the allowed limits, equilibrium (iii) occurs when Equations (v) and (vi) are satisfied, and, under these conditions, the $\Delta G - T$ lines for the oxidation of Fe and Mn intersect at 1800°C. Thus, as a consequence of the ability to vary a_M and a_{MO}, equilibrium (iii) can be established at any T and any p_{O_2} (within the aforementioned limits). This is in contrast to the situation illustrated in Figures 12.4 and 12.5, in which, if both metals and both oxides are present in their pure states, then an equilibrium such as (iii) can only be achieved at the single unique state (unique T and unique p_{O_2}) at which the Ellingham lines for the two oxidation reactions intersect with one another. The restrictions on general multicomponent multiphase equilibria are discussed in Section 13.4.

13.3 ALTERNATIVE STANDARD STATES

Up to this point, the standard state of a component of a system has been chosen as being the pure component in its stable state of existence at the temperature of interest. This is called the *Raoultian standard state*; in Figure 13.3, the Raoultian standard state for the component *B* is located at point *r*.

In situations in which the pure component exists in a physical state which differs from that of the solution, the Henrian standard state may be more convenient than the Raoultian standard state. Such situations include the solution of a gas in a solid or liquid solvent and the solution of a solid in a liquid solvent. The Henrian standard state is obtained from consideration of Henry's law, which, strictly being a limiting law obeyed by the solute *B at* infinite dilution, is expressed as

$$\frac{a_B}{X_B} \to \gamma_B^{\circ} \quad \text{as} \quad X_B \to 0 \tag{13.6}$$

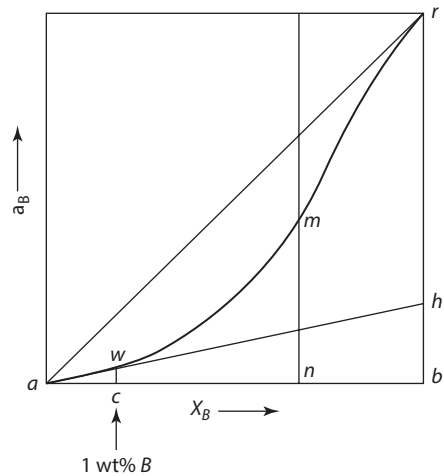

FIGURE 13.3 Illustration of the Raoultian, Henrian, and 1 wt% standard states for component B in a binary A–B system.

where:

a_B is the activity of B in the solution with respect to the Raoultian standard state

γ_B°, the Henry's law constant at the temperature T, is the constant activity coefficient which quantifies the difference between the Raoultian solution behavior of B and the Henrian solution behavior of B.

If the solute obeys Henry's law over a finite range of composition, then, over this range,

$$a_B = \gamma_B^\circ X_B$$

The Henrian standard state is obtained by extrapolating the Henry's law line to $X_B = 1$. This state (the point h in Figure 13.3) represents pure B in the hypothetical nonphysical state in which it would exist as a pure component, if it behaved as it does in a dilute solution. The activity of B in the Henrian standard state with respect to the Raoultian standard state having unit activity is given by Equation 13.6 as

$$a_B = \gamma_B^\circ$$

Thus, in Figure 13.3, if the length rb is unity, then $hb = \gamma_B^\circ$.

Having defined the Henrian standard state, the activity of B in a solution, with respect to the Henrian standard state having unit activity, is given by

$$h_B = f_B X_B \tag{13.7}$$

where h_B is the Henrian activity and f_B is the Henrian activity coefficient. In the range of composition in which the solute B obeys Henry's law, $f_B = 1$, and the solute exhibits Henrian ideality.

The mole fraction of B in an A–B solution is related to the weight percentage of B by

$$X_B = \frac{\dfrac{\text{wt\%}B}{\text{MW}_B}}{\dfrac{\text{wt\%}B}{\text{MW}_B} + \dfrac{(100 - \text{wt\%}B)}{\text{MW}_A}}$$

where MW_A and MW_B are, respectively, the molecular weights of A and B. Thus, in a dilute solution, as the mole fraction of B is virtually proportional to the weight percentage of B; that is,

$$X_B \sim \frac{\text{wt\%}B \times \text{MW}_A}{100 \times \text{MW}_B}$$

a third standard state can be introduced. This is the 1 wt% standard state, which is defined as

$$\frac{h_{B(1\text{ wt\%})}}{\text{wt\%}B} \to 1 \text{ as } \text{wt\%}B \to 0$$

and is located at the point on the Henry's law line which corresponds to a concentration of 1 wt% B (the point w in Figure 13.3). With respect to the 1 wt% standard state having unit activity, the activity of B, $h_{B(1\text{ wt\%})}$, is given by

$$h_{B(1\text{ wt\%})} = f_{B(1\text{ wt\%})}\text{wt\%}B \tag{13.8}$$

where $f_{B(1\text{ wt\%})}$ is the 1 wt% activity coefficient, and in the range of composition in which the solute B obeys Henry's law, $f_{B(1\text{ wt\%})} = 1$, and hence,

$$h_{B(1\text{ wt\%})} = \text{wt\%}B$$

which is of considerable practical convenience.

From consideration of the similar triangles *awc* and *ahb* in Figure 13.3, the activity of B in the 1 wt% standard state with respect to the Henrian standard state having unity activity is

$$h_{B(1\text{ wt\%})} = \frac{wc}{hb} = \frac{ac}{ab} = \frac{\text{MW}_A}{100\ \text{MW}_B}$$

and, with respect to the Raoultian standard state having unit activity, is

$$\frac{\gamma^{\circ}_B \text{MW}_A}{100\ \text{MW}_B}$$

The value of the equilibrium constant for any reaction, being equal to the quotient of the activities of the reactants and products at reaction equilibrium, necessarily

depends on the choice of standard states for the components. Similarly, the magnitude of ΔG° for the reaction depends on the choice of standard states and thus, in order to convert from the use of one standard state to another, it is necessary that the differences between the Gibbs free energies of the standard states be known.

For the change of standard state

$$B_{(\text{in the Raoultian standard state})} \rightarrow B_{(\text{in the Henrian standard state})}$$

$$\Delta G^\circ_{B(R\rightarrow H)} = G^\circ_{B(H)} - G^\circ_{B(R)} = RT \ln \frac{a_{B(\text{in the Henrian standard state})}}{a_{B(\text{in the Raoultian standard state})}}$$

where both activities are measured on the same activity scale. On either the Raoultian or Henrian scales,

$$\frac{a_{B(\text{in the Henrian standard state})}}{a_{B(\text{in the Raoultian standard state})}} = \frac{hb}{rb} = \gamma^\circ_B$$

and thus,

$$\Delta G^\circ_{B(R\rightarrow H)} = RT \ln \gamma^\circ_B \tag{13.9}$$

where γ°_B is the Henrian activity coefficient *at the temperature T.*

For the change of standard state

$$B_{(\text{in the Henrian standard state})} \rightarrow B_{(\text{in the 1 wt\% standard state})}$$

$$\Delta G^\circ_B\left(H \rightarrow 1 \text{ wt\%}\right) = G^\circ_{B(1\text{ wt\%})} - G^\circ_{B(H)} = RT \ln \frac{a_{B(\text{in the 1 wt\% standard state})}}{a_{B(\text{in the Henrian standard state})}}$$

where, again, both activities are measured on the same scale:

$$\frac{a_{B(\text{in the 1 wt\% standard state})}}{a_{B(\text{in the Henrian standard state})}} = \frac{wc}{hb} = \frac{ac}{ab} = \frac{\text{MW}_A}{100\text{MW}_B}$$

and thus,

$$\Delta G^\circ_{B(H\rightarrow 1\text{ wt\%})} = RT \ln\left(\frac{\text{MW}_A}{100\,\text{MW}_B}\right) \tag{13.10}$$

Combination of Equations 13.9 and 13.10 gives

$$\Delta G^\circ_{B(R\rightarrow 1\text{ wt\%})} = RT \ln\left(\frac{\gamma^\circ_B \text{MW}_A}{100\,\text{MW}_B}\right) \tag{13.11}$$

for the change of standardstate Raoultian → 1 wt%.

Example 13.2

Using the subscript *R* to denote the Raoultian standard state, the subscript *H* to denote the Henrian standard state, and the subscript wt% to denote the 1 wt% standard state, consider again the oxidation of metal M to form the oxide MO_2 at the temperature *T*:

$$\mathrm{M}_{(R)} + \mathrm{O}_{2(g)} = \mathrm{MO}_{2(R)}$$

For this equilibrium,

$$\Delta G^{\circ}_{(R)} = -RT \ln K_{(R)} = -RT \ln \frac{a_{\mathrm{MO_2}}}{a_{\mathrm{M}} p_{\mathrm{O_2}}}$$

If M occurs in a dilute solution, in which case it may be more convenient to use the Henrian standard state for M, then

$$\mathrm{M}_{(H)} + \mathrm{O}_{2(g)} = \mathrm{MO}_{2(R)}$$
$$\Delta G^{\circ}_{(H)} = \Delta G^{\circ}_{(R)} - \Delta G^{\circ}_{\mathrm{M}(R \to H)}$$

That is,

$$-RT \ln K_{(\mathrm{H})} = -RT \ln K_{(\mathrm{R})} - RT \ln \gamma^{\circ}_{\mathrm{M}}$$

or

$$RT \ln \frac{a_{\mathrm{MO_2}}}{h_{\mathrm{M}} p_{\mathrm{O_2}}} = RT \ln \frac{a_{\mathrm{MO_2}}}{a_{\mathrm{M}} p_{\mathrm{O_2}}} + RT \ln \gamma^{\circ}_{\mathrm{M}}$$

Thus,

$$a_{\mathrm{M}} = h_{\mathrm{M}} \gamma^{\circ}_{\mathrm{M}} \tag{13.12}$$

which relates the activity of M in solution with respect to the Raoultian standard state to the activity of M in solution with respect to the Henrian standard state; for example, in the case of composition *m* in Figure 13.3,

$$a_B = \frac{mn}{rb} = \frac{mn}{hb}\frac{hb}{rb} = h_B \gamma^{\circ}_B$$

Similarly, if it is convenient to use the 1 wt% standard state for M, then

$$\mathrm{M}_{(1\,\mathrm{wt\%})} + \mathrm{O}_{2(g)} = \mathrm{MO}_{2(R)}$$
$$\Delta G^{\circ}_{(1\,\mathrm{wt\%})} = \Delta G^{\circ}_{(R)} - \Delta G^{\circ}_{\mathrm{M}(R \to 1\,\mathrm{wt\%})}$$

or

$$-RT \ln K_{(1\,\mathrm{wt\%})} = -RT \ln K_{(R)} - RT \ln \frac{\gamma^{\circ}_{\mathrm{M}}\ \mathrm{MW}_{\mathrm{solvent}}}{100\ \mathrm{MW}_{\mathrm{M}}}$$

or

$$-RT\ln\frac{a_{MO_2}}{f_{M(1\,wt\%)}\times wt\%M\times p_{O_2}}=-RT\ln\frac{a_{MO_2}}{a_M p_{O_2}}-RT\ln\frac{\gamma^{\circ}_M\ MW_{solvent}}{100\ MW_M}$$

or

$$a_M=f_{M(1\,wt\%)}\cdot wt\%M\cdot\gamma^{\circ}_M\cdot\frac{MW_{solvent}}{100\ MW_M} \tag{13.13}$$

Example 13.3

The activity of silicon in binary Fe–Si liquid alloys, a_{Si}, is shown in Figure 13.4 at two temperatures. As is seen, Si exhibits considerable negative deviation from Raoult's law; for example, at $X_{Si}=0.1$ and 1420°C, $a_{Si}=0.00005$. Thus, in considering dilute solutions of Si in Fe, there is an advantage to using either the Henrian standard state or the 1 wt% standard state.

For the change of standard state from Raoultian to Henrian at the temperature T,

$$\Delta G^{\circ}_{Si(R\to H)}=RT\ln\gamma^{\circ}_{Si}$$

and the experimentally measured variation of $\log\gamma^{\circ}_{Si}$ with temperature is

$$\log\gamma^{\circ}_{Si}=-\frac{6230}{T}+0.37$$

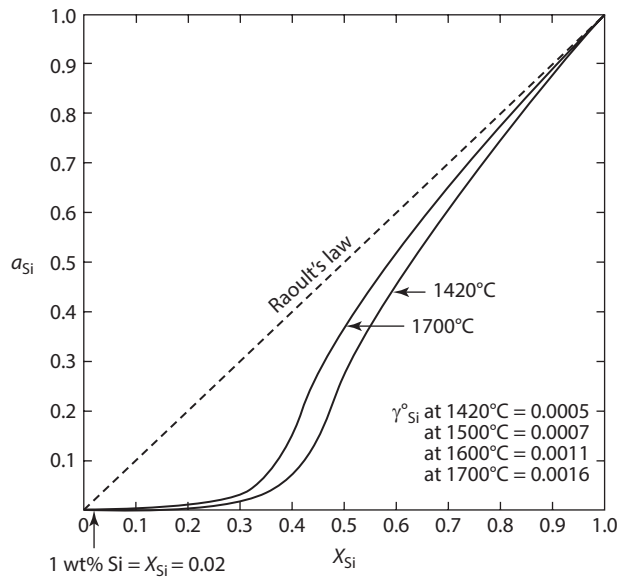

FIGURE 13.4 The activity of Si in Fe–Si melts at 1420°C and 1700°C.

and thus,

$$\Delta G^{\circ}_{\mathrm{Si}(R\rightarrow H)} = 8.3144T \times 2.303 \log \gamma^{\circ}_{Si}$$
$$= -119{,}300 + 7.08T \text{ J}$$

Also, for the change of standard state from Henrian to 1 wt% in Fe at the temperature T

$$\Delta G^{\circ}_{\mathrm{Si}(H\rightarrow 1\,\mathrm{wt\%})} = RT \ln \frac{\mathrm{MW_{Fe}}}{100\,\mathrm{MW_{Si}}}$$
$$= RT \ln\left(\frac{55.85}{100 \times 28.09}\right)$$
$$= -32.6T \text{ J}$$

so, for the change $\mathrm{Si}_{(R)} \rightarrow \mathrm{Si}_{(1\,\mathrm{wt\%\ in\ Fe})}$

$$\Delta G^{\circ}_{(R\rightarrow 1\,\mathrm{wt\%})} = \Delta G^{\circ}_{(R\rightarrow H)} + \Delta G^{\circ}_{(H\rightarrow 1\,\mathrm{wt\%})}$$
$$= -119{,}300 - 25.5T \text{ J} \qquad \text{(i)}$$

Now, given that a liquid Fe–Si alloy is in equilibrium with an SiO_2-saturated FeO–SiO_2 melt (in which $a_{SiO_2} = 1$) and an atmosphere containing oxygen, calculate the relationship between the equilibrium weight percentage of Si in the Fe–Si alloy and the oxygen pressure in the gaseous atmosphere. For the reaction

$$\mathrm{Si}_{(l)} + \mathrm{O}_{2(g)} = \mathrm{SiO}_{2(s)} \qquad \text{(ii)}$$

$\Delta G^{\circ}_{(\mathrm{ii})} = -952{,}700 + 204T\ J$ in the temperature range of 1700–2000 K. Thus, the standard Gibbs free energy for the reaction

$$\mathrm{Si}_{(1\,\mathrm{wt\%})} + \mathrm{O}_{2(g)} = \mathrm{SiO}_{2(s)} \qquad \text{(iii)}$$

is obtained as $\Delta G^{\circ}_{(\mathrm{ii})} - \Delta G^{\circ}_{(\mathrm{i})}$; namely

$$\Delta G^{\circ}_{(\mathrm{iii})} = -833{,}400 + 229.5T \text{ J}$$
$$= -RT \ln \frac{a_{\mathrm{SiO_2}}}{h_{\mathrm{Si}(1\,\mathrm{wt\%})} p_{\mathrm{O_2}}}$$

As $a_{\mathrm{SiO_2}} = 1$, then

$$\ln h_{\mathrm{Si}(1\,\mathrm{wt\%})} = -\frac{833{,}400}{8.3144T} + \frac{229.5}{8.3144} - \ln p_{\mathrm{O_2}}$$

If it can be assumed that Si in Fe obeys Henry's law over some initial range of composition, then, in this range, $h_{\mathrm{Si}(1\,\mathrm{wt\%})} = \mathrm{wt\%\ Si}$, and thus,

$$\ln (\mathrm{wt\%Si}) = -\frac{100{,}200}{T} + 27.60 - \ln p_{\mathrm{O_2}}$$

Thus, to produce an equilibrium melt containing 1 wt% Si at 1600°C, the partial pressure of oxygen must be 5.57×10^{-12} atm, and the oxygen pressure for any other weight percentage of Si at 1600°C is calculated from

$$p_{O_2} = \frac{5.57 \times 10^{-12}}{\text{wt\% Si}}$$

The error in this calculation caused by the assumption of Henrian behavior in some initial range of composition is demonstrated when the calculation is considered again in Section 13.9.

13.4 PHASE STABILITY DIAGRAMS: SI-C-O

In this section *phase stability diagrams* (also called *predominance diagrams*) are introduced. These are diagrams which are used in multicomponent, multiphase reacting systems to display regions in thermodynamic variable space where various phases in the system are likely to be found.

Consider equilibrium in the ternary system Si–C–O at 1000°C. The solid phases that can exist in this system are Si, SiO_2, SiC, and C, and the gas phase is a mixture of CO and CO_2. Just as fixing the activity of one component in a binary system fixes the activity of the other component, the fixing of the activities of two of the components in a ternary system fixes the activity of the third. Thus, when the activities of C and O_2 are fixed in the system Si–C–O, the activity of Si is fixed and a definite equilibrium state exists.

The two-dimensional representation of the phase stability can be considered in the following ways:

1. At constant temperature with a_C and p_{O_2} as the variables
2. At constant a_C (or constant p_{O_2}) with T and p_{O_2} (or a_C) as the variables

Application of the phase rule to a three-component system indicates that an equilibrium among five phases has no degrees of freedom. Thus, if a gas phase is always present,

- Four condensed phases can be in equilibrium with one another and with a gas phase at an invariant state ($\mathcal{F} = 0 = C + 2 - \Phi = 3 + 2 - 5$).
- Three condensed phases can be in equilibrium with one another and a gas phase at an arbitrarily chosen temperature ($\mathcal{F} = 1 = C + 2 - \Phi = 3 + 2 - 4$).
- Two condensed phases can be in equilibrium with one another and a gas phase at an arbitrarily chosen temperature and an arbitrarily chosen value of a_C or p_{O_2} ($\mathcal{F} = 2 = C + 2 - \Phi = 3 + 2 - 3$).
- One condensed phase can be in equilibrium with the gas phase at an arbitrarily chosen temperature and arbitrarily chosen values of a_C and p_{O_2} ($\mathcal{F} = 3 = C + 2 - \Phi = 3 + 2 - 2$).

Since four solid phases can exist, there are

- Four possible equilibria involving three condensed phases and a gas phase (found by taking four solid phases three at a time, or $4!/(3!\cdot 1!) = 4$)
- Six possible equilibria involving two condensed phases and a gas phase (found by taking four solid phases two at a time, or $4!/(2!\cdot 2!) = 6$)
- Four possible equilibria involving one condensed phase and the gas phase (found by taking four solid phases one at a time, or $4!/(1!\cdot 3!) = 4$)

13.4.1 Plots of log a_C and log p_{O_2} for Si-C-O

Consider the construction of the phase stability diagram for the system Si–C–O at 1000°C using log a_C and log p_{O_2} as the variables.

As sated above, there are six possible equilibria involving two condensed phases and a gas phase: namely,

1. Si–SiO_2–gas
2. Si–SiC–gas
3. SiC–SiO_2–gas
4. SiC–C–gas
5. SiO_2–C–gas
6. Si–C–gas

The four possible equilibria involving three condensed phases and a gas phase are

1. Si–SiO_2–SiC–gas
2. Si–SiC–C–gas
3. SiO_2–SiC–C–gas
4. Si–SiO_2–C–gas

Consider the equilibria between two condensed phases and the gas phase.

13.4.1.1 The Equilibrium Si–SiO_2–Gas Phase

For the reaction

$$\mathrm{Si}_{(s)} + \mathrm{O}_{2(g)} = \mathrm{SiO}_{2(s)} \tag{i}$$

$$\Delta G^{\circ}_{(\mathrm{i})1273\,\mathrm{K}} = -683{,}400\ \mathrm{J}$$

$$= -RT \ln \frac{1}{p_{O_2}}$$

$$= 8.3144 \times 1273 \times 2.303 \log p_{O_2}$$

or $\log p_{O_2} = -28.04$. Thus, at 1273 K, the equilibrium between Si and SiO_2 requires $\log p_{O_2} = -28.04$, and this equilibrium, which is drawn as the vertical line *AB* in

Figure 13.5a, is independent of a_C. At lower values of p_{O_2} (the abscissa), Si is stable relative to SiO_2 and, at higher values, SiO_2 is stable relative to Si.

13.4.1.2 The Equilibrium Si–SiC–Gas Phase

For the reaction

$$Si_{(s)} + C_{(s)} = SiC_{(s)} \tag{ii}$$

$$\Delta G^{\circ}_{(ii)1273\,K} = -63{,}300\ J$$

$$= -RT \ln \frac{1}{a_C}$$

$$= 8.3144 \times 1273 \times 2.303 \log a_C$$

or $\log a_C = -2.60$. Thus, at 1273 K, the equilibrium between Si and SiC requires $\log a_C = -2.60$, and this equilibrium, which is drawn as the horizontal line *CD* in Figure 13.5a, is independent of p_{O_2}. At lower values of a_C, Si is stable relative to SiC and, at higher values of a_C, SiC is stable relative to Si.

13.4.1.3 The Equilibrium SiC–SiO_2–Gas Phase

Lines *AB* and *CD* intersect at the point $P\left(\log p_{O_2} = -28.04,\quad \log a_C = -2.60\right)$, which is the unique state at which the three solid phases Si, SiC, and SiO_2 are in equilibrium with one another and with a gas phase at 1273 K. The variation of $\log a_C$ with $\log p_{O_2}$ required for the equilibrium SiC–SiO_2 must pass through this point. Combination of Equations (i) and (ii) gives

$$SiC_{(s)} + O_{2(g)} = SiO_{2(s)} + C_{(s)} \tag{iii}$$

for which

$$\Delta G^{\circ}_{(iii)1273\,K} = -620{,}100\ J$$

$$= -8.3144 \times 1273 \times 2.303 \log \frac{a_C}{p_{O_2}}$$

or

$$\log a_C = \log p_{O_2} + 25.44$$

which is drawn as line *EF* in Figure 13.5a. In states above this line, SiC is stable relative to SiO_2, and below the line, SiO_2 is stable relative to SiC.

13.4.1.4 The Equilibrium SiC–C–Gas Phase

The equilibrium between solid SiC and solid C is a phase equilibrium that exists only at $a_C = 1$, or $\log a_C = 0$. Thus, in Figure 13.5a, the equilibrium between SiC and C exists along the $\log a_C = 0$ line, at values of $\log p_{O_2}$ less than −25.44, the point of intersection of line *EF* with the $\log a_C = 0$ line.

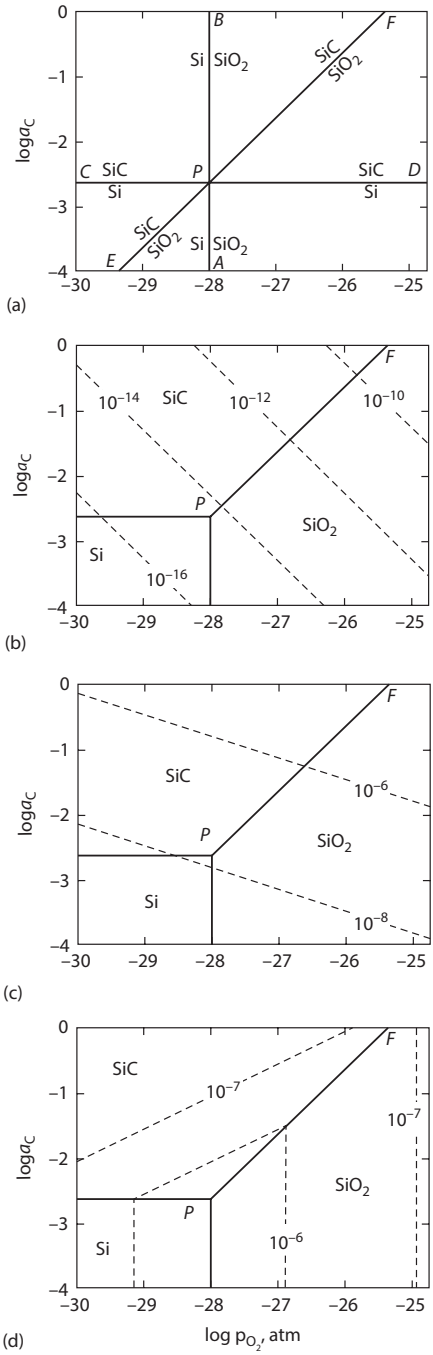

FIGURE 13.5 (a) Construction of the phase stability diagram for the system Si–C–O at 1273 K. (b) CO_2 isobars in the phase stability diagram for Si–C–O at 1273 K. (c) CO isobars in the phase stability diagram for Si–C–O at 1273 K. (d) SiO isobars in the phase stability diagram for Si–C–O at 1273 K.

13.4.1.5 The Equilibrium SiO_2–C–Gas Phase

As with the equilibrium between SiC and C, the phase equilibrium between SiO_2 and C requires $a_C = 1$ and thus occurs along the $\log a_C = 0$ line at values of $\log p_{O_2}$ greater than −25.44.

13.4.1.6 The Equilibrium Si–C–Gas Phase

The standard Gibbs free energy change at 1273 K for the reaction

$$Si_{(s)} + C_{(s)} = SiC_{(s)}$$

is $\Delta G^{\circ}_{(ii)1273\,K} = -63,300$ J, which, being negative, indicates that Si and C spontaneously react with one another to form SiC until either the C or the Si is consumed. Thus, Si and C cannot be in equilibrium with one another. If the molar ratio Si/C in the system is greater than 1, the C is consumed by the reaction and equilibrium between the product SiC and the remaining Si is attained, and if the ratio is less than one, the Si is consumed by the reaction and an equilibrium is attained between the SiC produced and the remaining C.

The solid carbon phase exists only along the $\log a_C = 0$ line, and thus, Figure 13.5a contains fields of stability of the single phases Si, SiO_2, and SiC. Consequently, of the six lines in the diagram radiating from point *P*, three represent *stable equilibria* involving two condensed phases and a gas phase, and three represent *metastable equilibria* involving two condensed phases and a gas phase. The problem is how to distinguish between the two types of equilibria. It is a property of such diagrams that the lines of metastable and stable equilibria radiate alternatively from a point such as *P* (see, for example, Figures 7.7 and 7.8a). Thus, one set of lines is *PA-PC-PF* and the other is *PE-PB-PD*. In Figure 13.5a, Si is stable relative to SiO_2 in states to the left of *PA* and is stable relative to SiC in states below *PC*. Thus, the line *PE* represents the *metastable* equilibrium between SiC and SiO_2. This identifies the stable equilibrium lines as being *PA-PC-PF* and, as shown in Figure 13.5b, defines the fields of stability of a single condensed phase with a gas phase, which, at constant temperature, have 2 degrees of freedom. These fields meet at lines that represent the equilibrium between two condensed phases and a gas phase (which, at constant temperature, have one degree of freedom), and the lines meet at points representing equilibrium among three condensed phases and a gas phase. The point *P* is the state of equilibrium of Si, SiC, SiO_2, and a gas phase, and the point *F* is the state of equilibrium of SiC, SiO_2, C, and a gas phase.

The partial pressures of CO and CO_2 are determined by the activities of carbon and oxygen in the system, and the iso-p_{CO_2} and iso-p_{CO} lines can be placed on the stability diagram as follows.

For the reaction

$$C_{(s)} + O_{2(g)} = CO_{2(g)} \tag{iv}$$

$$\Delta G^{\circ}_{(iv)1273\,K} = -395,200\ \text{J} = -8.3144 \times 1273 \times 2.303 \log \frac{p_{CO_2}}{a_C p_{O_2}}$$

Therefore,

$$16.21 = \log p_{CO_2} - \log a_C - \log p_{O_2}$$

or

$$\log a_C = -\log p_{O_2} - 16.21 + \log p_{CO_2}$$

Thus, as shown in Figure 13.5b, the CO_2 isobars in the phase stability diagram are lines with slopes of −1.

Similarly, for

$$C_{(s)} + \frac{1}{2}O_{2(g)} = CO_{(g)} \tag{v}$$

$$\Delta G^{\circ}_{(v)1273\,K} = -223,300\ \text{J} = -8.3144 \times 1273 \times 2.303 \log \frac{p_{CO}}{a_C p_{O_2}^{1/2}}$$

or

$$\log a_C = -\frac{1}{2}\log p_{O_2} - 9.16 - \log p_{CO}$$

and, as shown in Figure 13.5c, the CO isobars are lines with slopes of −½.

The gaseous species SiO also occurs in the system Si–C–O, and SiO isobars can be drawn on the stability diagram. Since the partial pressure of SiO is determined by the activity of Si and the partial pressure of oxygen, the individual single condensed-phase stability fields have to be considered separately, and each equilibrium must involve the condensed phase of interest, SiO gas, and C and/or O_2. In the field of stability of Si, the equilibrium is

$$Si_{(s)} + \frac{1}{2}O_{2(g)} = SiO_{(g)} \tag{vi}$$

for which

$$\Delta G^{\circ}_{(vi)1273\,K} = -209,200\ \text{J} = -8.3144 \times 1273 \times 2.303 \log \frac{p_{SiO}}{p_{O_2}^{1/2}}$$

or

$$\log p_{SiO} = \frac{1}{2}\log p_{O_2} + 8.59$$

Thus, as shown in Figure 13.5d, the SiO isobars in the stability field of Si are vertical lines, and p_{SiO} increases with increasing p_{O_2}.

In the SiO_2 field, the equilibrium is

$$SiO_{2(s)} = SiO_{(g)} + \frac{1}{2}O_{2(g)} \tag{vii}$$

for which combination of $\Delta G^{\circ}_{(vi)1273\,K}$ and $\Delta G^{\circ}_{(i)1273\,K}$ gives

$$\Delta G^{\circ}_{(vii)1273\,K} = -474,200\ \text{J} = -8.3144 \times 1273 \times 2.303 \log\left(p_{SiO}\, p_{O_2}^{1/2}\right)$$

which gives

$$\log p_{SiO} = -\frac{1}{2}\log p_{O_2} - 19.45$$

Thus, as shown in Figure 13.5d, the SiO isobars in the field of stability of SiO_2 are vertical lines and p_{SiO} decreases with increasing p_{O_2}.

In the field of stability of SiC, the equilibrium is

$$SiC_{(s)} + \frac{1}{2}O_{2(g)} = SiO_{(g)} + C_{(s)} \qquad \text{(viii)}$$

for which combination of $\Delta G^{\circ}_{(vi)1273\,K}$ and $\Delta G^{\circ}_{(ii)1273\,K}$ gives

$$\Delta G^{\circ}_{(viii)1273\,K} = -145,900\ \text{J} = -8.3144 \times 1273 \times 2.303 \log \frac{p_{SiO} \cdot a_C}{p_{O_2}^{1/2}}$$

or

$$\log a_C = \frac{1}{2}\log p_{O_2} - \log p_{SiO} + 5.99$$

Thus, as shown in Figure 13.5d, the SiO isobars in the field of stability of SiC are lines with slopes of ½.

13.4.2 Plots of $\log p_{CO} = \log p_{CO_2}$ Stability Diagram for Si-C-O

At any temperature, the maximum value of p_{SiO} occurs in states in which Si and SiO_2 are in equilibrium with a gas phase. The activities of carbon and oxygen used as the variables in the construction of Figure 13.5 are determined by the individual values of p_{CO} and p_{CO_2}, which establish the equilibria

$$CO + \frac{1}{2}O_2 = CO_2$$

and

$$C + CO_2 = 2CO$$

and thus, the phase stability diagram can be constructed using p_{CO} and p_{CO_2} as the variables. The equilibrium corresponding to Equation (i) is

$$Si_{(s)} + 2CO_{2(g)} = SiO_{2(s)} + 2CO_{(g)} \qquad \text{(ix)}$$

Combination of the Gibbs free energy changes for the reactions given by Equations (i), (iv), and (v) gives

$$\Delta G^{\circ}_{(\text{ix})1273\,\text{K}} = -339{,}600\ \text{J} = -8.3144 \times 1273 \times 2.303 \log \frac{p^2_{\text{CO}}}{p^2_{\text{CO}_2}}$$

which gives

$$\log p_{\text{CO}} = \log p_{\text{CO}_2} + 6.97$$

This is drawn as the line *AB* in Figure 13.6a (and corresponds to the line *AB* in Figure 13.5a). Above the line, Si is stable relative to SiO_2, and below the line, SiO_2 is stable relative to Si. The equivalent of the equilibrium given by Equation (ii) is

$$\text{Si}_{(s)} + 2\text{CO}_{(g)} = \text{SiC}_{(s)} + \text{CO}_{2(g)} \tag{x}$$

for which

$$\Delta G^{\circ}_{(\text{x})1273\,\text{K}} = -11{,}900\ \text{J} = -8.3144 \times 1273 \times 2.303 \log \frac{p_{\text{CO}_2}}{p^2_{\text{CO}}}$$

or

$$\log p_{\text{CO}} = \frac{1}{2} \log p_{\text{CO}_2} - 0.24$$

This is drawn as line *CD* in Figure 13.6a. Above the line, SiC is stable relative to Si, and below the line, Si is stable relative to SiC. The lines *AB* and *CD* intersect at *P*, which is thus the invariant point at which Si, SiC, SiO_2, and a gas phase are in equilibrium. The equivalent of the equilibrium given by Equation (iii) is

$$\text{SiC}_{(s)} + 3\text{CO}_{2(g)} = \text{SiO}_{2(s)} + 4\text{CO}_{(g)} \tag{xi}$$

for which

$$\Delta G^{\circ}_{(\text{xi})1273\,\text{K}} = -327{,}700\ \text{J} = -8.3144 \times 1273 \times 2.303 \log \frac{p^4_{\text{CO}}}{p^3_{\text{CO}_2}}$$

or

$$\log p_{\text{CO}} = 0.75 \log p_{\text{CO}_2} + 3.36$$

This is drawn as the line *EF* in Figure 13.6a. SiC is stable relative to SiO_2 above the line, and SiO_2 is stable relative to SiC below the line.

The *carbon line*, which is equivalent to the log $a_C = 0$ line in Figure 13.5, is obtained from

$$\text{C}_{(s)} + \text{CO}_{2(g)} = 2\text{CO}_{(g)} \tag{xii}$$

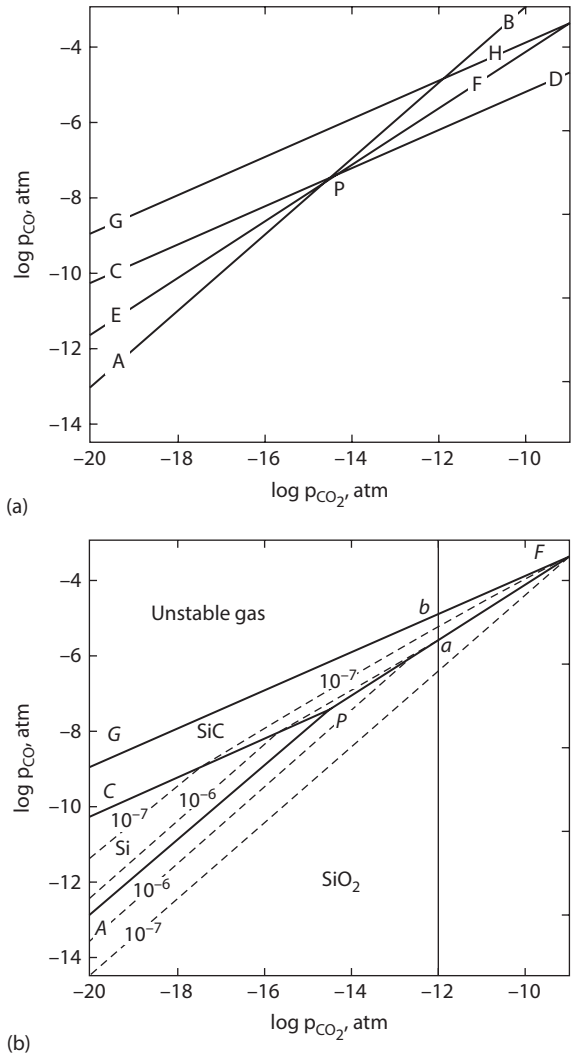

FIGURE 13.6 (a) Construction of the phase stability diagram for the system Si–C–O at 1273 K. (b) The phase stability diagram for the system Si–C–O at 1273 K showing the 10^{-6} and 10^{-7} atm SiO isobars.

for which

$$\Delta G^{\circ}_{(\text{xii})1273\,\text{K}} = -51,400\ \text{J} = -8.3144 \times 1273 \times 2.303 \log \frac{p^2_{\text{CO}}}{p_{\text{CO}_2}}$$

which gives

$$\log p_{\text{CO}} = \frac{1}{2} \log p_{\text{CO}_2} - 1.05$$

This is drawn as the line *GH* in Figure 13.6a.

The phase stability fields, identified in the same manner as was used in Figure 13.5a, are shown in Figure 13.6b. The Si phase field is bounded by *APC*, the SiC phase field is bounded by *CPFG*, and the SiO_2 phase field lies below the line *APF*. The region above *GF* is an unstable gas. Any gas in this region precipitates carbon according to

$$2CO_{(g)} \rightarrow CO_{2(g)} + C_{(s)}$$

until, thereby, the ratio p_{CO_2}/p_{CO} is required for equilibrium with C at $a_C = 1$ at 1273 K. The isobars for SiO gas are calculated as follows. In the field of stability of Si, the equivalent of the equilibrium given by Equation (vi) is

$$Si_{(s)} + CO_{2(g)} = SiO_{(g)} + CO_{(g)} \qquad \text{(xiii)}$$

for which

$$\Delta G^{\circ}_{(\text{xiii})1273\,\text{K}} = -37{,}300\ \text{J} = -8.3144 \times 1273 \times 2.303 \log \frac{p_{SiO}\, p_{CO}}{p_{CO_2}}$$

which gives

$$\log p_{CO} = \log p_{CO_2} + 1.53 - \log p_{SiO}$$

In the field of stability of SiO_2, the equivalent of the equilibrium given by Equation (vii) is

$$SiO_{2(s)} + CO_{(g)} = SiO_{(g)} + CO_{2(g)} \qquad \text{(xiv)}$$

for which

$$\Delta G^{\circ}_{(\text{xiv})1273\,\text{K}} = 302{,}300\ \text{J} = -8.3144 \times 1273 \times 2.303 \log \frac{p_{CO_2}\, p_{SiO}}{p_{CO}}$$

which gives

$$\log p_{CO} = \log p_{CO_2} + 12.40 + \log p_{SiO}$$

In the field of stability of SiC, the equilibrium equivalent to that given by Equation (viii) is

$$SiC_{(s)} + 2CO_{2(g)} = SiO_{(g)} + 3CO_{(g)} \qquad \text{(xv)}$$

for which

$$\Delta G^{\circ}_{(\text{xv})1273\,\text{K}} = -25{,}400\ \text{J} = -8.3144 \times 1273 \times 2.303 \log \frac{p^3_{CO}\, p_{SiO}}{p^2_{CO_2}}$$

which gives

$$\log p_{CO} = \frac{2}{3} \log p_{CO_2} - 0.35 + {}^{1} \log p$$

The 10^{-7} and 10^{-6} atm SiO isobars are shown in Figure 13.6b, and a comparison of Figures 13.5 and 13.6 shows that the latter is produced by distorting the former such that the CO isobars are horizontal lines and the CO_2 isobars are vertical lines. The points *P* and *F* in Figure 13.6b correspond to the points *P* and *F* in Figure 13.5. The full phase stability diagram is three-dimensional, with the axes being temperature and the activities of two components (a_C and p_{O_2}) or the partial pressures of CO and CO_2. Two-dimensional phase stability diagrams which show the influence of temperature can be drawn if the activity of one component is held constant.

13.4.3 Plots of $\log p_{CO}$ versus $\frac{1}{T}$ for Si-C-O

Consider the phase stability diagram using p_{CO} and $1/T$ as coordinates and drawn for a constant partial pressure of CO_2 of 10^{-12} atm. The diagram is drawn for temperatures in the range 1250–1990 K, and thus, since the melting temperature of Si is 1683 K, equilibria involving both solid and liquid Si will have to be considered. In Figure 13.7a, the vertical line at $T = 1683$ K represents the melting temperature of Si, and thus, liquid Si occurs to the left of the line and solid Si occurs to the right.

13.4.3.1 The Equilibrium $Si_{(s)}$–SiO_2–Gas Phase

The equilibrium is

$$Si_{(s)} + 2CO_{2(g)} = SiO_{2(s)} + 2CO_{(g)} \tag{xvi}$$

for which

$$\Delta G^{\circ}_{(xvi)} = -337{,}300 - 0.02T \text{ J}$$

Thus,

$$\frac{-337{,}300}{8.3144 \times 2.303T} - \frac{0.02}{8.3144 \times 2.303} = -\log \frac{p_{CO}^2}{p_{CO_2}^2}$$

which can be rearranged to give

$$\log p_{CO} = \frac{8807}{T} + 5.22 \times 10^{-4} + \log p_{CO_2}$$

This line, with $\log p_{CO_2} = -12$, is drawn as *AB* in Figure 13.7a. Silicon is stable relative to SiO_2 above the line, and SiO_2 is stable relative to Si below the line.

The equilibrium $Si_{(l)}$–SiO_2–gas phase: The equilibrium is

$$Si_{(l)} + 2CO_{2(g)} = SiO_{2(s)} + 2CO_{(g)} \tag{xvii}$$

for which

$$\Delta G^{\circ}_{(xvii)} = -387{,}900 + 30.18T \text{ J}$$

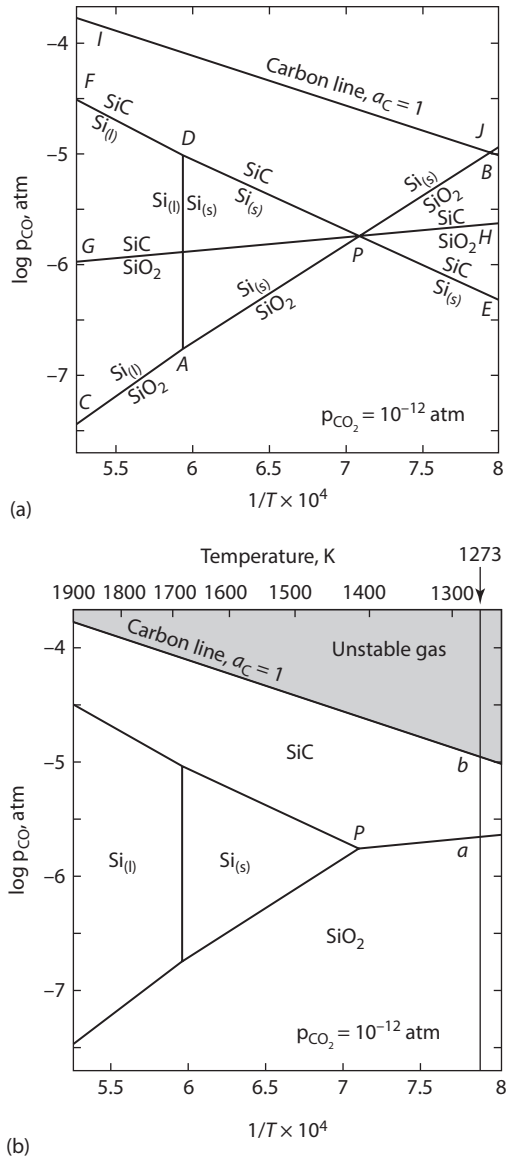

FIGURE 13.7 (a) Construction of the phase stability diagram for the system Si–C–O using $\log p_{CO}$ and $1/T$ as coordinates at a constant partial pressure of CO_2 of 10^{-12} atm. (b) The phase stability diagram for the system Si–C–O at a constant partial pressure of $CO_2 = 10^{-12}$ atm.

Thus,

$$\frac{-387,900}{8.3144 \times 2.303T} + \frac{30.18}{8.3144 \times 2.303} = -\log \frac{p_{CO}^2}{p_{CO_2}^2}$$

which gives

$$\log p_{CO} = \frac{10{,}130}{T} - 0.788 + \log p_{CO_2}$$

With $p_{CO_2} = 10^{-12}$ atm, this gives line *CA* in Figure 13.7a. Liquid Si is stable relative to SiO_2 above the line, and SiO_2 is stable relative to liquid Si below the line.

13.4.3.2 The Equilibrium $Si_{(s)}$–SiC–Gas Phase

The equilibrium is

$$Si_{(s)} + 2CO_{(g)} = SiC_{(s)} + CO_{2(g)} \qquad \text{(xviii)}$$

for which

$$\Delta G^{\circ}_{(\text{xviii})} = -243{,}750 + 182.11T \text{ J}$$

which yields

$$\log p_{CO} = -\frac{6364}{T} + 4.76 + \frac{1}{2}\log p_{CO_2}$$

With $\log p_{CO_2} = -12$, this gives line *DE* in Figure 13.7a. SiC is stable relative to solid Si above the line, and Si is stable relative to SiC below the line.

13.4.3.3 The Equilibrium $Si_{(l)}$–SiC–Gas Phase

The equilibrium is

$$Si_{(l)} + 2CO_{(g)} = SiC_{(s)} + CO_{2(g)} \qquad \text{(xix)}$$

for which

$$\Delta G^{\circ}_{(\text{xix})} = -293{,}300 + 211.5T \text{ J}$$

This gives

$$\log p_{CO} = -\frac{7659}{T} + 5.52 + \frac{1}{2}\log p_{CO_2}$$

which, with $\log p_{CO_2} = -12$, gives line *FD* in Figure 13.7a. Liquid Si is stable with respect to SiC below the line, and SiC is stable with respect to Si above the line.

13.4.3.4 The Equilibrium SiC–SiO_2–Gas Phase

The equilibrium is

$$SiC_{(s)} + 3CO_{2(g)} = SiO_{2(s)} + 4CO_{(g)} \qquad \text{(xx)}$$

which gives

$$\log p_{CO} = \frac{1221}{T} + 2.38 + 0.75\log p_{CO_2}$$

This is drawn, with $\log p_{CO_2} = -12$, as line *GH* in Figure 13.7a. SiC is stable relative to SiO_2 above the line, and SiO_2 is stable relative to SiC below the line.

The carbon line, at which $a_C = 1$, is determined by the equilibrium

$$C_{(s)} + CO_{2(g)} = 2CO_{(g)}$$

for which

$$\Delta G^\circ = 170,700 - 174.5T \text{ J}$$

which gives

$$\log p_{CO} = -\frac{4457}{T} + 4.55 + \frac{1}{2}\log p_{CO_2}$$

With $p_{CO_2} = 10^{-12}$ atm, this gives line *IJ* in Figure 13.7a. States above this line represent unstable gas. The stability fields are identified as follows:

1. In the area *APD*, solid silicon is stable with respect to SiO_2 and SiC, and thus, this area is the field of stability of solid Si.
2. In the areas *FDAC*, liquid silicon is stable with respect to SiC and SiO_2, and thus, this area is the field of stability of liquid Si.
3. In the area *FDPHJI*, SiC is stable with respect to Si and SiO_2, and thus, this area is the field of stability of SiC.
4. Below the line *CAPH*, SiO_2 is stable with respect to Si and SiC, and thus, this is the field of stability of SiO_2

These fields of stability are shown in Figure 13.7b. The phase stability diagram shows that, with $p_{CO_2} = 10^{-12}$ atm, 1410 K (the point *P*) is the minimum temperature at which silicon is stable, and that, with increasing temperature, the field of stability of silicon widens at the expense of SiC and SiO_2. The slopes of the lines in Figure 13.7 are related to the standard enthalpy changes for the equilibrium reactions; for example, the slope of the line dividing the solid Si and the SiO_2 fields (the line *AB* in Figure 13.7a) is obtained as $-\left(\Delta H^\circ/(2.303 \times 2 \times R)\right) = 337,300/\left(2.303 \times 2 \times R\right) = 8807$ for the reaction given by Equation (xvi). The points *a* and *b* on the 10^{-12} atm CO_2 isobar in Figure 13.6b correspond with the points *a* and *b* on the 1273 K isotherm in Figure 13.7b.

13.5 BINARY SYSTEMS CONTAINING COMPOUNDS

The phase relationships in a two-component system can be represented on an isobaric phase diagram using temperature and composition as coordinates, and these are the phase diagrams often encountered in materials science (see Chapter 10). If the two components react with one another to form compounds or intermetallic phases, then, in such systems, *chemical reaction equilibria* and *phase equilibria are* synonymous.

Consider the binary system *A–B*, the phase diagram for which is shown in Figure 13.8. The negative departures from ideality in the solid state are sufficiently

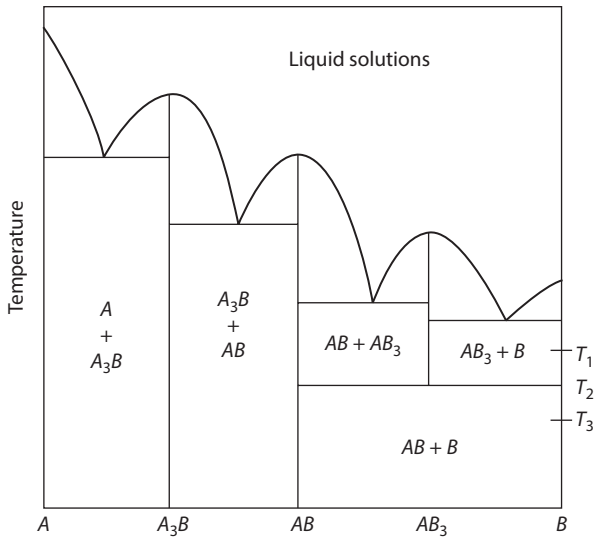

FIGURE 13.8 The phase diagram for the system *A*–*B* in which three stoichiometric compounds are formed.

large that stoichiometric compounds following the law of definite proportions are formed, with there being negligible solubility of *A* in *B*, or *B* in *A*, and negligible range of nonstoichiometry in the compounds AB_3, *AB*, and A_3B. Such compounds are called *Daltinides* (*after* John Dalton, 1766–1844). The system contains the equilibria

$$3A + B = A_3B$$

$$A + B = AB,$$

$$A + 3B = AB_3$$

In this analysis we assume that the total pressure of the system is due to the vapor pressure of the components, that is, the system is at very low total pressure. If one of the components (*B*) is appreciably *volatile* and the other (*A*) is not, then, the thermodynamics of the system can be determined from knowledge of the variation of p_B with composition. The variation of p_B with composition at the temperature T_1 is shown in Figure 13.9. In the range of composition between *B* and AB_3, virtually pure *B* exists in equilibrium with AB_3 (saturated with *B*), and, since pure *B* exists, the pressure exerted by the system is p_B^0, the saturated vapor pressure of *B* at the temperature T_1. In the range of composition between *AB* (saturated with *B*) and AB_3 (saturated with *A*), the constant pressure exerted by the system is p'_B, in the range between A_3B (saturated with *B*) and *AB* (saturated with *A*) it is p''_B, and in the range between *A* (saturated with *B*) and A_3B (saturated with *A*) it is p'''_B. In each of

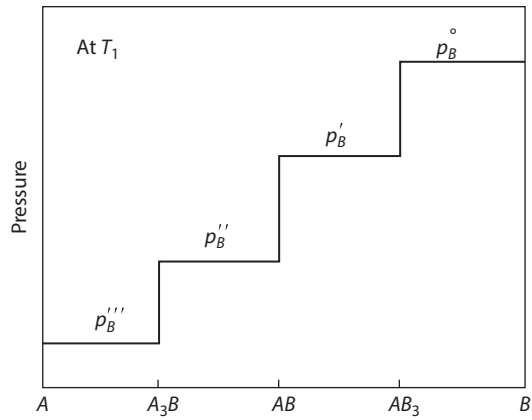

FIGURE 13.9 The variation, with composition, of the vapor pressure of component B in the system shown in Figure 13.8 at the temperature T_1.

these ranges of composition, the two-component, three-phase equilibrium has one degree of freedom, which is used when T_1 is specified, which requires that $P = p_B$ within these ranges at fixed temperature. The activity of B in the system, defined as p_B/p_B°, is thus

$$\frac{p_B^\circ}{p_B^\circ} = 1 \text{ in the range } AB_3 - B$$

$$\frac{p_B'}{p_B^\circ} \text{ in the range } AB - AB_3$$

$$\frac{p_B''}{p_B^\circ} \text{ in the range } A_3B - AB$$

$$\frac{p_B'''}{p_B^\circ} \text{ in the range } A - A_3B$$

Thus, since $\Delta\bar{G}_B^M = \bar{G}_B - G_B^\circ = RT \ln p_B / p_B^\circ$, the Gibbs free energy–composition diagram at the temperature T_1 is as shown in Figure 13.10. Since Figure 13.10 is drawn for 1 mole of the system, then

$hb = \Delta G_{(i)} = \Delta G$ for the reaction

0.75 mole A + 0.25 mole $B = A_{0.75}B_{0.25}$ or 0.25 moles of A_3B

$gc = \Delta G_{(ii)} = \Delta G$ for the reaction

0.5 mole A + 0.5 mole $B = A_{0.5}B_{0.5}$ or 0.5 moles of AB

$fd = \Delta G_{(iii)} = \Delta G$ for the reaction

0.25 mole A + 0.75 mole $B = A_{0.25}B_{0.75}$ or 0.25 moles of AB_3

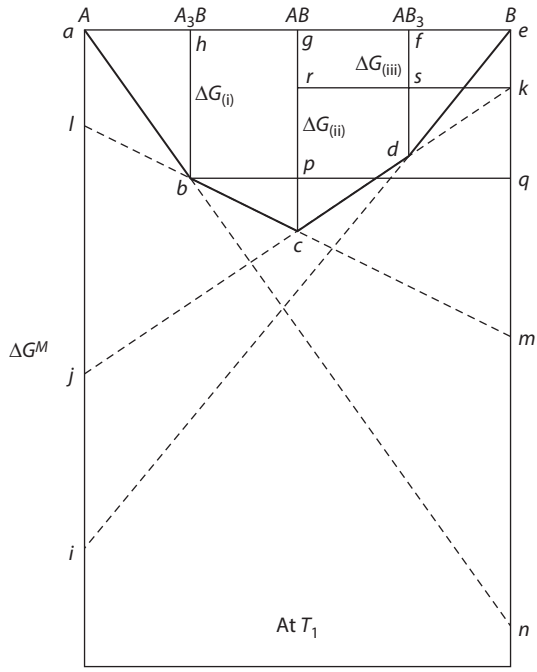

FIGURE 13.10 The molar Gibbs free energies at T_1 in the system shown in Figure 13.8.

These three changes in Gibbs free energy can be determined geometrically as follows:

$$ek = \Delta\overline{G}'^{M}_{B} = RT \ln \frac{p'_B}{p^\circ_B}$$

$$em = \Delta\overline{G}''^{M}_{B} = RT \ln \frac{p''_B}{p^\circ_B}$$

and

$$en = \Delta\overline{G}'''^{M}_{B} = RT \ln \frac{p'''_B}{p^\circ_B}$$

Thus, from consideration of the similar triangles *ahb* and *aen*,

$$\frac{\Delta G_{(i)}}{\Delta\overline{G}'''^{M}_{B}} = \frac{1}{4}$$

and hence,

$$\Delta G_{(\mathrm{i})} = \frac{1}{4}\Delta\overline{G}'''^{M}_{B}$$

Consideration of the similar triangles *bpc* and *bqm* gives

$$\frac{pc}{qm} = \frac{bp}{bq} = \frac{1}{3}$$

But

$$pc = gc - gp = \Delta G_{(\mathrm{ii})} - \Delta G_{(\mathrm{i})}$$

and

$$qm = em - eq = \Delta \bar{G}_B''^M - \Delta G_{(\mathrm{i})}$$

Thus,

$$3\left(\Delta G_{(\mathrm{ii})} - \Delta G_{(\mathrm{i})}\right) = \left(\Delta \bar{G}_B''^M - \Delta G_{(\mathrm{i})}\right)$$

or

$$\Delta G_{(\mathrm{ii})} = \frac{1}{3}\Delta \bar{G}_B''^M + \frac{2}{3}\Delta G_{(\mathrm{i})}$$

Consideration of the similar triangles *rck* and *sdk* gives

$$\frac{rc}{sd} = \frac{rk}{sk} = 2$$

But

$$rc = gc - gr = \Delta G_{(\mathrm{ii})} - \Delta \bar{G}_B'^M$$

and

$$sd = fd - fs = \Delta G_{(\mathrm{iii})} - \Delta \bar{G}_B'^M$$

such that

$$\Delta G_{(\mathrm{iii})} = \frac{1}{2}\Delta G_{(\mathrm{ii})} + \frac{1}{2}\Delta \bar{G}_B'^M$$

Thus,

$$\Delta G_{(\mathrm{i})} = \frac{1}{4} RT \ln \frac{p_B'''}{p_B^\circ}$$

$$\Delta G_{(\mathrm{ii})} = \frac{1}{3} RT \ln \frac{p_B''}{p_B^\circ} + \frac{1}{6} RT \ln \frac{p_B'''}{p_B^\circ}$$

and

$$\Delta G_{(\mathrm{iii})} = \frac{1}{6} RT \ln \frac{p_B''}{p_B^\circ} + \frac{1}{12} RT \ln \frac{p_B'''}{p_B^\circ} + \frac{1}{2} RT \ln \frac{p_B'}{p_B^\circ}$$

and hence for

$$3A + B = A_3B \qquad \Delta G^{\circ}_{(\mathrm{i})} = 4\Delta G_{(i)}$$

$$A + B = AB \quad \Delta G^{\circ}_{(\mathrm{ii})} = 2\Delta G_{(\mathrm{ii})} = \frac{2}{3}\Delta \bar{G}''^{M}_{B} + \frac{4}{3}\Delta G_{(i)}$$

$$A + 3B = AB_3 \quad \Delta G^{\circ}_{(\mathrm{iii})} = 4\Delta G_{(\mathrm{iii})} = 2\Delta G_{(\mathrm{ii})} + 2\Delta \bar{G}'^{M}_{B}$$

Figure 13.8 shows that, below the temperature T_2, the compound AB_3 is unstable with respect to AB and B, with the invariant equilibrium

$$AB_{(s)} + 2B_{(s)} = AB_{3(s)}$$

occurring at the temperature T_2. The standard Gibbs free energy change for this reaction is calculated as $\Delta G^{\circ}_{(\mathrm{iii})} - \Delta G^{\circ}_{(\mathrm{ii})}$, which equals $2RT \ln p'_B/p^{\circ}_B$. Thus, at $T > T_2$,

$$\Delta G^{\circ}_{(\mathrm{iii})} - \Delta G^{\circ}_{(\mathrm{ii})} < 0 \quad \text{and} \quad p'_B < p^{\circ}_B$$

at T_2,

$$\Delta G^{\circ}_{(\mathrm{iii})} - \Delta G^{\circ}_{(\mathrm{ii})} = 0 \quad \text{and} \quad p'_B = p^{\circ}_B$$

and at $T < T_2$,

$$\Delta G^{\circ}_{(\mathrm{iii})} - \Delta G^{\circ}_{(\mathrm{ii})} > 0 \quad \text{and} \quad p'_B > p^{\circ}_B$$

The variations of the Gibbs free energy of mixing with temperature at T_2 and T_3 are shown in Figure 13.11a and b, respectively, which illustrates graphically that at T_2,

$$\Delta G_{(\mathrm{iii})} = \frac{1}{2}\Delta G_{(\mathrm{ii})}$$

and at T_3,

$$\left|\Delta G_{(\mathrm{iii})}\right| < \left|\frac{1}{2}\Delta G_{(\mathrm{ii})}\right|$$

such that, in the range of composition B–AB, at temperatures below T_2, the system occurring as either $AB + AB_3$ or $AB_3 + B$ is metastable with respect to its occurrence as $AB + B$.

In considering the thermodynamic properties of a system such as that shown in Figure 13.8, two approaches can be made:

1. Consider the compound AB_3 to be an ordered solid solution of A and B in the molar ratio 1/3. Then, in Figure 13.10,

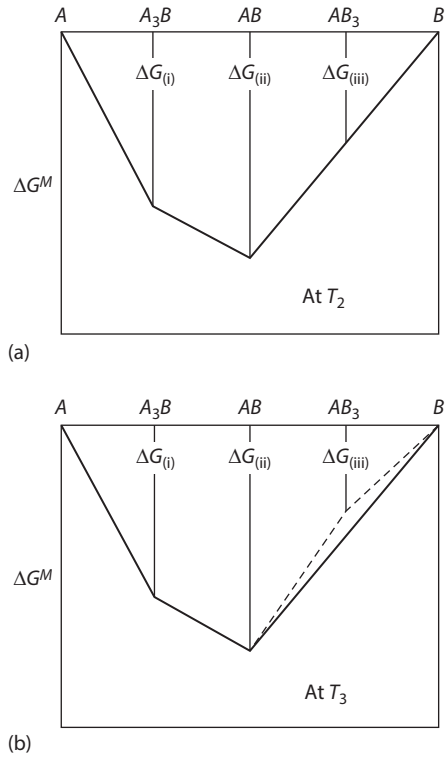

FIGURE 13.11 (a) The Gibbs free energies of mixing in the system shown in Figure 13.8 at the temperature T_2. (b) The Gibbs free energies of mixing in the system shown in Figure 13.8 at the temperature T_3.

$$fd = \Delta G^M = RT\left(X_A \ln a_A + X_B \ln a_B\right) = RT\left(0.25 \ln a_A + 0.75 \ln a_B\right)$$
$$= RT \ln a_A^{0.25} a_B^{0.75} \tag{i}$$

2. Consider the compound AB_3 to form as the product of the reaction

$$A + 3B = AB_3$$

for which the change in the standard Gibbs free energy is $\Delta G^\circ_{(\text{iii})}$. Then,

$$fd = 0.25\Delta G^\circ_{(\text{iii})} = -0.25RT \ln K_{(\text{iii})} = -RT \ln\left(\frac{a_{AB_3}}{a_A a_B^3}\right)^{0.25}$$
$$= RT \ln\left(\frac{a_A^{0.25} a_B^{0.75}}{a_{AB_3}^{0.25}}\right) \tag{ii}$$

Since AB_3 is a *line compound* (i.e., it has a negligible range of nonstoichiometry), it exists at a fixed composition and hence exists in a fixed state. If this fixed state is chosen as being the standard state, in which $a_{AB_3} = 1$, then Equation (ii) becomes

$$fd = 0.25\Delta G^{\circ}_{(\text{iii})} = RT \ln a_A^{0.25} a_B^{0.75}$$

which is identical with Equation (i). In both Equations (i) and (ii), the standard states of A and B are the pure solid elements at the temperature T. The variations of the activities of A and B in the compound AB_3 are limited by the separation of B and AB; for example, when AB_3 is in equilibrium with B, $a_B = 1$, and thus, $a_A = \exp\left(4\Delta G_{(\text{iii})}/RT\right) = \exp\left(\Delta G^{\circ}_{(\text{iii})}/RT\right)$ ($RT \ln a_A = ai$ in Figure 13.10). If the activity of B is decreased to a value less than unity, then AB_3 is no longer saturated with B, and the activity of A in the compound increases in accordance with Equation (i). The minimum activity of B in AB_3 is determined by the saturation of AB_3 with A, at which point the compound AB appears. The minimum activity which B may have is obtained from Figure 13.10 as $RT \ln a_B = ek$, and the corresponding maximum activity of A is obtained from $RT \ln a_A = aj$. Nonsaturation of AB_3 with either A or B occurs when the partial pressure of B exerted by the compound lies between the limits p'_B and p°_B. Similar consideration can be made with respect to the compounds AB and A_3B; for example, in Figure 13.10,

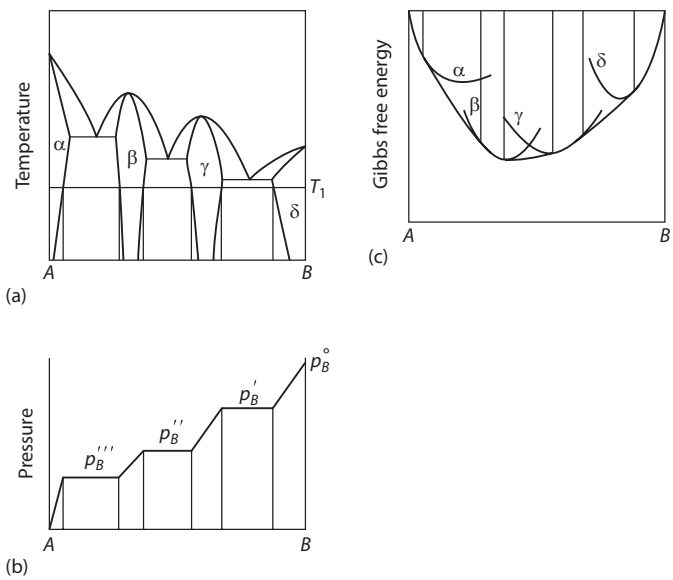

FIGURE 13.12 (a) The phase diagram for the system A–B. (b) The partial vapor pressure of B at the temperature T_1. (c) The molar Gibbs free energies of mixing at the temperature T_1.

$$gc = \Delta G^{\mathrm{M}} = \frac{1}{2}\Delta G^{\circ}_{(\mathrm{ii})} = RT \ln a_A^{0.5} a_B^{0.5}$$

and

$$hb = \Delta G^{\mathrm{M}} = 0.25\Delta G^{\circ}_{(i)} = RT \ln a_A^{0.75} a_B^{0.25}$$

In the preceding discussion, it was assumed that the intermediate phases were line compounds and that there was no solubility of A in B. If A and B are partially soluble in one another and the compounds A_2B and AB_2 (identified as phases β and γ, respectively) have measurable ranges of nonstoichiometry, the phase diagram is as shown in Figure 13.12a. Again, if B is appreciably volatile and A is not, then the variation of vapor pressure with composition at the temperature T_1 is as shown in Figure 13.12b, and the corresponding variation of the Gibbs free energy is as shown in Figure 13.12c.

13.5.1 Example Problem: The Binary Ga–GaP System

The phase diagram for the system Ga–GaP is shown in Figure 13.13. Calculate the partial pressure of phosphorus vapor, p_{P_2}, exerted by the GaP liquidus melt at 1273 K.

The standard Gibbs free energy change for the reaction

$$\mathrm{Ga}_{(l)} + \frac{1}{2}\mathrm{P}_{2(g)} = \mathrm{GaP}_{(s)}$$

is

$$\Delta G^{\circ} = -178{,}800 + 96.2T + 3.1T \ln T - 3.61 \times 10^{-3} T^2 - \frac{1.035 \times 10^5}{T}$$

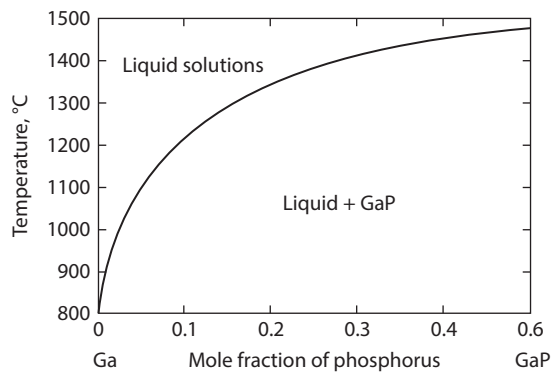

FIGURE 13.13 The phase diagram for the system Ga–GaP.

Solution

At 1273 K,

$$\Delta G^{\circ}_{1273\,\mathrm{K}} = -3.968 \times 10^{4}\ \mathrm{J} = -8.3144 \times 1273 \ln K_{1273\,\mathrm{K}}$$

which gives

$$K_{1273\,\mathrm{K}} = 24.97 = \frac{a_{\mathrm{GaP}}}{a_{\mathrm{Ga}}\, p_{\mathrm{P_2}}^{1/2}}$$

In the preceding expression, a_{Ga} is the activity of Ga in the liquidus melt with respect to liquid Ga as the standard state, and, since the liquidus melt is in equilibrium with pure solid GaP, the activity of GaP, a_{GaP}, is unity. The variation of the liquidus composition with temperature in the range of 1173–1373 K can be expressed as

$$\ln X_{\mathrm{P}} = -\frac{16{,}550}{T} + 9.902$$

which gives the liquidus composition at 1273 K as $X_{\mathrm{P}} = 0.045$. In view of the low solubility of the solute P, it can be assumed that the solvent Ga obeys Raoult's law, in which case the activity of Ga in the liquidus melt is 0.955, and hence the partial pressure of P_2 exerted by the liquidus melt is

$$p_{\mathrm{P_2}} = \left(\frac{1}{24.97 \times 0.955}\right)^{2}$$

$$= 1.76 \times 10^{-3}\ \mathrm{atm}$$

13.6 GRAPHICAL REPRESENTATION OF PHASE EQUILIBRIA

13.6.1 Phase Equilibria in the System Mg–Al–O

Consider the phase equilibria in the system Mg–Al–O at 1073 K. At 1073 K, liquid Mg and Al are completely miscible in one another, and MgO, Al_2O_3, and the *spinel*[1] $MgAl_2O_4$ occur as the products of oxidation of the metallic alloys. The stabilities of the oxides are determined by the activities of Al and Mg in the liquid metallic alloys and by the standard Gibbs free energies of formation of the oxides. For

$$2\mathrm{Al}_{(l)} + \frac{3}{2}\mathrm{O}_{2(g)} = \mathrm{Al_2O_{3(s)}} \qquad \text{(i)}$$

$$\Delta G^{\circ}_{(\mathrm{i}),1073\,\mathrm{K}} = -1.323{,}000\ \mathrm{J} = -RT \ln \frac{a_{\mathrm{Al_2O_3}}}{a_{\mathrm{Al}}^{2}\, p_{\mathrm{O_2}}^{3/2}}$$

[1] A spinel is a cubic oxide with the general formula AB_2O_4, where A is a divalent ion and B is a trivalent ion.

which gives

$$2\log a_{\mathrm{Al}} + 1.5\log p_{\mathrm{O_2}} - \log a_{\mathrm{Al_2O_3}} = -64.39 \tag{ia}$$

For

$$\mathrm{Mg}_{(l)} + \frac{1}{2}\mathrm{O}_{2(g)} = \mathrm{MgO}_{(s)}$$

$$\Delta G^{\circ}_{(\mathrm{ii}),1073\,\mathrm{K}} = -484{,}300\ \mathrm{J} = -RT\ln\frac{a_{\mathrm{MgO}}}{a_{\mathrm{Mg}}p_{\mathrm{O_2}}^{1/2}} \tag{ii}$$

which gives

$$\log p_{\mathrm{O_2}} = -2\log a_{\mathrm{Mg}} + 2\log a_{\mathrm{MgO}} - 47.14 \tag{iia}$$

For

$$\mathrm{Mg}_{(l)} + 2\mathrm{Al}_{(l)} + 2\mathrm{O}_{2(g)} = \mathrm{MgAl_2O_{4(s)}}$$

$$\Delta G^{\circ}_{(\mathrm{iii}),1073\,\mathrm{K}} = -1{,}854{,}000\ \mathrm{J} = -RT\ln\frac{a_{\mathrm{MgAl_2O_4}}}{a_{\mathrm{Mg}}a_{\mathrm{Al}}^{2}p_{\mathrm{O_2}}^{2}} \tag{iii}$$

which gives

$$\log p_{\mathrm{O_2}} = -\frac{1}{2}\left[\log a_{\mathrm{Mg}} + 2\log a_{\mathrm{Al}} - \log a_{\mathrm{MgAl_2O_4}} + 90.24\right] \tag{iiia}$$

Combination of the reactions given by Equations (i), (ii), and (iii) gives

$$\mathrm{MgO}_{(s)} + \mathrm{Al_2O_{3(s)}} = \mathrm{MgAl_2O_{4(s)}} \tag{iv}$$

for which

$$\Delta G^{\circ}_{(\mathrm{iv}),1073\,\mathrm{K}} = -46{,}700\ \mathrm{J} = -RT\ln\frac{a_{\mathrm{MgAl_2O_4}}}{a_{\mathrm{MgO}}a_{\mathrm{Al_2O_3}}}$$

or

$$\log a_{\mathrm{MgO}} + \log a_{\mathrm{Al_2O_3}} - \log a_{\mathrm{MgAl_2O_4}} = -2.273 \tag{iva}$$

The Gibbs free energy of mixing diagram for the system MgO–Al_2O_3 is shown in Figure 13.14. From $\Delta G^{\circ}_{(\mathrm{iv}),1073\,\mathrm{K}}$, the Gibbs free energy of formation of $(\mathrm{MgO})_{1/2}(\mathrm{Al_2O_3})_{1/2}$ is −23,350 J, and the existence of $MgAl_2O_4$ as a stable phase requires that the activities of both MgO and Al_2O_3 have values between $\log a = -2.273$ and $\log a = 0$, the values of which are determined by Equation (iva). From Equation (iva) and Figure 13.14, the logarithm of the activity of Al_2O_3 in $MgAl_2O_4$ (at $a_{\mathrm{MgAl_2O_4}} = 1$) which is saturated with MgO (at $a_{\mathrm{MgO}} = 1$) is −2.273, and, from symmetry, the logarithm of the activity of MgO in $MgAl_2O_4$ (at $a_{\mathrm{MgAl_2O_4}} = 1$) which is saturated with Al_2O_3 (at $a_{\mathrm{Al_2O_3}} = 1$) is −2.273. Thus, if the activity of either MgO or Al_2O_3 in the system is less than antilog (−2.273), the spinel of $MgAl_2O_4$ is not stable.

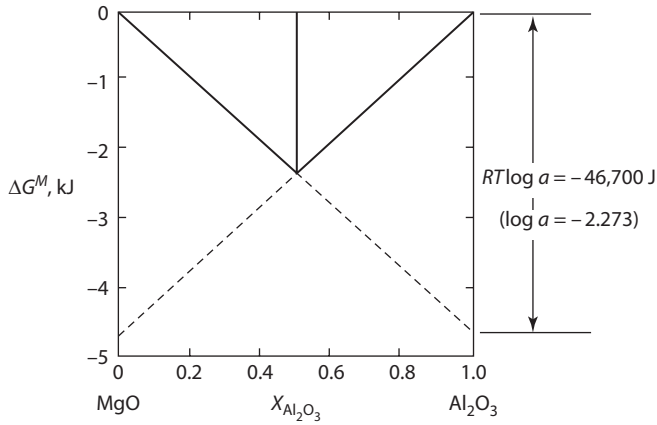

FIGURE 13.14 Molar Gibbs free energies of mixing in the system $MgO–Al_2O_3$ at 1073 K.

The measured activities of Mg and Al at 1073 K in the system Mg–Al have been fitted by the equations[2]

$$\log a_{Mg} = \log X_{Mg} - 0.68\left(1 - X_{Mg}\right)^3 \tag{v}$$

and

$$\log a_{Al} = \log\left(1 - X_{Mg}\right) - 1.02X_{Mg}^2 + 0.68X_{Mg}^3 \tag{vi}$$

The phase stability diagram for the system at 1073 K, using p_{O_2} and $\log a_{Mg}$ as coordinates, is shown in Figure 13.15a (the fixing of the activities of O_2 and Mg in the ternary system Mg–Al–O at constant temperature fixes the activity of Al). From Equation (iia), equilibrium between pure liquid Mg and MgO occurs at $\log p_{O_2} = -47.17$, which is shown as point *a* in Figure 13.15a. The three-phase equilibrium involving the Mg–Al melt, MgO, and the g as phase is determined by Equation (iia) and is shown as the line *ab* in Figure 13.15a. The addition of Al to the liquid alloy decreases a_{Mg} and hence increases the value of the pressure of oxygen required to maintain $a_{MgO} = 1$. Also, in moving along *ab* from *a* toward *b*, the activity of $a_{Al_2O_3}$, given by Equation (i), increases, and at point *b*, it reaches the value of antilog (–2.273), which with $a_{MgO} = 1$ makes $a_{MgAl_2O_4} = 1$. Thus, the four-phase equilibrium melt–MgO–$MgAl_2O_4$–gas occurs at the point *b*. The three-phase equilibrium involving the Mg–Al melt, $MgAl_2O_4$, and the gas phase, determined by Equation (iiia), occurs along the line *bd*. In moving along the line from *b* to *d*, the dilution of Mg in the melt causes a_{MgO} to decrease from unity at *b* and $a_{Al_2O_3}$ to increase, and at the point *d*, $a_{Al_2O_3} = 1$ and $\log a_{MgO} = -2.273$. Thus, *d* represents the four-phase equilibrium melt–Al_2O_3–$MgAl_2O_4$–gas. At activities of Mg less than that at *d*, the activity of MgO is less than antilog

[2] G. R. Belton and Y. K. Rao, "A Galvanic Study of Activities in Mg–Al Liquid Alloys," *Trans. Met. Soc.* (1969), vol. 245, p. 2189.

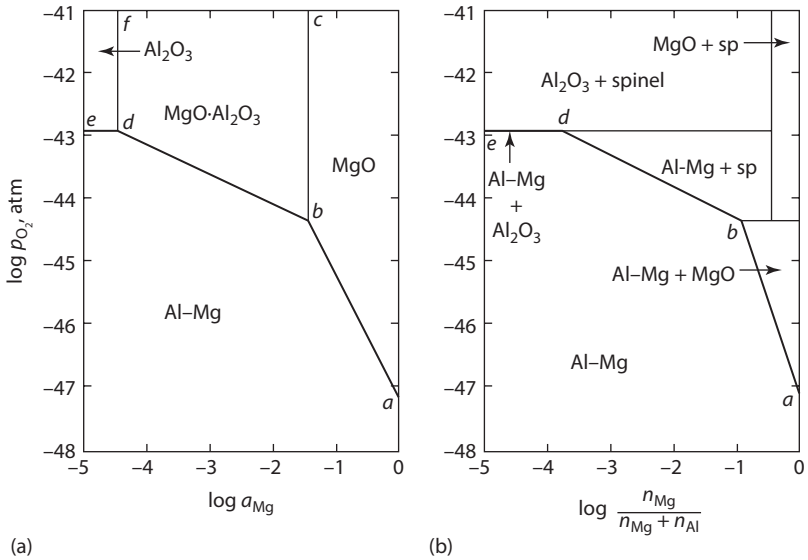

FIGURE 13.15 (a) The phase stability diagram for the system Al–Mg–O at 1073 K. (b) The phase diagram for the system Al–Mg–O at 1073 K.

(−2.273), and thus, the spinel $MgAl_2O_4$ is not stable. The line *ed* represents the equilibrium involving a melt, Al_2O_3, and a gas phase, given by Equation (ia). However, as $a_{Mg} = 5.75 \times 10^{-5}$ at point *d*, a_{Al} is virtually unity, and thus, the line *ed* is virtually horizontal at $\log p_{O_2}$ (obtained from Equation (ia)) = −42.93. The lines *df* and *bc* represent, respectively, the three-phase equilibria Al_2O_3–$MgAl_2O_4$–gas and $MgAl_2O_4$–MgO–gas. The lines in Figure 13.15a identify the fields of stability of Al–Mg liquid alloys, MgO, $MgAl_2O_4$, and Al_2O_3 at 1073 K.

The activity–composition relationships given by Equations (v) and (vi) allow the phase stability diagram presented as Figure 13.15a to be converted to the phase diagram shown in Figure 13.15b, in which $\log p_{O_2}$ and $\log n_{Mg}/(n_{Mg}+n_{Al})$ (where n_{Mg} and n_{Al} are, respectively, the numbers of moles of Mg and Al in the system) are used as coordinates. The line *ab* gives the compositions of the metallic melts saturated with MgO, the line *bd* gives the compositions of the melts saturated with $MgAl_2O_4$, and the line *ed* gives the compositions of the melts saturated with Al_2O_3.

Consider the sequence of oxidation of Al–Mg alloys of $X_{Mg} = 0.333$, 0.2, and 0.01 at 1073 K. With $X_{Mg} = 0.333$ and $\log p_{O_2} = -48$, the system exists at the state *a* in Figure 13.16. When the oxygen pressure is increased to $\log p_{O_2} = -45.6$, the system exists at *b*, in which state the alloy is in equilibrium with MgO. Further increase in the oxygen pressure causes the precipitation of MgO from the melt, which decreases the mole fraction of X_{Mg} in the melt and causes its composition to move along the MgO saturation line from *b* toward *c*. At $\log p_{O_2} = -44.3$, the melt of composition *c* is saturated with MgO, and further increase in the oxygen pressure causes all of the melt of composition *c* to react with all of the MgO at *d* to form the spinel $MgAl_2O_4$.

A melt of $X_{Mg} = 0.2$ equilibrated with oxygen at $\log p_{O_2} = -48$ exists at the state *e* in Figure 13.16, and increasing the oxygen pressure to $\log p_{O_2} = -45.1$ brings the alloy into equilibrium with MgO at the state *f*. Further increase in the oxygen pressure to $\log p_{O_2} = -44.3$ causes MgO to precipitate and moves the composition of the melt along the MgO saturation line from *f* to *c*. Further increase in the oxygen pressure causes all of the MgO to react with some of the melt to produce $MgAl_2O_4$ and a melt saturated with $MgAl_2O_4$. With further oxidation, $MgAl_2O_4$ is precipitated from the melt, and the composition of the melt is moved along the $MgAl_2O_4$ saturation line from *c* toward *i*. Although the precipitation of the spinel from the melt removes Al and Mg atoms from the melt in the ratio Al/Mg = 2, the values of X_{Mg} in the melts are low enough that the removal of Al atoms makes a negligible change in X_{Al} but causes a significant decrease in X_{Mg}. At $\log p_{O_2} = -42.9$, the melt at the state *i* is doubly saturated with Al_2O_3 and $MgAl_2O_4$, and further increase in the oxygen pressure causes the disappearance of the melt. Increasing the oxygen pressure exerted on a melt of $X_{Mg} = 0.01$ causes saturation of the melt with $MgAl_2O_4$ at $\log p_{O_2} = -43.8$ (the state *h*), and further increase in the oxygen pressure causes oxidation to proceed as described previously.

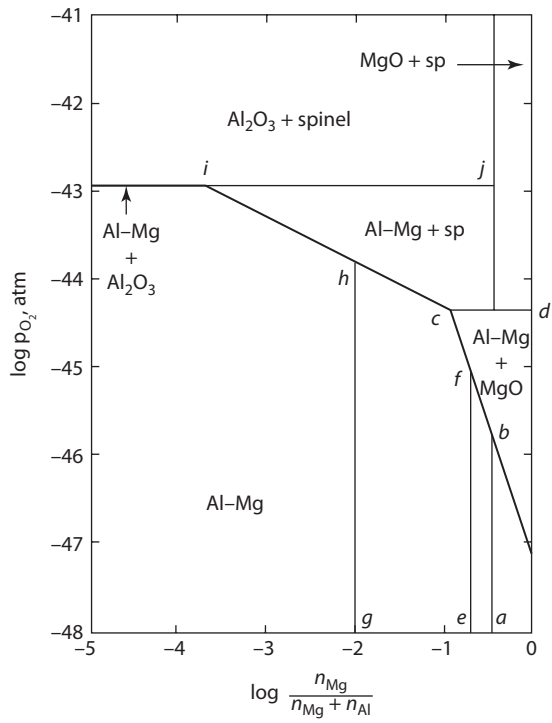

FIGURE 13.16 The influence of composition and oxygen pressure on the equilibrium states of existence in the system Mg–Al–O.

13.6.2 Phase Equilibria in the System Al–C–O–N Saturated with Carbon

Consider now, the phase stability in the system Al–C–O–N, saturated with carbon at 2000 K, and identify the conditions under which AlN can be contained in a graphite crucible at 2000 K without the formation of Al_4C_3. The solid phases that occur in the quaternary system are AlN, Al_4C_3, Al_4O_4C, and Al_2O_3, and since the system is saturated with graphite, the minimum number of phases that can coexist in equilibrium with one another is three (graphite, a gas phase, and a second condensed phase). The number of degrees of freedom available to this three-phase equilibrium is

$$\mathcal{F} = C + 2 - \Phi = 4 + 2 - 3 = 3$$

which can be selected as T, p_{O_2}, and p_{N_2}. An isothermal phase stability diagram can thus be constructed using $\log p_{N_2}$, and $\log p_{O_2}$ as coordinates. For

$$\begin{aligned} 4\mathrm{Al}_{(l)} + 3\mathrm{C}_{(s)} &= \mathrm{Al_4C_{3(s)}} \\ \Delta G^{\circ}_{(\mathrm{i}),2000\,\mathrm{K}} &= -74,060\ \mathrm{J} \end{aligned} \tag{i}$$

and thus, an equilibrium involving pure liquid Al, graphite, and solid Al_4C_3 does not exist at 2000 K. The activity of Al in carbon-saturated Al_4C_3 is obtained from

$$K_{(\mathrm{i}),2000\,\mathrm{K}} = \exp\left(\frac{74,060}{8.3144 \times 2000}\right) = 85.95 = \frac{a_{\mathrm{Al_4C_3}}}{a_{\mathrm{Al}}^4 a_{\mathrm{C}}^3} = \frac{1}{a_{\mathrm{Al}}^4}$$

which gives $a_{Al} = 0.327$, relative to pure liquid Al.

For

$$\begin{aligned} 4\mathrm{AlN}_{(s)} + 3\mathrm{C}_{(s)} &= \mathrm{Al_4C_{3(s)}} + 2\mathrm{N_{2(g)}} \\ \Delta G^{\circ}_{(\mathrm{ii}),2000\,\mathrm{K}} &= 917,900\ \mathrm{J} = -2 \times 8.3144 \times 2000 \times 2.303 \log p_{N_2} \end{aligned} \tag{ii}$$

which gives $\log p_{N_2} = -11.98$ for the equilibrium involving solid graphite, solid AlN, solid Al_4C_3, and a gas phase. The line representing this equilibrium is drawn as *ab* in Figure 13.17a. Graphite and AlN are stable relative to graphite and Al_4C_3 in states above the line, and graphite and Al_4C_3 are stable relative to graphite and AlN in states below the line.

For

$$\begin{aligned} \mathrm{Al_4O_4C_{(s)}} + 2\mathrm{C}_{(s)} &= \mathrm{Al_4C_{3(s)}} + 2\mathrm{O_{2(g)}} \\ \Delta G^{\circ}_{(\mathrm{iii}),2000\,\mathrm{K}} &= 1,333,000\ \mathrm{J} = -2 \times 8.3144 \times 2000 \times 2.303 \log p_{O_2} \end{aligned} \tag{iii}$$

which gives $\log p_{O_2} = -17.40$ for the equilibrium involving solid graphite, solid Al_4C_3, solid Al_4O_4C, and a gas phase. This is drawn as line *cd* in Figure 13.17a. To the left of this line, graphite and Al_4C_3 are stable relative to graphite and Al_4O_4C, and to the right of the line, the reverse is the case.

For

$$4Al_{(l)} + 2O_{2(g)} + C_{(s)} = Al_4O_4C_{(s)} \qquad \Delta G^\circ_{(iv),2000\,K} = -1,407,000\ J \tag{iv}$$

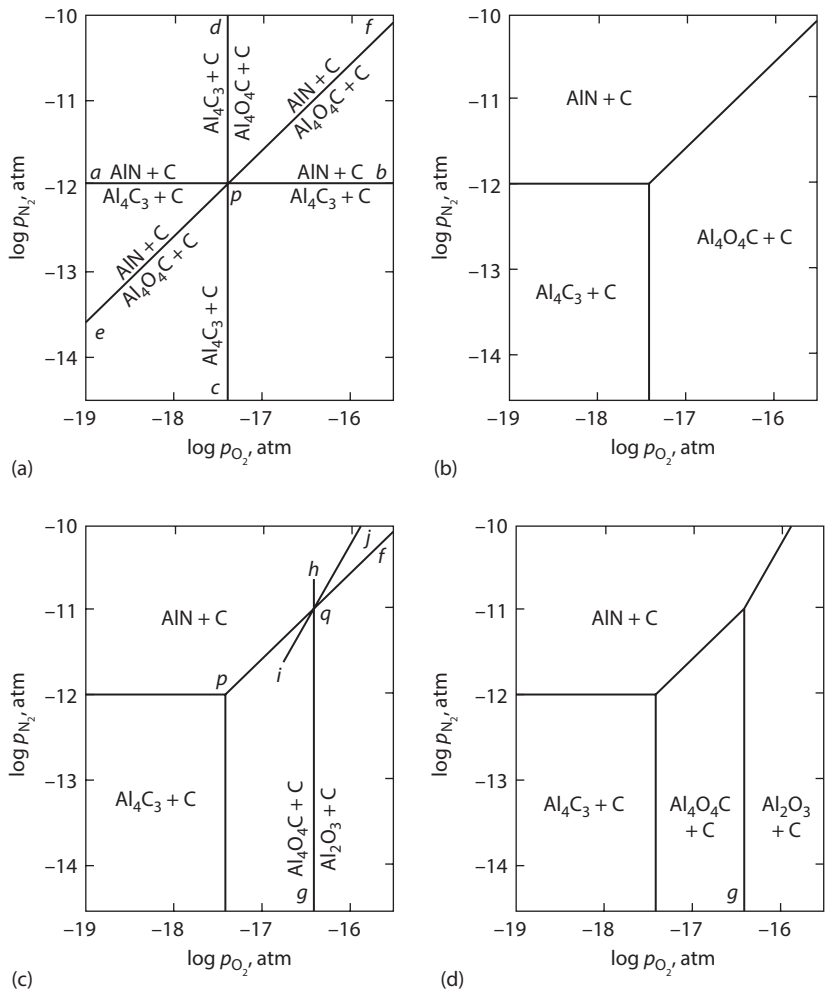

FIGURE 13.17 Construction of the phase stability diagram for the system Al–C–O–N saturated with carbon at 2000 K. (a), (b), and (c) are drawn from the various possible equilibrium equations and (d) is the final equilibrium diagram

and thus, for carbon-saturated Al_4O_4C,

$$K_{(\mathrm{iv}),2000\,\mathrm{K}} = \exp\left(\frac{1{,}407{,}000}{8.3144 \times 2000}\right) = 5.58 \times 10^{36} = \frac{1}{a_{\mathrm{Al}}^4 p_{\mathrm{O}_2}^2}$$

which, with $\log p_{\mathrm{O}_2} = -17.40$, gives $a_{\mathrm{Al}} = 0.327$. Thus, the activity of Al in C-saturated Al_4O_4C has the same value as that in C-saturated Al_4C_3. The point of intersection of lines *ab* and *cd* is the state in which the five-phase equilibrium involving four solid phases and a gas phase occurs.

For

$$\begin{gathered}\mathrm{Al_4O_4C}_{(s)} + 2\mathrm{N}_{2(g)} = \mathrm{C}_{(s)} + 2\mathrm{O}_{2(g)} + 4\mathrm{AlN}_{(s)} \\ \Delta G^{\circ}_{(\mathrm{v}),2000\,\mathrm{K}} = 415{,}000\ \mathrm{J} = -2 \times 8.3144 \times 2000 \times 2.303 \log \frac{p_{\mathrm{O}_2}}{p_{\mathrm{N}_2}}\end{gathered} \tag{v}$$

which gives

$$\log p_{\mathrm{N}_2} = \log p_{\mathrm{O}_2} + 5.42$$

for the equilibrium among graphite, solid AlN, solid Al_4O_4C, and a gas phase. This is drawn as line *ef* in Figure 13.17a. Carbon-saturated Al_4C_3 is stable relative to carbon-saturated Al_4O_4C above the line, with the reverse being the case below the line. Inspection of Figure 13.17a shows the following:

1. In the area below *ap* and to the left of *pc*, Al_4C_3 is stable with respect to AlN and Al_4O_4C.
2. In the area above *ap* and above *pf*, AlN is stable with respect to Al_4C_3 and Al_4O_4C.
3. In the area below *pf* and to the right of *pc*, Al_4O_4C is stable with respect to AlN and Al_4C_3.

Thus, without consideration of the stability of Al_2O_3, the fields of stability of AlN, Al_4C_3, and Al_4O_4C are as shown in Figure 13.17b.

For

$$\begin{gathered}2\mathrm{Al_2O_3}_{(s)} + \mathrm{C}_{(s)} = \mathrm{O}_{2(g)} + \mathrm{Al_4O_4C}_{(s)} \\ \Delta G^{\circ}_{(\mathrm{vi}),2000\,\mathrm{K}} = 630{,}800\ \mathrm{J} = -8.3144 \times 8.3144 \times 2000 \times 2.303 \log p_{\mathrm{O}_2}\end{gathered} \tag{vi}$$

which gives $\log p_{\mathrm{O}_2} = -16.47$ for the equilibrium among graphite Al_4O_4C, Al_2O_3, and a gas phase. This is drawn as the line *gh* in Figure 13.17c, and its point of intersection with *pf* is the state of the five-phase equilibrium among graphite, AlN, Al_4O_4C, Al_2O_3, and a gas phase.

For

$$Al_2O_{3(s)} + N_{2(g)} = 2AlN_{(s)} + 1.5O_{2(g)}$$

$$\Delta G^{\circ}_{(vii),2000\,K} = 522{,}900\ J = -8.3144 \times 2000 \times 2.303 \log \frac{p_{O_2}^{1.5}}{p_{N_2}} \qquad (vii)$$

which gives

$$\log p_{N_2} = 1.5 \log p_{O_2} + 13.65$$

for the equilibrium given by Equation (vii). This line, which is independent of the activity of C in the system, is drawn as *ij* in Figure 13.17c. Since the line *pq* represents a stable equilibrium, the other two lines radiating from the point *q* which represent stable equilibria are *qg* and *gj*, and the full phase stability diagram is shown in Figure 13.17d. The diagram shows that AlN can be heated in a graphite crucible without forming Al_4C_3 if the pressures of oxygen and nitrogen are such that the thermodynamic state lies in the field of stability of AlN.

13.7 THE FORMATION OF OXIDE PHASES OF VARIABLE COMPOSITION

Figure 13.18 shows the variation, with composition at a temperature *T*, of the molar Gibbs free energy of mixing for the metal M–oxygen system in which measurable solubility of oxygen in metallic M occurs and the oxides MO and M_3O_4 have variable compositions. Compounds with nonstoichiometric compositions are sometimes called *berthollides*, after Claude Louis Berthollet (1748–1822). Starting with pure M, increasing the pressure of oxygen causes the molar Gibbs free energy of mixing to move from *f* along the curve *fi* until, at $p_{O_2} = p_{O_2(M/MO)}$, the metal is saturated with oxygen and the metal-saturated MO phase of composition $M_b O_a$ appears. If the pure metal M and oxygen gas at 1 atm pressure at the temperature *T* are chosen as the standard states, then

$$\Delta G_{(\text{metal/saturated MO})} = jk = RT\left(b \ln a_M + a \ln p_{O_2}^{1/2}\right)$$

$$= RT \ln a_M^b p_{O_2}^{a/2}$$

From Figure 13.18, $fg = RT \ln a_M$ and $lm = RT \ln p_{O_{2(M/MO)}}$.

We can also write for the reaction

$$bM_{(s)} + \frac{1}{2} aO_{2(g)} = M_bO_{a(s)}$$

$$\Delta G^{\circ} = jk = RT \ln\left(\frac{a_M^b p_{O_2}^{a/2}}{a_{M_bO_a}}\right)$$

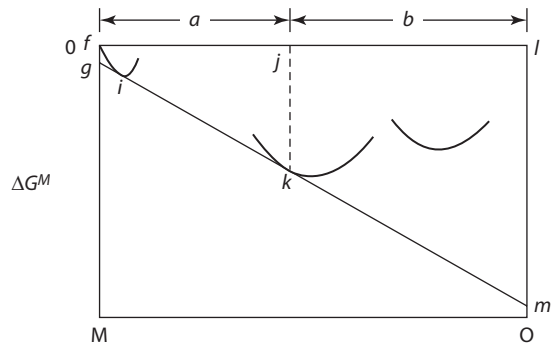

FIGURE 13.18 The Gibbs free energies of mixing of the system M–O which forms oxide phases of variable composition and which shows a significant solubility of oxygen in metallic M.

which, if the metal-saturated oxide is chosen as the standard state, is identical with the preceding expression.

It is convenient to write the reaction of the oxidation such that an integer number of gram-atoms of oxygen are consumed, For the consumption of one gram-atom of oxygen,

$$y\mathrm{M} + \frac{1}{2}\mathrm{O}_2 = \mathrm{M}_y\mathrm{O}, \qquad \text{where} \quad y = \frac{b}{a}$$

$$\Delta G^\circ = RT \ln\left(\frac{a_{\mathrm{M}}^{y} p_{\mathrm{O}_2}^{1/2}}{a_{\mathrm{M}_y\mathrm{O}}}\right)$$

or, for the consumption of 1 gram-mole of oxygen (2 gram-atoms),

$$\Delta G^\circ = RT \ln\left(\frac{a_{\mathrm{M}}^{2y} p_{\mathrm{O}_2}}{a_{\mathrm{M}_y\mathrm{O}}^{2}}\right)$$

If the solubility of oxygen in the metal is virtually zero, then *fg* in Figure 13.18 shrinks to a point, and Figure 13.18 is redrawn as Figure 13.19. In this case, choosing pure M, oxygen gas at 1 atm pressure and the temperature *T*, and the oxide of composition $\mathrm{M}_y\mathrm{O}$ as the standard states gives, for the oxidation,

$$y\mathrm{M} + \frac{1}{2}\mathrm{O}_2 = \mathrm{M}_y\mathrm{O}$$

$$\Delta G^\circ = RT \ln p_{\mathrm{O}_2(\mathrm{M/MO})}^{1/2}$$

where $p_{\mathrm{O}_2(\mathrm{M/MO})}$ is the pressure of oxygen required for equilibrium between the metal M and the metal-saturated oxide MO, given by $lm = RT \ln p_{\mathrm{O}_2(\mathrm{M/MO})}$.

If the oxygen pressure is increased to a value greater than $p_{\mathrm{O}_2(\mathrm{M/MO})}$, the metal phase disappears, the oxygen content of the MO phase increases, the molar Gibbs free energy of mixing of the system moves along the curve *kn*.

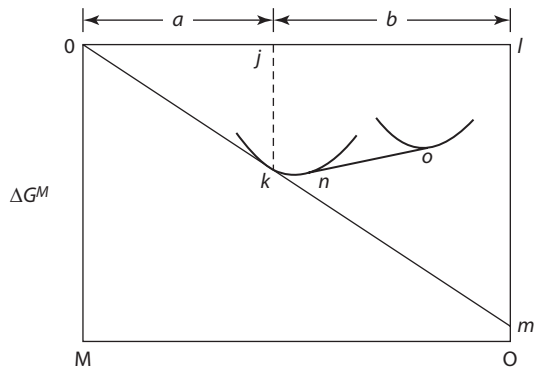

FIGURE 13.19 The Gibbs free energies of mixing of the system M–O which forms oxide phases of variable composition and which shows a negligible solubility of oxygen in metallic M.

13.7.1 The Fe-O System

In a classic investigation, Darken and Gurry[3] determined the phase relationships occurring in the system Fe–O by varying the oxygen pressure and temperature and observing the consequential changes in phase and phase composition. Their diagram, drawn for the components FeO and Fe_2O_3, is shown in Figure 13.20. Consider the wustite ("FeO")[4] phase field which, at 1100°C, extends from the composition *m* to the composition *n*. The variation of a_{Fe} in the wustite phase can be calculated from the experimentally determined variation of the composition of wustite with oxygen pressure using the Gibbs–Duhem equation:

$$X_{Fe} d \ln a_{Fe} + X_O d \ln a_O = 0$$

That is,

$$\log a_{Fe} = -\int \frac{X_O}{X_{Fe}} d \log a_O = -\int \frac{X_O}{X_{Fe}} d \log p_{O_2}^{1/2}$$

where the upper limit of integration is the oxygen pressure in equilibrium with the wustite composition of interest, and the lower limit is $p_{O_2(Fe/"FeO")}$ (the oxygen pressure at which wustite of composition *m* is in equilibrium with oxygen-saturated metallic iron), at which composition $a_{Fe} = 1$. Having thus determined the variations of a_{Fe} with composition, the corresponding variations of $a_{"FeO"}$ are determined as follows. If the standard state for oxygen gas is selected as being $p_{O_2(Fe/"FeO")}$ at the temperature of interest, then for

$$y\text{Fe}_{(s)} + \frac{1}{2}\text{O}_{2\left(g,\text{at } p_{O_2(Fe/"FeO")}\right)} = \text{Fe}_y\text{O}_{(s)}$$

[3] L. S. Darken and R. W. Gurry, "The System Iron–Oxygen, I: The Wustite Field and Related Equilibria," *J. Am. Chem. Soc.* (1945), vol. 67, p. 1398; "The System Iron–Oxygen, II: Equilibria and Thermodynamics of Liquid Oxide and Other Phases," *J. Am. Chem. Soc.* (1946), vol. 68, p. 798.

[4]

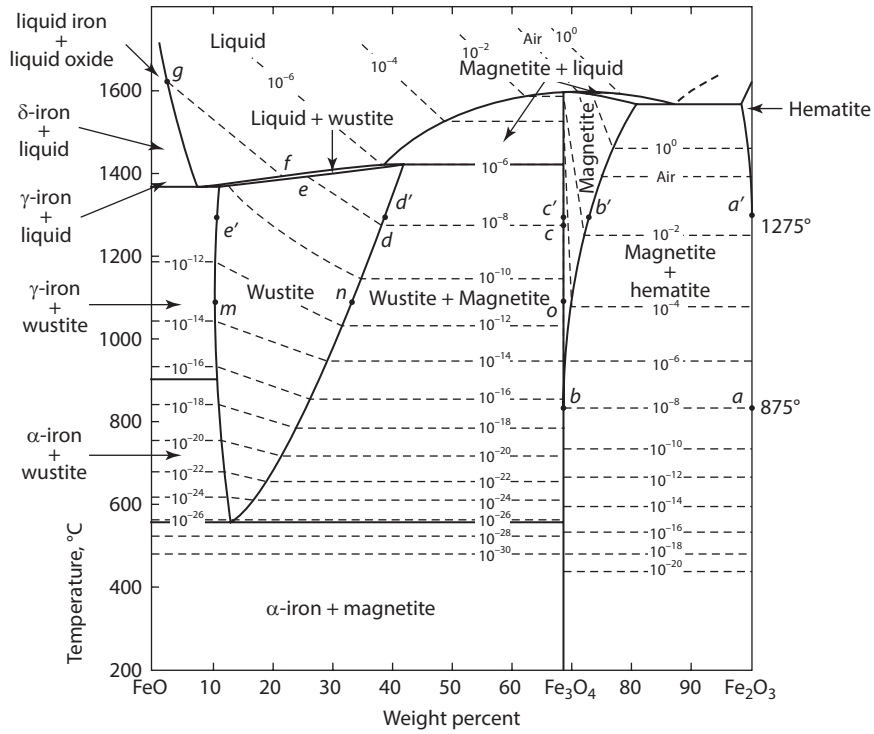

FIGURE 13.20 The phase diagram for the system FeO–Fe_2O_3 showing the positions of the oxygen (atm) isobars.

as the standard states are in equilibrium with one another, $\Delta G^\circ = 0$, and thus, $K = 1$,

$$a_{\text{"FeO"}} = a_{\text{Fe}} a_{\text{O}} \qquad \text{where } a_{\text{O}} = \left(\frac{p_{\text{O}_2}}{p_{\text{O}_2(\text{Fe}/\text{"FeO"})}} \right)^{1/2}$$

or

$$\log a_{\text{"FeO"}} = \log a_{\text{Fe}} + \log a_{\text{O}}$$

$$= -\int \frac{X_{\text{O}}}{X_{\text{Fe}}} d \log a_{\text{O}} + \int d \log a_{\text{O}}$$

$$= -\int \left(\frac{X_{\text{O}}}{X_{\text{Fe}}} - 1 \right) d \log p_{\text{O}_2}^{1/2}$$

in which the integration limits are the same as before.

The variations of a_{Fe}, $a_{\text{"FeO"}}$, and a_{O} across the wustite field at 1100°C, 1200°C, and 1300°C are shown in Figure 13.21, and from these variations, the molar Gibbs free energy curve for wustite, *kn* in Figure 13.19, can be determined. For a fixed composition, the partial molar heats of solution of metal and oxygen in the wustite can be obtained from the Gibbs–Helmholtz relationship as

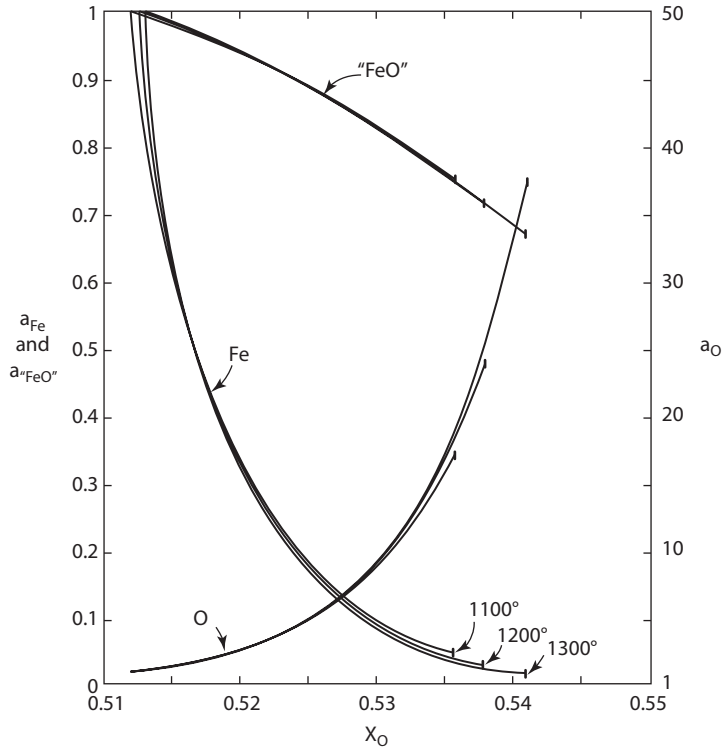

FIGURE 13.21 The activities of iron, oxygen, and iron-saturated wustite in the wustite phase field at several temperatures.

$$\Delta\bar{H}_{\mathrm{O}}^{\mathrm{M}} = R\frac{\partial \ln p_{\mathrm{O}_2}^{1/2}}{\partial\left(1/T\right)}$$

and

$$\Delta\bar{H}_{\mathrm{Fe}}^{\mathrm{M}} = R\frac{\partial \ln a_{\mathrm{Fe}}}{\partial\left(1/T\right)}$$

The variations of $\Delta\bar{H}_{\mathrm{O}}^{\mathrm{M}}$ and $\Delta\bar{H}_{\mathrm{Fe}}^{\mathrm{M}}$ with composition are shown in Figure 13.22. In Figure 13.21, at the composition of wustite $X_{\mathrm{O}} = 0.5175$, the activity of Fe is independent of temperature, and thus, as shown in Figure 13.22, the partial molar heat of mixing of Fe at this composition is zero.

At the temperature T, the limit of increase of p_{O_2} above homogeneous stable wustite is $p_{\mathrm{O}_2(\text{"FeO"}/\mathrm{Fe_3O_4})}$, the oxygen pressure at which wustite of composition n is in equilibrium with magnetite (Fe_3O_4) of composition o (Figure 13.20), and, if these compositions are chosen as the standard states, then for

$$3\,\text{"FeO"}_{(\text{saturated with oxygen})} + \frac{1}{2}\mathrm{O}_{2(g)} = \mathrm{FeO_3O_4}_{(\text{saturated with Fe})}$$

$$\Delta G^{\circ} = RT\ln p^{1/2}$$

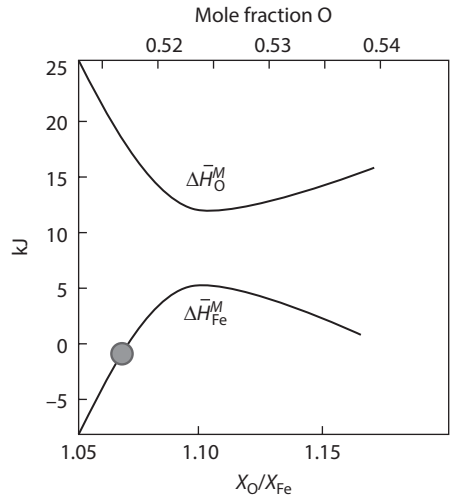

FIGURE 13.22 The partial molar heats of solution of iron and oxygen in wustite.

Figure 13.20 shows that the composition of wustite in equilibrium with magnetite varies significantly with temperature. Thus, the heat of formation of magnetite from wustite cannot be calculated by application of the Gibbs–Helmholtz equation to the variation of $p_{O_2("FeO"/Fe_3O_4)}$ with temperature (the Gibbs–Helmholtz partial differential is for constant total pressure and constant composition). However, since the composition of magnetite in equilibrium with wustite is independent of temperature, the change in enthalpy for the reaction

$$3Fe_{(s)} + 2O_{2(g)} = Fe_3O_{4(\text{saturated with Fe})}$$

can be obtained using the Gibbs–Helmholtz relationship; that is,

$$K = \frac{1}{a_{Fe}^3 p_{O_2}^2}$$

and thus,

$$\Delta H^\circ = -R\frac{d\ln K}{d(1/T)} = R\left[3\frac{d\ln a_{Fe}}{d(1/T)} + 2\frac{d\ln p_{O_2}}{d(1/T)}\right]$$

In this expression, a_{Fe} and p_{O_2} are the respective values for equilibrium between wustite and magnetite obtained from the data in Figure 13.21.

Below 550°C, homogeneous wustite is metastable with respect to iron and magnetite.

The common tangent drawn from pure Fe to the curve for the Gibbs free energy of magnetite lies below the curve of the Gibbs free energy for wustite. At 550°C, this common tangent becomes a "triple" common tangent and the two-component, four-phase equilibrium is invariant.

The FeO–Fe_2O_3 phase diagram at 1 atm total pressure shown in Figure 13.20 has, superimposed on it, oxygen isobars which trace the loci of variation of equilibrium composition with temperature under a fixed oxygen pressure in the system. For example, consider a small quantity of *hematite* (Fe_2O_3) at room temperature held in a gas reservoir of $p_{O_2} = 10^{-8}$ atm, the volume of which is sufficiently large that any oxygen gas produced by the reduction of the oxide has an insignificant effect on the pressure of oxygen in the gas reservoir. Let the oxide be heated slowly enough that equilibrium with the gas phase is maintained. From Figure 13.20, it is seen that the oxide remains as homogeneous hematite until 875°C is reached, at which temperature 10^{-8} atm is the invariant partial pressure of oxygen required for the equilibrium

$$2Fe_3O_4 + \frac{1}{2}O_2 = 3Fe_2O_3$$

At 875°C, magnetite of composition *b* is in equilibrium with hematite of composition *a*, and any increase in temperature upsets the equilibrium toward the magnetite side, with the consequent disappearance of the hematite phase. Further increase in temperature moves the composition of the oxide along the 10^{-8} atm isobar in the magnetite phase field until 1275°C is reached, at which temperature 10^{-8} atm is the invariant partial pressure of oxygen required for the equilibrium

$$3\,\text{"FeO"} + \frac{1}{2}O_2 = Fe_3O_4$$

At 1275°C wustite of composition *d* is in equilibrium with magnetite of composition *c*. Further increase in temperature causes the disappearance of the magnetite phase, and the composition of the solid homogeneous wustite moves along the 10^{-8} atm oxygen isobar until the solidus temperature of 1400°C is reached, in which state solid wustite of composition *e* melts to form a liquid oxide of composition *f* at $p_{O_2} = 10^{-8}$ atm. Continued increase in temperature moves the composition of the liquid oxide along the 10^{-8} atm isobar to saturation with iron at the temperature 1635°C, where the liquid oxide has the composition *g*, and oxygen-saturated liquid iron appears. In this state, the equilibrium

$$Fe_{(l)} + \frac{1}{2}O_{2(g)} = \text{"FeO"}_{(l)}$$

is established. An increase in temperature beyond 1635°C causes the disappearance of the liquid oxide phase and a decrease in the dissolved oxygen content of the liquid iron.

Similarly, isothermal *reduction of hematite* is achieved by decreasing the partial pressure of oxygen in the system. For example, from Figure 13.20, at 1300°C, hematite is the stable phase until the partial pressure of oxygen has been decreased to 1.34×10^{-2} atm, in which state magnetite of composition *b'* is in equilibrium with hematite of composition *a'*. Magnetite is then stable until the partial pressure of

oxygen has been decreased to 2.15×10^{-8} atm, where wustite of composition *d'* is in equilibrium with magnetite of composition *c'*. Wustite is then stable until the partial pressure of oxygen has been decreased to 1.95×10^{-11} atm, where solid iron appears in equilibrium with wustite of composition *e'*. Further decrease in the pressure of oxygen causes the disappearance of the oxide phase. Figure 13.23 shows the phase relationships in a plot of $\log p_{O_2}$ versus temperature *T*, and the paths *a–g* and *a'–e'* correspond to those in Figure 13.20. Since Figure 13.23 does not contain the compositions of the coexisting oxide phases, it is less useful than the normal composition–temperature phase diagram containing oxygen isobars. Figure 13.24 shows the phase equilibria on a plot of $1/T$ versus $\log p_{O_2}$. This plot can be converted to an Ellingham diagram, as shown in Figure 13.25. In this diagram, the paths *a–g* and *a'–e'* correspond to those in Figure 13.20. Except for the Fe_3O_4–Fe_2O_3 line in Figure 13.25, the lines are drawn for oxidation reactions involving the consumption of 1 mole of oxygen—that is, of the type

$$Fe_xO_y + O_2 = Fe_xO_{(2+y)}$$

in which the lower oxide of composition $Fe_x\ O_y$ is in equilibrium with the higher oxide of composition $Fe_x\ O_{(2+y)}$. The Fe_3O_4–Fe_2O_3 line is hypothetical and applies to the stoichiometric compounds (stoichiometric Fe_3O_4 contains Fe at a higher activity

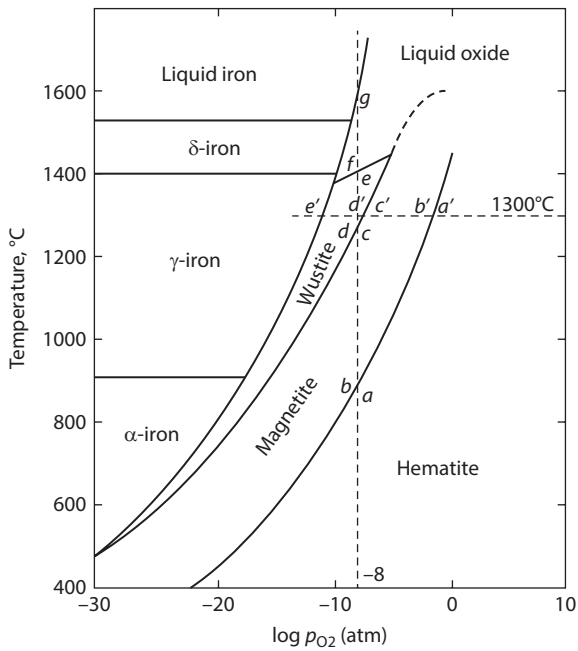

FIGURE 13.23 Phase stability in the system Fe–Fe_2O_3 as a function of temperature and $\log p_{O_2}$.

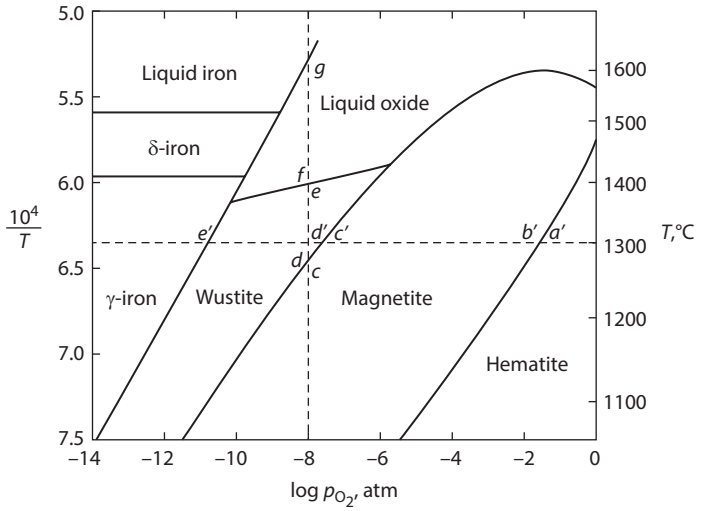

FIGURE 13.24 Phase stability in the system $Fe–Fe_2O_3$ as a function of log p_{O_2} and $1/T$.

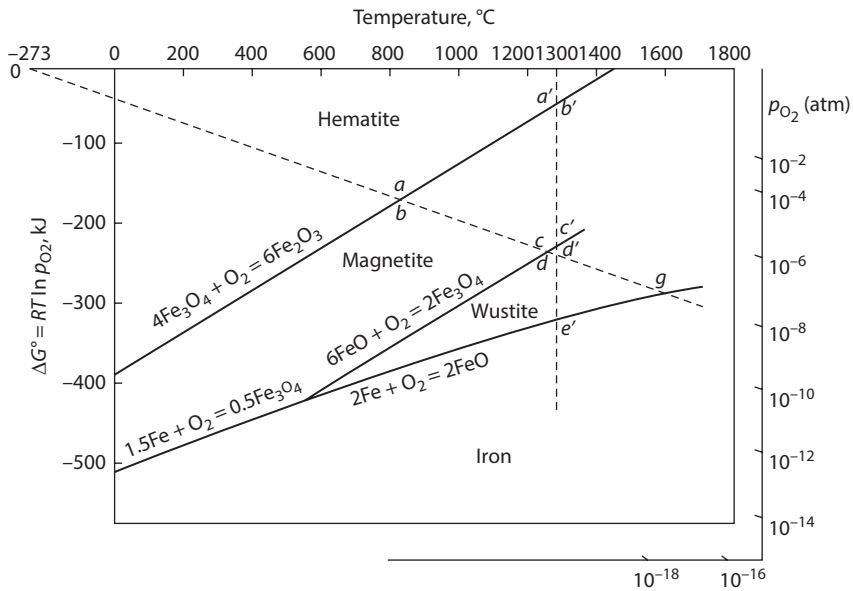

FIGURE 13.25 Phase stability in the system $Fe–Fe_2O_3$ as a function of ΔG° and temperature.

than does the composition in equilibrium with hematite). In the Ellingham diagram, lines that radiate from the origin ($\Delta G^\circ = 0$, $T = 0$ K) are oxygen isobars. The distinct advantage of the Ellingham-type representation of reaction and phase equilibria is its ability to indicate, at a glance, the relative stabilities of a large number of metal–oxygen systems, as shown in Figure 12.13.

13.8 THE SOLUBILITY OF GASES IN METALS

It is invariably found that molecular gases dissolve in metals as atoms. For example, if pure liquid Ag is brought into contact with oxygen gas at a relatively low pressure, the following series of events occur:

1. Molecules of O_2 striking the surface of the liquid Ag become *adsorbed* on the surface.
2. The adsorbed molecules *dissociate* to form O atoms adsorbed on the surface.
3. The adsorbed O atoms diffuse from the surface into the bulk melt.

The overall reaction can be written as

$$\frac{1}{2}\mathrm{O}_{2(g)} = [\mathrm{O}]_{\text{in Ag}}$$

and equilibrium is attained when the partial molar Gibbs free energy of oxygen in solution in the liquid Ag, $\overline{G}_{\mathrm{O}}$, is equal to the molar Gibbs free energy of oxygen in the gas phase, $\frac{1}{2}G_{\mathrm{O}_2}$. The standard state for a gas dissolved in a metal can be chosen as the 1 wt% standard state, discussed in Section 13.3, or as the 1 atom percent (at%) standard state, which is the point on the Henry's law line at a mole fraction of solute of 0.01. Thus, the standard change in the molar Gibbs free energy which occurs when a gaseous species A_2, at 1 atm pressure and the temperature T, is dissolved in a metal at the concentration $X_A = 0.01$ (1 at%), at the temperature T, according to

$$\frac{1}{2}\mathrm{A}_{2(g,P=1\text{ atm})} = [\mathrm{A}]_{(1\text{ at }\%)} \tag{13.14}$$

is

$$\Delta G^{\circ}_{1\text{ at }\%} = -RT\ln K_{1\text{ at }\%} = -RT\ln\frac{[h_{\mathrm{A}}]_{(1\text{ at }\%)}}{p^{1/2}_{\mathrm{A}_2}} \tag{13.15}$$

in which $[h_A]_{(1\text{ at}\%)}$ is the activity of A in solution in the metal relative to the 1 at% standard state. If the solute obeys Henry's law,

$$K_{1\text{ at }\%} = \frac{[\text{at }\%\ \mathrm{A}]}{p^{1/2}_{\mathrm{A}_2}} \tag{13.16}$$

If, however, the 1 wt% standard state is chosen for the solute, then for

$$\frac{1}{2}\mathrm{A}_{2(g,\,P=1\text{ atm})} = [\mathrm{A}]_{(1\text{ wt}\%)} \tag{13.17}$$

$$\Delta G^{\circ}_{1\text{ wt}\%} = -RT\ln K_{1\text{ wt}\%} = -RT\ln\frac{[h_{\mathrm{A}}]_{(1\text{ wt}\%)}}{p^{1/2}_{\mathrm{A}_2}} \tag{13.18}$$

in which $[h_A]_{(1\ wt\%)}$ is the activity of A in solution relative to the 1 wt% standard state. If Henry's law is obeyed,

$$K_{1\ wt\%} = \frac{[\text{wt\% A}]}{p_{A_2}^{1/2}} \tag{13.19}$$

For the solution of oxygen in liquid Ag in the range 1213 (the invariant temperature) –1573 K,

$$\Delta G^\circ_{1at\%} = -14{,}310 + 5.44T\text{J} \tag{i}$$

A concentration of 1 wt% O in Ag corresponds to a mole fraction of

$$\frac{\frac{1}{16}}{\frac{1}{16}+\frac{99}{107.9}} = 0.0638$$

and thus, the change in the molar Gibbs free energy for

$$[\text{O}]_{(\text{in Ag}\cdot 1\ \text{at \%})} = [\text{O}]_{(\text{in Ag}\cdot 1\ \text{wt\%})}$$

is

$$\Delta G^\circ_{(ii)} = -8.3144T \ln\frac{0.0638}{0.01} = -15.40T\ \text{J} \tag{ii}$$

The sum of $\Delta G^\circ_{1\ at\%}$ and $\Delta G^\circ_{(ii)}$ gives

$$\Delta G^\circ_{1\ wt\%} = -14{,}310 - 9.96T \tag{iii}$$

For the solution of oxygen in solid Ag in the range 573–1173 K,

$$\Delta G^\circ_{1\ at\%} = 49{,}620 - 15.77T\ \text{J} \tag{iv}$$

Oxygen obeys Henry's law in liquid Ag, and thus, from Equations (i), 13.15, and 13.16, the solubility of oxygen in liquid silver is

$$\text{at\% O} = p_{O_2}^{1/2}\ \exp\left(\frac{1721}{T} - 0.654\right) \tag{v}$$

and, from Equations (iv), 13.15, and 13.16, the solubility of oxygen in solid Ag is

$$\text{at\% O} = p_{O_2}^{1/2}\ \exp\left(-\frac{5967}{T} + 1.90\right) \tag{vi}$$

The phase equilibria in the system Ag–O at an oxygen pressure of 1 atm are shown in Figure 13.26. Equation (i) gives $\Delta H^\circ_{1\ at\%}$ for the change of state

$$\frac{1}{2}\text{O}_{2(g,P=1\ \text{atm})} = [\text{O}]_{(1\ \text{a}}$$

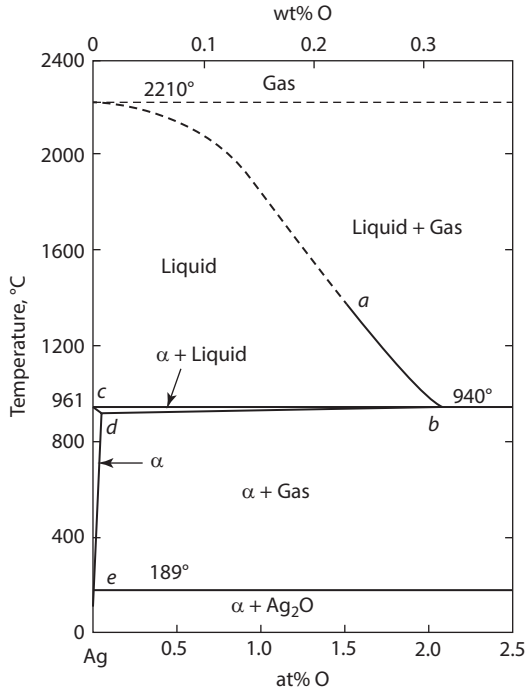

FIGURE 13.26 Phase equilibria in the system Ag–O at an oxygen pressure of 1 atm.

as −14,310 J. Thus, since the enthalpy change is negative, decreasing the temperature causes the equilibrium to shift to the right, with the consequence that, at constant oxygen pressure, the solubility of oxygen in liquid Ag increases with decreasing temperature. From Equation (v), and the data from Figure 13.26 the maximum solubility of O in liquid Ag is 2.14 at% at 940°C (state *b*). Equation (vi) gives the solubility of O in solid Ag at 940°C as 0.049 at% (the state *d*), and thus, the *invariant transformation* at 940°C can be written as:

$$\mathrm{Ag}_{(l,2.14\ \text{at\% O})} \rightarrow \mathrm{Ag}_{(s,0.049\ \text{at\% O})} + \mathrm{O}_{2(g,P=1\ \text{atm})}$$

The evolution of oxygen during the freezing of oxygen-containing liquid Ag causes the phenomenon of *spitting*, during which droplets of liquid silver are ejected from the freezing mass of liquid. Equation (iv) gives $\Delta H^{\circ}_{1\ \text{at\%}}$ for the change of state

$$\frac{1}{2}\mathrm{O}_{2(g,P=1\ \text{atm})} = \mathrm{O}_{1\ \text{at\%}\ \text{in solid Ag}}$$

as 49,620 J, which being positive requires that the solubility of O in solid Ag decreases with decreasing temperature. From Equation (vi), the solubility of O in solid Ag at an oxygen pressure of 1 atm decreases from 0.049 at% at 940°C to 1.7×10^{-5} at% at 189°C (the point *e* in Figure 13.26). ΔG° for the reaction

$$2\mathrm{Ag}_{(s)} + \frac{1}{2}\mathrm{O}_{2(g)} = \mathrm{Ag}_2\mathrm{O}_{(s)}$$

is written as

$$\Delta G^\circ = -30{,}540 + 66.11T \text{ J}$$

The temperature at which $p_{\mathrm{O}_2,\mathrm{eq}} = 1$ atm is thus 30,540/66.11 = 462 K (189°C), and the three-phase invariant equilibrium is shown at 189°C in Figure 13.26. The solubility of oxygen in Ag is shown as a function of temperature and oxygen pressure in Figure 13.27. On a plot of log (at% O) versus inverse temperature, the oxygen isobars in a single-phase field are parallel lines, the slopes of which are determined by the molar enthalpies of the solution of oxygen. From Equation (v), the slope of the lines in the phase field of liquid silver is 1721, and from Equation (vi), the slope in the phase field of solid silver is −5967. The points *b* and *d* on the 1 atm isobar at 940°C correspond with the points *b* and *d* in Figure 13.26. Increasing the oxygen pressure decreases the temperature at which the equilibrium involving liquid Ag, solid Ag, and O_2 gas occurs and increases the temperature at which the equilibrium involving solid Ag, Ag_2O, and O_2 gas occurs. The two temperatures coincide at 508°C when the

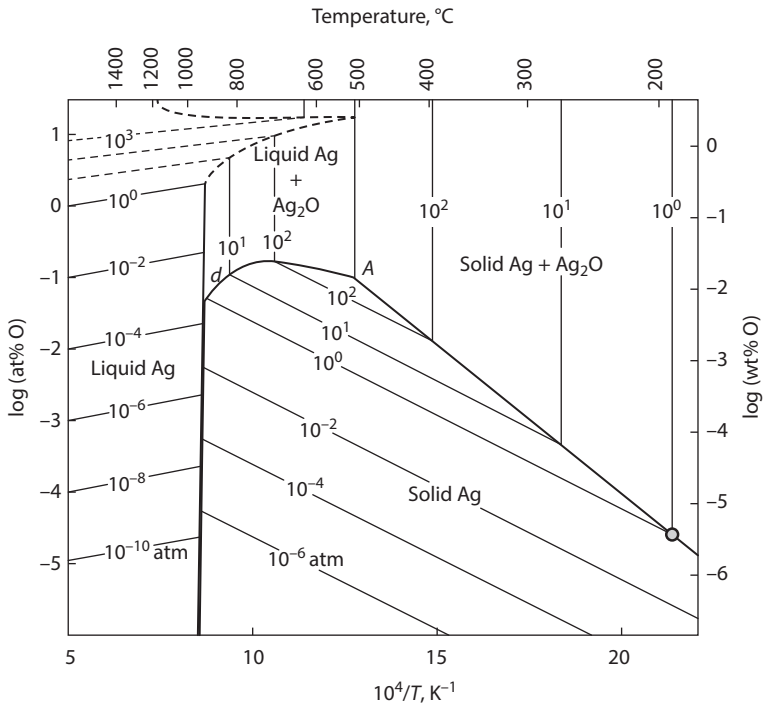

FIGURE 13.27 The solubility of oxygen in silver as a function of oxygen pressure and temperature.

oxygen pressure is 414 atm (the state *A* in Figure 13.27). This four-phase equilibrium in a binary system has zero degrees of freedom. Recasting Equation 13.16 as

$$\left[\text{at\% A}\right] = k(T)\, p_{\text{A}_2}^{1/2} \tag{13.20}$$

gives an equation known as *Sieverts' law* (Adolf Sieverts, 1874–1947) and the temperature-dependent constant in Equation 13.20, $k(T)$, which is known as *Sieverts' constant*, is evaluated as the concentration of A in the metal equilibrated, at the temperature T, with gaseous A_2 at 1 atm pressure. Sieverts measured the solubility of oxygen in liquid Ag in 1907.[5]

13.9 SUMMARY

1. Reaction equilibrium in the reaction

   $$aA + bB = cC + dD$$

   is established when the reaction has proceeded to the extent that

   $$a\bar{G}_A + b\bar{G}_B = c\bar{G}_C + d\bar{G}_D$$

   That is, ΔG for the reaction is zero.
2. The state of reaction equilibrium is determined by the standard Gibbs free energy change for the reaction, ΔG°, via

   $$\Delta G^\circ = -RT \ln K$$

   where K is the equilibrium constant for the reaction given by the quotient of the activities of the reactants and products at reaction equilibrium, raised to their stoichiometric coefficients; that is,

   $$K = \frac{a_C^c a_D^d}{a_A^a a_B^b}$$

3. The *Raoultian standard state* of a thermodynamic component is the pure component in its stable state of existence at the temperature of interest. The *Henrian standard state* is obtained from consideration of Henry's law, which, strictly being a limiting law obeyed by the solute B at infinite dilution, is expressed as

   $$\frac{a_B}{X_B} \to \gamma_B^\circ \quad \text{as} \quad X_B \to 0$$

   where γ_B° is the constant activity coefficient which quantifies the difference between Raoultian and Henrian solution behavior of B. If the solute obeys Henry's law over a finite range of composition, then, over this range,

   $$a_B = \gamma_B^\circ X_B$$

[5] A. Sieverts and J. Hagenacker, "Über die Loslichkeit von Wasserstoff und Sauerstoff in festem und geschmolzenem Silber," *Z. Phys. Chem.* (1907), vol. 68, p. 115.

4. The Henrian standard state is obtained by extrapolating the Henry's law line to $X_B = 1$, and the activity of B in the Henrian standard state with respect to the Raoultian standard state having unit activity is

$$a_B = \gamma_B^\circ$$

The activity of B in a solution with respect to the Henrian standard state having unit activity is given by

$$h_B = f_B X_B$$

where h_B is the Henrian activity and f_B is the Henrian activity coefficient. In the range of composition in which B obeys Henry's law, $f_B = 1$.

5. The *1 wt% standard state* is defined as

$$\frac{h_{B(1\text{ wt\%})}}{\text{wt\% } B} \to 1 \quad \text{as} \quad \text{wt\% } B \to 0$$

and is located at that point on the Henry's law line which corresponds to a concentration of 1 wt% B. With respect to the 1 wt% standard state having unit activity, the activity of B, $h_{B(1\text{ wt\%})}$, is given by

$$h_{B(1\text{ wt\%})} = f_{B(1\text{ wt\%})}\text{wt\% } B$$

where $f_{B(1\text{ wt\%})}$ is the 1 wt% activity coefficient. The activities are related via

$$a_B = h_B \gamma_B^\circ$$

and

$$a_B = f_{B(1\text{ wt\%})} \cdot \text{wt\% } B \cdot \gamma_B^\circ \cdot \frac{\text{MW}_{\text{solvent}}}{100\ \text{MW}_B}$$

6. The Gibbs equilibrium phase rule is

$$\mathcal{F} = C + 2 - \Phi$$

where:

C is the number of components in the system

$\mathcal{F}$ is the number of degrees of freedom available to the equilibrium involving Φ phases

With R independent reaction equilibria involving N species, the Gibbs equilibrium phase rule is

$$\mathcal{F} = (N - R) + 2 - \Phi$$

where $C = N - R$

7. The equilibria among the phases Fe, FeO (wustite), Fe_3O_4 (magnetite) and Fe_2O_3 (hematite) were examined as an example of phase equilibria with oxide phases of varying composition.

13.10 CONCEPTS AND TERMS INTRODUCED IN THIS CHAPTER

The reader should write out brief definitions or descriptions of the following terms. Where appropriate, equations may be used.

Activity quotient
Adsorbed atoms
Alternate standard state
Berthollides
Components
Compound
Daltonides
Gibbs equilibrium phase rule
Hematite
Henrian standard state
Infinite dilution
Law of definite proportions
Magnetite
Nonstoichiometric compound
Phase stability diagram
Raoultian standard state
Sieverts' constant
Sieverts' law
Solubility of gases in solids
Solution thermodynamics
Stoichiometric compound
Thermodynamic degree of freedom
Volatile
Wustite

13.11 QUALITATIVE EXAMPLE PROBLEMS

QUALITATIVE PROBLEM 1

a. Find the point *e* in Figure 13.26 and locate its corresponding location on Figure 13.27.
b. What phase(s) is (are) present at point *e*?
c. Apply the Gibbs equilibrium phase rule to the system at this point.
d. What phase(s) is (are) present at point *b* in Figure 13.27?
e. If the temperature is raised slightly at point *b*, what phases will be present?
f. Apply the Gibbs equilibrium phase rule to the system at this slightly higher temperature.

SOLUTION TO QUALITATIVE PROBLEM 1

a.

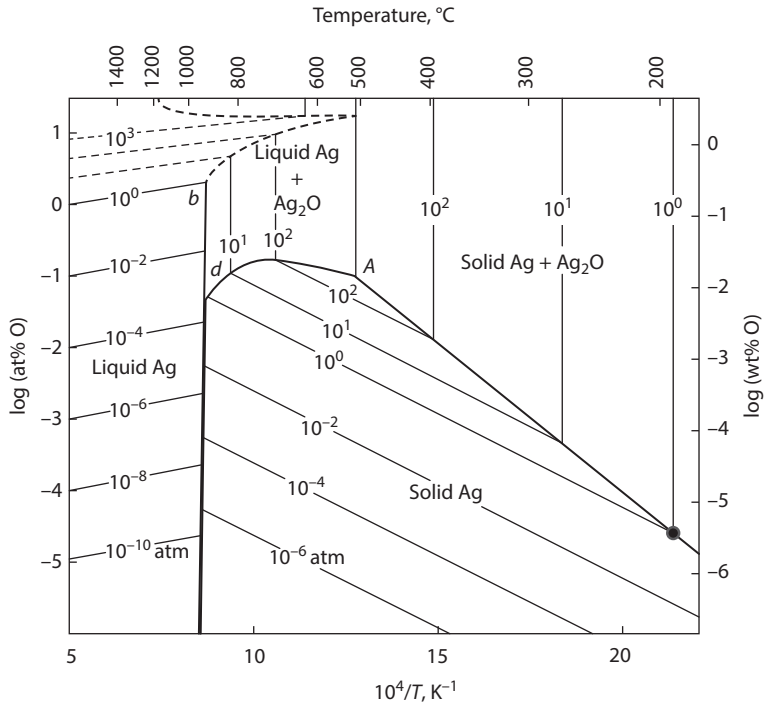

FIGURE 13.28 Point e from Figure 13.26 is plotted here at $P = 1$ atm.

b. $Ag_{(s)}$, $Ag_2O_{(s)}$, and the O_2 gas phase.

c. In Figure 13.26, the pressure is fixed.

There are three phases, $Ag_{(s)}$, O_2 gas and $Ag_2O_{(s)}$.

There are two components, C

$$\mathcal{F} = C + 1 - \Phi$$

$$\mathcal{F} = 2 + 1 - 3 = 0$$

For the fixed pressure of 1 atm the point *e* lies on an *invariant temperature*.

d. $Ag_{(l)}$, $Ag_2O_{(s)}$, and O_2 gas.

e. $Ag_{(l)}$ and $O_{2(g)}$.

f. $\mathcal{F} = C + 2 - \Phi = 2 + 2 - 2 = 2$

This is no longer an *invariant* condition. Both the temperature and the partial pressure of O_2 can change and the state remains $Ag_{(l)}$ and $O_{2(g)}$.

QUALITATIVE PROBLEM 2

The molar Gibbs free energy of mixing of Al_2O_3 and MgO at 1073 K is shown in Figure 13.14.

Delineate the phase fields as the composition varies from $X = 0$ to $X = 1$.

SOLUTION TO QUALITATIVE PROBLEM 2

$$X_{Al_2O_3} = 0 \quad \text{only MgO}$$

$$0 < X_{Al_2O_3} < 0.5 \qquad \text{MgO and } MgAl_2O_4$$

$$0.5 < X_{Al_2O_3} < 1 \qquad MgAl_2O_4 \text{ and } Al_2O_3$$

$$X_{Al_2O_3} = 1 \quad \text{only } Al_2O_3$$

Note: The diagram in Figure 13.14 is only approximate. There must be some solubility (however small) of each of the components in each other as well as in the spinel phase.

13.12 QUANTITATIVE EXAMPLE PROBLEMS

QUANTITATIVE PROBLEM 1

In a dew-point experiment, a Cu–Zn alloy is placed in one end of an evacuated and closed tube and is heated to 900°C. When the other end of the tube is cooled to 740° C Zn vapor begins to condense. Calculate the activity of Zn in the alloy relative to pure zinc.

SOLUTION TO QUANTITATIVE PROBLEM 1

See Table A.4

$$\text{At } 740°C = 1013 \text{ K} \qquad \ln p^{\circ}_{Zn} = -\frac{15,250}{1013} - 1.255 \ln (1013) + 21.79$$

$$p^{\circ}_{Zn,1013\,K} = 0.142 \text{ atm}$$

$$\text{At } 900°C = 1173 \text{ K} \qquad \ln p^{\circ}_{Zn} = -\frac{15,250}{1173} - 1.255 \ln (1173) + 21.79$$

$$p^{\circ}_{Zn,1173\,K} = 0.923 \text{ atm}$$

$$\therefore a_{Zn}(\text{in the alloy}) = \frac{0.142}{0.923} = 0.154$$

QUANTITATIVE PROBLEM 2

Determine the conditions under which an Fe–Cr–O melt is in equilibrium with

1. Solid Cr_2O_3
2. Solid $FeO{\cdot}Cr_2O_3$

at 1600°C. For

$$2\mathrm{Cr}_{(s)} + \frac{3}{2}\mathrm{O}_{2(g)} = \mathrm{Cr}_2\mathrm{O}_{3(s)}, \quad \Delta G^\circ_{(\mathrm{i})} = -1{,}120{,}300 + 259.8T \text{ J} \tag{i}$$

and for

$$\frac{1}{2}\mathrm{O}_{2(g)} = [\mathrm{O}]_{(1 \text{ wt\% in Fe})}, \quad \Delta G^\circ_{(\mathrm{ii})} = -111{,}070 - 5.87T \text{ J} \tag{ii}$$

SOLUTION TO QUANTITATIVE PROBLEM 2

At 1600°C, Fe–Cr melts exhibit Raoultian ideality, and the molar heat of melting of Cr, at its equilibrium melting temperature of 2173 K, is 21,000 J. Thus, for $\mathrm{Cr}_{(s)} = \mathrm{Cr}_{(l)}$,

$$\Delta G^\circ_m = \Delta H^\circ_m - T\frac{\Delta H^\circ_m}{T_m} = 21{,}000 - 9.66T \text{ J}$$

and for $\mathrm{Cr}_{(l)} = [\mathrm{Cr}]_{(1 \text{ wt\% in Fe})}$,

$$\Delta G = RT \ln \frac{55.85}{100 \times 52.01} = -37.70T \text{ J}$$

Therefore, for $\mathrm{Cr}_{(s)}$ — $[\mathrm{Cr}]_{(1 \text{ wt\% in Fe})}$,

$$\Delta G^\circ_{(\mathrm{iii})} = 21{,}000 - 47.36T \text{ J} \tag{iii}$$

The standard Gibbs free energy change for the reaction

$$2[\mathrm{Cr}]_{(1 \text{ wt\%})} + 3[\mathrm{O}]_{(1 \text{ wt\%})} = \mathrm{Cr}_2\mathrm{O}_{3(s)} \tag{iv}$$

is thus

$$\begin{aligned}\Delta G^\circ_{(\mathrm{iv})} &= \Delta G^\circ_{(\mathrm{i})} - 3\Delta G^\circ_{(\mathrm{ii})} - 2\Delta G^\circ_{(\mathrm{iii})} \\ &= -829{,}090 + 372.13T \text{ J} \\ &= -RT \ln \frac{a_{\mathrm{Cr_2O_3}}}{h^2_{\mathrm{Cr}(1 \text{ wt\%})} \cdot h^3_{\mathrm{O}(1 \text{ wt\%})}}\end{aligned}$$

or, at 1873 K,

$$\log \frac{h^2_{\mathrm{Cr}(1 \text{ wt\%})} \cdot h^3_{\mathrm{O}(1 \text{ wt\%})}}{a_{\mathrm{Cr_2O_3}}} = -3.68 \tag{v}$$

Saturation of the melt with solid $\mathrm{Cr}_2\mathrm{O}_3$ occurs at $a_{\mathrm{Cr_2O_3}} = 1$, and, if the interactions between Cr and O in solution are ignored, and it is assumed that oxygen obeys Henry's law, Equation (v) can be written as

$$\log[\text{wt\% Cr}] = -1.5 \log[\text{wt\% O}] - 1.84 \tag{vi}$$

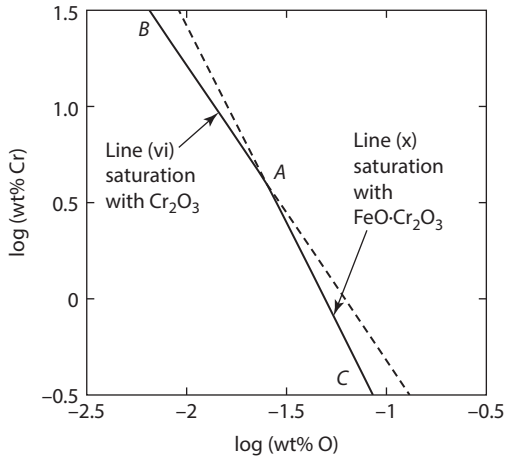

FIGURE 13.29 The variations of the concentrations of Cr with the concentrations of O in Fe saturated with Cr_2O_3 and $FeO{\cdot}Cr_2O_3$ at 1600°C.

which is the variation of [wt% Cr] with [wt% O] in liquid iron required for equilibrium with solid Cr_2O_3 at 1600°C. Equation (vi) is drawn as line (vi) in Figure 13.29.

For

$$\begin{gathered}\mathrm{Fe}_{(l)} + 2\mathrm{Cr}_{(s)} + 2\mathrm{O}_{2(g)} = \mathrm{FeO}\cdot\mathrm{Cr_2O_{3(s)}} \\ \Delta G^{\circ}_{(\mathrm{vii})} = -1{,}409{,}420 + 318.07T \text{ J}\end{gathered} \tag{vii}$$

and thus, for the reaction

$$\begin{gathered}\mathrm{Fe}_{(l)} + 2\left[\mathrm{Cr}\right]_{(1\text{ wt\%})} + 4\left[\mathrm{O}\right]_{(1\text{ wt\%})} = \mathrm{FeO}\cdot\mathrm{Cr_2O_{3(s)}} \\ \Delta G^{\circ}_{(\mathrm{viii})} = \Delta G^{\circ}_{(\mathrm{vii})} - 2\Delta G^{\circ}_{(\mathrm{iii})} - 4\Delta G^{\circ}_{(\mathrm{ii})} \\ = -1{,}007{,}140 + 436.27T \text{ J} \\ = -RT\ln\frac{a_{\mathrm{FeO}\cdot\mathrm{Cr_2O_3}}}{a_{\mathrm{Fe}}\cdot h^{2}_{\mathrm{Cr}(1\text{ wt\%})}\cdot h^{4}_{\mathrm{O}(1\text{ wt\%})}}\end{gathered} \tag{viii}$$

or, at 1873 K,

$$\log\frac{a_{\mathrm{Fe}}\cdot h^{2}_{\mathrm{Cr}(1\text{ wt\%})}\cdot h^{4}_{\mathrm{O}(1\text{ wt\%})}}{a_{\mathrm{FeO}\cdot\mathrm{Cr_2O_3}}} = -5.30 \tag{ix}$$

Saturation of the melt with $FeO{\cdot}Cr_2O_3$ occurs at $a_{\mathrm{FeO}\cdot\mathrm{Cr_2O_3}} = 1$ and, with the same assumptions as before, and $a_{\mathrm{Fe}} = X_{\mathrm{Fe}} = 1 - X_{\mathrm{Cr}}$, the variation of [wt% Cr] with [wt% O] required for equilibrium with solid $FeO{\cdot}Cr_2O_3$ at 1600°C is

$$\log\left(1 - X_{\mathrm{Cr}}\right) + 2\log\left[\mathrm{wt\%Cr}\right] + 4\log\left[\mathrm{wt\%O}\right] = -5.30 \tag{x}$$

In solutions sufficiently dilute that $X_{Fe} \sim 1$, Equation (x) can be simplified as

$$\log\left[\text{wt\% Cr}\right] = -2\log\left[\text{wt\% O}\right] - 2.65 \qquad \text{(xi)}$$

Equation (xi) is drawn as line (x) in Figure 13.29. Lines (vi) and (x) intersect at the point *A*, log [wt% Cr] = 0.59, log [wt% O] = −1.62 (wt% O = 0.024, wt% Cr = 3.89), which is the composition of the melt which is simultaneously saturated with solid Cr_2O_3 and $FeO{\cdot}Cr_2O_3$. From the phase rule, equilibrium in a three-component system (Fe–Cr–O) among four phases (liquid Fe–Cr–O, solid Cr_2O_3, solid $FeO{\cdot}Cr_2O_3$, and a gas phase) has one degree of freedom, which, in the present case, has been used by specifying the temperature to be 1873 K. Thus, the activities of Fe, Cr, and O are uniquely fixed, and hence [wt% Cr] and [wt% O] are uniquely fixed. The equilibrium oxygen pressure in the gas phase is obtained from Equation (ii) as

$$\Delta G^{\circ}_{(\text{ii}),1873\text{K}} = -122{,}065\ \text{J} = -8.3144 \times 1873 \ln \frac{\left[\text{wt\% O}\right]}{p_{O_2}^{1/2}}$$

which, with [wt% O] = 0.024, gives $p_{O_2(\text{eq})} = 8.96 \times 10^{-11}$ atm. The positions of the lines in Figure 13.29 are such that, in melts of [wt% Cr] > 3.89, Cr_2O_3 is the stable phase in equilibrium with saturated melts along the line *AB* and, in melts in which [wt% Cr] < 3.89, $FeO{\cdot}Cr_2O_3$ is the stable phase in equilibrium with saturated melts along the line *AC*. Alternatively, Cr_2O_3 is the stable phase in equilibrium with saturated melts of [wt% O] < 0.024, and $FeO{\cdot}Cr_2O_3$ is the stable phase in equilibrium with saturated melts of [wt% O] > 0.024. Consider a melt in which log [wt% Cr] = 1.5. From Figure 13.29, or Equation (vi), the oxygen content at this chromium level required for equilibrium with Cr_2O_3 (at the point *B* in Figure 13.29) is 5.93×10^{-3} wt%, or log [wt% O] = −2.25. From Equation (v), the activity of Cr_2O_3 in this melt with respect to solid Cr_2O_3 is unity, and hence the melt is saturated with respect to solid Cr_2O_3. However, from Equation (ix), in the same melt (i.e., $X_{Fe} = 0.668$, [wt% Cr] = 31.6, [wt% O] = 0.00593), the activity of $FeO{\cdot}Cr_2O_3$ with respect to solid $FeO{\cdot}Cr_2O_3$ is only 0.2. Thus, the melt is saturated with respect to Cr_2O_3 and is undersaturated with respect to $FeO{\cdot}Cr_2O_3$. Moving along the line *BA* from *B* toward *A*, $a_{Cr_2O_3} = 1$, and $a_{FeO{\cdot}Cr_2O_3} = 1$ increases from 0.2 at *B* to unity at *A* in the doubly saturated melt. Consider a melt in which log [wt% Cr] = −0.5. From Figure 13.29, the oxygen content required for saturation with $FeO{\cdot}Cr_2O_3$ is 0.084 wt% (log [wt% O] = −1.075 at the point *C* in Figure 13.29). From Equation (ix), the activity of $FeO{\cdot}Cr_2O_3$ in this melt is unity. However, from Equation (v), the activity of Cr_2O_3 in the melt, with respect to solid Cr_2O_3, is only 0.285. Thus, this melt is saturated with $FeO{\cdot}Cr_2O_3$ and is undersaturated with Cr_2O_3. On moving along the line *CA* from *C* toward *A*, $a_{FeO{\cdot}Cr_2O_3}$ is unity and $a_{Cr_2O_3}$ increases from 0.285 at *C* to unity at *A*.

PROBLEMS

13.1 Air at atmospheric pressure is blown over a Cu-rich copper–gold liquid solution at 1500 K. If only the copper is oxidized (to form pure solid

Cu_2O), calculate the minimum activity of Cu which can be obtained in the solution.

13.2 Magnesium can be removed from Mg–Al liquid solution by selectively forming the chloride $MgCl_2$. Calculate the activity of Mg in the liquid Mg–Al system which can be achieved at 800°C by reacting the solution with an H_2–HCl gas mixture containing hydrogen at essentially 1 atm pressure and $p_{HCl} = 10^{-5}$ atm to form pure liquid $MgCl_2$.

13.3 The partial pressure of oxygen in equilibrium with pure liquid lead and pure liquid lead oxide at 1200 K is 2.16×10^{-9} atm. When SiO_2 is added to the liquid PbO to form a lead silicate melt, the oxygen pressure in equilibrium with pure liquid lead and the silicate melt is decreased to 5.41×10^{-10} atm. Calculate the activity of PbO in the lead silicate melt.

13.4 Copper, present as an impurity in liquid Pb, can be removed by adding PbS to the Cu–Pb alloy and allowing the exchange reaction

$$2Cu_{(s)} + PbS_{(s)} = Cu_2S_{(s)} + Pb_{(l)}$$

to come to equilibrium.

The solid sulfides are mutually immiscible, Pb is insoluble in solid Cu, and the Cu liquidus, below 850°C, can be represented by

$$\log X_{Cu} = -\frac{3500}{T} + 2.261$$

where X_{Cu} is the solubility of Cu in liquid Pb. If Cu obeys Henry's law in liquid Pb, calculate the extent to which Cu can be removed from liquid Pb by this process at 800°C. Would the extent of purification of the lead be increased by increasing or by decreasing the temperature?

13.5 A CH_4–H_2 gas mixture at 1 atm total pressure, in which $p_{H_2} = 0.957$ atm, is equilibrated with an Fe–C alloy at 1000 K. Calculate the activity of C with respect to graphite in the alloy. What would the value of p_{H_2} in the gas mixture (at $P_{total} = 1$ atm) have to be in order to saturate the Fe with graphite a t 1000 K?

13.6 Calculate the activity of FeO in an FeO–Al_2O_3–SiO_2 melt below which the FeO cannot be reduced to pure liquid iron by a CO–CO_2 mixture of $p_{CO}/p_{CO_2} = 10^5$ at 1600°C.

13.7 A piece of iron is to be heat treated at 1000 K in a CO–CO_2–H_2O–H_2 gas mixture at 1 atm pressure. The gas mixture is produced by mixing CO_2 and H_2 and allowing the equilibrium $CO_2 + H_2 = CO + H_2O$ to establish. Calculate (a) the minimum H_2/CO_2 ratio in the inlet gas which can be admitted to the furnace without oxidizing the iron, (b) the activity of carbon (with respect to graphite) in the equilibrated gas of this initial minimum H_2/CO_2 ratio, (c) the total pressure to which the equilibrated gas would have to be raised to saturate the iron with graphite at 1000 K,

and (d) the effect, on the partial pressure of oxygen in the equilibrated gas, of this increase in total pressure.

13.8 An Fe–Mn solid solution containing $X_{Mn} = 0.001$ is in equilibrium with an FeO–MnO solid solution and an oxygen-containing gaseous atmosphere at 1000 K. How many degrees of freedom does the equilibrium have? What is the composition of the equilibrium oxide solution, and what is the partial pressure of oxygen in the gas phase? Assume that both solid solutions are Raoultian in their behavior.

13.9 The elements A and B, which are both solid at 1000°C, form two stoichiometric compounds A_2B and AB_2, which are also both solid at 1000°C. The system A–B does not contain any solid solutions. A has an immeasurably small vapor pressure at 1000°C, and, for the change of state $B_{(s)} = B_{(v)}$,

$$\Delta G^\circ = 187,220 - 108.80T \text{ J}$$

The vapor pressure exerted by an equilibrated AB_2–A_2B mixture is given by

$$\log p(\text{atm}) = -\frac{11,242}{T} + 6.53$$

and the vapor pressure exerted by an equilibrated A–A_2B mixture is given by

$$\log p(\text{atm}) = -\frac{12,603}{T} + 6.9$$

From these data, calculate the standard Gibbs free energies of formation of A_2B and AB_2.

13.10 For the change of standard state $V_{(s)} = V_{(1\text{ wt\% in Fe})}$

$$\Delta G^\circ = -15,480 - 45.61T \text{ J}$$

Calculate the value of γ_V° at 1600°C. If a liquid Fe–V solution is equilibrated with pure solid VO and a gas containing $p_{O_2} = 4.72 \times 10^{-10}$ atm, calculate the activity of V in the liquid solution (a) with respect to solid V as the standard state, (b) with respect to liquid V as the standard state, (c) with respect to the Henrian standard state, and (d) with respect to the 1 wt% in iron standard state.

13.11 When an Fe–P liquid solution is equilibrated at 1900 K with solid CaO, solid $3CaO{\cdot}P_2O_5$, and a gas phase containing $p_{O_2} = 10^{-10}$ atm, the activity of P in the iron, with respect to the 1 wt% in Fe standard state, is 20. Given that $\Delta G^\circ_{1900\,K} = -564,600$ J for

$$3CaO_{(s)} + P_2O_{5(g)} = 3CaO \cdot P_2O_{5(s)}$$

and $\Delta G^\circ = -122,200 - 19.22$T J for

$$\frac{1}{2}P_{2(g)} = P_{(1\text{ wt\% in Fe})}$$

calculate $\Delta G^{\circ}_{1900\,\mathrm{K}}$ for the reaction

$$P_{2(g)} + \frac{5}{2}O_{2(g)} = P_2O_{5(g)}$$

13.12 Liquid iron, contained in an Al_2O_3 crucible under a gaseous atmosphere of $p_{O_2} = 3 \times 10^{-12}$ atm at 1600°C, contains its equilibrium contents of dissolved oxygen and aluminum. To what value must p_{O_2} be raised in order that solid hercynite ($FeO{\cdot}Al_2O_3$) appears in equilibrium with the melt and with solid Al_2O_3? What is the activity of Al (with respect to the 1 wt% in Fe standard state) in this state? How many degrees of freedom does this equilibrium have at 1600°C? Given

$$\frac{1}{2}O_{2(g)} = O_{(1\text{ wt\% in Fe})} \quad \Delta G^{\circ} = -111{,}070 - 5.87T \text{ J}$$

$$Al_{(l)} = Al_{(1\text{ wt\% in Fe})} \quad \Delta G^{\circ} = -43{,}100 - 32.26T \text{ J}$$

$$FeO \cdot Al_2O_{3(s)} = Fe_{(l)} + O_{(1\text{ wt\% in Fe})} + Al_2O_{3(s)}$$

$$\Delta G^{\circ} = 146{,}230 - 54.35T \text{ J}$$

13.13 UC_2 can be equilibrated with UC and C at high temperature and can be equilibrated with U_2C_3 and C at lower temperatures. Calculate the maximum and minimum temperatures at which UC_2 can exist.

13.14 In the Pidgeon process for the production of magnesium, dolomite ($CaO{\cdot}MgO$) is reduced by silicon to form magnesium vapor and $2CaO{\cdot}SiO_2$. Calculate the equilibrium pressure of magnesium vapor produced by this reaction at 1200°C. The Gibbs free energy of formation of dolomite from CaO and MgO is small enough that it can be ignored.

13.15 What is the minimum value that the activity of MgO can have in $MgO{\cdot}Al_2O_3$ at 1000°C?

13.16 A mixture of ZnO and graphite is placed in an evacuated vessel and heated to 1200 K. Calculate the partial pressures of Zn, CO, and CO_2 that are developed.

13.17 An assemblage of solid CaO, MgO, $3CaO{\cdot}Al_2O_3$, and liquid Al exerts an equilibrium vapor pressure of Mg of 0.035 atm at 1300 K. Write the equation for the appropriate reaction equilibrium. Calculate the standard Gibbs free energy of formation of $3CaO{\cdot}Al_2O_3$ from CaO and Al_2O_3 and the activity of Al_2O_3 in CaO-saturated $3CaO{\cdot}Al_2O_3$ at 1300 K.

13.18 It is required that PbO be eliminated from an ore containing PbO, PbS, and $PbSO_4$ by converting it to PbS or $PbSO_4$ by reaction with an SO_2–O_2 gas. Although the pressure of O_2 in the gas can vary within wide limits, the partial pressure of SO_2 may not be higher than 0.5 atm. Calculate the maximum temperature at which it can be guaranteed that the PbO phase will be eliminated.

13.19 Cementite, Fe_3C, is metastable with respect to carbon-saturated α-iron and graphite at 950 K and 1 atm pressure. Given that the molar volumes of α-Fe, graphite, and Fe_3C at 950 K are, respectively, 7.32, 5.40, and 23.92 cm^3/mole, calculate the pressure, at 950 K, at which Fe_3C is in equilibrium with carbon-saturated α-Fe and graphite. At what temperature, at 1 atm pressure, is carbon-saturated γ-Fe and graphite in equilibrium with cementite?

13.20 An experiment is being conducted on an equilibrated mixture of CaO and $CaCO_3$ contained in a closed vessel at 1200 K. The mixture is contaminated by iron in the form of hematite (Fe_2O_3). The contaminant would not be harmful to the experiment if it occurred as either wustite (FeO) or as cementite (Fe_3C). The necessary changes in the chemical form of the contaminant can be effected by admitting CO gas to the vessel. Calculate the allowable limits of p_{CO} in the vessel for the occurrence of the contaminant as (a) wustite and (b) cementite.

13.21 A Cu–Au alloy of $X_{Cu} = 0.5$ is being annealed at 600°C in deoxidized argon. The argon is deoxidized by being passed over heated pure copper turnings prior to its admission to the annealing furnace. The solid Cu–Au system is virtually regular in its solution behavior, with a molar Gibbs excess free energy of mixing given by

$$G^{XS} = -28,280 X_{Cu} X_{Au} \text{ J}$$

Assuming that equilibrium is attained in the deoxidizing furnace, calculate the maximum temperature at which the deoxidizing furnace can be operated without causing oxidation of the copper in the Cu–Au alloy being annealed.

13.22 A crucible containing 100.0 g of silver at 1000°C is placed in the reaction chamber of a Sieverts' apparatus. The chamber is evacuated and filled with 50 cm^3 (STP) of argon, which measures the dead volume of the chamber. An external manometer reads the pressure of argon as 0.9 atm. The chamber is reevacuated and filled with oxygen, and it is found that 251.5 cm^3 (STP) is required to produce a gas pressure of 0.9 atm in the chamber. Calculate the solubility of O in the Ag (as atom percent) and calculate the value of the Sieverts' law constant at 1000°C.

13.23 Silicon and manganese are commonly used together as deoxidizers for liquid steel. At 1600°C,

$$[\text{Mn}]_{(1 \text{ wt\% in Fe})} + [\text{O}]_{(1 \text{ wt\% in Fe})} = \text{MnO}_{(s)}$$

$$[\text{Si}]_{(1 \text{ wt\% in Fe})} + 2[\text{O}]_{(1 \text{ wt\% in Fe})} = \text{SiO}_{2(s)}$$

The values of the equilibrium constants show that SiO_2 is considerably more stable than MnO. Why, then, is a mixture of Mn and Si more effective as a deoxidizing agent than Si alone? The activities of MnO and SiO_2, with respect to solids as the standard states in MnO–SiO_2 melts at 1600°C, are shown in Figure 13.30.

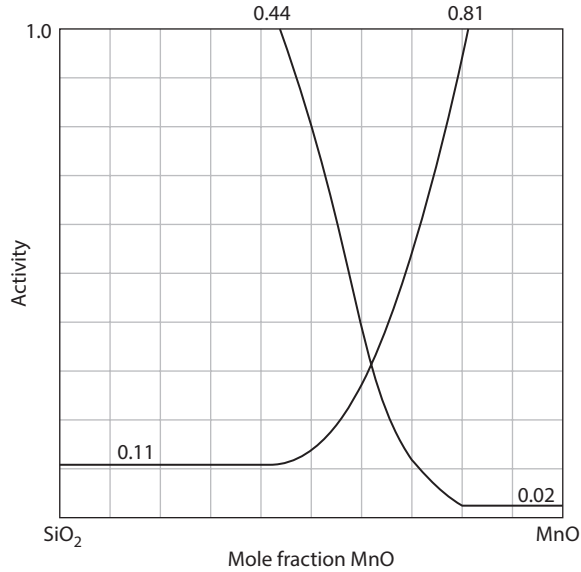

FIGURE 13.30 Activities in the system MnO–SiO_2 at 1600°C.

14 Electrochemistry

14.1 INTRODUCTION

Chemical reactions, in which products form from reactants, may involve changes in the state of oxidation, (*valence state)*, of some or all of the participating atoms. By convention, the valence state of an atom in a compound is determined by the number of electrons that surround the nucleus of the atom. The assignment of a valence state is not influenced by the nature of the bonding between the constituent atoms. For example, the bonding in the HF molecule is considered to be 50% ionic in character and 50% covalent in character. Here, *ionic character* implies complete electron transfer from the H atom to the F atom to form the ions H^+ and F^-. The *covalent character* implies complete electron sharing to give a normal covalent HF molecule, which has zero electric dipole moment. Nevertheless, the valence states of H and F in HF are denoted as +1 and −1 respectively.

Changes in the valence state of an element are caused by the addition or removal of electrons. The thermodynamic driving force of any reaction must be related in some way to the ease with which the required changes of the valence of the participating atoms can occur—that is, to the ease with which the necessary transfer of electrons can occur. For example, the reaction

$$AO + B = BO + A$$

involves a decrease in the valence state of A from +2 to 0 and an increase in the valence state of B from 0 to +2. The valence state of O is unchanged. The reaction involves the transfer of two electrons from B to A and hence can be written as

$$A^{2+} + B = B^{2+} + A$$

The change in free energy is thus a manifestation of the energetics of electron transfer. The reaction equation, written as the sum of

$$A^{2+} + 2e^- = A$$

and

$$B - 2e^- = B^{2+}$$

suggests the possibility of conducting the reaction as shown in Figure 14.1. A mixture of A + AO and a mixture of B + BO are joined by two connections *a* and *b*, where *a* is an electron conductor through which *only* electrons can pass and *b* is an ionic

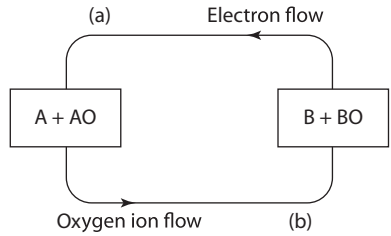

FIGURE 14.1 A schematic representation of an electrolytic reaction. (a) Path for the flow of electrons, (b) path for the flow of oxygen ions.

conductor through which *only* oxygen ions can pass. The spontaneous reaction thus occurs in the following manner. Two electrons leave a B atom, travel from right to left along *a* and, on arrival at the A + AO mixture, where they convert an A^{2+} ion to an A atom. Simultaneously, an O^{2-} ion leaves the A + AO mixture and passes through *b* to the B + BO mixture. Charge neutrality in the overall system is thus maintained, and the overall reaction can be written as

$$A^{2+}O^{2-} + B = B^{2+}O^{2-} + A$$

As a result of its being conducted in an electrochemical manner, this reaction is called an *electrochemical reaction*. The driving force for the transport of electrons along *a* is manifested as an electric voltage (or difference in electric potential) which can be measured by placing an external opposing voltage in the circuit *a* and adjusting this voltage until no electric current flows, at which point the electrochemical reaction ceases. At this point, the external voltage exactly balances the voltage generated by the electrochemical system; that is, the thermodynamic driving force for the chemical reaction is exactly balanced by the externally applied electric driving force. Knowledge of the mathematical relationship between these two types of forces allows the thermodynamic driving force for the chemical reaction (ΔG for the reaction) to be measured. Furthermore, whereas in Chapter 12, it was seen that pure A, pure AO, pure B, and pure BO are in thermodynamic equilibrium only at the unique temperature at which the two Ellingham lines intersect (if, indeed, they do intersect), it is now seen that the four phases can be brought into electrochemical equilibrium at a variety of temperatures by balancing the chemical driving force with an opposing electric driving force. In these cases, the Gibbs Equilibrium Phase Rule is changed to be:

$$\Phi + \mathcal{F} = C + 3$$

to account for the added intensive electric field (potential) term.

The properties of systems such as this are examined in this chapter.

14.2 THE RELATIONSHIP BETWEEN CHEMICAL AND ELECTRICAL DRIVING FORCES

In Section 5.4 it was seen that when a system undergoes a *reversible* process at constant temperature and pressure, the decrease in the Gibbs free energy of the system equals w'_{max}, the work (other than the work of expansion) done by the system. For an increment of such a process,

$$-dG' = \delta w'_{max}$$

Consider a system that performs electrical work by transporting an electric charge across a voltage difference—that is, from one electric potential to another. The work performed is obtained as the product of the charge transported, q (coulombs), and the electric potential difference, $\Delta\phi$ (volts). The unit of such work is the joule, which is equal to a volt times a coulomb. A system that is capable of performing electrical work as the result of the occurrence of a chemical reaction is called a *galvanic cell*. The overall chemical reaction is represented by an equation called the *cell reaction*. The charge carried by 1 g-ion (i.e., Avogadro's number of ions) of unit positive charge is 96,487 coulombs and is called Faraday's constant (Michael Faraday, 1791–1867), denoted as *f*. Thus, if dn g-ions of valence z are transported through a voltage difference $\Delta\phi$ maintained between the electrodes of a cell, then

$$\delta w' = zf\Delta\phi dn$$

If the transport is conducted reversibly, the electric potential difference between the electrodes of the cell is called the *electromotive force* (EMF), $\boldsymbol{\varepsilon}$, of the cell, then

$$\delta w'_{max} = zf \cdot \varepsilon \cdot dn = -dG' \tag{14.1}$$

For the transport of 1 mole of ions, Equation 14.1 becomes

$$\Delta G = -zf\varepsilon \tag{14.2}$$

which is known as the *Nernst equation*.

Consider the familiar Daniell cell (John Frederick Daniell, 1790–1845) shown in Figure 14.2. This cell consists of a zinc electrode partially immersed in an acidified aqueous solution of $ZnSO_4$ and a copper electrode partially immersed in an acidified aqueous solution of $CuSO_4$. The two aqueous solutions, which constitute the electrolyte of the galvanic cell (i.e., the medium through which ionic current flows, but not the electrons), are prevented from mixing by the insertion between them of a *porous diaphragm*.

Consider the processes which occur when a metal is immersed in an electrolyte. The asymmetric forces at the interface between the metal and the electrolyte cause

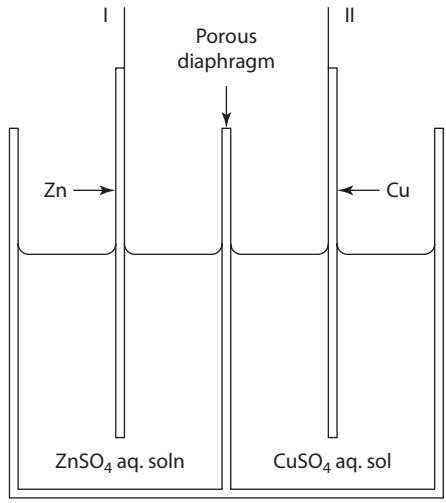

FIGURE 14.2 The Daniell cell.

the rearrangement of the solvent dipoles and the charged species in such a manner that the electrolyte side of the interface becomes electrically charged. The electric field produced operates across the interface, and, depending on the direction of the field, free electrons in the metal either move toward or away from the interface until a charge is induced in the metal which is equal and opposite to that on the electrolyte side of the interface. This separation of charge causes the development of a difference in electric potential between the interface and the bulk of the electrolyte far removed from the interface. Figure 14.3a shows the nature of the variation of electric potential with distance away from the interface into the electrolyte when the metal acquires a negative charge. Figure 14.3b shows the corresponding variation when the metal (Cu in the Daniel cell) acquires a positive charge. The difference between the potential at the metal, ϕ^M, and the potential in the bulk of the electrolyte, ϕ^e, is called the *absolute potential* of the electrode. In the Daniell cell, before external electrical contact is made between the electrodes, the zinc electrode acquires an excess of electrons, and the copper has a deficit of electrons. This causes the variation of electric potential from the zinc electrode through the electrolyte to the copper electrode to be as shown schematically in Figure 14.4. The equilibrium

$$\mathrm{Zn}^{2+} + 2e^- = \mathrm{Zn}$$

is established at the zinc–electrolyte interface when

$$\mu_{\mathrm{Zn}^{2+}}\left(\text{in the electrolyte}\right) = \mu_{\mathrm{Zn}^{2+}}\left(\text{in the electrode}\right)$$

and

$$\mu_{\mathrm{Zn}^{2+}} + 2\mu_{e^-}^{\mathrm{Zn}} = \mu_{\mathrm{Zn}}$$

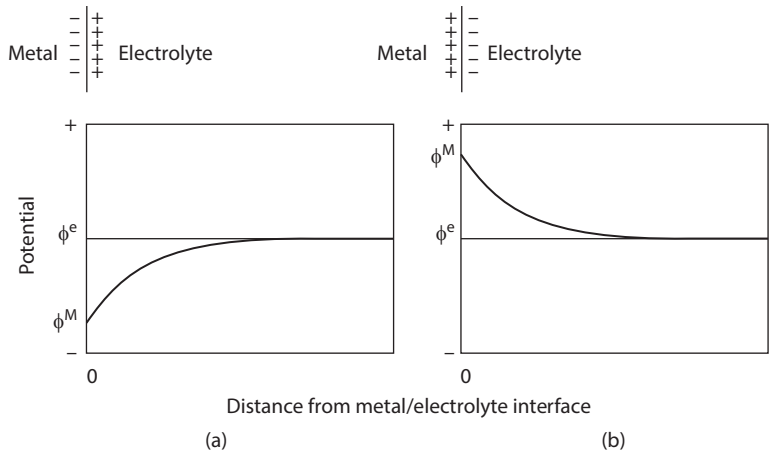

FIGURE 14.3 A schematic representation of the variation, with distance from the metal/electrolyte interface, of the potential when (a) the metal electrode acquires a negative charge, and (b) when the electrode acquires a positive charge.

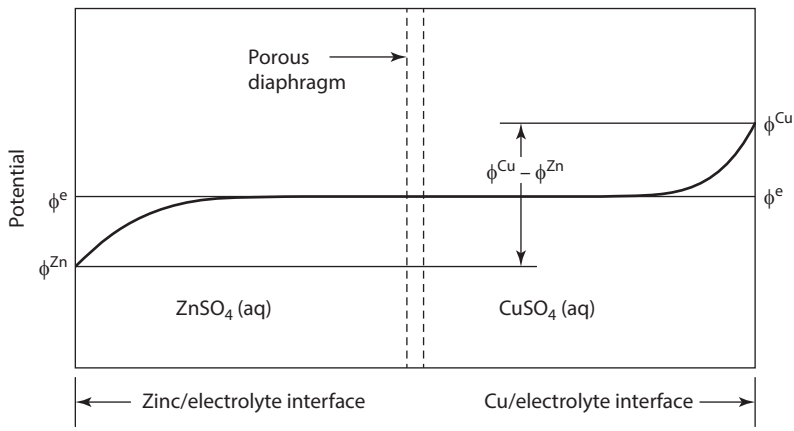

FIGURE 14.4 A schematic representation of the variation of potential with position in a Daniell cell. The open cell EMF of the cell is given by $\phi^{Cu} - \phi^{Zn}$.

where:

μ_{Zn} is the chemical potential of the zinc atoms in the electrode.

$\mu_{Zn^{2+}}$ is the chemical potential of the zinc ions in the solution and in the electrode.

$\mu_{e^-}^{Zn}$ is the chemical potential of the electrons in the zinc electrode.

It is seen that the value of $\mu_{Zn^{2+}(\text{in solution})}$, which is determined by the concentration of $ZnSO_4$ in the solution, determines the equilibrium value of $\mu_{e^-}^{Zn}$.

Similarly, the equilibrium

$$Cu^{2+} + 2e^- = Cu$$

is established at the copper–electrolyte interface when

$$\mu_{Cu^{2+}}\left(\text{in the solution}\right) = \mu_{Cu^{2+}}\left(\text{in the copper electrode}\right)$$

and

$$\mu_{Cu^{2+}} + 2\mu_{e^-}^{Cu} = \mu_{Cu}$$

Again it is seen that the equilibrium value of $\mu_{e^-}^{Cu}$ is determined by the concentration of $CuSO_4$ in the electrolyte. If identical pieces of metal wire are joined to each of the electrodes as extensions, as shown in Figure 14.2 (I and II), then since both the wire–Zn electrode and the wire–Cu electrode are electrical conductors,

$$\mu^{I} = \mu_{e^-}^{Zn} \quad \text{and} \quad \mu^{II} = \mu_{e^-}^{Cu}$$

The reversible transfer of *dn* moles of electrons from the electric potential ϕ^{Zn} to the electric potential ϕ^{Cu} involves the performance of work $\delta w'_{max}$ given by

$$\delta w'_{max} = zf \cdot \left(\phi^{Cu} - \phi^{Zn}\right) \cdot dn$$

The reversible transfer of *dn* moles of electrons from the chemical potential μ^{I} to μ^{II} at constant temperature and pressure also involves the performance of work $\delta w'_{max}$ and a decrease in the Gibbs free energy, *dG′*, of the system according to

$$\delta w'_{max} = -dG' = -\left(\mu^{II} - \mu^{I}\right) dn$$

Thus,

$$\left(\mu^{II} - \mu^{I}\right) = zf\left(\phi^{Cu} - \phi^{Zn}\right) \tag{14.3}$$

where, for electrons, *z* has the value of minus unity. Equation 14.3 relates the chemical potential difference and the electric potential difference for electron transfer. The difference $\phi^{Cu} - \phi^{Zn}$ is called the *open-circuit EMF*, ε, of the Daniell cell.

When an opposing electric potential of magnitude ε is applied externally between the electrodes I and II, the entire system is at equilibrium. This is because the *chemical driving force* of the cell is exactly balanced by the *external opposing voltage*. If the magnitude of the external opposing voltage is decreased, equilibrium no longer exists, and electronic current flows through the external circuit from I to II, with the equivalent ionic current flowing through the cell.

In the Daniell cell, the ionic current through the cell involves the transport of SO_4^{2-} ions from the solution in the $CuSO_4$ compartment (*the catholyte*) to the $ZnSO_4$ compartment (*the anolyte*) at a rate equal to that of the addition of Zn^{2+} ions to the anolyte and, hence, equal to the rate of removal of Cu^{2+} ions from the catholyte. As the cell reaction proceeds, the concentration of $CuSO_4$ in the catholyte decreases, and the concentration of $ZnSO_4$ in the anolyte increases. As has been seen, the equilibrium values of μ^{I} and μ^{II}, and hence the value of ε, depend on the concentrations of $ZnSO_4$ and $CuSO_4$ in the electrolyte, and thus, eventually, in the absence of unfavorable

kinetic factors, the EMF of the cell decreases to the value of the externally applied opposing voltage, at which point the passage of electric current ceases and a new equilibrium is established. If, however, by appropriate addition and removal, the concentrations of $ZnSO_4$ and $CuSO_4$ in their respective compartments are maintained constant, the cell reaction continues indefinitely. When the externally applied voltage is finitely less than the EMF of the cell, a finite current flows and the cell reaction proceeds irreversibly. In such a situation, less than maximum work is obtained since the electrons in the external circuit are being transported through a smaller difference in voltage. In the limit of decrease of the external voltage—that is, when the external voltage is zero and the cell is short-circuited—the degree of irreversibility of the reaction is maximized, no work is done, and the decrease in the Gibbs free energy of the system appears entirely as thermal energy. This system corresponds to that of placing a piece of zinc in an aqueous solution of $CuSO_4$.

For the production of maximum work, the cell must be operated reversibly, in which case the externally applied voltage must be only infinitesimally smaller than the EMF of the cell, giving an infinitesimal flow of current in the forward direction. If the cell can be operated reversibly, then an infinitesimal increase in the magnitude of the external voltage reverses the direction of the current flow and the direction of the cell reaction. The cell thus becomes current consuming rather than current producing; that is, it becomes an *electrolysis cell* instead of a galvanic cell. This scheme is illustrated in Figure 14.5.

When operating as a galvanic cell, the anodic oxidation reaction

$$\mathrm{Zn} = \mathrm{Zn}^{2+} + 2e^-$$

occurs at the Zn anode and the cathodic reduction reaction

$$\mathrm{Cu}^{2+} + 2e^- = \mathrm{Cu}$$

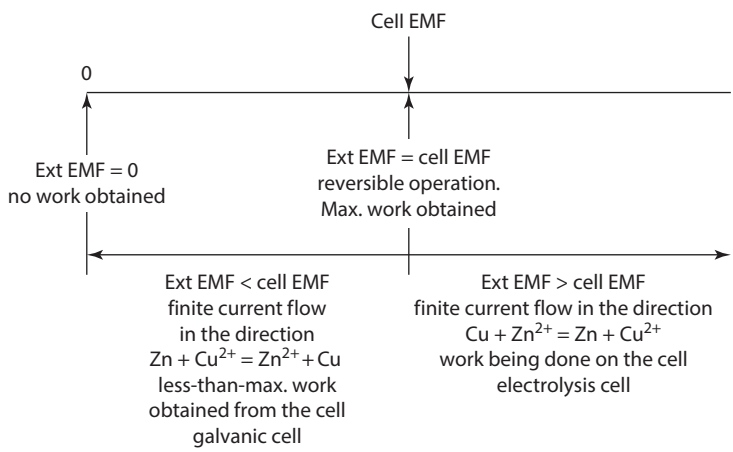

FIGURE 14.5 The relationship of a current-producing cell (a galvanic cell) to a current-consuming cell (an electrolysis cell).

occurs at the Cu cathode. The overall cell reaction is the sum of these, which gives

$$Zn + CuSO_4 = Cu + ZnSO_4$$

In shorthand notation, this is written as

$$Zn\left|Zn^{2+}\left(\text{aqueous solution}\right)\right.\vdots\left.Cu^{2+}\left(\text{aqueous solution}\right)\right|Cu$$

where the full vertical lines indicate phase boundaries in the cell and the dashed vertical line represents the porous diaphragm separating the two aqueous solutions.

14.3 THE EFFECT OF CONCENTRATION ON EMF

In the preceding section, it was seen that the EMF of a Daniell cell is dependent on the concentrations of $CuSO_4$ and $ZnSO_4$ in the catholyte and anolyte, respectively. The quantitative relationship between the concentration, or correctly, the activity, and the EMF can be introduced as follows. Consider the reaction

$$Zn + CuSO_4 = Cu + ZnSO_4$$

Although it was assumed that the reaction, as written, proceeds spontaneously from left to right, the direction depends on the states of the reactants and products. Consider the reactants and products to occur in their standard states at 298 K. Then,

$$Zn_{(s)} + CuSO_4\left(\text{saturated aqueous solution}\right)$$

$$= Cu_{(s)} + ZnSO_4\left(\text{saturated aqueous solution}\right)$$

which is thermodynamically equivalent to

$$Zn_{(s)} + CuSO_{4(s)} = Cu_{(s)} + ZnSO_{4(s)}$$

At 298 K, $\Delta G = \Delta G^{\circ}_{298\,\mathrm{K}} = -213{,}040$ J, and thus, from Equation 14.2,

$$\varepsilon^{\circ} = -\frac{\Delta G^{\circ}}{zf} = \frac{213{,}040}{2 \times 96{,}487} = 1.104 \text{ volts}$$

where ε°, is the EMF of the cell when the reactants and products occur in their designated standard states, and is termed the *standard EMF* of the cell. Thus, when Zn is immersed in a saturated aqueous solution of $ZnSO_4$ and Cu is immersed into a saturated aqueous solution of $CuSO_4$, the externally applied voltage that is required to balance the chemical driving force of the cell reaction at 298 K is 1.104 volts.

For the general reaction

$$aA + bB = cC + dD$$

when the reactants and products do not occur in their standard states, it was shown in Chapter 13 that:

$$\Delta G = \Delta G^\circ + RT \ln \frac{a_C^c a_D^d}{a_A^a a_B^b} \tag{13.4}$$

and, from Equation 14.2, the EMF of the cell in which the preceding reaction is occurring electrochemically is

$$\varepsilon = \varepsilon^\circ - \frac{RT}{zf} \ln \frac{a_C^c a_D^d}{a_A^a a_B^b} \tag{14.4}$$

Thus, with pure Zn and Cu in the Daniell cell, the EMF is given as

$$\varepsilon = \varepsilon^\circ - \frac{RT}{2f} \ln \frac{a_{\mathrm{ZnSO_4}}}{a_{\mathrm{CuSO_4}}}$$

which, at 298 K, gives

$$\varepsilon = 1.104 - 0.01284 \ln \frac{a_{\mathrm{ZnSO_4}}}{a_{\mathrm{CuSO_4}}}$$

In order that the EMF of the cell be zero, the activity quotient must be

$$e^{\frac{1.104}{0.01284}} = 2.2 \cdot 10^{37}$$

Thus, if the $ZnSO_4$ solution is saturated (i.e., $a_{\mathrm{ZnSO_4}} = 1$), then it is required that the activity of $CuSO_4$ in the catholyte, with respect to the saturated solution as the standard state, be 5×10^{-38} in order that the occurrence of equilibrium does not require a backing EMF in the external circuit between the electrodes. The concentration gradient that exists across the porous diaphragm causes the diffusion of ions from one compartment to the other, and since diffusion is an *irreversible process*, the concentration gradient gives rise to a potential known as the *liquid junction potential*. This liquid junction potential must be minimized by such means as the use of a *salt bridge* between the anolyte and the catholyte.

14.4 FORMATION CELLS

An example of a cell without a liquid junction is the cell

$$\mathrm{Pb}_{(l)} \left| \mathrm{PbO}_{(l)} \right| \mathrm{O}_{2(g)}, (\mathrm{Pt})$$

in which the anode is liquid lead, the cathode is oxygen gas bubbled over an inert platinum wire immersed into the electrolyte, and the electrolyte is liquid lead oxide. In this cell, the driving force of the cell reaction

$$\mathrm{Pb}_{(l)} + \frac{1}{2} \mathrm{O}_{2(g)} = \mathrm{PbO}_{(l)}$$

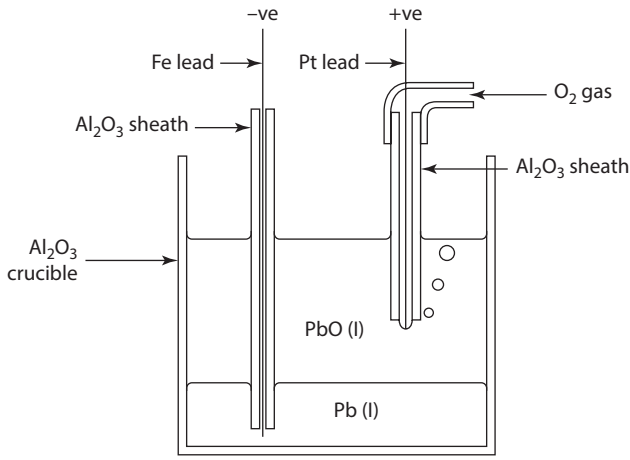

FIGURE 14.6 A lead oxide formation cell.

is the *formation* of $PbO_{(l)}$. The driving force can be balanced by the application of an opposing voltage between the electrodes. Such a cell, which is an example of a formation cell, is illustrated in Figure 14.6.[1]
Oxidation occurs at the liquid lead anode,

$$Pb = Pb^{2+} + 2e^-$$

and reduction occurs at the oxygen cathode,

$$\frac{1}{2}O_2 + 2e^- = O^{2-}$$

With a pure liquid lead anode, pure liquid PbO electrolyte, and oxygen gas at 1 atm pressure at the cathode, the standard Gibbs free energy of formation of lead oxide is obtained as

$$\Delta G^\circ = -2f\varepsilon^\circ$$

Maintaining the oxygen pressure constant at 1 atm and varying the temperature of the cell facilitate the determination of the variation of ΔG° with T. The addition to the electrolyte of a second oxide which

1 Must be chemically more stable than PbO and
2 Must not introduce any electronic conductivity (e.g., SiO_2)

influences the EMF of the cell according to

$$\varepsilon = \varepsilon^\circ - \frac{RT}{2f}\ln\frac{a_{PbO(\text{in } PbO-SiO_2)}}{p_{O_2}^{1/2}}$$

[1] R. Sridhar and J. H. E. Jeffes, "Thermodynamics of PbO and PbO–SiO_2 Melts," *Trans. Inst. Min. Metall. Ser. C* (1967), vol. 76, pp. 44–50.

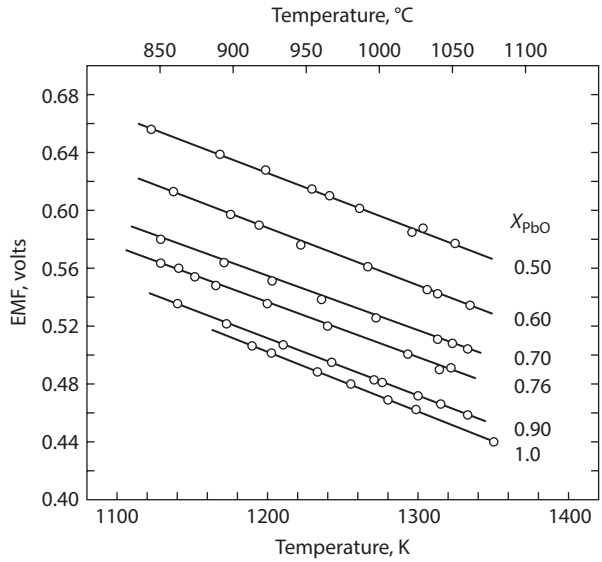

FIGURE 14.7 The variation, with temperature and silica of the electrolyte, of the EMF of the cell $PbO_{(l)}$ | $PbO–SiO_{2(l)}$ | $O_{2(1\ atm)}$, Pt. (R. Sridhar and J. H. E. Jeffes, op. cit.)

Thus, measurement of the EMF of the cell as a function of the concentration of PbO in the lead silicate from pure PbO to saturation with SiO_2 allows the determination of the variation of a_{PbO} with composition. Hence, *via* the Gibbs–Duhem relationship, the variation of a_{SiO_2} with composition can also be determined. The variation of ε° with temperature and composition of the lead silicate melts, obtained by Sridhar and Jeffes, are shown in Figure 14.7. The variation of ε° with temperature (the line in Figure 14.7 for $X_{PbO} = 1$) gives

$$\Delta G^\circ = -181,200 + 68.03T \text{ J}$$

for the cell reaction

$$Pb_{(l)} + \frac{1}{2}O_{2(g)} = PbO_{(l)}$$

14.5 CONCENTRATION CELLS

A cell that has identical electrodes inserted into solutions differing only in concentration is called a *concentration cell*.

Consider the cell

Cu | $CuSO_4$ (aq. sol'n, low concentration) | $CuSO_4$ (aq. sol'n, high concentration) | Cu

The cell reaction is

$$CuSO_4\left(\text{at high concentration}\right) \rightarrow CuSO_4\left(\text{at low concentration}\right)$$

that is, the spontaneous process is the *dilution* of $CuSO_4$. The standard EMF of such a cell is zero, and thus, the EMF is

$$\varepsilon = -\frac{RT}{2f}\ln\frac{a_{CuSO_4}\left(\text{low concentration}\right)}{a_{CuSO_4}\left(\text{high concentration}\right)}$$

If one of the aqueous solutions (say the high-concentration solution) contains $CuSO_4$ in its standard state, then

$$\varepsilon = -\frac{RT}{2f}\ln a_{CuSo_4\left(\text{low concentration}\right)} = \frac{\Delta\bar{G}^{M}_{CuSO_4}}{2f}$$

Thus, an electrochemical measurement allows the determination of the partial molal Gibbs free energy of solution of $CuSO_4$ in water. Such a cell suffers from the disadvantage of having a liquid junction potential.

A form of concentration cell of considerable importance in materials applications is the *oxygen concentration cell* which uses lime-stabilized zirconia as a *solid electrolyte*. The phase diagram for the system ZrO_2–CaO, presented as Figure 14.8, shows that the substitution of Ca^{2+} ions for Zr^{4+} ions stabilizes the high-temperature cubic polymorph of ZrO_2, and solid solutions containing up to 20 mole percent CaO can be formed. Electroneutrality in the solid solution requires that an oxygen vacancy be formed in the crystal lattice for every substitution of Ca^{2+} for Zr^{4+}, and thus, when the stabilized cubic zirconia contains x mole percent of CaO, $0.5x\%$ of the oxygen lattice sites are vacant; for example, with 20 mole percent CaO, 10% of the oxygen sites in the crystal lattice are vacant. This causes the diffusivity of oxygen in the solid solution to be high enough that, within certain ranges of oxygen pressure and temperature, the cubic solid solution is an ionic conductor in which the oxygen ion is the only mobile species.

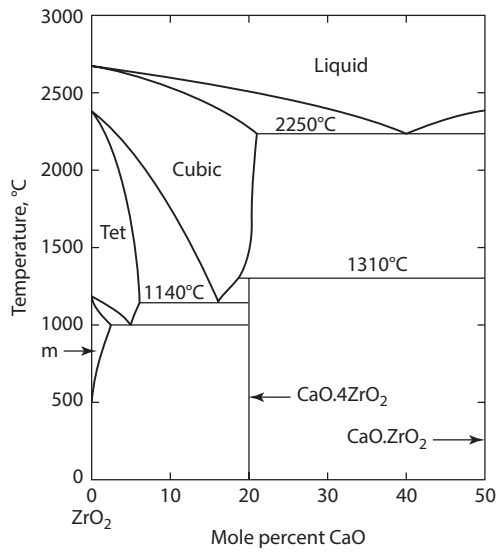

FIGURE 14.8 The phase diagram for the system ZrO –CaO (m = monoclinic polymorph, tet = tetragonal polymorph).

Thus, a cell is constructed as follows:

$$\mathrm{O_2}\left(g, \text{lower pressure I}\right), \mathrm{Pt}\left|\mathrm{CaO-ZrO_2}\right|\mathrm{Pt}, \mathrm{O_2}\left(g, \text{higher pressure II}\right)$$

in which the cell reaction is

$$\mathrm{O_2}\left(g, \text{pressure II}\right) \rightarrow \mathrm{O_2}\left(g, \text{pressure I}\right)$$

has the EMF

$$\varepsilon = -\frac{RT}{4f}\ln\frac{p_{\mathrm{O_2(I)}}}{p_{\mathrm{O_2(II)}}}$$

In the operation of the cell, oxygen ions are transported through the electrolyte from the cathode to the anode (or oxygen vacancies diffuse in the reverse direction), and electrons are transported through the external circuit from the anode to the cathode. The oxygen pressures at the electrodes can be fixed by using metal–metal oxide couples; for example, using the couples X–XO and Y–YO, the cell becomes

$$\mathrm{X}\left|\mathrm{XO}\right|\mathrm{CaO-ZrO_2}\left|\mathrm{YO}\right|\mathrm{Y}$$

At the temperature T, the lower anode oxygen pressure $p_{\mathrm{O_2(X/XO)}}$ is fixed by the establishment of the chemical equilibrium

$$\mathrm{X}_{(s)} + \frac{1}{2}\mathrm{O}_{2(g)} = \mathrm{XO}_{(s)}$$

and the higher cathode oxygen pressure $p_{\mathrm{O_2(Y/YO)}}$ is fixed by the establishment of the chemical equilibrium

$$\mathrm{Y}_{(s)} + \frac{1}{2}\mathrm{O}_{2(g)} = \mathrm{YO}_{(s)}$$

Thus, the anode half-cell reaction can equivalently be regarded as being

$$\mathrm{X} + \frac{1}{2}\mathrm{O_2}\left(\text{at } p_{\mathrm{O_2(eq.}T\mathrm{, X/XO)}}\right) = \mathrm{XO}$$

or

$$\mathrm{O^{2-}} - 2e^- = \frac{1}{2}\mathrm{O_2}\left(\text{at } p_{\mathrm{O_2(eq.}T\mathrm{, X/XO)}}\right)$$

and, similarly, the cathode half-cell reaction can equivalently be regarded as being

$$\mathrm{YO} = \mathrm{Y} + \frac{1}{2}\mathrm{O_2}\left(\text{at } p_{\mathrm{O_2(eq.}T\mathrm{,Y/YO)}}\right)$$

or

$$\frac{1}{2}\mathrm{O_2}\left(\text{at } p_{\mathrm{O_2(eq.}T\mathrm{,Y/YO)}}\right) + 2e^- = \mathrm{O^{2-}}$$

The cell reaction is thus

$$\mathrm{YO} + \mathrm{X} = \mathrm{XO} + \mathrm{Y} \tag{i}$$

or

$$\frac{1}{2}\mathrm{O_2}\left(\text{at } p_{\mathrm{O_2}(\text{eq.}T,\mathrm{Y/YO})}\right) = \frac{1}{2}\mathrm{O_2}\left(\text{at } p_{\mathrm{O_2}(\text{eq.}T,\mathrm{X/XO})}\right) \tag{ii}$$

Thus, whereas the chemical equilibrium between the pure reactants and products

$$\mathrm{YO} + \mathrm{X} = \mathrm{XO} + \mathrm{Y}$$

could be obtained only at the single invariant temperature (e.g., at T_E in Figure 12.4) in which state

$$p_{\mathrm{O_2}(\text{eq.}T,\mathrm{X/XO})} = p_{\mathrm{O_2}(\text{eq.}T,\mathrm{Y/YO})}$$

the electrochemical equilibrium

$$\mathrm{YO} + \mathrm{X} = \mathrm{XO} + \mathrm{Y}$$

can be obtained at any temperature (within the limits imposed by the performance of the ZrO_2–CaO electrolyte) by placing an external voltage in opposition to the chemical driving force of the cell. For either Equation (i) or (ii), the chemical driving force is

$$\Delta G = RT \ln \frac{p^{1/2}_{\mathrm{O_2}(\text{eq.}T,\mathrm{X/XO})}}{p^{1/2}_{\mathrm{O_2}(\text{eq.}T,\mathrm{Y/YO})}}$$

and hence the cell EMF is

$$\varepsilon = -\frac{RT}{2f} \ln \frac{p^{1/2}_{\mathrm{O_2}(\text{eq.}T,\mathrm{X/XO})}}{p^{1/2}_{\mathrm{O_2}(\text{eq.}T,\mathrm{Y/YO})}}$$

or

$$\varepsilon = -\frac{RT}{4f} \ln \frac{p_{\mathrm{O_2}(\text{eq.}T,\mathrm{X/XO})}}{p_{\mathrm{O_2}(\text{eq.}T,\mathrm{Y/YO})}} \tag{iii}$$

If one of the metals—say, X—is dissolved in an inert solvent, where the requirement for "inertness" is that the equilibrium oxygen pressure for the solvent metal–solvent metal oxide equilibrium is considerably higher than $p_{\mathrm{O_2}(\text{eq.}T,\mathrm{X/XO})}$, then the activity of X in the alloy can be obtained as follows. If X in solution is denoted $\underline{\mathrm{X}}$, then the EMF of the cell

$$\underline{\mathrm{X}}\,|\,\mathrm{XO}\,|\,\mathrm{CaO} - \mathrm{ZrO_2}\,|\,\mathrm{Y}\,|\,\mathrm{YO}$$

is

$$\varepsilon' = -\frac{RT}{4f}\ln\frac{p_{O_2(\text{eq.}T,\underline{X}/XO)}}{p_{O_2(\text{eq.}T,Y/YO)}} \tag{iv}$$

At the temperature T,

$$a_X p^{1/2}_{O_2(\underline{X},XO)} = p^{1/2}_{O_2(X,XO)}$$

combination of Equations (iii) and (iv) gives

$$\varepsilon - \varepsilon' = -\frac{RT}{4f}\ln a_X$$

and thus, measurement of the variation of ε' with the composition of the alloy allows the determination of the activity–composition relationship of X in the alloy.

More simply, if the cell is

$$X\ |XO|\,CaO - ZrO_2\,|\underline{X}|\,XO$$

then

$$\varepsilon = \frac{RT}{2f}\ln\frac{p^{1/2}_{O_2(\text{eq.}T,\underline{X}/XO)}}{p^{1/2}_{O_2(\text{eq.T},X/XO)}} = -\frac{RT}{2f}\ln a_X = -\frac{\Delta\bar{G}^{M}_X}{2f}$$

Similarly, if the metal oxide XO is dissolved in an inert oxide solvent, then, denoting dissolved XO as $\underline{XO}$, for the cell

$$X\,|\underline{XO}|\,CaO - ZrO_2\,|X|\,XO$$

$$\varepsilon = -\frac{RT}{2f}\ln\frac{p^{1/2}_{O_2(\text{eq.}T,X/XO)}}{p^{1/2}_{O_2(\text{eq.}T,X/XO)}}$$

and, since

$$a_{\underline{XO}} = \frac{p^{1/2}_{O_2(\text{eq.}T,X/XO)}}{p^{1/2}_{O_2(\text{eq.}T,X/XO)}}$$

then

$$\varepsilon = -\frac{RT}{2f}\ln a_{XO}$$

This technique has been used by Kozuka and Samis[2] to measure the activities of PbO in the melt in the system $PbO–SiO_2$ using the cell

[2] Z. Kozuka and C. S. Samis, "Thermodynamic Properties of Molten $PbO–SiO_2$ Systems," *Met. Trans.* (1970), vol. 1, (4) p. 871.

$$\mathrm{Pb}_{(l)}\left|\mathrm{PbO}_{(l,\text{in pbO}-\mathrm{SiO}_2)}\right|\mathrm{CaO}-\mathrm{ZrO}_2\left|\mathrm{Pb}_{(l)}\right|\mathrm{PbO}_{(l)}$$

Their experimental cell is illustrated in Figure 14.9, and their results, at 1000°C, are shown, in comparison with those obtained by Sridhar and Jeffes, in Figure 14.10.

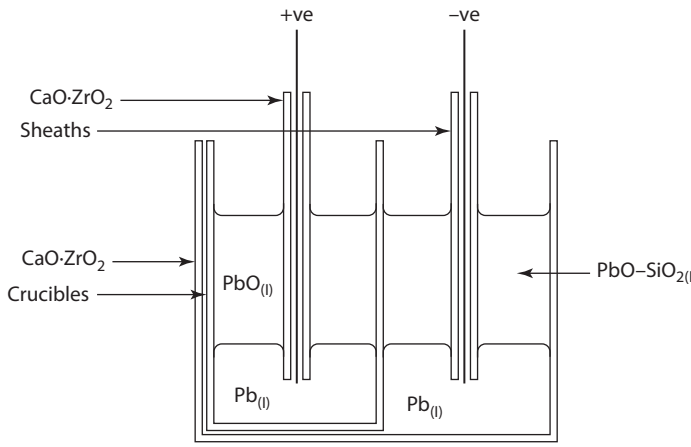

FIGURE 14.9 A lead oxide concentration cell using stabilized zirconia as the solid-state electrolyte.

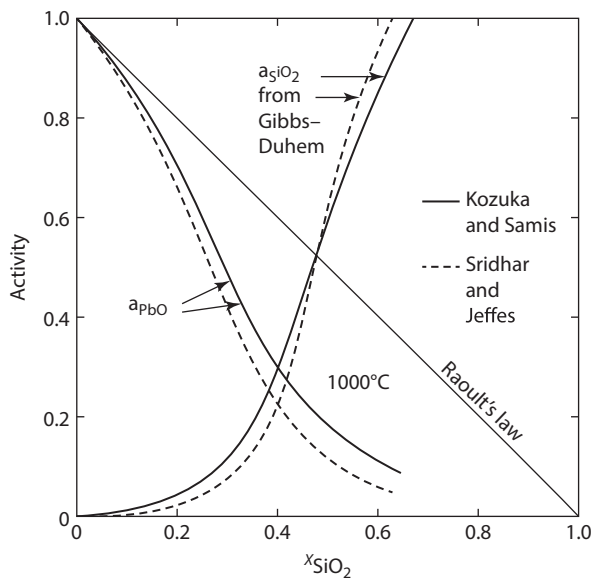

FIGURE 14.10 The activities of PbO in liquid PbO–SiO_2 determined from a PbO concentration cell. (From: Z. Kozuka and C. S. Samis, op. cit.

14.6 THE TEMPERATURE COEFFICIENT OF THE EMF

For any cell reaction at constant temperature and pressure,

$$\Delta G = -zf\varepsilon$$

Differentiation with respect to temperature at constant pressure gives

$$\left(\frac{\partial \Delta G}{\partial T}\right)_P = -zf\left(\frac{\partial \varepsilon}{\partial T}\right)_P = -\Delta S$$

Thus, for the cell reaction,

$$\Delta S = zf\left(\frac{\partial \varepsilon}{\partial T}\right)_P \tag{14.5}$$

and

$$\Delta H = -zf\varepsilon + zfT\left(\frac{\partial \varepsilon}{\partial T}\right)_P \tag{14.6}$$

From Equation 14.5, the slopes of the lines in Figure 14.7 are equal to $\Delta S/zf$ for the cell reaction in the formation cell $Pb + ½O2 = PbO$. The slope of the line for $X_{PbO} = 1$ gives

$$\Delta S_{(a)} = S^{\circ}_{PbO(l)} - S^{\circ}_{Pb(l)} - \frac{1}{2}S^{\circ}_{O_2(g)}$$

and the slopes of the lines for melts of $X_{PbO} < 1$ give

$$\Delta S_{(b)} = \bar{S}_{PbO \text{ at } X_{PbO}} - S^{\circ}_{Pb(l)} - \frac{1}{2}S^{\circ}_{O_2(g)}$$

Thus, the partial molar entropy of mixing of PbO in a melt of composition X_{PbO}, $\Delta\bar{S}^{M}_{PbO}$, is given by $\Delta S_{(b)} - \Delta S_{(a)}$. Both of the values of ΔS are negative since in each of the reaction the oxygen gas is consumed. $\Delta S_{(b)} - \Delta S_{(a)} > 0$ since the entropy of the solution of Si in PbO is greater than that of pure PbO.

In *concentration cells* such as

$$A\left|A^{z+}X^{z-}\right|A\left(\text{in an A–B alloy}\right)$$

since

$$\varepsilon = -\frac{RT}{zf}\ln a_A$$

the partial molar properties of A in the A–B alloy are obtained as

$$\Delta\bar{S}^{M}_{A} = zf\frac{\partial \varepsilon}{\partial T}$$

and

$$\Delta\bar{H}_{\mathrm{A}}^{\mathrm{M}} = -zf\varepsilon + zfT\frac{\partial\varepsilon}{dT}$$

Alternatively, from measurements on formation cells of the type

$$\mathrm{A}\left|\mathrm{A}^{2+}\mathrm{X}^{2-}\right|X_{2(g,1\ \mathrm{atm})}$$

for which

$$\varepsilon_{(\mathrm{i})} = \varepsilon^{\circ}$$

and measurements on cells of the type

$$\mathrm{A}\left(\text{in A–B alloy}\right)\left|\mathrm{A}^{2+}\mathrm{X}^{2-}\right|\mathrm{X}_{2(g,1\ \mathrm{atm})}$$

for which

$$\varepsilon_{(\mathrm{ii})} = \varepsilon^{\circ} - \frac{RT}{2f}\ln\left(\frac{1}{a_{\mathrm{A}}}\right)$$

the value of a_A is obtained from

$$\varepsilon_{(\mathrm{ii})} - \varepsilon_{(\mathrm{i})} = \frac{RT}{2f}\ln a_{\mathrm{A}}$$

Variation with temperature then gives

$$\Delta\bar{S}_{\mathrm{A}}^{\mathrm{M}} = 2f\frac{\partial}{\partial T}\left(\varepsilon_{(\mathrm{i})} - \varepsilon_{(\mathrm{ii})}\right)$$

and

$$\Delta\bar{H}_{\mathrm{A}}^{\mathrm{M}} = 2f\left(\varepsilon_{(\mathrm{ii})} - \varepsilon_{(\mathrm{i})}\right) - 2fT\frac{\partial}{\partial T}\left(\varepsilon_{(\mathrm{ii})} - \varepsilon_{(\mathrm{i})}\right)$$

Belton and Rao[3] measured the EMFs of the cells

$$\mathrm{Mg}_{(l)}\left|\mathrm{MgCl}_{2(l)}\right|\mathrm{Cl}_{2(g,1\ \mathrm{atm})}$$

and

$$\mathrm{Mg}\left(\text{in Mg–Al}\right)_{(l)}\left|\mathrm{MgCl}_{2(l)}\right|\mathrm{Cl}_{2(g,1\ \mathrm{atm})}$$

[3] G. R. Belton and Y. K. Rao, "A Galvanic Cell Study of Activities in Mg–Al Liquid Alloys," *Trans. Met. Soc. AIME* (1969), vol. 245, p. 2189.

in the range of temperature 700°C–1000°C with Mg–Al alloys in the range $X_{Mg} = 0.096 - 0.969$. With pure Mg as the anode, they obtained

$$\varepsilon^\circ = 3.135 - 6.5 \times 10^{-4} T \,(\text{volts})$$

which gives, for the reaction

$$Mg_{(l)} + Cl_{2(g)} = MgCl_{2(l)}$$

$$\Delta G^\circ = -604{,}970 + 125.4T \text{ J}$$

Thus, temperature coefficients of the EMF of cells allows for the calculation of activities and related thermodynamics variables of the electrode components.

14.7 THERMAL ENERGY (HEAT) EFFECTS

In examining the properties of enthalpy, H, in Chapter 5, it was noted that the change in the enthalpy of a system equals the *thermal energy* entering or leaving the system during a constant-pressure process only if the work of volume change (the PdV work) is the sole form of work performed on or by the system. If an electrochemical reaction is conducted in a galvanic cell, as a result of which electrical work is performed, $\Delta H \neq q_P$.

For a change of state at constant temperature and pressure, Equation 5.6 gave

$$\Delta G = q - w + P\Delta V - T\Delta S$$

$$= q - w' - T\Delta S$$

where w' is the sum of all the non-PV work terms.

If $w' = 0$, then, $q = \Delta G + T\Delta S = \Delta H$. But, if the process, which involves the performance of work w', is conducted reversibly, in which case $-w' = -w'_{\max} = \Delta G$, then

$$q = T\Delta S$$

Consider the Daniel cell reaction $Zn + CuSO_4 = Cu + ZnSO_4$. When the reactants and products are in their standard states (pure metals and saturated aqueous solutions), the change in the Gibbs free energy for the cell reaction is

$$\Delta G^\circ = -208{,}800 - 13.9T \text{ J}$$

If the reaction occurs as a result of placing pure solid zinc into a saturated copper sulfate solution at 25°C, in which case the reaction proceeds spontaneously and w' is zero, then, for the formation of saturated zinc sulfate solid and copper, per mole of the reaction,

$$\Delta H^\circ = -208{,}800 \text{ J}$$

which is the thermal energy that *flows from* the system into the constant temperature heat reservoir.

However, if the reaction is conducted reversibly in a Daniell cell, in which case

$$w' = -\Delta G^\circ = 208{,}800 + 13.9 \times 298$$

then $q = T\Delta S = 13.9 \times 298 = +4140$ J is the thermal energy that *is transferred into* the system from the constant temperature reservoir.

14.8 THE THERMODYNAMICS OF AQUEOUS SOLUTIONS

The composition of an aqueous solution is usually expressed in terms of the molality, m, or the molarity, M, where the molality is the number of moles of solute present per 1000 g of solvent, and the molarity is the number of moles of solute present in 1 liter of solution.

Mole fraction, molality, and molarity are related as follows. Consider an aqueous solution of m_i moles of solute i in 1000 g of H_2O, such that the solution is m_i molal. Since the molecular weight of H_2O is 18, 1000 g of H_2O contains 1000/18 g-moles, and hence,

$$X_i = \frac{n_i}{n_i + n_{H_2O}} = \frac{m_i}{m_i + 1000/18}$$

Consider an M_i molar solution that contains M_i moles of solute i per liter of solution—that is, in 1000ρ g of the solution, where ρ is the density of the solution in g/cm^3. The number of g-moles of H_2O in the liter of solutions is $(1000\rho - M_i\,\mathrm{MW}_i)/18$, where MW_i is the molecular weight of i, and thus,

$$X_i = \frac{n_i}{n_i + n_{H_2O}} = \frac{M_i}{M_i + \left(1000\rho - M_i \mathrm{MW}_i\right)/18}$$

As the solution tends toward infinite dilution,

$$m_i \to \frac{1000 X_i}{18} \quad \text{and} \quad M_i \to \frac{1000\rho X_i}{18}$$

In dilute solutions, molality and molarity are essentially equal to one another; for example, an aqueous solution of NaCl of $X_{NaCl} = 10^{-3}$ is 0.0556 molal and 0.0554 molar.

In the case of dilute solutes in liquid metals, it is convenient to define the 1 wt% standard state, and hence the 1 wt% activity scale, as

$$h_{i(1\,\mathrm{wt\%})} \to [\mathrm{wt\%}i] \quad \text{as} \quad [\mathrm{wt\%}i] \to 0$$

with the 1 wt% standard state located on the Henry's law line at 1 wt%. It is also convenient, in aqueous solutions, to define the analogous unit molality standard state, and hence unit molality activity scale, as

$$a_{i(m)} \to m_i \text{ as } m_i \to 0$$

where $a_{i(m)}$ is the activity of the solute with respect to the unit molality standard state, and the unit molality standard state is located on the Henry's law line at $m_i = 1$. As before, deviations from ideality are accommodated by introducing an activity coefficient defined as

$$\gamma_{i(m)} = \frac{a_{i(m)}}{m_i}$$

Consider the electrolyte (or salt) $A_a Y_y$, which, when dissolved in water, dissociates to form A^{z+} cations and Y^{z-} cations according to

$$A_a Y_y = aA^{z+} + yY^{z-}$$

When m moles of $A_a Y_y$ are dissolved in n moles of H_2O, the solution formed can be considered either

1. A solution containing m moles of the component $A_a Y_y$ and n moles of H_2O, or
2. A solution of am moles of A^{z+} and ym moles of Y^{z-} in n moles of H_2O

In case 1, the variation of the Gibbs free energy of the solution with composition at constant T and P is given by Equation 9.16 as

$$dG' = \bar{G}_{A_a Y_y} dm + \bar{G}_{H_2O} dn \tag{i}$$

In case 2, the stoichiometry of the dissociation is such that the number of moles of A^{z+}, m_A^{z+}, is am and the number of moles of Y^{z-}, m_Y^{z-}, is ym. Thus,

$$dm_A^{z+} = a\,dm \quad \text{and} \quad dm_{Y^{z-}} = y\,dm$$

and, at constant T and P,

$$\begin{aligned} dG' &= \bar{G}_{A^{z+}} dm_{A^{z+}} + \bar{G}_{A^{z+}} dm_{A^{z+}} + \bar{G}_{H_2O} dn \\ &= \left(a\bar{G}_{A^{z+}} + y\bar{G}_{A^{z+}}\right) dm + \bar{G}_{H_2O} dn \end{aligned} \tag{ii}$$

By definition,

$$\bar{G}_{A_a Y_y} = \left(\frac{\partial G'}{\partial m}\right)_{T,P,n}$$

$$\bar{G}_{A^{z+}} = \left(\frac{\partial G'}{\partial m_{A^{z+}}}\right)_{T,P,n,m_{Y^{z-}}}$$

and

$$\bar{G}_{Y^{z-}} = \left(\frac{\partial G'}{\partial m_{Y^{z-}}}\right)_{T,P,n,m_{A^{z+}}}$$

Since m can be varied at constant n, $\bar{G}_{\mathrm{A}_a\mathrm{Y}_y}$ can be determined experimentally. However, since $m_{\mathrm{A}^{z+}}$ an $m_{\mathrm{Y}^{z-}}$ cannot be varied independently, neither $\bar{G}_{\mathrm{A}^{z+}}$ nor $\bar{G}_{\mathrm{Y}^{z-}}$ can be measured. Combination of Equations (i) and (ii) gives

$$\bar{G}_{\mathrm{A}_a\mathrm{Y}_y} = a\bar{G}_{\mathrm{A}^{z+}} + y\bar{G}_{\mathrm{Y}^{z-}} \tag{iii}$$

which shows that, although neither $\bar{G}_{\mathrm{A}^{z+}}$ nor $y\bar{G}_{\mathrm{Y}^{z-}}$ can be measured, the combination given by Equation (iii) can be measured.

If the component $\mathrm{A}_a\,\mathrm{Y}_y$ occurs in the unit molality standard state, Equation (iii) is written as

$$G^{\circ}_{\mathrm{A}_a\mathrm{Y}_y} = aG^{\circ}_{\mathrm{A}^{z+}} + yG^{\circ}_{\mathrm{Y}^{z-}} \tag{iv}$$

and subtraction of Equations (iv) from (iii), noting that

$$\bar{G}_i - G^{\circ}_i = RT\ln a_i$$

gives, on rearrangement,

$$a_{\mathrm{A}_a\mathrm{Y}_y} = a^a_{A^{z+}} + a^y_{\mathrm{Y}^{z-}} \tag{v}$$

Thus, again, although neither $a_{A^{z+}}$ nor $a_{\mathrm{Y}^{z-}}$ can be measured experimentally, which necessarily means that neither $a_{A^{z+}}$ nor $a_{\mathrm{Y}^{z-}}$ has any physical significance, the product given by Equation (v) can be measured and does have a physical significance. Equation (v) can be written as

$$\begin{aligned} a_{\mathrm{A}_a\mathrm{Y}_y} &= \left(\gamma_{\mathrm{A}^{z+}} m_{\mathrm{A}^{z+}}\right)^a \left(\gamma_{\mathrm{Y}^{z-}} m_{\mathrm{Y}^{z-}}\right)^y \\ &= \gamma^a_{\mathrm{A}^{z+}}\gamma^y_{\mathrm{A}^{z-}} m^a_{\mathrm{A}^{z+}} m^y_{\mathrm{Y}^{z-}} \end{aligned} \tag{vi}$$

The mean ionic molality, $m_{\pm}$, is defined as

$$m_{\pm} = \left(m^a_{\mathrm{A}^{z+}} m^y_{\mathrm{Y}^{z-}}\right)^{\frac{1}{(a+y)}} \tag{vii}$$

and the mean ion activity coefficient, $\gamma_{\pm}$, is defined as

$$\gamma_{\pm} = \left(\gamma^a_{\mathrm{A}^{z+}}\gamma^y_{\mathrm{Y}^{z-}}\right)^{\frac{1}{(a+y)}} \tag{viii}$$

Thus, substitution of Equations (vii) and (viii) in Equation (vi) gives

$$a_{\mathrm{A}_a\mathrm{Y}_y} = \left(\gamma_{\pm} m_{\pm}\right)^{a+y} \tag{ix}$$

Consider an m molar solution of NaCl. Since $\left|\underline{z}^+\right|$ and $\left|\underline{z}^-\right| = 1$ and $a = y = 1$, Equation (ix) gives

$$a_{\mathrm{NaCl}_{(m)}} = \left(\gamma_{\pm} m_{\pm}\right)^2$$

and Equation (vii) gives

$$m_{\pm} = (mm)^{1/2}$$

Thus,

$$a_{\mathrm{NaCl}_{(m)}} = \left(\gamma_{\pm} m_{\mathrm{NaCl}}\right)^2$$

and Henrian behavior follows

$$a_{\mathrm{NaCl}_{(m)}} = m^2_{\mathrm{NaCl}}$$

In an m molal solution of $CaCl_2$, since $|z^+| = 2, |z^-| = 1, \quad a = 1, \quad \text{and} \quad y = 2,$

$$a_{\mathrm{CaCl_2}_{(m)}} = \left(\gamma_{\pm} m_{\pm}\right)^3$$

$$m_{\pm} = \left[m(2m)^2\right]^{1/3}$$

and thus,

$$a_{\mathrm{CaCl_2}_{(m)}} = 4\left(\gamma_{\pm} m_{\mathrm{CaCl_2}}\right)^3$$

Similarly, in an m molal solution of $Fe_2(SO_4)_3$,

$$a_{\mathrm{Fe_2(SO_4)_3}_{(m)}} = 36\left(\gamma_{\pm} m_{\mathrm{Fe_2(SO_4)_3}}\right)^5$$

14.9 THE GIBBS FREE ENERGY OF FORMATION OF IONS AND STANDARD REDUCTION POTENTIALS

Consider the cell

$$\mathrm{Pt, H_{2(g)} \left| HCl_{(aqueous)} \right| Hg_2Cl_{2(s)} \mid Hg_{(l)}}$$

set up as shown in Figure 14.11. The half-cell reaction at the anode is

$$\frac{1}{2}\mathrm{H_2} = \mathrm{H^+} + e^-$$

and the Hg_2Cl_2 (*calomel*) half-cell reaction at the cathode is

$$\frac{1}{2}\mathrm{Hg_2Cl_2} + e^- = \mathrm{Hg} + \mathrm{Cl^-}$$

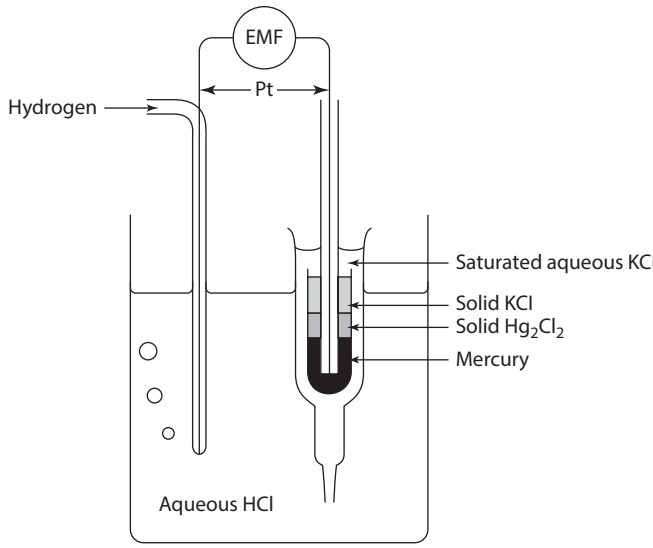

FIGURE 14.11 The calomel cell, Pt, $H_{2(g)} \mid HCl_{(aq)} \mid Hg_2Cl_2(s) \mid Hg_{(l)}$.

The overall reaction is thus

$$\frac{1}{2}H_{2(g)} + \frac{1}{2}Hg_2Cl_{2(s)} = Hg_{(l)} + HCl_{(m)} \tag{i}$$

with Hg and Hg_2Cl_2 occurring at unit activity and $p_{H_2} = 1$ atm. The EMF of the cell is

$$\varepsilon = \varepsilon^\circ - \frac{RT}{f}\ln a_{HCl_{(m)}}$$

$$= \varepsilon^\circ - \frac{RT}{f}\ln\left(\gamma_\pm m_{HCl}\right)^2$$

This expression can be rearranged as

$$\varepsilon + \frac{2RT}{f}\ln m_{HCl} = \varepsilon^\circ - \frac{2RT}{f}\ln\gamma_\pm \tag{ii}$$

in which the measurable quantities occur on the left-hand side. Extrapolation of the term $\varepsilon + 2RT\ln m_{HCl}$ to infinite dilution, where $\gamma_\pm \to 1$, allows the calculation of ε° and hence, from Equation (ii), the calculation of the variation of $\gamma_\pm$ with m_{HCl}. The value of ε° at 298 K has been determined to be 0.26796 volts, and the variation of $a_{HCl_{(m)}}$ with m^2_{HCl} is as shown in Figure 14.12. Since $\varepsilon^\circ = 0.26796$ volts,

$$\Delta G^\circ_{(i),298\,K} = -f\varepsilon^\circ = -96{,}487 \times 0.26796 = -25{,}855\ \text{J}$$

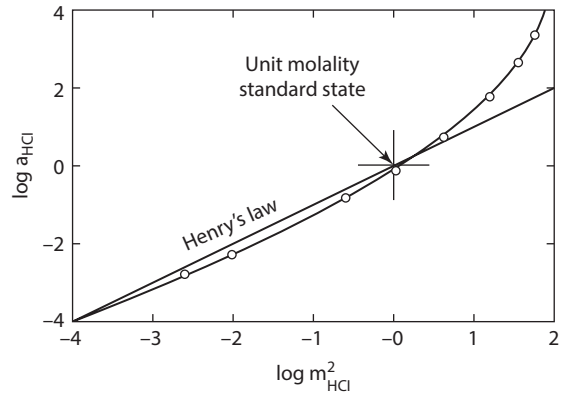

FIGURE 14.12 The activity of HCl in aqueous solution.

For

$$\mathrm{Hg}_{(l)} + \frac{1}{2}\mathrm{Cl}_{2(g)} = \frac{1}{2}\mathrm{Hg}_2\mathrm{Cl}_{2(s)} \tag{iii}$$

$$\Delta G^{\circ}_{(\mathrm{iii}),298\ \mathrm{K}} = -105,320\ \mathrm{J}$$

and thus, for

$$\frac{1}{2}\mathrm{H}_{2(g)} + \frac{1}{2}\mathrm{Cl}_{2(g)} = \mathrm{HCl}_{(m)}$$

$$\begin{aligned}\Delta G^{\circ}_{(\mathrm{iv})} &= \Delta G^{\circ}_{(\mathrm{i})} + \Delta G^{\circ}_{(\mathrm{iii})} \\ &= -25,855 - 105,320\ \mathrm{J} \\ &= -131,175\ \mathrm{J}\end{aligned} \tag{iv}$$

Thus, the standard Gibbs free energy of formation of HCl in aqueous solution at unit activity from H_2 gas and Cl_2 gas, each at 1 atm pressure, is −131,175 J at 298 K. For

$$\frac{1}{2}\mathrm{H}_{2(g)} + \frac{1}{2}\mathrm{Cl}_{2(g)} = \mathrm{HCl}_{(g)} \tag{v}$$

$$\Delta G^{\circ}_{(\mathrm{v}),298\ \mathrm{K}} = -94,540\ \mathrm{J}$$

and hence, for the change of state

$$\mathrm{HCl}_{(g)} = \mathrm{HCl}_{(m)}$$

$$\Delta G^{\circ}_{298\,\mathrm{K}} = -131{,}175 + 94{,}540$$

$$= -36{,}635 \text{ J}$$

$$= -8.3144 \times 298 \ln \frac{a_{\mathrm{HCl}(m)}}{p_{\mathrm{HCl}}}$$

Thus, at 298 K, an aqueous solution of HCl at unit activity exerts a partial vapor pressure of HCl of 3.79×10^{-7} atm.

From Equation (iv), the standard EMF of the cell

$$\mathrm{Pt}, \mathrm{H}_{2(g)} \left| \mathrm{HCl}_{(m)} \right| \mathrm{Cl}_{2(g)}, \mathrm{Pt}$$

is

$$\varepsilon^{\circ} = \frac{-\Delta G^{\circ}_{(\mathrm{iv})}}{f} = \frac{131{,}175}{96{,}487} = 1.3595 \text{ volts}$$

and the cell reaction

$$\frac{1}{2}\mathrm{H}_{2(g)} + \frac{1}{2}\mathrm{Cl}_{2(g)} = \mathrm{HCl}_{(m)}$$

or

$$\frac{1}{2}\mathrm{H}_{2(g)} + \frac{1}{2}\mathrm{Cl}_{2(g)} = \mathrm{H}^{+}_{(m)} + \mathrm{Cl}^{-}_{(m)} \tag{vi}$$

is the sum of the half-cell reactions

$$\frac{1}{2}\mathrm{H}_{2(g)} = \mathrm{H}^{+} + e^{-} \tag{vii}$$

and

$$\frac{1}{2}\mathrm{Cl}_{2} + e^{-} = \mathrm{Cl}^{-} \tag{viii}$$

14.9.1 Single Electrode Potential

It is now convenient to introduce the concept of a *half-cell*, or *single electrode potential*, the sum of which, in any cell, equals the EMF of the cell. This concept is useful in spite of the fact that it is impossible to construct, and hence to measure the potential of, a cell with a single electrode. In order to give meaning to the concept, it is necessary to choose a particular standard single electrode and arbitrarily assign it a potential of zero. In aqueous solutions, this standard single electrode is the *standard hydrogen electrode* (SHE), in which hydrogen gas at 1 atm pressure, in contact with a platinum wire, is bubbled through an aqueous solution containing hydrogen ions at unit activity.

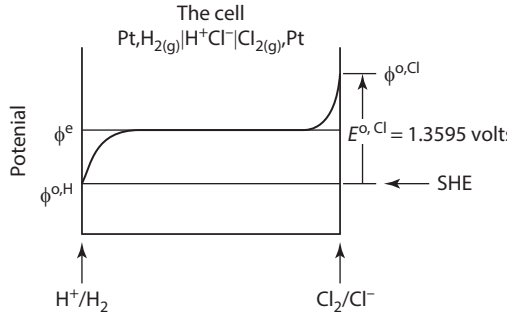

FIGURE 14.13 The relationship of the standard reduction potential of Cl to the standard hydrogen electrode and the absolute potentials in the cell $\mathrm{Pt, H_{2(g,1\,atm)}}\left|\mathrm{H^{+}_{(m)}Cl^{-}_{(m)}}\right|\mathrm{Cl_{2(g,1\,atm)}, Pt}$.

In the SHE, hydrogen gas in its standard state is arbitrarily placed at the same potential as hydrogen ions in their standard state in aqueous solution. Consider the cell

$$\mathrm{Pt, H_{2(g,1\,atm)}}\left|\mathrm{H^{+}_{(m)}Cl^{-}_{(m)}}\right|\mathrm{Cl_{2(g,1\,atm)}, Pt}$$

The variation of the potential with distance from the hydrogen gas–electrolyte interface to the chlorine gas–electrolyte interface is shown schematically in Figure 14.13. Although the value of $\phi^{\circ,e}$ is not known, the difference between $\phi^{\circ,\mathrm{Cl}}$ and $\phi^{\circ,\mathrm{H}}$ is experimentally measured as 1.3595 volts. Thus, if the absolute potential $\phi^{\circ,\mathrm{H}}$ is arbitrarily assigned the value zero, the standard electrode potential at which the reduction of $\frac{1}{2}\mathrm{Cl_2}$ to $\mathrm{Cl^-}$ occurs at the cathode is 1.3595 volts. Thus, with the standard oxidation (and hence reduction) potential of hydrogen being zero, then, algebraically, from Figure 14.13, the standard EMF of the cell, ε°, is obtained as the standard reduction potential of the cathode minus the standard reduction potential at the anode; that is,

$$\varepsilon^{\circ} = \varepsilon^{\circ,\mathrm{Cl}} - \varepsilon^{\circ,\mathrm{H}}$$

$$= 1.3595 \text{ volts}$$

Consider, again, the Daniell cell with pure Zn and Cu as electrodes and $\mathrm{Zn^{2+}}$ and $\mathrm{Cu^{2+}}$ ions at unity molality. Figure 14.14a shows a schematic variation of the potential through the electrolyte in the subcell which has the cell reaction

$$\mathrm{Zn_{(s)} + 2H^{+}_{(m)} = 2Zn^{2+}_{(m)} + H_{2(}}$$

and Figure 14.14b shows the corresponding variation through the subcell which has the cell reaction

$$\mathrm{H_{2(g)} + Cu^{2+}_{(m)} = 2H^{+}_{(m)} + Cu_{(s)}}$$

With reference to the SHE, as shown, the standard reduction potential for $\mathrm{Cu^{2+}}$ is given by $\phi^{\circ,\mathrm{Cu}} - \phi^{\circ,\mathrm{H}}$, which is experimentally measured as 0.337 volts. The standard reduction potential of copper is thus 0.337 volts. Also, with respect to the SHE, the

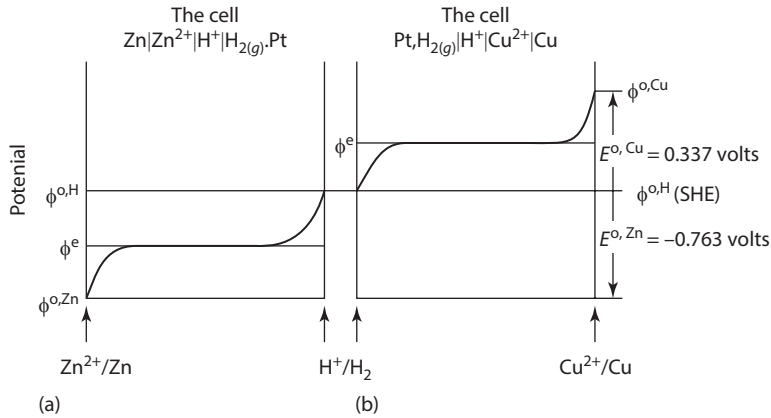

FIGURE 14.14 The relationship of the standard reduction potentials of (a) Zn and (b) Cu to the standard hydrogen electrode and the absolute potentials in the cells Zn | Zn^{2+} | H^+ | $H_{2(g)}$, Pt, and Pt, $H_{2(g)}$ | H^+ | Cu^{2+} | Cu.

standard oxidation potential for Zn is measured experimentally as $\phi^{\circ,H} - \phi^{\circ,Zn} = 0.763$. Thus, the standard reduction potential of Zn, $\varepsilon^{\circ,Zn}$, is -0.763 volts, and the standard EMF of the Daniell cell is the standard reduction potential of Cu minus the standard reduction potential of Zn; that is,

$$\varepsilon^{\circ} = 0.337 - (-0.763) = 1.100 \text{ volts}$$

The systematic list of standard reduction potentials, part of which is presented as Table 14.1, is called the *electrochemical series.*

14.9.2 Solubility Products

From Table 14.1, the standard reduction potential for sodium, $\varepsilon^{\circ,Na}$, is -2.714 volts, and the standard reduction potential for chlorine, $\varepsilon^{\circ,Cl}$, is 1.3595 volts. Thus, for the equilibrium

$$Na = Na^+ + e^-$$

$$\Delta G^{\circ} = -f\varepsilon^{\circ,Na} = -96,487 \times 2.714 = -261,870 \text{ J}$$

and for

$$\frac{1}{2}Cl_2 + e^- = Cl^-$$

$$\Delta G^{\circ} = -f\varepsilon^{\circ,Cl} = -96,487 \times 1.3595 = -131,170 \text{ J}$$

TABLE 14.1
Standard Electrode Potentials at 298 K, 1 atm

Electrode Reaction	ε°, volts
Acid Solutions	
$F_2 + 2e^- = 2F^-$	2.65
$S_2O_8^{2-} + 2e^- = 2SO_4^{2-}$	1.98
$Co^{3+} + e^- = Co^{2+}$	1.82
$Ce^{4+} + e^{-=} Ce^{3+}$	1.61
$½Cl_2 + e^- = Cl^-$	1.3595
$Cr_2O_7^{2-} + 14H^+ + e^- = 2Cr^3 + 7H_2O$	1.33
$MnO_2 + 4H^+ + 2e^- = Mn^{2+} + 2H_2O$	1.23
$Br_2(l) + 2e^- = Br^-$	1.0652
$2Hg^{2+} + 2e^- = Hg_2^{2+}$	0.92
$Hg^{2+} + 2e^- = Hg$	0.854
$Ag^+ + e^- = Ag$	0.7991
$Fe^{3+} + e^- = Fe^{2+}$	0.771
$I_2 + 2e^- = 2I^-$	0.5355
$Fe(CN)_6^{3-} + e^- = Fe(CN)_6^{4-}$	0.36
$Cu^{2+} + 2e^- = Cu$	0.337
$S_4O_6^{2-} + 2e^- = 2S_2O_3^{2-}$	0.17
$Cu^{2+} + e^- = Cu^+$	0.153
$Sn^{4+} + 2e^- = Sn^{2+}$	0.15
$S + 2H^+ + e^- = H_2S$	0.141
$2H^+ + e^- = H_2$	0.000
$Fe^{3+} + 3e^- = Fe$	−0.036
$Pb^{2+} + 2e^- = Pb$	−0.126
$Sn^{2+} + 2e^- = Sn$	−0.136
$Cd^{2+} + 2e^- = Cd$	−0.403
$Cr^{3+} + e^- = Cr^{2+}$	−0.41
$Fe^{2+} + 2e^- = Fe$	−0.440
$Zn^{2+} + 2e^- = Zn$	−0.763
$Al^{3+} + 3e^- = Al$	−1.66
$½H_2 + e^- = H^-$	−2.25
$Mg^{2+} + 2e^- = Mg$	−2.37
$Na^+ + e^- = Na$	−2.714
$Ca^{2+} + 2e^- = Ca$	−2.87
$Ba^{2+} + 2e^- = Ba$	−2.90
$Cs^+ + e^- = Cs$	−2.923
$K^+ + e^- = K$	−2.925
$Li^+ + e^- = Li$	−3.045
Basic Solutions	
$O_3 + H_2O + 2e^{-=} O_2 + 2OH^-$	1.24
$Fe(OH)_3 + e^{-=} OH^- + Fe(OH)_2$	−0.56

(*Continued*)

TABLE 14.1 (*Continued*)
Standard Electrode Potentials at 298 K, 1 atm

Electrode Reaction	ε°_{x}, volts
$Ni(OH)_2 + 2e^- = Ni + 2OH^-$	−0.72
$2H_2O + 2e^- = H_2 + 2OH^-$	−0.828
$SO_4^{2-} + H_2O + 2e^- = 2OH^- + SO_3^{2-}$	−0.93
$CNO^- + H_2O + 2e^- = 2OH^- + CN^-$	−0.97
$ZnO_2^{2-} + 2H_2O + 2e^- = Zn + 4OH^-$	−1.216
$Cr(OH)_3 + 3e^- = Cr + 3OH^-$	−1.3
$Ca(OH)_2 + 2e^- = Ca + 2OH^+$	−3.03

Note: Standard state is 1 molal.

Summing gives

$$\Delta G^{\circ}_{(\mathrm{i})} = -261{,}870 - 131{,}170 = -393{,}040 \text{ J}$$

for the reaction

$$\mathrm{Na}_{(s)} + \frac{1}{2}\mathrm{Cl}_{2(g)} = \mathrm{Na}^{+}_{(m)} + \mathrm{Cl}^{-}_{(m)} \tag{i}$$

For the reaction

$$\mathrm{Na}_{(s)} + \frac{1}{2}\mathrm{Cl}_{2(g)} = \mathrm{NaCl}_{(s)} \tag{ii}$$

$$\Delta G^{\circ}_{(\mathrm{ii}),298\ \mathrm{K}} = -385{,}310 \text{ J}$$

and combination of Equations (i) and (ii) gives

$$\mathrm{NaCl}_{(s)} = \mathrm{Na}^{+}_{(m)} + \mathrm{Cl}^{-}_{(m)} \tag{iii}$$

for which

$$\begin{aligned}\Delta G^{\circ}_{(\mathrm{iii})} &= \Delta G^{\circ}_{(\mathrm{i})} - \Delta G^{\circ}_{(\mathrm{ii})} \\ &= -393{,}040 + 385{,}310 \\ &= -8.3144 \times 298 \ln \frac{\left(\gamma^{\pm} m_{\mathrm{NaCl}}\right)^2}{a_{\mathrm{NaCl}}}\end{aligned}$$

In Equation (iii), the standard state on the left-hand side is pure solid NaCl, and the standard state on the right-hand side is the unit molality standard state. Saturation of

the aqueous solution occurs when NaCl has dissolved to the extent that the activity of NaCl in the solution, with respect to solid NaCl as the standard state, is unity. In this state,

$$\left(\gamma_{\pm} m_{\mathrm{NaCl}}\right)^2 = 22.6$$

or

$$\gamma_{\pm} m_{\mathrm{NaCl}} = 4.76$$

Thus, if the ions in the solution are behaving ideally, the saturated aqueous solution of NaCl at 298 K is 4.76 molal. When the activity of NaCl in the solution is unity with respect to solid NaCl as the standard state, the term $(\gamma_{\pm}\, m_{\mathrm{NaCl}})^2$ is called the *solubility product*, K_{sp}. Thus, generally, for the salt $\mathrm{A}_a\,\mathrm{Y}_y$,

$$K_{\mathrm{sp}} = \left(\gamma_{\pm} m_{\pm}\right)^{a+y} = \exp\frac{-\Delta G^{\circ}_{298\,\mathrm{K}}}{298R}$$

where $\Delta G^{\circ}_{298\,\mathrm{K}}$ is the standard Gibbs free energy change for the change of state

$$\mathrm{A}_a\mathrm{Y}_{y(\mathrm{Raoultian})} = a\mathrm{A}^{z+}_{(m)} + y\mathrm{Y}^{z-}_{(m)}$$

Example 14.1

Calculate the molalities of H^+ and OH^- in water at 298 K.

Solution

In Table 14.1, the standard reduction potential for the half-cell reaction

$$\mathrm{H_2O}_{(l)} + e^- = \frac{1}{2}\mathrm{H}_{2(g)} + \mathrm{OH}^-_{(m)}$$

is −0.828 volts, and the standard reduction potential for the reaction

$$H^+_{(m)} + e^- = \frac{1}{2}\mathrm{H}_{2(g)}$$

is zero. Summing gives

$$\mathrm{H_2O}_{(l)} = H^+_{(m)} + \mathrm{OH}^-_{(m)}$$

for which

$$\begin{aligned}\Delta G^{\circ}_{298\,\mathrm{K}} &= -f\varepsilon^{\circ} = -96487\times(-0.828)\\ &= 79{,}900\ \mathrm{J}\\ &= -8.3144\times 298\ln\left(\gamma\ \ m\ \ m\ \ \right)\end{aligned}$$

Thus, presuming that $\gamma_{\pm} = 1$,

$$m_{H^+} m_{OH^-} = 9.88 \times 10^{-15}$$

or, from the stoichiometry of the dissociation, as $m_{H^+} = m_{OH^-}$,

$$m_{H^+} = m_{OH^-} \approx 10^{-7}$$

At a molality of 10^{-7}, the assumption that $\gamma_{\pm} = 1$ is reasonable.

14.9.3 The Influence of Acidity

The single electrode potential for the half-cell reaction

$$H^+_{(m)} + e^- = \frac{1}{2} H_{2(g)}$$

is

$$\varepsilon^H = \varepsilon^{\circ,H} - \frac{RT}{f} \ln \frac{p_{H_2}^{1/2}}{m_{H^+}}$$

$\varepsilon^{\circ,H} = 0$ and thus,

$$\varepsilon^H = -\frac{RT}{f} \ln \frac{p_{H_2}^{1/2}}{m_{H^+}} \tag{i}$$

that is, for a fixed pressure of hydrogen gas, ε^H is a linear function of the logarithm of the molality of the hydrogen ions. The concentration of hydrogen ions in an aqueous solution determines the acidity of the solution, and, conventionally, acidity is quantified by the definition of pH, as

$$\text{pH} = -\log\left[H^+\right] \tag{ii}$$

$[H^+]$ is the *molarity* of the hydrogen ions—that is, the number of moles of H^+ per liter of solution. Substitution of Equation (ii) into Equation (i) would require that either the half-cell reduction potential be determined with reference to the unit molarity standard state, or that pH be defined as $-\log\left(m_{H^+}\right)$. Since in dilute solutions, molality and molarity are virtually identical, this theoretical difficulty is of no practical significance. In the following discussions, the unit molarity standard state will be used for ions in solution. This standard state is defined as

$$a_{A^{z+}} \to \left[A^{z+}\right] \quad \text{as } \left[A^{z+}\right] \to 0$$

Furthermore, in the following discussions, it will be assumed that all ions in aqueous solutions behave ideally, in which case

$$a_{A^{z+}} = \left[A^{z+}\right] \sim m$$

With this understanding, Equation (i) becomes

$$\varepsilon^{H} = -\frac{RT}{f} \ln \frac{p_{H_2}^{1/2}}{\left[H^+\right]}$$

which, with Equation (ii), becomes

$$\varepsilon^{H} = -\frac{2.303 \times 8.3144 \times 298}{2 \times 96,487} \log p_{H_2} + \frac{2.303 \times 8.314 \times 298}{96,487} \log\left[H^+\right]$$

$$= -0.0591(\text{pH}) - 0.0296 \log p_{H_2}$$

or, with $p_{H_2} = 1$ atm, the reduction potential of hydrogen varies with pH as

$$\varepsilon^{H} = -0.0591(\text{pH})$$

In the previous example, it was found that the molality (and hence the molarity) of H^+ in H_2O at 298 K is 10^{-7}. Thus, the pH of H_2O at 298 K is 7, and the reduction potential of hydrogen in water is $-0.0591 \times 7 = -0.414$ volts. The hydrogen electrode has its standard reduction potential of 0 at pH = 0—that is, at $[H^+] = 1$.

14.10 BATTERIES

In the previous several sections, the thermodynamics of electrochemical cells and the details of how chemical energy can be converted into electrical energy or work and *vice-versa* have been explored. One major application of such electrochemical cells is the field of batteries. Batteries are devices in which electrochemical cells are utilized to both store energy and produce electrical energy on demand.

There are two basic kinds of batteries: those that are rechargeable (called secondary batteries) and those that are not rechargeable (called primary batteries). Electrochemical cells may have solid or liquid electrolytes. Some need a constant supply of fuel for their electrode reactions. Such cells are called *fuel cell*s and are therefore open systems from the thermodynamic point of view.

The engineering details of batteries will not be discussed in this text. However, in the following subsections, the thermodynamic systems of three that have been used in batteries will be discussed. The nomenclature of batteries can be confusing. In this text, the anode is the electrode where oxidation occurs, whether on discharging or charging.

The EMF of a battery equals the standard electrode potential of the cathode minus the standard electrode potential of the anode.

14.10.1 Lead-Acid Battery

The lead acid batteries are well known to automobile owners! This is a rechargeable battery. It is composed of lead (as the anode), lead oxide (PbO_2) as the cathode, and sulfuric acid as the electrolyte. During discharging of the battery, lead is oxidized

at the anode and the electrons flow from the anode to the cathode, where the lead^{+4} cations are reduced to lead^{+2}. During charging, the sulfate anions are oxidized at the anode and the electrons flow from the cathode to the anode.

The lead-acid battery can be represented in the standard galvanic cell format:[4]

$$\mathrm{Pb}\ \left|\mathrm{H_2SO_{4(aq)}}\right|\ \mathrm{PbO_2}$$

The cell reactions in this battery are unusual in that they involve reactions of both of the electrodes with the same electrolyte, i.e., the Pb anode and the PbO_2 cathode both react with sulfuric acid to form $PbSO_4$.

A simplified view of this cell during discharging is:

$$\text{At the anode:}\quad \mathrm{Pb + SO_4^- \rightarrow PbSO_4 + 2}e \qquad -0.356\ \mathrm{V}$$

$$\text{At the cathode:}\quad \mathrm{PbO_2 + 4H^+ + SO_4^- + 2}e^- \rightarrow \mathrm{PbSO_4 + 2H_2O} \qquad +1.685\ \mathrm{V}$$

The overall cell reaction is written as:

$$\mathrm{Pb + PbO_2 + 2H_2SO_4 \rightarrow 2PbSO_4 + 2H_2O} \qquad +2.041\ \mathrm{V}$$

It can be seen that as written, the metallic lead is oxidized and the lead^{+4} cations of the oxide are reduced.

14.10.2 Nickel Cadmium Battery

A common battery for use in small devices is the nickel–cadmium battery.

The nickel–cadmium battery can be represented in the standard galvanic cell format:

$$\mathrm{Cd}\left|\ \mathrm{KOH_{(aq)}}\right|\mathrm{NiO(OH)}$$

Where the KOH acts as the aqueous electrolyte

During discharging of the battery, the reactions are written as:

$$\text{At anode:}\quad \mathrm{Cd + 2(OH)^- \rightarrow Cd(OH)_2 + 2}e^- \qquad -0.76\ \mathrm{V}$$

$$\text{At cathode:}\quad \mathrm{2NiO(OH) + 2H_2O + 2}e^- \rightarrow \mathrm{2Ni(OH)_2 : 2(OH)^-} \qquad +0.49\ \mathrm{V}$$

This yields an overall reaction given as follows:

$$\mathrm{Cd + 2NiO(OH) + 2H_2O \rightarrow Cd(OH)_2 + 2Ni(OH)_2} \qquad +1.25\ \mathrm{V}$$

The ΔG° of this overall reaction can be calculated. See Problem 14.10.

[4] The inclusion of the lead acid cell is due to the suggestion of Dr. Anthony Petric, Emeritus Professor, McMaster University, and notes he supplied were utilized.

14.10.3 Lithium Ion Batteries

In the last decades of the twentieth century, Li-ion batteries were discovered and commercialized. In these rechargeable batteries, the Li^{+1} ion moves between the electrodes during the discharging and charging cycles through a solid electrolyte. When arriving at the electrode the Li^{+1} ion "intercalates" into the solid electrode. This process is possible since the Li^{+1} ions are small and the electrodes are made of solids whose crystal structures have large spacing between a certain set of planes (e.g. the basal planes in graphite).

The overall process during discharging can be summarized as follows:

At the anode: Li atoms are oxidized to $Li^{+1} + e^-$
At the cathode: Li^{+1} is reduced to the Li atom.

There are at least two intercalation phase transformations in these batteries which bring with them the possibility of microstructure changes such as the production of Li dendrites which can cause shorting of the battery.

14.11 POURBAIX DIAGRAMS

Pourbaix diagrams,[5] or *potential-pH* diagrams, are graphical representations of thermodynamic and electrochemical equilibria occurring in aqueous systems. They are thus the electrochemical analogs of the chemical phase stability diagrams discussed in Section 13.4.

Consider the cell

$$\mathrm{Pt}, \mathrm{H}_{2(g)} \left| \mathrm{H_2O} \right| \mathrm{O}_{2(g)}, \mathrm{Pt}$$

The galvanic cell reaction

$$\mathrm{H}_{2(g)} + \frac{1}{2}\mathrm{O}_{2(g)} = \mathrm{H_2O}_{(l)} \tag{i}$$

is the sum of the half-cell reactions

$$\mathrm{H}_2 = 2\mathrm{H}^+ + 2e^- \tag{ii}$$

and

$$\frac{1}{2}\mathrm{O}_2 + 2\mathrm{H}^+ + 2e^- = \mathrm{H_2O} \tag{iii}$$

Thus,

$$\Delta G^\circ_{(\mathrm{i})} = \Delta G^\circ_{(\mathrm{ii})} + \Delta G^\circ_{(\mathrm{iii})}$$

[5] M. Pourbaix, *Atlas of Electrochemical Equilibria in Aqueous Solutions*, National Association of Corrosion Engineers, Houston, TX, 1974.

$\Delta G^{\circ}_{(i)298\,K} = -237{,}190$ J, and by convention, $\Delta G^{\circ}_{(ii)298\,K} = 0$. Thus, the standard reduction potential for the reaction given by Equation (iii) is

$$\varepsilon^{\circ}_{(iii)} = \frac{-\Delta G^{\circ}_{(iii)}}{2f}$$

$$= \frac{237{,}190}{2f}$$

$$= 1.229 \text{ volts}$$

With all of the reactants and products occurring in their standard states, electrochemical equilibrium is established when the backing EMF applied to the cell is 1.229 volts. If the backing EMF is less than this value, the cell is a current-producing galvanic cell and the cell reaction occurring is

$$H_{2(g)} + \frac{1}{2}O_{2(g)} \rightarrow H_2O_{(l)}$$

with the oxidation $H_2 \rightarrow 2H^+ + 2e^-$ occurring at the anode and the reduction reaction $\frac{1}{2}O_2 + 2H^+ + 2e^- \rightarrow H_2O$ occurring at the cathode. However, if the backing EMF is greater than 1.229 volts, the cell is a current-consuming *electrolysis cell* and the cell reaction occurring is

$$H_2O_{(l)} \rightarrow H_{2(g)} + \frac{1}{2}O_{2(g)}$$

with the oxidation reaction $H_2O \rightarrow \frac{1}{2}O_2 + 2H^+ + 2e^-$ occurring at the anode and the reduction reaction $2H^+ + 2e^- \rightarrow H_2$ occurring at the cathode. Thus, with hydrogen gas and hydrogen ions at unit activity, electrochemical equilibrium is established at the hydrogen electrode when the electrode is at zero potential. If the potential of the electrode is increased to a value above zero, the anodic reaction $H_2 \rightarrow 2H^+ + 2e^-$ occurs, and if the potential of the electrode is decreased to a value less than zero, the cathodic reaction $2H^+ + 2e^- \rightarrow H_2$ occurs.

Similarly, with oxygen at unit pressure and hydrogen ions at unit activity, electrochemical equilibrium at the oxygen electrode is established when the electrode potential is 1.229 volts. If the potential of the electrode is increased above 1.229 volts, the anodic reaction $H_2O \rightarrow \frac{1}{2}O_2 + 2H^+ + 2e^-$ occurs, and if the potential of the electrode is decreased below 1.229 volts, the cathodic reaction $\frac{1}{2}O_2 + 2H^+ + 2e^- \rightarrow H_2O$ occurs. Thus, generally, if the potential, ε, of an electrode at equilibrium with the electrolyte is increased, an anodic oxidation reaction occurs, and if it is decreased, a cathodic reduction reaction occurs.

Since both half-cell reactions (i) and (ii) involve hydrogen ions, the half-cell potentials are functions of the pH of the aqueous solution. At the hydrogen electrode, at 298 K, the electrochemical equilibrium

$$H^+ + e^- = \frac{1}{2}H_2 \qquad \text{(a)}$$

is established at

$$\varepsilon_{(a)} = -\frac{RT}{f}\ln\frac{p_{H_2}^{1/2}}{e\left[H^+\right]}$$

$$= -0.0591(\text{pH}) - 0.0298\log p_{H_2}$$

which, with $p_{H_2} = 1\,\text{atm}$, is drawn as line *a* in Figure 14.15. (Note the change from natural to common log) At the oxygen electrode, at 298 K, the electrochemical equilibrium

$$\frac{1}{2}O_2 + 2H^+ + 2e^- = H_2O \qquad \text{(b)}$$

is established at

$$\varepsilon_{(b)} = 1.299 - \frac{RT}{2f}\ln\frac{1}{[H^+]^2 p_{O_2}^{1/2}}$$

$$= 1.229 - 0.0591\,\text{pH} + 0.0148\log p_{O_2}$$

which, with $p_{O_2} = 1\,\text{atm}$, is drawn as line *b* in Figure 14.15.

Lines *a* and *b* in Figure 14.15 define the *domain of thermodynamic stability of water* in aqueous solutions under a pressure of 1 atm of H_2 and 1 atm of O_2. Below line *a*, the equilibrium pressure of hydrogen gas is greater than 1 atm, and thus, hydrogen is cathodically evolved from an aqueous solution, the potential of which is moved below line *a* when the pressure of hydrogen at the electrode is 1 atm. Similarly, above line *b*, the equilibrium pressure of oxygen gas is greater than 1 atm, and thus, oxygen gas is anodically evolved from an aqueous solution at an electrode,

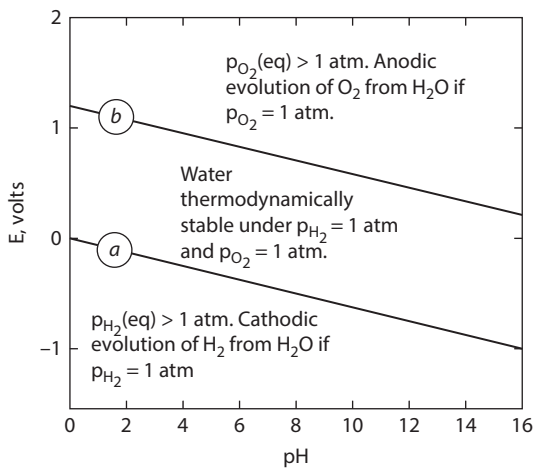

FIGURE 14.15 The domain of thermodynamic stability of water.

the potential of which is moved above line *b* when the oxygen pressure at the electrode is 1 atm. Water is thermodynamically stable between lines *a* and *b* with oxygen and hydrogen pressures of 1 atm.

14.11.1 The Pourbaix Diagram for Aluminum

The species participating in the various chemical and electrochemical equilibria are the solids Al and Al_2O_3 and the ions Al^{3+} and AlO_2^-. The pertinent standard Gibbs free energies of formation are

Reaction	$\Delta G^\circ_{298K,}$ J
Al	0
$\frac{1}{2}H_{2(g)} = H^+_{(m)} + e^-$	0
$2Al_{(s)} + 3/20_{2(g)} = Al_2O_{3(s)}$	−1,608,900
$Al_{(s)} = Al^{3+}_{(m)} + 3e^-$	−481,200
$Al_{(s)} + O_{2(g)} + e^- = AlO^-_{2(m)}$	−839,800
$H_{2(g)} + \frac{1}{2}O_{2(g)} = H_2O_{(l)}$	−237,200

Consider first the equilibrium which occurs between the ions in solution. Since reduction potentials are being used, the equations for the electrochemical equilibria are set up with the higher oxidation state on the left and the lower oxidation state on the right—that is, with the balancing electronic charge on the left-hand side of the equation.

14.11.1.1 The Equilibrium between the Two Dissolved Substances

14.11.1.1.1 The Equilibrium between Al^{3+} and AlO_2^-

$$Al^{3+} \longleftrightarrow AlO_2^-$$

The procedure for deriving the expression for the equilibrium is as follows:

1. Balance the oxygen with H_2O; that is,

$$Al^{3+} + 2H_2O \longleftrightarrow AlO_2^-$$

2. Balance the hydrogen with H^+; that is,

$$Al^{3+} + 2H_2O \longleftrightarrow AlO_2^- + 4H^+$$

3. If necessary, balance the charge with e^-.

This step is not necessary with Al^{3+} and AlO_2^-, as the equilibrium is not electrochemical. The desired expression is thus

$$Al^{3+} + 2H_2O = AlO_2^- + 4H^+ \tag{i}$$

for which

$$\Delta G^\circ_{(i)} = (-839{,}800) - (2 \times -237{,}200) - (-481{,}200)$$
$$= 115{,}800 \text{ J}$$
$$= -8.3144 \times 298 \times 2.303 \log \frac{[H^+]^4 [AlO_2^-]}{[Al^{3+}]}$$

Thus,

$$-20.29 = 4 \log [H^+] + \log \frac{[AlO_2^-]}{[Al^{3+}]}$$

or

$$\log \frac{[Al^{3+}]}{[AlO_2^-]} = 20.29 - 4 \text{ pH}$$

Thus, $[Al^{3+}] = [AlO_2^-]$ at pH = 5.07 and pH = 5.07 is drawn as line 1 in Figure 14.16a. At values of pH > 5.07, $[AlO_2^-] > [Al^{3+}]$, and at values of pH < 5.07, $[Al^{3+}] > [AlO_2^-]$.

14.11.1.2 The Equilibrium between the Two Solids

14.11.1.2.1 The Equilibrium between Al and Al_2O_3

With the higher oxidation state on the left and the lower oxidation state on the right, the procedure for deriving the expression for the equilibrium begins with

$$Al_2O_3 \longleftrightarrow 2Al$$

Then, as before, balance the oxygen with H_2O; that is,

$$Al_2O_3 \longleftrightarrow 2Al + 3H_2O$$

balance the hydrogen with H^+; that is,

$$Al_2O_3 + 6H^+ \longleftrightarrow 2Al + 3H_2O$$

and balance the charge with e^-; that is,

$$Al_2O_3 + 6H^+ + 6e^- \longleftrightarrow 3H_2O + 2Al$$

The required equilibrium is thus

$$Al_2O_3 + 6H^+ + 6e^- = 3H_2O + 2Al \qquad \text{(ii)}$$

for which

$$\begin{aligned}\Delta G^\circ_{(ii)} &= (3\times -237,200) - (-1,608,900)\\ &= 897,300 \text{ J}\\ &= -zf\varepsilon^\circ_{(ii)} = -6\times 96,487\varepsilon^\circ_{(ii)}\end{aligned}$$

Thus, $\varepsilon^\circ_{(ii)} = -1.55$ volts and, with $a_{Al} = a_{Al_2O_3} = 1$,

$$\begin{aligned}\varepsilon_{(ii)} &= \varepsilon^\circ_{(ii)} - \frac{RT}{zf}\ln\frac{1}{\left[H^+\right]^6}\\ &= -1.55 + \frac{8.3144\times 298\times 2.303\times 6}{6\times 96,487}\log\left[H^+\right]\\ &= -1.55 - 0.0591 \text{ pH volts}\end{aligned}$$

This is drawn as line 2 in Figure 14.16a and is the line along which Al is in equilibrium with Al_2O_3. Al is the stable solid phase in states below line 2 (at lower values of pH and at more negative electrode potentials), and Al_2O_3 is the stable solid in states above the line.

14.11.1.3 One Solid in Equilibrium with a Dissolved Substance

14.11.1.3.1 The Equilibrium between Al and Al^{3+}

The equilibrium is

$$Al^{3+} + 3e^- = Al \qquad \text{(iii)}$$

for which

$$\Delta G^\circ_{(iii)} = 481,200 \text{ J}$$

Thus,

$$\varepsilon^\circ_{(iii)} = \frac{-481,200}{3\times 96,487} = -1.66 \text{ volts}$$

Then, with $a_{Al} = 1$,

$$\varepsilon_{(iii)} = -1.66 - \frac{8.3144\times 298\times 2.303}{3\times 96,487}\log\frac{1}{\left[Al^{3+}\right]}$$

The variation of the concentration of $Al^{3}+$ ions in equilibrium with Al is thus

$$\varepsilon_{(iii)} = -1.66 + 1.971 \times 10^{-2} \log\left[Al^{3+}\right]$$

With $[Al^{3+}] = 1$ mole per liter, this equation is drawn as line 3 in Figure 14.16a. The concentration of $Al^{3}+$ in equilibrium is independent of pH and decreases with increasingly negative values of ε.

14.11.1.3.2 The Equilibrium between Al_2O_3 and Al^{3+}

The sequence in the derivation of the equilibrium equation is

$$Al_2O_3 \longleftrightarrow 2Al^{3+}$$

$$Al_2O_3 \longleftrightarrow 2Al^{3+} + 3H_2O$$

$$6H^{+} + Al_2O_3 \longleftrightarrow 2Al^{3+} + 3H_2O$$

Balancing the charge with e^{-} is not necessary, and the required expression is thus

$$6H^{+} + Al_2O_3 = 2Al^{3+} + 3H_2O \qquad \text{(iv)}$$

for which

$$\Delta G^{\circ}_{(iv)} = (3 \times -237,200) + (2 \times -481,200) - (-1,608,900)$$
$$= -65,100 \text{ J}$$

which, with $a_{Al_2O_3} = 1$, gives

$$-65,100 = -8.3144 \times 298 \times 2.303 \log \frac{\left[Al^{3+}\right]^2}{\left[H^{+}\right]^6}$$

or

$$\log\left[Al^{3+}\right] = 5.70 - 3\ pH$$

which is the variation of the concentration of Al^{3+} ions in equilibrium with Al_2O_3. This equilibrium is independent of the electrode potential, and line 4 in Figure 14.16a, at pH = 1.9, represents a concentration of Al^{3+} of 1 mole per liter in equilibrium with Al_2O_3.

14.11.1.3.3 The Equilibrium between Al and AlO_2^-

$$AlO_2^- \longleftrightarrow Al$$

$$AlO_2^- \longleftrightarrow Al + 2H_2O$$

$$AlO_2^- + 4H^+ \longleftrightarrow Al + 2H_2O$$

$$AlO_2^- + 4H^+ + 3e^- \longleftrightarrow Al + 2H_2O$$

The equilibrium is thus

$$AlO_2^- + 4H^+ + 3e^- = Al + 2H_2O \qquad \text{(v)}$$

for which

$$\Delta G^\circ_{(v)} = (2 \times -237,200) + 839,800$$
$$= 365,400 \text{ J}$$

Thus,

$$\varepsilon^\circ_{(v)} = \frac{-365,400}{3 \times 96,487} = -1.26 \text{ volts}$$

With $a_{Al} = 1$,

$$\varepsilon_{(v)} = -1.26 - \frac{8.3144 \times 298 \times 2.303}{3 \times 96,487} \log \frac{1}{\left[H^+\right]^4 \left[AlO_2^-\right]}$$

which gives the variation of the concentration of AlO_2^- ions in equilibrium with Al as

$$\varepsilon_{(v)} = -1.26 - 0.0789\text{pH} + 0.0198 \log \left[AlO_2^-\right]$$

This equation, with $\left[AlO_2^-\right] = 1$ mole per liter, is drawn as line 5 in Figure 14.16a. The equilibrium is dependent on both pH and ε.

14.11.1.3.4 The Equilibrium between Al_2O_3 and AlO_2^-:

$$Al_2O_3 \longleftrightarrow 2AlO_2^-$$
$$H_2O + Al_2O_3 \longleftrightarrow 2AlO_2^-$$
$$H_2O + Al_2O_3 \longleftrightarrow 2AlO_2^- + 2H^+$$

The equilibrium is thus

$$H_2O + Al_2O_3 = 2AlO_2^- + 2H^+ \qquad \text{(vi)}$$

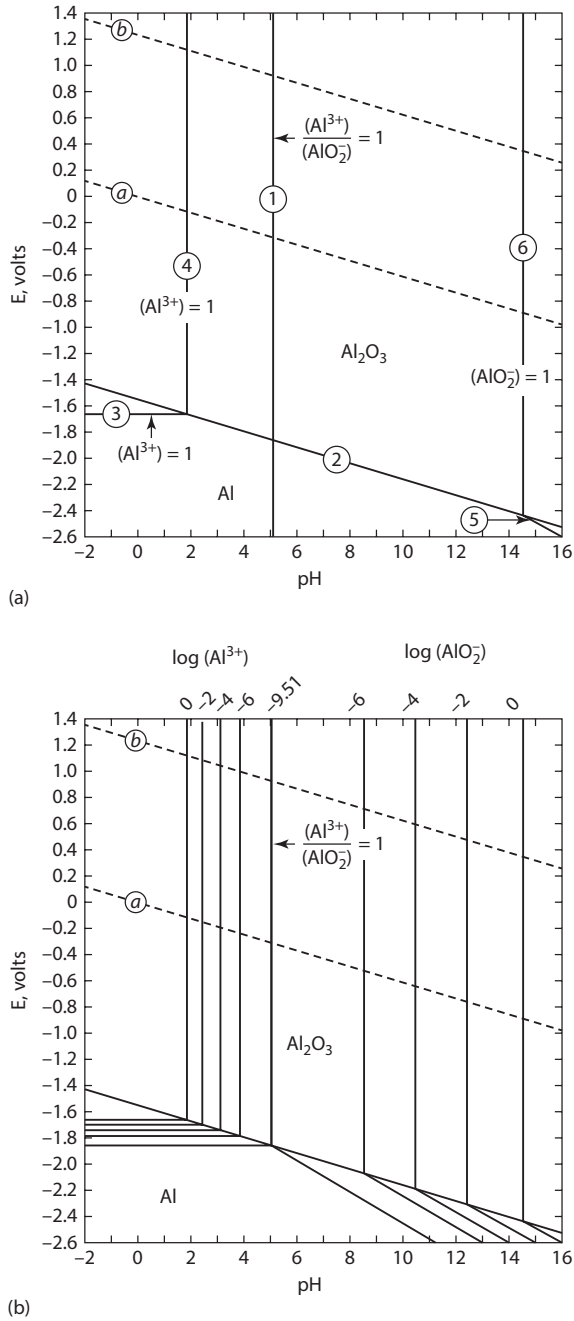

FIGURE 14.16 (a) Construction of the Pourbaix diagram for Al. (b) The Pourbaix diagram for Al. See Figure 14.15

for which

$$\Delta G^{\circ}_{(vi)} = 166{,}500 \text{ J}$$

This gives

$$\log\left[AlO_2^-\right] = pH - 14.59$$

as the variation of the concentration of AlO_2^- in equilibrium with Al_2O_3. This equation, with $\left[AlO_2^-\right] = 1$ mole per liter is drawn as line 6 in Figure 14.16a at pH = 14.59.

The Pourbaix diagram for Al, containing iso-concentrations lines for Al^{3+} and AlO_2^- in the fields of stability of Al and Al_2O_3, is shown in Figure 14.16b. At pH = 5.07 in the Al_2O_3 field of stability $\left[Al^{3+}\right] = \left[AlO_2^-\right] = 3.10 \times 10^{-10}$ moles per liter. However, in the Al stability field, the 3×10^{-10} moles of Al^{3+} per liter iso-concentration line occurs at $\varepsilon = -1.85$ volts, and the 3×10^{-10} moles of AlO_2^- per liter iso-concentration lines lies at $\varepsilon = -1.45 - 0.0789$ pH. The domain of thermodynamic stability of water at hydrogen and oxygen pressures of 1 atm is defined by the lines *a* and *b*, and the position of line *a* relative to line 2 in Figure 14.16a illustrates why Al metal cannot be produced by electrolysis of aqueous solutions. With a hydrogen pressure of 1 atm, attempts to decrease the potential of an electrode to a value less than that given by line *a* cause the cathodic evolution of hydrogen gas from the electrolyte.

14.11.1.4 The Solubility of Alumina in Aqueous Solutions

Alumina dissolves in aqueous solutions to form Al^{3+} ions according to

$$Al_2O_3 + 6H^+ = 2Al^{3+} + 3H_2O$$

and to form AlO_2^- ions according to

$$Al_2O_3 + H_2O = 2AlO_2^- + 2H^+$$

The solubility, as Al^{3+}, which varies with pH as

$$\log\left[Al^{3+}\right] = 5.70 - 3\,pH$$

and as AlO_2^-, which varies with pH as

$$\log\left[AlO_2^-\right] = pH - 14.59$$

is shown in Figure 14.17. The solubility of Al_2O_3 as AlO_2^- decreases by 10 orders of magnitude when the pH is decreased from 14 to 5, and this behavior is made use of in the Bayer process for the separation of Al_2O_3 from bauxite. Bauxite, which is the principal aluminum ore, is a mixture of aluminum monohydrate and aluminum trihydrate containing up to 60% Al_2O_3 with Fe_2O_3 as the main impurity. The ore is digested in a

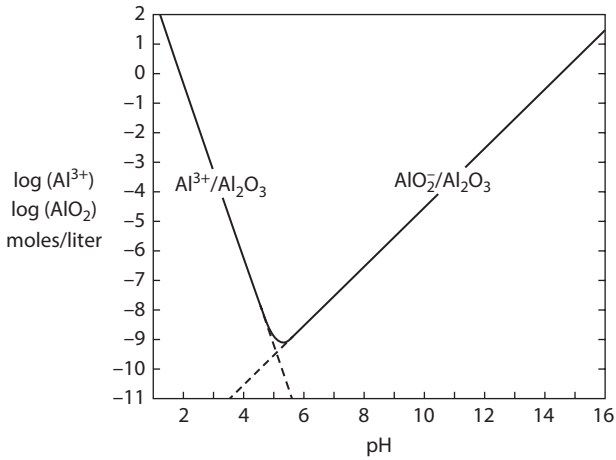

FIGURE 14.17 The solubility of Al_2O_3 in aqueous solution.

strong caustic solution at a temperature between 150°C and 250°C and a pressure high enough to suppress boiling. The alumina dissolves as AlO_2^-, and the insoluble residue of Fe_2O_3 (red mud) is removed from the solution by filtration. The pH of the solution is then decreased by adding water, and seed crystals of $Al(OH)_3$ are added. The decreasing solubility causes the precipitation of $Al(OH)_3$ by the hydrolysis reaction

$$NaAlO_2 + 2H_2O = NaOH + Al(OH)_3$$

The strong caustic solution is regenerated by the removal of water by boiling, and the precipitated hydrate is then calcined at 1200°C–1350°C to form α-Al_2O_3.

14.12 SUMMARY

1. A system that is capable of performing electrical work as the result of the occurrence of a chemical reaction is called a galvanic cell, and the overall chemical reaction is represented by an equation called the cell reaction.
   - If, in such a reaction, dn g-ions of valence z are transported through a voltage difference $\Delta\phi$ maintained between the electrodes of the cell, then

$$\delta w' = zf\Delta\phi dn$$

     where f is Faraday's constant (= 96,487 coulombs/mole).
   - If the transportation is conducted reversibly, in which case the electric potential difference between the electrodes of the cell is called the electromotive force (EMF), ε, of the cell, then

$$\delta w'_{\max} = zf\varepsilon dn = -dG'$$

     and, for the transportation of 1 mole of ions,

$$\Delta G = -zf\varepsilon$$

2. If the reaction

$$aA + bB = cC + dD$$

is conducted in an electrochemical cell, the EMF of the cell is given by

$$\varepsilon = \varepsilon^\circ - \frac{RT}{zf} \ln \frac{a_C^c a_D^d}{a_A^a a_B^b}$$

where the standard EMF of the cell, ε°, is given by

$$\varepsilon^\circ = -\frac{\Delta G^\circ}{zf}$$

3. For any cell reaction at constant temperature and pressure,

$$\Delta G = -zf\varepsilon$$

Thus, the molar entropy change for the cell reaction is

$$\Delta S = zf\left(\frac{\partial \varepsilon}{\partial T}\right)_P$$

and the molar enthalpy change for the cell reaction is

$$\Delta H = -zf\varepsilon + zfT\left(\frac{\partial \varepsilon}{\partial T}\right)_P$$

4. The cell reactions for three types of batteries (Lead Acid, Nickel Cadmium and Lithium Ion) are presented and discussed.
5. The composition of an aqueous solution is usually expressed in terms of the molality, m, or the molarity, M, where molality is the number of moles of solute present per 1000 g of solvent and molarity is the number of moles of solute present in 1 liter of solution. The unit molality activity scale (which is analogous to the 1 wt% activity scale) is defined as

$$a_{i(m)} \to m_i \quad \text{as} \quad m_i \to 0$$

where $a_{i(m)}$ is the activity of the solute with respect to the unit molality standard state, and the unit molality standard state is located on the Henry's law line at $m_i = 1$. Deviation from ideality is accommodated by an activity coefficient defined as

$$\gamma_{i(m)} = \frac{a_{i(m)}}{m_i}$$

6. The mean ionic molality, $m_{\pm}$, of the electrolyte (or salt) $A_a\ Y_y$ when dissolved in water is defined by

$$m_{\pm} = \left(m^a_{A^{z+}} m^y_{Y^{z-}} \right)^{\frac{1}{a+y}}$$

and the mean ion activity coefficient, $\gamma_{\pm}$, is defined as

$$\gamma_{\pm} = \left(\gamma^a_{A^{z+}} \gamma^y_{Y^{z-}} \right)^{\frac{1}{a+y}}$$

The activity of the dissolved salt is thus

$$a_{A_a Y_y} = \left(\gamma_{\pm} m_{\pm} \right)^{a+y}$$

7. Any cell reaction is the sum of two half-cell reactions, and the SHE, at which the half-cell reaction

$$H^+_{(\text{aqueous}, m=1)} + e^- = \frac{1}{2} H_{2(g, P=1\ \text{atm})}$$

occurs is assigned a potential of zero. This facilitates the assignment of standard reduction half-cell potentials to all other half-cell reactions. The electrochemical series is produced by listing the half-cell reactions in decreasing order of the magnitudes of their standard reduction half-cell potentials.
8. The influence of electrode potential and pH on the phase equilibria and solubilities in aqueous electrochemical systems can be presented graphically by Pourbaix diagrams.

14.13 CONCEPTS AND TERMS INTRODUCED IN THIS CHAPTER

The reader should write out brief definitions or descriptions of the following terms. Where appropriate, equations may be used.

Absolute potential
Anodic oxidation reaction
Anolyte
Cathodic reduction reaction
Catholyte
Cell reaction
Charge neutrality
Concentration cell
Covalent character
Daniell cell

Electric potential
Electric work
Electrochemical reaction
Electrochemical series
Electrode
Electrolysis
Electrolysis cell
Electrolyte
Electromotive force (EMF)
Faraday's constant (ʃ; 96,487 coulombs/mole)
Formation cell
Galvanic cell
Ionic character
Liquid junction potential
Molality
Molarity
Nernst equation
Open-circuit EMF
Porous diaphragm
Salt bridge
Single electrode potential
Solubility product
Standard EMF of the cell
Standard hydrogen electrode (SHE)

14.14 QUALITATIVE EXAMPLE PROBLEM

QUALITATIVE PROBLEM

Calculate the solubility of AgBr in water at 298 K.

SOLUTION TO QUALITATIVE PROBLEM

From Table 14.1, $\varepsilon^{\circ,\mathrm{Ag}} = 0.7991$ volts and $\varepsilon^{\circ,\mathrm{Br}} = 1.0652$ volts. Therefore, for the reaction

$$\mathrm{Ag}_{(s)} + \frac{1}{2}\mathrm{Br}_{2(l)} = \mathrm{Ag}^{+}_{(m)} + \mathrm{Br}^{-}_{(m)}$$

$$\Delta G^{\circ}_{298\,\mathrm{K}} = -f\left(-0.7991 + 1.0652\right) = 25{,}675\ \mathrm{J}$$

For

$$\mathrm{Ag}_{(s)} + \frac{1}{2}\mathrm{Br}_{2(l)} = \mathrm{AgBr}_{(s)}$$

$$\Delta G^{\circ}_{298\,\mathrm{K}} = -95{,}670\ \mathrm{J}$$

and hence for

$$\mathrm{AgBr}_{(s)} = \mathrm{Ag}^{+}_{(m)} + \mathrm{Br}^{-}_{(m)}$$

$$\begin{aligned}\Delta G^{\circ}_{298\,\mathrm{K}} &= 25{,}675 + 95{,}670 \\ &= 121{,}345\ \mathrm{J} \\ &= -8.3144 \times 298 \ln K_{\mathrm{sp}}\end{aligned}$$

Thus, $K_{\mathrm{sp}} = (\gamma_{\pm}\, m_{\mathrm{AgBr}})^2 = 5.4 \times 10^{-22}$ or $m_{\mathrm{AgBr}} = 2.3 \times 10^{-11}$, which indicates that AgBr is virtually insoluble in water.

14.15 QUANTITATIVE EXAMPLE PROBLEMS

QUANTITATIVE PROBLEM 1

Fayalite, $2\mathrm{FeO}\cdot\mathrm{SiO}_2$, is the only iron silicate compound formed by reaction of FeO with SiO_2 at a total pressure of 1 atm, and the standard Gibbs free energy change for the reaction

$$2\mathrm{FeO}_{(s)} + \mathrm{SiO}_{2(s)} = 2\mathrm{FeO}\cdot\mathrm{SiO}_{2(s)}$$

is −11,070 J at 1200 K. Calculate the EMF of the cell

$$\mathrm{Fe}\,|\,\mathrm{SiO}_2\,|\,2\mathrm{FeO}\cdot\mathrm{SiO}_2\ \|\ \mathrm{CaO}-\mathrm{ZrO}_2\,|\,\mathrm{FeO}\,|\,\mathrm{Fe}$$

at 1200 K.

SOLUTION TO QUANTITATIVE PROBLEM 1

This is an oxygen concentration cell in which the cell reaction can be written as

$$\mathrm{O}_2\left(\text{higher pressure at the cathode}\right) \rightarrow \mathrm{O}_2\left(\text{lower pressure at the anode}\right) \qquad \text{(i)}$$

for which the EMF is

$$\varepsilon = -\frac{RT}{4f}\ln\frac{p_{\mathrm{O}_2}\left(\text{at the anode}\right)}{p_{\mathrm{O}_2}\left(\text{at the cathode}\right)} \qquad \text{(ii)}$$

The oxygen pressure at the electrodes are fixed by the chemical equilibrium

$$\mathrm{Fe} + \frac{1}{2}\mathrm{O}_2 = \mathrm{FeO} \qquad \text{(iii)}$$

for which

$$K_{(\text{iii})} = \frac{a_{\text{FeO}}}{a_{\text{Fe}} p_{\text{O}_2}^{1/2}}$$

At the cathode, the activity of FeO with respect to Fe-saturated pure FeO is unity, and at the anode, the activity of FeO is that occurring in $2\text{FeO}\cdot\text{SiO}_2$ saturated with Fe and SiO_2. As

$$K_{(\text{iii})} = \frac{a_{\text{FeO(cathode)}}}{a_{\text{Fe(cathode)}} p_{\text{O}_2\,\text{(cathode)}}^{1/2}} = \frac{a_{\text{FeO(anode)}}}{a_{\text{Fe(anode)}} p_{\text{O}_2\,\text{(anode)}}}$$

and

$$a_{\text{Fe(anode)}} = a_{\text{Fe(cathode)}} = a_{\text{FeO(cathode)}} = 1$$

$$\frac{p_{\text{O}_2\,\text{(anode)}}}{p_{\text{O}_2\,\text{(cathode)}}} = a_{\text{FeO(anode)}}^2$$

and hence, in Equation (ii),

$$\varepsilon = -\frac{RT}{4f} \ln a_{\text{FeO(anode)}}^2$$

For $2\text{FeO} + \text{SiO}_2 = 2\text{FeO}\cdot\text{SiO}_2$,

$$\Delta G_{1200\,\text{K}}^{\circ} = -11{,}070 \text{ J}$$

$$= -8.3144 \times 1200 \ln \frac{a_{2\text{FeO}\cdot\text{SiO}_2}}{a_{\text{FeO}}^2 a_{\text{SiO}_2}}$$

Thus, at the anode, with $a_{2\text{FeO}\cdot\text{SiO}_2} = a_{\text{SiO}_2} = 1$,

$$a_{\text{FeO(anode)}} = 0.574$$

and thus,

$$\varepsilon = -\frac{8.3144 \times 1200}{4 \times 96{,}487} \ln (0.574)^2$$

$$= 0.0287 \text{ volts}$$

Alternatively, the anode half-cell reaction can be written as

$$\text{O}^{2-} = \frac{1}{2}\text{O}_{2(\text{eq.Fe/FeO})} + 2e^-$$

and the cathode half-cell reaction can be written as

$$\frac{1}{2}\text{O}_{2(\text{eq.Fe/FeO})} + 2e^- = \text{O}^{2-}$$

or, at the anode,

$$2\text{Fe} + 2\text{O}^{2-} + \text{SiO}_2 = 2\text{FeO}\cdot\text{SiO}_2 + 4e^-$$

and, at the cathode,

$$2\text{FeO} + 4e^- = 2\text{Fe} + 2\text{O}^{2-}$$

summation of which gives the cell reaction as

$$2\text{FeO} + \text{SiO}_2 = 2\text{FeO}\cdot\text{SiO}_2$$

The Gibbs free energy change for the cell reaction is

$$\Delta G^\circ = -zf\varepsilon^\circ = -11{,}070 \text{ J}$$

and thus,

$$\varepsilon = \frac{-\Delta G^\circ}{4f} = \frac{11{,}070}{4\times 96{,}487} = 0.0287 \text{ volts}$$

QUANTITATIVE PROBLEM 2

A waste liquor consists of a 0.5 molal solution of $CaCl_2$ in water. Calculate the minimum work, per mole of $CaCl_2$, required to separate the liquor into anhydrous $CaCl_2$ and pure water at atmospheric temperature and pressure. The mean ionic activity coefficient of 0.5 molal $CaCl_2$ is 0.448.

SOLUTION TO QUANTITATIVE PROBLEM 2

The minimum work is that required when the separation is conducted reversibly; that is, $w = -\Delta G$ for the process. Further, 0.5 molal $CaCl_2$ comprises 0.5 moles of $CaCl_2$ and 1000 g of H_2O or 0.5 moles of $CaCl_2$ and 1000/18 = 55.55 moles of water. Thus, 1 mole of $CaCl_2$ exists in 111.1 moles of water, and the mole fraction of water is 111.1/112.1 = 0.991.

1. Move 1 mole of dissolved $CaCl_2$ from a concentration of 0.5 molar to the 1 molal standard state.

$$\Delta G_{(1)} = RT \ln \frac{a_{\text{CaCl}_2(m=1)}}{a_{\text{CaCl}_2(m=0.5)}}$$

$$= -RT \ln 4\left(\gamma^{\pm} m_{\text{CaCl}_2}\right)^3$$

$$= -8.3144 \times 298 \ln\left[4\times(0.448\times 0.5)^3\right] = 7686 \text{ J}$$

2. Transfer the 1 mole of Ca^{2+} ions from the 1 molal standard state to solid Ca at 298 K. From Table 14.1, $\varepsilon^{\circ,Ca} = -2.87$ volts. Therefore, for the reaction

$$Ca^{2+}_{(m)} + 2e^- = Ca_{(s)}$$

$$\Delta G_{(2)} = -(2 \times 96{,}487 \times -2.87) = 553{,}835 \text{ J}$$

3. Transfer the 2 moles of Cl^{2-} ions from the 1 molal standard state to Cl_2 gas at 1 atm pressure at 298 K. From Table 14.1, $\varepsilon^{\circ,Cl} = 1.3595$ volts. Therefore, for the reaction

$$2Cl^-_{(m)} = Cl_{2(g)} + 2e^-$$

$$\Delta G_{(3)} = -(2 \times 96{,}487 \times -1.3595) = 262{,}348 \text{ J}$$

4. Transfer 111.1 moles of H_2O from a mole fraction of 0.991 to a mole fraction of 1.0. Assuming Raoultian behavior,

$$\Delta G_{(4)} = -n_{H_2O} RT \ln X_{H_2O}$$

$$= -111.1 \times 8.3144 \times 298 \ln 0.991 = 2486 \text{ J}$$

5. Allow the 1 mole of solid Ca to react with the mole of gaseous Cl_2 to form 1 mole of solid $CaCl_2$ at 298 K. For the reaction

$$Ca_{(s)} + Cl_{2(g)} = CaCl_{2(s)}$$

$$\Delta G_{(5)} = \Delta G^{\circ}_{298K} = -752{,}100 \text{ J}$$

Thus, the change in the Gibbs free energy for the separation process is

$$\Delta G_{(1)} + \Delta G_{(2)} + \Delta G_{(3)} + \Delta G_{(4)} + \Delta G_{(5)} = 74{,}255 \text{ J}$$

which is the minimum amount of work required per mole of $CaCl_2$ separated.

PROBLEMS

14.1 The EMF of the galvanic cell

$$Pb_{(s)} \left| PbCl_{2(s)} \right| HCl_{(\text{aqueous})} \left| AgCl_{(s)} \right| Ag_{(s)}$$

where all of the components are present as pure solids in contact with an HCl electrolyte, is 0.490 volts at 25°C and, at that temperature, the temperature coefficient of the EMF is -1.84×10^{-4} volts/degree. Write the cell reaction and calculate the Gibbs free energy change and the change in entropy for the cell reaction at 298 K.

14.2 At 298 K, the EMF of the cell

$$\mathrm{Pb}\,|\,\mathrm{PbCl_2}\,|\,\mathrm{Hg_2Cl_2}\,|\,\mathrm{Hg}$$

is +0.5357 volts and the temperature coefficient of the EMF is 1.45×10^{-4} volts/degree. Calculate (*a*) the maximum work available from the cell at 298 K per mole of Pb reacted, (*b*) the change in entropy for the cell reaction, and (*c*) the heat absorbed by the cell at 298 K per mole of Pb reacted when the cell is operating reversibly.

The Hg electrode in the cell is replaced by an Hg–X alloy in which $X_{\mathrm{Hg}}=0.3$ and where *X* is inert. The EMF of the cell at 298 K is found to increase by 0.0089 volts. Calculate (*d*) the activity of Hg in the alloy at 298 K.

14.3 The solid-state electrochemical cell

$$(\mathrm{Pt}),\mathrm{O_2}(\text{gas at } p_{\mathrm{O_2}})\,|\,\mathrm{CaO-ZrO_2}\,|\,\mathrm{Fe}\,|\,\mathrm{FeO},(\mathrm{Pt})$$

is built to measure the partial pressure of oxygen in gases. Write an equation relating the oxygen pressure and temperature of the gas to the EMF to the cell.

14.4 The EMF of the cell

$$\mathrm{Ag}_{(s)}\,|\,\mathrm{AgCl}_{(s)}\,|\,\mathrm{Cl}_{2(g,1\mathrm{atm})},\mathrm{Pt}$$

is found to be

$$\varepsilon(\text{volts})=0.977+57\times10^{-4}(350-T)-4.8\times10^{-7}(350-T)^2$$

in the temperature range = 100°–450°C. Calculate the value of Δc_p for the cell reaction.

14.5 A galvanic cell is set up with electrodes of solid aluminum and solid aluminum-zinc alloy and an electrolyte of molten $AlCl_3$–NaCl. When the mole fraction of Al in the alloy electrode is 0.38, the EMF of the cell is 7.43 millivolts at 380°C, and the temperature coefficient of the EMF is 2.9×10^{-5} volts/degree. Calculate (*a*) the activity of Al in the alloy, (*b*) the partial molar entropy of mixing of Al in the alloy, and (*c*) the partial molar enthalpy of mixing of Al in the alloy.

14.6 By measuring the EMFs of cells of the type

$$\mathrm{Ni}_{(s)}\,|\,\mathrm{NiO}_{(s)}\,|\,\mathrm{CaO-ZrO_2}\,|\,\mathrm{Cu}_{(l)}\quad\text{containing dissolved oxygen}$$

it has been established that $e_{\mathrm{O}}^{\mathrm{O}}$ in liquid copper at 1363 K is −0.16 and that the standard Gibbs free energy change for

$$\frac{1}{2}\mathrm{O}_{2(g)}=[\mathrm{O}]_{1\text{ wt\% in Cu}}$$

is $\Delta G^\circ=-74{,}105+10.76T$ J. If the EMF of such a cell is 0.222 volts at 1363 K, calculate (*a*) the activity of oxygen in the liquid copper cathode with respect to a standard state of oxygen gas at 1 atm pressure, (*b*) the

activity of Cu_2O in the cathode metal with respect to Cu-saturated pure solid Cu_2O, (*c*) the weight percentage of oxygen dissolved in the copper cathode, (*d*) the maximum solubility of oxygen in liquid copper at 1363 K.

14.7 Calculate the conditions under which an aqueous solution of $[Pb^{2+}] = 1$ mole/liter is in equilibrium with metallic Pb and solid PbO at 298 K. Is any other lead ion present in significant concentration in this solution?

Species	$\Delta G^{\circ}_{298\,K}$ J
$PbO_{(s)}$	−189,300
$Pb^{2+}_{(m)}$	−24,310
$Pb^{4+}_{(m)}$	+302,500
$HPbO^{-}_{2(m)}$	−339,000
$PbO^{2-}_{3(m)}$	−277,570
$PbO^{4-}_{4(m)}$	−28,210
$H_2O_{(l)}$	−237,190

14.8 Aluminum can be produced by electrolysis of Al_2O_3 dissolved in molten cryolite, $3NaF{\cdot}A1F_3$. If inert electrodes are used in an electrolysis cell and the cryolite is saturated with Al_2O_3 at 1000°C, what is the decomposition voltage of the Al_2O_3? The Hall-Heroult process for electrolysis of Al_2O_3 uses graphite as the anode material, and the gas which is evolved at the anode is essentially pure CO_2 at 1 atm pressure. Calculate the decomposition voltage of Al_2O_3 in an Al_2O_3-saturated $3NaF{\cdot}AlF_3$ electrolyte at 1000°C in the Hall-Heroult cell.

14.9 At 298 K the solubility of Cl_2 in H_2O, under a partial pressure of $Cl_2 = 1$ atm, is 0.0618 molal. Calculate the standard Gibbs free energy of formation of an aqueous solution of chlorine and calculate the change in the Gibbs free energy to form a solution of chlorine which is 0.01 molal. Ideal solution behavior can be assumed.

14.10* Calculate the Gibbs free energy change at 298 K and one atmosphere pressure for the overall reaction of a Ni-Cd battery. See Section 14.10.2.

14.11* A copper wire is immersed in a strong acid (e.g. HCl). Will the copper wire dissolve? Explain.

14.12* A zinc wire is immersed in a strong acid (e.g. HCl). Will the zinc wire dissolve? Explain.

* New problem in this edition.

15 More Binary System Solution Models

15.1 INTRODUCTION

In Chapter 9, the *ideal* and r*egular* solution models were developed, and in Chapter 10, they were applied to both the liquid and solid state solutions and utilized to produce temperature *versus* composition equilibrium phase diagrams in Binary alloy systems. This chapter briefly reviews these models in their application to *condensed* binary alloys. This is followed by several enhanced models of solutions, namely, a sub-regular model as well as statistical models of solutions. Finally, the Landau approach of including the effect of ordering processes by means of the thermodynamic variable of order parameter to solid solutions is presented and discussed.

15.2 REVIEW OF IDEAL AND REGULAR SOLUTION MODELS

15.2.1 The Gaseous State: Ideal Solutions

The ideal solution model of the gaseous phase posits that there are no interactions between the constituents (atoms or molecules) that compose the gas. This means that the Gibbs free energy of mixing of a gas, $\Delta G^{M,\mathrm{id}}(g)$ is determined solely by its temperature, T, and its entropy of mixing, $\Delta S^{M,\mathrm{id}}(g)$, that is

$$\Delta G^{M,\mathrm{id}}(g) = -T\ \Delta S^{M,\mathrm{id}}(g) \tag{15.1}$$

Figure 15.1 shows a plot of $\Delta G^{M,\mathrm{id}}(g)$ *versus* composition for a gas composed of the constituents A and B at two different temperatures. It can be seen that the greater the temperature, the more negative is the value of $\Delta G^{M,\mathrm{id}}(g)$ at any given composition. This diagram shows that at all temperatures >0 K the ideal *solution* model for an ideal gas predicts the complete random distribution of its constituents.

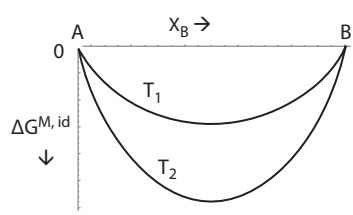

FIGURE 15.1 Plots of the Gibbs free energy of mixing of an ideal solution at two temperatures, T_1 and T_2, where $T_1 < T_2$.

At 0 K, $\Delta G^{M,\mathrm{id}}(g)=0$ for all compositions. This implies (hypothetically), that whatever state the gas is in when it reaches 0 K it will remain in that state, since there is no energetic driving force ($\Delta G^{M,\mathrm{id}}(g)=0$) for it to change. However, if the gas were to obey the *Third Law of Thermodynamics*, it would separate into its constituent components.

15.2.2 The Condensed State: Ideal Solutions

The assumption of no constituent interactions that is used to define an ideal gas case is of course not valid, since all gases can be condensed to their liquid state at low temperatures and/or high pressures. The very process of condensing shows that constituents *do interact*, and in passing from the gaseous to liquid state the interaction is such that the *internal energy* of the system is lowered.

The *ideal solution model* of condensed *binary alloys* assumes that there is no difference in the interaction between different types of constituents (A and B) than between the same types of constituents (A and A or B and B). There is therefore no energy term that needs to be included in the formulation of the Gibbs free energy of *mixing* of ideal condensed solutions. This means that the Gibbs free energy of mixing of condensed phases, $\Delta G^{M,\mathrm{id}}(c)$ is determined solely by its temperature, T, and its entropy of mixing, $\Delta S^{M,\mathrm{id}}(c)$, that is, as was the case for ideal mixtures of gases.

$$\Delta G^{M,\mathrm{id}}(c) = -T\ \Delta S^{M,\mathrm{id}}(c) \tag{15.2}$$

Figure 15.1 can also be used to display the variation of $\Delta G^{M,\mathrm{id}}(c)$ versus composition for a condensed phase composed of the constituents A and B at two different temperatures. As for the gaseous phase, it shows that the greater the temperature, the more negative is the value of $\Delta G^{M,\mathrm{id}}(c)$ at any given composition. This diagram shows that at all temperatures >0 K the ideal solution model for a condensed phase predicts complete random distribution of its constituents.

Let us consider a crystalline phase. At 0 K, $\Delta G^{M,\mathrm{id}}{}_{(\mathrm{crystal})}=0$ at all compositions. This means that whatever state the crystalline phase is in when it reaches 0 K it should remain in that state, using the Gibbs free energy criterion of equilibrium, since there is no energetic driving force for it to change. The ground state would be highly degenerate, as it may be composed of many combinations of the distributions of its constituents in the solid solutions with different entropies in equilibrium with each other. However, if we invoke the *Third Law of Thermodynamics*, the ground state should be composed of pure A phase and a pure B phase since these phases would have zero configurational entropy of 0 K. Of course this state can only be reached if there is the ability of the constituents to inter-diffuse in the solid state at extremely low temperatures!

15.2.3 The Condensed State: Regular Solutions

The regular solution model for condensed phases was discussed in detail in Chapter 9 and applied to phase equilibria of binary component, multi-phase systems in Chapter 10.

From Equation 9.56 the expression for the change in Gibbs free energy of mixing of a condensed phase following the regular solution behavior

$$\Delta G^M = \alpha X_A X_B - T\Delta S^{M,\text{ideal}} \tag{9.56}$$

The term $\alpha X_A X_B$ accounts for interaction among the constituents and is identified as the *excess Gibbs free energy of mixing*. In this case, the excess *Gibbs free energy* is equal to the enthalpy of mixing of the constituents. That is,

$$G^{XS} = \Delta H^M = \alpha X_A X_B$$

Since the enthalpy of mixing of non-ideal solutions can be either positive or negative, the term α may be either positive or negative. In the regular solution model, α is independent of temperature and composition of the alloy.

15.2.3.1 Regular Solutions with Positive Deviation from Ideality

The phase diagram for solid solutions with positive deviation from ideality ($\alpha > 0$) is shown in Figure 15.2. The following features are of note:

- The phase boundary is symmetrical about 50% B
- At high temperatures ($T > T_C$) the alloy forms a solid solution with complete solid-state miscibility. For this to occur, the constituents A and B must have the same crystal structure.
- At temperatures below T_C, the high-temperature phase decomposes into two phases, of A-enriched and B-enriched regions.
- At 0 K the ground state of the alloy is seen to consist of a two-phase mixture of pure A and pure B phases.
- The slopes of the phase boundaries at $X_B = 0$ and 1 are infinite.

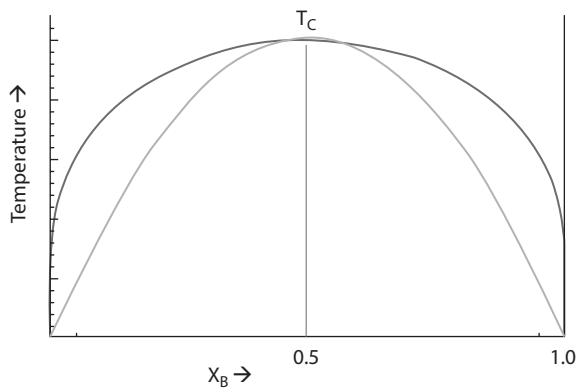

FIGURE 15.2 The regular solution phase diagram with positive deviation from ideality, along with its corresponding spinodal curve.

As shown in Chapter 9, the temperature of the critical point is proportional to the regular solution constant α,

$$T_{cr} = \frac{\alpha}{2R} \tag{9.70}$$

The spinodal curve displays the limits of stability of the homogeneous phase on cooling. The high-temperature homogeneous single phase can be brought below the phase boundary without decomposition (*thermodynamically metastable*) but when it reaches the spinodal the homogeneous phase is *thermodynamically unstable*.

It can be seen in Figure 15.2 that a 50% B alloy has its *phase boundary* and *instability curve* (the spinodal) at the same temperature, namely its critical temperature. At this composition and temperature, the alloy may be considered to undergo a *higher-order transition*.

15.2.3.2 Regular Solutions with Negative Deviation from Ideality

For regular solutions with negative deviations from ideality ($\alpha < 0$), the homogeneous single solid solution curve remains and no phase boundary appears above $T = 0$ K for the ordered phase. See Figure 15.3. The negative term $\alpha X_A X_B$ merely lowers the Gibbs free energy of mixing curve with respect to the ideal solution curve. By invoking the *Third Law of Thermodynamics* it could be imagined that at 0 K there are three ground state phases, namely, the pure A phase, fully ordered A-B compound(s) and the pure B phase. All other compositions would be two-phase mixtures of the appropriate ground state phases.

15.3 SUB-REGULAR SOLUTION MODELS

In the regular solution model, the constant value of α, which, *via* Equation 9.66, gives a parabolic-like variation of G^{XS} and ΔG^M which are symmetrical about the composition $X_B = 0.5$. Using such models in Chapter 10, many different phase diagram topologies and types of invariant transitions were able to be obtained by varying the regular solution constants α_L and α_S of the liquid and the solid solutions.

The *regular solution constant* is independent of composition. The model can be made more flexible by allowing α to vary with composition such as done by Borelius,[1] who wrote:

$$G^{XS} = \Delta H^M = A_1 X_A^n X_B + A_2 X_A^{n-1} X_B^2 + \cdots + A_n X_A X_B^n \tag{15.3}$$

where n is the number of terms utilized in the expansion of the term ΔH^M as a function of composition.

For $n = 2$, this reduces to

$$G^{XS} = \Delta H^M = A_1 X_A^2 X_B + A_2 X_A X_B^2 \tag{15.4}$$

It can be seen that for $A_1 = A_2$, the equation reduces to that of the regular solution model, with $A_1 = \alpha$.

[1] G. Borelius, "The Theory of the Conversions of Metal Mix Phases, III Condition Diagram of Partially Controlled Mix Phases," *Annalen der Physik* (1935), vol. 24(6), pp. 489–506.

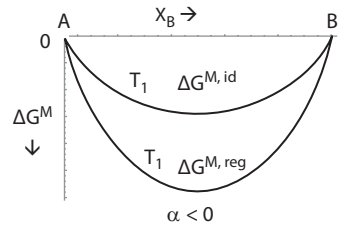

FIGURE 15.3 Plot of the Gibbs free energy of mixing of a regular solution at temperature T_1, with $a<0$, compared with the Gibbs free energy of mixing of an ideal solution at the same temperature T_1.

A model similar to that of the Borelius sub-regular solution can be made by expanding α in terms of X_B as follows:

$$\alpha = a + bX_B + cX_B^2 + dX_B^3 + \cdots \tag{15.5}$$

If we set all the constants in Equation 15.5 equal to zero except a and b we obtain the molar excess Gibbs free energy of formation of a binary A–B solution to be:

$$G^{XS} = H^M = (a + bX_B)X_A X_B \tag{15.6}$$

Equation 15.6 is an empirical equation; that is, the constants a and b have little physical significance; they are parameters, the values of which can be adjusted in an attempt to fit the equation to experimentally measured data. The application of Equations 9.27a and 9.27b to Equation 15.6 gives the partial molar excess Gibbs free energies of the components A and B as

$$\bar{G}_A^{XS} = aX_B^2 + bX_B^2(X_B - X_A) \tag{15.7}$$

and

$$\bar{G}_B^{XS} = aX_A^2 + 2bX_A^2 X_B \tag{15.8}$$

The maxima and/or minima in the curves occur at

$$\frac{dG^{XS}}{dX_B} = 0 \tag{15.9}$$

which, from Equation 15.6, written as

$$G^{XS} = aX_B + (b-a)X_B^2 - bX_B^3$$

gives

$$\frac{dG^{XS}}{dX_B} = a + 2(b-a)X_B - 3bX_B^2 = 0$$

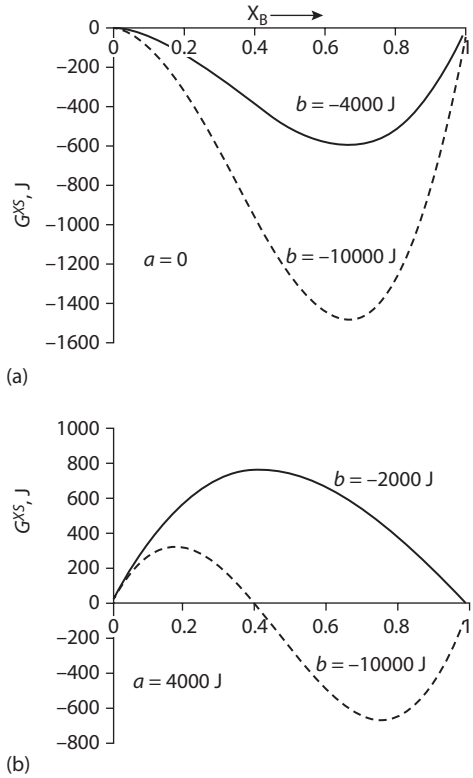

FIGURE 15.4 Excess molar Gibbs free energy curves generated by a sub-regular solution model for various values of a and b of Equation 15.6 in (a) the value of a is zero, while in (b) the value of a is 4000 J. The values of b for the plots are shown in the Figure.

or

$$X_B = \frac{2(b-a) \pm 2\sqrt{b^2 + ab + a^2}}{6b} \tag{15.10}$$

Thus, as shown in Figure 15.4a with $a = 0$ and $b \neq 0$, the minimum in the curve occurs at $X_B = ⅔$.

In Figure 15.4b, with $a = 4000$ J and $b = -10{,}000$ J, a maximum occurs in the curve at $X_B = 0.17$ and a minimum occurs at $X_B = 0.76$. If, however, $b = -2{,}000$ J, no minimum occurs, only a maximum.

The flexibility of the model can be seen nicely in Figure 15.4b, where the sign of the enthalpy of mixing varies from positive values at low values of X_B to negative values at larger X_B. This allows for phase diagrams that would display atomic ordering at some compositions and phase decomposition in other compositions, which cannot be done if only one interaction energy term is used. Meijerling[2] used such an arrangement of the heat of solution in AlCu alloys to explain phase transformations in that alloy.[3]

[2] L. Meijerling, *Rev. Met.* (1952), vol. 49, p. 906.

[3] See also *Report on Precipitation*, H. K. Hardy and T. J. Heal, *Prog. Met. Phys.* (1954), vol. 5, pp.143–278.

The influence of temperature on the behavior of sub-regular solutions is accommodated by introducing a third constant, τ, to give the molar excess Gibbs free energy of mixing as

$$G^{XS} = (a_0 + b_0 X_B) X_A X_B \left(1 - \frac{T}{\tau}\right) \tag{15.11}$$

The molar excess entropy of mixing is thus

$$\begin{aligned} S^{XS} &= -\frac{\partial G^{XS}}{\partial T} \\ &= \frac{(a_0 + b_0) X_A X_B}{\tau} \end{aligned} \tag{15.12}$$

and the molar enthalpy of mixing (which is also the molar excess enthalpy of mixing) is given by

$$\begin{aligned} \Delta H^M &= G^{XS} + TS^{XS} \\ &= (a_0 + b_0 X_B) X_A X_B \left(2 - \frac{T}{\tau}\right) \end{aligned} \tag{15.13}$$

15.4 STATISTICAL MODELS OF SOLUTIONS

Understanding the behavior of regular solutions can be enhanced by the application of the statistical mixing model, introduced in Chapter 4, to two-component alloys. In these alloys, it is assumed that the components have equal molar volumes, that is, they do not exhibit a change in molar volume when mixed, $\Delta \bar{V}_i^M = 0$. In both the pure state and in solution, the interatomic forces are assumed to exist only between neighboring atoms (the near-neighbor model), in which case the energy of the solution is the sum of the interatomic near-neighbor bond energies.

Consider one mole of a mixed crystal containing N_A atoms of A and N_B atoms of B, such that

$$X_A = \frac{N_A}{N_A + N_B} = \frac{N_A}{N_O} \quad \text{and} \quad X_B = \frac{N_B}{N_O} \tag{15.14}$$

where N_O is Avogadro's number. The mixed crystal, or solid solution, contains three types of atomic bonds:

1. A–A bonds with energy E_{AA}
2. B–B bonds with energy E_{BB}
3. A–B bonds with energy E_{AB}

By considering the zero of energy to be that when the atoms are infinitely far apart, the bond energies E_{AA}, E_{BB}, and E_{AB} are *negative quantities.*

Let the coordination number of an atom in the crystal be z; that is, each atom has z nearest neighbors. If, in the solution, there are P_{AA} A–A bonds, P_{BB} B–B bonds, and P_{AB} A–B bonds, the energy of the solution, E[4], is obtained as the linear combination

$$E = P_{AA}E_{AA} + P_{BB}E_{BB} + P_{AB}E_{AB} \tag{15.15}$$

and the problem of calculating E becomes one of calculating the values of P_{AA}, P_{BB}, and P_{AB}.

$$\text{The number of } A \text{ atoms} \times \text{the number of bonds per atom}$$

$$= \text{The number of } A-B \text{ bonds} + 2 \times \text{the number of } A-A \text{ bonds}$$

(The factor 2 arises because each A–A bond involves two A atoms). Thus,

$$zN_A = P_{AB} + 2P_{AA} \tag{15.16}$$

or

$$P_{AA} = \frac{zN_A}{2} - \frac{P_{AB}}{2} \tag{15.17}$$

Similarly, for B, $zN_B = P_{AB} + 2P_{BB}$, or

$$P_{BB} = \frac{zN_B}{2} - \frac{P_{AB}}{2} \tag{15.18}$$

The substitution of Equations 15.17 and 15.18 into Equation 15.15 gives

$$\begin{aligned} E &= \left(\frac{zN_A}{2} - \frac{P_{AB}}{2}\right)E_{AA} + \left(\frac{zN_B}{2} - \frac{P_{AB}}{2}\right)E_{BB} + P_{AB}E_{AB} \\ &= \frac{1}{2}zN_AE_{AA} + \frac{1}{2}zN_BE_{BB} + P_{AB}\left[E_{AB} - \frac{1}{2}(E_{AA} + E_{BB})\right] \end{aligned} \tag{15.19}$$

Consider now the energies of the pure components before mixing. With N_A atoms in pure A,

$$2 \times \text{The number of } A-A \text{ bonds} = \text{The number of atoms} \times \text{the number of bonds per atom}$$

That is,

$$P_{AA} = \frac{1}{2}zN_A \tag{15.20}$$

and similarly, for N_B atoms in pure B,

$$P_{BB} = \frac{1}{2}zN_B \tag{15.21}$$

[4] E is the contribution to the internal energy of the interaction energy.

Thus,

$$\Delta E^M = \left(\text{The energy of the solution}\right) - \left(\text{The energy of the unimixed components}\right)$$
$$= P_{AB}\left[E_{AB} - \frac{1}{2}(E_{AA} + E_{BB})\right] \tag{15.22}$$

For the mixing process,

$$\Delta H^M = \Delta E^M + P\Delta V^M$$

and, since it has been stipulated that $\Delta V^M = 0$, then

$$\Delta H^M = \Delta E^M = P_{AB}\left[E_{AB} - \frac{1}{2}(E_{AA} + E_{BB})\right] \tag{15.23}$$

Equation 15.23 shows that, for given values of E_{AA}, E_{BB}, and E_{AB}, ΔH^M depends on P_{AB}, and further that, for the solution to be ideal (i.e., for $\Delta H^M = 0$),

$$E_{AB} = \frac{(E_{AA} + E_{BB})}{2} \tag{15.24}$$

This is a somewhat less stringent condition than the one used in the preliminary discussion in Section 9.2 which suggested that ideal mixing required the condition $E_{AB} = E_{AA} = E_{BB}$. Thus it is seen that a sufficient condition for ideal behavior is that E_{AB} be the average of E_{AA} and E_{BB}.

If $|E_{AB}| > |\frac{1}{2}(E_{AA} + E_{BB})|$, then, from Equation 15.23, ΔH^M is a negative quantity, corresponding to *negative deviations* from Raoultian ideal behavior.

If $|E_{AB}| < |\frac{1}{2}(E_{AA} + E_{BB})|$, then ΔH^M is a positive quantity, corresponding to *positive deviations* from Raoultian ideality.

If $\Delta H^M = 0$, then the mixing of the N_A atoms with the N_B atoms of B is random, in which case Equation 9.45 gives

$$\Delta S^M = \Delta S^{M,\text{id}} = -R(X_A \ln X_A + X_B \ln X_B)$$

In solutions that exhibit relatively small deviations from ideal behavior (i.e., $|\Delta H^M| \leq RT$), it can be assumed that the mixing of the atoms is also approximately random, in which case P_{AB} can be calculated as follows.

Consider two neighboring lattice sites in the crystal denoted as 1 and 2. The probability that site 1 is occupied by an A atom is

$$\frac{\text{The number of } A \text{ atoms in the crystal}}{\text{The number of lattice sites in the crystal}} = \frac{N_A}{N_0} = X_A \tag{15.25}$$

and similarly, the probability that site 2 is occupied by a B atom is X_B. The probability that site 1 is occupied by an A atom and site 2 is simultaneously occupied by a B atom is thus $X_A X_B$. But the probability that site 1 is occupied by a B atom and

site 2 is simultaneously occupied by an A atom is also $X_A\,X_B$. Thus, the probability that a neighboring pair of sites contains an A–B pair is $2X_A\,X_B$. By a similar argument, the probability that the neighboring sites contain an A–A pair is X_A^2 and that the neighboring sites contain a B–B pair is X_B^2. The probability that the neighboring sites contain an A–B pair or an A–A pair or a B–B pair is

$$X_A^2 + 2X_AX_B + X_B^2 = (X_A + X_B)^2 = 1 \tag{15.26}$$

Since a mole of crystal contains ½ zN_O pairs of lattice sites, then

$$\text{The number of } A-B \text{ pairs} = \text{The number of pairs of sites} \times \text{the probability of an } A-B \text{ pair} \tag{15.27}$$

That is,

$$P_{AB} = \frac{1}{2} zN_O \times 2X_AX_B = zN_OX_AX_B \tag{15.28}$$

Similarly,

$$P_{AA} = \frac{1}{2} zN_O \times X_A^2 = \frac{1}{2} zN_OX_A^2 \tag{15.29a}$$

and

$$P_{BB} = \frac{1}{2} zN_OX_B^2 \tag{15.29b}$$

Substituting Equation 15.28 into 15.23 gives

$$\Delta H^M = zN_OX_AX_B\left[E_{AB} - \frac{1}{2}(E_{AA} + E_{BB})\right] \tag{15.30}$$

and if we set W_1 as

$$W_1 = \left[E_{AB} - \frac{1}{2}(E_{AA} + E_{BB})\right] \tag{15.31}$$

then

$$\Delta H^M = zN_OW_1X_AX_B \tag{15.32}$$

which shows that ΔH^M is a parabolic function of composition. Since random mixing is assumed, the statistical model corresponds to the *regular solution model*; that is,

$$\Delta H^M = G^{XS} = zN_OW_1X_AX_B \tag{15.33}$$

Thus, $zN_O\,W_1 = \alpha$.

Note, as defined by Equation 15.31, $W_1 < 0$ favors atomic ordering.

The applicability of the statistical model to actual solutions decreases as the magnitude of W_1 increases; that is, if the magnitude of E_{AB} is significantly greater or less than the average of E_{AA} and E_{BB}, then random mixing of the A and B atoms cannot be assumed. The equilibrium configuration of a solution at constant T and P is that which minimizes the Gibbs free energy, G, where $G = H - TS$ is measured relative to the unmixed components. As has been seen, the minimization of G occurs as a compromise between the minimization of H and the maximization of S. If $|E_{AB}| > |\frac{1}{2}(E_{AA} + E_{BB})|$, then the minimization of H corresponds to the maximization of the number of A–B pairs (complete ordering of the solution). On the contrary, the maximization of S corresponds to completely random mixing. The minimization of G thus occurs as a *compromise* between the maximization of P_{AB} (the tendency toward which increases with increasingly negative values of W_1) and random mixing (the tendency toward which increases with increasing temperature). The critical parameters are thus W_1 and T, and, if W_1 is appreciably negative and the temperature is not too high, then the value of P_{AB} will be greater than that for random mixing, in which case the assumption of random mixing is not valid.

Similarly, if $|E_{AB}| < |\frac{1}{2}(E_{AA} + E_{BB})|$, then the minimization of H corresponds to the minimization of the number of A–B pairs (complete clustering in the solution), and the minimization of G occurs as a compromise between the minimization of P_{AB} (the tendency toward which increases with increasingly positive values of W_1) and random mixing. Thus, if W_1 is appreciably positive and the temperature is not too high, then the value of P_{AB} will be less than that for random mixing, in which case the assumption of random mixing is again invalid.

In order for the statistical model—and hence, the regular solution model—to be applicable, it is necessary that the aforementioned compromise be such that the equilibrium solution configuration is not too distant from random mixing. Since the contribution of the entropy to the Gibbs free energy is dependent on temperature, it can be noted that:

1. For any value of W_1, more nearly random mixing occurs as the temperature is increased.
2. For any given temperature, more nearly random mixing occurs with smaller values of W_1.

15.5 THE ATOMIC ORDER PARAMETER

As mentioned above, a major flaw in the regular solution model is that, in counting neighbors to obtain the enthalpy of mixing as well as the entropy of mixing, it is assumed that the atoms are randomly placed on the lattice. But, if the expression

$$E_{AB} - \frac{1}{2}(E_{AA} + E_{BB}) \tag{15.34}$$

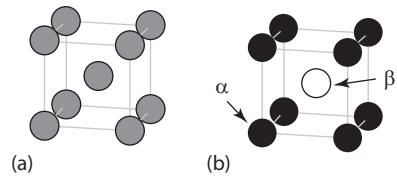

FIGURE 15.5 (a) BCC (A2) and (b) CsCl (B2) structures. The white and black atoms are randomly arranged in the BCC structure, but in the CsCl structure, the black atoms (*A* atoms) sit on the α sites and the white atoms (*B* atoms) are on the β sites.

is not zero, the atoms will not be randomly arranged! For atomic ordering transformations, this can be improved by including a thermodynamic variable that accounts for the nonrandom configuration of the atoms. This factor is the *long-range order parameter* (LRO), η.

Consider the ordering transformation of a random *A*–*B* solution phase (fully disordered) with a BCC (A2) structure to the fully ordered phase with the CsCl (B2) structure (Figure 15.5). In (a) the gray atoms represent random missing of A and B atoms.

The LRO parameter η is defined to be

$$\eta \equiv \frac{r_\alpha - X_A}{Y_\beta} = \frac{r_\beta - X_B}{Y_\alpha} \tag{15.35}$$

where r_α (r_β) is the fraction of α (β) sites that are "rightly" occupied, X_i is the fraction of the *i*th component, and Y_α (Y_β) is the fraction of α (β) sites in the lattice. For the BCC → B2 transformation, Y_α and Y_β are ½. Thus, for an equiatomic alloy ($X_A = X_B = ½$), we have

$$\eta = 2r_\alpha - 1 = 2r_\beta - 1 \tag{15.36}$$

- If all the α sites are occupied by *A* atoms, $r_\alpha = 1$ and $\eta = 1$.
- If all the α sites are occupied by *B* atoms, $r_\alpha = 0$ and $\eta = -1$.
- If the α sites are randomly occupied, $r_\alpha = ½$ and $\eta = 0$.

The case for $\eta = -1$ corresponds to a *translational domain* of the B2-ordered system.

The expression for the enthalpy of formation of a system from the pure *A* and pure *B* components was given previously (15.36) as

$$\Delta H^M = zN_O X_A X_B W_1$$

where $W_1 = E_{AB} - ½(E_{AA} + E_{BB})$. For $W_1 < 0$, atomic ordering is favored. This assumed a random distribution of A and B atoms on the crystalline sites. For $W_1 = 0$, the atoms are randomly arranged. and for $W_1 > 0$, clustering is favored.

This equation yields a value of $\Delta H^M = 2N_O W_1$ for the equiatomic ordered B2 alloy.

But of course, the atoms do not occupy the atomic sites randomly for the case $W_1 < 0$. If we include the effect of atomic ordering on the occupation of the sites, ΔH^M is written as:

$$\Delta H^M = zN_O W_1 \left(X_A X_B + \frac{\eta^2}{4} \right) \tag{15.37}$$

For a full order of an equiatomic alloy, this yields $\Delta H^M = zN_O W_1/2 = 4N_O W_1$. This value is twice as *negative* as the expression which does not include the order parameter.

The effect of atomic ordering in an equiatomic alloy also can be included in the entropy of mixing as follows:

$$\begin{aligned} \Delta S^M(\eta) = -\frac{N_O k_B}{2} \Bigg\{ & \left(X_A + \frac{\eta}{2} \right) \ln \left(X_A + \frac{\eta}{2} \right) + \left(X_B - \frac{\eta}{2} \right) \ln \left(X_B - \frac{\eta}{2} \right) \\ & + \left(X_A - \frac{\eta}{2} \right) \ln \left(X_A - \frac{\eta}{2} \right) + \left(X_B + \frac{\eta}{2} \right) \ln \left(X_B + \frac{\eta}{2} \right) \Bigg\} \end{aligned} \tag{15.38}$$

For full order of an equiatomic alloy this yields $\Delta S_{\text{conf}} = 0$, since the pure elements have zero configurational entropy and the fully ordered B2 phase also has zero configurational entropy.

Combining the expressions for enthalpy of mixing and the entropy of mixing we obtain:

$$\begin{aligned} \Delta G^M(\eta, T) = zN_O W_1 \left(X_A X_B + \frac{\eta^2}{4} \right) + \frac{Nk_B T}{2} \Bigg\{ & \left(X_A + \frac{\eta}{2} \right) \ln \left(X_A + \frac{\eta}{2} \right) \\ & + \left(X_B - \frac{\eta}{2} \right) \ln \left(X_B - \frac{\eta}{2} \right) + \left(X_A - \frac{\eta}{2} \right) \ln \left(X_A - \frac{\eta}{2} \right) + \left(X_B + \frac{\eta}{2} \right) \ln \left(X_B + \frac{\eta}{2} \right) \Bigg\} \end{aligned} \tag{15.39}$$

Since $\Delta G^M = \Delta G^M(T, P, \eta)$ at constant P and T we find its minimum by taking its derivative with respect to η and set it equal to zero:

$$\frac{\partial \Delta G^M}{\partial \eta} = \frac{zN_O W_1 \eta}{2} + \frac{N_O k_B T}{2} \ln \left(\frac{1+\eta}{1-\eta} \right) = 0 \tag{15.40}$$

This *transcendental equation* can be solved graphically, and its solution for the equiatomic case is shown in Figure 15.6.

As η approaches zero, the temperature approaches the transition temperature. T_0. For small values of η,

$$\ln \left(\frac{1+\eta}{1-\eta} \right) = 2 \left[\eta + \frac{\eta^3}{3} + \cdots \right] \approx 2\eta \tag{15.41}$$

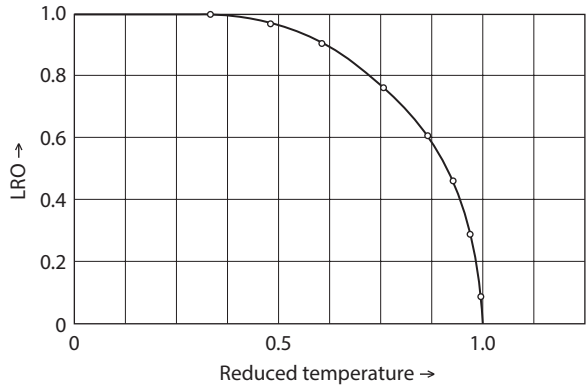

FIGURE 15.6 The atomic LRO parameter η vs. normalized temperature plot for a Bragg–Williams model. Note the infinite slope as T/T_0 approaches 1 and the zero slope as T approaches 0 K.

Thus,

$$\frac{zN_O W_1 \eta}{2} + \frac{2N_O k_B T \eta}{2} = 0 \tag{15.42}$$

which yields

$$T_0 = -\frac{4W_1}{k_B} \tag{15.43}$$

This model produces an atomic ordering phase transition for the equiatomic alloy at T_0. Above this temperature, the equilibrium phase is atomically *disordered* BCC. Below this temperature, the equilibrium phase is *atomically ordered* CsCl with an LRO parameter η that increases continuously with decreasing temperature and which approaches unity as T approaches 0 K, consistent with the Third Law of Thermodynamics. The slope of the η versus T curve at 0 K is zero and at the transition temperature is minus infinity. See Problem 15.8.

The Gibbs free energy of mixing, ΔG^M, versus the order parameter, η is plotted in Figure 15.7 for several temperatures. At temperatures above T_0, the minimum in ΔG^M occurs at $\eta = 0$; that is, the disordered phase is the stable one. Below T_0, two minima appear at $\pm\eta_{eq}$. A maximum appears at $\eta = 0$, showing that the disordered phase is unstable below T_0. As the temperature is lowered, η_{eq} (the value of η at the minimum in the curve) increases until, at $T = 0$ K, $\eta_{eq} = 1$. Plots such as this will be discussed in more detail in Section 15.6. For now, we notice that ΔG^M versus η can be written in a Taylor series form as follows:

$$\Delta G^M = b\eta^2 + c\eta^4 \tag{15.44}$$

where b is a function of T, and c is considered to be a positive constant.

By including the atomic order parameter as a thermodynamic variable, this model allows for a phase transition to occur in ordering solutions. The transition is one

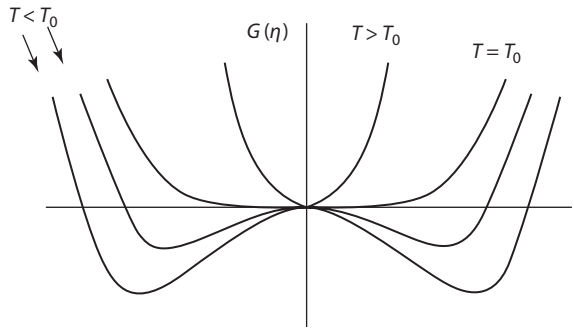

FIGURE 15.7 Gibbs free energy of mixing, ΔG^M, vs. order parameter at various temperatures relative to the critical temperature.

between zero and nonzero values of the order parameter and occurs at a temperature that is proportional to the interaction energy, W_1.

15.5.1 Statistical Models Including Second-Neighbor Interactions

Another extension of this solution model can be made by adding second-neighbor interactions. Previously, we defined first-neighbor interactions as

$$W_1 = E_{AB}^{(1)} - \frac{1}{2}\left(E_{AA}^{(1)} + E_{BB}^{(1)}\right) \tag{15.45}$$

Second-neighbor interaction energies can be written as

$$W_2 = E_{AB}^{(2)} - \frac{1}{2}\left(E_{AA}^{(2)} + E_{BB}^{(2)}\right) \tag{15.46}$$

This expression can be added to the one for the heat of transformation used previously to obtain

$$\Delta H^M = N_O X_A X_B \left[z_1 W_1 + z_2 W_2\right] + \frac{N_O \eta^2}{4}\left[z_1 W_1 - z_2 W_2\right] \tag{15.47}$$

It can be seen from Figure 15.5 that for the B2-ordered structure, although $W_1 < 0$ (favoring opposite first neighbors), $W_2 > 0$ (favoring the same second neighbors). See Problem 15.1. See Ino.[5] Details and further work on other structures can be found in Soffa, Laughlin, and Singh,[6] where the authors analyze the transformations FCC → $L1_2$ and FCC → $L1_0$.

[5] H. Ino, "A Pairwise Interaction Model For Decomposition And Ordering Processes in B.C.C. Binary Alloys and Its Application to the Fe-Be System," *Acta Met.* (1978), vol. 26, pp. 827–834.

[6] W. Soffa, D. E. Laughlin, and N. Singh, "Interplay of Ordering and Spinodal Decomposition in the Formation of Ordered Precipitates in Binary Fee Alloys: Role of Second Nearest-Neighbor Interactions," *Philos. Mag.* (2010), vol. 90(1–4), pp. 287–304.; W. A. Soffa, D. E. Laughlin, N. Singh, "Re-examination of A1 → L10 Ordering: Generalized Bragg–Williams Model with Elastic Relaxation," in *Solid–Solid Phase Transformations in Inorganic Materials*, edited by Y. Bréchet, et al. Trans Tech, Enfield, NH, 2011, pp. 608–617.

15.6 LANDAU THEORY OF ORDERED SOLUTIONS

We have discussed the Ehrenfest designation of transitions being either *first order* or *second (higher) order*. In Chapter 8, it was shown that the van der Waals equation for a nonideal gas gave rise to a phase change in the system and that such a change could be either a *first-order* one or a *continuous* one. In this section, we introduce another model of the thermodynamics of a solution phase that enables phase transitions and also allows for both first- and higher-order transitions. This model is the Landau model of phase transitions.

In the late 1930s, Lev Davidovich Landau (1908–1968) proposed that many phase transitions can be characterized by a parameter, η, which describes an important property that is characteristic of the system under study (e.g. atomic order, polarization, magnetic moment, density, strain, etc.). This parameter has nonzero values below a certain temperature, T_0, and is zero above this temperature. It is called an *order parameter*, and it describes the evolution of the system in terms of measurable physical parameters. It has an equilibrium value for a given system which is a function of temperature and pressure. The parameter is usually normalized such that in the ordered state the order parameter approaches unity ($\eta = 1$) as T approaches 0 K, and above the transition temperature the parameter is equal to zero. The way that it varies in the vicinity of the critical point serves as a useful basis for classifying the nature of the phase transition/transformation. Both first-order and higher-order transitions can be modeled, though the original model of Landau was focused on the *higher-order transitions*. In Section 15.5, the atomic order parameter was utilized to investigate equilibrium states in regular solutions that exhibit negative deviations from ideality. Figure 15.6 is a plot of the atomic order parameter *versus* temperature for such systems.

The effect of order parameter on the thermodynamics of a system is tracked as an excess term in the Gibbs excess free energy. Landau's model is that the excess free energy between the ordered ($\eta > 0$) and disordered states ($\eta = 0$), $G^{XS}(\eta)$, can be expanded in a *power series* in the order parameter in the neighborhood of the critical point.

Landau wrote the excess free energy as

$$G^{XS}(\eta) = G(\eta \neq 0) - G(\eta = 0)$$

$$G^{XS}(\eta) = A\eta^2 + B\eta^3 + C\eta^4 + D\eta^5 + E\eta^6 + \cdots \tag{15.48}$$

where the coefficients A, B, C, … may be functions of temperature, T, and/or pressure, P. At constant pressure, the term A can be taken as a linear function of temperature given by

$$A = a(T - T_C) \tag{15.49}$$

where T_c is the critical temperature and the coefficient a being *a positive constant*. B, C, D, and E are taken as constants in the first approximation. It can be seen that A changes sign on passing through the temperature T_C.

- When $T > T_C$, $A > 0$.
- When $T = T_C$, $A = 0$.
- When $T < T_C$, $A < 0$.

The curvature of the plot of G^{XS} versus order parameter is proportional to its second derivative, $\dfrac{\partial^2 G^{XS}(\eta)}{\partial \eta^2}$

$$\frac{\partial^2 G^{XS}(\eta)}{\partial \eta^2} = 2a(T - T_C) + 12C\eta^2$$

At $\eta = 0$,

$$\left(\frac{\partial^2 G^{XS}(\eta)}{\partial \eta^2}\right)_{\eta=0} = 2a(T - T_C) > 0, \quad \text{for} \quad T > T_C$$

- Above T_C, since $a > 0$, the curvature of the plot is positive. G^{XS} displays a minimum.
- At T_C, the curvature becomes 0, signifying an impending *instability* of the high-temperature phase.
- Below T_C, the curvature is negative and thus G^{XS} displays a maximum. This means that the disordered phase is *unstable* and the ordered phase forms (see Figure 15.8).

Different specific cases of the Landau model will be investigated in the text and problems at the end of this chapter.

15.6.1 The 2-4 Model

In this case, the values of the coefficients in Equation 15.48 are, $B = 0$, $C > 0$, and $D = E = 0$. Hence

$$G^{XS}(\eta) = a(T - T_C)\eta^2 + C\eta^4 \tag{15.50}$$

When $B = D = 0$, $G^{XS}(\eta)$ is an *even function* of η; that is,

$$G^{XS}(+\eta) = G^{XS}(-\eta)$$

This means that the entire plot of G^{XS} *versus* order parameter is symmetric about the ordinate.

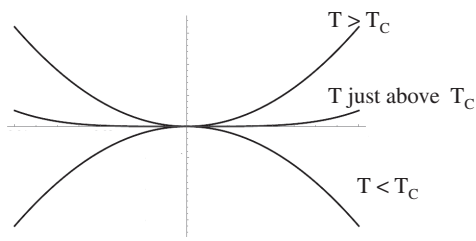

FIGURE 15.8 G^{XS} (η) near $\eta = 0$, showing the effect of temperature on the curvature and hence the stability of the phase being modeled.

As mentioned previously, $A = a(T - T_C)$ changes sign at $T = T_C$.

The behavior of $G^{XS}(\eta)$ as a function of temperature and the variation of the order parameter with temperature is shown in Figure 15.9. Above T_C (T_1 and T_2), $G^{XS}(0)$ is the only *extremum* (a minimum), and therefore, the equilibrium state is disordered. Thus, the A and B atoms are distributed randomly on the atomic sites. See Figure 15.5a. At T_C, the curvature of $G^{XS}(0)$ equals zero, which means that the disordered phase is unstable. Below T_C (e.g. T_3 and T_4), there are two states with nonzero equilibrium order parameters. It can be seen from the figure that the minimum in $G^{XS}(\eta)$ occurs at larger η as the temperature is decreased.

Other thermodynamic aspects of this system will now be investigated.

The excess free energy is written as

$$G^{XS}(\eta) = a(T - T_C)\eta^2 + C\eta^4 \tag{15.51}$$

To obtain the equilibrium state, the excess free energy is minimized with respect to η by taking the first derivative and setting it equal to zero.

$$\frac{\partial G^{XS}(\eta)}{\partial \eta} = 2a(T - T_C)\eta + 4C\eta^3 = 0$$

The three solutions to this equation are extrema.

$$\eta_{eq} = 0 \quad \text{and} \quad \eta_{eq}^2 = -\frac{a(T - T_C)}{2C}$$

To determine if the solutions are maxima or minima the sign of the curvature is determined.

The sign of the curvature of the plots are evaluated as

$$\left(\frac{\partial^2 G^{XS}}{\partial \eta^2}\right)_{\eta=0} = 2a(T - T_C) + 12C\eta^2 \tag{15.52}$$

For the solution $\eta_{eq} = 0$, when $T > T_C$ the curvature is positive which means that the function is a minimum, and hence the disordered phase is the stable state.

For the solution $\eta_{eq} = 0$, when $T < T_C$ the curvature is negative, which means that the function is a maximum, and the disordered phase is unstable with respect to those states with minima values.

Real values of η_{eq} other than $\eta_{eq} = 0$ occur at $\eta_{eq}^2 = -\frac{a(T - T_C)}{2C}$ which can be seen to be minima when $T < T_C$. The two solutions $\pm\eta_{eq}$ have equal absolute values (Figure 15.9) and correspond to different translational domains of the low-temperature ordered phase.

Invoking the Third Law of Thermodynamics, $\eta = 1$ at $T = 0$ and thus

$$T_C = 2C/a \tag{15.53}$$

and thus, for the nonzero solutions,

$$\eta_{eq}^2 = \frac{T_C - T}{T_C} = 1 - \frac{T}{T} \tag{15.54}$$

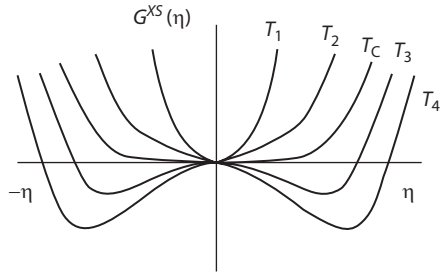

FIGURE 15.9 The excess Gibbs free energy for the 2-4 case (A and $C \neq 0$) of the Landau expansion. At T_C the disordered phase becomes unstable (curvature = 0). In the figure, $T_1 > T_2 > T_C > T_3 > T_4$.

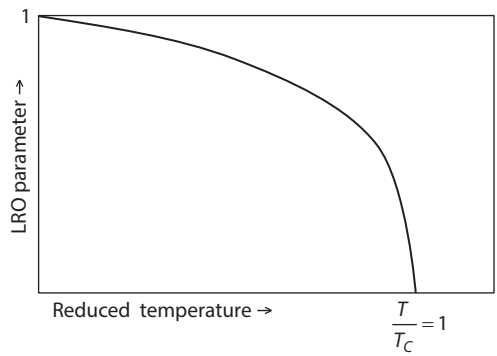

FIGURE 15.10 The order parameter vs. reduced temperature (T/T_C) plot for the Landau 2–4 case of Figure 15.9. Note that the slope at $T = 0$ is not zero in this Landau model.

The equilibrium plot of the order parameter, η, is shown in Figure 15.10.
The 2-4 Landau model gives rise is to a *continuous phase transition* at T_C. The behavior is essentially identical to that of the Ehrenfest second-order transition.

The excess Gibbs free energy, G^{XS}, for $T < T_C$ is found by substituting the equilibrium value $\eta_{eq}^2 = 1 - \dfrac{T}{T_C}$ into Equation 15.51. Thus,

$$G^{XS} = -\frac{a(T_C - T)^2}{2T_C} \tag{15.55}$$

Since $a > 0$, $G^{XS} < 0$ for all $T < T_C$. A negative excess value of G^{XS} is expected for the stable low-temperature-ordered phase.

The *excess entropy* of the system can be found as

$$S^{XS} = -\frac{\partial G^{XS}}{\partial T} = -a\frac{(T_C - T)}{T_C} \tag{15.56}$$

The *excess entropy* varies continuously through the transition temperature, as should be the case for a *second-order (continuous) transition*. Below T_C, the sign of S^{XS} is

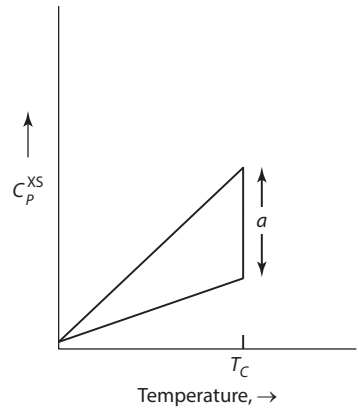

FIGURE 15.11 Plot of excess heat capacity vs. temperature for the Landau 2-4. Note the finite discontinuity at the critical temperature.

negative since the excess is with respect to the disordered phase, and the configurational entropy of the *ordered phase* is *less than* that of the disordered one.

The *excess heat capacity* of the ordered phase relative to the disordered phase at constant pressure for $T < T_C$ is given as

$$C_P^{XS} = T\left(\frac{\partial S^{XS}}{\partial T}\right) = \frac{aT}{T_C} \tag{15.57}$$

and is plotted in Figure 15.11.

At T_C, the value of C_P^{XS} is larger than the value of the disordered phase by an amount a. Just above T_C, the excess value of the heat capacity drops to the value of the disordered phase. This produces a finite discontinuity in the heat capacity plot consistent with the transition being *second order* (the heat capacity is proportional to the second derivative of the energy term $C_P = T\left(\partial^2 G / \partial T^2\right)$), which first becomes discontinuous at the transition temperature.

The excess heat capacity is positive because it takes more thermal energy to increase the temperature of the low-temperature-ordered phase than that of the disordered phase, since the thermal energy must also be utilized to decrease the order of the system. The heat capacity above T_C is that of the high-temperature phase.

Finally, the excess enthalpy H^{XS} can be shown (see Problem 15.3) to be

$$H^{XS} = \frac{a}{2}\frac{\left(T^2 - T_C^2\right)}{T_C} \tag{15.58}$$

This equation shows that the transition has no *latent enthalpy of transformation*, which is a signature of a *second-order transition*.

15.6.1.1 Excursus on T_C

The temperature denoted as T_C in the 2-4 case is a *critical temperature*, in the sense that at that temperature, the phase becomes unstable. For the 2-4 case, T_C is *critical* for the disordered state on cooling from above

state on heating from below T_C. These critical temperatures can be denoted as T_i^- and T_i^+ respectively.

For the 2-4 case

$$T_i^- = T_C = T_i^+$$

For first-order transitions these relationships are not valid. They are different from each other as well as from the equilibrium transition temperature, which is no longer a *critical temperature*. For first order transitions the transition temperature is denoted as T_0. Thus, for first-order transitions:

$$T_i^- < T_0 < T_i^+$$

15.6.2 The 2-3-4 Model

The excess Gibbs free energy function for the 2-3-4 case is written as:

$$G^{XS} = a\left(T - T_i^-\right)\eta^2 + B\eta^3 + C\eta^4 \tag{15.59}$$

where $a > 0$, $B < 0$ and $C > 0$.

This function is not symmetric about the ordinate. To determine if the equation produces a *first-order transformation*, a temperature T_0 for which the ordered phase is in equilibrium with the disordered phase must exist. If such a temperature exists, the two phases have *the same value* of excess free energy, namely zero. That is, since at this temperature the excess free energy of the disordered phase is zero (since $\eta = 0$) so is the excess free energy of the ordered phase. See Figure 15.12, for $T = T_0$.

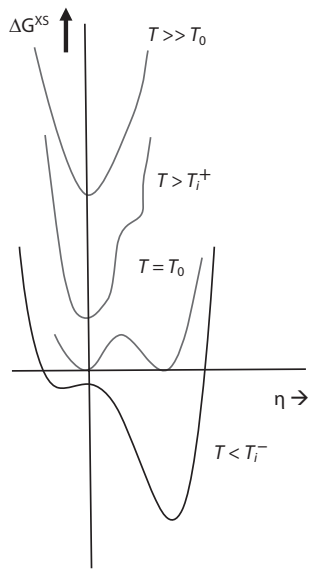

FIGURE 15.12 G^{XS} plots for the Landau 2-3-4 model shown at four different temperatures. The disordered phase exhibits a instability temperature T_i^- and the ordered phase exhibits an instability temperature on heating, T_i^+.

$$G^{XS} = a\left(T_0 - T_i^-\right)\eta^2 + B\eta^3 + C\eta^4 = 0 \tag{15.60}$$

Since the ordered phase is in equilibrium

$$\frac{\partial G^{XS}}{\partial \eta} = 0 = 2a\left(T_0 - T_i^-\right)\eta + 3B\eta^2 + 4C\eta^3 = 0 \tag{15.61}$$

Solving these equations simultaneously yields the following:

$$\eta_{eq}\left(T_0\right) = -\frac{B}{2C} \tag{15.62}$$

and inserting this value into the solution for $T - T_i^-$ at $T = T_0$

$$T_0 - T_i^- = \frac{B^2}{4Ca} \tag{15.63}$$

The instability temperature on cooling for the disordered phase is therefore seen to be less than the equilibrium transition temperature.

The value of T_i^- can be found by taking the first derivative of Equation 15.59 and setting it equal to zero, and inserting $T=0$ into it, since by the Third Law of Thermodynamics at $T=0$, $\eta=1$.

$$\frac{\partial G^{XS}}{\partial \eta} = 0 = 2a\left(0 - T_i^-\right)(1) + 3B(1) + 4C(1) = 0 \tag{15.64}$$

$$T_i^- = \frac{3B + 4C}{2a} \tag{15.65}$$

(Note that if we set $B=0$, the same value for the instability temperature (T_C) is obtained as for the 2-4 case).

Now, the temperature T_0 can be found by inserting Equation 15.65 into Equation 15.63:

$$T_0 = \frac{B^2}{4Ca} + \frac{3B + 4C}{2a}$$

Thus, we see that:

$$T_i^- < T_0 < T_i^+$$

(The value of T_i^+ will be determined in Problem 15.5)

Now, the values of the order parameter at these special temperatures will be calculated.

The value of the order parameter at T_0 was found in Equation 15.62 to be $-\frac{B}{2C}$

The value of the order parameter at T_i^- can be found by inserting T_i^- into Equation 15.59.

This yields:

$$\eta_{eq}\left(T_i^-\right) = -\frac{3B}{4C} \tag{15.66}$$

Finally, it can be shown (see Problem 15.5) that

$$\eta_{eq}\left(T_i^+\right) = -\frac{3B}{8C} \tag{15.67}$$

and

$$T_i^+ = T_i^- + \frac{9B^2}{32Ca} = \frac{3B+4C}{2a} + \frac{9B^2}{32Ca} \tag{15.68}$$

Summarizing these results, we have

$$\begin{aligned} T_i^- &= \frac{3B+4C}{2a} \\ T_0 &= T_i^- + \frac{B^2}{4Ca} \\ T_i^+ &= T_i^- + \frac{9B^2}{32Ca} \end{aligned} \tag{15.69}$$

and

$$\begin{aligned} \eta_{eq}\left(T_i^-\right) &= -\frac{3B}{4C} \\ \eta_{eq}\left(T_0\right) &= -\frac{2B}{4C} \\ \eta_{eq}\left(T_i^+\right) &= -\frac{1.5B}{4C} \end{aligned} \tag{15.70}$$

See Figure 15.13.
Consider the excess Gibbs free energy curves of Figure 15.12.

a. At very high temperatures ($T \gg T_0$) the curve has but one real extremum, being a minimum at $\eta = 0$. This curve represents the disordered phase.
b. As the temperature is decreased, to just above T_0 a second extrema becomes real, and represents relative a minimum the *ordered phase*. The state at $\eta = 0$ is the stable state just above T_0.
c. Continuing to decrease the temperature produces two minima and a maximum. The two minima have the same value of Gibbs excess free energy and are therefore in equilibrium. This occurs at $T = T_0$.
d. Finally, with further decrease in temperature, the extremum at $\eta = 0$ becomes a maximum, indicating the disordered phase has become unstable and the

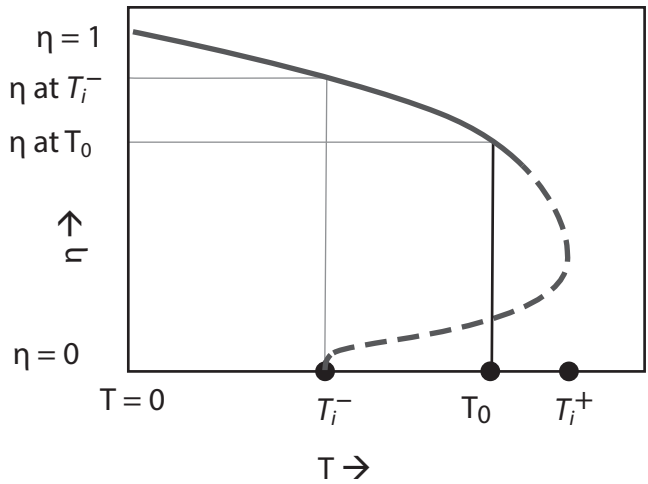

FIGURE 15.13 The order parameter value *versus* temperature for the 2-3-4 model. Equilibrium values are solid. Not to scale.

ordered phase is the equilibrium state. The transition to this state is *continuous*, but since it occurs away from equilibrium is not considered to be second order (or *higher order*) in the Ehrenfest designation.

Consider now Figure 15.13. At 0 K, the stable state is one in which the order parameter equals unity. As the temperature increases, the equilibrium order parameter decreases because of the increasing effect of entropy. At T_0, if the system remains in equilibrium, it will be in equilibrium with the disordered phase. This transition is a *first-order transition*. Increasing the temperature further, the disordered phase is the only stable phase.

If, however, as the temperature reached T_0, the disordered phase does not form, the ordered phase could remain as a *metastable state* (dashed curve). However, once the temperature reached T_i^+ the ordered phase becomes *unstable* and transforms to the disordered phase.

Now consider the system as it cools from far above $T = T_0$. There is no effect as the temperature passes T_i^+ since that temperature refers to the *ordered phase*. When the temperature reaches T_0, the ordered phase may form and be in equilibrium with the disordered phase. Subsequent cooling will increase the equilibrium order parameter until it reaches unity at 0 K.

If, however, as the temperature of the disordered phase reached T_0, and the ordered phase does not form, the disordered phase could remain as a *metastable state* (dashed curve). However, once the temperature reached T_i^-, the disordered phase becomes unstable and transforms into the ordered phase.

A final word about the instability temperatures. These are *thermodynamic instability* temperatures, not *kinetic* ones. Thus, it is possible for a disordered alloy to be cooled rapidly below its instability temperature, T_i^-, and remain disordered because of the lack of thermal energy to allow for the ordering process to occur. However this

will most likely have sufficient energy to allow for the continuous transition to occur at the instability temperature T_i^+.

15.6.3 The 2-4-6 Model

For this case, $A \neq 0$, $C < 0$, and $E > 0$. The excess Gibbs free energy function is written as:

$$G^{XS} = a\left(T - T_i^-\right)\eta^2 + C\eta^4 + E\eta^6 \tag{15.71}$$

Like the 2-4 case, the free energy in 2-4-6 case is symmetrical about $\eta = 0$. As previously, only the quadric term is given a temperature dependence, and $C < 0$ and $E > 0$ are taken to be independent of T and P. The sixth-order term ensures the proper thermodynamic behavior at low temperatures, yielding real solutions for the order parameter (Figure 15.14).

An interesting feature of this case is that even though the excess free energy of the low-temperature phase is symmetric about $\eta = 0$, the phase transition is *first order* for $C < 0$. At $T = T_0$ there are three minima with equal values of the excess free energy: two at nonzero order parameters and one at the disordered state ($\eta = 0$). This is the temperature of a *first-order transition* since the ordered and disordered phases are in equilibrium.

If the temperature is raised above T_0 the three minima remain, but the minima with nonzero order parameter have values of the excess free energy that are greater than the minima at zero order parameter. These ordered states are *metastable states* which appear only on *heating* the ordered phase rapidly (non-equilibrium process). At the temperature T_i^+, the metastable ordered phases become unstable and must disappear. This state has a horizontal inflection point.

As the temperature is lowered from T_0, the three minima remain in the excess free energy plot, but now the two minima with nonzero values of the order have the lower energy. These are now stable states, and the disordered phase (zero order parameter) is metastable.

If, however, the metastable disordered phase remains, eventually, on cooling, it reaches a temperature where the minimum at zero-order parameter becomes an

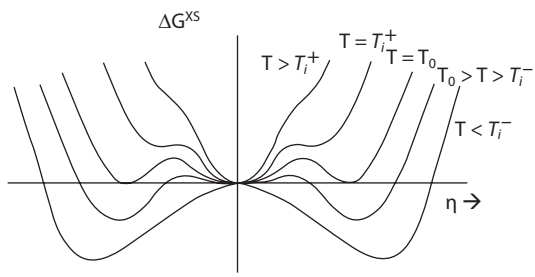

FIGURE 15.14 The excess Gibbs free energy for the Landau 2-4-6 case (A, C and $E \neq 0$, but $C < 0$). At T_0 the disordered phase has the same free energy as the two variants of the ordered phase.

inflection point and the phase becomes unstable. This temperature is denoted as T_i^-. At this temperature the metastable disordered state becomes unstable to any fluctuation in order parameter and hence the ordered phase will form continuously from the disordered phases. Note that this continuous transformation is away from the equilibrium transition temperature and is not considered a higher-order transition.

The values of η^2 for the special temperatures of the transition will now be determined.

The order parameter at any T can be found setting the first derivative of Equation 15.71 equal to zero.

$$\frac{\partial G^{\text{XS}}}{\partial \eta} = 0 = 2a\left(T - T_i^-\right)\eta + 4C\eta^3 + 6E\eta^5 = 0 \tag{15.72}$$

$$\text{For } T = 0,\ \eta^2 = 1,\ \text{so } T_i^- = \frac{2C + 3E}{a} \tag{15.73}$$

Equation 15.72 has the following solutions for $\eta \geq 0$. They are:

$$\eta = 0 \text{ and } \eta^2 = \frac{-2C \pm \sqrt{4C^2 - 12aE\left(T - T_i^-\right)}}{6E} \tag{15.74}$$

For the solutions to be real,

$$4C^2 - 12aE\left(T - T_i^-\right) > 0 \tag{15.75}$$

At T_0, the excess Gibbs free energy of the disordered phase is equal to zero (since $\eta = 0$) and since it is in equilibrium with the ordered phase the excess Gibbs free energy of the ordered phase must also be zero.

$$G^{xs} = a\left(T_0 - T_i^-\right)\eta^2 + C\eta^4 + E\eta^6 = 0 \tag{15.76}$$

Since the ordered phase is in equilibrium,

$$\frac{\partial G^{\text{XS}}}{\partial \eta} = 0 = 2a\left(T_0 - T_i^-\right)\eta + 4C\eta^3 + 6E\eta^5 = 0 \tag{15.77}$$

These equations are solved simultaneously.

On eliminating E, $\eta^2 = -\dfrac{2a\left(T_0 - T_i^-\right)}{C}$ is obtained.

On eliminating $a\left(T_0 - T_i^-\right)$, the following is obtained

$$\eta^2\left(T_0\right) = -\frac{C}{2E} \tag{15.78}$$

Also, $-\dfrac{2a\left(T_0 - T_i^-\right)}{C} = -\dfrac{C}{2E}$

$$T_0 = T_i^- + \frac{C^2}{4aE} \tag{15.79}$$

At the *instability temperature* on cooling, $T = T_i^-$, the first derivative of the excess Gibbs free energy of the ordered phase equals to zero.

$$\frac{\partial G^{\text{XS}}}{\partial \eta} = 0 = 2a\left(T_i^- - T_i^-\right)\eta + 4C\eta^3 + 6E\eta^5 = 0 \tag{15.80}$$

$$\eta^2\left(T_i^-\right) = -\frac{4C}{6E} = -\frac{2C}{3E} \tag{15.81}$$

The *instability temperature* on heating, T_i^+ can be found from the general solution of Equation 15.72, whose solution becomes imaginary at T_i^+ (see Equation 15.75).

$$4C^2 - 12aE\left(T_i^+ - T_i^-\right) = 0 \tag{15.82}$$

$$T^+ = T_i^- + \frac{C^2}{3aE} \tag{15.83}$$

$$\eta^2(T^+) = -\frac{2C}{3E} \tag{15.84}$$

Summarizing these results for the 2-4-6 Landau case:

$$\begin{aligned} T_i^- &= \frac{2C + 3E}{a} \\ T_0 &= T_i^- + \frac{C^2}{4aE} \\ T_i^+ &= T_i^- + \frac{C^2}{3aE} \end{aligned} \tag{15.85}$$

and

$$\begin{aligned} \eta_{\text{eq}}\left(T_i^-\right) &= -\frac{4C}{6E} \\ \eta_{\text{eq}}\left(T_0\right) &= -\frac{3C}{6E} \\ \eta_{\text{eq}}\left(T_i^+\right) &= -\frac{2C}{6E} \end{aligned} \tag{15.86}$$

The order parameter versus Temperature plot will be similar to Figure 5.13, but the above values of the order parameter at the critical temperatures would be inserted on the figure.

15.6.4 Concluding Remarks on the Landau Model

In each of the three cases of the Landau models examined above, it can be seen that the η versus T plot has a nonzero slope as T approaches absolute zero (Figures 15.10 and 15.13). This violates the Third Law of Thermodynamics and is discussed further in Qualitative Problem 1 of this chapter.

Although the Landau approach to the modeling of phase transformations is simple, some important thermodynamic functions and properties can be modeled, such as:

- The excess Gibbs free energy of the solution as a function of temperature and order parameter
- The equilibrium order parameter dependence on temperature
- The enthalpy change of the phase transition
- The entropy change of the phase transition
- The heat capacity change of the phase transition
- The Ehrenfest order of the phase transition

The Landau model is used in many fields and can be extended to nonhomogeneous phases by adding gradient terms of the order parameter. In addition, two or more order parameters may be included in the expansion and the interaction of the different types of order can be examined (see Qualitative Problem 2).

15.7 SUMMARY

1. The ideal and regular solution models are reviewed with the aim of showing how they can be extended.
2. The version of a sub-regular solution model is introduced in which the value of α, of the regular solution model is assumed to be a linear function of composition, being given by $\alpha = a + bX_B$. The variation of the molar excess Gibbs free energy of mixing is thus given by $G^{XS} = (a + bX_B)X_A X_B$. This can give rise to asymmetric dependence of the molar properties of formation. The constants a and b are curve-fitting parameters and have no physical significance.
3. Regular solution behavior is predicted by a statistical solution model in which it is assumed that the atoms mix randomly and that the energy of the solution is the sum of the individual interatomic bond energies in the solution. Random mixing can be assumed only if, in the system A–B, the A–B bond energy is not significantly different from the average of the A–A and B–B bond energies in the pure components. For any such deviation, the validity of the assumption of random mixing increases with increasing temperature.
4. This statistical solution model can be improved by adding the effect of second-nearest neighbors. In the case of solutions with ordering tendency (negative deviations from Raoultian behavior), the model for both the molar enthalpy and molar entropy of formation can be improved by adding an LRO parameter to the molar enthalpy and molar entropy terms.

5. The Landau model of the excess free energy was introduced and several cases of it were examined.
   - The 2-4 case shows a second-order transition and the various thermodynamic variables were derived from the model
   - The 2-3-4 case shows first-order behavior of the transformation. However, it was shown to exhibit instability temperatures for both the disordered phase on cooling and the ordered phase on heating. The transformation precedes continuously in these cases.
   - Although the transformations are continuous at the instability temperatures, since they are not the equilibrium temperature they are not second or even higher-order transformations.
   - The 2-4-6 case was shown to exhibit first-order behavior for $C < 0$.

15.8 CONCEPTS AND TERMS INTRODUCED IN THIS CHAPTER

The reader should write out brief definitions or descriptions of the following terms. Where appropriate, equations may be used.

Instability temperature
Kinetic instability
Landau model of free energy
Metastable phase
Nearest neighbors
Next nearest neighbors
Sub-regular solution model
Symmetrical excess Gibbs free energy
Thermodynamic instability

15.9 QUALITATIVE EXAMPLE PROBLEMS

QUALITATIVE EXAMPLE PROBLEM 1

Calculate the slope of the η versus temperature plot for the 2-4 model of a transition as the temperature approaches 0 K. Discuss this in terms of the Third Law prediction.

SOLUTION TO QUALITATIVE PROBLEM 1

$$\eta = \left(1 - \frac{T}{T_C}\right)^{\frac{1}{2}} \left(\text{see Equation } 15.54\right)$$

$$\frac{\partial \eta}{\partial T} = -\frac{1}{2T_C}\left(1 - \frac{T}{T_C}\right)^{-\frac{1}{2}}$$

$$\text{The limit of } \frac{\partial \eta}{\partial T} \text{ as } T \to 0 = -\frac{1}{2T_C}\left(1 - \frac{T}{T_C}\right)^{-\frac{1}{2}} = -\frac{1}{2T_C} < 0$$

The slope of the variation of the order parameter η with temperature as $\eta \rightarrow 1$ at $T = 0$ K is negative in this model, which is at variance with the predicted slope of zero according to the requirements of the Third Law of Thermodynamics.

QUALITATIVE EXAMPLE PROBLEM 2

The Landau expansion for a higher-order transition is written as

$$G^{\mathrm{XS}} = A\eta^2 + C\eta^4 \, (C > 0)$$

The Landau expansion that includes a second-order parameter (strain) can be written as:

$$G^{\mathrm{XS}} = A\eta^2 + C\eta^4 + \lambda\varepsilon_S\eta^2 + \frac{1}{2}C_{\mathrm{El}}\varepsilon_S^2 \quad (C > 0)$$

where:

ε_S is the strain in the phase

λ is the coupling constant between the strain and the order parameter η

C_{El} is an elastic constant

Show that this coupling can change the phase transition into a first-order transition and delineate

under what conditions this occurs.

SOLUTION TO QUALITATIVE PROBLEM 2

First, minimize the free energy with respect to the strain

$$\frac{\partial G^{\mathrm{XS}}}{\partial \varepsilon_S} = 0 = \lambda\eta^2 + C_{\mathrm{El}}\varepsilon_S$$

$$\varepsilon_S^* = -\frac{\lambda\eta^2}{C_{\mathrm{El}}}$$

Where ε_S^* is the critical value of the strain.

Now substitute this value in the free energy and obtain

$$G^{\mathrm{XS}} = A\eta^2 + C\eta^4 + \lambda\left(-\frac{\lambda\eta^2}{\mathrm{C_{El}}}\right)\eta^2 + \frac{1}{2}\mathrm{C_{El}}\left(-\frac{\lambda\eta^2}{\mathrm{C_{El}}}\right)^2$$

$$= A\eta^2 + \left(C + \lambda^2\left(-\frac{1}{\mathrm{C_{El}}}\right) + \frac{\lambda^2}{2\mathrm{C_{El}}}\right)\eta^4$$

$$= A\eta^2 + \left(C - \frac{\lambda^2}{2\mathrm{C_{El}}}\right)\eta^4$$

If the coupling term λ is positive and large or if the elastic constant is small, the term multiplying η^4 may become negative. This is no longer a higher-order transition. When the second term becomes negative, we must include an η^6 term for stability.

PROBLEMS

15.1* Two ordered structures that can form from the BCC structure are the B2 structure and the B32 structure. See below.

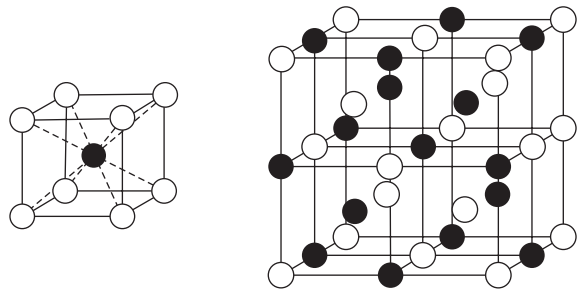

a. If only first neighbor interactions contribute to the enthalpy of the phase, which structure has the lowest energy?
b. If second neighbor interactions are included in the enthalpy which phase is stable?

15.2* Two ordered structures that can form from the FCC structure are the $L1_2$ structure and the $D0_{22}$ structure. See below.

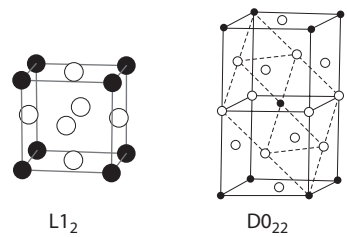

a. If only first neighbor interactions contribute to the enthalpy of the phase which structure has the lowest energy?
b. If second neighbor interactions are included in the enthalpy which phase is stable?

15.3* Find the expression for ΔH^M for the transformation of the disordered BCC phase of composition $X_B = 0.25$ to the B2 phase of the same composition, assuming the ordered phase obtains its highest order parameter for the composition 25% B.

15.4 The excess Gibbs free energy as a function of order parameter for a solution is written as:

$$G^{XS} = G_{ord} - G_{dis} = a(T - T_C)\eta^2 + C\eta^4$$

where G_{dis} is the free energy of the disordered phase and a and C are positive constants.

a. Obtain an expression for the excess entropy of the equilibrium ordered phase as a function of temperature.
b. Determine the value of $\Delta C_P = C_P^{ord} - C_P^{dis}$ at the transition temperature T_C.

15.5* The Landau expression for the excess Gibbs free energy of a first-order transition is written as:

$$G^{XS} = G_{ord} - G_{dis} = a\left(T - T_i^-\right)\eta^2 + B\eta^3 + C\eta^4$$

The ordered phase can be superheated above its equilibrium transition temperature T_0 until it becomes unstable at T_i^-.

a. Determine the value T_i^- in terms of its instability temperature on cooling, T_i^-
b. Determine the value of its order parameter when the phase becomes unstable.

15.6 Using the equation: $G^{XS}(\eta) = a(T - T_0)\eta^2 + C\eta^4$
show that the excess enthalpy for the Landau model with $B = 0$ and $C > 0$ is

$$\Delta H^{XS} = \frac{a}{2}\frac{\left(T^2 - T_C^2\right)}{T_C}$$

15.7 The Gibbs energy of a phase can be written in terms of its order parameter as:

$$G^{XS} = a(T - T_C)\eta^2 + E\eta^6$$

where $a > 0$ and $b > 0$

a. What is the temperature T_0 where the disordered phase has the same Gibbs Energy as the equilibrium ordered phase? Show work.

15.8* The LRO parameter, η, versus temperature plot of an ordered phase is shown in Figure 15.6.

1. Explain why the LRO parameter goes to unity at $T = 0$ K.
2. The slope of the LRO versus T plot goes to 0 as T approaches 0. Show why this is true.

Hint: Start by writing $G = G(\eta, T)$ and take the full differential dG. By the time you finish, you will have to use a form of L'Hôpital's rule:

$$\lim \text{ of } \frac{f(x)}{g(x)} \text{ as } x \to 0 = \frac{f'(x)}{g'(x)}$$

15.9 The Gibbs energy as a function of order parameter for a solution is written as:

$$G = a(T - T_C)\eta^2 + C\eta^4 + E\eta^6$$

For this case assume $C < 0$ and a and E are positive.

a. Find the nonzero value of the order parameter of the solution that has the same Gibbs Energy as that of the disordered solution.
b. Sketch the Gibbs Energy vs. η curve for the temperature in question in (a). This temperature can be called T_0
c. Determine if the transformation for this alloy is first order. Explain.
d. Calculate the heat of transformation, ΔH_0, for this disorder/order transformation in terms of a, η_0 and T_0, where η_0 is the order parameter at the equilibrium transition temperature T_0.

* New problem in this edition.

Appendix A
Selected Thermodynamic and Thermochemical Data

TABLE A.1: THE STANDARD GIBBS FREE ENERGY CHANGES FOR SEVERAL REACTIONS

This table lists the standard Gibbs free energy changes for selected reactions in the form

$$\Delta G_T^\circ = A + BT \text{ J}$$

or

$$\Delta G_T^\circ = A + BT \ln T + CT \text{ J}$$

and lists the range of temperature in which the expression is valid.

Example: For the oxidation of solid copper to form solid cuprous oxide according to

$$2\text{Cu}_{(s)} + \frac{1}{2}\text{O}_{2(g)} = \text{Cu}_2\text{O}_{(s)}$$

$$\Delta G^\circ = -162,200 + 69.24T \text{ J}$$

in the range 298–1356 K. Thus, at the melting temperature of Cu, 1356 K,

$$\Delta G_{1356\text{K}}^\circ = -162,200 + 69.24 \times 1356$$

$$= -68,310 \text{ J}$$

For the oxidation of liquid copper to form solid cuprous oxide according to

$$2\text{Cu}_{(l)} + \frac{1}{2}\text{O}_{2(g)} = \text{Cu}_2\text{O}_{(s)}$$

$$\Delta G_T^\circ = -188,300 + 88.48T \text{ J}$$

in the range 1356–1509 K. Thus, at 1356 K

$$\Delta G^{\circ}_{1356\text{K}} = -188{,}300 + 88.48 \times 1356 \text{ J}$$

$$= -68{,}321 \text{ J}$$

TABLE A.1
The Standard Gibbs Free Energy Changes for Several Reactions (Standard States Are Noted by Subscript)

Reaction	ΔG°, joules	Range, K
$2Ag_{(s)} + ½O_{2(g)} = Ag_2O_{(s)}$	$-30{,}540 + 66.11\,T$	298–463
$Al_{(l)} = [Al]_{(1\text{ wt\% in Fe})}$	$-43{,}100 - 32.26\,T$	
$2Al_{(l)} + 1.50_{2(g)} = Al_2O_{3(s)}$	$-1{,}687{,}200 + 326.8\,T$	993–2327
$C_{(s)} + ½O_{2(g)} = CO_{(g)}$	$-111{,}700 - 87.65\,T$	298–2000
$C_{(s)} + O_{2(g)} = CO_{2(g)}$	$-394{,}100 - 0.84\,T$	298–2000
$C_{(s)} + ½O_{2(g)} + ½S_{2(g)} = COS_{(g)}$	$-202{,}800 - 9.96\,T$	773–2000
$C_{(gr)} + 2H_{2(g)} = CH_{4(g)}$	$-91{,}040 + 110.7\,T$	773–2000
$C_{(gr)} = [C]_{(1\text{ wt\% in Fe})}$	$22{,}600 - 42.26\,T$	
$CaO_{(s)} + CO_{2(g)} = CaCO_{3(s)}$	$-168{,}400 + 144\,T$	449–1150
$2CaO_{(s)} + SiO_{2(s)} = 2CaO{\cdot}SiO_{2(s)}$	$-118{,}800 - 11.30\,T$	298–2400
$CoO_{(s)} + SO_{3(g)} = CoSO_{4(s)}$	$-227{,}860 + 165.3\,T$	298–1230
$2Cr_{(s)} + 1.5O_{2(g)} = Cr_2O_{3(s)}$	$-1{,}110{,}100 + 247.3\,T$	298–1793
$2Cu_{(s)} + ½O_{2(g)} = Cu_2O_{(s)}$	$-162{,}200 + 69.24\,T$	298–1356
$2Cu_{(l)} + ½O_{2(g)} = Cu_2O_{(s)}$	$-188{,}300 + 88.48\,T$	1356–1509
$2Cu_{(s)} + ½S_{2(g)} = Cu_2S_{(s)}$	$-131{,}800 + 30.79\,T$	708–1356
$3Fe_{(\alpha)} + C_{(gr)} = Fe_3C_{(s)}$	$29{,}040 - 28.03\,T$	298–1000
$3Fe_{(\gamma)} + C_{(gr)} = Fe_3C_{(s)}$	$11{,}234 - 11.00\,T$	1000–1137
$Fe_{(s)} + ½O_{2(g)} = FeO_{(s)}$	$-263{,}700 + 64.35\,T$	298–1644
$Fe_{(l)} + ½O_{2(g)} = FeO_{(s)}$	$-256{,}000 + 53.68\,T$	1808–2000
$3Fe_{(s)} + 2O_{2(g)} = Fe_3O_{4(s)}$	$-1{,}102{,}200 + 307.4\,T$	298–1808
$Fe_{(s)} + ½S_{2(g)} = FeS_{(s)}$	$-150{,}200 + 52.55\,T$	412–1179
$H_{2(g)} + Cl_{2(g)} = 2HCl_{(g)}$	$-188{,}200 - 12.80\,T$	298–2000
$H_{2(g)} + I_{2(g)} = 2HI_{(g)}$	$-8370 - 17.65\,T$	298–2000
$H_{2(g)} + ½O_{2(g)} = H_2O_{(g)}$	$-247{,}500 + 55.85\,T$	298–2000
$Hg_{(v)} + ½O_{2(g)} = HgO_{(s)}$	$-152{,}200 + 207.2\,T$	
$Li_{(g)} + ½Br_{2(g)} = LiBr_{(g)}$	$-333{,}900 + 42.09\,T$	1289–2000
$Mg_{(l)} + Cl_{2(g)} = MgCl_{2(l)}$	$-603{,}200 + 121.43\,T$	987–1368
$Mg_{(g)} + ½O_{2(g)} = MgO_{(s)}$	$-729{,}600 + 204\,T$	1363–2200
$2MgO_{(s)} + SiO_{2(s)} = Mg_2SiO_{4(s)}$	$-67{,}200 + 4.31\,T$	298–2171
$MgO_{(s)} + CO_{2(g)} = MgCO_{3(s)}$	$-117{,}600 + 170\,T$	298–1000
$MgO_{(s)} + Al_2O_{3(s)} = MgO{\cdot}Al_2O_{3(s)}$	$-35{,}560 - 2.09\,T$	298–1698
$Mn_{(s)} + ½O_{2(g)} = MnO_{(s)}$	$-388{,}900 + 76.32\,T$	298–1517

(*Continued*)

TABLE A.1 (*Continued*)
The Standard Gibbs Free Energy Changes for Several Reactions (Standard States Are Noted by Subscript)

Reaction	ΔG°, joules	Range, K
$N_{2(g)} + 3H_{2(g)} = 2NH_{3(g)}$	$-87{,}030 + 25.8\,T \ln T + 31.7\,T$	298–2000
$2Ni_{(s)} + O_{2(g)} = 2NiO_{(s)}$	$-471{,}200 + 172\,T$	298–1726
$2Ni_{(l)} + O_{2(g)} = 2NiO_{(s)}$	$-506{,}180 + 192.2\,T$	1726–2200
$\frac{1}{2}O_{2(g)} = [O]_{(1\ wt\%\ in\ Fe)}$	$-111{,}070 - 5.87\,T$	
$Pb_{(l)} + \frac{1}{2}O_{2(g)} = PbO_{(s)}$	$-208{,}700 + 91.75\,T$	600–1158
$Pb_{(l)} + \frac{1}{2}O_{2(g)} = PbO_{(l)}$	$-181{,}200 + 68.03\,T$	1158–1808
$Pb_{(l)} + \frac{1}{2}S_{2(g)} = PbS_{(s)}$	$-163{,}200 + 88.03\,T$	600–1386
$PbO_{(s)} + SO_{2(g)} + \frac{1}{2}O_{2(g)} = PbSO_{4(s)}$	$-401{,}200 + 261.5\,T$	298–1158
$PCl_{3(g)} + Cl_{2(g)} = PCl_{5(g)}$	$-95{,}600 - 7.94\,T \ln T + 235.2\,T$	298–1000
$\frac{1}{2}S_{2(g)} + O_{2(g)} = SO_{2(g)}$	$-361{,}700 + 76.68\,T$	718–2000
$Si_{(s)} + O_{2(g)} = SiO_{2(s)}$	$-907{,}100 + 175\,T$	298–1685
$3Si_{(s)} + 2N_{2(g)} = Si_3N_{4(s)}$	$-723{,}800 + 315.1\,T$	298–1685
$Sn_{(l)} + Cl_{2(g)} = SnCl_{2(l)}$	$-333{,}000 + 118.4\,T$	520–925
$SO_{2(g)} + \frac{1}{2}O_{2(g)} = SO_{3(g)}$	$-94{,}600 + 89.37\,T$	298–2000
$U_{(l)} + C_{(gr)} = UC_{(s)}$	$-102{,}900 + 5.02\,T$	1408–2500
$2U_{(l)} + 3C_{(gr)} = U_2C_{3(s)}$	$-236{,}800 + 25.1\,T$	1408–2500
$U_{(l)} + 2C_{(gr)} = UC_{2(s)}$	$-115{,}900 + 10.9\,T$	1408–2500
$V_{(s)} + \frac{1}{2}O_{2(g)} = VO_{(s)}$	$-424{,}700 + 80.04\,T$	298–2000
$Zn_{(v)} + \frac{1}{2}O_{2(g)} = ZnO_{(s)}$	$-460{,}200 + 198\,T$	1243–1973

TABLE A.2: THE CONSTANT-PRESSURE MOLAR HEAT CAPACITIES OF VARIOUS SUBSTANCES

The constant-pressure molar heat capacities are presented as

$$c_p = a + bT + cT^{-2}\ \text{J/K}$$

or as

$$c_p = a + bT + cT^{-2} + dT^2\ \text{J/K}$$

and the table includes the ranges of temperature in which the expressions are valid.

Example: For Ag in the range 298–1234 K

$$c_p = 21.30 + 8.54 \times 10^{-3} T + 1.51 \times 10^{5} T^{-2}\ \text{J/K}$$

and for graphite in the range 298–1100 K

$$c_p = 0.11 + 38.94 \times 10^{-3} T - 1.48 \times 10^{5} T^{-2} - 17.38 \times 10^{-6} T^{2}\ \text{J/K}$$

TABLE A.2
The Constant-Pressure Molar Heat Capacities of Various Substances ($c_p = a + bT + cT^{-2}$ J/mole·K)

Substance	a	$b \times 10^3$	$c \times 10^{-5}$	Range, K	Remarks
$Ag_{(s)}$	21.30	8.54	1.51	298–1234 (T_m)	
$Ag_{(l)}$	30.50	–	–	1234–1600	
$Al_{(s)}$	20.67	12.38	–	298–933 (T_m)	
$Al_{(l)}$	29.3	–	–	933–1600	
$Al_2O_{3(s)}$	106.6	17.78	−28.53	298–2325 (T_m)	
$Ba_{(\alpha)}$	−473.2	1587.0	128.2	298–648	
$Ba_{(\beta)}$	−5.69	80.33	–	648–1003	
$BaO_{(s)}$	53.30	4.35	−8.30	298–2286 (T_m)	
$BaTiO_{3(s)}$	121.46	8.54	−19.16	298–1800	
$C_{(graphite)}$	0.11	38.94	−1.48	298–1100	$-17.38 \times 10^{-6}T^2$
$C_{(graphite)}$	24.43	0.44	−31.63	1100–4000	
$C_{(diamond)}$	9.12	13.22	−6.19	298–1200	
$CO_{(g)}$	28.41	4.10	−0.46	298–2500	
$CO_{2(g)}$	44.14	9.04	−8.54	298–2500	
$Ca_{(\alpha)}$	25.37	−7.26	–γ	298–716	$23.72 \times 10^{-6}T^2$
$Ca_{(\beta)}$	−0.36	41.25	–	716–1115	
$CaO_{(s)}$	49.62	4.51	−6.95	298–1177	
$CaTiO_{3(s)}$	127.49	5.69	−27.99	298–1530	
$Cr_{(s)}$	24.43	9.87	−3.68	298–2130 (T_m)	
Cr_2O_3	119.37	9.30	−15.65	298–1800	
$Cu_{(s)}$	22.64	6.28	–	298–1356 (T_m)	
$Fe_{(\alpha/\delta)}$	37.12	6.17	–	298–1183/1664–1809	
$Fe_{(\gamma)}$	24.47	γ.45	–	1183–1664	
$Fe_{(l)}$	41.8	–	–	1809–1873	
$H_2O_{(g)}$	30.00	10.71	0.33	298–2500	
$O_{2(g)}$	29.96	4.18	−1.67	298–3000	
$2MgO{\cdot}2Al_2O_3{\cdot}5SiO_2$	626.34	91.21	−200.83	298–1738 (T_m)	
$N_{2(g)}$	27.87	4.27	–	298–2500	
$Si_3N_{4(g)}$	70.54	98.74	–	298–900	
$SiO_{2(\alpha\text{-quartz})}$	43.89	1.00	−6.02	298–847	
$Ti_{(s)}$	22.09	10.46	–	298–1155	
$TiO_{2(rutile)}$	75.19	1.17	−18.20	298–1800	
$Zr_{(\alpha)}$	21.97	11.63	–	298–1136	
$Zr_{(\beta)}$	23.22	4.64	–	1136–2128	
$ZrO_{2(\alpha)}$	69.62	7.53	−14.06	298–1478	
$ZrO_{2(\beta)}$	74.48	–	–	1478–2950 (T_m)	

TABLE A.3: THE STANDARD MOLAR HEATS OF FORMATION AND MOLAR ENTROPIES OF VARIOUS SUBSTANCES AT 298 K

Example: For the reaction

$$2\mathrm{Al}_{(s)} + \frac{3}{2}\mathrm{O}_{2(g)} = \mathrm{Al}_2\mathrm{O}_{3(s)}$$

$$\Delta H^{\circ}_{298\,\mathrm{K}} = -1{,}675{,}700\ \mathrm{J}$$

which is thus the standard molar heat of the formation of Al_2O_3 at 298 K. The molar entropy of Al_2O_3 at 298 K is 50.9 J/K. By convention, the standard molar enthalpies of elements in their standard states at 298 K are assigned the value of zero.

TABLE A.3
The Standard Molar Heats of Formation and Molar Entropies of Various Substances at 298 K

Substance	ΔH°_{298}, J	S°_{298}, J/K
Al_2O_3	−1,675,700	50.9
Ba	–	62.4
BaO	−548,100	72.1
$BaTiO_3$	−1,653,100	107.9
$C_{(graphite)}$	–	5.73
$C_{(diamond)}$	1,900	2.43
CH_4	−74,800	186.3
CO	−110,500	197.5
CO_2	−393,500	213.7
Ca	–	41.6
CaO	−634,900	38.1
$CaTiO_3$	−1,660,600	93.7
$3CaO{\cdot}Al_2O_3{\cdot}3SiO_2$	−6,646,300	241.4
$CaO{\cdot}Al_2O_3{\cdot}SiO_2$	−3,293,200	144.8
$CaO{\cdot}Al_3O_3{\cdot}2SiO_2$	−4,223,700	202.5
$2CaO{\cdot}Al_2O_3{\cdot}SiO_2$	−3,989,400	198.3
Cr_2O_3	−1,134,700	81.2
$H_2O_{(g)}$	−241,800	232.9
N_2	–	191.5
O_2	–	205.1
$SiO_{2(\alpha\text{-quartz})}$	−910,900	41.5
Si_3N_4	−744,800	113.0
Ti	–	30.7
TiO	−543,000	34.7
Ti_2O_3	−1,521,000	77.2
Ti_3O_5	−2,459,000	129.4

(*Continued*)

TABLE A.3 (*Continued*)
The Standard Molar Heats of Formation and Molar Entropies of Various Substances at 298 K

Substance	ΔH°_{298}, J	S°_{298}, J/K
TiO_2	−944,000	50.6
Zr	–	39.0
ZrO_2	−1,100,800	50.4

TABLE A.4: THE SATURATED VAPOR PRESSURES OF VARIOUS SUBSTANCES

The saturated (equilibrium) vapor pressures of substances, in the stated ranges of temperatures, are presented in the form

$$\ln p(\text{atm}) = -\frac{A}{T} + B\ln T + C$$

Example: The saturated vapor pressure exerted by liquid CaF_2 in the range of temperature 1691–2783 K is given by

$$\ln p(\text{atm}) = -\frac{50,200}{T} - 4.525\ln T + 53.96$$

Thus, at its normal boiling temperature of 2783 K, the saturated vapor pressure of liquid CaF_2 is

$$\ln p(\text{atm}) = -\frac{50,200}{2783} - 4.525\ln 2783 + 53.96$$
$$= 0$$

i.e., at the normal boiling temperature, the saturated vapor pressure is 1 atm.

TABLE A.4
The Saturated Vapor Pressures of Various Substances $\left[\ln p(\text{atm}) = -\frac{A}{T} + B\ln T + C\right]$

Substance	*A*	*B*	*C*	Range, K
$CaF_{2(\alpha)}$	54,350	−4.525	56.57	298–1430
$CaF_{2(\beta)}$	53,780	−4.525	56.08	1430–1691 (T_m)
$CaF_{2(l)}$	50,200	−4.525	53.96	1691–2783 (T_b)
$Fe_{(l)}$	45,390	−1.27	23.93	1809 (T_m)–3330 (T_b)
$Hg_{(l)}$	7611	−0.795	17.168	298–630 (T_b)
$Mn_{(l)}$	33,440	−3.02	37.68	1517 (T_m)–2348 (T_b)
$SiCl_{4(l)}$	3620	–	10.96	273–333 (T_b)
$Zn_{(l)}$	15,250	−1.255	21.79	693 (T_m)–1177 (T_b)

TABLE A.5: MOLAR HEATS OF MELTING AND TRANSFORMATION

Example: At the melting temperature of 1234 K, the enthalpy change for

$$Ag_{(s)} \rightarrow Ag_{(l)}$$

is 11,090 J. Thus at 1234 K, the molar heat of melting of Ag is 11,090 J. The change in molar entropy due to melting at 1234 K is thus

$$\frac{\Delta H_m}{T_m} = \frac{11{,}090}{1234} = 8.987 \text{ J/K}$$

At 1187 K, the enthalpy change for the transformation

$$Fe_{(\alpha)} \rightarrow Fe_{(\gamma)}$$

is 670 J. The corresponding change in the molar entropy at 1187 K is thus

$$\Delta S_{\text{trans}} = \frac{\Delta H_{\text{trans}}}{T_{\text{trans}}} = \frac{670}{1187} = 0.56 \text{ J/K}$$

TABLE A.5
Molar Heats of Melting and Transformation

Substance	Trans	ΔH_{trans}, J	$T_{\text{trans, K}}$
Ag	$s \rightarrow l$	11,090	1234
Al	$s \rightarrow l$	10,700	934
Al_2O_3	$s \rightarrow l$	107,500	2324
Au	$s \rightarrow l$	12,600	1338
Ba	$\alpha \rightarrow \beta$	630	648
Ba	$\beta \rightarrow l$	7650	1003
Cu	$s \rightarrow l$	12,970	1356
Ca	$\alpha \rightarrow \beta$	900	716
CaF_2	$s \rightarrow l$	31,200	1691
Fe	$\alpha \rightarrow \gamma$	670	1183
Fe	$\gamma \rightarrow \delta$	840	1664
Fe	$\delta \rightarrow l$	13,770	1809
H_2O	$s \rightarrow l$	6008	273
$K_2O{\cdot}B_2O_3$	$s \rightarrow l$	62,800	1220
MgF_2	$s \rightarrow l$	58,160	1563
$Na_2O{\cdot}B_2O_3$	$s \rightarrow l$	67,000	1240
Pb	$s \rightarrow l$	4810	600
PbO	$s \rightarrow l$	27,480	1158
Si	$s \rightarrow l$	50,200	1658
V	$s \rightarrow l$	22,840	2193
Zr	$\alpha \rightarrow \beta$	3900	1136
ZrO_2	$\alpha \rightarrow \beta$	5900	1478

Appendix B
Useful Mathematical Relationships

1. The total derivative of $B = B(X, Y, Z)$:

For $B = B(X, Y, Z)$

$$dB = \left(\frac{\partial B}{\partial X}\right)_{Y,Z} dX + \left(\frac{\partial B}{\partial Y}\right)_{X,Z} dY + \left(\frac{\partial B}{\partial Z}\right)_{X,Y} dZ$$

$$dB = MdX + NdY + PdZ$$

where $\left(\frac{\partial B}{\partial X}\right)_{Y,Z}$, $\left(\frac{\partial B}{\partial Y}\right)_{X,Z}$, and $\left(\frac{\partial B}{\partial Z}\right)_{X,Y}$ are partial derivatives of B.

B is the dependent variable, and X, Y, and Z are independent variables.

2. Criteria for $dB = f(X, Y, Z)$ to be an exact differential:

$$dB = \left(\frac{\partial B}{\partial X}\right)_{Y,Z} dX + \left(\frac{\partial B}{\partial Y}\right)_{X,Z} dY + \left(\frac{\partial B}{\partial Z}\right)_{X,Y} dZ$$

B is exact if

$$\left(\frac{\partial\left(\frac{\partial B}{\partial X}\right)_{Y,Z}}{\partial Y}\right)_{X,Z} = \left(\frac{\partial\left(\frac{\partial B}{\partial Y}\right)_{X,Z}}{\partial X}\right)_{Y,Z}$$

$$\left(\frac{\partial\left(\frac{\partial B}{\partial X}\right)_{Y,Z}}{\partial Z}\right)_{X,Y} = \left(\frac{\partial\left(\frac{\partial B}{\partial Z}\right)_{X,Y}}{\partial X}\right)_{Y,Z}$$

$$\left(\frac{\partial\left(\frac{\partial B}{\partial Y}\right)_{X,Y}}{\partial Z}\right)_{X,Y} = \left(\frac{\partial\left(\frac{\partial B}{\partial Z}\right)_{X,Y}}{\partial Y}\right)_{X,Z}$$

3. If B is an exact, then dB is an exact total derivative:

$$\oint dB = 0$$

and

$\int_1^2 dB = B_2 - B_1$ and is independent of the path.

4. Inverse or reciprocal relationships among partial differentials:

For $B = B(X,Y,Z)$

$$\left(\frac{\partial B}{\partial X}\right)_{Y,Z} = \left(\frac{\partial X}{\partial B}\right)_{Y,Z}^{-1} = \frac{1}{\left(\frac{\partial X}{\partial B}\right)_{Y,Z}}$$

$$\left(\frac{\partial B}{\partial Y}\right)_{X,Z} = \left(\frac{\partial Y}{\partial B}\right)_{X,Z}^{-1} = \frac{1}{\left(\frac{\partial Y}{\partial B}\right)_{X,Z}}$$

$$\left(\frac{\partial B}{\partial Z}\right)_{X,Y} = \left(\frac{\partial Z}{\partial B}\right)_{X,Y}^{-1} = \frac{1}{\left(\frac{\partial Z}{\partial B}\right)_{X,Y}}$$

5. Two chain rules for partial differentials:

i. For $B = B(X,Y,Z)$ and X and Y are the independent variables:

$$\left(\frac{\partial B}{\partial Y}\right)_Z = \left(\frac{\partial B}{\partial X}\right)_Z \left(\frac{\partial X}{\partial Y}\right)_Z$$

Used in Qualitative Problem 2 of Chapter 1.

ii. For $B = B(X,Y,Z)$ and X and Y are the independent variables:

$$\left(\frac{\partial B}{\partial X}\right)_Z = \left(\frac{\partial B}{\partial X}\right)_Y + \left(\frac{\partial B}{\partial Y}\right)_X \left(\frac{\partial Y}{\partial X}\right)_Z$$

6. Ratio relations (cycle rule) for partial differentials:

For $X = X(Y,Z)$

$$\left(\frac{\partial X}{\partial Y}\right)_Z \left(\frac{\partial Y}{\partial Z}\right)_X \left(\frac{\partial Z}{\partial X}\right)_Y = -1$$

Used in Problem 1.7* to show that the expression $\frac{\alpha_P}{\beta_T \gamma_V} = P$ is valid for an ideal gas.

7. Useful approximations:

$$e^x \approx (1+x) \quad \text{for small } x$$
$$e^{-x} \approx (1-x) \quad \text{for small } x$$
$$\frac{1}{1+x} \approx 1-x \quad \text{for small } x$$

$\ln X! \approx X \ln X - X$ (James Stirling's (1692–1770) Approximation).

Appendix C
The Generation of Additional Thermodynamic Potentials as Legendre Transformations

We have found for a simple thermodynamic system that the internal energy U is a function of the independent variables entropy and volume, viz. $U = U(S, V)$. This appendix details the mathematical method used in Chapter 5 to obtain the other thermodynamic potentials of the simple system. We also give a method to obtain all of the thermodynamic potentials for any number of dependent variables.

The variation of the dependent variable y with the independent variable x can be represented as the locus of points satisfying the relation $y = y(x)$, as shown in Figure C.1.

It can also be shown as the envelope of a family of tangent lines shown in Figure C.2.

In Figure C.1, every point in the plane is described by two coordinates x and y, and every line in the plane in Figure C.2 can be described by two numbers m and ψ, where m is the slope of the line and ψ is the intercept of the line with the y-axis. Then, just as the relation $y = y(x)$ selects a subset of all possible points (x, y), a relation $\psi = \psi(m)$ selects a subset of all possible lines (m, ψ). Knowledge of the intercept ψ of the tangent lines as a function of the slope m allows the construction of the family of tangent lines and thus the curve for which they are the envelope. Thus, the relationship

$$\psi = \psi(m) \tag{C.1}$$

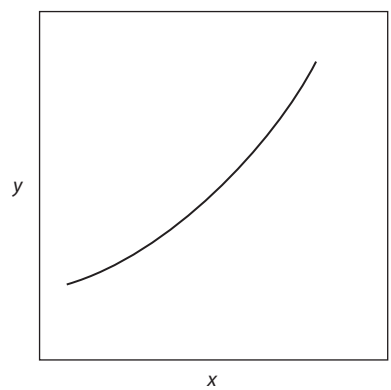

FIGURE C.1 The locus of points satisfying the relation $y = y(x)$.

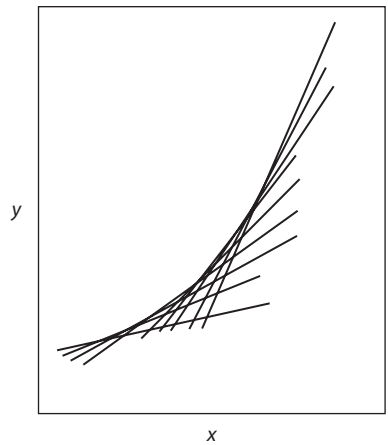

FIGURE C.2 The family of tangent lines $\psi = \psi(m)$.

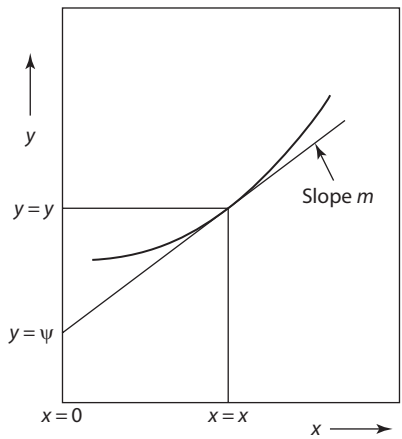

FIGURE C.3 Geometry procedure for obtaining ψ, the Legendre transform of y.

is equivalent to the relation $y = y(x)$, and in Equation C.1, m is the independent variable. The computation of the relation $\psi = \psi(m)$ from the known relation $y = y(x)$ is known as a Legendre transformation. Figure C.3 shows a tangent line of slope m going through the points x, y.

If the intercept with the y-axis is ψ, then

$$m = \frac{y - \psi}{x - 0} \tag{C.2}$$

or

$$\psi = y - mx \tag{C.3}$$

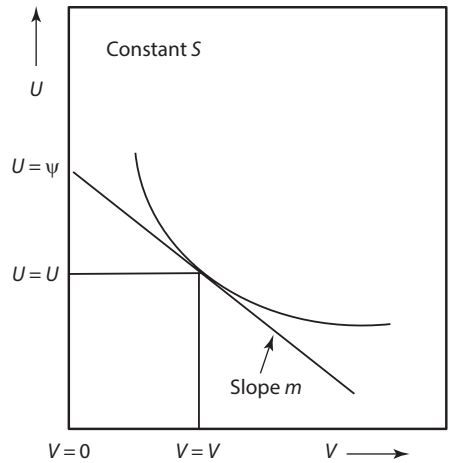

FIGURE C.4 Geometry procedure for obtaining ψ, the Legendre transform of U at constant S.

Differentiation of the known equation $y = y(x)$ gives $m = m(x)$, and elimination of x and y gives the desired relation ψ and m. The function ψ is known as the Legendre transform of y (Adrien-Marie Legendre, 1752–1833).

Equation 3.12 gives the variation of the dependent variable U on the independent variables S and V for a closed system of fixed composition which is undergoing a process involving a change of volume against the external pressure as the only form of work performed on, or by, the system.

$$dU = TdS - PdV \tag{3.12}$$

A schematic variation of U with V at constant S is shown in Figure C.4.

Using the geometry procedure outlined in Figure C.3 gives

$$m = \frac{U - \psi}{V - 0}$$

which rearranges to give

$$\psi = U - mV \tag{C.4}$$

From Equation 3.12, the slope of the line, m, is $\left(\frac{\partial U}{\partial V}\right)_S = -P$, and thus, Equation C.4 becomes

$$\psi = U + PV$$

This thermodynamic potential is called the enthalpy H (see Equation 2.4). The enthalpy H is thus a Legendre transform of the internal energy U, given as

$$H = U + PV \tag{C.5}$$

Differentiation of Equation C.5 gives

$$dH = dU + PdV + VdP$$

which, in combination with Equation 3.12, gives

$$dH = TdS + VdP \tag{C.6}$$

which is an expression for the variation of the dependent variable H with the independent variables S and P. Since H is a state function, we can write

$$dH = \left(\frac{\partial H}{\partial S}\right)_P dS + \left(\frac{\partial H}{\partial P}\right)_S dP$$

Comparison of this equation with Equation C.6 gives the thermodynamic definitions of T and V as

$$T = \left(\frac{\partial H}{\partial S}\right)_P$$

and

$$V = \left(\frac{\partial H}{\partial P}\right)_S$$

Figure C.5 shows a schematic variation of U with S at constant V, and the geometry procedure gives

$$m = \frac{U - \psi}{S - 0}$$

or

$$\psi = U - mS \tag{C.7}$$

From Equation 3.12, the slope of the line, m, is $\left(\frac{\partial U}{\partial S}\right)_V = T$, and thus, Equation C.7 becomes

$$\psi = U - TS \tag{C.8}$$

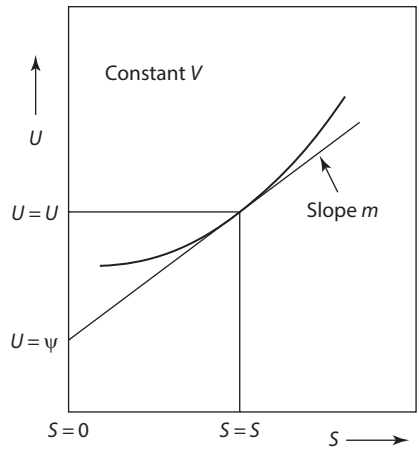

FIGURE C.5 Geometry procedure for obtaining ψ, the Legendre transform of U at constant V.

which is called the Helmholtz free energy A (see Equation 5.1). The Helmholtz free energy is thus *another* Legendre transform of the internal energy U, given as

$$A = U - TS \tag{C.9}$$

Differentiation of Equation C.9 gives

$$dA = dU - TdS - SdT$$

which, in combination with Equation 3.12, gives

$$dA = -SdT - PdV \tag{C.10}$$

which is an expression for the variation of A, as the dependent variable, with the independent variables T and V. Since A is a state function (and therefore an exact differential), we can write

$$dA = \left(\frac{\partial A}{\partial T}\right)_V dT + \left(\frac{\partial A}{\partial V}\right)_T dV$$

Comparison of this equation with Equation C.10 gives the thermodynamic definition of S and P as

$$S = -\left(\frac{\partial A}{\partial T}\right)_V$$

and

$$P = -\left(\frac{\partial A}{\partial V}\right)_T$$

The thermodynamic variable, which is dependent on T and P, is obtained as a Legendre transform of A in which V in Equation C.10 is replaced by P. The variation of A with V at constant T gives

$$m = \left(\frac{A - \psi}{V - 0} \right)$$

or

$$\psi = A - mV \tag{C.11}$$

From Equation C.10, $m = \left(\frac{dA}{dV} \right)_T = -P$. Thus, Equation C.11 becomes

$$\psi = A + PV = U - TS + PV = H - TS$$

which is called the Gibbs free energy G (defined in Section 5.4).

$$G = H - TS \tag{C.12}$$

Differentiation of Equation C.12 gives

$$dG = dH - TdS - SdT$$

which, in combination with Equation C.6, gives

$$dG = -SdT + VdP \tag{C.13}$$

which is an expression for the variation of G, the dependent variable, on T and P as the independent variables. Comparison of Equation C.13 with

$$dG = \left(\frac{\partial G}{\partial T} \right)_P dT + \left(\frac{\partial G}{\partial P} \right)_T dP$$

gives the thermodynamic definitions of S and V as

$$S = -\left(\frac{\partial G}{\partial T} \right)_P$$

and

$$V = \left(\frac{\partial G}{\partial P} \right)_T$$

Thus, starting with the first law as

$$dU = TdS - PdV \tag{3.12}$$

we have $U = U(S,V)$

$$H = H(S,P)$$
$$A = A(T,V)$$
$$\text{and} \quad G = G(T,P)$$

Now suppose the first law is written to include another form of work that may be performed on or by the system

$$dU = TdS - PdV + Xdy$$

where X is the force applied by or on the system and y is the resulting displacement. We now have

$$U = U(S,V,y)$$
$$H = H(S,P,y)$$
$$A = A(T,V,y)$$
$$\text{and} \quad G = G(T,P,y)$$

From this, the following additional fundamental equations can be obtained

$$\begin{aligned} dU &= TdS - PdV + Xdy \\ dH &= TdS + VdP + Xdy \\ dA &= -SdT - PdV + Xdy \\ dG &= -SdT + VdP + Xdy \end{aligned} \tag{C.14}$$

We may also form the Legendre transforms of the internal energy by considering the additional work term*[1]

$$\begin{aligned} dU'' &= TdS - PdV - ydX \\ dH'' &= TdS + VdP - ydX \\ dA'' &= -SdT - PdV - ydX \\ dG'' &= -SdT + VdP - ydX \end{aligned} \tag{C.15}$$

These have been primed to distinguish them from Equation C.14. We see that the addition of another independent variable to the first law increases the number of fundamental equations to eight. Since each member of the thermodynamic conjugate pairs of variables in the first law may be considered as a dependent variable, there will be 2^n fundamental equations for the first law written with n terms.

[1] The double prime is used to distinguish these terms from dU, dH, dA, and dG.

We now look at a specific application of the three-term first law, namely, the equation that includes magnetic terms. We have seen that the magnetic work done on or by the system can be written as

$$\delta w_{\text{mag}} = \mu_0 V \mathcal{H} dM$$

where V is the volume, and we assume $\vec{\mathcal{H}} \,//\, \vec{M}$

We write the first law as

$$dU_{\text{mag}} = TdS - PdV + \mu_0 V \mathcal{H} d\boldsymbol{M}$$

and obtain the other three magnetic fundamental equations as

$$\begin{aligned} dH_{\text{mag}} &= TdS + VdP + \mu_0 V \mathcal{H} d\boldsymbol{M} \\ dA_{\text{mag}} &= -SdT - PdV + \mu_0 V \mathcal{H} d\boldsymbol{M} \\ dG_{\text{mag}} &= -SdT + VdP + \mu_0 V \mathcal{H} d\boldsymbol{M} \end{aligned} \tag{C.16}$$

As above, we also get the following additional fundamental equations:

$$\begin{aligned} dU''_{\text{mag}} &= TdS - PdV - \mu_0 V \boldsymbol{M} d\mathcal{H} \\ dH''_{\text{mag}} &= TdS + VdP - \mu_0 V \boldsymbol{M} d\mathcal{H} \\ dA''_{\text{mag}} &= -SdT - PdV - \mu_0 V \boldsymbol{M} d\mathcal{H} \\ dG''_{\text{mag}} &= -SdT + VdP - \mu_0 V \boldsymbol{M} d\mathcal{H} \end{aligned} \tag{C.17}$$

Which fundamental equation one uses in dealing with a magnetic system depends on which of the thermodynamic variables are the independent ones (see Equations 5.11).

Nomenclature

LIST OF SYMBOLS

a	van der Waals constant
a_i	the activity of species i with reference to a specified standard state
A	Helmholtz free energy (or work function)
b	van der Waals constant
C	the number of components
C	heat capacity
c_p	constant-pressure molar heat capacity
c_v	constant-volume molar heat capacity
E^*	activation energy for an atom to leave surface
$\mathcal{F}$	the number of degrees of freedom of an equilibrium
f	Faraday's constant
f	fugacity
f_i	the Henrian activity coefficient of the species i
$f_{i\,(\mathrm{wt\%})}$	the activity coefficient of the species i with respect to the 1 weight percent standard state
G	Gibbs free energy
$\mathcal{H}$	magnetic field
H	enthalpy
h_i	the Henrian activity of the species i
$h_{i\,(\mathrm{wt\%})}$	the activity of the species i with respect to the 1 weight percent standard state
K	the equilibrium constant
k_B	Boltzmann's constant
$\boldsymbol{M}$	magnetization
m	mass
n	the number of moles
n_i	the number of moles of the species i
N_O	Avogadro's number
P	pressure
p_i	the partial pressure of the species i
p_i°	the saturated vapor pressure of the species i
q	heat
R	the gas constant
S	entropy
T_c	critical temperature
T_m	melting temperature
T_b	boiling temperature
T_o	Transition Temperature
U	internal energy
V	volume

w	work
X_i	the mole fraction of the species i
$\mathcal{Z}$	partition function
Z	the compressibility factor
α_P	coefficient of thermal expansion
α	the regular solution constant
β_S	adiabatic compressibility
β_T	coefficient of isothermal compressibility
β	equals $(k_B T)^{-1}$
γ	ratio of c_p to c_v
γ_i	the activity coefficient of the species i
γ_i°	the Henry's law activity coefficient
γ_V	thermal coefficient of pressure
ε_i	the energy of the ith energy level
ε_j^i	the interaction parameter of i on j
ε	electromotive force
$\varepsilon^{\circ,A}$	standard reduction potential of the species A
γ	surface energy
η	efficiency of heat engine
η	generalized order parameter
μ_0	permeability of vacuum
μ_i	the chemical potential of the species i
σ	stress
ϕ	the number of phases occurring in a system
Ω	possible number of arrangements of microstates
(s)	solid
(l)	liquid
(g)	gas

NOTATION FOR EXTENSIVE THERMODYNAMIC PROPERTIES (EXEMPLIFIED BY *G*, THE GIBBS FREE ENERGY)

G'	the Gibbs free energy of the system containing n moles
G	the Gibbs free energy per mole of the system
ΔG	the change in G due to a specified change in the state of the system
ΔG^M	the integral molar Gibbs free energy change due to mixing of the components to form a solution
$\Delta G^{M,\text{id}}$	the integral molar Gibbs free energy change due to mixing of the components to form an ideal solution the molar Gibbs free energy of the species i
G_i°	the molar Gibbs free energy of the species i in its designated standard state
$\bar{G}_i$	the partial molar Gibbs free energy of i in some specified solution
$\Delta \bar{G}_i^M$	$= \bar{G}_i - G_i^\circ$, the partial molar Gibbs free energy of mixing of i
G^{XS}	$= \Delta G^M - \Delta G^{M,\text{id}}$, the integral excess molar Gibbs free energy of a solution
$\bar{G}_i^{\text{xs}}$	the partial molar excess Gibbs free energy of mixing of i
ΔG_m	the molar Gibbs free energy of melting
ΔG_b	the molar Gibbs free energy of boiling
ΔG°	

Answers to Selected Problems

CHAPTER 1

1.1 The principal curvatures are proportional to the second derivatives:

$$\left(\frac{\partial^2 V}{\partial P^2}\right)_T = \beta_T^2 V > 0 \quad \text{and} \quad \left(\frac{\partial^2 V}{\partial T^2}\right)_P = \alpha_P^2 V > 0.$$

1.4 $\dfrac{\alpha_P}{\beta_T} = \dfrac{R}{V}$

1.5* $\alpha_P = \dfrac{1}{V}\left(\dfrac{\partial V}{\partial T}\right)_P = \dfrac{R(V-b)V^2}{RTV^3 - 2a(V-b)^2}$

1.8* $P = -\dfrac{1}{\beta_T}\ln\left(\dfrac{V}{V_0}\right) + P_0$

CHAPTER 2

2.1 (1a) 22.5 liters, (2a) $w = 9244$ J, (3a) $q = 9244$ J, (4a) $\Delta U = 0$, (5a) $\Delta H = 0$
(1b) 19.13 liters, (2b) $w = 5130$ J, (3b) $q = 0$, (4b) $\Delta U = -5130$ J, (5b) $\Delta H = -8549$ J

2.2 (a) $w = 2270$ J, $q = 5675$ J; (b) $w = 0$, $q = 6809$ J; (c) $w = -3278$ J, $q = -13.492$ J

2.3 $V = 1.52$ liters, $w = 8.7$ J

2.4 $T = 1620$ K

2.6 (a) +123.48 kJ, (b) −22.45 kJ, (c) 0. Total work = 101.03 kJ done by the system.

2.7 $P = 0.3$ atm

2.8 $\Delta U = 0 \quad \left(\text{a state function}\right)$

$$\sum w_i = RT_A - 2RT_A \ln(2)$$

$$\sum q_i = (C_V + R)T_A - 2RT_A \ln(2) - C_V T_A = RT_A - 2RT_A \ln(2)$$

2.9 $w = \displaystyle\int_0^{M_f} \mu_0 V \mathcal{H} \cdot d\boldsymbol{M} = \int_0^{M_f} \mu_0 V \frac{T\boldsymbol{M}}{C} \cdot d\boldsymbol{M} = \mu_0 V \frac{TM_f^2}{2C} = \mu_0 V \frac{\mathcal{H}_f M_f}{2}$

2.12 $\gamma_{gb} = 2\gamma_{\alpha/L}\cos\left(\frac{\theta_{\text{groove}}}{2}\right)$

2.13* $\Delta H = 42,750$ J

2.14* For adiabatic expansion: $PV^{\gamma} = \text{constant} = K$

$$w = \int_{V_1}^{V_2} P\,dV = \int_{V_1}^{V_2} KV^{-\gamma}\,dV = \frac{KV^{-\gamma+1}}{1-\gamma}\Big|_{V_1}^{V_2}$$

$$= \frac{P_2V_2 - P_1V_1}{1-\gamma}$$

CHAPTER 3

3.1 a. 5.76 J/K, (b) 0 J/K. (c) −8.65 J/K

3.2 a. $\Delta U = \Delta H = q = w = 0$, $\Delta S = 9.13$ J/K
b. $\Delta U = q =$ 1247 J, $\Delta H = 2078$ J, $w = 0$, $\Delta S = 3.59$ J/K
c. $\Delta U = \Delta H = 0$, $q = w = 3654$ J, $\Delta S = 9.13$ J/K
d. $\Delta U = -1247$ J, $\Delta H = q = -2078$ J, $w = -831$ J, $\Delta S = -5.98$ J/K
totals: $\Delta U = \Delta H = 0$, $w = q = 2823$ J, $\Delta S = 15.88$ J/K

3.3 $T_1 = 300$ K, $T_2 = 600$ K. The isothermal expansion is conducted at 300 K.

3.4 $\Delta H = 42{,}750$ J, $\Delta S = 59.7$ J/K

3.5 The final temperature is 323.32 K, which is >323 K because the heat capacity increases with increasing temperature. Thus, the decrease in temperature caused by withdrawing heat q from hot copper is less than the increase in temperature caused by adding heat q to cold copper. The quantity of heat transferred is 1,233 J and $\Delta S_{\text{irr}} = 0.6$ J/K.

3.6 $T_f = \left(T_1^{C_1}T_2^{C_2}\right)^{\frac{1}{C_1+C_2}}$, $w = q_2 - q_1 = [-C_2(T_f - T_2)] - [C_1(T_f - T_1)]$

3.8 (a) −22.01 J/K, (b) −20.18 J/K

3.9 $w = (t_2 - t_1)\Delta S$, the area of the box in the T - S Plot

3.10* $\Delta S^{\text{Fe}}_{300\text{K}\to1500\text{K}} = 65.43$ J/K

3.13*

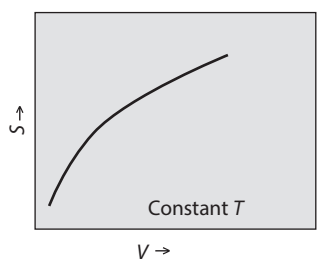

CHAPTER 4

4.1 (*a*) $R \ln 4$, (*b*) $R \ln 8$, (*c*) 0, (*d*) $R \ln (32/27)$

4.2 The total number of distinguishable complexions is

$$\frac{(2n)!}{n!n!} \tag{i}$$

and, with n being a multiple of 4, the number of complexions in the most probable distribution is

$$\left[\frac{n!}{(0.5n)!(0.5n)!}\right]\left[\frac{n!}{(0.5n)!(0.5n)!}\right] \tag{ii}$$

The ratio of (ii) to (i) decreases with increasing n.

4.3 $\Delta S_{\text{conf}} = 1.02\,\text{J/K}$

4.4 65.0 grams

4.5 a. $Z = \sum \exp\left(\frac{\varepsilon_i}{k_B T}\right) = \exp\left(\frac{\varepsilon^{\uparrow}}{k_B T}\right) + \exp\left(\frac{\varepsilon^{\downarrow}}{k_B T}\right)$

b. at high T: equal numbers up and down

at low temperatures: all up

4.7* (*a*) $U = \frac{3}{2}RT$ (*b*) $c_V = \left(\frac{\partial U}{\partial T}\right)_V = \frac{3}{2}R$

Looks to be a monatomic ideal gas.

CHAPTER 5

5.1

$$\text{Use the third } TdS \text{ equation } TdS = \frac{c_V \beta_T}{\alpha_P} dP + \frac{c_p}{V\alpha_P} dV$$

$$\text{at constant } P \quad dS = \frac{c_p}{TV\alpha_P} dV \quad \therefore \left(\frac{\partial S}{\partial V}\right)_P = \frac{c_p}{TV\alpha_P}$$

5.2

$$\text{Use the third } TdS \text{ equation} \qquad TdS = \frac{c_V \beta_T}{\alpha_P} dP + \frac{c_p}{V\alpha_P} dV$$

$$\text{at constant } V \quad dS = \frac{c_V \beta_T}{T\alpha_P} dP \qquad \therefore \left(\frac{\partial S}{\partial P}\right)_V = \frac{c_V \beta_T}{T\alpha_P}$$

$$\text{But} \quad c_V = c_P - \frac{VT\alpha_P^2}{\beta_T} \qquad \therefore \left(\frac{\partial S}{\partial P}\right)_V = \frac{c_P \beta_T}{T\alpha_P} - \alpha_P V$$

5.3

$$dA = \left(\frac{\partial A}{\partial T}\right)_V dT + \left(\frac{\partial A}{\partial V}\right)_T dV \quad \therefore \left(\frac{\partial A}{\partial P}\right)_V = \left(\frac{\partial A}{\partial T}\right)_V \left(\frac{\partial T}{\partial P}\right)_V$$

$$\left(\frac{\partial A}{\partial T}\right)_V = -S \quad \text{and} \quad \left(\frac{\partial T}{\partial P}\right)_V = \frac{\beta_T}{\alpha_P} \quad \therefore \left(\frac{\partial A}{\partial P}\right)_V = -\frac{S\beta_T}{\alpha_P}$$

5.6

$$dH = TdS + VdP$$

$$\therefore \left(\frac{\partial H}{\partial V}\right)_S = V\left(\frac{\partial P}{\partial V}\right)_S$$

From the third TdS equation: $\left(\frac{\partial P}{\partial V}\right)_S = -\frac{c_P}{c_V V \beta_T}$

$$\therefore \left(\frac{\partial H}{\partial V}\right)_S = V\left(-\frac{c_P}{c_V V \beta_T}\right) = -\frac{c_P}{c_V \beta_T}$$

5.7

$$c_p = \left(\frac{\partial H}{\partial T}\right)_P \therefore \left(\frac{\partial c_p}{\partial P}\right)_T = \left[\frac{\partial}{\partial P}\left(\frac{\partial H}{\partial T}\right)_P\right]_T = \left[\frac{\partial}{\partial T}\left(\frac{\partial H}{\partial P}\right)_T\right]_P$$

$$\left(\frac{\partial H}{\partial P}\right)_T = T\left(\frac{\partial S}{\partial P}\right)_T + V \quad \text{and} \quad \left(\frac{\partial S}{\partial P}\right)_T = -\left(\frac{\partial V}{\partial T}\right)_P$$

$$\therefore \left(\frac{\partial c_p}{\partial P}\right)_T = \frac{\partial}{\partial T}\left[-T\left(\frac{\partial V}{\partial T}\right)_P + V\right]_P$$

$$= \frac{\partial}{\partial T}\left[-T\alpha_P V + V\right]_P$$

$$= -\alpha_P V - TV\frac{d\alpha_P}{dT} - T\alpha_P^2 V + \alpha_P V$$

$$= -TV\left(\alpha_P^2 + \frac{d\alpha_P}{dT}\right)$$

5.8

$$\left(\frac{\partial S}{\partial T}\right)_P = \frac{c_p}{T} \quad \text{and} \quad \left(\frac{\partial S}{\partial P}\right)_T = -\left(\frac{\partial V}{\partial T}\right)_P = -\alpha_P V$$

$$\therefore \left(\frac{\partial T}{\partial P}\right)_S = \frac{\left(\frac{\partial S}{\partial P}\right)_T}{\left(\frac{\partial S}{\partial T}\right)_P} = \frac{\alpha_P V T}{c_p}$$

5.9 From the third *TdS* equation:

$$TdS = 0 = \frac{c_V \beta_T}{\alpha_P} dP + \frac{c_P}{\alpha V} dV$$

$$\therefore \left(\frac{\partial P}{\partial V}\right)_S = -\frac{\dfrac{c_P}{\alpha_P V}}{\dfrac{c_V \beta_T}{\alpha_P}} = -\frac{c_P}{V c_V \beta_T}$$

5.10

$$dG = -SdT + VdP$$

$$\therefore \left(\frac{\partial G}{\partial P}\right)_T = V \quad \text{and} \quad \left(\frac{\partial^2 G}{\partial P^2}\right)_T = \left(\frac{\partial V}{\partial P}\right)_T$$

$$dA = -SdT - PdV$$

$$\therefore \left(\frac{\partial A}{\partial V}\right)_T = -P \quad \text{and} \quad \left(\frac{\partial^2 A}{\partial V^2}\right)_T = -\left(\frac{\partial P}{\partial V}\right)_T = -\frac{1}{\left(\dfrac{\partial^2 G}{\partial P^2}\right)_T}$$

5.12 a. l. $\Delta U = \Delta H = 0$, $\Delta S = R \ln 4$, $\Delta A = \Delta G = -T\Delta S = -RT \ln 4$
2. $\Delta U = \Delta H = 0$, $\Delta S = R \ln 8$, $\Delta A = \Delta G = -RT \ln 8$
3. $\Delta U = \Delta H = \Delta S = \Delta A = \Delta H = 0$
4. $\Delta U = \Delta H = 0$, $\Delta S = R \ln(32/27)$, $\Delta A = \Delta G = -RT \ln (32/27)$

b. $\Delta U = \Delta H = 0$, $\Delta S = R \ln(V_2/V_1) = R \ln 2$, $\Delta A = \Delta G = -RT \ln 2$

c. $\Delta U = c_v(T_2 - T_1)$, $\Delta H = c_p(T_2 - T_1)$, $\Delta S = 0$, $\Delta A = \Delta U - S(T_2 - T_1)$, $\Delta G = \Delta H - S(T_2 - T_1)$

d. $\Delta U = c_v(T_2 - T_1), \Delta H = c_p(T_2 - T_1), \Delta S = c_p \ln(T_2/T_1), \Delta A = \Delta U - (T_2 - T_1)$ $S_1 - T_2 \Delta S$, $\Delta G = \Delta H - (T_2 - T_1)S_1 - T_2 \Delta S$

e. $\Delta U = c_v(T_2 - T_1), \Delta H = c_p(T_2 - T_1), \Delta S = c_v \ln(T_2/T_1), \Delta A = \Delta U - (T_2 - T_1)$ $S_1 - T_2 \Delta S$, $\Delta G = \Delta H - (T_2 - T_1)S_1 - T_2 \Delta S$

5.14

$$\left(\frac{\partial T}{\partial P}\right)_{S,\mathcal{H}} = \left(\frac{\partial V}{\partial S}\right)_{P,\mathcal{H}}$$

$$\left(\frac{\partial V}{\partial \mathcal{H}}\right)_{S,P} = -\mu_0 V \left(\frac{\partial \boldsymbol{M}}{\partial P}\right)_{S,\mathcal{H}}$$

$$\left(\frac{\partial T}{\partial \mathcal{H}}\right)_{S,P} = -\mu_0 V \left(\frac{\partial \boldsymbol{M}}{\partial S}\right)_{P,\mathcal{H}}$$

5.15

$$\left(\frac{\partial S}{\partial V}\right)_{T,\boldsymbol{M}} = \left(\frac{\partial P}{\partial T}\right)_{V,\boldsymbol{M}}$$

$$\left(\frac{\partial S}{\partial \boldsymbol{M}}\right)_{T,V} = -\mu_0 V\left(\frac{\partial \boldsymbol{\mathcal{H}}}{\partial T}\right)_{\boldsymbol{M},V}$$

$$\left(\frac{\partial P}{\partial \boldsymbol{M}}\right)_{V,T} = -\mu_0 V\left(\frac{\partial \boldsymbol{\mathcal{H}}}{\partial V}\right)_{\boldsymbol{M},T}$$

5.17* A, the Helmholtz free energy
5.18* G, the Gibbs free energy
5.22*

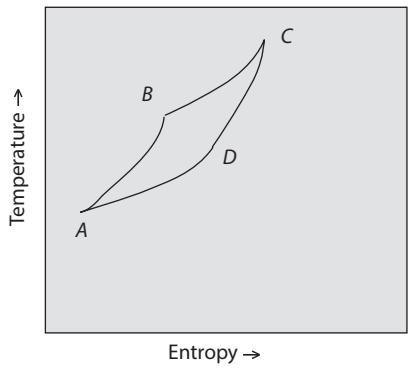

CHAPTER 6

6.1 $\Delta H_{1600} = -1.086 \times 10^6$ J, $\Delta S_{1600} = -178.5$ J/K
6.2 $H_{\text{diamond, 1000}} - H_{\text{graphite, 1000}} = 1037$ J. Thus, the oxidation of diamond at 1000 K is 1037 J/mole more exothermic than the oxidation of graphite.
6.3 $\Delta H_{1000} = -80{,}194$ J, $\Delta S_{1000} = 4.05$ J/K
6.4 Increasing the pressure to 1000 atm increases the molar enthalpy by 612.1 J. This increase in molar enthalpy is achieved by increasing the temperature of Cu from 298 to 323 K at a pressure of 1 atm.
6.5 (a) $\Delta H = -435{,}000$ J, $\Delta S = -94.75$ J/K; (b) $\Delta H = -355{,}000$ J, $\Delta S = -75.35$ J/K; (c) $\Delta H = -373{,}000$ J, $\Delta S = -80.15$ J/K
6.6 15.1 kg
6.7 (a) 4745 K, (b) 2485 K
6.8 $\Delta G_{800} = -1.805 \times 10^6$ J. If it is assumed that Δc_p for the reaction is zero, $\Delta G_{800} = \Delta H_{298} - 800\Delta S$ is calculated as -1.811×10^6 J, which involves a 0.3% error.
6.9 $a = 3$, $b = c = 2$, $\Delta H_{298} = 99{,}700$ J, $\Delta S_{298} = 125.8$ J/K, $\Delta G_{298} = 62{,}210$ J

6.10 1675 kJ

6.11 $d\Omega = SdT + PdV + Nd\mu$

$$\Omega = \Omega(T, V, m)$$

6.16* a. $c_P - c_V = RT\alpha_P$

b. For an ideal gas: $\alpha_P = \dfrac{1}{T} \quad \therefore c_P = c_V = R$

6.17*a.

i. Amorphous solid to atomic ordered crystal.
$\Delta H < 0 \; + \Delta S < 0$

ii. Amorphous solid to random crystal.
$\Delta H < 0 + \Delta S < 0$

iii. Amorphous solid to liquid.
$\Delta H > 0 + \Delta S > 0$

iii. Random crystal to liquid
$\Delta H > 0 + \Delta S > 0$

b. The atomically ordered crystalline phase since it has zero configurational entropy and negative enthalpy.

6.18* At A: amorphous ferromagnet
At B: amorphous paramagnet
At C: crystalline ferromagnet
At D: liquid paramagnetic

CHAPTER 7

7.1 (a) The triple point for α-β-vapor is $T = 1163$ K, $p = 2.52 \times 10^{-10}$ atm, and the triple point for β-liquid-vapor is $T = 1689$ K, $p = 8.35 \times 10^{-5}$ atm. (b) $T_b = 2776$ K. (c) $\Delta H_{(\alpha \to \beta)} = 4739$ J, $\Delta H_m = 29{,}770$ J.

7.2 $p_{\mathrm{Hg},373\ \mathrm{K}} = 3.55 \times 10^{-4}$ atm

7.3 Condensation begins at 328 K; at 280 K, 82.5% of the $SiCl_4$ has condensed.

7.4 Equation (i) gives the vapor pressure of solid zinc.

7.5 $\Delta H_b = 342$ kJ

7.6 $p_{\mathrm{CO_2},298\mathrm{K},(l)} = 78.3$ atm. The triple point pressure is 5.14 atm, and, as the 1 atm isobar does not pass through the liquid phase field, liquid CO_2 is not stable at atmospheric pressure.

7.7 $P = 2831$ atm

7.8 The slopes of the lines at the triple point are obtained from $dP/dT = \Delta S/\Delta V$.

7.9 $T_b = 523$ K

7.12

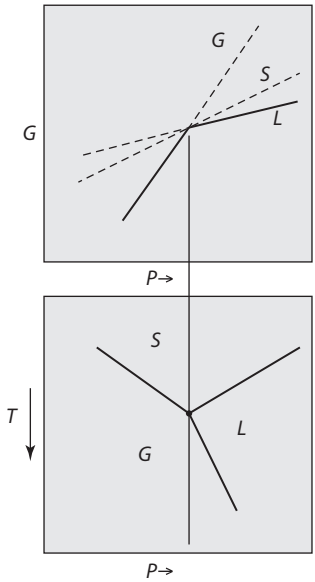

7.13

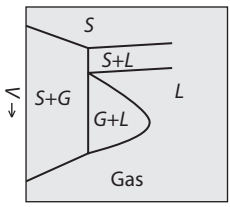

7.15* This transformation is neither a *first-order* or *second-order* transformation according to their definitions. The heat capacity starts to rise at temperatures well below the transformation temperature, in contrast to that of *first-order* transformations. However, the heat capacity does not have a finite drop at the transformation temperature, as *second-order* ones display. The transformation is best called a *continuous* or *higher-order* transformation.

7.16* $\Delta H = 43{,}272$ J/mole

CHAPTER 8

8.1 The van der Waals equation containing the reduced variables is

$$\left(P_R + \frac{3}{V_R^2}\right)(3V_R - 1) = 8T_R$$

$$Z_{\text{cr}} = 0.375;\ \left(\partial U / \partial V\right)_T = a / V^2$$

8.2 $n_A/n_B = 1$, $P = 1.414$ atm

8.3 The tank contains 565 moles of van der Waals oxygen and 511 moles of ideal gas oxygen. As the gas is purchased by the tank load, the same price purchases more moles of a van der Waals gas than it does an ideal gas.

8.4 $w = -1385$ J

8.5 (a) $b = 0.0567$ *l*/mole, $a = 6.77$ l^2atm/mole^2; (b) 0.170 *l*/mole; (c) P (van der Waals) = 65.5 atm, P (ideal gas) = 82.1 atm

8.6 With the virial equation $w = -301$ kJ, with the van der Waals equation $w = -309$ kJ, with the ideal gas law $w = -272$ kJ

8.7 (a) $f = 688$ atm, (b) $P = 1083$ atm, (c) $\Delta G = 16{,}190$ J with an nonideal contribution of 790 J

8.9*

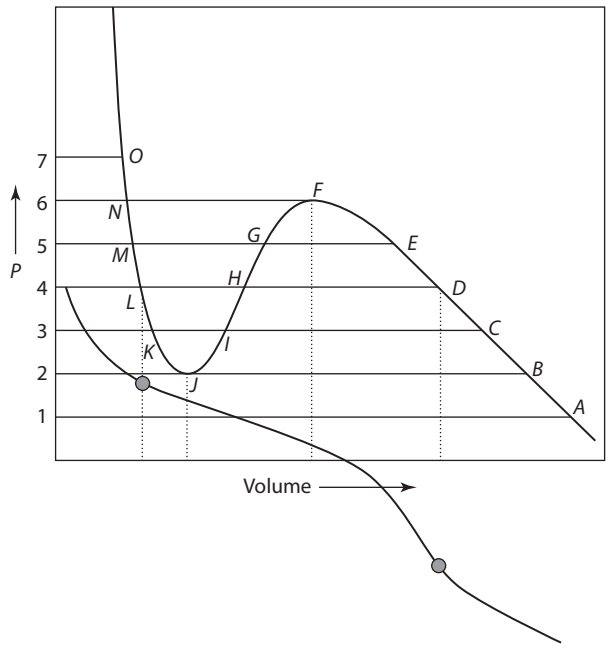

8.10 $$dP = \frac{R}{V-b}dT + \left(-\frac{RT}{(V-b)^2} + \frac{2a}{V^3}\right)dV$$

8.11* $$dP = \left[\frac{R}{V} + \frac{B'(T)R}{V^2} + \frac{RT}{V^2}\left(\frac{\partial B'(T)}{\partial T}\right)\right]dT - \left[\frac{RT}{V^2} + \frac{2B'(T)RT}{V^3}\right]dV$$

8.12 $$Z_{cr} = \frac{P_{cr}V_{cr}}{RT_{cr}} = \frac{a}{27b^2}\cdot 3b \cdot \frac{1}{R}\cdot\frac{27bR}{8a} = \frac{3}{8} = 0.375$$

$$w = \int_{V_1}^{V_2} P\,dV = \int_{V_1}^{V_2} \left(\frac{nRT}{(V - nb)} - \frac{n^2 a}{V^2} \right) dV$$

8.14* (a)

$$w = nRT \ln \frac{(V_2 - nb)}{(V_1 - nb)} + n^2 a \left(\frac{1}{V_2} - \frac{1}{V_1} \right)$$

(b) negative

8.16* $V_{cr} = \dfrac{b(m-1)}{m+1}$

For $m = -2$, $V_{cr} = 3b$

CHAPTER 9

9.1 $\Delta H = 117{,}400$ J, $\Delta S = 59.63$ J/K

9.2 $\gamma_{Mn} = 1.08$

9.3 (a) The average value of Ω is 4396 ± 6 J, which indicates that, with respect to the behavior of G^{xs}, the solution is regular. (b) $\bar{G}_{Fe}^{xs} = 1582$ J and $\bar{G}_{Mn}^{xs} = 703$ (c) $\Delta G^M = -9.370$ J. (d) $p_{Mn} = 0.0118$ atm and $p_{Fe} = 3.68 \times 10^{-5}$ atm.

9.4 73,380 J

9.5 $\Omega = -4578$ J, $a_{Sn} = 0.418$

9.6 a. $\Delta G^{M,id}(X_B = 0.5) = -RT\Delta S^M(X_B = 0.5)$

$$= -8314 * \left(\frac{1}{2} \ln \frac{1}{2} + \frac{1}{2} \ln \frac{1}{2} \right) = -5763 \text{ J}$$

$$\Delta \bar{G}_B = RT \ln a_B = -5763 \text{ J}$$

$$a_B(X_B = 0.5) = \exp\left(-\frac{5763}{8314} \right) = 0.5$$

b. $\Delta \bar{G}_B = RT \ln a_B = -1609$ J

$$a_B = \exp\left(-\frac{1609}{8314} \right) = 0.844$$

9.8 The temperature is increased by 2.37 degrees (K).

9.10 $\ln \gamma_{Cd} = 0.425\, X_{Zn}^2 + 0.30 X_{Zn}^3$, $a_{Cd} = 0.577$

9.11 $a_{Au} = 0.695$, $a_{Ni} = 0.87$

9.14 $a_B = \gamma_B X_B$. This is Henry's law.

We cannot determine the value of the constant γ_B.

9.15 $a_B = 0.824$

9.17* $\dfrac{dT^{\text{Binodal}}}{dX_B} \to \infty$ as $X_B \to 0$ and $\dfrac{dT^{\text{Binodal}}}{dX_B} \to \infty$ as $X_B \to 1$

9.18*

$$\text{as} \quad X_B \to 0 \qquad T^{\text{spinodal}} = 4T_C$$

$$\text{as} \quad X_B \to 1 \qquad T^{\text{spinodal}} = -4T_C$$

9.19* $\dfrac{Y_1}{Y_2} = \sqrt{3}$

CHAPTER 10

10.1 $T = 1317$ K, $X_{CaF_2} = 0.53$
10.2 (a) −11,140 J, (b) zero
10.3 (a) 2418 K, (b)$X_{Al_2O_3} = 0.62$, (c) 2444 K, (d) $X_{Al_2O_3} = 0.38$
10.4 −814 J
10.5 $\Omega_l = 38{,}096$ J, $T_{cr} = 2291$ K
10.6 (a) $\Delta H^{\circ}_{m,Ge}$ from liquidus = 21,527 J, (b) $\Delta H^{\circ}_{m,Ge}$ from solidus = 33,111 J
10.7 The maximum solubility of CaO in MgO is $X_{CaO} = 0.066$, and the maximum solubility of MgO in CaO is $X_{MgO} = 0.15$.
10.14*

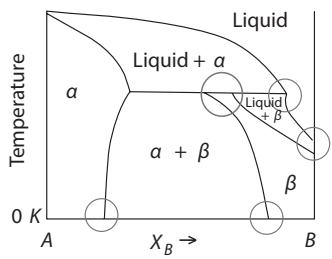

CHAPTER 11

11.1 $X_{CO_2} = X_{H_2} = 0.182$, $X_{H_2O} = 0.0677$, $X_{CO} = 0.568$
11.2 43,800 J
11.3 $CO_2/H_2 = 1.276$
11.4 1771 K
11.5 $P_T = 0.192$ atm, $T = 791$ K
11.6 (a) $p_N = 5.94 \times 10^{-6}$ atm, (b) $P_T = 3.18 \times 10^{-9}$ atm
11.7 13.3 atm, $\Delta H^{\circ}_{573\,K} = -50{,}900$ J, $\Delta H^{\circ}_{573\,K} = -1107$ J/K

11.8 $PCl_5/PCl_3 = 0.371$

11.9 At $P_T = 1$ atm, $p_{H_2} = 1.12 \times 10^{-8}$ atm, $p_{O_2} = 0.0756$ atm

At $P_T = 10$ atm, $p_{H_2} = 3.56 \times 10^{-8}$ atm, $p_{O_2} = 0.756$ atm

11.10 $X_{H_2} = X_{I_2} = 0.165$, $X_{HI} = 0.669$, $T = 918$ K

11.11 $$p_{CO} = \frac{1}{\left(K_P^{\frac{1}{4}} + 1\right)} \qquad p_{CO_2} = \frac{K_P^{\frac{1}{4}}}{\left(K_P^{\frac{1}{4}} + 1\right)}$$

11.12 $K_P = 13.12$

11.13* $p_H = 1.67 \times 10^{-3}$ atm

CHAPTER 12

12.1 $T = 565$ K

12.2 $T_{m,Ni} = 1731$ K, $\Delta H^\circ_{m,Ni} = 17{,}490$ J, $\Delta S^\circ_{m,Ni} = 10.1$ J/K

12.3 (a) $T = 462$ K, (b) $T = 421$ K

12.4 $p_{H_2O} = 1.32 \times 10^{-3}$ atm, and the oxidation reaction is exothermic.

12.5

$$K_P = \exp\left(-\frac{26{,}720}{8.3144 \times 900}\right) = 0.028 = \frac{p_{HCl}^2}{p_{H_2}}$$

$$\text{In the exit gas, } \frac{p_{HCl}^2}{p_{H_2}} = \frac{0.07^2}{0.5} = 0.0098.$$

Since this is less than K_P, equilibrium has not been attained.

12.6 The FeO disappears.

12.7 $p_{Mg} = 2.53 \times 10^{-2}$ atm

12.8 (a) $T = 1166$ K, (b) $p_{CO_2} = 0.053$ atm, (c) $p_{CO_2} = 1.23$ atm

12.9 $P = 1$ atm, ($p_{SO_3} = 7.99 \times 10^{-2}$ atm, $p_{SO_2} = 0.612$ atm, $p_{O_2} = 0.306$ atm)

12.10 99.1% of the sulfur is removed, and p_{S_2} in the effluent gas is 6.3×10^{-11} atm.

12.11 $\Delta G^\circ = 282{,}000 - 123T$ J

12.12 0.76 moles of CH_4 are consumed per mole of Fe produced.

12.13 Equation (i) for solid Mg, Equation (ii) for gaseous Mg, Equation (iii) for liquid Mg, $T_{m,Mg} = 930$ K, $T_{b,Mg} = 1372$ K

12.14 54.92 g of Zn are oxidized to form ZnO and 29.78 g of Zn are evaporated, which leaves 115.3 g of metallic Zn in the crucible.

12.15 4.76 moles of $CaCO_3$ are decomposed per mole of CH_4 burned.

12.16 $X_{Hg} = 0.0152$, $X_{O_2} = 0.0051$

12.17 $P_T = 1.68$ atm, $p_{CO} = 1.03$ atm, $p_{CO_2} = 0.65$ atm

12.19* For the reaction $B + 2AO = 2A + BO_2$, we have:

$N = 4$, $R = 1$, $\phi = 4$, and therefore, $\mathcal{F} = (4-1) + 2 - 4 = 1$. One degree of freedom.

CHAPTER 13

13.1 $a_{Cu} = 0.159$
13.2 $a_{Mg} = 6.4 \times 10^{-4}$
13.3 $a_{PbO} = 0.5$
13.4 $X_{Cu} = 0.018$. Increasing T decreases the extent to which Cu is removed.
13.5 $a_C = 0.5$, $p_{H_2} = 0.92$ atm
13.6 $a_{FeO} = 6.2 \times 10^{-5}$
13.8 With $C = 3$ and $\phi = 3$, $\mathcal{F} = 2$, which are used by specifying $T = 1000$ K and $[X_{Mn}] = 0.001$. $(X_{FeO}) = 1.22 \times 10^{-3}$, $p_{O_2} = 2.33 \times 10^{-27}$ atm
13.9 For $2A + B = A_2B$, $\Delta G^\circ_{1273K} = -24{,}370$ J; for $A + 2B = A_2B$, $\Delta G^\circ_{1273K} = -23{,}190$ J
13.10 (a) 10^{-3}, (b) 8.07×10^{-4}, (c) 7.14×10^{-3}, (d) 0.65
13.11 $\Delta G^\circ = -567{,}500$ J
13.12 $p_{O_2} = 5.17 \times 10^{-10}$ atm; $h_{Al(1\ wt\%\ in\ Fe)} = 7.2 \times 10^{-6}$; $C = 3$, $\phi = 4$, and therefore, $\mathcal{F} = 1$ which is fixed by specifying $T = 1600°C$.
13.13 $T_{max} = 2211$ K, $T_{min} = 1515$ K
13.14 $p_{Mg} = 0.053$ atm
13.15 $a_{MgO}(min) = 0.027$
13.16 $p_{CO} = 0.739$ atm, $p_{CO_2} = 0.013$ atm, $p_{Zn} = 0.766$ atm
13.17 $a_{Al_2O_3} = 0.129$
13.18 $T_{max} = 1108$ K
13.19 $P = 6917$ atm
13.20 Wustite $0.904 < p_{CO} < 3.196$ atm, cementite $7.43 < p_{CO} < 8.14$ atm
13.21 $T_{max} = 1026$ K
13.22 [wt% O] = 1.9, $k = 2.0$

CHAPTER 14

14.1 $Pb_{(s)} + 2AgCl(s) = 2Ag(s) + PbCl2(s)$, $\Delta G° = -94{,}560$ J, $\Delta S° = -35.5$ J/K
14.2 (a) −103,400 J, (b) 27.98 J/K, (c) 8338 J/mole of Pb, (d) $a_{Hg} = 0.71$
14.3 $$\ln p_{O_2}(\text{atm}) = \frac{46{,}620E}{T} + \frac{63{,}440}{T} - 15.48$$
14.4 $\Delta Cp = -0.093$ J/K
14.5 (a) $a_{Al} = 0.673$, (b) $\Delta \bar{G}^M_{Al} = -2150$ J, (c) $\Delta \bar{H}^M_{Al} = 3329$ J
14.6 (a) $1.62 \times 10{-}6$, (b) 0.5, (c) 0.266 wt%, (d) 0.602 wt%
14.7 pH = 6.33, $\varepsilon = -0.126$ volts. Other ions: $[Pb^{4+}] = 3.05 \times 10^{-62}$ moles/liter, $HPbO_2^- = 10^{-9}$ moles/liter, $PbO_3^{2-} = 2.5 \times 10^{-47}$ moles/liter, $\left[PbO_4^{4-}\right] = 6 \times 10^{-221}$ moles/liter
14.8 2.20 volts, 1.17 volts
14.9 $\Delta G° = +6897$ J, $\Delta G = -4513$
14.10* $\Delta G^\circ = -241{,}217$ J
14.12* $\Delta G^\circ = -147{,}239$ J; The reaction will happen and Zn will dissolve.

CHAPTER 15

15.3 $\Delta H^M = 8N_O W_1\left(\frac{3}{16}+\frac{1}{16}\right) = 2N_O W_1$ at $25\%\, B$

15.4* (a) $S^{XS} = \frac{a^2(T-T_C)}{2B}$ (b) $C_P^{ord} - C_P^{dis} = a$

15.9 a. $T = T_C + \frac{C^2}{4aE}$

b.

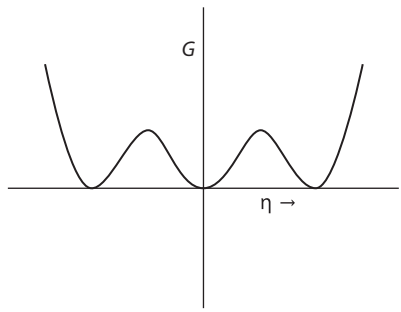

c. First order

d. $\Delta H = T_0 a\left(\frac{C}{2E}\right) < 0$ since $C < 0$

e. Exothermic

Index

Note: **Bold** page numbers refer to tables; *italic* page numbers refer to figures and page numbers followed by "n" denote endnotes.

A–A bond energy 292, 293, 309, 310, 602, 603, 605, 623
A–B bond energy 291, 292, 293, 301, 302, 306, 309, 310, 312, 324, 331, 345, *346,* 348, 349, 351, 354, 359, 362, 364, 366, *368*, 374, 375, *480*, 481, 499, *500, 506*, 558, 600, 602, 603, 605, 606, 607, 623
absolute potential 545, 568, *568,* 569, *569*
activation energy 290, 291
activity 294–296, 307, *308*, 309, 310–314, *311*, 317, 318, *318*, *319*, 326, *327*, *328*, 329, 331, *335*, 345, *346*, 347, 348, 350, 356, *357*, 469, 470, 471, 472, *473*, 476, 483, 484, *484*, 486, 490, 491, 492, 496, 501, 506, 508, 509, 510, 511, 513, 515, 516, 520, *520*, 523, 525, 526, 529, 530, 536, 549, 550, 555, 556, *557*, 560, 561, 562, 563, 565, 566, *566*, 567, 572, 577
  coefficient 307, 309, 317, 318, *319,* 332, 333, 480–482, 529, 530, 562, 563, 587, 588
  quotient 471, 550
  thermodynamic 343–344, *344*, 351–353, *354*
  thermodynamic of nonideal gases 272–280, *275, 278*
adiabatic boundaries 4
adiabatic expansion of ideal gas 36, 39, *39,* 40, 43, 65–69, 73
adiabatic process 29, 40, 41, 42, 65, 191, 192
  changes of state 26
  compression 74
  expansion 36
  irreversible expansion 66–68
  reversible expansion 37–39, 66
Al-C-O-N system, and phase equilibria in 513–516, *514*
allotropy 173, *173, 174,* 183, 187, 188, 229, 230
alloy 15, 190, 191, 232, *299,* 310, 320, 358, 362, 370, 475, 476, *476,* 478, 479, 484, 485, 508, 510–512, 555, 556, 558–560, 596–599, 601, 602, 607–609, 619
AlN 513–516
alternate standard state 479–486
aluminum, Pourbaix diagrams for 579–586, *584*
anodic oxidation reaction 548, 577
anolyte 547, 549, 550
anticlockwise rotation 474, 479
aqueous solution 544, 548, 549, 553, 560, 567, 568, 572, 573, 577, 578, 585–586, *586*, 587
  HCl 565, *566*
  thermodynamics 561–564
aspects of entropy 18, 96, 123, 157, 190, 191, 231, 320
atomic order parameter 189, 606–611
auxiliary functions 132
Avogadro, Lorenzo 12
Avogadro's number 8, 12n3, 111, 117, 194, 306, 403, 544, 602

barocaloric effect 156, 157, 191
batteries, EMF 574–576
B–B bond energy 292, 293, 309, 310, 602, 603, 605, 623
BCD 266
Beattie–Bridgeman equation 271
Beattie, James A. 271
Bennett, L.H. 371n4
Berthelot equation 271
Berthelot, Pierre Eugène Marcellin 271
Berthollet, Claude Louis 516
berthollides 516
Bi–Cd system 358, *359,* 388–390
binary alloy systems 370, 596, 597
binary systems 14, 104, *295*, 297, 342–375, 486, 529, 596–624
  containing compounds 499–508
  the Ga-GaP system *507,* 507–508
  phase diagrams of 499, *500, 506,* 507
Binodal 329, 333
blast furnace 444
body-centered cubic (BCC) 31, 195, 196, 231–233, 373, 607, *607,* 609
Boltzmann distribution 107–111
Boltzmann equation 113, 123
Boltzmann, Ludwig Eduard 94, 97, 106, 110, 123, 131, 306
bond energy 103, 292, 293, 309, 310, 602, 623
Borelius, G. 599–600, 599n1, 600
Boudouard, Octave Leopold 444
Boudouard reaction 444
boundaries 3, 4, 9, 231, 235, 259, 329, 372, 373, *373,* 374, 375, 549, 598, 599

Boyle, Robert 9, 11
Boyle's law 9, 11
Bridgeman, Oscar C. 271

Cahn, Anne Hessing 267n3, 371n4
Cahn, John Werner 267n3, 371n4
Callen, Herbert Bernard 5, 5n2
calomel cell 564, *565*
caloric theory 24
calorie 24
capillarity, and local equilibrium 224
carbonates 426, 430
carbon oxides 140, 444–450, *444*, *449–, 451*
carbon-oxygen reactions 450
Carnot cycle *69,* 70–72, *72,* 73, 75, *75,* 76
Carnot, Nicolas Leonard Sadi 69
catalyst 393
cathodic reduction reaction 548, 577
catholyte 547, 549, 550
cell reaction 544, 547–550, 552, 554–555, 558, 560, 567–568, 575–577, 586–588
Celsius, Anders 11
charge neutrality 543
Charles, Jacques-Alexandre-Cesar 10
Charles' law 10, 11
chemical affinity 184, 393, 435
chemical driving force 184, 216, 254, 543, 544–549, 547, 550, 551, 555
chemical potential 97, 131, 132, 140–143, 159, 215, 216, 222, 248, 254, 297, 298, 301, 342, 347, 394, 398, 427, 469, 546, 547
chemical reaction 31–32, 58, 79, 132, 140, 142, 143, 174, 177, 184, 186, 200, 393–396, *396,* 397, 399, 402–404, 406, 432, 456, 469, 499, 542–544, 560, 586
  application of First Law 31–32
chemical species 14, 132, 141, 142, 216, 254, 290, 402, 427, 579
chemical work 143
chlorination 193, 403, 568, 569
Clapeyron, Benoft Paul Emile 223
Clapeyron equation 223, 225–227, 232
classical thermodynamics 4, 5, 34, 94, 96, 99, 107, 120, 122, 186
Clausius-Clapeyron equation 227
Clausius, Rudolf Julius Emanuel 71, 227
closed systems 3, 29, 30, *79,* 83, 97, 100, *111,* 121, 123, 131, 133, 135, 139–140, 142–144, 157–160, 174, 198–200, 216, 251, 439
  enthalpy 132–133
  Gibbs free energy 137–138, 140–142, 251
  Gibbs-Helmholtz equation 158–159
  Helmholtz free energy 133–137, *135–137*
  Maxwell's relations (*see* Maxwell's relations)
  overview 131–132
  potential 23, 26
  thermodynamic relations 143–144
CO_2-CO gas mixture 411–413, 447, *451*, *452*
coefficient of thermal expansion, IO 4, 8, 11, 188, 199
common tangent 323, 326, *327, 328,* 353, 354, 364, 366, 379, 521
component 4, 13–16, 29, 122, 159, 188, 189, 215, 216, 222, 225, 248–249, 251–257, 281, 290, 292, *292,* 294–299, *299,* 300–304, 306, 307, 309, 310, *311,* 313, *322,* 326, *327, 328,* 331–333, 342–344, *344,* 345, 347, 348, 351, 353, 356, 364, 366, *368,* 393, 416, 427n1, 429, 469–530, 560, 562, 563, 597, 600, 602–604, 606, 607, 623
compound 122, 171–173, *173,* 174, *174,* 176, 187, 190, 194, *195,* 200, 298, 310, 342, 372, *372,* 456, 499–508, 516, 523, 542, 599
compressibility factor 260, 261, *261,* 264, 274, 281
concentration cell 552–557, *557,* 558
condensation 227, 258, 281, 288, 290, 291
condensed and gaseous phases
  and carbon oxides 444–450
  chlorination of iron 231
  description 426
  effect of phase transformations 441–443
  Ellingham diagrams 433–445, *441–444,* 447, 448, *449,* 456
  Gibbs free energy change with temperature 432–433, 501, *502*
  graphical representation of 450–455, *452, 455,* 508–516
condensed-phase reactions 426–431, 455
condensed solutions
  binary systems containing compounds 499–508
  criteria for 470–479
  dilute solute 293, 480–481
  Gibbs equilibrium phase rule 530
  graphical representation of 508–516
  and phase stability diagrams 486–499
  solubility of gases in metals 525–529
  standard state of 479–486
condensed state 455
  ideal solution model 597
  regular solution model 597–599
configurational entropy 82, 95, 96, 100–104, *104,* 105–106, 122, 123, 186, 190–192, 290, 292, 305, 310, 320, 399, 597, 608, 615
  of differing atoms in a crystal 100–104, *101, 104*
  of magnetic spins 105–106, *106*
congruent solidification 364
congruent temperature *372*
conservation of energy 3

constant-pressure molar heat capacities 43, 120, 171, *173, 174*, 176, 194, 205, 389, 631, **632**
constant-pressure processes 30–32, 42, 43, 560
constant-temperature heat reservoir 59, 60, 62, 62n3, 83, 561
constant-volume processes 29–30, 42, 43, 87
constituent 4, 24, 95, 96, 123, 171, 262, 290, 542, 596–598
constitution of materials 215
constraints on system 215, 248, 249
continuous transition *see* higher-order transition
conversion of energy 3, 4
$2CO + O_2 = 2CO_2$ 444, 446–449, *451*, 454
copper, oxidation 442–443, *442–443*, 629
corresponding states 119, 260, 261, *261,* 281
covalent character 542
C_P, relationship with C_v 34–35
criterion for equilibrium 79, 83, 131, 132, 135, *136,* 201, 237, 426, 470
critical point 259, 260, *260,* 263, 264, **264,** 268, 270, 271, 368, 599, 611
CsCl structure 607, *607,* 609
curvature of Gibbs free energy plots 218, 220, 233, 235, 323, 326, 371, 375, 612, *612, 614*
C_v, relationship with C_P 34–35
cyclic process 29, 53, 69–71, 75, *75*

Daltinides 500
Dalton, John 253, 500
Dalton's law of partial pressure 252–253, 281
Daniell cell 544–545, *545–546,* 547, 549–550, 561, 568–569
Daniell, John Frederick 544
Darken, L. S. 311, 311n2, 518, 518n3
Debye model of heat capacity *119,* 120, *120,* 124, 186
Debye, Peter Joseph William 118–120, 124
decomposition of a solid 190
degree of irreversibility 57, 59–61, 77, 78, 82, 83, 548
degree, of mixed-up-ness 96, 97, 100, 113
DeHoff, Robert *118, 171, 228*
dependent thermodynamic variables 5, 9
deviation from ideality 257–262, 281, 295, *308,* 309, 310, 313, 314, *315,* 316, *320,* 343, *343,* 344, *344,* 358–362, 562, 587, *598,* 598–599, 604, 611
Dewar flask 24n1
diathermal boundaries 9
Dieterici, Conrad 271
Dieterici equation 271
dilute solute, and reaction equilibria 293, 480, 481, 483, 484, 561, 573
discontinuos transformation (transition) 172, 220, 237, 271
disordered phase 609, 612, 613, *614,* 615, 616, *616,* 617–620, *620,* 621, 624
dissipation of energy 59
driving force 61, 82, 184, 215, 216, 254, 542–551, 555, 597
Duhem Pierre Maurice Marie 5
Dulong and Petit's Law 118, 119
Dulong, Pierre Louis 170
dynamic energy 23
dynamic equilibrium 290, 394

efficiency of engine 69
Ehrenfest, Paul 220, 611, 614, 619, 623
Einstein, Albert 115–118, *118,* 119, *119,* 124, 171, 186
Einstein crystal 115
Einstein model of heat capacity 118, *118*
Einstein solid 115, 116
electric field 26, 41, 113, 157, 237, 543, 545
electric potential 26, 543–545, 547, 586
electric work 544, 560, 574, 586
electrochemical reaction 543, 560
electrochemical series 569, 588
electrochemistry 542–588
  and aqueous solution 561–564
  batteries 574–576
  chemical and electrical driving forces 544–549
  concentration cell 552–557, *557,* 558
  EMF (*see* electromotive force (EMF))
  formation cells 550–552, *551*
  Gibbs free energy of formation of ions and standard reduction potentials 564–574
  overview 542–543
  Pourbaix diagrams (*see* Pourbaix diagrams)
electrode 544–546, *546,* 547, 550–552, 554, 560, 567–569, **570–571,** 573–579, 581, 582, 585, 586, 588
electrolysis 585
electrolysis cell 548, *548,* 577
electrolyte 544, 545, *546,* 547, 550, 551, *552,* 553–555, *557,* 562, 568, 574–577, 585, 588
electrolytic reaction 542, *543*
electromotive force (EMF)
  batteries 574–576
  effect of concentration on 549–550
  temperature coefficient of 558–560
Ellingham diagrams 433–441, *444,* 445, *449,* 448, 456, 523, 524, 543
  intersection 436–441, *438–440*
  silver oxidation reaction *434,* 434–436, *436, 437*
Ellingham, Harold Johann Thomas 433, 433n2, 441, *441,* 442, *442,* 443, *443,* 444, *444,* 445, 447, 448, *449,* 456, 479, 543
EMF *see* electromotive force (EMF)

endothermic 174, 183, 223, 230, 310, 401, 402, 414, 445, 310
process 27, 183
energy barrier 266, 293
energy conversion 3, 4
energy equation (internal energy) 157
enthalpy 23, 34, 43, 51, 90, 160, 169–201, 170, *175*, *177*, *178, 179,* 182, *182*, 195, 200, 220, 225, 229, 230, *230*, 256, 281, 304, 309, 310, *320*, 321, *321,* 330, 371, 393, 529, 633, 403–406, 432, 434, 435, 437, 441, 442, 456, 499, 521, 527, 560, 587, 598, 601, 602, 606, 607, 608, 615, 623, 635, 642
changes of reactions *33,* 33–34
constant pressure processes 30–32
definition 132–133
energy equation 157–158
of freezing *33,* 33–34, 96, 192
as function of temperature and composition 174–183, *175, 177–178,* **178,** *181–182*
and ideal solutions 302–304, *304*
influence of pressure 198–200
of melting *33,* 33–34, 95, 96, *175,* 180, 182, 183, 192, 195, 201, 219, *230,* 441, 635
mixing of ideal gases 255–257
entropy 17, 18, 57, 62–68, 71, 75, 76, 78, 79, *79*, 81, *81*, 82, 83, 94, 95–96, 97, 107, 113, 114, 123, 131, 133, 135, *136,* 138, 146–152, *156*, 157, 169–201, 216, 217, 219, *219*, 220, 231, 232, 235, 237, 281, 290, 292, 310, *320*, 329, 330, 331, 333, 343, 344, 366, 368, 375, 399, 400, 401, 403–406, 434, 435, 437, 441, 442, 456, 465, 558, 587, 596, 597, 602, 606, 608, 614, 615, 619, 623, 633, **633–634**, 639
aspects of 18, 96, 123, 157, 190–191, 231, 320
and atomic scale disorder 95–96
of boiling 196–198, *197, 198*
and Boltzmann distribution 107–111, *110*
and Boltzmann equation 113, 123
configurational 100–104
and criterion for equilibrium 79, *79,* 83
of differing atoms in a crystal 100–104, *101, 104*
heat flow and production of 120–122
of ideal gases 257
ideal solutions 304–306, *306*
and identical particles 100
influence of pressure 198–200
magnetic 105–106, *106*, 122, 153, 156, *156*, 191, 231
of melting 195–196, *196*
and microstate 96–97
as “mixed-up-ness” 95–97, 100, 113
of mixing ideal gases 100–104, *104*, 257
quantification of irreversibility *59,* 59–60
in space 100
spin 105–106, *106,* 123, 156, 157, 191, 231, 232, 320
temperature dependence 194–195
and temperature effect *110, 111,* 111–113, 152, 153, *153,* 194–198, *195–198*
thermal 82, 96, 97, 100, 122, 123, 157, 190, 196
thermal equilibrium 216
vibrational 190, 231, 232
vs. internal energy 189–190, *190*
vs. temperature plots 189, *191*
and working of heat engine 57, 68, 76, 113, 123
environment 3, 191
equation of state 5, 8–13, 131, 132, 157, 158, 250, 261, 262, 262n2, 271, 272, 274, 277, 281
equiatomic alloy 607–609
equilibrium 3–6, *6,* 8–9, 12, 13–16, *16,* 17, 18, 24, 33, *33,* 37, 57, 58–62, 65, 66, 76, 79, 82, 83, 95–98, 100, 101, 103, 105–107, 113, 121–123, 131, 132, 134, 135, *136, 137,* 138, 140, 141, 159, 170, 175, *175,* 176, 182–184, 186, 187, 190–194, 201, 215–237, 248–249, 254, *258,* 259, *260,* 264, 266, 267, 281, 290, 291, 293, 294, 310, 324, 326, 329, 342, 347, 351, 353, 356, *361,* 362, 364, 366, 368, 371, *372,* 373–375, 386, 393–415, 426–431, *431,* 434, 437, 439, 440, 444, 445, 446, 447–450, *451, 452,* 453–456, 469–476, 478, 479, 481, 483, 485–493, 495–501, 504, 506, 508, 510–512, *512,* 513, 514, *514,* 515–519, 521–525, 527–530, 543, 545–548, 550, 554, 555, 569, 577–585, 596, 597, 606, 609, 611, 613, 614, 616–619, *619,* 620, 621, 623, 624, 634
constant (*see* equilibrium constant)
phase diagram 13–16, *14, 16,* 186, 215, 326, 362, 373, 486–499, 596
with single dissolved substance 581–585
state 3–6, *6,* 8, 13, 14, 17, 37, 57–59, 61, 62, 65, 79, 82, 97, 100, 103, 106, 107, 113, 122, 131, *137,* 170, 201, 215, 216, 234, *258,* 259, 264, 266, 267, 295, 310, 324, 393, 394, 397, 399, *405,* 413, 440, 455, 469, 470, 486, *512,* 611, 613, 619
between two dissolved substances 579–580
between two solids 580–581
equilibrium constant
constant pressure, K_P 394, 398–402, 405–411, 413, 414
mole fraction, K_x 403, 414
eutectic phase diagram *352, 354,* 370, 372–373, *373,* 374

eutectoid phase diagram *352, 354,* 370, 372–373, *373,* 374
evaporation 225, 227, 229, 240, 270, 290–293
exact differential equation 5, 5n1, 7, 75, 145, 636, 643
excess free energy 611, 613, 616, 618, 620, 624
exchange energy 105, 215
exchange field 105
exothermic 34, 175, 309, 310, 332, 371, 401, *401,* 414
  process 27, 175
expansion 8, 9, 11, *28,* 34, 36, 39, *39,* 40, 43, 61, *61,* 63–69, 73, 78, 83, 132, 138, 147, 152, 156, 188, 199, 201, 216, 251, 271, 277, 279, 280, 544, 599, *614,* 623
  adiabatic 36, 39, *39,* 40, 43, 65–69, 73
  free 36, 61, 63, 64, 66–67, 78
  isothermal 39, *39,* 61–64, 73, 78, 147, 148, 277, 279
extensive thermodynamic variables 13, 18, 256, 296
external field 5, 235, 237
external opposing voltage 543, 547, 548

face-centered cubic (FCC) 195, 196, 231–233, *233,* 610
Faraday, Michael 544
Faraday's constant 544, 586
FCC *see* face-centered cubic
Fe C (metastable) phase diagram 373–374, *374*
Fe–O system 518–524, *519–521,* 523, *524*
ferromagnet 154
ferromagnetic phases 373, 374
field variable 5, *155*
First Law of Thermodynamics 4, 17, 18, 23–44, 56, 62, 63, 67, 68, 70, 71, 77, 80–83, 94, 96, 131, 137–139, 143, 146, 175, 201, 644–646
  constant-pressure processes 30–32
  constant-volume processes 29–30
  electrical work on dielectric material 41
  heat and work 23–24
  heat capacity 32–36
  internal energy and 25–29
  magnetic work on paramagnetic material 40–41
  overview 23
  reversible adiabatic processes 37–38
  reversible isothermal process 38–40, *39*
  and Second Law 80–82
  work to create or extend surface 41–42
first-order phase transition 220, 266, 611, 616, 619, 620
Flory-Huggins model 329–331, 330n4
Flory, P. J. 329
forbidden energy bands 97
formation cells 550–552, *551,* 558, 559
free expansion 36, 61, 64, 66–67, 78
  ideal gas 63
friction 4, 23
fugacity 272–281, 294, 331, 393
function of state 5, 23, 42, 43, 75, 78, 97, 260
fundamental equation 131–160, 215, 251, 254, 304, 645, 646

The Ga-GaP system *507,* 507–508
galvanic cell reaction 132, 544, 548, *548,* 560, 575–577, 586
gas
  constant, R 12, 110, 250, 306
  ideal gases (*see* ideal gases; reaction equilibria)
  ideal solution model 596–597
  mixture and equilibrium constant (*see* gas mixture and equilibrium constant)
gaseous reaction 402, 426
gas mixture and equilibrium constant 394–399, 414
  as compromise between enthalpy and entropy 403–406, *404, 405*
  description 400–402
  in H_2O-H_2 and CO_2-CO mixtures 411–413
  overview 393
  pressure effect on 402–403
  in $SO_2(g)$-$SO_{2(}g)$-$O_2(g)$ 406–411
  temperature effect on 400–402
Gay-Lussac, Joseph-Luis 11
Gibbs-Duhem equation ideal solutions 296–297, 310–314, *311,* 398, 552
  Henry's and Raoult's laws 290–294, *292, 294,* 312
Gibbs equilibrium phase rule 248–249, 353, 375, 406, 429, 440, 456, 530, 543
  with reactions 429, 456
Gibbs free energy 123, 137–141, *141,* 142, 158–160, 185, *185,* 189, 201, 215–221, *218,* 220, 221–225, *226,* 233, *233,* 234–237, 248, 251, 253–257, 264, 266, *266,* 268, 272, 275, 276, 280, 281, 297, 298–301, 307, 310, 312–314, *315,* 316, *320,* 321–324, *322, 325,* 326, *327, 328,* 329, 330–332, 342–375, 393–396, *396,* 397, 402–406, 412, 426–430, 432–433, 438, *438,* 439, 442, 445, 446, 447, 455, 456, 469–474, 482, 485, 490, 493, 501, 502, 504, 505, *505, 506,* 507–509, *510,* 516, *517, 518,* 519, 521, 525, 526, 529, 544, 547, 548, 551, 553, 560, 562, 564–574, 579, 596, *596,* 597–600, *600, 601,* 602, 606, 609, *610,* 614, *614,* 616, 618, 620, *620,* 621–623, 629–630, **630–631,** 644
  2-3-4 case *616,* 616–620
  2-4 case 612–616, *615*

Gibbs free energy (*cont.*)
2-4-6 case *620,* 620–622
changes for selected reactions 629–630, **630–631**
change with temperature 432–433
composition 501, *502*
with constant pressure 216–221, *217–219, 221*
constant-pressure molar heat capacities 120, 171, 173, *174,* 176, 194, 631, **632**
criteria for phase stability in 324–329, *325, 327–329*
due to chemical reaction 31–32, 140, 393–397, 403, 404, 432–433, 456, 469
as function of temperature and pressure 222–225, *223, 224*
graphical representation Gibbs free energy composition 351–353
graphical representation, of phase equilibria 229
liquid and solid standard states 345–351
magnetic field on *P-T* diagram 234–235, *235*
of mixing ideal gases 256–257
molar *601,* 602, 606, 609, *610*
molar entropies of various substances molar heat 631, **632,** 633, **633–**634(*see also* Molar heat capacity)
overview 342–343
phase diagram (*see* phase diagram)
with pressure at constant 221–222, *222*
pressure at constant temperature 221–222, *222*
saturated (equilibrium) vapor pressures 634, **634**
solid-solid equilibria 229–234, *231, 233, 234*
temperature at constant pressure 216–221, *217–219, 221*
and thermodynamic activity 343–344, 351–353
vapor and condensed phase 225–229, *226, 228*
Gibbs free energy of formation and ideal solutions 307, 347, 354
change in *299,* 299–300
of ions and standard reduction potentials 564–574
molar 298–299, *299,* 629–630, **630–631**
nonideal solutions 307–310, *308,* 315
overview 301
partial molar 298–299, 600
regular solutions *321,* 321–324, *322*
tangential intercepts 301
Gibbs free energy of mixing 256–257, 300, 301, 310, 312–314, 316, *320,* 321–324, *325,* 326, *327, 328,* 329, 343–345, 347, 348, *349,* 350–352, *352,* 353, 354, *354, 357, 358,* 362, *363, 365,* 366, *367, 369,* 371, 504, 509, 516–517, *517, 518,* 596, *596,* 597–600, *600,* 602, 609, *610,* 623
ideal gases 256–257
Gibbs–Helmholtz equation 158–160, 184, 302, 400, 432, 519, 521
Gibbs, Josiah Willard 95, 133
Gibbs-Konovalov rule 373
glass 24n1, 186, 192
Goodman, D. A. 371
graphical representation, of phase equilibria 229
in Al-C-O-N system 513–516, *514*
in Mg-Al-O system 508–512, *510–512*
Guggenheim, Edward Armand 192n3
Gurry, R.W. 311, 311n2, 518, 518n3

half-cell reactions 554, 564, 567, 572, 573, 576, 577, 588, 591
Hardy, H. K. 601n3
Heal, T. J. 601n3
heat 3, 4, 9, 12, 17, 23–24, 27, *27,* 28, 57, 59, *59,* 60, *61,* 62–65, 67, *68,* 68–71, 76–78, 83, 96, 97, 101, 120–122, 124, 133, 134, 137, 157, 159, 215, 219, 227, *228,* 230, 256, 270, 326, 332, 333, 348, 371, 375, 388, 393, 402, 408, 445, 519, 520, *521,* 560–561, 601, 610, 633, **633–634,** 635, **635**
flow and entropy production 120–122
mechanical equivalent of and work 24
process 27–29, *28*
relationship between work and 23–24
heat capacity 32–36, 42, 43, 114–120, *120,* 140, 152, 156, 169–201, 218, 219, *219,* 220, 229, 233, 235, 389, 432, 456, 615, *615,* 623, 631, **632**
constant magnetic field 156
constant magnetization 189
constant pressure 169–170
empirical representation of 170–174, *171–174*
function of temperature 115–120, *118–120*
molar 33, 42, 43, 117, 118, 120, *120,* 164, 170, 171, *171,* 172, *173, 174,* 176, 194, 219, 229, 432, 456, 631, **632**
overview 169–170
theoretical calculation of 199–200
heat engine 4, 17, 57, *68,* 68–71, *69,* 76
heat pump 70
heat reservoir 59, *59,* 60, 62, 62n3, 63–65, 68–70, 78, 83, 96, 134, 137, 561
Helmholtz free energy 112, 132, 133–137, 159, 160, 170, 189, 643
hematite 31, 522, 524, 530
Henrian standard state 479–484, 529–530
Henry's law 290–294, *292, 294,* 312, 331, 344, 350, 351, 479–481, 485, 525, 526, 529, 530, 534, 561–562, 587
ideal solution 290–294, *292, 294,* 312
Hess, Germain 32
Hess' law of constant heat summation 32
heterogeneous system 14
higher-order phase transformation

higher-order transitions 220, 237, 271, 599, 609, 611, 614, 619–621, 625, 626
H_2O-H_2 gas mixture 411–413
homogeneous system 14n6, 141, 215, 324
horizontal inflection point 326, 620
Huggins, M. L. 329
hydroxides 430
hyper-peritectic reaction 370
hypo-peritectic reaction 370

ideal gases 9–13, 34–40, 43, 61–67, 73, 74, 78, 147–151, 157, 158, 199, 200, 250, 251–257, 262, 270, 272, 274, 277, 278, *278,* 279–281, 393, 414, 438, *438,* 596, 597
  adiabatic expansion of 66–68
  Dalton's law of partial pressures 252–253
  enthalpy of mixing 255–256
  entropy of 257
  equations of state for 9–12, *10,* 250, 257–262, *258–261,* 271–272
  free expansion of 63
  Gibbs free energy of mixing 256–257, 504, 509, 516, 517, *517, 518*
  internal energy 255
  isothermal expansion of 61–63
  law 12, 250
  mixing equations of state for 312–314
  mixtures of 251–255
  mole fraction 251–252
  nonideal gases 271–280, 611
  overview 250
  of *P-V-T* relationships 250
  partial molar quantities *253,* 253–255
  reversible isothermal compression 38–40, *39,* 64–65
  temperature 73
  thermodynamic treatment of 272–280, *275, 278*
ideal solution 301–307, 313, 314, 332, 345–351, 596, *596,* 597, 599, 600
  change in volume 301–302, *304*
  condensed state 597
  enthalpy of formation 302–304, *306*
  entropy of formation 304–306
  gaseous state 596–597
  Gibbs-Duhem equation 296–297, 310–314, *311*
  Gibbs free energy of formation (*see* Gibbs free energy of formation and ideal solutions)
  Gibbs free energy of mixing 596, *596,* 597–600, 602, 609, *610,* 623
  Henry's and Raoult's laws 290–294, *292, 294,* 312, 344, 350, 351
  Raoult's law and Henry's law (*see* Henry's law; Raoult's law)
  sub-regular solution models 599–602
  total molar Gibbs free energy of mixing 312–314, *314, 315,* 596, *596,* 597–600, *600,* 602, 609, *610,* 623
impermeable boundaries 3, 4
independent thermodynamic variables 5, 123, 135, 144
infinite dilution 479, 529, 561, 565
Ino, H. 610, 610n5
intensive thermodynamic variables 7, 13, 16, 140, 141, 215
interaction among particles 257
interaction parameter 610, 623
internal energy
  energy equation 157
  and First Law of thermodynamics 25–29
  ideal gases 255
  system 597, 603n4, 639, 642, 643, 645
  vs. entropy 189–190, *190*
internal equilibrium 17, 18, 186, 190, 192–194, 201
invariant reaction 370, 374
ionic character 542
iron, solid-solid equilibria *231,* 231–233, *233*
irreversible processes 57–59, 68, 76, 83, 87, 120, 122, 236, 257, 550
  comparison with reversible process 64
  vs. reversible process 63
isentropic process 66, 149–151
isobaric 29, 42, 138, 149–151, 158, 159, 199, 201, 260, 342, 343, 345, 499
isochoric 42
isolated systems 3, 42, 59, 79, 96–107, 111, 131, 215, 216
  configurational entropy (*see* configurational entropy)
  discretation of energy *98,* 98–100, *99*
  microcanonical ensemble 106–107
isothermal process
  compression 64–65
  expansion *61,* 61–63

Jeffes, J. H. E. 552, 557
Joule, definition 24, 36
Joule, James Prescott 24–26, 29, 36, 78

Kamerlingh Onnes equation 271
Kelvin, degree 12n4
Kelvin, Lord 73
kinetic energy 23, 26, 96
kinetic theory of gases 94
Kirchhoff's law 183, 432
Konovalov, Dmitri Petrovich 371
Kopp, Emile 170–171
Kopp rule 171
Kozuka, Z 556

Landau, Lev Davidovich 611–624
model of Gibbs free energy 611, 613, *614,* 614–623, *620*
theory on phase transformations 611–623
latent heat of melting 205, 219
Laughlin, D. E. 232, 373, 610
law of corresponding states 119, 260, *261,* 281
law of definite proportions 500
law of Dulong and Petit 118
laws of thermodynamics 16–17, 57, 80–83, 131, 186
Fisrt Law 4, 17, 18, 23–44, 56, 62, 63, 67, 68, 70, 71, 77, 80–83, 94, 96, 131, 137–139, 143, 146, 175, 201, 644–646
Second Law 17, 18, 57–83, 94, 107, 131, 133, 134, 139, 143, 186
Third Law 17, 18, 82, 114, 154, 156, 169–201, 217, 220, 597, 599, 609, 613, 617, 623
Zeroth law 12, 16, 17
lead acid batteries 574–575, 587
Le Chatelier, Henry Louis 184
Le Chatelier's principle 182, 222, 402, 407, 408, 414, 421, 445
Legendre transformations *639–641,* 639–646, *643*
liquid junction potential 550, 553
liquid standard states 345–351, *346*
liquidus 342, 345–351, 353, 356, 358–362, 364, 366, 368, 371, *372,* 375, 379, 386, 388, 390, 507, 508
lines 358–362, *360, 361*
temperature 342, 359, 381, 383
liquidus curves 345–351, 356, 358, 359, 361, 366, 371, *372*
for ideal solutions 345–351, *346*
liquid-vapor equilibrium *260*
lithium ion batteries 576, 587
local equilibrium 224
log pressure vs 1/T phase diagram 454, *455*
long-range order parameter (LRO) 607, 609, *609,* 623
low-temperature regions, in phase diagrams *266*
LRO *see* long-range order parameter (LRO)

macroscopic thermodynamic variables 96, 394
macrostate 96, 98–100, 103, 108, 110, 111, 122, 123
magnetic entropy 105–106, *106*, 122, 153, 156, *156*, 191, 231
magnetic field 5, 40, 41, 56, 105, 106, 113, 132, 139, 140, 153, 156, *156,* 157
P-T diagram 234–235
magnetic susceptibility 234, 235, *235*
magnetic work, on paramagnetic material 40–41
magnetite 520–523, 530
magnetization 40, 106, 153, 154, *154,* 156, 189
magnetocaloric 153, 156, 157
Massalski, T. B. 232, 373
mathematical relationships 543, 636–638
maximum work 77–78, 548
Maxwell construction 267
Maxwell, James Clerk 144–158, 160, 188, 198, 199
Maxwell's relations
energy equation (internal energy) 157
enthalpy energy equation 157–158
magnetic relation 153–154, *154*
S and *Vas* dependent variables 152–153, *153*
S, V and *M* with independent variables *T, P* and **H** 154–157, *155, 156*
T and *Pas* independent variables 152–153, *153*
TdS equation 146–151
mechanical equivalent of heat 24
Meijerling, J. L. 601
melting temperature 15, 95, 96, 172, 175, *175,* 180, 182, *182,* 183, 194, 195, 217–221, 223, 229, *230,* 236, 345, 348, 353, 362, 364, 366, *368,* 441–443, 496, 629, 635
metal-carbon-oxygen equilibria 450–455, *452, 455*
metallic glass 192
metastable equilibria 490
metastable extension *224,* 225, 271
metastable phase 373
metastable solution 324, 329, 599
metastable state 224, 619, 620
metatectic diagram 374
metatectic phase diagram 374
Mg-Al-O system, and phase equilibria in 508–512, *510–512*
microcanonical ensemble 106–107
microscopic thermodynamic variables 5, 394
microstate, and entropy 96–97, 100, 105–107, 120, 122, 123
mixtures, of ideal gases 251–256, 281, 414
Dalton's law of partial pressure 252–253
mole fraction 251–252
partial molar quantities *253,* 253–255, 597
molal 253n1, 553, 561, 564, 572
porous diaphragm 36, 544, 549, 550
molality 561–563, 568, 571–574, 587, 588
molar enthalpy of melting 183, 219, 602, 623, 633
molar enthalpy of mixing 256, 303, 309, *320,* 528, 587, 602
molar free energy of melting 345, 362, 364, 368, 623
molar heat capacity 33, 42, 43, 117, 118, 120, *120,* 164, 170, 171, *171,* 172, *173, 174,* 176, 194, 219, 229, 389, 432, 456, 631, **632**
constant-pressure capacities 32, 120, 139, 158, 159, 216–221, 631, **632**
of formation 298–301, 307, 321–324, 564–574, 633, **633–634**
of melting and transformation 635, **635**

molarity 561, 573, 574, 587
mole fraction 104, 251–253, 281, 291, 292, 307, 402, 403, 414, *418,* 478, 481, 511, 525, 526, 561
monotectic equilibrium *361,* 362, 366, 368
monotectic phase diagram *361,* 370, 374
monotectoid equilibrium 370, 374
monotectoid phase diagram 370, 374
most probable state 101, 103, 106, 113, 122

natural processes 57–59, 61
near-neighbor model 602
Nernst equation 544
Nernst heat theorem 185
Nernst-Planck-Simon statement 186, 201
Nernst, Walther Hermann 185, 186, 201
nickel–cadmium battery 575
nomographic scale 437, 439, *440,* 448, 450, 456, 473
nonequilibrium state 58, 59, 61, 79, 122, 236
nonideal gases 611
  equations of state for 257–262, *258–261,* 271–272
  thermodynamic treatment of 272–280, *275, 278*
nonideal solutions 307–310, *308,* 315, 332, 598
nonstoichiometric compound 516

one-component simple system 15, 152, 215–237
Onnes, Heike Kamerlingh 271
open-circuit EMF 547
open systems 4, 97, 140, 142, 143, 574
ordered phase 295, 310, 599, 607, 612, 613, 615, 616, *616,* 617–620, *620,* 621, 622, 624
order parameter 154, 189, 596, 606–610, *610,* 611–613, *614,* 617, *619,* 620–623
  definition 611
  vs. G^{xs} 612, 613
  vs. reduced temperature 614, *614,* 617, 619, *619,* 620–623
oxidation 31, 176, 177, 182, *182,* 406, 426, 430, 433, *436,* 436, *437,* 437, 440, *441,* 442, 455, 456, 472, 474, 478, 479, 483, 508, 511, 512, 517, 523, 542, 548, 568, 569, 574, 577, 579, 580, 629
  effect of pressure 445–447
  Ellingham diagram *434,* 434–435
  example 442–443, *443*
  of pure solid phase 434, 455, 456, 472
oxygen concentration cell 553

paramagnet 98, 105, 106, 156, 157, 191
  BCC phase 373
partial molar quantities 251, *253,* 253–255, 597, 600, 611
  ideal gases *253,* 253–255
partial pressure 251, 252–253, 256, 281, 294, 393, 398, 402, 406, 409, 411–413, 426, 430, *452,* 455, 470, 472, 477, 478, 486, 490, 491, 496, *497,* 506–508, 522, 523
partition function 109, 111, 113, 115, 126, 131, 291
path 5–7, 15, 25, 26, 28, *28,* 29, 31, 32, 39, *39,* 42, 43, *47, 54,* 61, 66, 75, 77, 78, 82, 83, 236, 260, 266, 523, *543,* 637
Pelton, A. D. 366n2
perfect gas 250, 260
peritectic phase diagrams 366, 368–369, *369,* 370, 374
peritectoid phase diagrams 370, 374
permeable boundaries 3, 4
perpetual motion 71
  first kind 71
  second kind 71
Petit, Alexis Therese 118, 119, 170, 171
phase, definition 14, 14n6, 215
phase diagram 13–16, 186, 215, 224, *224,* 229, 231, *231,* 233, *234,* 236, 237, 260, 267, 271, 326, *327, 328,* 329, *330,* 342–375, 386, 388, 499, *500, 506,* 507, *507,* 511, *511, 519,* 522, 523, 553, *553,* 596, 598, *598,* 599, 601
  of binary system 362–370
  binary temperature-composition 370–372
  calculations 353–362, *357, 358,* 388–390
  eutectic and eutectoid *352, 354,* 370, 372–373, *373,* 374
  low-temperature regions in 266, *266*
  magnetic transformations and *373,* 373–374
  monotectic *361,* 370, 374
  monotectoid 370, 374
  peritectic and peritectoid 366, 368, 369, *369,* 370, 374
  of regular solutions 362–370
  syntectic 368
  system ZrO2–CaO 386–388, 553, *553*
phase equilibrium 215–237, 426–428, 469, 476, 488, 490
phase separation 260, 310, 324, 325
phase stability diagrams 486–499, 510, 511, 513, 514, 516, 576
phase transformations 441–443, *441*
  capillarity and local equilibrium 224
  with change in composition 143, 371
  definitions 623
  Landau theory 611–623
  with no change in composition 253, 441
  surface energy 41–42
phenomenological 94
Planck, Max Karl Ernst Ludwig 115, 126, 186, 201
polymers 329–331, 333

polymorphism 173, 174, 229
porous diaphragm 544, 549, 550
potential energy 23, 25, 26, 290, 292, 293
potential-pH diagrams *see* Pourbaix diagrams
Pourbaix diagrams 576–579, *578*
  for aluminum 579–586, *584*
  equilibrium, between two dissolved substances 579–580
  equilibrium, between two solids 580–581
  equilibrium, with single dissolved substance 581–585
  solubility of alumina in aqueous solutions 585–586, *586*
  thermal energy (heat) effects 560–561
predominance diagrams *see* phase stability diagrams
pressure, definition 12, 15, 43, 56, 295, 393, 402, 414
pressure, thermal coefficient 189
principle of Clausius 71
principle of Kelvin and Planck 71
principle of Le Chatelier 222
property matrix 153
P-T diagram, magnetic field on 234–235, *235*
pure species 426–427, 429, 455
P-V-T relationships, in ideal gases 250, 271

quasi-static process 61

Raoult, François-Marie 292
Raoultian ideality 353, 390, 604, 623
Raoultian ideal solutions 345, 353, 390, 604
  liquid 345
  solid 345
Raoultian standard state 479–483, 529–530
Raoult's law 290–294, *292, 294,* 301, 307, 312, 331, 332, 344, 350–351, 353, 484, 508
  atomic order parameter 189, 606–611
  Flory-Huggins model 329–331
  ideal solution 290–294, *292, 294,* 312
  regular solution 314–320, *318–320*
  second-neighbor interactions 610
  statistical models 602–606
  sub-regular solution models 599–602
  thermodynamic activity of component in 294–296, *295, 296*
Raynor, G.V. 352n1
reactants, and products 174, 176, *178,* 179, 182, 186, 201, 205, 393, 395, 398, 402, 406, 413, 426, 432, 441, *442,* 456, 469, 471, *473,* 481, 529, 542, 549, 550, 555, 560, 577
reaction equilibria 403, 426, 445, 469–530
  binary systems containing compounds 499–508
  and carbon oxides 444–450
  and chlorination of iron 231
  in condensed and gaseous phases 427–431, *431*
  in condensed solution 470–479
  criteria for 470–479
  description 469–470
  and dilute solute 480–481
  effect of phase transformations 441–443
  Ellingham diagrams 433–441, 523, 524
  enthalpy and entropy 403–406
  in gas mixture and equilibrium constant as compromise between 403–406, *404, 405*
  and Gibbs equilibrium phase rule 406, 429, 440, 456, 530
  and Gibbs free energy change with temperature 432–433
  graphical representation of 450–455, *452, 455,* 508–516
  H_2O-H_2 and CO_2-CO mixtures 411–413
  overview 469–470
  oxide phases formation 516–524
  and phase stability diagrams 486–499
  pressure effect on 402–403
  solubility of gases in metals 525–529
  in $SO_2(g)$-$SO_{2(}g)$-$O_2(g)$ 406–411
  standard state of 479–486
  temperature effect on 400–402
reactive systems 429
real gas 36, 250, 257–262, 264, 281
reduction, of oxide 430, 444, 522
reference state 201, 251, 345
region of instability 264
Regnault, Henri Victor 11
regular solutions 314–324, 326, *327, 328,* 329–331, *330,* 333, 342, 358, *360, 361,* 362–370, 374, 596–599, *600,* 602, 605, 606, 611, 623
  atomic order parameter 606–610
  Flory-Huggins model 329–331
  Gibbs free energy of formation *321,* 321–324, *322*
  ideal solution 314–320, *318–320*
  model 597–598
  with negative deviations from ideality 599
  with positive deviation from ideality *598,* 598–599
  second-neighbor interactions 610
  statistical models 602–606
regular solutions, of Gibbs free energy *321,* 321–324, *322,* 362–370
  criteria for phase stability in 324–329, *325, 327–329*
reversible adiabatic processes 66
reversible and irreversible expansion of an ideal gas 64
  free expansion of 63
  isothermal expansion of 61–63

reversible processes 37, 61, 64, 66, 68, 75, 76, 82, 83, 134, 236, 544
comparison with irreversible expansions 64
isothermal 38–40, *39*
isothermal compression 64–65, 74
isothermal expansion *61,* 61–63
vs. irreversible process 57–59, 63
Richards, Joseph W. 184, 186, 195, 201
Richardson, Frederick Denys 437, *440*
Richardson nomographic scale 437, 439, *440,* 448, 450, 456
Richards' rule (JW) 196
Richards, Theodore William 184, 186, 201
Rothery, William Hume 351, 351n1
Rumford, Count *see* Thomson, Sir Benjamin

salt bridge 550
Samis, C. S. 556
S and *Vas* dependent variables 80–82, 131, 152–153, *153,* 641, 644
saturated solution 550
saturated vapor pressures 15, 227, 229, 236, 258, 268–270, 281, 290–292, 294, 295, 412, 426–428, 455, 500, 634, **634**
and Gibbs free energy 268, 426, 427, 455
Second Law of Thermodynamics 17, 18, 57–83, 94, 107, 131, 133, 134, 139, 143, 186
adiabatic expansion of ideal gas 66–68
amount of work 77–78
description 57
entropy and criterion for equilibrium 79, *79*
entropy and quantification of *59,* 59–60
and First Law 80–82
free expansion of ideal gas 63
isothermal expansion of ideal gas *61,* 61–63
overview 57
reversible and irreversible expansion 64
reversible isothermal compression 65
spontaneous/natural/irreversible processes 57–59
thermodynamic temperature scale 71–74, *72*
and working of heat engine *68,* 68–71, *69*
second-neighbor interaction energies 610
second order phase transformation (transition) 219, *219,* 220, 611, 612, 614, 615, 618, 619, 624
semipermeable boundaries 4
SHE *see* standard hydrogen electrode (SHE)
SiC–C–gas phase 487, 488, *489*
Si–C–gas phase 487, 490–492
Si–C–O 486, 487, *489,* 491, *494, 497*
phase stability diagram 487–499, *489, 494*
SiC–SiO_2–gas phase 487, 488, 498–499
Sieverts, Adolf 529
Sieverts' constant 529
Sieverts' law 529
Simon, Sir Francis 190, 192, 201
simple system 3, 5, 8, 17, 29, 32, 40, 42, 80, 122, 123, 131, 133, 137, 139, 140, 143, 145, 146, 152, 160, 169, 170, 189, *190,* 215, 216, 218, 220, 237, 639
simple thermodynamic systems 3, 639
Singh, N. S. 610
single electrode potential solid 567–569, *568–569,* 573
influence 573–574
SiO_2–C–gas phase 487, 490
Si–SiC–gas phase 487, 488
$Si_{(l)}$–SiC–gas phase 498
$Si_{(s)}$–SiC–gas phase 498
Si–SiO_2–gas phase 487–488
Si–SiO_2–SiC–gas phase 496–498
Soffa, W. A. 610
solid equilibria 224, 229–234
solid–solid equilibria 229–234, *230*
iron *231,* 231–233, *233*
zirconia 233–234, *234*
solid standard states 345–351
solidus curves 348, 364, 366, 368
for ideal solutions 345–351, *346*
temperature 342
solubility of gases 525–529
in metals 525–529, *527–528*
in solids 525–529
solubility product 569–573, **570–571**
solution thermodynamics 290, 358, 470
$SO_2(g)$-$SO_{2(}g)$-$O_2(g)$ system, effect of temperature and pressure changes 406–411
specific heat 33, *115*
spina 267
spin entropy 123, 153, 156, 157, 191, 231, 232
spinodal *266, 267,* 271, 326, 329, *330,* 333, *598,* 599
spin system 105–106, *106,* 113, 122, 123, 153, 154, 156, 157, 191, 231, 232, 320
spontaneous processes 17, 57–60, 79, 94, 135
types 59
Sridhar, R. 552, 557
stable equilibria 490, 516
stable solution 322–324, 329
stable state 176, 201, 266, 322, 329, 342, 345, 366, 437, 479, 529, 613, 618–620
standard EMF, of cell 549, 553, 567–569, 587
standard Gibbs free energy 470–472, 474, 485, 490, 504, 505, 507, 508, 529
change 393, 395, 400, 406, 412, 429, 430, 432–433, 438, 442, 447, 456, 471, 472, 474, 485, 490, 504, 505, 507, 529, 551, 566, 572, 629–630, **630–631**
standard hydrogen electrode (SHE) 567–568, *568–569,* 588

standard state 251, 255, 272, 280, 281, 294, 295, 331, 345–351, 353, 358, 362, 364, 395, 413, 429, 437, 445, 455, 469, 471, 472, 479–486, 506, 508, 516–520, 525, 526, 529, 530, 549, 550, 553, 560–563, 568, 571–573, 577, 587, **630–631,** 633
standard temperature pressure (STP) 12, 13
state variable 7, 12–14, 23, 28–31, 68, 133, 144, 220, 235, 237, 248, 254
statistical interpretation of entropy 94–124
  and atomic scale disorder 95–96
  and Boltzmann distribution 107–111, *110*
  and Boltzmann equation 107–111, *110*
  configurational entropy 100–104 (*see also* configurational entropy)
  heat flow and production of 120–122
  and identical particles 119
  and microstate 96–97
  overview 94–95, *95*
  and temperature effect *110–111,* 111–113, 115–120, *118–120*
  thermal equilibrium 95, 96
statistical models, regular solution 596, 602–606
statistical thermodynamics 82, 94–97, 103, 124
steam engine 68, 69
Stirling, James 194
Stirling's approximation 107, 305, 305n1
stoichiometric compound 190, 500, *500,* 523
stoichiometry 394, 406, 409, 562, 573
sublimation 15, 225, 227
sub-regular solution models 596, 599–602, 623
supercritical fluid 260, *260*
superheated steam 69
surroundings 3, 4, 9, 17, 27, 34, 48, 57, 63, 67, 68, 70, 79, 80, 131, 133, 142, 215, 309
S, V and *M* with independent variables *T, P* and **H** 154–157, *155, 156*
syntectic phase diagram 368
system 3–6, 8, 9, 12–16, *16,* 17, 18, 23–27, *27,* 28–34, 36–44, 56, 57–61, 63, 68, 70, 75–78, *79,* 80–83, 94–98, *99,* 100, 101, 103–108, 110, 111, *111,* 112, 113–115, 117, 120–123, 131–135, *136,* 137, *137,* 138, 139–146, 152, 154, 157–160, 169, 170, 172, 174, 175, 177, 182, 183, 189, *190,* 191, *191,* 192, 194, 198–201, 215–237, 248–252, 254, 258–260, 263, 264, 266, 267, 295, *295, 296,* 297, 301, 306, 307, *308,* 309, 310, 313, *314, 315,* 318, *318–320,* 322, *322,* 323, 324, 326, *327, 328,* 332, 333, 342–375, 386, 393–397, 399, 402, 403, 406–408, 426, 427–431, 434, 437, 439, 445, 450–455, 469–530, 543, 544, 547, 548, *553,* 556, 560, 561, 574, 586, 588, 596–624, 639, 640, 645, 646
  internal energy 597, 603n4, 639, 642, 643, 645
  phase diagram 386–388
  simple 3, 5, 8, 17, 29, 32, 40, 42, 80, 122, 123, 131, 133, 137, 139, 140, 143, 145, 146, 152, 160, 169, 170, 189, *190,* 215, 216, 218, 220, 237, 639
  SO_2(g)-SO_2(g)-O_2(g) 406–411
  ZrO2-CaO 553, *553*
system variable 32

T and *P as* independent variables 148, 152–153, *153*, 229, 264, 296, 297, 323, 562, 612, 620, 644
T_C (critical temperature) *258,* 262, *265, 266,* 281, 325, 326, 329, 333, 364, 366, 374, 599, *610,* 615, *615*, 616, 622
TdS equation
  first TdS equation 146–148
  second TdS equation 148–150
  third TdS equation 150–151
temperature 3–6, 9, *10,* 11–16, *16,* 17, 18, *20,* 24, 26, 27, 29, 32–34, 36, 39, 41–43, 58–60, 62–65, 67, 69–75, 77, 80, 82, 83, 94, 95, *95,* 96, 101, 110, 111–114, *114,* 115–121, 124, 131–135, *135, 136,* 137, *137,* 139–141, 146–153, *154,* 156, *156,* 157–159, 169–183, *181,* 182, *182,* 183–185, *185,* 186–189, *190,* 191, *191,* 192–201, 215–230, *230,* 231–233, *233, 234,* 235, *235,* 236, 237, 248, 250, 252, 253, 255, 257, 258, *258,* 259, 260, *261,* 262, 263, *263,* 264, *265, 266,* 267–269, *269,* 270–273, 277, 280, 281, 290–294, 296–299, *299,* 300, 301, 303, 305–307, 309, 310, 313–319, 321, 322, *322,* 323–326, *327, 328,* 329, 332, 333, 342, 343, 345, *346,* 347, 348, *349,* 351–354, *355,* 356, *356,* 358, 359, 362, *363,* 364, *365,* 366, *367,* 368, *368, 369,* 370–375, 386, 388–390, 393–395, 398–402, 405, *405,* 406–411, 414, 415, 426–430, *431,* 432–435, 437, 438, *438,* 439–443, 445–449, 448, 449, *451,* 452, *452,* 453–456, 467, 469–475, 479, 480, 482–486, 490, 492, 496, 499–501, *501,* 504, *505,* 506, *506,* 507, 508, 510, 516–518, 520–523, *524,* 525–528, *528,* 529, 543, 544, 547, 551, 552, *552,* 553–556, 558–561, 586, 587, 596, *596,* 597–599, 602, 606, 608, 609, *609,* 610, *610,* 611, 612, *612,* 613, *614,* 615, *615,* 616, *616,* 617–619, *619,* 620–624, 629, 631, 634, 635
  definition 4, 215
  dependence of the standard free energy change 432–433

entropy 111–113, 152, 153, *153,* 194–198, *195–198*
Gibbs free energy (*see* Gibbs free energy)
influence *110, 111,* 111–113
instability *266,* 599, *616,* 617, 619, 620, 622, 624
vs. composition phase diagram 342, 343, 358, 370, 371, *372,* 373, *374,* 500, *501,* 552, *552*
thermal energy (heat) effects 3, 4, 9, 12, 17, 23, 24, 24n1, 27, 28, 30–32, 34, 38, 39, 42, 43, 57–59, *59,* 60, 62, 62n3, 63–66, *68,* 69–71, 74–78, 82, 83, 94–96, 114, 120–123, 133, 134, 137, 142, 157, 169, 172, 174–176, 215, 219, 220, 223, 309, 402, 403, 407, 548, 560–561, 615, 619
thermal entropy 82, 96, 97, 100, 122, 123, 157, 190, 196
thermal equilibrium 12, 16, 24, *61,* 92, 121, 216
and Boltzmann equation 113, 123
thermochemical calorie 24
thermodynamic activity 294–296, 343–344, 351–353
of component in solution 294–296, *295, 296*
and Gibbs free energy composition 343–344, 351–353
of nonideal gases 272–280, *275, 278*
thermodynamics 4, 12, 16–18, 23–44, 56–83, 94–97, 103, 107, 114, 124, 131, 133–134, 137–139, 143, 146, 154, 156, 169–201, 217, 220, 294–296, 343–344, 351–353, 597, 599, 609, 613, 617, 623, 644–646
aqueous solution 561–564
chemical potential 140–143
for closed system 139–140, *141,* 439 (*see also* closed system)
components 13–16, *14, 16*
definition 3, 94
degree of freedom 225
field variables 5, 155
fundamental equations 139–140, 215, 251
potential (*see* internal energy)
state 4–8, *6*
state functions 17, 57, 68, 82, 94, 144, 298
state variable 7, 13, 23, 29–31, 68, 144, 220, 248, 254
temperature scale 71–74, *72*
treatment of ideal gases 272–280, *275, 278*
thermos flask 24n1
Third Law constraint 310, 364, 366, 373
Third Law of Thermodynamics 17, 18, 82, 114, 154, 156, 169–201, 217, 220, 597, 599, 609, 613, 617, 623
constraints on phase diagram 364, 366, 373
contradictions to 192–194
development of 184–186, *185*
experimental verification of 186–188, *187*
influence of pressure on 198–200
physical consequences 188–192
statement 186
Thomson, Sir Benjamin 23
Thomson, William *see* Lord Kelvin
Thomson, W. T. 36
total molar Gibbs free energy of mixing, ideal solution 312–314, *314, 315*
transcendental equation 608
transition states 220, 232, 266, 611, 619, 620
Trouton, Frederick Thomas 196, 201
Trouton' rule 196, *197*
2-4 model 612–616, *615*
2-4-6 model *620,* 620–622
two state system 113–115, *114, 115*
2-3-4 model *616,* 616–620

unique partial pressure 455, 470
universe 3, 17, 18, 27, 57, 63, 64, 67, 68, 77, 96, 131
unstable phase 236
unstable solution 324, 329
unstable state 236, 268

valence state 542
van der Waals fluid (gas) 262–271, *263,* **264, 265,** *265–269*
van der Waals, Johannes Diderik 262, 281, 290, 611
van't Hoff equation 400–401
van't Hoff, Jacobus Henricus 218, 400, 401
van't Hoff rule 218
vapor and condensed phase 225–229, *226, 228*
equilibrium between 225–229
graphical representation 229
vapor pressure 15, 135, 227, *228,* 229, 232–234, 236, 258, 268, 269, *269,* 270, 281, 290–292, *292,* 294, *294,* 295, *308,* 331, 412, 426–428, 430, 455, 469, 500, *501, 506,* 507, 567
saturated 634, **634**
vapor species 427
Vegard, Lars 302
Vegard's law 302
vibrational entropy 190, 231, 232
virial equation 271, 274–275, 277, 281
volatile 500, 507
V-P-T space 6, *6,* 8

Wagner, Carl 370
weight–pulley–heat reservoir arrangement 59, *59*

work 3, 4, 9, 12–13, 17, 23–30, 34, 36–38, 40–44, 56, 57, 59, *59,* 60, 62–68, *68,* 69–71, 74–78, 80, 82, 83, 94, 131–134, 138, 139, 142, 143, 146, 159, 170, 234, 251, 277, 278, 280, 544, 547, 548, 560, 574, 586, 610, 641, 645, 646
  changes of state 26–27, *27*
  function 133, 134
  and heat 23–24, 27–29
  units of energy 12–13
wustite 518–520, *520,* 521, *521,* 522, 523, 530

Zemansky, Mark W 147
Zeroth Law 12, 16, 17
zirconia, solid-solid equilibria 233–234, *234*